

2008-01-01

A Study Of The Interaction Of Thioindigo Dye, With Several Inorganic Host Materials

Alejandra Ramirez

University of Texas at El Paso, aleramirez@miners.utep.edu

Follow this and additional works at: https://digitalcommons.utep.edu/open_etd



Part of the [Inorganic Chemistry Commons](#), [Materials Science and Engineering Commons](#), [Mechanics of Materials Commons](#), and the [Organic Chemistry Commons](#)

Recommended Citation

Ramirez, Alejandra, "A Study Of The Interaction Of Thioindigo Dye, With Several Inorganic Host Materials" (2008). *Open Access Theses & Dissertations*. 339.

https://digitalcommons.utep.edu/open_etd/339

A STUDY OF THE INTERACTION OF THIOINDIGO DYE, WITH
SEVERAL INORGANIC HOST MATERIALS

ALEJANDRA RAMIREZ

Materials Science and Engineering

APPROVED:

Russell R. Chianelli, Ph.D., Chair

Keith H. Pannell, Ph.D.

Felicia S. Manciu, Ph.D.

Lori A. Polette-Niewold, Ph.D.

Lawrence E. Murr, Ph.D.

Patricia D. Witherspoon, Ph.D.
Dean of the Graduate School

DEDICATION

Für meinen Dennis

A STUDY OF THE INTERACTION OF THIOINDIGO DYE, WITH
SEVERAL INORGANIC HOST MATERIALS

by

ALEJANDRA RAMIREZ , B.S., M.S.

DISSERTATION

Presented to the Faculty of the Graduate School of

The University of Texas at El Paso

in Partial Fulfillment

of the Requirements

for the Degree of

DOCTOR OF PHILOSOPHY

Materials Science and Engineering

THE UNIVERSITY OF TEXAS AT EL PASO

December 2008

ACKNOWLEDGEMENTS

I would like to thank my committee members for their time, support and technical assistance. I also would like to thank Dr. Chianelli for the opportunity to work in his group and learn new techniques to approach research. My sincere gratitude to Dr. Komarneni whom I met at a materials conference and expressed interest in my project and later gave me the opportunity to test some of these materials. Special thanks to Dr. Pannell for investing so much time with me discussing this work. His guidance and love for science has helped me enormously. My sincere thanks to Dr. Polette-Niewold and Dr. Williams from Maya Pigments Inc. for general information regarding Maya Blue, and allowing me the use of their laboratory installations. My thanks to Dr. Manciu for her availability at all times in the analysis of countless samples, Swati Kumar, and to Candice Sifuentes for their work in the preparation of some of the samples tested. Thanks to David Williams and Manny Alvarado for their support at all times in general discussions about Maya Blue, writing tutorials, and testing countless models in Cerius² and Materials Studio software. Thanks, also, to Kristen Gonzalez, Harold Kelley and Manuel Ramos for their support and help at all times and to the rest of the Materials Research and Technology Institute group and Dr. Pannell's group for their friendship and valuable discussions.

ABSTRACT

Maya Blue has been the focus of numerous studies and is believed to be a mixture of palygorskite clay and indigo dye.^{1,2} Several derivatives of this pigment have been developed with intriguing properties. For instance, the dye thioindigo reacts with the palygorskite clay to exhibit a broad range of colors from red to blue under UV-Vis excitation. Based on FT-Raman and computer simulation, previous work performed in our group could relate indigo and thioindigo interaction to the aluminum sites in the framework.^{3,4}

The work performed with other inorganic host materials such as, layer structures and zeolites have displayed reversible acid indicator properties, similar to the ones observed in concentrated sulfuric acid. Spectroscopic analyses and computer modeling of the above mentioned interactions have been evaluated. Results obtained by these techniques showed that in dehydrated materials a disturbance of thioindigo C=O at 1655 cm^{-1} to lower frequencies occurs, due to the C=O---Lewis acid sites (LAS) interaction. In the presence of water, a smaller C=O shift due to C=O---HO(H)LAS was observed. Moreover, displacement of the 001 plane in some layer materials confirmed the effect of water on the color changes displayed by UV-Vis spectroscopy.

Based on these premises, it was concluded that weak electron donor-acceptor interactions took place between thioindigo functional groups (electron donors) and LAS of the aluminum silicate framework (electron acceptor). LAS (extra-framework aluminum and exchangeable cations) high hydration enthalpy made them extremely susceptible to

water molecules (electron donors); generating a hydrogen bond between the two sites. The reversibility of these chromatic hybrid materials could have potential applications as water sensors and charge transfer photosensitizers in nanocrystalline TiO_2 -based solar cells.

TABLE OF CONTENTS

ACKNOWLEDGEMENTS	iv
ABSTRACT	v
TABLE OF CONTENTS	vii
LIST OF TABLES	ix
APPENDIX TABLES	x
LIST OF FIGURES	xvii
APPENDIX FIGURES	xxxiii
LIST OF EQUATIONS	xxxix
CHAPTER	
1. INTRODUCTION	1
1.1 Background	1
1.2 Research Objectives	4
2. METHODOLOGY	5
2.1 Materials Sampling	5
2.2 Sample Preparation	6
2.3 Instrumentation	9
3. CHEMICAL AND STRUCTURAL CHARACTERISTICS OF STARTING MATERIALS	13
3.1 Thioindigo Dye	13
3.2 Inorganic Host Materials	18
4. RESULTS AND DISCUSSION	38

4.1 Chemical Analysis by Wide Range X-Ray Fluorescence Spectrometry (WD-XRF)	38
4.2 Physical Properties	38
4.3 Diffuse Reflectance Ultraviolet-Visible Spectroscopy	43
4.4 Structural Analysis by Fourier-Transformed Infrared Spectroscopy	85
4.5 Structural Analysis by X-ray Powder Diffraction	133
4.6 Chemical Analysis by Energy Dispersive Analysis (EDAX)	158
4.7 Magic Angle Nuclear Magnetic Resonance (MAS-NMR)	162
4.8 DFT Method For Calculation of Optical Spectra	169
5. CONCLUSIONS	172
6. INDUSTRIAL APPLICATION	189
6.1 Introduction	189
6.2 Experimental	190
6.3 Results and Discussion	190
6.4 Conclusions	191
LIST OF REFERENCES	192
APPENDIX A	202
APPENDIX B	208
CURRICULUM VITAE	297

LIST OF TABLES

Table 1 Main cation properties	33
Table 2 Observed vibrational assignments for palygorskite and sepiolite clays.	87
Table 3 Observed vibrational assignments for Na ⁺ -montmorillonite clays.....	90
Table 4 Observed vibrational assignments for Ca ²⁺ -montmorillonite clays.	91
Table 5 Observed vibrational assignments for three low charge fluorinated micas.....	93
Table 6 Observed vibrational assignments for several faujasite synthetic zeolites.	95
Table 7 Observed vibrational assignments for mordenite synthetic zeolites	96
Table 8 Observed vibrational assignments for LTA synthetic zeolites	97
Table 9 Fundamental frequencies (cm ⁻¹) in pyridine.	99
Table 10 D spacing values for the studied montmorillonite clays.	136
Table 11 d spacing values for the studied mica clays.	139
Table 12 Summary of Chemical Analysis for CBV21A exchanged with different cations by EDAX.....	158
Table 13 NMR resonances of several natural occurring clay minerals.....	165
Table 14 NMR spectra and color changes observed in several natural occurring clay minerals.....	174
Table 15 Cation content in natural occurring clay minerals.....	175
Table 16 Color changes related to exchangeable cation.....	183

APPENDIX TABLES

Table A. 1 WD-XRF chemical analysis clays and synthetic aluminosilicates used in this study.....	202
Table A. 2 WD-XRF Chemical analysis of synthetic zeolites used in this study.	203
Table A. 3 WD-XRF Chemical analysis of synthetic zeolites used in this study.	204
Table A. 4 List of natural occurring clay minerals used in this research. Chemical formula derived from WD-XRF measurements, pore size and general structure based on literature.	205
Table A. 5 List of synthetic zeolites used in this research. Chemical formula derived from WD-XRF measurements, pore size and general structure based on literature. ...	206
Table A. 6 List of synthetic swelling micas used in this research. Chemical formula derived from WD-XRF measurements, pore size and general structure based on literature.	207
Table B. 1 Peak fit statistics of thioindigo	208
Table B. 2 Peak fit statistics of Palygorskite / 0.5 mol % thioindigo unheated.....	209
Table B. 3 Peak fit statistics of Palygorskite / 0.5 mol % thioindigo heated at 413K for nine hours.	210
Table B. 4 Peak fit statistics of Palygorskite / 0.5 mol % thioindigo heated at 413K for nine hours / hydrated.....	211
Table B. 5 Peak fit statistics of Palygorskite / 0.5 mol % thioindigo unheated / exposed to vacuum.....	212
Table B. 6 Peak fit statistics of Sepiolite / 0.5 mol % thioindigo unheated.....	213

Table B. 7 Peak fit statistics of Sepiolite / 0.5 mol % thioindigo heated at 413K for nine hours.	214
Table B. 8 Peak fit statistics of Sepiolite / 0.5 mol % thioindigo heated at 413K for nine hours / hydrated.	215
Table B. 9 Peak fit statistics of Bentolite L [®] / 0.5 mol % thioindigo unheated.....	216
Table B. 10 Peak fit statistics of Bentolite L [®] / 0.5 mol % thioindigo heated at 413K for nine hours.	217
Table B. 11 Peak fit statistics of Bentolite L [®] / 0.5 mol % thioindigo heated at 413K for nine hours / hydrated.....	218
Table B. 12 Peak fit statistics of Ca-MMT (Texas) / 0.5 mol % thioindigo unheated. ..	219
Table B. 13 Peak fit statistics of Ca-MMT (Texas) / 0.5 mol % thioindigo heated at 413K for nine hours.	220
Table B. 14 Peak fit statistics of Ca-MMT (Texas) / 0.5 mol % thioindigo heated at 413K for nine hours / hydrated.	221
Table B. 15 Peak fit statistics of Na-MMT (Kunipia) / 0.5 mol % thioindigo unheated.	222
Table B. 16 Peak fit statistics of Na-MMT (Kunipia) / 0.5 mol % thioindigo heated at 413K for nine hours.	223
Table B. 17 Peak fit statistics of Na-MMT (Kunipia) / 0.5 mol % thioindigo heated at 413K for nine hours / hydrated.	224
Table B. 18 Peak fit statistics of Na-MMT (Wyoming) / 0.5 mol % thioindigo unheated.	225
Table B. 19 Peak fit statistics of Na-MMT (Wyoming) / 0.5 mol % thioindigo heated at 413K for nine hours.	226

Table B. 20 Peak fit statistics of Na-MMT (Wyoming) / 0.5 mol % thioindigo heated at 413K for nine hours / hydrated.	227
Table B. 21 Peak fit statistics of YN6 / 0.5 mol % thioindigo unheated.	228
Table B. 22 Peak fit statistics of YN6 / 0.5 mol % thioindigo heated at 413K for nine hours.	229
Table B. 23 Peak fit statistics of YN8 / 0.5 mol % thioindigo unheated.	230
Table B. 24 Peak fit statistics of YN8 / 0.5 mol % thioindigo heated at 413K for nine hours.	231
Table B. 25 Peak fit statistics of Na-Ts / 0.5 mol % thioindigo unheated.....	232
Table B. 26 Peak fit statistics of Na-Ts / 0.5 mol % thioindigo heated at 413K for nine hours.	233
Table B. 27 Peak fit statistics of Talc / 0.5 mol % thioindigo unheated.	234
Table B. 28 Peak fit statistics of Talc / 0.5 mol % thioindigo heated at 413K for nine hours.	235
Table B. 29 Peak fit statistics of 4A / 0.5 mol % thioindigo unheated.....	236
Table B. 30 Peak fit statistics of 4A / 0.5 mol % thioindigo heated at 413K for nine hours.	237
Table B. 31 Peak fit statistics of 5A / 0.5 mol % thioindigo unheated.....	238
Table B. 32 Peak fit statistics of 5A / 0.5 mol % thioindigo heated at 413K for nine hours.	239
Table B. 33 Peak fit statistics of NaY / 0.5 mol % thioindigo unheated.	240
Table B. 34 Peak fit statistics of NaY / 0.5 mol % thioindigo heated at 413K for nine hours.	241

Table B. 35 Peak fit statistics of NaY / 0.5 mol % thioindigo heated at 413K for nine hours / hydrated.	242
Table B. 36 Peak fit statistics of 13X / 0.5 mol % thioindigo unheated.	243
Table B. 37 Peak fit statistics of 13X / 0.5 mol % thioindigo heated at 413K for nine hours.	244
Table B. 38 Peak fit statistics of 13X / 0.5 mol % thioindigo heated at 413K for nine hours / hydrated.	245
Table B. 39 Peak fit statistics of LZY62 / 0.5 mol % thioindigo unheated.	246
Table B. 40 Peak fit statistics of LZY62 / 0.5 mol % thioindigo heated at 413K for nine hours.	247
Table B. 41 Peak fit statistics of LZY62 / 0.5 mol % thioindigo heated at 413K for nine hours / hydrated.	248
Table B. 42 Peak fit statistics of Zeolon [®] / 0.5 mol % thioindigo unheated.	249
Table B. 43 Peak fit statistics of Zeolon [®] / 0.5 mol % thioindigo heated at 413K for nine hours.	250
Table B. 44 Peak fit statistics of Zeolon [®] / 0.5 mol % thioindigo heated at 413K for nine hours / hydrated.	251
Table B. 45 Peak fit statistics of CBV21A / NH ₄ / 0.5 mol % thioindigo unheated.	252
Table B. 46 Peak fit statistics of CBV21A / NH ₄ / 0.5 mol % thioindigo heated at 413K for nine hours.	253
Table B. 47 Peak fit statistics of CBV21A / NH ₄ / 0.5 mol % thioindigo heated at 413K for nine hours / hydrated.	254
Table B. 48 Peak fit statistics of CBV21A / Al / 0.5 mol % thioindigo unheated.	255

Table B. 49 Peak fit statistics of CBV21A / Al / 0.5 mol % thioindigo heated at 413K for nine hours.	256
Table B. 50 Peak fit statistics of CBV21A / Al / 0.5 mol % thioindigo heated at 413K for nine hours / hydrated.....	257
Table B. 51 Peak fit statistics of CBV21A / Al / 0.5 mol % thioindigo heated at 413K for nine hours / hydrated for 1 week.	258
Table B. 52 Peak fit statistics of CBV21A / Ca / 0.5 mol % thioindigo unheated.	259
Table B. 53 Peak fit statistics of CBV21A / Ca / 0.5 mol % thioindigo heated at 413K for nine hours.	260
Table B. 54 Peak fit statistics of CBV21A / Ca / 0.5 mol % thioindigo heated at 413K for nine hours / hydrated.....	261
Table B. 55 Peak fit statistics of CBV21A / K / 0.5 mol % thioindigo unheated.	262
Table B. 56 Peak fit statistics of CBV21A / K / 0.5 mol % thioindigo heated at 413K for nine hours.	263
Table B. 57 Peak fit statistics of CBV21A / K / 0.5 mol % thioindigo heated at 413K for nine hours / hydrated.....	264
Table B. 58 Peak fit statistics of CBV21A / Na / 0.5 mol % thioindigo unheated.	265
Table B. 59 Peak fit statistics of CBV21A / Na / 0.5 mol % thioindigo heated at 413K for nine hours.	266
Table B. 60 Peak fit statistics of CBV21A / Na / 0.5 mol % thioindigo heated at 413K for nine hours / hydrated.....	267
Table B. 61 Peak fit statistics of CBV21A / H / 0.5 mol % thioindigo unheated.	268

Table B. 62 Peak fit statistics of CBV21A / H / 0.5 mol % thioindigo heated at 413K for nine hours.	269
Table B. 63 Peak fit statistics of CBV21A / H / 0.5 mol % thioindigo heated at 413K for nine hours / hydrated.....	270
Table B. 64 Peak fit statistics of CBV21A / H(HCL) / 0.5 mol % thioindigo unheated.	271
Table B. 65 Peak fit statistics of CBV21A / H(HCL) / 0.5 mol % thioindigo heated at 413K for nine hours.	272
Table B. 66 Peak fit statistics of CBV21A / H(HCL) / 0.5 mol % thioindigo heated at 413K for nine hours / hydrated.	273
Table B. 67 Peak fit statistics of CBV10A / H / 0.5 mol % thioindigo unheated.	274
Table B. 68 Peak fit statistics of CBV10A / H / 0.5 mol % thioindigo heated at 413K for nine hours.	275
Table B. 69 Peak fit statistics of CBV10A / H / 0.5 mol % thioindigo heated at 413K for nine hours / hydrated.....	276
Table B. 70 Peak fit statistics of CBV10A / H(HCl) / 0.5 mol % thioindigo unheated... ..	277
Table B. 71 Peak fit statistics of CBV10A / H(HCl) / 0.5 mol % thioindigo heated at 413K for nine hours.	278
Table B. 72 Peak fit statistics of CBV10A / H(HCl) / 0.5 mol % thioindigo heated at 413K for nine hours / hydrated.	279
Table B. 73 Peak fit statistics of CBV10A / NH ₄ / 0.5 mol % thioindigo unheated.	280
Table B. 74 Peak fit statistics of CBV10A / NH ₄ / 0.5 mol % thioindigo heated at 413K for nine hours.	281

Table B. 75 Peak fit statistics of CBV10A / NH ₄ / 0.5 mol % thioindigo heated at 413K for nine hours / hydrated.	282
Table B. 76 Peak fit statistics of CBV10A / Na / 0.5 mol % thioindigo unheated.	283
Table B. 77 Peak fit statistics of CBV10A / Na / 0.5 mol % thioindigo heated at 413K for nine hours.	284
Table B. 78 Peak fit statistics of CBV10A / Na / 0.5 mol % thioindigo heated at 413K for nine hours / hydrated.....	285
Table B. 79 Peak fit statistics of MA-1 / 0.5 mol % thioindigo unheated.....	286
Table B. 80 Peak fit statistics of MA-1 / 0.5 mol % thioindigo heated at 413K for nine hours.	287
Table B. 81 Peak fit statistics of MS-1 / 0.5 mol % thioindigo unheated.....	288
Table B. 82 Peak fit statistics of MS-1 / 0.5 mol % thioindigo heated at 413K for nine hours.	289
Table B. 83 Peak fit statistics of MAS-1 / 0.5 mol % thioindigo unheated.	290
Table B. 84 Peak fit statistics of MAS-1 / 0.5 mol % thioindigo heated at 413K for nine hours.	291
Table B. 85 Peak fit statistics of pretreated palygorskite / 0.5 mol % thioindigo heated at 413K for nine hours.	292
Table B. 86 Peak fit statistics of pretreated palygorskite / 0.5 mol % thioindigo unheated.	293
Table B. 87 Peak fit statistics of thioindigo in concentrated sulfuric acid.....	294
Table B. 88 Peak fit statistics of thioindigo interaction with concentrated sulfuric acid, after water addition.....	296

LIST OF FIGURES

Figure 1 Mural from Bonampak, Palenque (Classic period, 200 B.C. - 900 A.C.).	1
Figure 2 Trans -Thioindigo molecule (the most stable conformation). C= gray, H= white, S= yellow, and O= red. [Materials Studio v4.0].	13
Figure 3 Thioindigo crystal structure [Materials Studio v4.0].	14
Figure 4 Synthesis of thioindigo by oxidation [Image courtesy of M. Saunbury, <i>et al.</i>].	15
Figure 5 Representing the four forms at which the isomers could exist in solution. No double bond present [Image courtesy of G.M. Wyman, <i>et al.</i>].	16
Figure 6 (a) Highest Occupied Molecular Orbital (HOMO) location on the sulfur and C=C bond of thioindigo. (b)Lowest Unoccupied Molecular Orbital (LUMO) location on C-C single bond and oxygen bond of thioindigo [Cerius ² accelrys software].	17
Figure 7 (left) Palygorskite unit cell, visualization on 001 plane. (right) Block unit representation showing dimension of channels [Image courtesy of the Coastal and Marine Geology Program].	19
Figure 8 (right) Sepiolite orthorhombic unit cell.(left) Schematic 001 plane representation of the cross-section of a sepiolite fiber [Image courtesy of Coastal and Marine Geology Program].	20
Figure 9 Octahedral ribbon for palygorskite [Image courtesy of Suarez <i>et al.</i>].	21
Figure 10 Talc unit cell displaying 2:1 arrangement [Materials Studio v4.0].	22
Figure 11 Montmorillonite structure displaying building units of tetrahedral and octahedral sheets [Materials Studio v4.0].	23

Figure 12 Meier's secondary building units of zeolite frameworks [Image courtesy of J.V. Smith].	26
Figure 13 Visualization of Faujasite framework in (left) tetrahedral arrangement, and (right) secondary building units of sodalite and hexagonal prism linked together [Image courtesy of G. Bergerhoff <i>et al.</i>].	27
Figure 14 Visualization of LTA framework in (left) tetrahedral arrangement, and (right) secondary building units of sodalite and cubes linked together [Image courtesy of T.B. Reed <i>et al.</i> ⁵⁵].	28
Figure 15 Visualization of MOR framework in (left) tetrahedral arrangement, and (right) secondary building units of 4 different secondary building units linked together [Image courtesy of W.M. Meier].	29
Figure 16 (left) Substitution of ions of different charge. (right) Interlayer cation compensation charge imbalance originated in 2:1 [Image courtesy of B.Velde].	30
Figure 17 Trioctahedral and dioctahedral substitution exclusively in octahedral sites...	31
Figure 18 Location of cations in internal layers (absorbed) and surface of layersilicate clay mineral (adsorbed) [Image courtesy of B. Velde].	32
Figure 19 Hydrolysis of a hydrated cation [Image courtesy of G. Wulfsberg].	34
Figure 20 (Top) Brønsted acid site (H^+) in a tetrahedral site.(bottom) Lewis acid hydrated.	35
Figure 21 Pure thioindigo color and samples prepared with 0.5 mol % thioindigo in different host materials before thermal treatment.	39
Figure 22 Colors observed in pure thioindigo and 0.5 mol %thioindigo in different host materials heated at 413K for nine hours.....	40

Figure 23 High moisture effect in thioindigo and 0.5 mol %thioindigo in different host materials at 413K for nine hours.	41
Figure 24 Example of color change of 0.5 mol %thioindigo in Bentolite L [®] UNHEATED when exposed to three different levels of moisture.	42
Figure 25 (Top) Color variation of palygorskite / 0.5 mol % thioindigo unheated and heated at 413K for nine hours, hydrated after heat treatment and hydrated after exposure to vacuum. (Bottom) Diffuse Reflectance UV-Vis spectra of the above mentioned samples and thioindigo starting material.	45
Figure 26 Comparison of (a) pretreated palygorskite (833K for 16h) / 0.5 mol % thioindigo heated at 413K for nine hours, and (b) palygorskite / 0.5 mol % thioindigo heated at 413K for nine hours.	46
Figure 27 (Top) Color variation of sepiolite / 0.5 mol % thioindigo unheated and heated at 413K for nine hours, hydrated after heat treatment and hydrated after exposure to vacuum. (Bottom) UV-Vis spectra of the above mentioned samples and thioindigo starting material.....	48
Figure 28 Effect of moisture in montmorillonite clays.	49
Figure 29 (Top) Color variations of (Ca ²⁺ -MMT) bentolite L [®] / 0.5 mol % thioindigo unheated, dehydrated at 413K for nine hours and hydrated after heat treatment (Bottom) UV-Vis spectra of the above mentioned samples and thioindigo starting material.	50
Figure 30 (Top) Color variations of Ca ²⁺ -MMT (Texas deposit) / 0.5 mol % thioindigo unheated, dehydrated at 413K for nine hours and hydrated after heat treatment	

(Bottom) UV-Vis spectra of the above mentioned samples and thioindigo starting material.	51
Figure 31 (Top) Color variations of Na ⁺ -MMT (Wyoming deposit) / 0.5 mol % thioindigo unheated, dehydrated at 413K for nine hours and hydrated after heat treatment (Bottom) UV-Vis spectra of the above mentioned samples and thioindigo starting material.	52
Figure 32 (Top) Color variations of Na ⁺ -MMT (Kunipia deposit) / 0.5 mol % thioindigo unheated, dehydrated at 413K for nine hours and hydrated after heat treatment (Bottom) UV-Vis spectra of the above mentioned samples and thioindigo starting material.	53
Figure 33 (Top) Color variations of Talc / 0.5 mol % thioindigo unheated, dehydrated at 413K for nine hours and hydrated after heat treatment (Bottom) UV-Vis spectra of the above mentioned samples and thioindigo starting material.....	54
Figure 34 (Top) Color variations of YN6 / 0.5 mol % thioindigo unheated, dehydrated at 413K for nine hours and hydrated after heat treatment (Bottom) UV-Vis spectra of the above mentioned samples and thioindigo starting material.....	55
Figure 35 (Top) Color variations of YN8 / 0.5 mol % thioindigo unheated, dehydrated at 413K for nine hours and hydrated after heat treatment (Bottom) UV-Vis spectra of the above mentioned samples and thioindigo starting material.....	56
Figure 36 (Top) Color variations of Na-Ts / 0.5 mol % thioindigo unheated, dehydrated at 413K for nine hours and hydrated after heat treatment (Bottom) UV-Vis spectra of the above mentioned samples and thioindigo starting material.....	57

Figure 37 Reversible color changes in presence of water of 0.5 mol % thioindigo in Na ⁺ -FAU (NaY), Na ⁺ ,Ca ²⁺ -FAU (13X), NH ₄ ⁺ -FAU (LZY-62) and H ⁺ -FAU heated at 413K for nine hours.	58
Figure 38 (Top) Color variations of Valfor CP300-35 [®] (H ⁺ -FAU) / 0.5 mol % thioindigo unheated, dehydrated at 413K for nine hours and hydrated after heat treatment (Bottom) UV-Vis spectra of the above mentioned samples and thioindigo starting material.	59
Figure 39 (Top) Color variations of LZY-62 (NH ₄ ⁺ -FAU) / 0.5 mol % thioindigo unheated, dehydrated at 413K for nine hours and hydrated after heat treatment (Bottom) UV-Vis spectra of the above mentioned samples and thioindigo starting material.	60
Figure 40 (Top) Color variations of 13X (Na ⁺ ,Ca ²⁺ -FAU) / 0.5 mol % thioindigo unheated, dehydrated at 413K for nine hours and hydrated after heat treatment (Bottom) UV-Vis spectra of the above mentioned samples and thioindigo starting material.	61
Figure 41 (Top) Color variations of NaY (Na ⁺ -FAU) / 0.5 mol % thioindigo unheated, dehydrated at 413K for nine hours and hydrated after heat treatment (Bottom) UV-Vis spectra of the above mentioned samples and thioindigo starting material.	62
Figure 42 (Top) Color variations of 4A (Na ⁺ -FAU) / 0.5 mol % thioindigo unheated, dehydrated at 413K for nine hours and hydrated after heat treatment (Bottom) UV-Vis spectra of the above mentioned samples and thioindigo starting material.	64
Figure 43 (Top) Color variations of 5A (Na ⁺ -FAU) / 0.5 mol % thioindigo unheated, dehydrated at 413K for nine hours and hydrated after heat treatment (Bottom) UV-Vis spectra of the above mentioned samples and thioindigo starting material.	65

Figure 44 (Top) Color variations of Zeolon [®] (Na ⁺ -MOR) / 0.5 mol % thioindigo unheated, dehydrated at 413K for nine hours and hydrated after heat treatment (Bottom) UV-Vis spectra of the above mentioned samples and thioindigo starting material.	67
Figure 45 Color changes of samples prepared with 0.5 mol % thioindigo in CBV10A (Na ⁺ -MOR), CBV21A (Na ⁺ -MOR) and Zeolon [®] (Na ⁺ -MOR) with different Si/Al ratios... 68	
Figure 46 (Top) Color variations of CBV10A (Na ⁺ -MOR) / 0.5 mol % thioindigo unheated, dehydrated at 413K for nine hours and hydrated after heat treatment (Bottom) UV-Vis spectra of the above mentioned samples and thioindigo starting material.	69
Figure 47 (Top) Color variations of CBV21A (Na ⁺ -MOR) / 0.5 mol % thioindigo unheated, dehydrated at 413K for nine hours and hydrated after heat treatment (Bottom) UV-Vis spectra of the above mentioned samples and thioindigo starting material.	70
Figure 48 (Top) Color variations of MA-1 / 0.5 mol % thioindigo unheated, dehydrated at 413K for nine hours and hydrated after heat treatment (Bottom) UV-Vis spectra of the above mentioned samples and thioindigo starting material.....	72
Figure 49 (Top) Color variations of MS-1 / 0.5 mol % thioindigo unheated, dehydrated at 413K for nine hours and hydrated after heat treatment (Bottom) UV-Vis spectra of the above mentioned samples and thioindigo starting material.....	73
Figure 50 (Top) Color variations of MAS-1 / 0.5 mol % thioindigo unheated, dehydrated at 413K for nine hours and hydrated after heat treatment (Bottom) UV-Vis spectra of the above mentioned samples and thioindigo starting material.....	74

Figure 51 (Top) Color change of thioindigo with concentrated sulfuric acid. (Bottom) UV-Vis spectra of (a) concentrated sulfuric acid reaction with thioindigo and (b) concentrated sulfuric acid reaction with thioindigo after water addition.....	76
Figure 52 (Top) Color changes observed in heated samples of CBV21A (MOR) exchanged with different cations (K^+ , Na^+ , Ca^{2+} , NH_4^+ , Al^{3+} and H^+) and mixed with 0.5 mol% thioindigo. (Bottom) UV-Vis Spectra of the above mentioned samples.	77
Figure 53 Color changes observed in 0.5 mol % thioindigo in exchanged zeolites unheated, dehydrated at 413K for nine hours and hydrated.	78
Figure 54 (Top) Color changes observed in 0.5 mol % thioindigo in K^+ -MOR unheated (21AK+dye Unheated), dehydrated at 413K for nine hours (21AK+dye Dehydrated) and hydrated (21AK+dye Hydrated). (Bottom) UV-Vis spectra of the above mentioned samples.....	79
Figure 55 UV-Vis spectra of color change observed during hydration of 0.5 mol % thioindigo in Na^+ -MOR (21ANa+dye Hydrated). Hydrated sample was compared with heated mixture at 413K for nine hours (21ANa+dye Dehydrated) and unheated mixture (21ANa+dye Unheated).	80
Figure 56 UV-Vis spectra of color change observed during hydration of 0.5 mol % thioindigo in Ca^{2+} MOR (21ACa ²⁺ +dye Hydrated). Hydrated sample was compared with heated mixture at 413K for nine hours (21ACa ²⁺ +dye Dehydrated) and unheated mixture (21ACa ²⁺ +dye Unheated).	81
Figure 57 UV-Vis spectra of color change observed during hydration of 0.5 mol % thioindigo in NH_4^+ MOR (21ANH ₄ ⁺ +dye Hydrated). Hydrated sample was compared with	

heated mixture at 413K for nine hours (21ANH ₄ ⁺ +dye Dehydrated) and unheated mixture (21ANH ₄ ⁺ +dye Unheated).	82
Figure 58 UV-Vis spectra of color change observed during hydration of 0.5 mol % thioindigo in Al ³⁺ -MOR (21AAI+dye Hydrated). Hydrated sample was compared with heated mixture at 413K for nine hours (21AAI+dye Dehydrated) and unheated mixture (21AAI+dye Unheated).	83
Figure 59 UV-Vis spectra of color change observed during hydration of 0.5 mol % thioindigo in H ⁺ -MOR (21AH+dye Hydrated). Hydrated sample was compared with heated mixture at 413K for nine hours (21AH+dye Dehydrated) and unheated mixture (21AH+dye Unheated).	84
Figure 60 Trioctahedral arrangement for sepiolite clay [Image courtesy of Suarez <i>et al.</i>].	86
Figure 61 FTIR spectra for palygorskite and sepiolite clays with KBr support.	87
Figure 62 Dioctahedral arrangement in Na ⁺ and Ca ²⁺ - Montmorillonite clays	88
Figure 63 FTIR spectra for Na ⁺ -montmorillonite clays in KBr support.	90
Figure 64 FTIR spectra for Ca ²⁺ -montmorillonite clays in KBr support.	91
Figure 65 FTIR spectra for three low charge synthetic micas (YN6, YN8 and Na-Ts) ..	93
Figure 66 FTIR spectra of several faujasite sieves with different cations (KBr support): Valfor CP300-35 (H ⁺ -FAU), LZY-62 (NH ₄ ⁺ -FAU), NaY (Na ⁺ -FAU), 13X (Ca ²⁺ , Na ⁺ -FAU).	95
Figure 67 FTIR spectra of several mordenite synthetic zeolites with different cations (KBr support): Zeolon [®] (Na ⁺ -MOR), CBV21A (NH ₄ ⁺ -MOR), CBV10A (Na ⁺ -MOR).	96

Figure 68 FTIR spectra of several LTA synthetic zeolites with different concentrations of sodium cation (KBr support): 4A (0.6 moles Na ⁺ -LTA), 5A (0.2moles Na ⁺ -LTA).	97
Figure 69 FTIR spectra of simulated pyridine by Gaussian 3.0.....	98
Figure 70 FTIR comparison of palygorskite raw material [Palygorskite Raw] and pyridine adsorption on palygorskite [Paly-PY] (KBr support).	100
Figure 71 FTIR comparison of sepiolite raw material [Sepiolite Raw] and pyridine adsorption on sepiolite [Sepio-PY] (KBr support).....	101
Figure 72 FTIR comparison of bentolite raw material [Bentolite L [®] Raw] and pyridine adsorption on bentolite [Bentolite L [®] -PY] (KBr support).....	102
Figure 73 FTIR comparison of Ca ²⁺ -MMT raw material [Ca-MMT Raw] and pyridine adsorption on Ca ²⁺ -MMT [Ca-MMT -PY] (KBr support).	103
Figure 74 FTIR comparison of Na ⁺ -MMT (Wyoming deposit) raw material [Na-MMT(W) Raw] and pyridine adsorption [Na-MMT(W) -PY] (KBr support).....	104
Figure 75 FTIR comparison of Na ⁺ -MMT (Kunipia deposit) raw material [Na-MMT(K) Raw] and pyridine adsorption [Na-MMT(K) -PY] (KBr support).....	105
Figure 76 FTIR comparison of Valfor CP300-35 (H ⁺ -MOR) raw material [Valfor CP300-35Raw] and pyridine adsorption [Valfor CP300-35-PY] (KBr support).....	106
Figure 77 FTIR spectra of pyridine adsorption in CBV21A [NH ₄ ⁺ -MOR] (KBr support).	108
Figure 78 FTIR spectra of pyridine adsorption in CBV21A [Na ⁺ -MOR] (KBr support).	109
Figure 79 FTIR spectra of pyridine adsorption in Zeolon [®] (Na ⁺ -MOR) with KBr support.	110

Figure 80 FTIR spectra of palygorskite raw material, thioindigo raw material, 0.5 mol % thioindigo/palygorskite mixture heated (paly+dye H), and unheated (paly+dye UN). All of the above mentioned samples mixed with KBr as support.	112
Figure 81 FTIR spectra of palygorskite raw material, thioindigo raw material, 0.5 mol % thioindigo/palygorskite mixture heated [paly+dye D (blue)], unheated [paly+dye UN (pink)] and vacuum [paly+dye UN vacuum (purple)]. Mineral oil as support.	113
Figure 82 FTIR spectra of sepiolite raw material, thioindigo raw material, 0.5 mol % thioindigo/sepiolite mixture heated (sepio+dye D magenta) unheated (sepio+dye UN pink) and heated mixture hydrated (sepio+dye D purple). Mineral oil as support.....	115
Figure 83 FTIR spectra of bentolite L [®] raw material, thioindigo raw material, 0.5 mol % thioindigo/bentolite L [®] mixture heated (bentolite L +dye D blue) and unheated (bentolite L+dye UN purple). Mineral oil as support.	117
Figure 84 FTIR spectra of Ca-MMT (Texas deposit) raw material, thioindigo raw material, 0.5 mol % thioindigo/ Ca-MMT mixture heated (Ca-MMT +dye D blue) and unheated (Ca-MMT+dye UN purple). Mineral oil as support.	118
Figure 85 FTIR spectra of Na ⁺ -MMT (Wyoming deposit) raw material, thioindigo raw material, 0.5 mol % thioindigo/ Na ⁺ -MMT mixture heated (Na-MMT +dye D purple) and unheated (Na-MMT+dye UN purple). Mineral oil as support.	119
Figure 86 FTIR spectra of Na-MMT (Kunipia deposit) raw material, thioindigo raw material, 0.5 mol % thioindigo/ Na-MMT mixture heated (Na-MMT +dye D purple) and unheated (Na-MMT+dye UN purple). Mineral oil as support.	120

Figure 87 FTIR spectra of NaY raw material, thioindigo raw material, 0.5 mol % thioindigo/ NaY mixture heated (NaY +dye D purple) and unheated (NaY +dye UN red). Mineral oil as support.	121
Figure 88 FTIR spectra of Valfor CP300-35 raw material, thioindigo raw material, 0.5 mol % thioindigo/Valfor mixture heated (Valfor +dye D purple), and hydrated (Valfor +dye UN pink). Mineral oil as support.	123
Figure 89 FTIR spectra of Zeolon [®] raw material, thioindigo raw material, 0.5 mol % thioindigo/ Zeolon [®] mixture heated (Zeolon [®] +dye D purple), and hydrated (Zeolon [®] +dye UN pink). Mineral oil as support.	125
Figure 90 FTIR spectra of starting materials thioindigo and K ⁺ -MOR (21AK Raw) and 0.5 mol % thioindigo mixture with K ⁺ -MOR heated at 413K for nine hours (21AK+dye dehydrated) and unheated (21AK+dye Unheated) with Mineral Oil as support.....	127
Figure 91 FTIR spectra of starting materials thioindigo and Ca ²⁺ -MOR (21ACa Raw) and 0.5 mol % thioindigo mixture with Ca ²⁺ -MOR heated at 413K for nine hours (21ACa+dye dehydrated) and unheated (21ACa+dye unheated) with Mineral Oil as support.	128
Figure 92 FTIR spectra of starting materials thioindigo and Na ⁺ -MOR (21ANa Raw) and 0.5 mol % thioindigo mixture with Na ²⁺ -MOR heated at 413K for nine hours (21ANa+dye dehydrated) and unheated (21ANa+dye unheated) with Mineral Oil as support.	129
Figure 93 FTIR spectra of starting materials thioindigo and NH ₄ ⁺ -MOR (21ANH4 Raw) and 0.5 mol % thioindigo mixture with NH ₄ ⁺ -MOR heated at 413K for nine hours (21ANH4+dye dehydrated) and unheated (21ANH4+dye unheated) with Mineral Oil as support.	130

Figure 94 FTIR spectra of starting materials thioindigo and Al^{3+} -MOR (21AAI Raw) and 0.5 mol % thioindigo mixture with Al^{3+} -MOR heated at 413K for nine hours (21AAI+dye dehydrated) and unheated (21AAI+dye unheated) with Mineral Oil as support.	131
Figure 95 FTIR spectra of starting materials thioindigo and H^{+} -MOR (21AH Raw) and 0.5 mol % thioindigo mixture with H^{+} -MOR heated at 413K for nine hours (21AH+dye dehydrated) and unheated (21AH+dye unheated) with Mineral Oil as support.	132
Figure 96 XRD pattern comparison of (a) thioindigo raw material, (b) thioindigo - triclinic simulated by Materials Studio v4.0 software.	133
Figure 97 XRD pattern comparison of (a) palygorskite raw material, (b) palygorskite-orthorhombic (c) palygorskite -monoclinic and (d) α -quartz-trigonal. [Simulation of palygorskite and quartz unit cells by Cerius ² accelrys software].....	134
Figure 98 XRD pattern comparison of (a) sepiolite raw material, (b) α -quartz-trigonal, (c) calcite -trigonal, (d) sepiolite - monoclinic. [Simulation of sepiolite, quartz and calcite unit cells by Materials Studio v4.0 software].	135
Figure 99 Powder X-ray diffraction pattern of (a) Na^{+} -MMT (Kunipia deposit) raw material, (b) Na^{+} -MMT (Wyoming deposit) raw material, (c) Ca^{2+} -MMT (Texas deposit) raw material, and (d) Ca^{2+} -MMT (bentolite L [®]).	138
Figure 100 Powder X-ray diffraction pattern of (a) YN6 raw material, (b) YN8 raw material, and (c) Sodium Trisilic (Na-Ts) raw material.....	140
Figure 101 Powder X-ray diffraction pattern of Talc raw material.....	141
Figure 102 Powder X-ray diffraction pattern of (a) [Na^{+} -LTA] 4A Raw material, (b) [Na^{+} -LTA] 5A Raw material (c) LTA framework by Materials Studio v4.0 software.	142

Figure 103 Powder X-ray diffraction pattern of (a) [H ⁺ -FAU] Vallfor CP300-35 [®] Raw material, (b) [Na ⁺ -FAU] NaY Raw material (c) [NH ₄ ⁺ -FAU] LZY-62 Raw material, (d) [Na ⁺ ,Ca ²⁺ -FAU] 13X Raw material and (e) FAU framework by Materials Studio v4.0 software.....	143
Figure 104 Powder X-ray diffraction pattern of (a) [Na ⁺ -MOR] CBV10A Raw material, (b) [NH ₄ ⁺ -MOR] CBV21A Raw material (c) [Na ⁺ -MOR] Zeolon [®] Raw material and (e) MOR framework by Materials Studio v4.0 software. (Calcite-standard).	144
Figure 105 Powder X-ray diffraction pattern of (a) MS-1 Raw material, (b) MA-1 Raw material (c) MAS-1 Raw material.	145
Figure 106 Powder X-ray diffraction pattern of (a) [NH ₄ ⁺ -MOR] CBV21A Raw material, (b) [H ⁺ -MOR] CBV21A (c) MOR framework by Materials Studio v4.0 software.....	146
Figure 107 Powder X-ray diffraction pattern of (a) Zeolon [®] 1223K 16h, (b) Zeolon [®] Raw material.	147
Figure 108 Powder X-ray diffraction pattern of (a) Palygorskite heated at 823K for sixteen hours. (b) Palygorskite raw material (c) trigonal α-Quartz simulated by Materials Studio v4.0. software.....	148
Figure 109 X-ray powder diffraction of (a) palygorskite +dye dehydrated [blue], (b) palygorskite +dye unheated [magenta], (c) palygorskite raw material and (d) thioindigo raw material.....	149
Figure 110 X-ray powder diffraction of (a) sepiolite +dye dehydrated [purple], (b) sepiolite +dye unheated [magenta], (c) sepiolite raw material and (d) thioindigo raw material.	150

Figure 111 Powder X-ray diffraction pattern of (a) thioindigo, (b) bentolite L [®] +dye dehydrated [purple], (c) [Ca ²⁺ -MMT] bentolite L [®] raw material, and (d) bentolite L [®] +dye hydrated [red].	152
Figure 112 Powder X-ray diffraction pattern of (a) thioindigo, (b) Ca ²⁺ -MMT +dye dehydrated [purple], (c) Ca ²⁺ -MMT (Texas) raw material, and (d) Ca ²⁺ -MMT +dye hydrated [red].	153
Figure 113 Powder X-ray diffraction pattern of (a) thioindigo, (b) Na ⁺ -MMT +dye dehydrated [purple], (c) Na ⁺ -MMT (Wyoming) raw material, and (d) Na ⁺ -MMT +dye hydrated [red].	154
Figure 114 Powder X-ray diffraction pattern of (a) thioindigo, (b) Na ⁺ -MMT +dye dehydrated [purple], (c) Na ⁺ -MMT +dye hydrated [red],(d) Na ⁺ -MMT (Kunipia) raw material.	155
Figure 115 Powder X-ray diffraction pattern of (a) thioindigo, (b) YN8 +dye dehydrated [pink] and (c) [Na ⁺ -LTA] YN8 raw material.	156
Figure 116 Powder X-ray diffraction pattern of (a) thioindigo, (b) YN6 +dye dehydrated [pink] and (c) [Na ⁺ -Mica] YN6 raw material.	157
Figure 117 Sodium cation exchanged in Na ⁺ -MOR.	159
Figure 118 Calcium cation exchange for Ca ²⁺ [MOR].	160
Figure 119 Potassium cation exchanged in K ⁺ -MOR.	160
Figure 120 Aluminum cation exchanged in Al ³⁺ -MOR.	161
Figure 121 Hydrogen cation exchanged in H ⁺ -MOR.	161
Figure 122 ²⁷ Al magic angle spinning-nuclear magnetic resonance of (a) palygorskite and (b) sepiolite.	162

Figure 123 ^{27}Al magic angle spinning-nuclear magnetic resonance of (a) Ca^{2+} -MMT (Bentolite L [®]) and (b) Ca^{2+} -MMT (Texas deposit).....	163
Figure 124 ^{27}Al magic angle spinning-nuclear magnetic resonance of (a) Na^{+} -MMT (Kunipia deposit) and (b) Na^{+} -MMT (Wyoming deposit).....	164
Figure 125 ^{27}Al magic angle spinning-nuclear magnetic resonance of (a) palygorskite from MinTech; (b) palygorskite / 0.5 mol % thioindigo heated at 413K for nine hours; (c) palygorskite/ 1 mol %thioindigo heated at 413K for nine hours.....	166
Figure 126 ^{27}Al magic angle spinning-nuclear magnetic resonance of (a) sepiolite (Pansil) from Tolsa; (b) Sepiolite / 0.5 mol % thioindigo heated at 413K for nine hours; (c) Sepiolite/ 1 mol %thioindigo heated at 413K for nine hours.....	167
Figure 127 ^{27}Al magic angle spinning-nuclear magnetic resonance of (a) sepiolite (Pansil) from Tolsa; (b) Sepiolite dehydrated at 413K for nine hours	168
Figure 128 Ammonium cation interaction with one thioindigo molecule.	170
Figure 129 UV-Vis spectra simulated and experimental for 0.5 mol % thioindigo in NH_4^{+} -MOR.....	170
Figure 130 Hydrogen interaction with one thioindigo molecule.	171
Figure 131 UV-Vis spectra simulated and experimental for 0.5 mol % thioindigo in H^{+} -MOR.....	171
Figure 132 (Left) Lewis Acid Site (LAS) present in palygorskite. (Right) Lewis Acid Site (LAS) present in sepiolite.	176
Figure 133 Schematic representation of possible explanation for color changes in sepiolite.....	177
Figure 134 Acid Sites present in Ca^{2+} -Montmorillonite clays (Ca^{2+} -MMT).....	178

Figure 135 (Top) Schematic representation of tetrahedral sites in Ca^{2+} -MMT structure. Interaction with H and Al-LAS. (Bottom) Hydrated sites of $\text{C}=\text{O}---\text{H}(\text{HO})\text{Al-LAS}$ interaction.....	179
Figure 136 Acid Sites present in Na^{+} -Montmorillonite clays (Na^{+} -MMT).	180
Figure 137 (Top) Schematic representations of tetrahedral sites in Na^{+} -MMT structure. Interaction with Na^{+} -LAS. (Bottom) Hydrated sites of $\text{C}=\text{O}---\text{H}(\text{HO})\text{Na}^{+}$ -LAS interaction.	181
Figure 138 Acid Sites present in silicon-aluminum tetrahedral framework of synthetic zeolite.....	182
Figure 139 (a) Brønsted acid sites and (b) Ammonium exchange in silicon-aluminum tetrahedral framework.	184
Figure 140 (Top) Schematic representation of tetrahedral sites in synthetic zeolites. Interaction with H^{+} -LAS. (Bottom) Hydrated sites of $\text{C}=\text{O}---\text{H}(\text{HO})\text{H}^{+}$ -LAS interaction.	185
Figure 141 (Top) Schematic representation of tetrahedral sites in synthetic zeolites. Interaction with NH_4^{+} -LAS. (Bottom) Hydrated sites of $\text{C}=\text{O}---\text{H}(\text{HO}) \text{NH}_4^{+}$ -LAS interaction.....	186
Figure 142 (Left) Mordenite (MOR) unit Cell with 1 molecule of thioindigo inserted in the channels. (Right) Linde Type A (LTA) unite cell with 0 molecules of thioindigo inserted in the channels by Monte Carlo Simulation [Cerius ² Software].....	187
Figure 143 Faujasite (FAU) unit cell with 11.7 molecules of thioindigo inserted in the channels by Monte Carlo Simulation [Cerius ² Software].	188
Figure 144 Injection molding samples (left) Valfor CP300-35 (H^{+} -MMT) / 0.5 % thioindigo and (right). Bentolite L (Ca^{2+} -MMT) / 0.5 mol % thioindigo.....	191

APPENDIX FIGURES

Figure B. 1 Peak fit of thioindigo	208
Figure B. 2 Peak fit of Palygorskite / 0.5 mol % thioindigo unheated.	209
Figure B. 3 Peak fit of Palygorskite / 0.5 mol % thioindigo heated at 413K for nine hours.	210
Figure B. 4 Peak fit of Palygorskite / 0.5 mol % thioindigo heated at 413K for nine hours / hydrated.	211
Figure B. 5 Peak fit of Palygorskite / 0.5 mol % thioindigo unheated / exposed to vacuum.....	212
Figure B. 6 Peak fit of Sepiolite / 0.5 mol % thioindigo unheated.	213
Figure B. 7 Peak fit of Sepiolite / 0.5 mol % thioindigo heated at 413K for nine hours.	214
Figure B. 8 Peak fit of Sepiolite / 0.5 mol % thioindigo heated at 413K for nine hours / hydrated.	215
Figure B. 9 Peak fit of Bentolite L [®] / 0.5 mol % thioindigo unheated.	216
Figure B. 10 Peak fit of Bentolite L [®] / 0.5 mol % thioindigo heated at 413K for nine hours.	217
Figure B. 11 Peak fit of Bentolite L [®] / 0.5 mol % thioindigo heated at 413K for nine hours / hydrated.	218
Figure B. 12 Peak fit of Ca-MMT (Texas) / 0.5 mol % thioindigo unheated.....	219
Figure B. 13 Peak fit of Ca-MMT (Texas) / 0.5 mol % thioindigo heated at 413K for nine hours.	220

Figure B. 14 Peak fit of Ca-MMT (Texas) / 0.5 mol % thioindigo heated at 413K for nine hours / hydrated.	221
Figure B. 15 Peak fit of Na-MMT (Kunipia) / 0.5 mol % thioindigo unheated.....	222
Figure B. 16 Peak fit of Na-MMT (Kunipia) / 0.5 mol % thioindigo heated at 413K for nine hours.	223
Figure B. 17 Peak fit of Na-MMT (Kunipia) / 0.5 mol % thioindigo heated at 413K for nine hours / hydrated.....	224
Figure B. 18 Peak fit of Na-MMT (Wyoming) / 0.5 mol % thioindigo unheated.....	225
Figure B. 19 Peak fit of Na-MMT (Wyoming) / 0.5 mol % thioindigo heated at 413K for nine hours.	226
Figure B. 20 Peak fit of Na-MMT (Wyoming) / 0.5 mol % thioindigo heated at 413K for nine hours / hydrated.....	227
Figure B. 21 Peak fit of YN6 / 0.5 mol % thioindigo unheated.....	228
Figure B. 22 Peak fit of YN6 / 0.5 mol % thioindigo heated at 413K for nine hours.....	229
Figure B. 23 Peak fit of YN8 / 0.5 mol % thioindigo unheated.....	230
Figure B. 24 Peak fit of YN8 / 0.5 mol % thioindigo heated at 413K for nine hours.....	231
Figure B. 25 Peak fit of Na-Ts / 0.5 mol % thioindigo unheated.	232
Figure B. 26 Peak fit of Na-Ts / 0.5 mol % thioindigo heated at 413K for nine hours..	233
Figure B. 27 Peak fit of Talc / 0.5 mol % thioindigo unheated.	234
Figure B. 28 Peak fit of Talc / 0.5 mol % thioindigo heated at 413K for nine hours.....	235
Figure B. 29 Peak fit of 4A / 0.5 mol % thioindigo unheated.	236
Figure B. 30 Peak fit of 4A / 0.5 mol % thioindigo heated at 413K for nine hours.	237
Figure B. 31 Peak fit of 5A / 0.5 mol % thioindigo unheated.	238

Figure B. 32 Peak fit of 5A / 0.5 mol % thioindigo heated at 413K for nine hours.	239
Figure B. 33 Peak fit of NaY / 0.5 mol % thioindigo unheated.....	240
Figure B. 34 Peak fit of NaY / 0.5 mol % thioindigo heated at 413K for nine hours.....	241
Figure B. 35 Peak fit of NaY / 0.5 mol % thioindigo heated at 413K for nine hours / hydrated.	242
Figure B. 36 Peak fit of 13X / 0.5 mol % thioindigo unheated.	243
Figure B. 37 Peak fit of 13X / 0.5 mol % thioindigo heated at 413K for nine hours.	244
Figure B. 38 Peak fit of 13X / 0.5 mol % thioindigo heated at 413K for nine hours / hydrated.	245
Figure B. 39 Peak fit of LZV62 / 0.5 mol % thioindigo unheated.	246
Figure B. 40 Peak fit of LZV62 / 0.5 mol % thioindigo heated at 413K for nine hours.	247
Figure B. 41 Peak fit of LZV62 / 0.5 mol % thioindigo heated at 413K for nine hours / hydrated.	248
Figure B. 42 Peak fit of Zeolon [®] / 0.5 mol % thioindigo unheated.	249
Figure B. 43 Peak fit of Zeolon [®] / 0.5 mol % thioindigo heated at 413K for nine hours.	250
Figure B. 44 Peak fit of Zeolon [®] / 0.5 mol % thioindigo heated at 413K for nine hours / hydrated.	251
Figure B. 45 Peak fit of CBV21A / NH ₄ / 0.5 mol % thioindigo unheated.....	252
Figure B. 46 Peak fit of CBV21A / NH ₄ / 0.5 mol % thioindigo heated at 413K for nine hours.	253
Figure B. 47 Peak fit of CBV21A / NH ₄ / 0.5 mol % thioindigo heated at 413K for nine hours / hydrated.	254

Figure B. 48 Peak fit of CBV21A / Al / 0.5 mol % thioindigo unheated.....	255
Figure B. 49 Peak fit of CBV21A / Al / 0.5 mol % thioindigo heated at 413K for nine hours.	256
Figure B. 50 Peak fit of CBV21A / Al / 0.5 mol % thioindigo heated at 413K for nine hours / hydrated.	257
Figure B. 51 Peak fit of CBV21A / Al / 0.5 mol % thioindigo heated at 413K for nine hours / hydrated for 1 week.....	258
Figure B. 52 Peak fit of CBV21A / Ca / 0.5 mol % thioindigo unheated.	259
Figure B. 53 Peak fit of CBV21A / Ca / 0.5 mol % thioindigo heated at 413K for nine hours.	260
Figure B. 54 Peak fit of CBV21A / Ca / 0.5 mol % thioindigo heated at 413K for nine hours / hydrated.	261
Figure B. 55 Peak fit of CBV21A / K / 0.5 mol % thioindigo unheated.....	262
Figure B. 56 Peak fit of CBV21A / K / 0.5 mol % thioindigo heated at 413K for nine hours.	263
Figure B. 57 Peak fit of CBV21A / K / 0.5 mol % thioindigo heated at 413K for nine hours / hydrated.	264
Figure B. 58 Peak fit of CBV21A / Na / 0.5 mol % thioindigo unheated.	265
Figure B. 59 Peak fit of CBV21A / Na / 0.5 mol % thioindigo heated at 413K for nine hours.	266
Figure B. 60 Peak fit of CBV21A / Na / 0.5 mol % thioindigo heated at 413K for nine hours / hydrated.	267
Figure B. 61 Peak fit of CBV21A / H / 0.5 mol % thioindigo unheated.	268

Figure B. 62 Peak fit of CBV21A / H / 0.5 mol % thioindigo heated at 413K for nine hours.	269
Figure B. 63 Peak fit of CBV21A / H / 0.5 mol % thioindigo heated at 413K for nine hours / hydrated.	270
Figure B. 64 Peak fit of CBV21A / H(HCL) / 0.5 mol % thioindigo unheated.	271
Figure B. 65 Peak fit of CBV21A / H(HCL) / 0.5 mol % thioindigo heated at 413K for nine hours.	272
Figure B. 66 Peak fit of CBV21A / H(HCL) / 0.5 mol % thioindigo heated at 413K for nine hours / hydrated.....	273
Figure B. 67 Peak fit of CBV10A / H / 0.5 mol % thioindigo unheated.	274
Figure B. 68 Peak fit of CBV10A / H / 0.5 mol % thioindigo heated at 413K for nine hours.	275
Figure B. 69 Peak fit of CBV10A / H / 0.5 mol % thioindigo heated at 413K for nine hours / hydrated.	276
Figure B. 70 Peak fit of CBV10A / H(HCl) / 0.5 mol % thioindigo unheated.	277
Figure B. 71 Peak fit of CBV10A / H(HCl) / 0.5 mol % thioindigo heated at 413K for nine hours.	278
Figure B. 72 Peak fit of CBV10A / H(HCl) / 0.5 mol % thioindigo heated at 413K for nine hours / hydrated.	279
Figure B. 73 Peak fit of CBV10A / NH ₄ / 0.5 mol % thioindigo unheated.....	280
Figure B. 74 Peak fit of CBV10A / NH ₄ / 0.5 mol % thioindigo heated at 413K for nine hours.	281

Figure B. 75 Peak fit of CBV10A / NH ₄ / 0.5 mol % thioindigo heated at 413K for nine hours / hydrated.	282
Figure B. 76 Peak fit of CBV10A / Na / 0.5 mol % thioindigo unheated.	283
Figure B. 77 Peak fit of CBV10A / Na / 0.5 mol % thioindigo heated at 413K for nine hours.	284
Figure B. 78 Peak fit of CBV10A / Na / 0.5 mol % thioindigo heated at 413K for nine hours / hydrated.	285
Figure B. 79 Peak fit of MA-1 / 0.5 mol % thioindigo unheated.	286
Figure B. 80 Peak fit of MA-1 / 0.5 mol % thioindigo heated at 413K for nine hours. ...	287
Figure B. 81 Peak fit of MS-1 / 0.5 mol % thiondigo unheated.	288
Figure B. 82 Peak fit of MS-1 / 0.5 mol % thioindigo heated at 413K for nine hours. ...	289
Figure B. 83 Peak fit of MAS-1 / 0.5 mol % thioindigo unheated.	290
Figure B. 84 Peak fit of MAS-1 / 0.5 mol % thioindigo heated at 413K for nine hours. ...	291
Figure B. 85 Peak fit of pretreated palygorskite / 0.5 mol % thioindigo heated at 413K for nine hours.	292
Figure B. 86 Peak fit of pretreated palygorskite / 0.5 mol % thioindigo unheated.	293
Figure B. 87 Peak fit of thioindigo in concentrated sulfuric acid.	294
Figure B. 88 Peak fit of thioindigo interaction with concentrated sulfuric acid, after water addition.	296

LIST OF EQUATIONS

Equation 1 32

Equation 2 33

CHAPTER 1

INTRODUCTION

1.1 Background

Natural dyes have been widely used after their discovery in 2600 B.C.⁵ The method of synthesis is through the fermentation and extraction from roots and leaves of different plants and insects.⁶ By the end of the nineteenth century, synthetic production of these organic dyes substituted the natural dye extraction from inexpensive starting materials. Adolf von Baeyer, among others, was at the forefront of this work.⁷ Today, dyes are synthesized in large quantities through large-scale industrial processes, based upon the original synthetic pathways. A problem with these organic dyes is their gradual degradation; one major step towards the solution of this problem was discovered by chance in America (Figure 1).



Figure 1 Mural from Bonampak, Palenque (Classic period, 200 B.C. - 900 A.C.)⁸.

Mayans, at the peak of their civilization (250 - 900 A.C.), extracted indigo dye from the leaves of *indigofera suffruticosa*.⁹ This Mesoamerican pigment became what is known today as Maya Blue;¹ it has been the focus of numerous studies and is a mixture of indigo and palygorskite/sepiolite clays.^{1,10}

Palygorskite and Sepiolite belong to a phyllosilicate group, which are naturally occurring hydrated magnesium silicates with varying compositions based on the region. Palygorskite has been found to be the main component in Maya Blue pigment. The second component, indigo, is a common organic dye with the chemical formula $C_{16}H_{10}N_2O_2$.¹¹

Several theories have been proposed that seek to explain the shades and longevity of the blue pigments. G. Chiari *et al.*¹² have proposed that indigo resides in the surface grooves (half channels) of palygorskite, since zeolitic water is still inside the channels at 100°C, which they get from their interpretation of their thermogravimetric analysis. The binding of indigo is possibly explained by hydrogen bonding with the structural water or hydroxyl groups in the clay. Using thermogravimetric analysis (TGA), nuclear magnetic resonance (NMR) and textural analysis techniques, B. Hubbard *et al.*¹³ proposed that indigo molecules, via the carbonyl and amine moieties, are anchored in the entrance of the channels through hydrogen bonds with silanol groups. A. Domenech *et al.*¹⁴ proposed that varying amounts of dehydroindigo, the oxidized form of indigo, in the mixture, causes the different shades of blue observed in samples of Maya Blue. L.A. Polette-Niewold *et al.*¹¹ proposed that oxidation of indigo to

dehydroindigo does occur during the production of the pigment and the chemical interaction between the carbonyl oxygen of the dehydroindigo binds to the surface Al^{3+} in the Si-O lattice. This is a plausible explanation of the observed phenomena.

Several derivatives of the Maya Blue pigment have been developed and more intriguing properties have been found. For instance, the dye thioindigo reacts with palygorskite clay to exhibit a broad range of colors from red to purple under thermal treatment and UV excitation. In the case of sepiolite, color change is not as drastic, and for faujasite synthetic zeolites, color change is reversible.

The immobilization of thioindigo on SiO_2 , Al_2O_3 and bentonite was first recorded by G.M. Schwab *et al.*¹⁵ where color changes from red to blue were detected. Conversely, H.D. Breuer *et al.*¹⁶ observed photoisomerization from *trans* to *cis* of thioindigo molecule and an energetically stable *cis*- thioindigo was preferentially absorbed on the Al_2O_3 surface rather than the *trans* counterpart. Using tetrachloro derivatives of thioindigo, D. Reinen *et al.*¹⁷ reported similar changes in color and suggested different hydrogen bonding patterns of thioindigo with palygorskite as the basis for the different colors. This team also reported that thioindigo derivatives bound to palygorskite are weaker than indigo. Analogous results were obtained by R. Hoppe *et al.*,¹⁸ where bathochromic shifts under visible excitation inducing a surface reaction of thioindigo with a zeolite (faujasite structure) were observed. Concluding silanol interaction could be responsible for this behavior, but no reversible color change was detected.

1.2 Research Objectives

The issue addressed in this paper was the nature of the interaction between inorganic host materials and a small dye molecule such as thioindigo. The root of this is the clay's organic interaction in Maya pigments, but the scope of this paper includes other materials. In addition, the organic molecular interaction with a concentrated acid was also described.

Several characterization techniques such as, wide range X-ray fluorescence spectrometry, diffuse reflectance and transmission ultraviolet-visible spectroscopy, electron dispersive X-ray analysis, Fourier transformed infrared spectroscopy, magic angle nuclear magnetic resonance and X-ray diffraction were used to examine the samples. Moreover, computer simulation helped enormously to draw further conclusions observed experimentally.

CHAPTER 2

METHODOLOGY

2.1 Materials Sampling

Thioindigo dye was obtained from TCI America Inc. and was used as received.

Inorganic host materials were obtained from several providers and a complete list of information is listed in Appendix A. All materials were used as received.

A number of inorganic salts for cationic exchange such as, KCl (Fischer Scientific), CaCl_2 (EM Science), $\text{Al}_2(\text{SO}_4)_3$ (Sigma-Aldrich), NH_4Cl (J.T. Baker) and NaNO_3 (Fischer Scientific) were used as received.

Solvents such as: Ethanol reagent grade (Sigma-Aldrich), 98.7% sulfuric acid (EM Science) and HCl (Sigma-Aldrich) were used without further purification. Pyridine (Sigma-Aldrich) was dried overnight with KOH (Sigma-Aldrich) and purified by distillation under N_2 gas.¹⁹

2.2 Sample Preparation

2.2.1 Thioindigo

Thioindigo was reported by Brode *et al.*²⁰ to present bathochromic shifts around 666nm when in contact with a concentrated solution of sulfuric acid. This reaction was reproduced with ~1 mg of thioindigo added to 2 mL of 98.7% sulfuric acid in a beaker. The blue greenish solution was stirred and measured under UV-Vis spectroscopy.

2.2.2 Inorganic Host Materials

A number of inorganic materials used in these experiments were synthesized by Penn State University or pretreated at UTEP before mixed with thioindigo. The following section describes the procedures used which were: synthetic route for swelling micas, neutral templating route for mesoporous zeolites, cationic exchange zeolites and high temperature treatment. Additionally, the surface acidity evaluation was performed.

Synthetic Route for Swelling Micas

YN6 and YN8 synthetic swelling micas and mesoporous zeolites (MS-1, MAS-1 and MA-1) were prepared by Penn State University using the following methodology: YN6 and YN8 were synthesized by mixing in a stoichiometric ratio sodium fluoride, silicic acid and aluminum chloride. Once homogenized the mixture was placed in a platinum crucible and heated at 1123K for five hours, then it was cooled down to room

temperature and washed several times with deionized water using centrifugation. The white powder was dried prior to being used as a host with thioindigo.²¹

Neutral Templating Route for Mesoporous Zeolites

Mesoporous zeolites of silica (MS-1), alumina (MAS-1) and aluminosilicate (1:1 Si:Al atomic ratio) were synthesized by tetraethoxysilane, Al isopropoxide, and a mixture of tetraethoxysilane and Al isopropoxide, respectively, using a neutral templating route. This route entailed the addition of 1 mol of alkoxide to a solution of 0.27 moles of dodecylamine, 9.09 moles of ethanol and 29.6 moles of deionized water under vigorous stirring for thirty minutes and kept aside at room temperature for thirty-five hours. After this time the sample was transferred to a glass plate and air dried. The neutral template was heated at 773K for four hours in order to remove the organic matter.²²

Cationic Exchange Zeolite

One cation exchange mordenite was prepared from synthetic zeolite CBV21A (Si/Al = 9.5). The method involved 5 g of sample two times washed with 250 mL of 0.2 M solution [KCl, CaCl₂, Al₂(SO₄)₃, NH₄Cl, NaNO₃, and HCl] containing the desired cation at 373K for 1 hour. All solutions were prepared with ultra pure water to avoid contamination by other cations. The slurry solution was then filtered in a fluorocarbon filter membrane (Chemplast, Inc.), washed several times and centrifuged at 1000 rpm

(International centrifuge, model CM). The slurry solution was then dried at 413K in a tube furnace (Lindberg/Blue M) with an electronic thermocouple (Omega Engineering DP900) and the powder collected.²³ Moreover, hydrogen cation exchange was also performed through a different procedure where an NH_4^+ -MOR sample was calcined in an air stream at 873K for three hours.²⁴

High Temperature Treatment

In order to reduce the pore size of the crystal structure, zeolon[®] and palygorskite were exposed to 1223K and 823K , respectively, for a time period of fifteen hours.

Surface Acidity Evaluation

Inorganic materials were treated with pyridine following the sample preparation by C. Ravindra Reddy *et al.*²⁵ where a fast pyridine evaluation was performed. Samples (~50 mg each) were set to dry at 413K for one hour before pyridine adsorption. This thermal treatment allowed a closer evaluation of the framework Brønsted acids, instead of the hydration protons that could give similar vibration in FTIR. After thermal treatment, samples were set in a crucible individually with 0.2 - 0.5 mL of pyridine. The crucible was then placed in a tubular furnace at 413K for one hour to remove physisorbed pyridine. After this time samples were left inside a desiccator for further FTIR analysis.

2.2.3 Inorganic Host Materials Treated with Thioindigo

6 wt. % thioindigo was added to 94 wt. % inorganic host materials (including pretreated samples) in a glass mortar and finely ground until a homogenous mixture was obtained. The mixture was placed in a ceramic crucible and heated in a tube furnace at 413K for nine hours. Evaluation of stability was performed by soxhlet ethanol extraction with cellulose thimbles. High hydration environment was fabricated with a glass desiccator and water instead of desiccant.

2.3 Instrumentation

2.3.1 Wide Range X-Ray Fluorescence Spectrometry (WD-XRF)

Minerals were analyzed using a WD-XRF Axios Panalytical spectrophotometer by an external company (SGS Mineral Services Analytical). Sample preparation required the formation of a homogenous glass disk by the fusion of 0.2 g to 0.5 g of a clay powder sample, with 7 g of lithium tetraborate/ lithium metaborate (50/50). The loss on ignition (LOI) at 1000°C was gravimetrically determined separately. The LOI was included in the calculations.

2.3.2 Diffuse Reflectance Ultraviolet- Visible Spectroscopy

Diffuse reflectivity measurements were recorded using a Shimadzu 3101 spectrophotometer with a 50 cm integrating sphere or Ulbricht sphere (a sphere with a fully reflective inner surface) and BaSO₄ as a standard for 100% reflectance. Reflectance values were acquired from 200 to 800 nm, which were then converted to absorption using the Kubelka-Munk method.

2.3.3 Transmission Ultraviolet-Visible Spectroscopy

Liquid UV-Vis spectra were recorded with a Varian Cary 50 Conc. spectrophotometer using a 1.00 cm fused quartz absorption cell over the entire wavelength range (200 - 800 nm).

2.3.4 Fourier Transformed Infrared Spectroscopy (FTIR)

FTIR measurements were carried out with two different experimental setups. The first setup was a Bruker IFS 66v spectrometer equipped with a DTGS detector and a potassium bromide beamsplitter. The samples for the IR studies were prepared in the form of pellets by embedding the pigments in a polycrystalline potassium bromide matrix. An accumulation of 256 scans was performed for each spectrum from 400 to 4000 cm⁻¹. The data were normalized at each frequency to a vacuum throughout spectrum.

The second equipment was a Thermo Nicolet Nexus 470 FTIR spectrometer. Samples were embedded in mineral oil and smeared between two sodium chloride windows and supported by a metallic sample holder. The spectrum was recorded from 400 to 4000 cm^{-1} with an accumulation of 60 scans.

2.3.5 X-ray Powder Diffraction

Starting materials were characterized by a Scintag XDS 2000 seal tube diffractometer with a copper $\text{K}\alpha$ source. Calcium carbonate and quartz were used as internal standards. Experimental parameters involved diffraction angles between 5 - 50 degrees, a step size 0.02 degrees per sec. and a time scan of 1.5 sec. Braggs Law ($\lambda = 2d\sin\theta$) was used to compute the spacing. Characterization was performed by comparison of XRD results with reported patterns from the inorganic crystallographic database.

2.3.6 Electron Dispersive X-ray Analysis (EDAX)

Chemical analysis was performed in a Hitachi S-4800 high performance scanning electron microscope at 20 kV voltage in high resolution mode with carbon plates for sample loading and an EDAX detector. Gold sputtering for 120 seconds was carried out for all samples tested to improve conductivity. Sensitivity of this technique is 1000 ppm (0.1 wt.%), with a lateral and depth spatial resolution approximately 1 μm .²⁶

2.3.7 Magic Angle Nuclear Magnetic Resonance (MAS-NMR)

²⁷Al MAS-NMR spectra were obtained at 94.7 MHz using a 360 MHz Tecmag NMR system, equipped with a 5 mm Doty SuperSonic probe. The operating conditions of the spectrometer were: a pulse width of 1.1 µsec; the solution for a 90 degree pulse of 6.5 µsec, a solid 45 degree pulse of ($I = 5/2$); the pulse length was 15 degrees and the delay was 0.3 seconds; number of transients was 2000 or higher, and a spinning speed in the range of 8.2 to 10 kHz. Chemical shifts were measured relative to 1 M aqueous Al nitrate solution.

2.3.8 Computer Simulation

We have chosen a semi-empirical calculation method called ZINDO (Zerners Intermediate Neglect of Differential Overlap)²⁷ through the CERIUS² modeling platform, to perform excited states calculations and geometry optimization. Moreover, the adsorption of thioindigo molecule into a 3D inorganic framework was performed by a Monte Carlo method with a similar platform. A newer version of this platform called Materials Studio (MS) was also used to performed similar calculations for some other systems. In this case, the semi-empirical molecular orbital application was called VAMP²⁸. This application was carried out using a Hamiltonian of neglect of diatomic differential overlap (NDDO) for best results. NDDO is a basic approximation for neglecting less important integrals.²⁹

CHAPTER 3

CHEMICAL AND STRUCTURAL CHARACTERISTICS OF STARTING MATERIALS

3.1 Thioindigo Dye

Thioindigo belongs to a group of derivatives with structurally related compounds usually formed of two nuclei (heterocyclic or homocyclic), united by a double bond and conjugated by both sides with a carbonyl group.³⁰ The chromophoric center responsible for the color in these dyes is mainly the electronic excitation of the π - π^* transition.³¹ In the case of thioindigo, two carbonyl and sulfur moieties are present in the chromophoric center of the molecule. Thioindigo molecule proportions are 15.17 Å (length), 7.42 Å (width) and 3.4 Å (thickness) (see Figure 2).³²

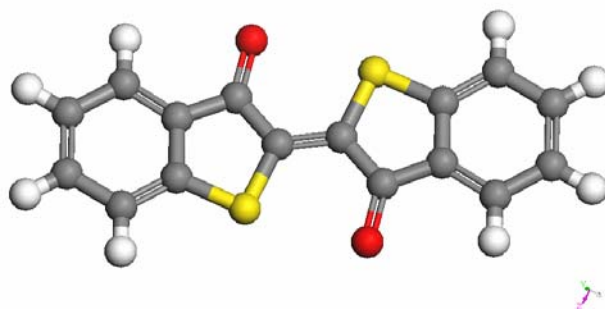


Figure 2 Trans -Thioindigo molecule (the most stable conformation). C= gray, H= white, S= yellow, and O= red. [Materials Studio v4.0].

Thioindigo forms dark red crystals by sublimation at 563K with a structural formula $C_{16}H_{10}S_2O_2$. It crystallizes in a monoclinic arrangement elongated in the a-axis, with a space group of $P2_1/n$ and cell parameters $a = 3.981(3)$, $b = 20.65(2)$, $c = 7.930(7)\text{\AA}$, $\beta = 98.84(5)^\circ$ (see Figure 3).³³

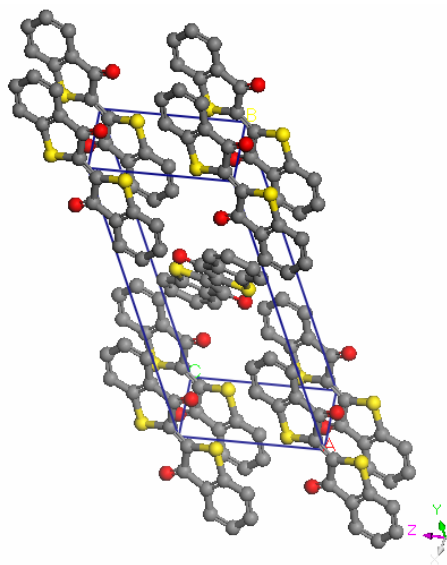


Figure 3 Thioindigo crystal structure [Materials Studio v4.0].

Thioindigo can be obtained by three different procedures. (1) Oxidation of benzo[b]thiophene-3-ol(thioindoxyl) II, or its carboxylic acid by ferricyanide, sulphur, or by nitro-substituted arenesulphonic acids (III) (Figure 4). (2) Condensation of thioindoxyl with its 2,2-dibromo derivative or with phenyliminothioisatin. (3) Reaction with thiosalicyclic acid with 1,2-dichloroethene followed by dehydration with chlorosulphonic acid.³⁰

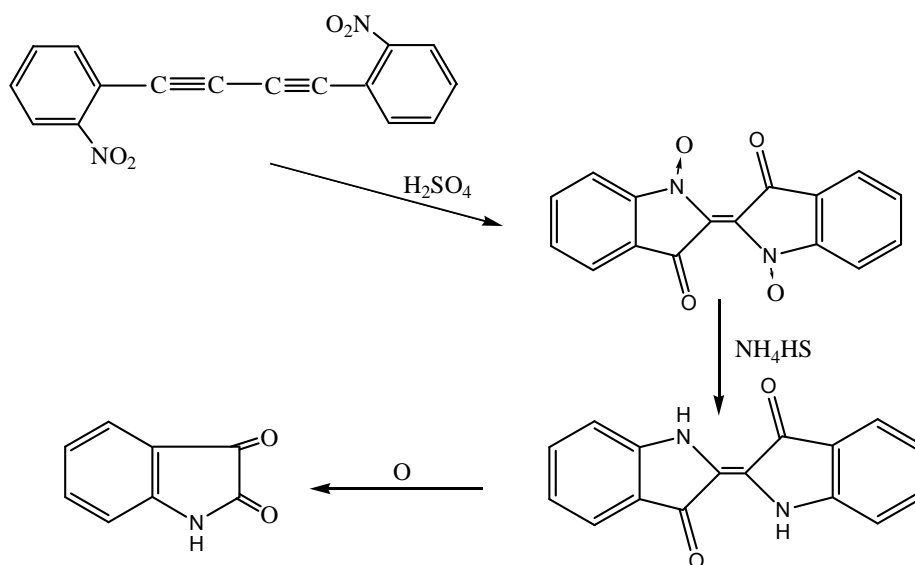


Figure 4 Synthesis of thioindigo by oxidation [Image courtesy of M. Saunbury, *et al.*³⁰].

Trans-thioindigo is found to be a stable isomer in the solid state and is believed to be mostly due to the electrostatic charges on the slightly negative and positive charges of oxygen and sulfur atoms, preventing isomerization.³⁴

In solution, the electrostatic forces mentioned previously are lost, and thioindigo, for example, in benzene is found to change from *trans* red-purple ($\lambda_{\text{max}} \approx 545 \text{ nm}$) to *cis* orange-yellow (Figure 5) ($\lambda_{\text{max}} \approx 485 \text{ nm}$) for a short period when exposed to visible light.^{30,35} In the eighties, a vast amount of research was performed using thioindigo, mainly to pursue alternative photochromic materials suitable for electronic applications. However, its use in the liquid state made it difficult to handle. Accordingly, research focused in the immobilization of thioindigo in different solids such as Al_2O_3 , SiO_2 , etc. G.M. Wyman *et al.*³⁶ successfully separated the red-purple solution (*trans*) and the orange-yellow solution (*cis*) isomers in a silica gel column when thioindigo/benzene was

irradiated ($\lambda_{\text{max.}} > 520 \text{ nm}$) for 20 min. Moreover, the same authors also reported thioindigo bathochromic shifts up to 666 nm when reacted with concentrated sulfuric acid.²⁰

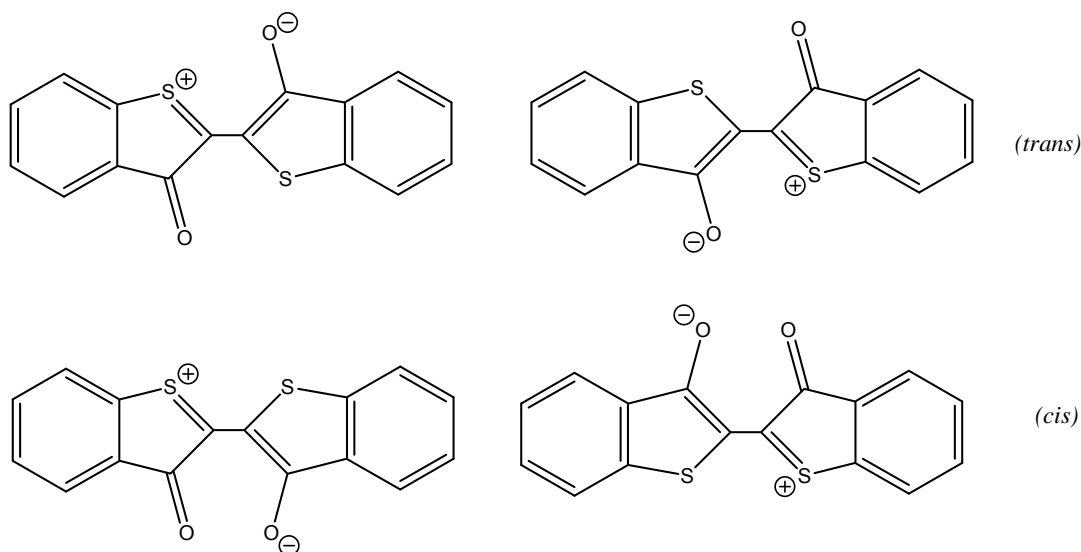


Figure 5 Representing the four forms at which the isomers could exist in solution. No double bond present [Image courtesy of G.M. Wyman, *et al.*³⁶].

Molecular Orbitals of Thioindigo

In order to better understand color changes occurring in these systems, the HOMO (Highest Occupied Molecular Orbital)-LUMO (Lowest Unoccupied Molecular Orbital) excitations have to be looked at closely. This energy difference is what defines color in molecules, and is easily affected by molecular isomerization, conjugation, electron donating substituents and more. As mentioned before, *cis*- thioindigo isomer in benzene has been reported to occur at higher energies ($\lambda_{\text{max}} = 470 \text{ nm}$), displaying a red-orange color.

Using TD-DFT (Time Dependent - Density Functional Theory), Jacquemin *et al.*³⁵ identified the full π orbital (HOMO) on the sulfur and the central C=C bond, whereas the empty π^* orbital (LUMO) was centered on the single C-C bonds and oxygen atoms. Based on the electron-donating substitution of the HOMO and LUMO of some aluminum complexes, Chai *et al.*³⁷ observed by UV-Vis spectroscopy, the raise of LUMO energy leading to a blue (hypsochromic) shift in the emission. On the other hand, the raise of HOMO energy resulted in a red (bathochromic) shift. Location of HOMO and LUMO for thioindigo (Figure 6), given by ZINDO, are in agreement with the information previously reported by Fabian *et al.*³⁸

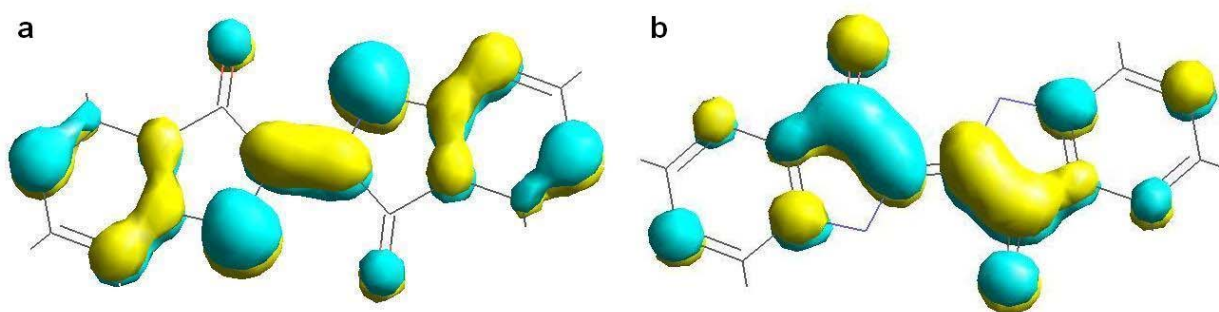


Figure 6 (a) Highest Occupied Molecular Orbital (HOMO) location on the sulfur and C=C bond of thioindigo. (b) Lowest Unoccupied Molecular Orbital (LUMO) location on C-C single bond and oxygen bond of thioindigo [Cerius² accelrys software].

3.2 Inorganic Host Materials

3.2.1 Natural Occurring Clay Minerals

Palygorskite and Sepiolite Clays

Clays are naturally occurring minerals with varying compositions. Palygorskite with a general formula, $(R^{2+}, R^{3+})_5(Si, R^{3+})_8O_{20}(OH)_4M^{n+}(H_2O)_4$ with cation substitution $Ca^{2+}, Mg^{2+}, Fe^{2+}(R^{2+}), Al^{3+}, Fe^{3+}(R^{3+})$, and sepiolite $[(R^{2+}, R^{3+}, R^{2+}, R^{3+})_8(H_2O)_4(OH)_4(Si, Al)_{10}O_{30}]$,³⁹ exhibit a fibrous structure-like ribbons where silicon atoms coordinate tetrahedrally with basal oxygens forming pyroxene chains periodically inverted. At the same time, and in order to balance the oxygen negative charge, apical oxygens bind to aluminum atoms forming non-continuous octahedral chains.⁴⁰

Palygorskite is a mixture of two polymorphs, one with monoclinic unit cell, space group $C2/m$, cell parameters $a = 13.24$, $b = 17.89$, $c = 5.21$ Å and an orthorhombic unit cell with a space group $P2_1/b2/m2/n$ and cell parameters $a = 12.762$, $b = 17.882$, $c = 5.249$ Å. Conversely, sepiolite is orthorhombic, with a space group $P2_1/n2/c2/n$ and cell parameters $a = 14.66$, $b = 26.71$, $c = 5.26$ Å.⁴¹

Palygorskite and sepiolite are built of two types of discontinued polyhedral building blocks, one octahedral sheet is bonded between two tetrahedral sheets on each side, forming micro-channels throughout the structure,¹³ with tunnel measurements along the yz axis of 6.4 x 3.7 Å for palygorskite, and 10.7 x 3.7 Å for sepiolite.⁴² Correspondingly, palygorskite and sepiolite contain three forms of water in their structure: zeolitic water, coordinated water and structural which is water, coordinated at two positions to the magnesium/aluminum ion in the crystal lattice (see Figure 7). The difference in channel size between the two clays allows the storage of 5 zeolitic waters for palygorskite,¹³ and 8 zeolitic waters for sepiolite, per formula unit.

Thermal analysis of palygorskite by G. Chiari *et al.*⁴³ reported the reversible process up to 623K. At 393K, 6.3% weight loss is detected for free pore water and surface water. Over the range 393-573K and with 4% weight loss, zeolitic water is removed. Below 603K hydroxyl groups are still unmodified, and at higher temperatures structural water is removed.⁴⁴

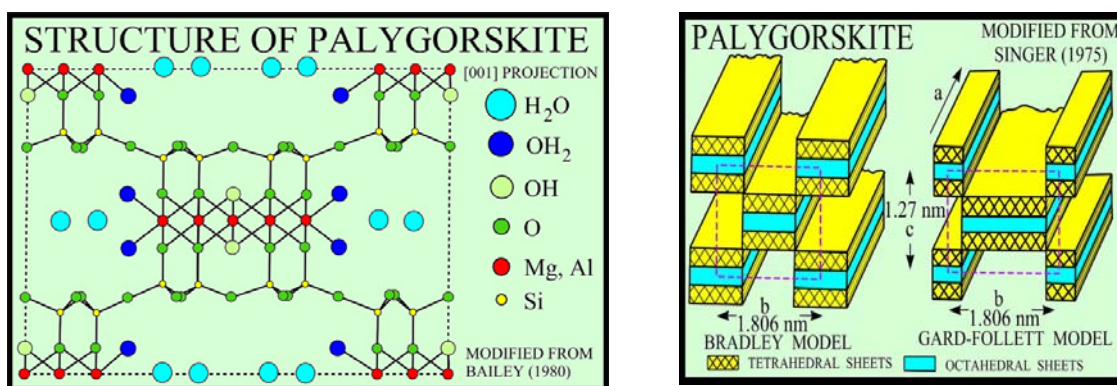


Figure 7 (left) Palygorskite unit cell, visualization on 001 plane. (right) Block unit representation showing dimension of channels [Image courtesy of the Coastal and Marine Geology Program].⁴⁵

Sepiolite thermal analysis by U. Shuali *et al.*⁴⁶ reported a 18.6% weight loss in a range of temperatures between 298 and 513K, together with an endothermic peak at 413K, which is characteristic of absorbed water and some zeolitic water as well. At 623-773K several sepiolites show two endothermic peaks and 5.3% weight loss in TG is detected; this was related to a change in the bonding energy of bound water, due to the formation of a stable new phase of sepiolite anhydrite ($\text{Mg}_8\text{Si}_{12}\text{O}_{30}(\text{OH})_4$) at 623K.⁴⁷

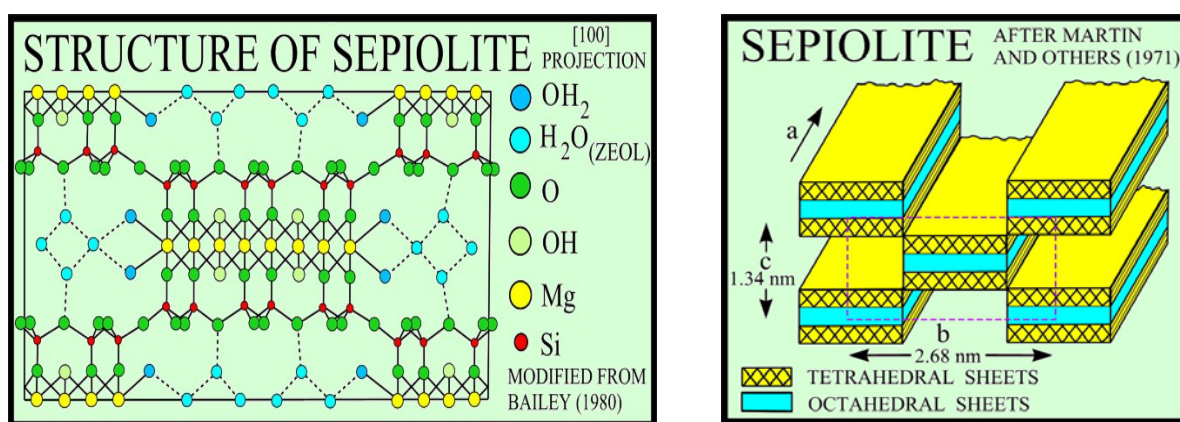


Figure 8 (right) Sepiolite orthorhombic unit cell.(left) Schematic 001 plane representation of the cross-section of a sepiolite fiber [Image courtesy of Coastal and Marine Geology Program].⁴⁵

Using FTIR and elemental chemical analysis Serna *et al.*⁴⁸ helped to elucidate the distribution of metals inside the structure bonded to coordinated (bonded) water and structural water (hydroxyl groups). In general, palygorskite clay contains Mg^{2+} located in the external octahedral sites bound to 2 structural waters (M3 position). Moreover, Al^{3+} and Fe^{3+} are found in the inner octahedral sites, bound to 2 hydroxyl groups when a high concentration of Fe^{3+} is found (M2 position) This arrangement is called dioctahedral, where two trivalent cations (2R^{3+}) are occupying two of the three octahedral sites available.⁴⁰

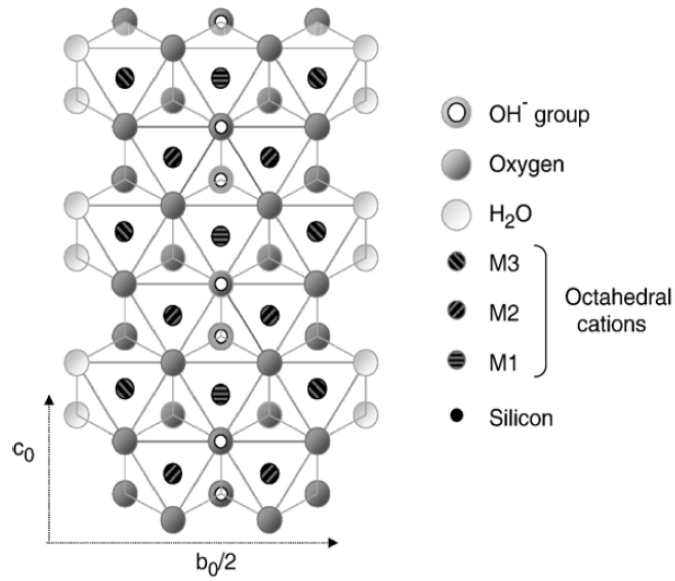


Figure 9 Octahedral ribbon for palygorskite [Image courtesy of Suarez *et al.* ⁴⁴].

In the case of sepiolite, Mg²⁺ cations are reported in the inner octahedral sites, forming an trioctahedral arrangement,⁴⁹ where three divalent cations (3R²⁺) occupy the three octahedral sites available (M3 and M1 positions).

Neutral Layer Clays (Charge almost zero)

Most clays that belong to this group present dioctahedral or trioctahedral character. Talc belongs to this group and would be tested in this research. Its main characteristic is the zero charge imbalances due to low aluminum substitution in its layers; therefore, no cations are present between the interlayer and no hydration takes place. This gives talc the slippery and dry property.⁴⁰

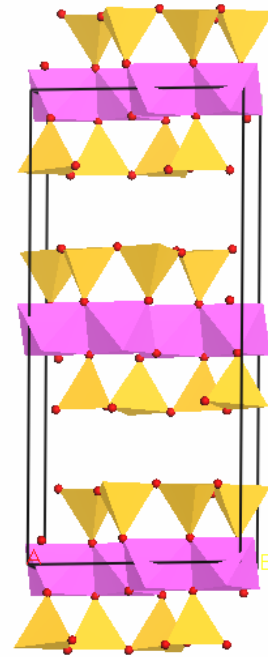


Figure 10 Talc unit cell displaying 2:1 arrangement [Materials Studio v4.0].

Low Charge Swelling Minerals: Smectites (Charge between 0.7 to 0.2)

This group of minerals with a 10 Å layer structure and an excess charge of 0.7 to 0.2 allow hydrated cations between the layers. This characteristic causes the layers to expand from a monohydrated state (one water layer around the cation) of d spacing 12.5 Å to 15.2 Å for a trihydrated state (three water layers around the cation). The maximum expansion smectite clays can handle are 17 Å, when measured with ethylene glycol. Clay minerals that belong to this group are montmorillonite clays, among others.⁴⁰

Montmorillonite Clays

Montmorillonite is a clay mineral with expandable layers, with continual polyhedral sheets, consisting primarily of one octahedral between two tetrahedral sheets (2:1 minerals). The octahedral sheets contain varied hexa-coordinate ions, forming dioctahedral and trioctahedral arrangements.

As in most of the aluminosilicates, substitution of aluminum in the silicon tetrahedral sites is observed, generating negative charges between the layers, this charge is neutralized by the proximity of exchangeable cations in the layers (Figure 11).

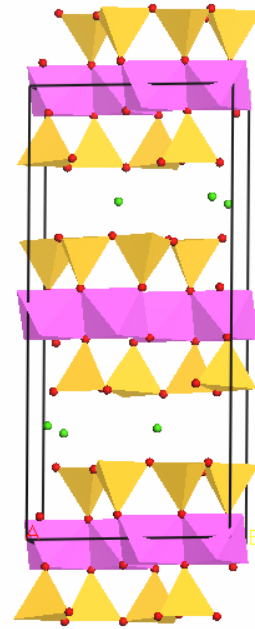


Figure 11 Montmorillonite structure displaying building units of tetrahedral and octahedral sheets [Materials Studio v4.0].

High Charge Mica Group (Charge almost 1)

Charge imbalance in this group is from 0.8 to 1, normally for dioctahedral substitution. Due to the high charge imbalance the cation in the interlayer is strongly bound, usually potassium is the cation present in this type of mineral, due to its high polarizability these clays typically do not expand.⁴⁰ However, recent research in synthetic micas, have manipulated these properties by inserting other cations less polarizable such as sodium, and giving mica the property to expand.²¹

Low Charge Synthetic Swelling Micas

Low charge synthetic micas derived from the reduction of the high interlayer charge by hydroxylation (oxygen from tetrahedral sites replaced by OH), or by silification (Al^{3+} in tetrahedral sites substituted by Si^{4+}). In addition, a less polarizing cation such as sodium improves mica swelling with polar solvents.⁵⁰ In this research two low charge swelling micas (YN6 and YN8) prepared by Dr. Komarneni and his group were tested. In YN6 ($\text{Na}_{0.125} \text{Al}_{0.125} \text{Si}_{7.875} \text{Mg}_6 \text{O}_{20} \text{F}_4$) and YN8 ($\text{Na}_{0.5} \text{Al}_{0.5} \text{Si}_{7.5} \text{Mg}_6 \text{O}_{20} \text{F}_7$) fluorine anion was used to lower the high charge of the mica clays instead of OH.²¹

3.2.2 Synthetic Aluminosilicates

Zeolites are crystalline aluminosilicates with a general formula, $M_{x/n}[(AlO_2)_x(SiO_2)_y] \cdot mH_2O$, where cations (M) balance the negative charge created in the framework. In general, these crystalline minerals consist of building blocks of $[SiO_4]$ and $[AlO_5]$, tetrahedrally coordinated and corner sharing. The substitution of Si(IV) by Al(III) in the tetrahedral sites creates an electrical imbalance in the $[AlO_5]$ building block; hence, to preserve the neutral charge, exchangeable cations are held within the zeolite.⁵¹

Differences in topology help to classify the structural variety found in zeolites. Simple Secondary Building Units (SBU) were chosen by W.M. Meier⁵² to explain in a simple way the complicated structures of zeolites. SBU are the smallest number of building units (Figure 12) from which zeolites are mostly formed; for example, in the case of modernite, the framework can be made only by 5-1 units. For some other zeolites more than one SBU is involved; for example, faujasite with four SBU of 4-, 6-, 8- rings and 6-6 hexagonal prisms, and Linde zeolite A, with 4-, 6-, 8- and 4-4 cubic units.

Ring size in the structure is defined by the amount of tetrahedrals sharing corners. Six tetrahedral groups form a hexagon where twenty four form a truncated octahedron shape, called a sodalite unit or β -cage.⁵³

Three zeolite groups will be discussed in this research, such as: faujasite (FAU), Linde Type A (LTA) and mordenite (MOR).

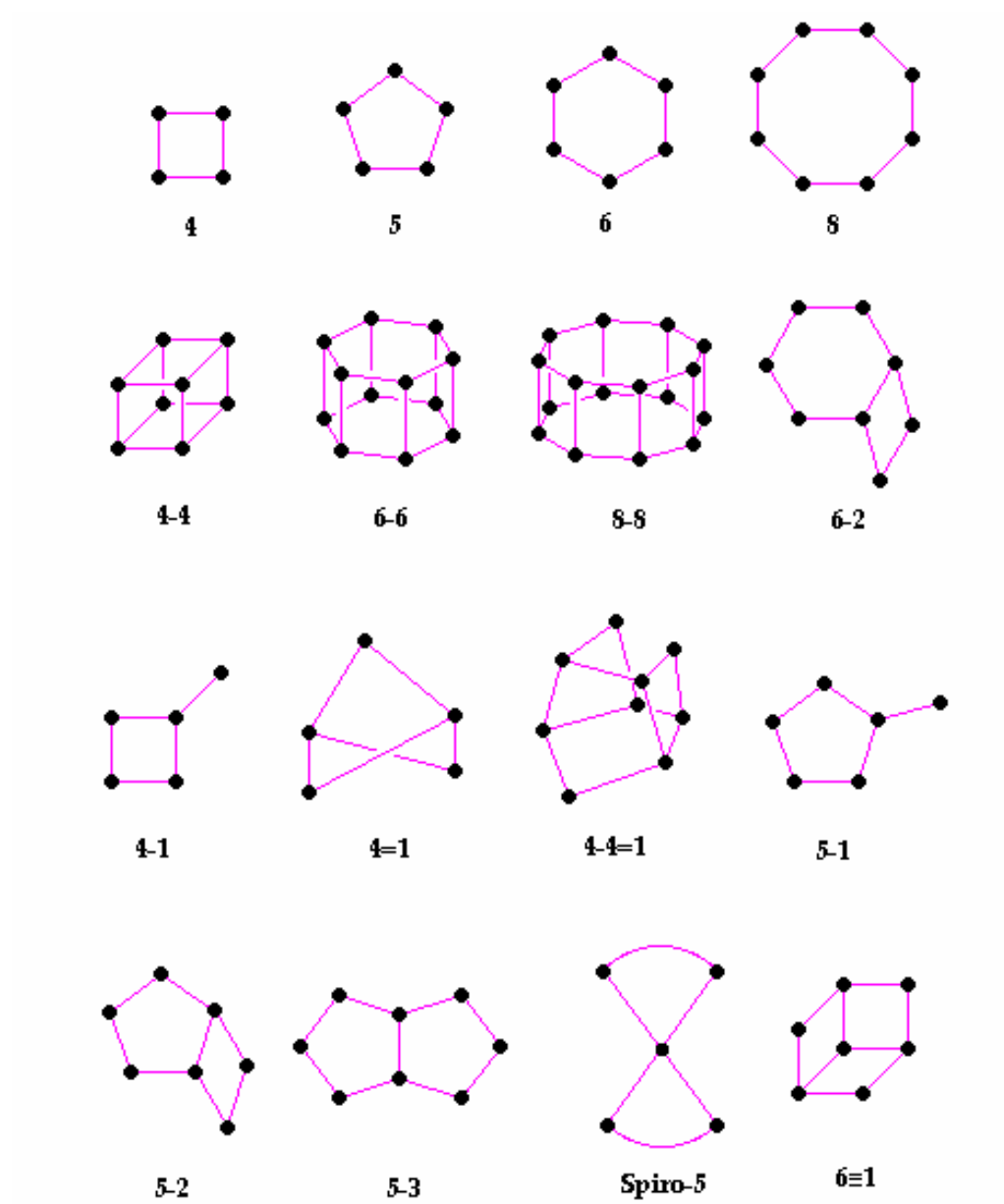


Figure 12 Meier's secondary building units of zeolite frameworks [Image courtesy of J.V. Smith⁵¹].

Faujasite (FAU)

Faujasite is the proper name given to the natural occurring mineral with a cubic unit cell, cell parameters $a = 27.4\text{\AA}$ and space group $Fd3m$.⁴⁰ Zeolite falling into this category have a similar framework such as X and Y. However, in the case of Linde Type A (LTA), some variations in the crystal structure are found. For zeolite X and Y, the unit cell consists of sodalite units linked to hexagonal prisms (6-6 SBU, see (Figure 12). The tetrahedral array of this structure encloses a large supercage (α -cage) which is entered through a twelve-ring window (Figure 13).⁵³

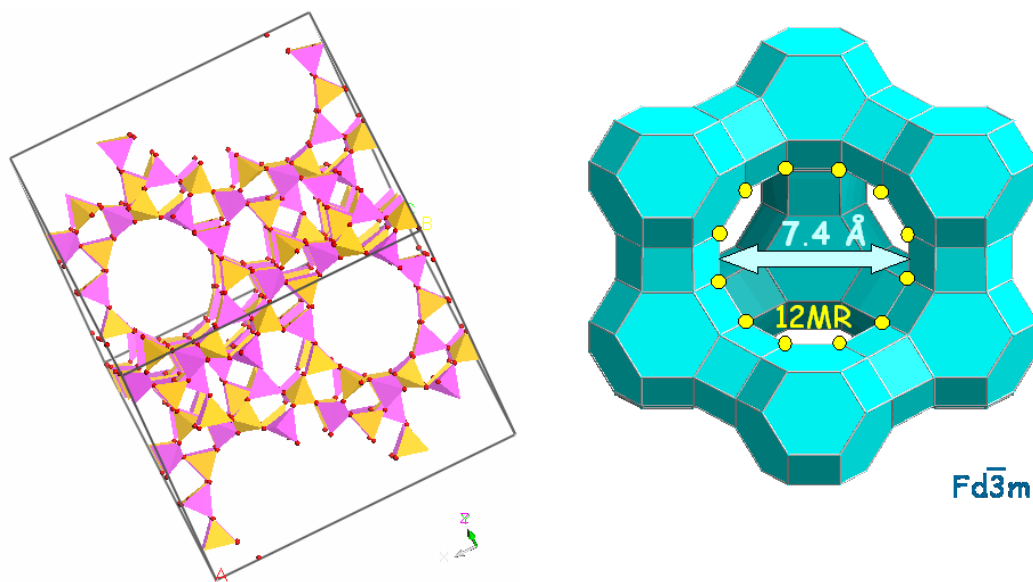


Figure 13 Visualization of Faujasite framework in (left) tetrahedral arrangement, and (right) secondary building units of sodalite and hexagonal prism linked together [Image courtesy of G. Bergerhoff *et al.*⁵⁴].

Linde Type A (LTA)

Linde Type A is a member of the faujasite group; however, there are small differences that characterize this zeolite. LTA crystallizes in a cubic arrangement with cell parameters $a = 11.9\text{\AA}$, and space group $Pm\bar{3}m$.⁵⁵ In the framework, sodalite units are modified to the 4-ring found in the truncated octahedron at the corner of the unit cell and replaced by a 4-4 secondary building unit, forming a center cage with a shape of a truncated cubooctahedron with twelve 4-rings, eight 6-rings and six 8-rings. These cages are connected in three directions by windows of 8-ring (Figure 14).⁵¹

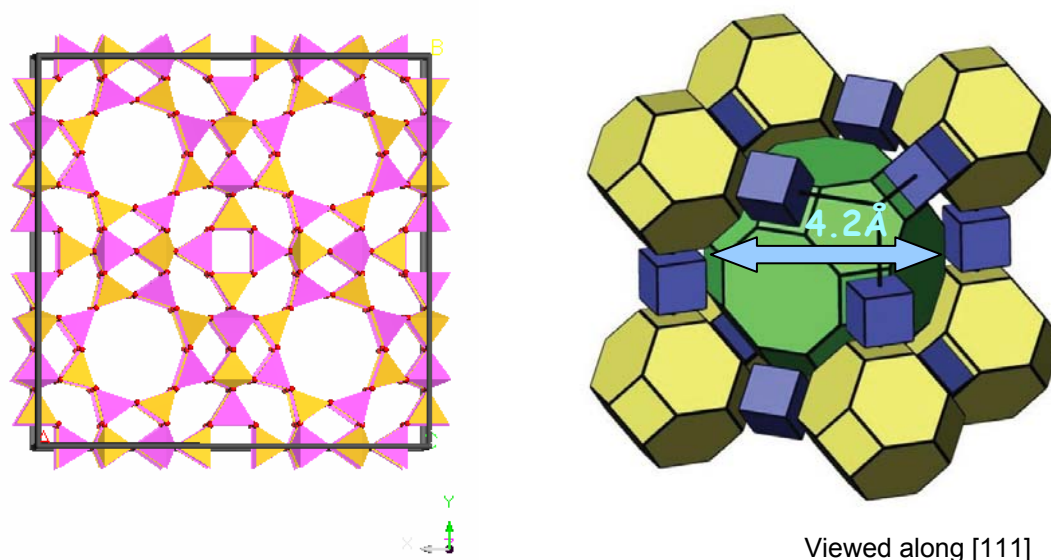


Figure 14 Visualization of LTA framework in (left) tetrahedral arrangement, and (right) secondary building units of sodalite and cubes linked together [Image courtesy of T.B. Reed *et al.*⁵⁵].

Modernite

Modernite is orthorhombic, cell parameters of $a = 18.1$, $b = 20.5$ and $c = 7.5\text{\AA}$, and space group $Cmcm$.⁵⁶ The framework of modernite is composed of horizontal 4-rings and tilted 5-rings sharing an edge. Together these units form a 12-ring in interconnected zig-zag channels made up of 5-, 6-, 8-rings. Pairs of 5-rings connected to other 5 rings form vertical strips of high rigidity. These strips can be arranged in different ways to form other members of the modernite group.⁵¹

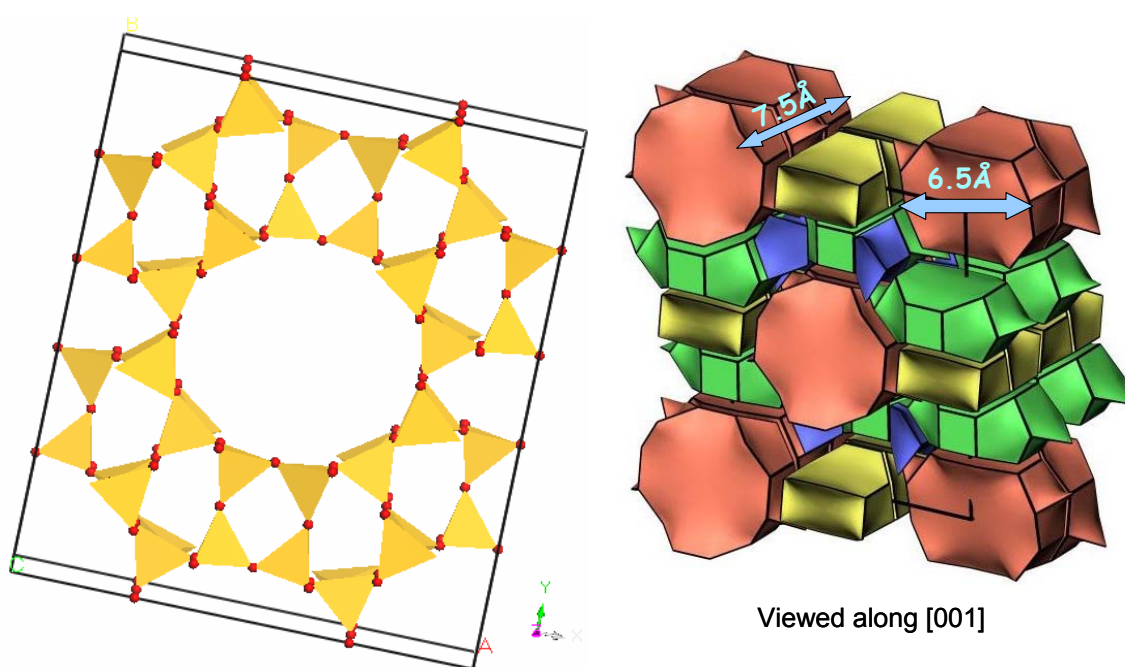


Figure 15 Visualization of MOR framework in (left) tetrahedral arrangement, and (right) secondary building units of 4 different secondary building units linked together [Image courtesy of W.M. Meier].⁵⁶

3.2.3 Charge Imbalance Substitution in Inorganic Host Materials

As indicated by B. Velde⁴⁰ there are four types of substitutions that can create charge imbalance in natural occurring clays: constant ionic site occupation, interlayer substitution, non-stoichiometric substitution and di and trioctahedral substitution.

Constant ionic occupation is created by the substitution of silicon in the tetrahedral sites by aluminum. This substitution is then compensated by another substitution in the octahedral site, thus leaving a electrostatic balance in the clay. Figure 16 illustrates this situation.

Interlayer substitution refers to the charge imbalance originated in either tetrahedral or octahedral site of the clay, this extra charge is compensated by the introduction of an external ion which neutralizes the charge. Figure 16 illustrates this situation.

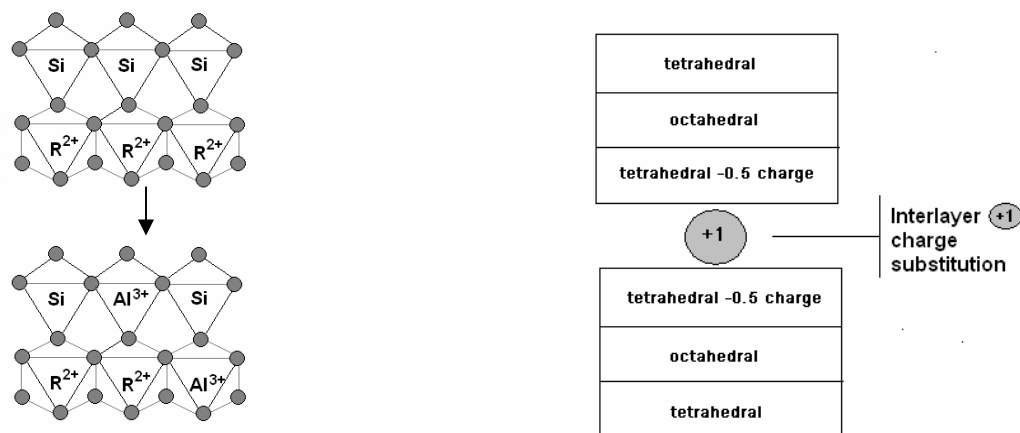


Figure 16 (left) Substitution of ions of different charge. (right) Interlayer cation compensation charge imbalance originated in 2:1 [Image courtesy of B.Velde⁴⁰].

Non-stoichiometric, dioctahedral and trioctahedral substitution is a major subdivision among clay minerals defining the composition and therefore their origin. The main characteristic of this substitution is that its changes exclusively take place in octahedral sites of the structure. Substitution of 3 R^{2+} cations (called trioctahedral) to complete an overall charge of +6, or substitution of 2 R^{3+} cations (called dioctahedral) leaving an octahedral site empty.⁴⁰ Figure 17 illustrates this situation.

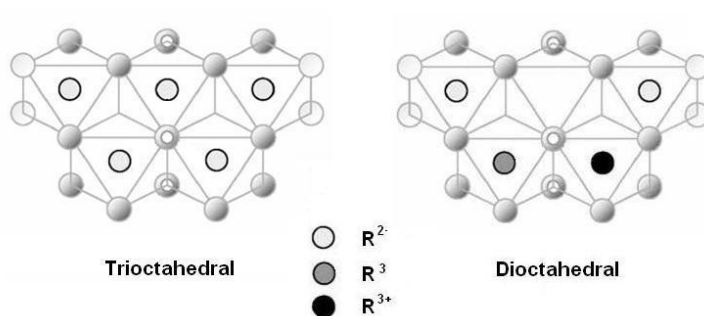


Figure 17 Trioctahedral and dioctahedral substitution exclusively in octahedral sites.

Now that the origin of the negative charge in the framework has been explained, interlayer substitution will be reviewed more closely in this section since this effect is responsible for the cations detected in most of the materials evaluated.

Exchangeable Cations in Inorganic Host Materials

In accordance with B. Velde⁴⁰, cations are fixed in two different sites in clay minerals: surface and interlayers (montmorillonites) or channels - cages (palygorskite - sepiolite and synthetic zeolites), as indicated in Figure 18 where absorbed and adsorbed cations are displayed.

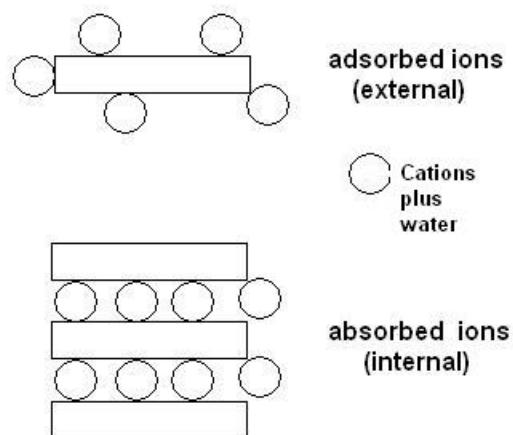


Figure 18 Location of cations in internal layers (absorbed) and surface of layersilicate clay mineral (adsorbed) [Image courtesy of B. Velde⁴⁰].

Polarizing Power of the Cations

Polarizing power is influenced by the charge and the ionic radius of the cation. To quantify this effect a function called ionic potential (ϕ) is widely used and is defined as:

$$\phi = \frac{z^+}{r}$$

Equation 1

where z^+ is the charge of the cation and r its radius. Table 1 displays a variety of cations properties.

Table 1 Main cation properties

Ionic species	r (nm)*	\square (nm ⁻¹)	$\Delta H_{\text{hydration}}$ (KJ/mol)	pka	Ref.
NH ₄ ⁺	0.143	6.99	-	9.25	57,58
H ⁺	~	~	-1075	-	59
Li ⁺	0.0588	17.0	-515	13.6	60,61,58
Na ⁺	0.100	10.5	-405	14.2	59,60,58
K ⁺	0.153	7.00	-321	14.5	59,60,58
Ca ²⁺	0.1000	20.0	-1592	12.8	59,60,58
Mg ²⁺	0.0645	31.0	-1922	11.4	59,60,58
Be ²⁺	0.0313	64.0	-2487	6.2	59,60,58
Al ³⁺	0.0500	60.0	-4613	5.14	60,62,63
B ³⁺	0.0200	150	-	-	59,64
Si ⁴⁺	0.0400	100	-	9.66	60,62,63

* value calculated from \square

In this data it is clear that the charge to ionic radius ratio enhances the ionic potential and therefore the covalent character. An example of this covalent character is the melting points of two oxides such as, Al₂O₃ and MgO, where Al₂O₃ presents lower melting point due to its higher covalent character.⁵⁹

Cations have a large tendency to hydrate accordingly to their ionic radius and charge, as observed by Latimer⁶⁵, with low electronegative elements. Latimer's equation relates these variables as follow;⁵⁹

$$\Delta H_{\text{hyd}} = \frac{-60.900z^2}{(r + 50)} \quad \text{Equation 2}$$

where z is the charge of the cation and r its radius in picometers. According to G. Wulfborg⁵⁹ electronegativity increases the hydration energy of the cation of similar ionic potential, which suggest there is not only an electrostatic attraction between the metal and negative charge of the water molecule but a covalent character in the bond, where

an unshared electron pair of the water molecules is shared with the ion, as illustrated in Figure 19.

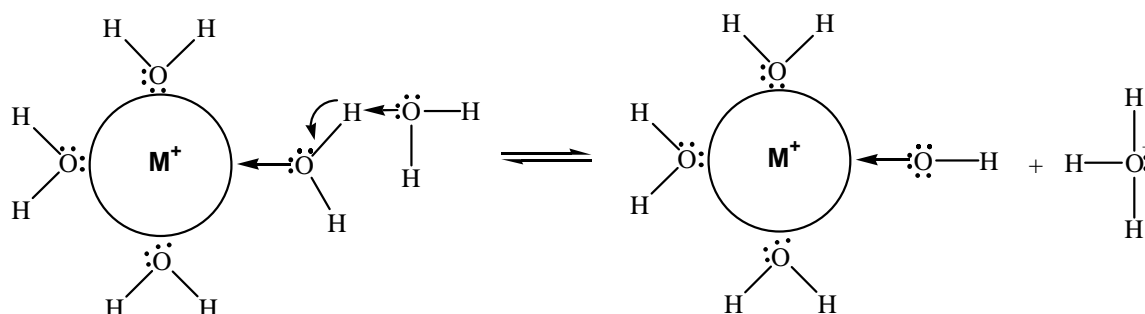


Figure 19 Hydrolysis of a hydrated cation [Image courtesy of G. Wulfsberg⁵⁹].

The process of hydration is well known to be a Lewis acid - base process where metal ions act as Lewis acids and water molecules as Lewis bases. The O-H bond then polarizes and becomes acidic.⁶⁶ This behavior was detected by C. Ravindra Reddy *et al.*²⁵ in cation exchanged montmorillonite clay, where adsorbed pyridine (weak base) reacted with the O-H water surrounding the cations to form pyridinium at room temperature. Moreover, the water interaction with a high ionic potential cation such as aluminum increased the strength of the electron withdrawing observed in the esterification of succinic acid.

3.2.4 Brønsted and Lewis Acids Sites

The acidity of natural and synthetic aluminosilicates is an important reactivity factor for catalytic materials and sorbent applications.⁶⁷ This acidity results from the presence of surface groups such as siloxanes, silanols, aluminols, Al-O, and Mg-O, usually found at the edges of the aluminosilicate framework.⁶⁸

In order to differentiate between both acid sites present in aluminosilicates, both terminologies have been used in the catalysis field. Brønsted acids refer to the hydrogen ion attracted to the negatively charged oxygen, which is attached to aluminum and silicon atoms (Figure 20-top), and Lewis acids refer to the active aluminum site, when H₂O has been removed (Figure 20-bottom).

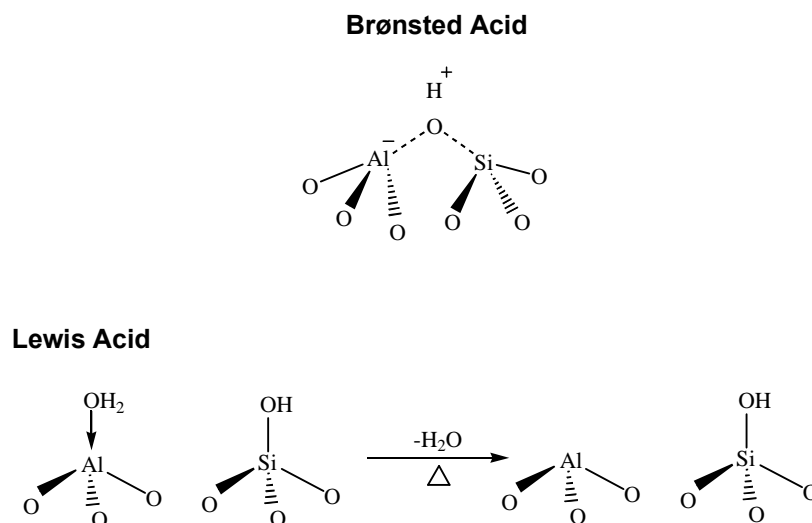


Figure 20 (Top) Brønsted acid site (H⁺) in a tetrahedral site.(bottom) Lewis acid hydrated.

However, this classification is slightly obsolete when evaluating an inorganic material, mostly because it is not including other acidic species also present in the host, such as cations. As mentioned before these cations also have presented a Lewis acid character.⁶⁶

Elemental analysis normally describes the surface Si/Al ratio, which portrays acid sites density; however, this type of analysis can not distinguish between aluminum incorporated in the framework, as cation aluminum, or aluminum oxide, this being an important factor to determine catalytic activity. Therefore, different spectroscopic techniques such as FTIR and MAS-NMR have been used for qualitative and quantitative characterization of active acid sites.⁶⁹

The activity and strength studies for sepiolite and palygorskite by U. Shuali *et al.*⁶⁸ revealed the presence of more Brønsted than Lewis acids at 423K by the decomposition products of cumene. The strength of the active sites was determined by FTIR vibration modes of pyridine, triphenylpyridine and n-butylamine adsorbed in the clays. Weak-medium surface Brønsted acid sites were detected at room temperature until 373K. The interaction was mainly due to the hydrogen bonding between nitrogen (proton acceptor) and hydrogen (proton donor) from zeolitic water and bound water. At higher temperatures (623K) and after the loss of water, Lewis acids sites were detected by the binding of nitrogen to aluminum and magnesium. Similar strength experiments for zeolite NaY by F. Mauge *et al.*⁷⁰ revealed the absence of certain representative vibration modes of Brønsted (1655 and 1620 cm⁻¹) and Lewis (1610 cm⁻¹) active sites.

Pyridine adsorption by L. Pinard *et al.*⁷¹ confirmed this statement by the absence of pyridinium ions in the Brønsted sites (1455 cm^{-1}), and pyridine coordinated at Lewis sites (1545 cm^{-1}).

CHAPTER 4

RESULTS AND DISCUSSION

4.1 Chemical Analysis by Wide Range X-Ray Fluorescence Spectrometry (WD-*XRF*).

The complete elemental chemical analysis for all natural occurring clay minerals and synthetic aluminosilicates is shown in Appendix A.

4.2 Physical Properties

4.2.1 Inorganic Host Materials Treated with Thioindigo

A display of different shades of color were observed when 0.5 mol % thioindigo interacted with different inorganic hosts before thermal treatment (Figure 21).



Figure 21 Pure thioindigo color and samples prepared with 0.5 mol % thioindigo in different host materials before thermal treatment.

A variety of color changes were noticed in samples thermally treated at 413K for nine hours (Figure 22).



Figure 22 Colors observed in pure thioindigo and 0.5 mol % thioindigo in different host materials heated at 413K for nine hours.

High moisture effect was also observed in some of the thermally heated samples, as seen in Figure 23.



Figure 23 High moisture effect in thioindigo and 0.5 mol % thioindigo in different host materials at 413K for nine hours.

Water content in sepiolite and montmorillonite clays was noticed to color change the unheated dye composite with time. Evaporation of loosely bound water from Lewis acid sites (LAS) could be responsible for this behavior; therefore leaving the tightly bound water – LAS to interact with C=O, this effect was displayed as a purple color in the samples.



Figure 24 Example of color change of 0.5 mol %thioindigo in Bentolite L[®] UNHEATED when exposed to three different levels of moisture.

Palygorskite, bentolite L[®], Ca-MMT (Wyoming Deposit) and Valfor CP300-35[®] mixed with 0.5 mol % thioindigo exhibited blue color change when exposed to vacuum for more than 3 hrs. Nevertheless, the blue color observed in these samples was not stable once the vacuum was removed, exhibiting a purple color. This purple color could be related to hydrogen bonding between the C=O and the H₂O surrounding the active sites. Moreover, the color change observed in this experiment seemed to be associated to surface active sites easily approach by moisture. In the case of palygorskite, temperature seemed to play an important role as a driving force to locate thioindigo in active sites less susceptible to moisture. Conversely, the amount and the type of cations present in the inorganic materials, and a more open type of structure, were two factors in the fast hydration of the mixture.

4.3 Diffusive Reflectance Ultraviolet- Visible Spectroscopy

4.3.1 Thioindigo

The decomposition of the diffuse reflectance UV-Vis spectra was better evaluated using multiple Voigt bands by peak fit v4.11 software. These bands revealed that thioindigo absorption band best fitted with two main π - π^* transitions bands at 504 nm ($A = 0.7$) and 578 nm ($A = 0.6$) in the visible region (see Figure B.1). However, these values seemed to vary in the references reviewed.⁷² On the other hand, it is known that diffuse reflectance UV-Vis spectrophotometers have poor reproducibility depending on (a) limitations in method and apparatus, (b) variations in the surface treatment and (c) differences in extrapolations used in the Kramers-Kronig dispersion relation.⁷³ In conclusion, these values reported were specific for thioindigo from TCI America and the spectrophotometer used for this specific analysis (see Chapter 2, Section 2.3.1).

4.3.2 Inorganic Host Materials Treated with Thioindigo

Palygorskite - Thioindigo Interaction

Thioindigo reacts with palygorskite to exhibit a non-reversible broad range of colors, from red-pink to purple-blue. Palygorskite a natural occurring clay with a Si/Al ratio = 5.68 was mixed with 0.5 mol % thioindigo and heated at 413K for nine hours. This mixture displayed a bathochromic shift to a bright purple-blue color identified by peak fit v4.11 software as four main absorption bands 468 nm ($A = 0.09$), 570 nm ($A = 0.46$), 568 nm ($A = 0.72$) and 629 nm ($A = 0.48$) in the visible region (see Figure B.3). The thermally treated palygorskite mixture, was the most stable of all mixtures tested, when exposed to a slight hydration displayed a small reduction in absorbance values 468 nm ($A = 0.08$), 565 nm ($A = 0.41$), 568 nm ($A = 0.67$) and 628 nm ($A = 0.48$) was observed (see Figure B.4); conversely, palygorskite mixture upon prolonged evacuation, displayed a bright blue color; however, once the sample was removed from evacuation, a purple color was observed. UV-Vis spectra of the dull purple color revealed no change in wavelength with a reduction in absorbance values 466 nm ($A = 0.065$), 569 nm ($A = 0.32$), 568 nm ($A = 0.66$) and 625 nm ($A = 0.34$) (see Figure B.5).

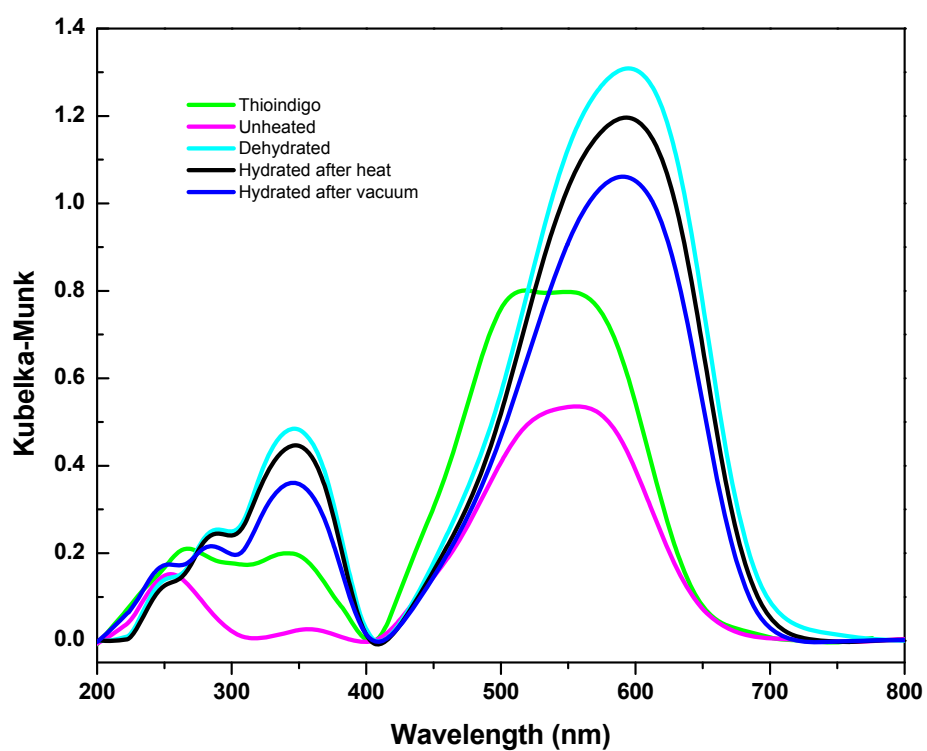
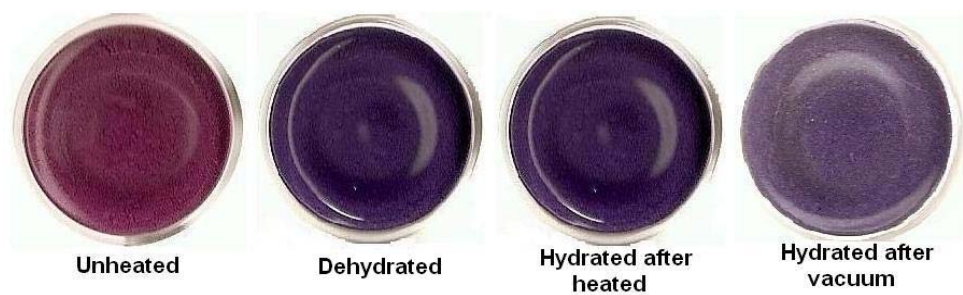


Figure 25 (Top) Color variation of palygorskite / 0.5 mol % thioindigo unheated and heated at 413K for nine hours, hydrated after heat treatment and hydrated after exposure to vacuum. (Bottom) Diffuse Reflectance UV-Vis spectra of the above mentioned samples and thioindigo starting material.

A pretreated palygorskite at 833K mixed with 0.5 mol % thioindigo and heated at 413K for nine hours displayed a red color with two main absorbance bands at 512 nm ($A = 0.36$) and 571 nm ($A = 0.69$) (see Figure B.85). This red color was not stable after washing with ethanol soxhlet extraction. On the other hand, palygorskite blue color was demonstrated to be stable in ethanol soxhlet extraction.⁷⁴

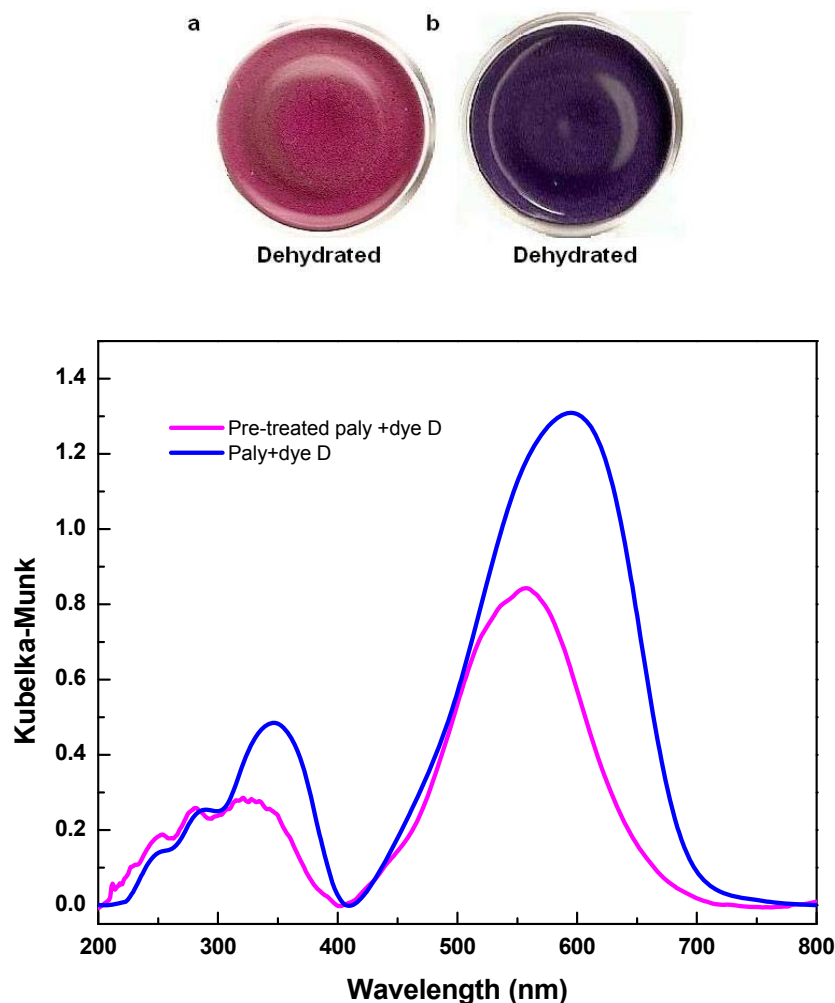


Figure 26 Comparison of (a) pretreated palygorskite (833K for 16h) / 0.5 mol % thioindigo heated at 413K for nine hours, and (b) palygorskite / 0.5 mol % thioindigo heated at 413K for nine hours.

Sepiolite-Thioindigo Interaction

Sepiolite, a natural occurring clay with a Si/Al ratio = 15 mixed with 0.5 mol % thioindigo exhibited a magenta color shade with two main absorption bands at 526 nm ($A = 0.80$) and 584 nm ($A = 0.75$) when thermally treated (see Figure B.7). The slight hydration of sepiolite displayed a reduction in the absorbance of the two bands at 526 nm ($A = 0.65$) and 570 nm ($A = 0.54$) and the appearance of a new band at 610 nm ($A = 0.52$) (see Figure B.8). This new band was responsible for the color change magenta to purple exhibited in sepiolite. This bright purple color was also observed in the unheated mixture after some time exposed to air. Further hydration of either sample reduced absorbance to lower values similar to the unheated sample. The behavior of these samples after time was very puzzling. In the case of the heated sample color change from magenta to purple could be explained as the LAS hydration, forming a thin hydration sphere around them. For the unheated sample color change (light pink to purple), a possible reason could be the dehydration of the excess water in the LAS due to the dry climate of El Paso, thus leaving only a thin water layer between thioindigo and the LAS displayed as a purple color.

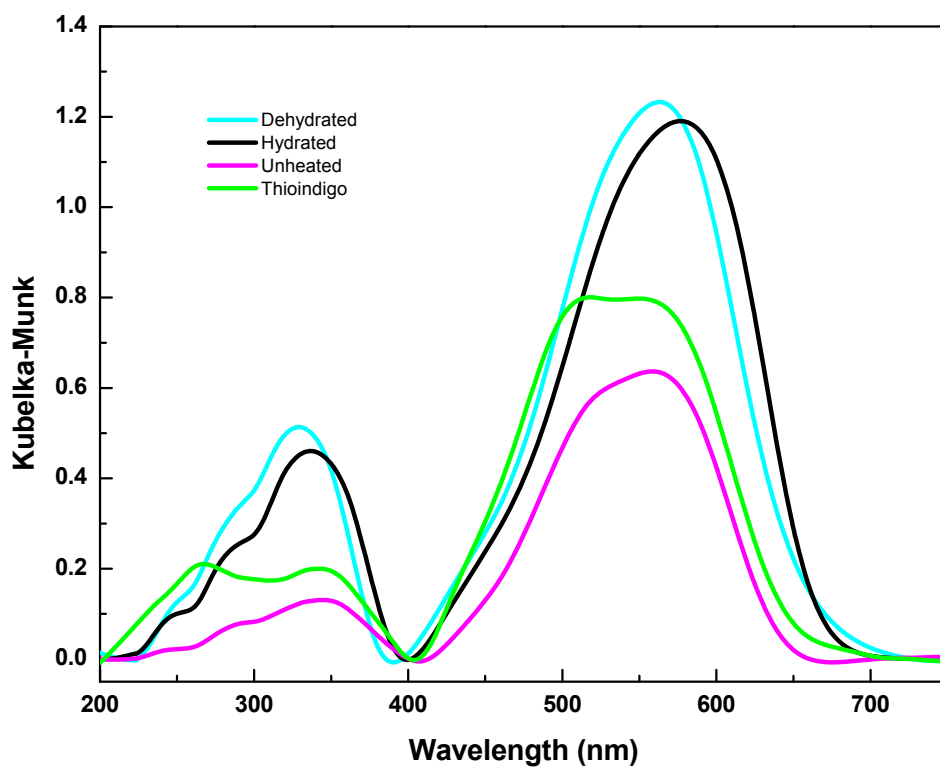


Figure 27 (Top) Color variation of sepiolite / 0.5 mol % thioindigo unheated and heated at 413K for nine hours, hydrated after heat treatment and hydrated after exposure to vacuum. (Bottom) UV-Vis spectra of the above mentioned samples and thioindigo starting material.

Montmorillonite clays –Thioindigo Interaction

Ca²⁺-MMT (Bentolite L[®] and Texas deposit) and Na⁺-MMT (Wyoming and Kunipia deposit) displayed reversible color changes when exposed to different levels of moisture.

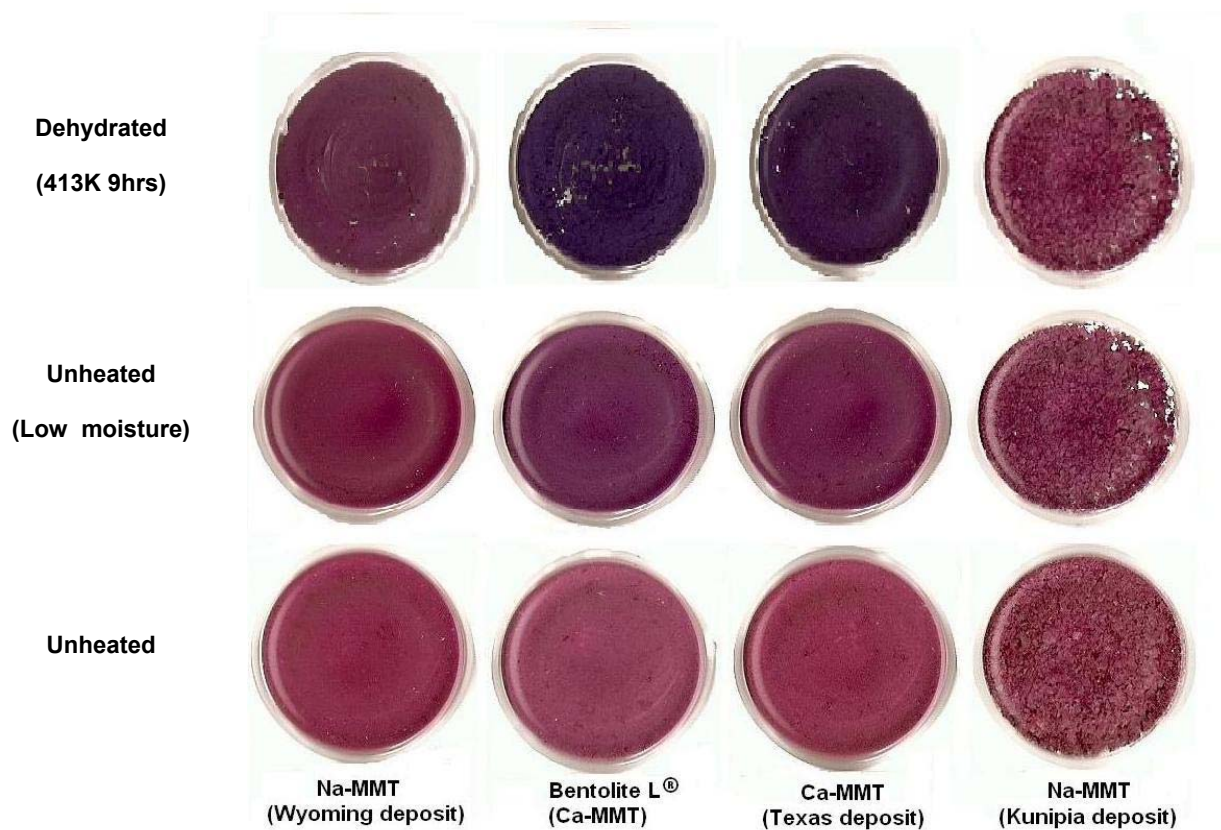


Figure 28 Effect of moisture in montmorillonite clays.

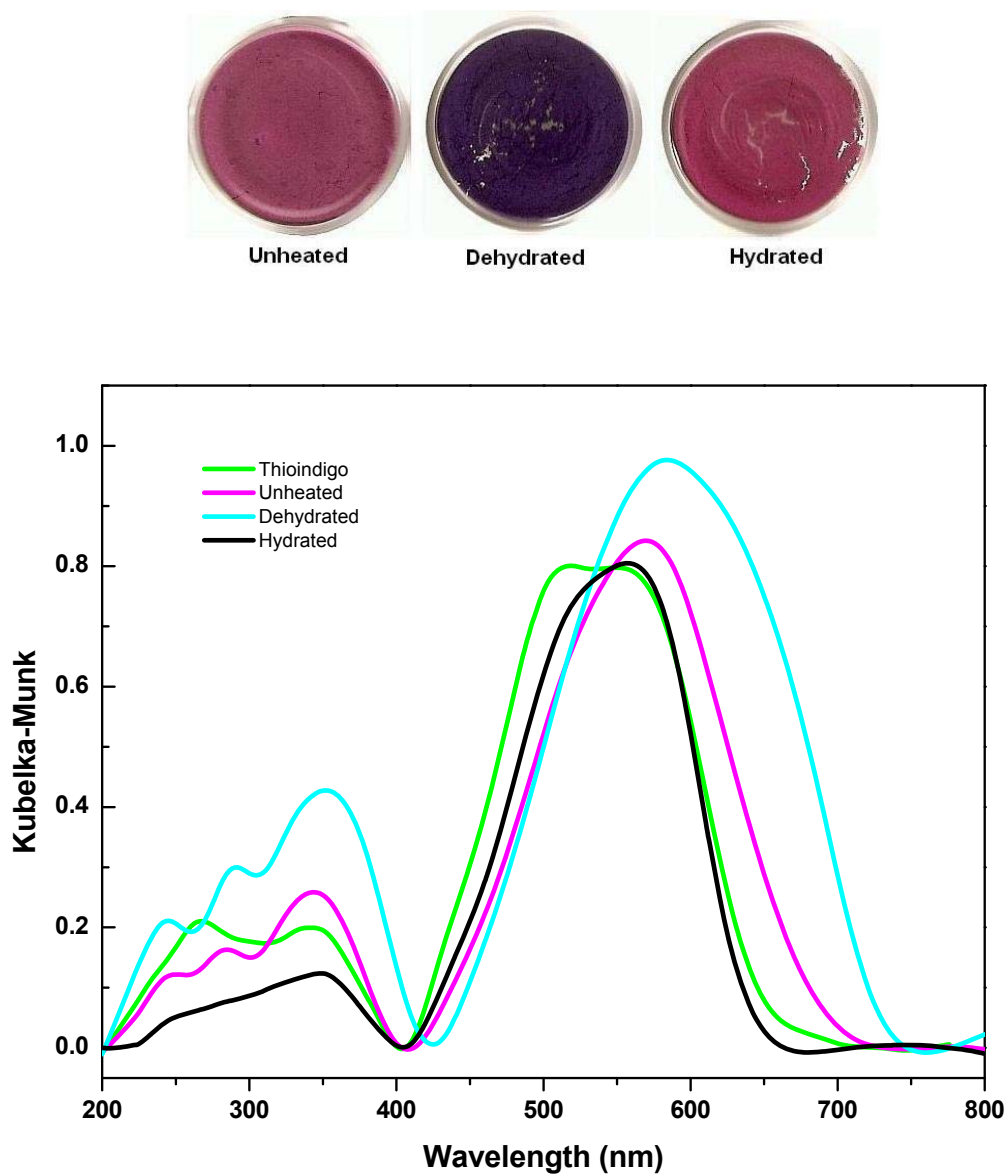


Figure 29 (Top) Color variations of (Ca²⁺-MMT) bentonite L[®] / 0.5 mol % thioindigo unheated, dehydrated at 413K for nine hours and hydrated after heat treatment (Bottom) UV-Vis spectra of the above mentioned samples and thioindigo starting material.

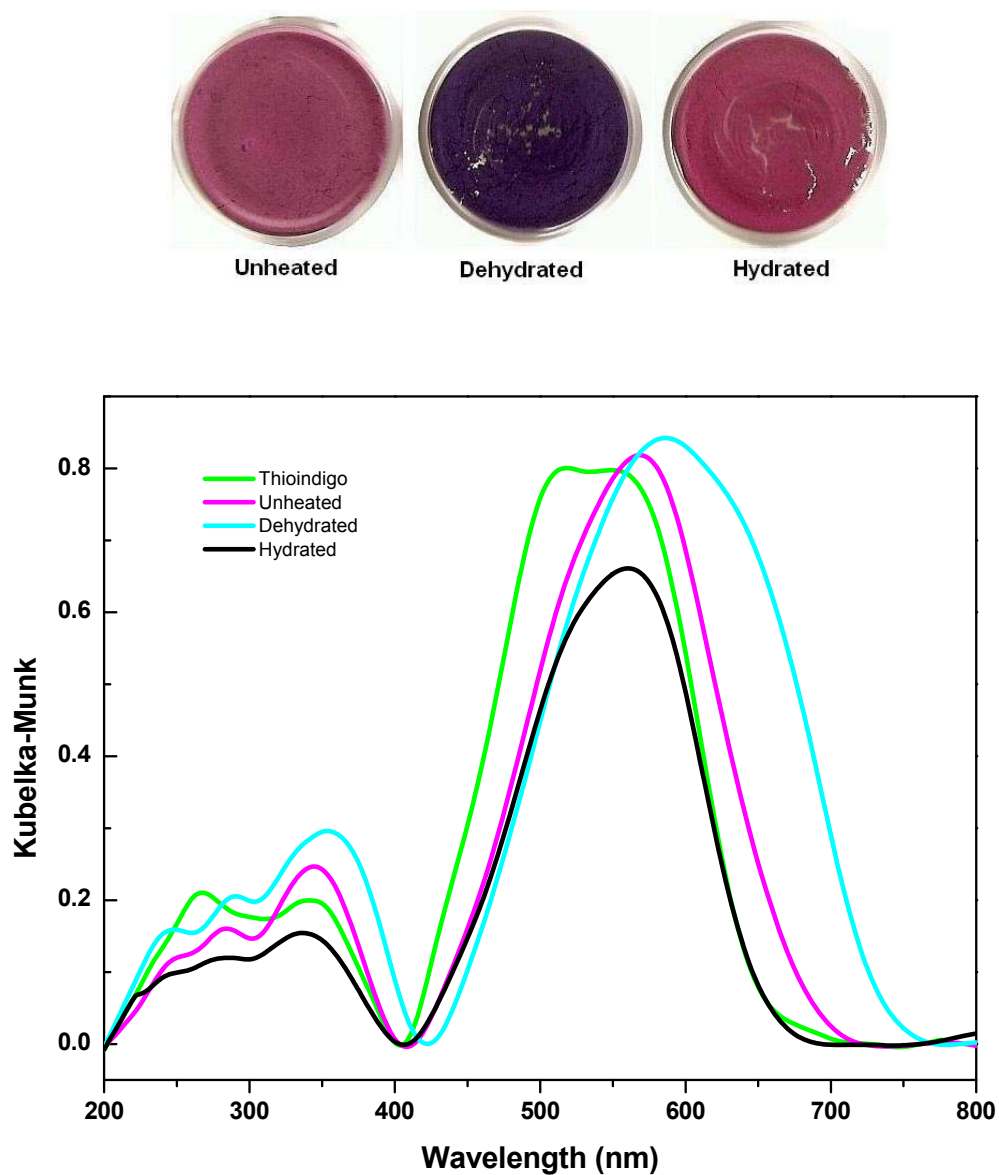


Figure 30 (Top) Color variations of Ca^{2+} -MMT (Texas deposit) / 0.5 mol % thioindigo unheated, dehydrated at 413K for nine hours and hydrated after heat treatment (Bottom) UV-Vis spectra of the above mentioned samples and thioindigo starting material.

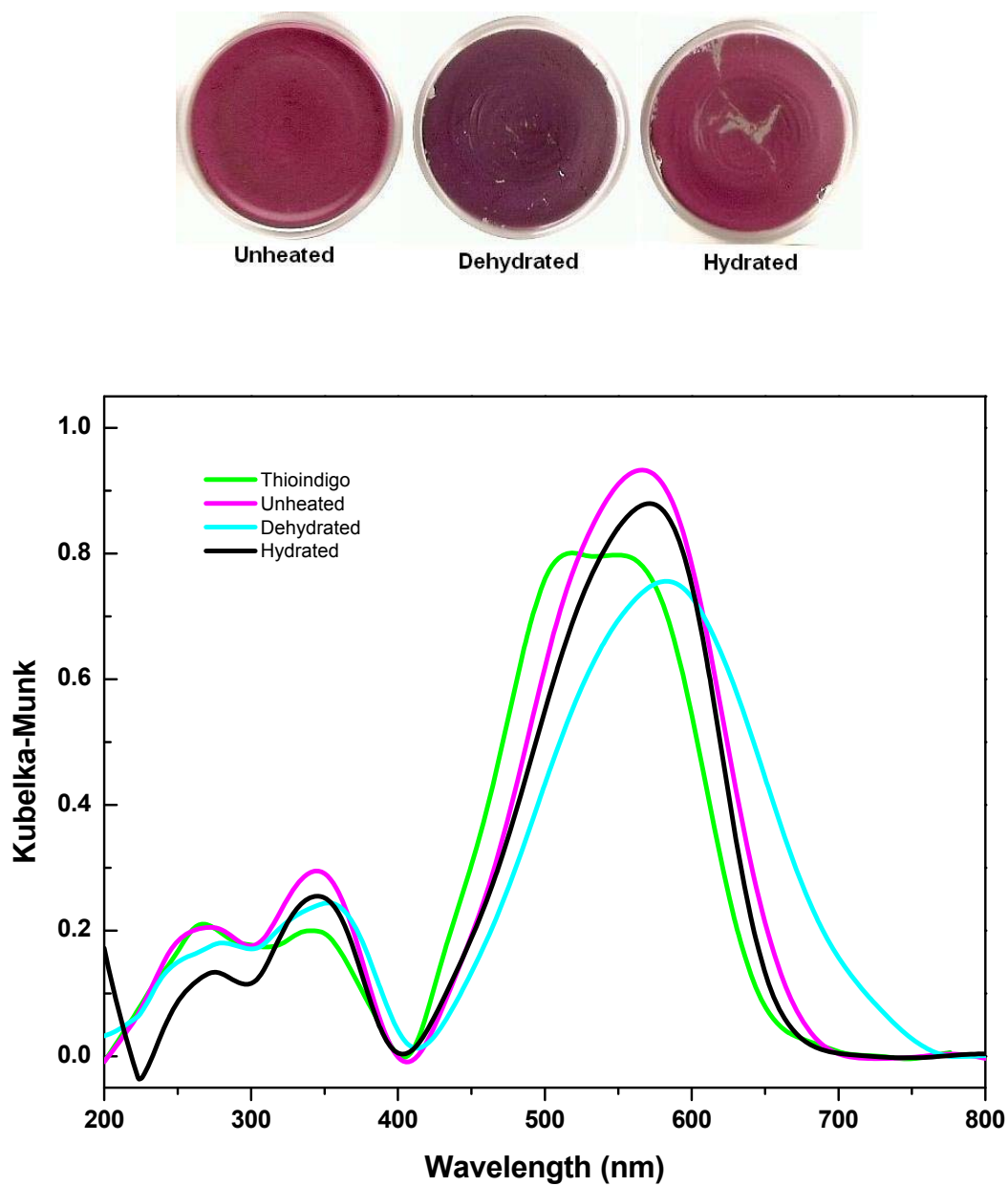


Figure 31 (Top) Color variations of Na^+ -MMT (Wyoming deposit) / 0.5 mol % thioindigo unheated, dehydrated at 413K for nine hours and hydrated after heat treatment (Bottom) UV-Vis spectra of the above mentioned samples and thioindigo starting material.

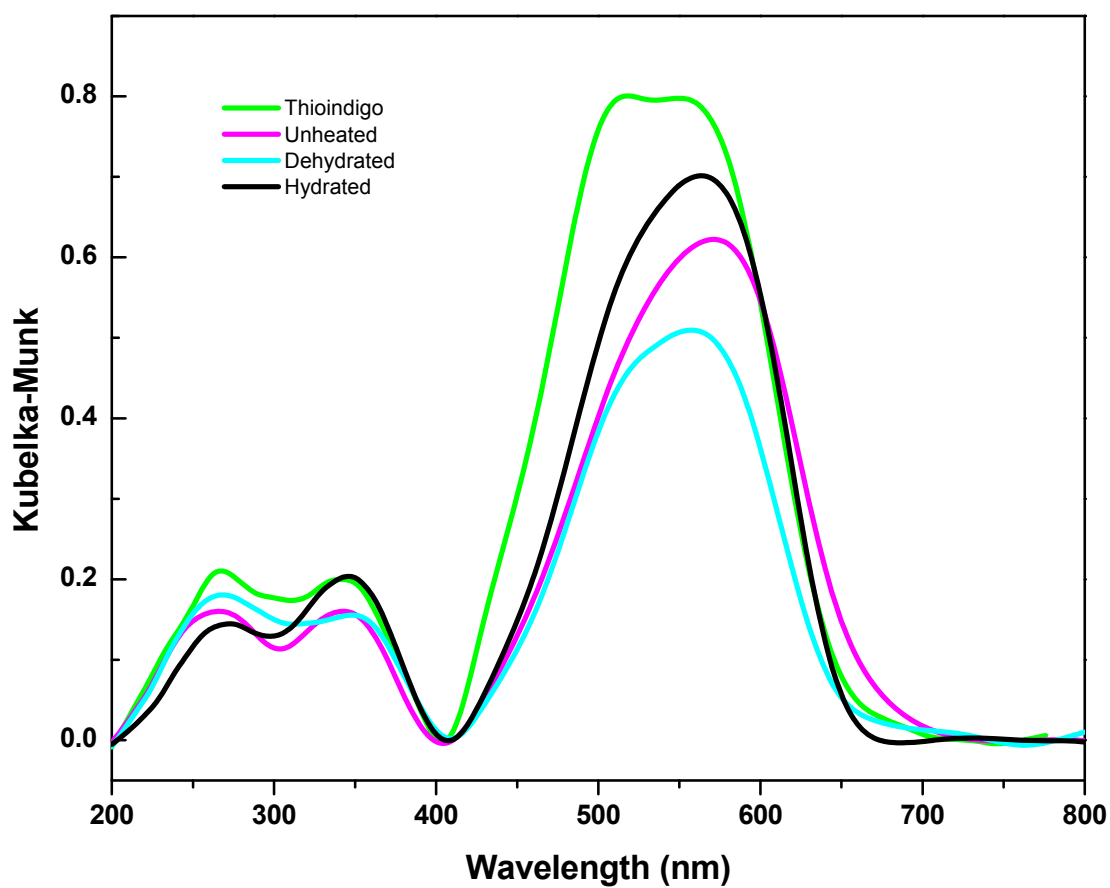


Figure 32 (Top) Color variations of Na^+ -MMT (Kunipia deposit) / 0.5 mol % thioindigo unheated, dehydrated at 413K for nine hours and hydrated after heat treatment (Bottom) UV-Vis spectra of the above mentioned samples and thioindigo starting material.

Neutral layer clays (Talc) – Thioindigo Interaction

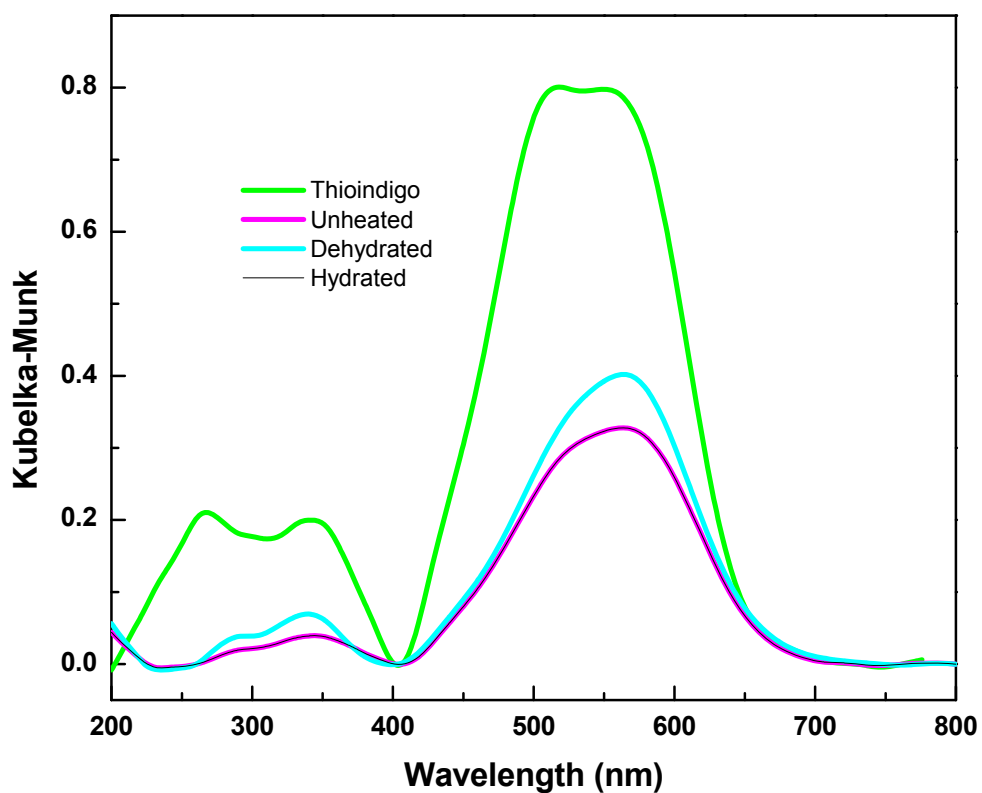


Figure 33 (Top) Color variations of Talc / 0.5 mol % thioindigo unheated, dehydrated at 413K for nine hours and hydrated after heat treatment (Bottom) UV-Vis spectra of the above mentioned samples and thioindigo starting material.

Synthetic Swelling Micac (YN6, YN8 and Na-Ts)- Thioindigo Interaction

No major color change was observed with YN6 Si/Al = 63 and YN8 Si/Al = 15, however, the presence of the 579 nm band was more predominant than the 505 nm band (see Figure B.22).

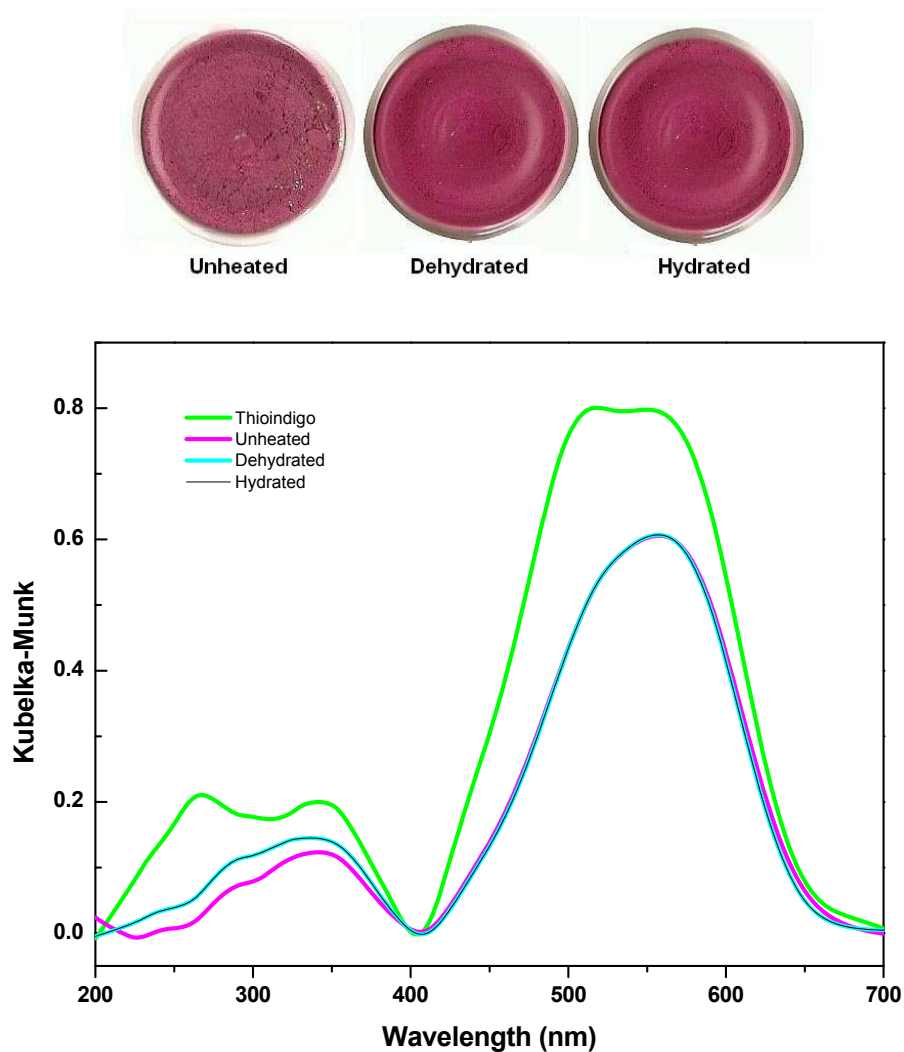


Figure 34 (Top) Color variations of YN6 / 0.5 mol % thioindigo unheated, dehydrated at 413K for nine hours and hydrated after heat treatment (Bottom) UV-Vis spectra of the above mentioned samples and thioindigo starting material.

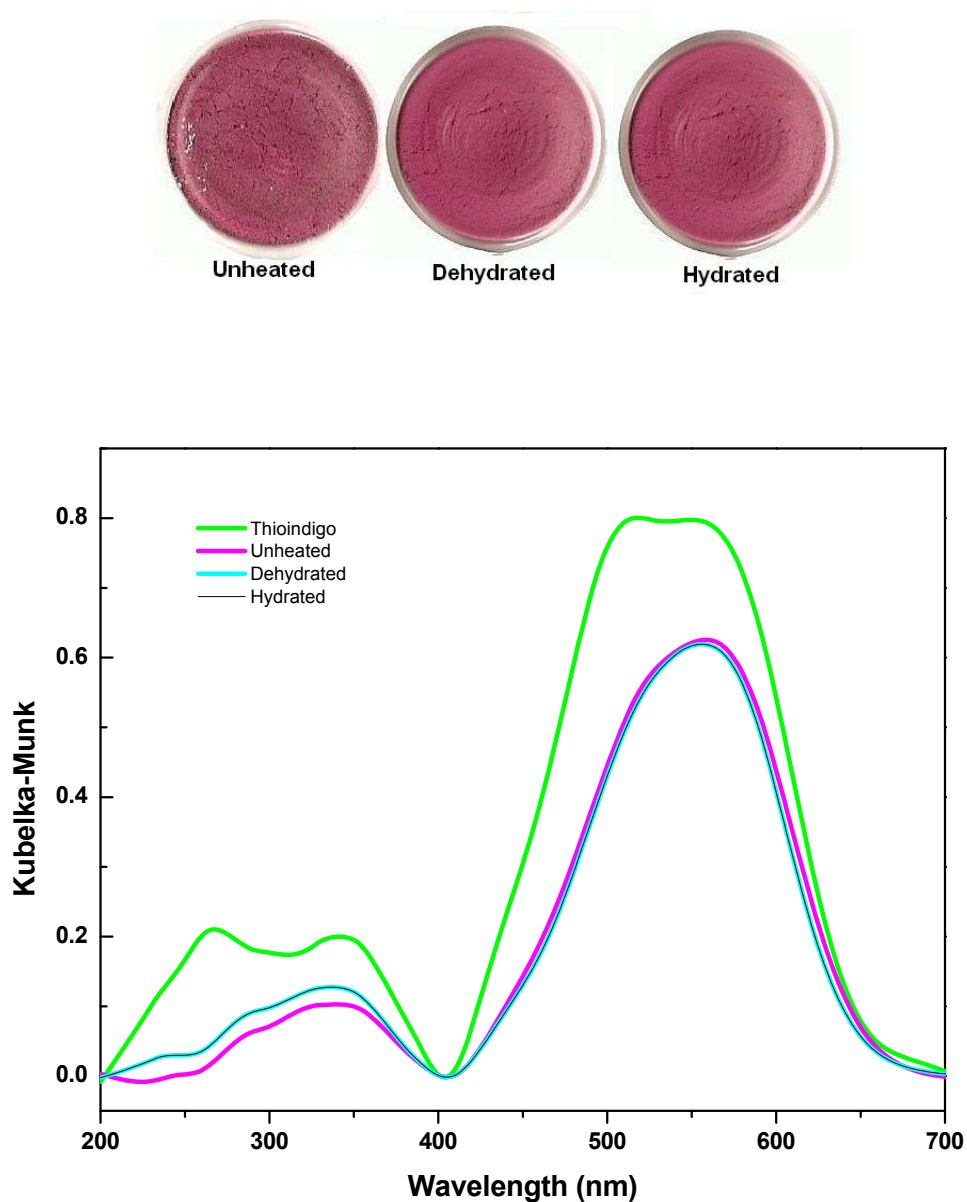


Figure 35 (Top) Color variations of YN8 / 0.5 mol % thioindigo unheated, dehydrated at 413K for nine hours and hydrated after heat treatment (Bottom) UV-Vis spectra of the above mentioned samples and thioindigo starting material.

In the case of Na-Ts Si/Al = 608 a similar effect is observed, however the color was observed to be more red than for YN6 and YN8.

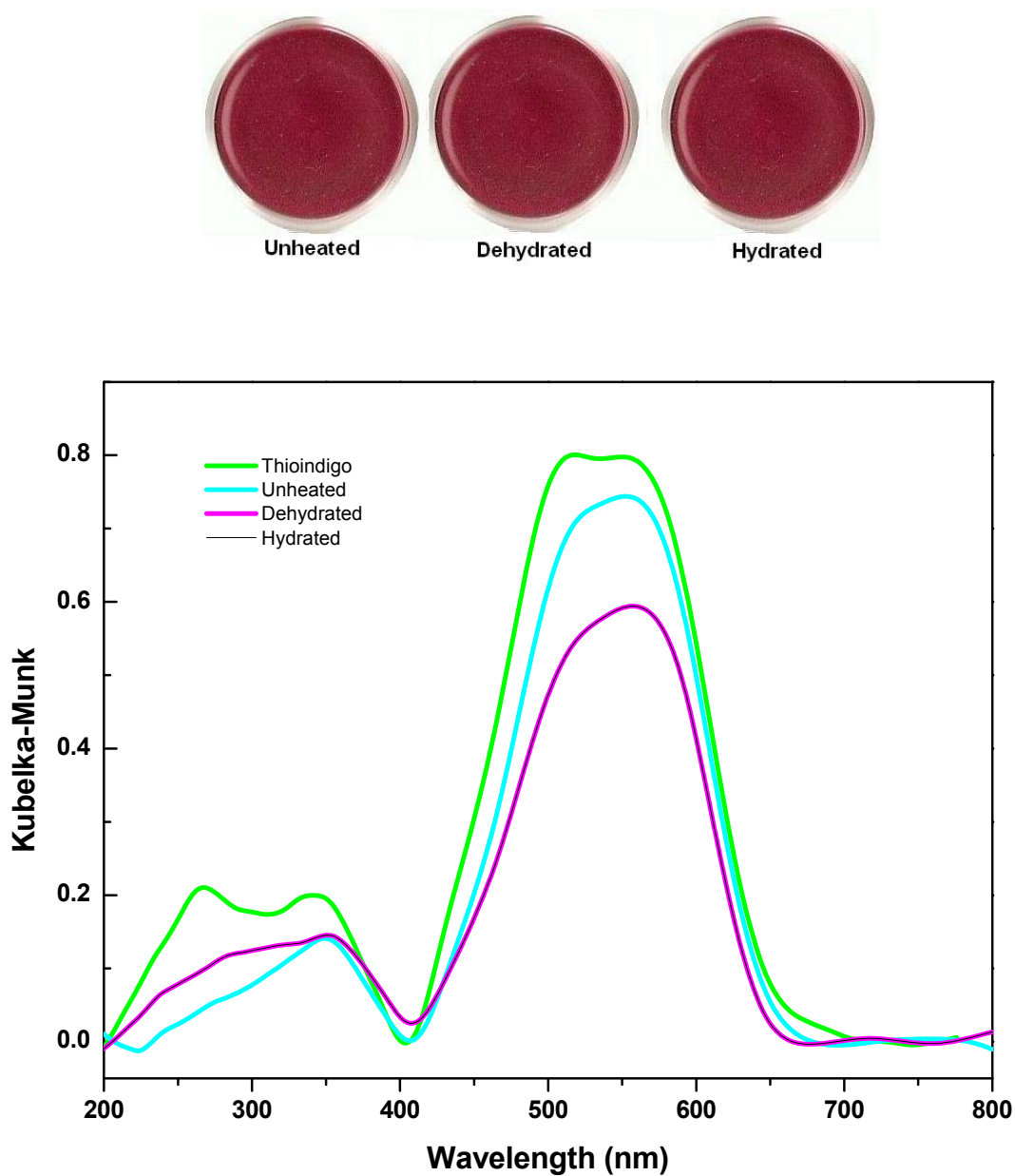


Figure 36 (Top) Color variations of Na-Ts / 0.5 mol % thioindigo unheated, dehydrated at 413K for nine hours and hydrated after heat treatment (Bottom) UV-Vis spectra of the above mentioned samples and thioindigo starting material.

Synthetic Zeolites, Faujasite (FAU)

Faujasite (FAU) synthetic zeolites with a range of Si/Al ratio from 2 to 4, when mixed with 0.5 mol % thioindigo, also revealed reversible color changes related to water absorption. Additionally, cation substitution was detected to have an effect in the color shades obtained after thermal treatment (Figure 37).



Figure 37 Reversible color changes in presence of water of 0.5 mol % thioindigo in Na⁺-FAU (NaY), Na⁺,Ca²⁺-FAU (13X), NH₄⁺-FAU (LZY-62) and H⁺-FAU heated at 413K for nine hours.

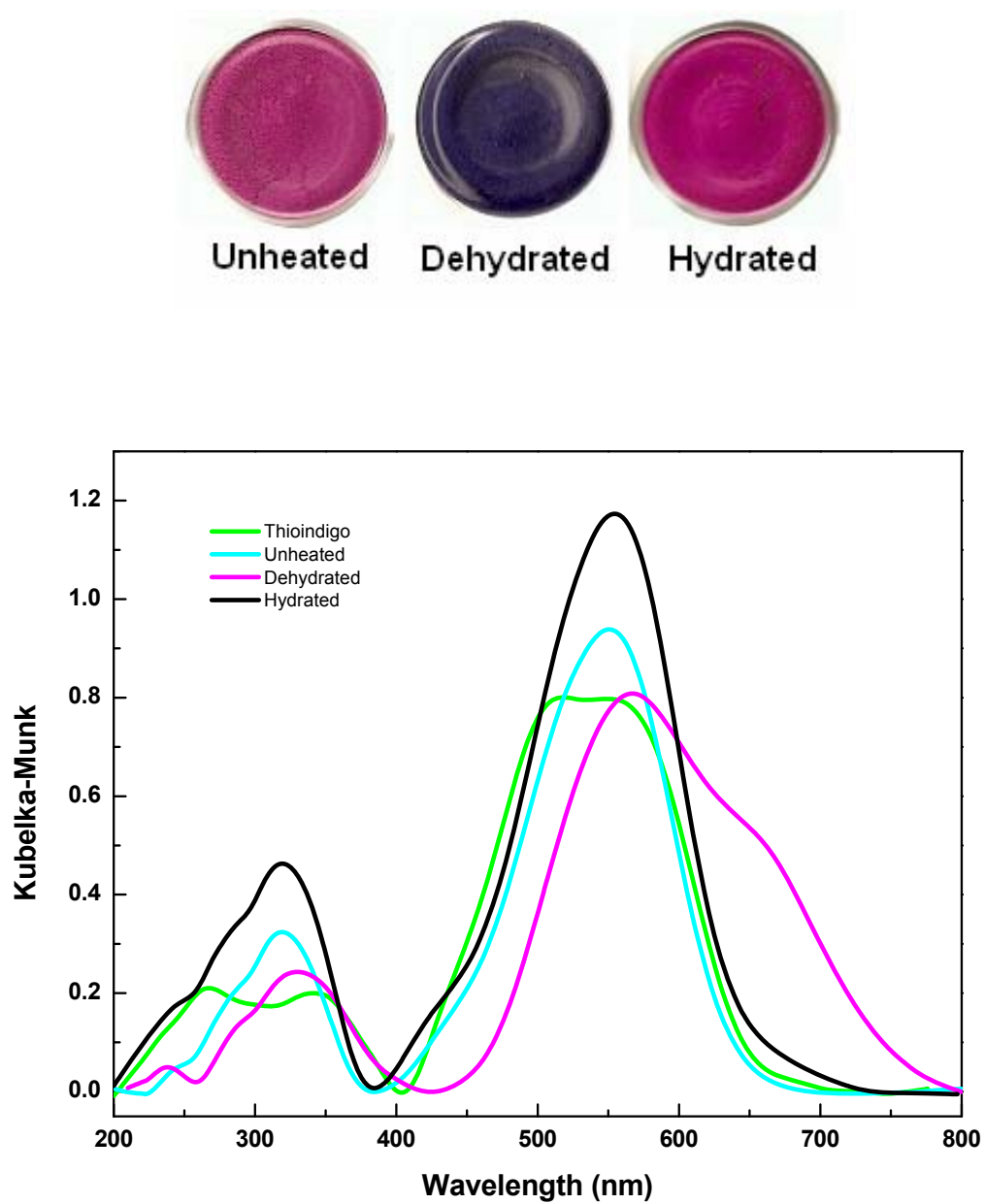


Figure 38 (Top) Color variations of Valfor CP300-35[®] (H⁺-FAU) / 0.5 mol % thioindigo unheated, dehydrated at 413K for nine hours and hydrated after heat treatment (Bottom) UV-Vis spectra of the above mentioned samples and thioindigo starting material.

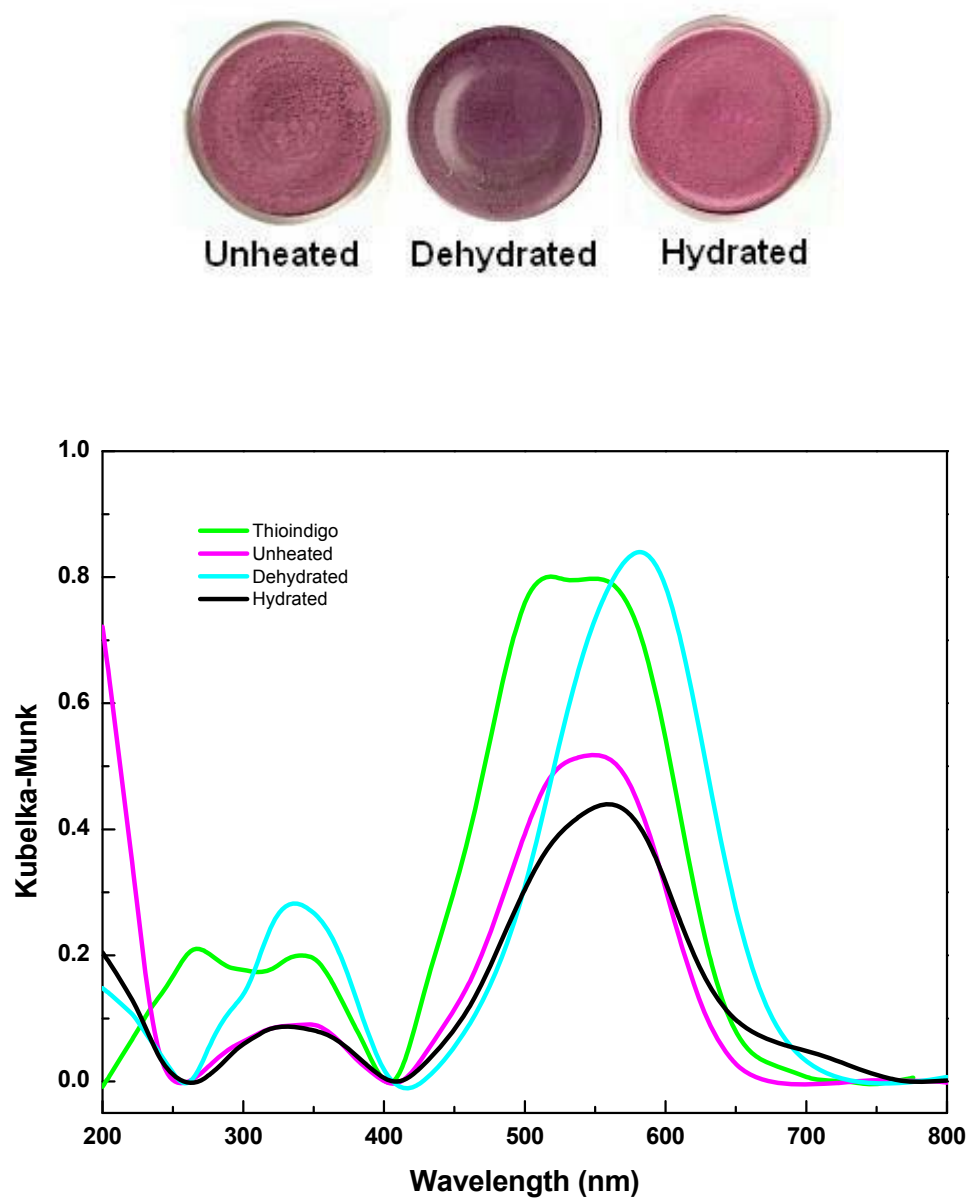


Figure 39 (Top) Color variations of LZY-62 (NH₄⁺-FAU) / 0.5 mol % thioindigo unheated, dehydrated at 413K for nine hours and hydrated after heat treatment (Bottom) UV-Vis spectra of the above mentioned samples and thioindigo starting material.

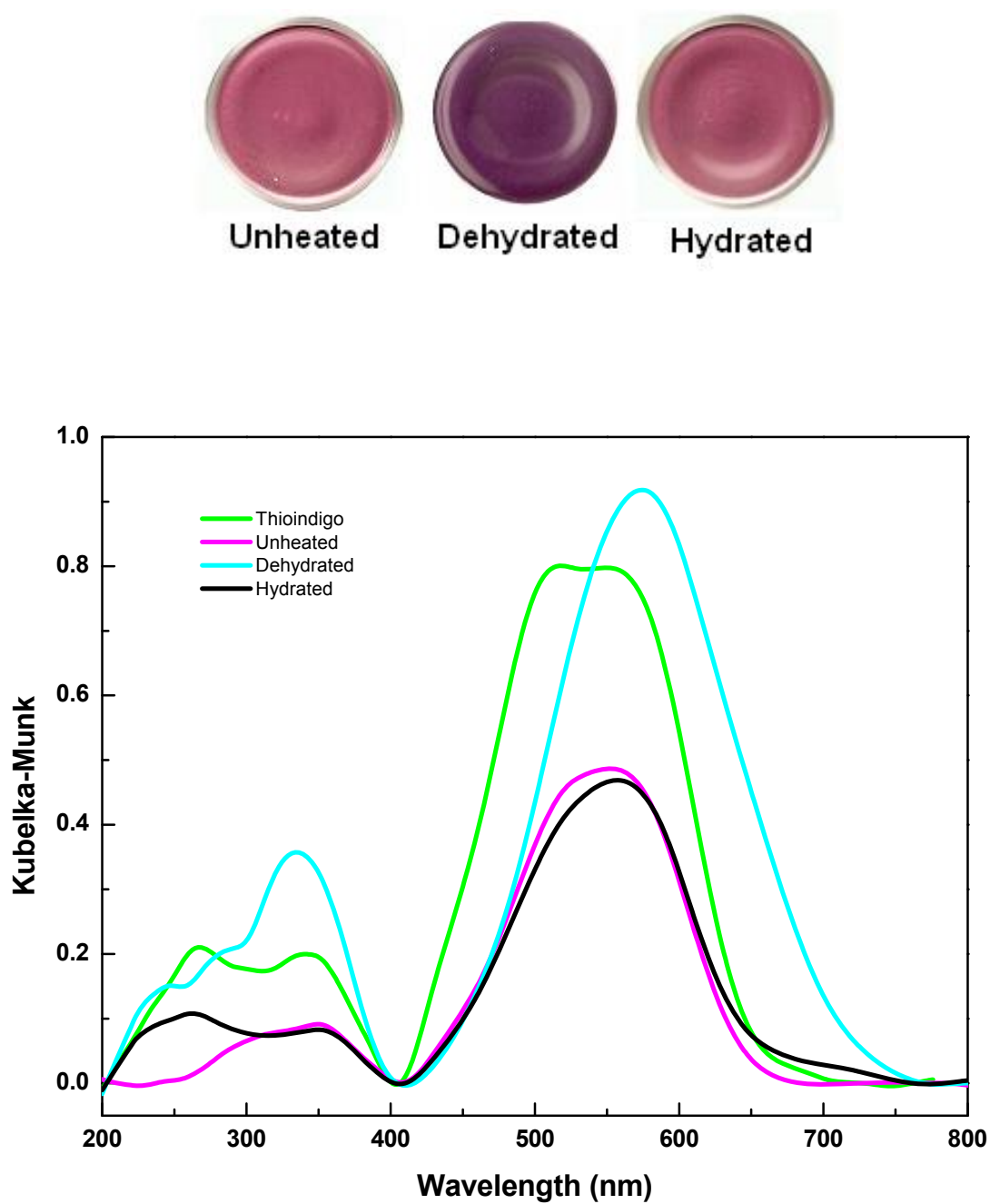


Figure 40 (Top) Color variations of 13X (Na^+ , Ca^{2+} -FAU) / 0.5 mol % thioindigo unheated, dehydrated at 413K for nine hours and hydrated after heat treatment (Bottom) UV-Vis spectra of the above mentioned samples and thioindigo starting material.

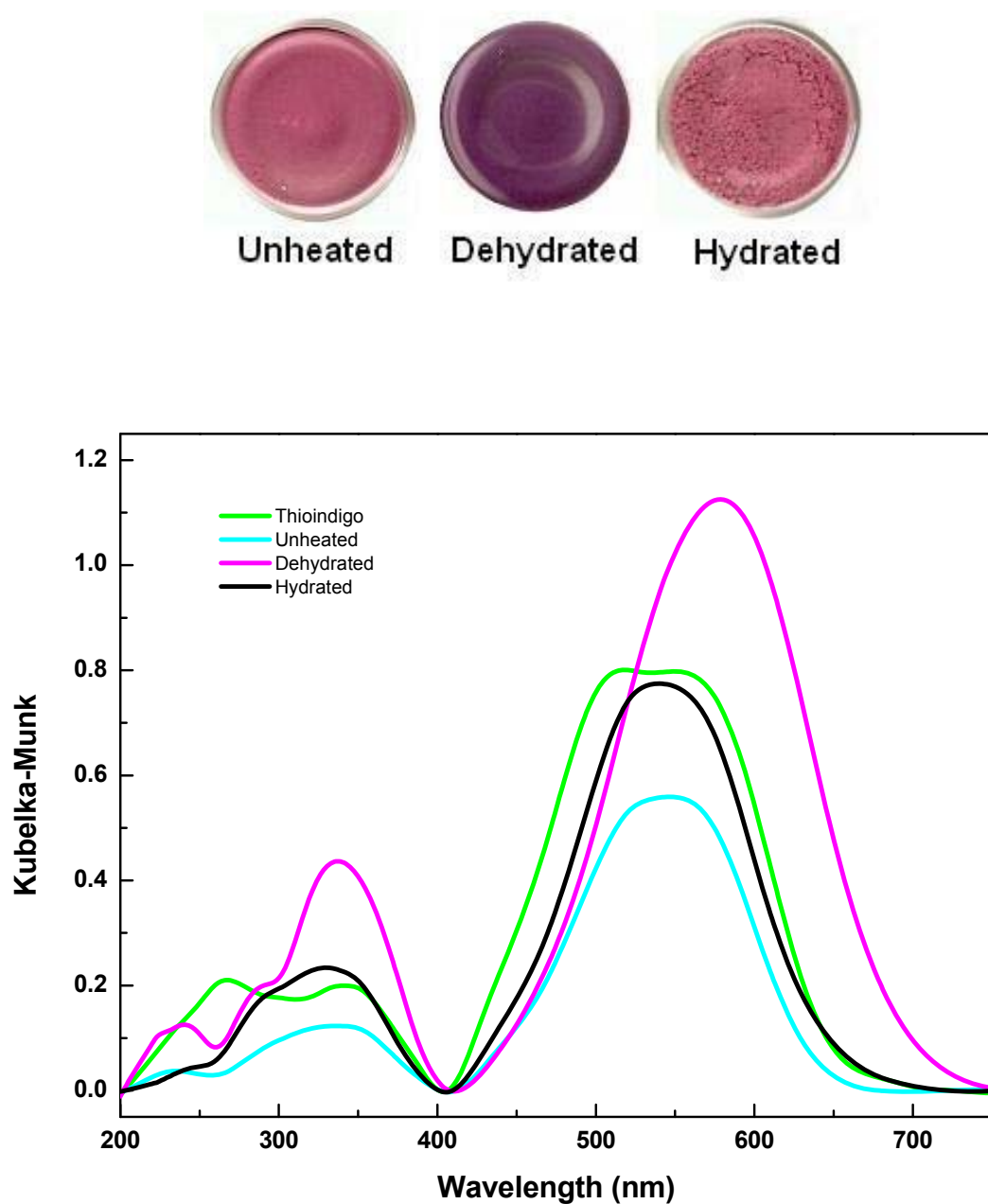


Figure 41 (Top) Color variations of NaY (Na^+ -FAU) / 0.5 mol % thioindigo unheated, dehydrated at 413K for nine hours and hydrated after heat treatment (Bottom) UV-Vis spectra of the above mentioned samples and thioindigo starting material.

Synthetic Zeolites, Linde Type A (LTA)

4A and 5A Linde Type A zeolites (LTA) with a Si/Al ratio = 1.00, exhibited a bright pink color when mixed with thioindigo and no further color changes were perceived with temperature. This behavior could be explained by the small dimensions of the pore cages (4.2 Å) in comparison with thioindigo molecule proportions (15.17 Å (length), 7.42 Å (width) and 3.4 Å (thickness)³², thus not allowing the entrance of the dye inside the cages and therefore no major interaction took place. In addition the predominance of the 577 nm band was also observed (see Figure B.30 and B.32).

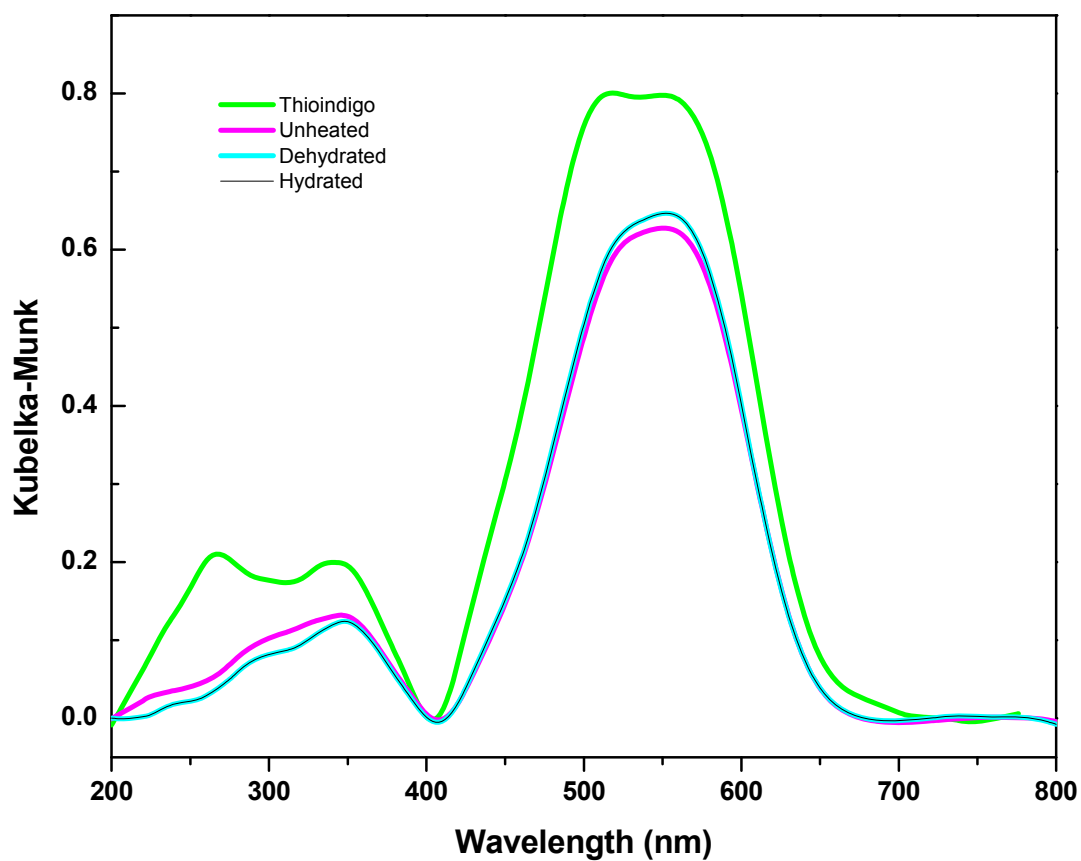
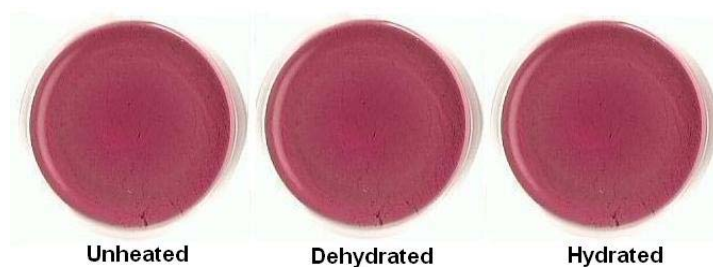


Figure 42 (Top) Color variations of 4A (Na^+ -FAU) / 0.5 mol % thioindigo unheated, dehydrated at 413K for nine hours and hydrated after heat treatment (Bottom) UV-Vis spectra of the above mentioned samples and thioindigo starting material.

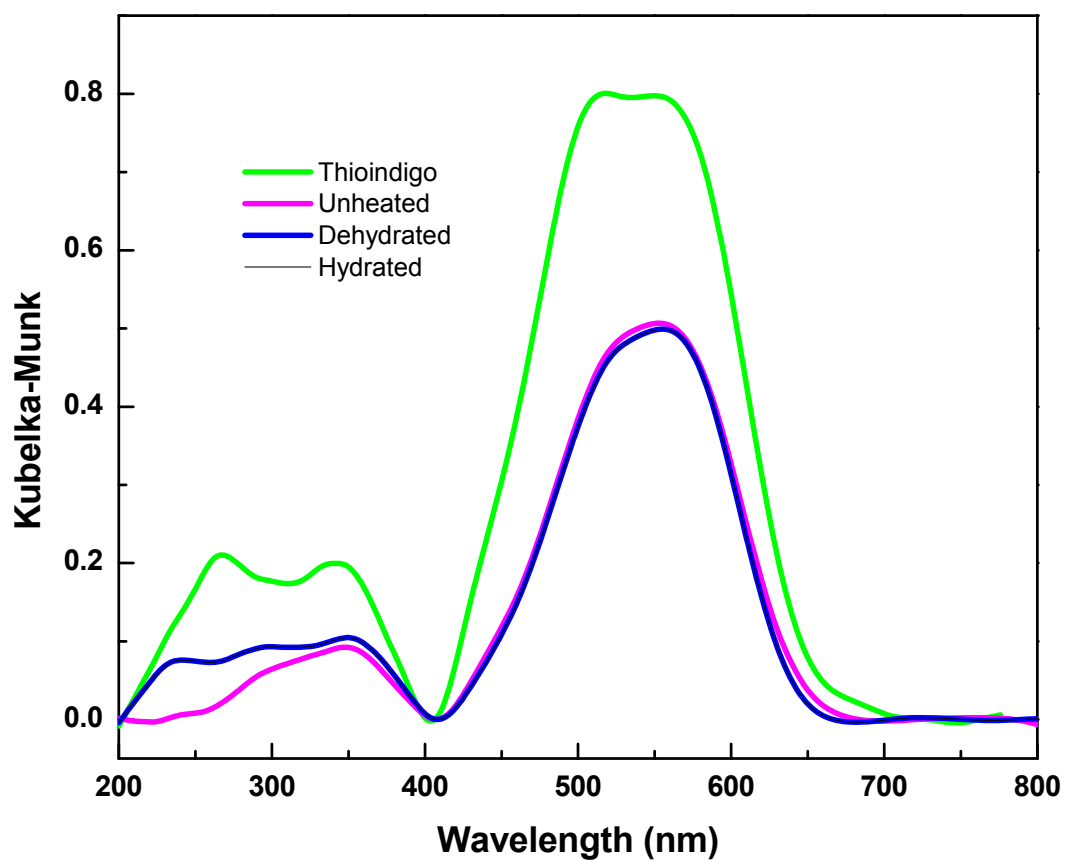


Figure 43 (Top) Color variations of 5A (Na^+ -FAU) / 0.5 mol % thioindigo unheated, dehydrated at 413K for nine hours and hydrated after heat treatment (Bottom) UV-Vis spectra of the above mentioned samples and thioindigo starting material.

Synthetic Zeolite, Mordenite (MOR)

Zeolon[®] a mordenite type zeolite with a Si/Al ratio = 2.5, was noticed to have more stability towards moisture than other zeolites tested; the main reason could be its cylindrical pore shape similar to palygorskite shape. Due to the low amount of zeolon[®] available and the item was not longer available; two other mordenites were tested for further analysis. Nevertheless, zeolon[®] exhibited two broad bands at 573 nm ($A = 0.51$) and 676 nm ($A = 0.33$) (see Figure B.43). The intensity of these bands was lower than expected; however, this could be due to an aged sample instead of a freshly prepared sample.

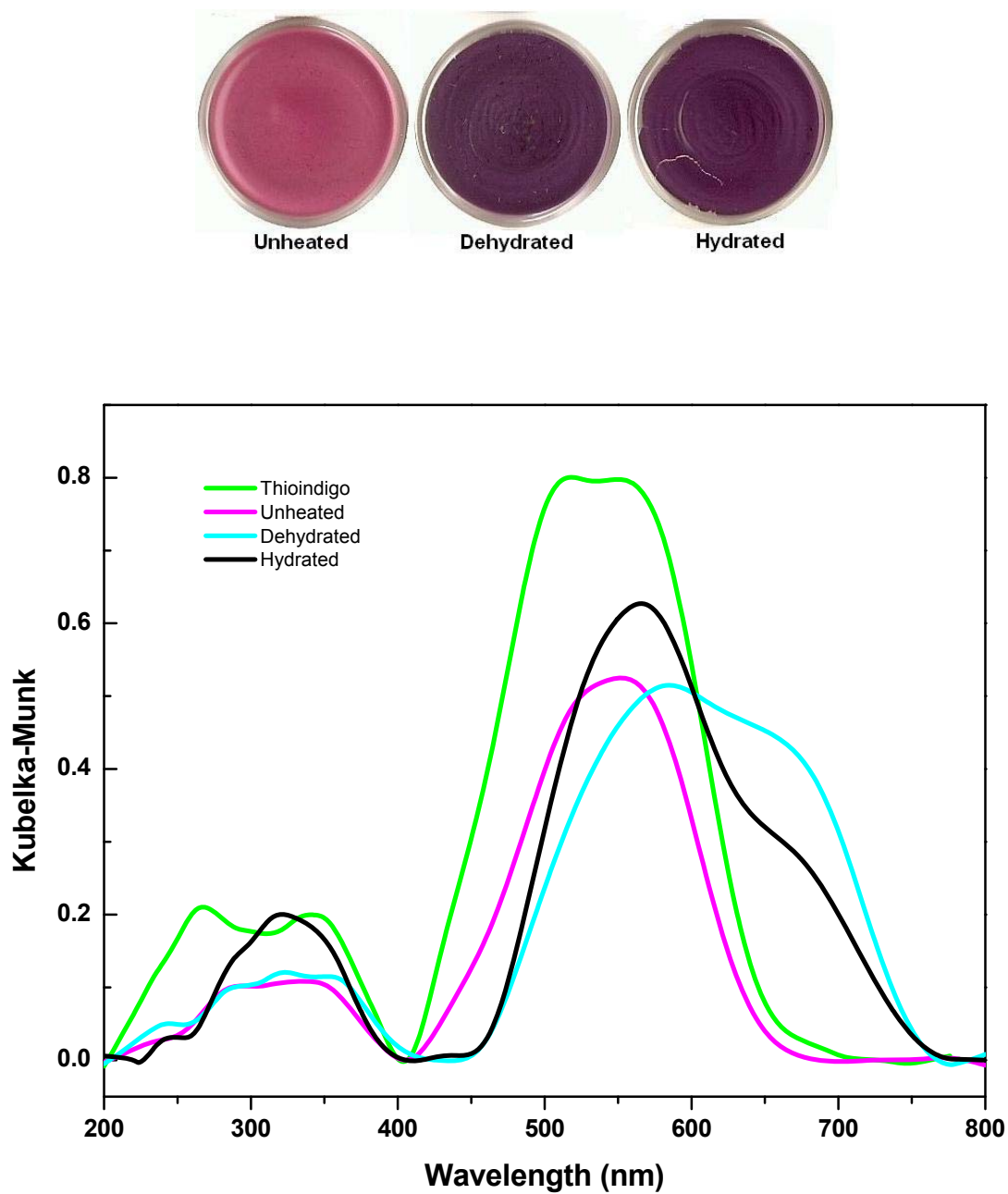


Figure 44 (Top) Color variations of Zeolon® ($\text{Na}^+\text{-MOR}$) / 0.5 mol % thioindigo unheated, dehydrated at 413K for nine hours and hydrated after heat treatment (Bottom) UV-Vis spectra of the above mentioned samples and thioindigo starting material.

CBV21A (NH_4^+ -MOR) Si/Al ratio = 9.5 and CBV10A (Na^+ -MOR) Si/Al ratio = 4.0 mixed with 0.5 % mol thioindigo displayed different colors, however when similar cations were present in the framework analogous colors were observed. Si/Al ratio difference between these two mordenites did not play a significant role in the colors observed, however when compared to zeolon[®] (Na^+ -MOR) Si/Al = 7.3, the difference was more drastic, since zeolon[®] exhibited a darker color.



Figure 45 Color changes of samples prepared with 0.5 mol % thioindigo in CBV10A (Na^+ -MOR), CBV21A (Na^+ -MOR) and Zeolon[®] (Na^+ -MOR) with different Si/Al ratios.

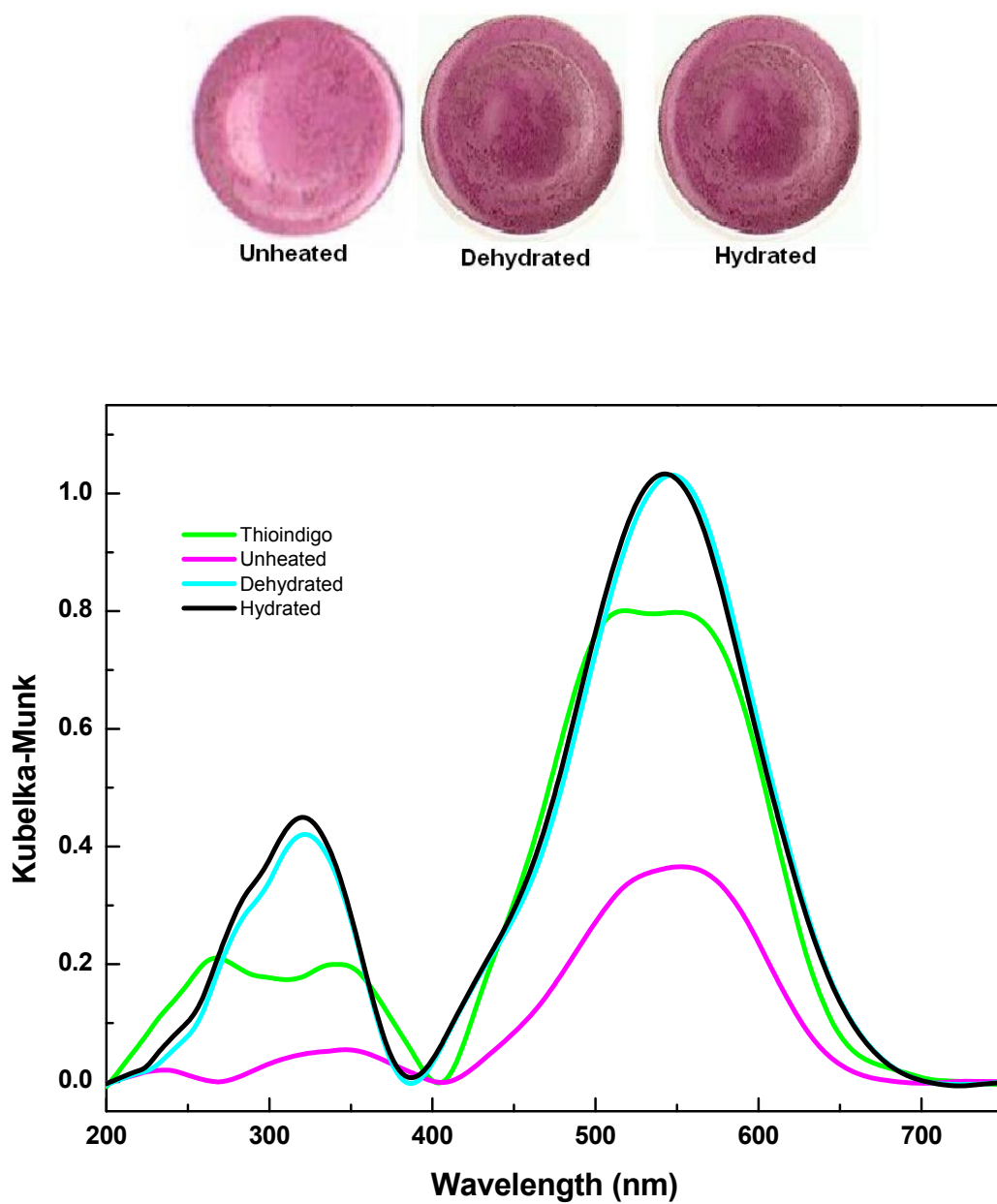


Figure 46 (Top) Color variations of CBV10A (Na⁺-MOR) / 0.5 mol % thioindigo unheated, dehydrated at 413K for nine hours and hydrated after heat treatment (Bottom) UV-Vis spectra of the above mentioned samples and thioindigo starting material.

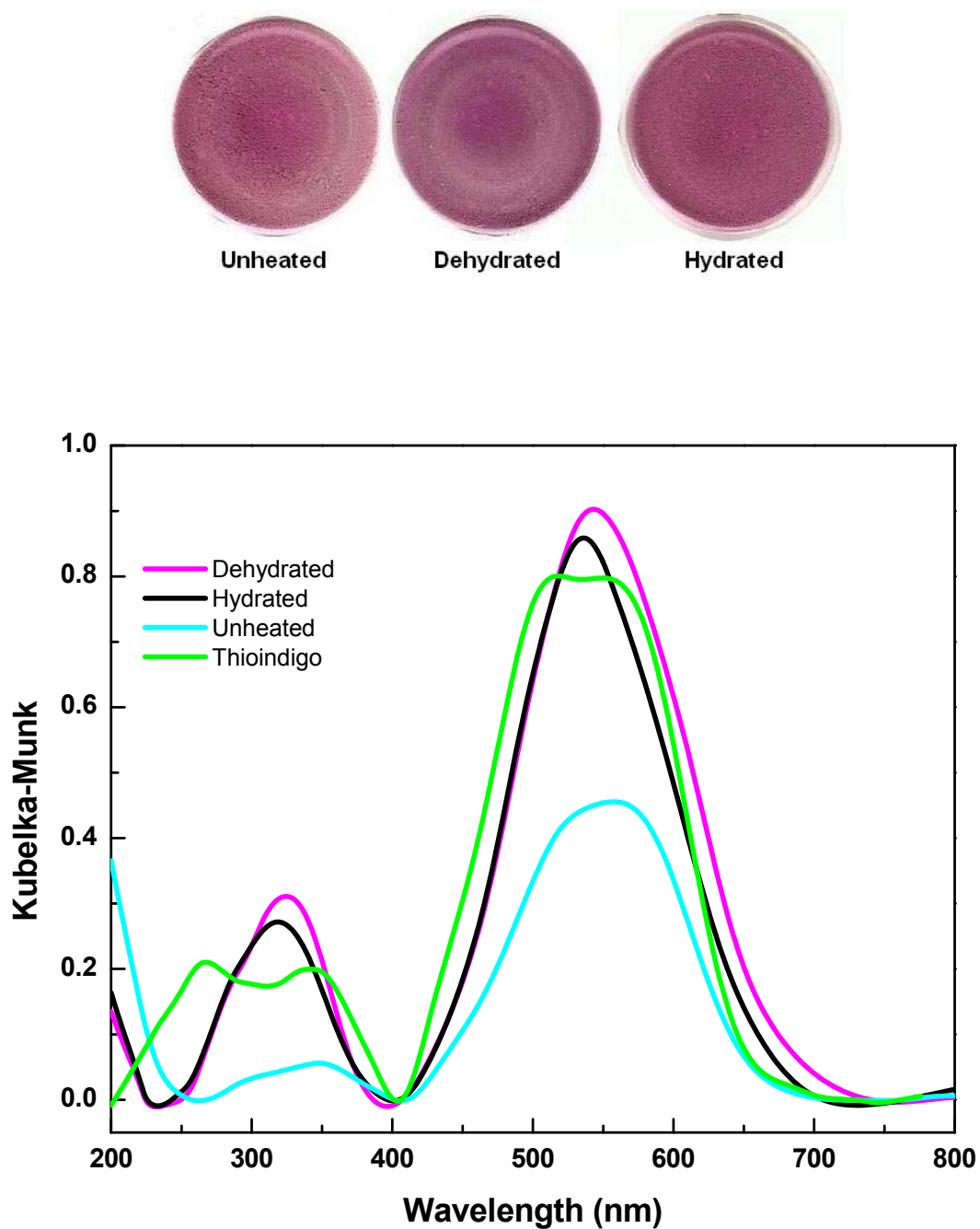


Figure 47 (Top) Color variations of CBV21A (Na⁺-MOR) / 0.5 mol % thioindigo unheated, dehydrated at 413K for nine hours and hydrated after heat treatment (Bottom) UV-Vis spectra of the above mentioned samples and thioindigo starting material.

Mesoporous Zeolites

Mesoporous zeolites such as, aluminum silicates, aluminum oxide and silicon oxide displayed different colors shades when in contact with thioindigo. Samples behaved differently when heated: Aluminum oxide exhibited a bright pink color with two bands at 552 nm ($A = 0.45$) and 678 nm ($A = 0.05$) with no changes when hydrated (see Figure B.80). In the case of silicon oxide and aluminum, silicon (1:1) a bright magenta with three bands at 502 nm ($A = 0.38$), 554 nm ($A = 0.66$) and 604 nm ($A = 0.38$) and for the later a bright red color with three bands at 507 nm ($A = 0.40$), 548 nm ($A = 0.57$) and 587 nm ($A = 0.35$) were observed (see Figure B.82 and B.84).

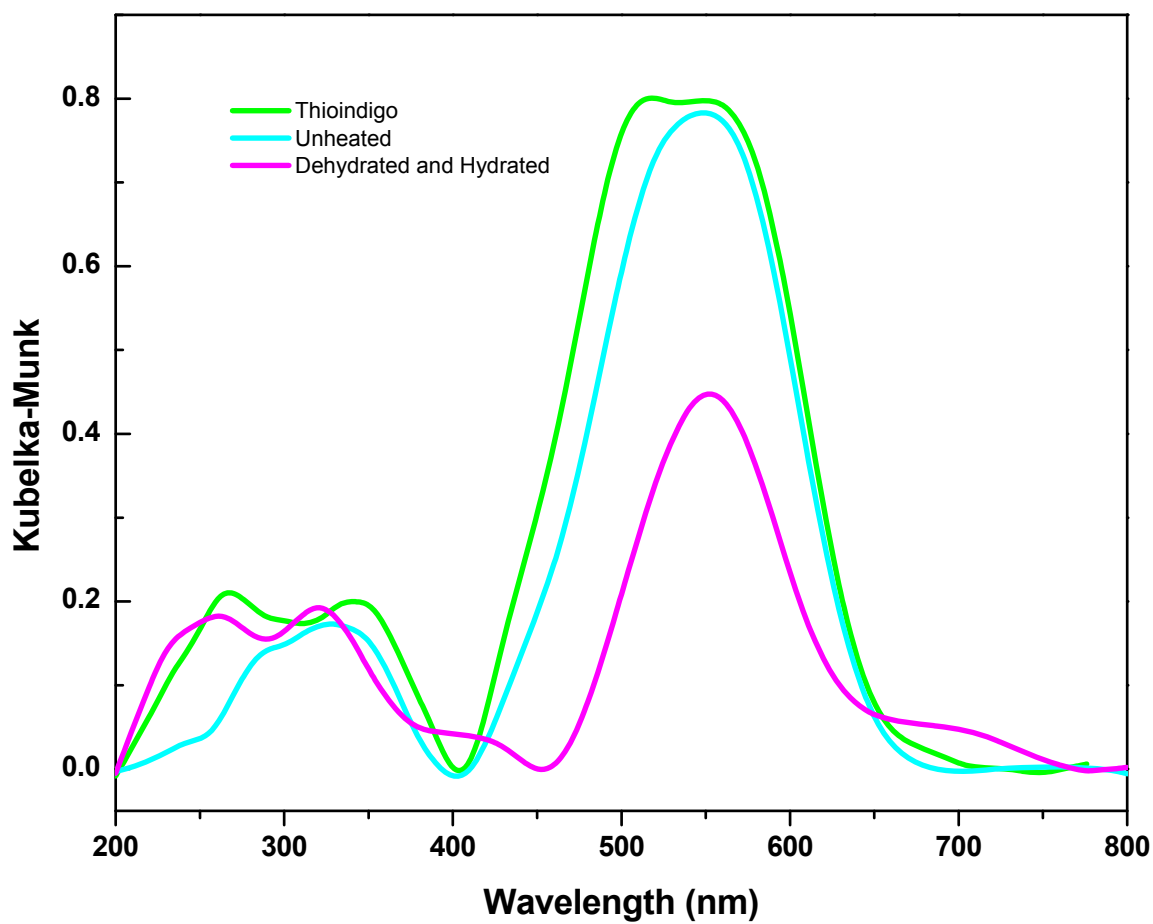


Figure 48 (Top) Color variations of MA-1 / 0.5 mol % thioindigo unheated, dehydrated at 413K for nine hours and hydrated after heat treatment (Bottom) UV-Vis spectra of the above mentioned samples and thioindigo starting material.

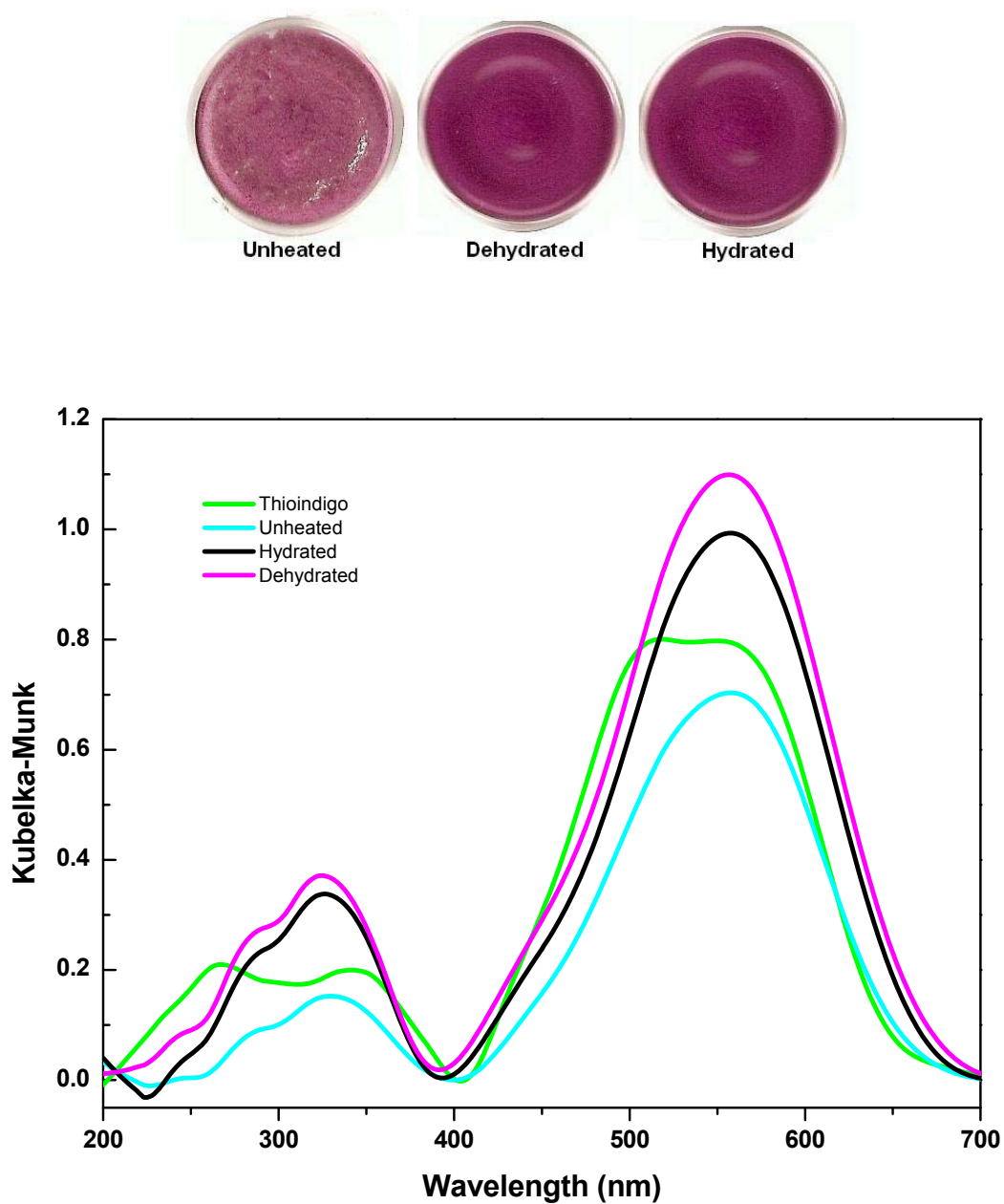


Figure 49 (Top) Color variations of MS-1 / 0.5 mol % thioindigo unheated, dehydrated at 413K for nine hours and hydrated after heat treatment (Bottom) UV-Vis spectra of the above mentioned samples and thioindigo starting material.

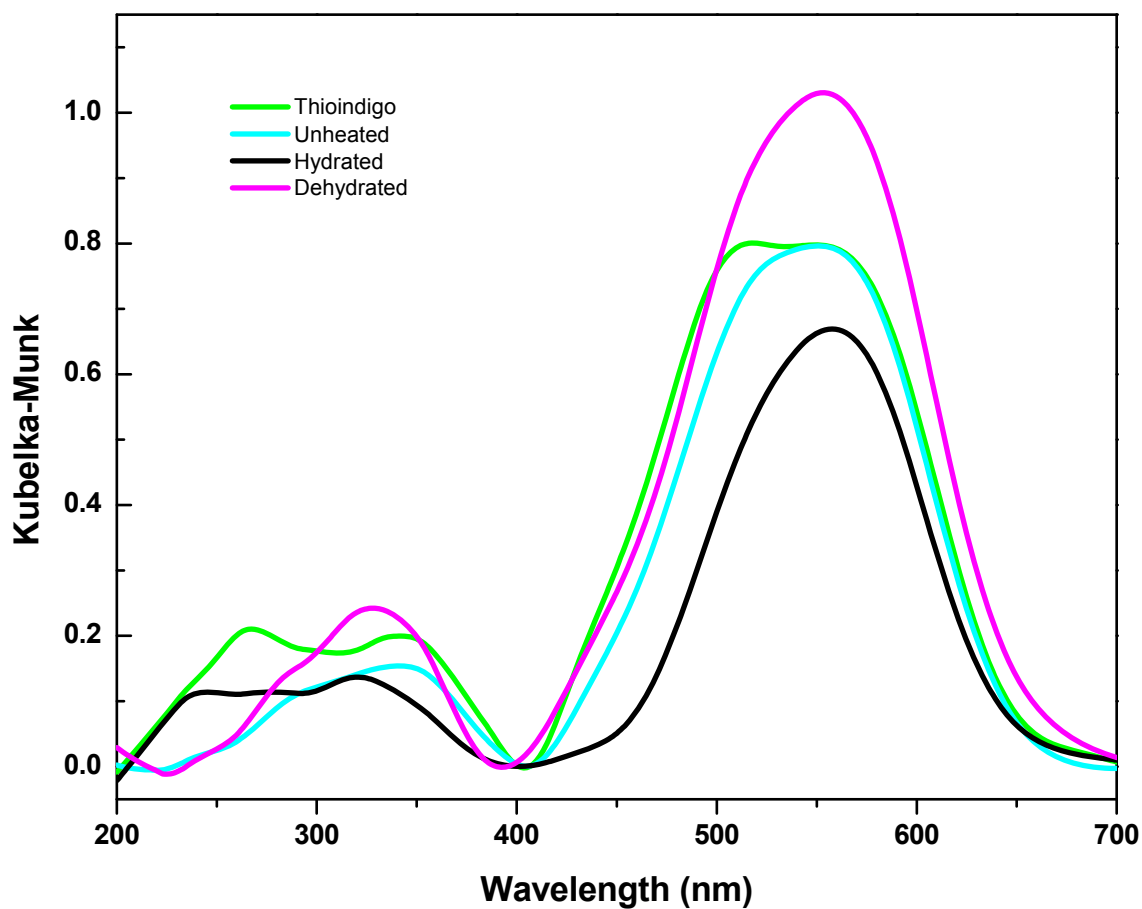


Figure 50 (Top) Color variations of MAS-1 / 0.5 mol % thioindigo unheated, dehydrated at 413K for nine hours and hydrated after heat treatment (Bottom) UV-Vis spectra of the above mentioned samples and thioindigo starting material.

4.3.3 Sulfuric Acid Treated with Thioindigo

A bright blue-green color was displayed when thioindigo reacted with concentrated sulfuric acid (98.7%). The UV-Vis spectra of the blue-greenish solution with a concentration of 4.4×10^{-5} M (taken from measurements by Brode *et al.*²⁰) revealed 7 bands separated in two broad peaks from 425 nm ($A = 0.40$) to 439 nm ($A = 0.41$) and 582 nm ($A = 0.31$) to 700 nm ($A = 0.20$) (see Figure B.87). In addition a large absorption was also observed in the ultraviolet region with an extinction coefficient (ϵ) value of $17,647 \text{ L mol}^{-1}$ based on measurements by Brode *et al.*²⁰ The bright blue-greenish color was noted to change to red suspended particles when small amount of water was added to the solution, eventually the red suspended particles precipitated after some time. Nevertheless a UV-Vis of this reddish solution was obtained at 529 nm ($A = 0.03$) and 587 nm ($A = 0.01$). UV-Vis spectrum illustrated in Figure 51 was normalized for better visualization.

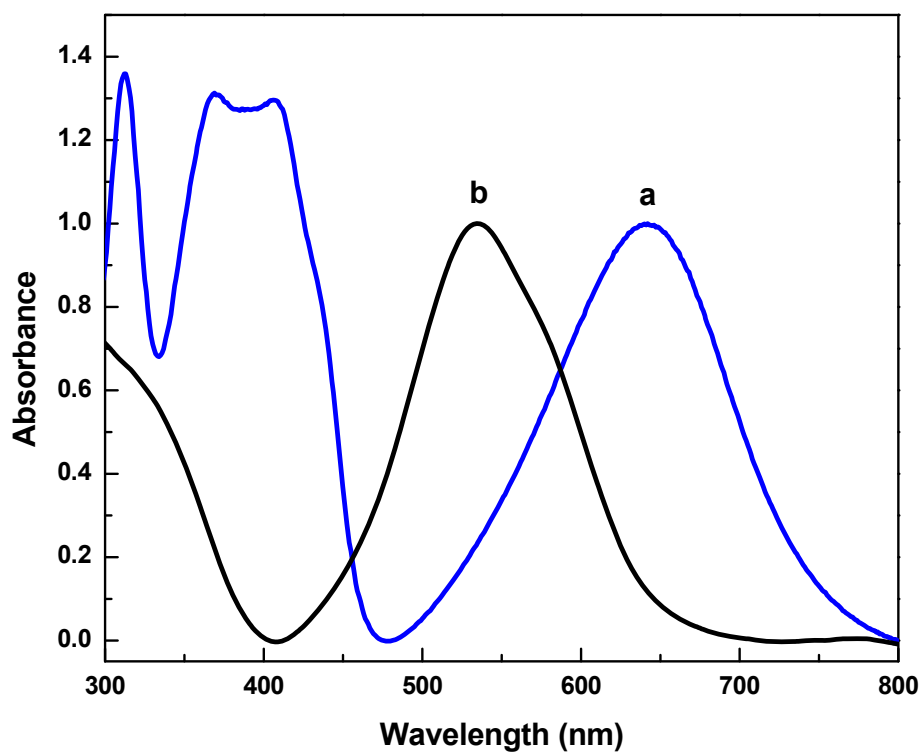


Figure 51 (Top) Color change of thioindigo with concentrated sulfuric acid. (Bottom) UV-Vis spectra of (a) concentrated sulfuric acid reaction with thioindigo and (b) concentrated sulfuric acid reaction with thioindigo after water addition.

4.3.4 Cation Exchanged Mordenite Treated with Thioindigo

Exchanged mordenites, (K^+ , Na^+ , Ca^{2+} , NH_4^+ , H^+ , Al^{3+} -MOR) combined with 0.5 mol % thioindigo at 413K for nine hours, displayed a variety of color changes depending on the exchanged cation, as shown in Figure 52.

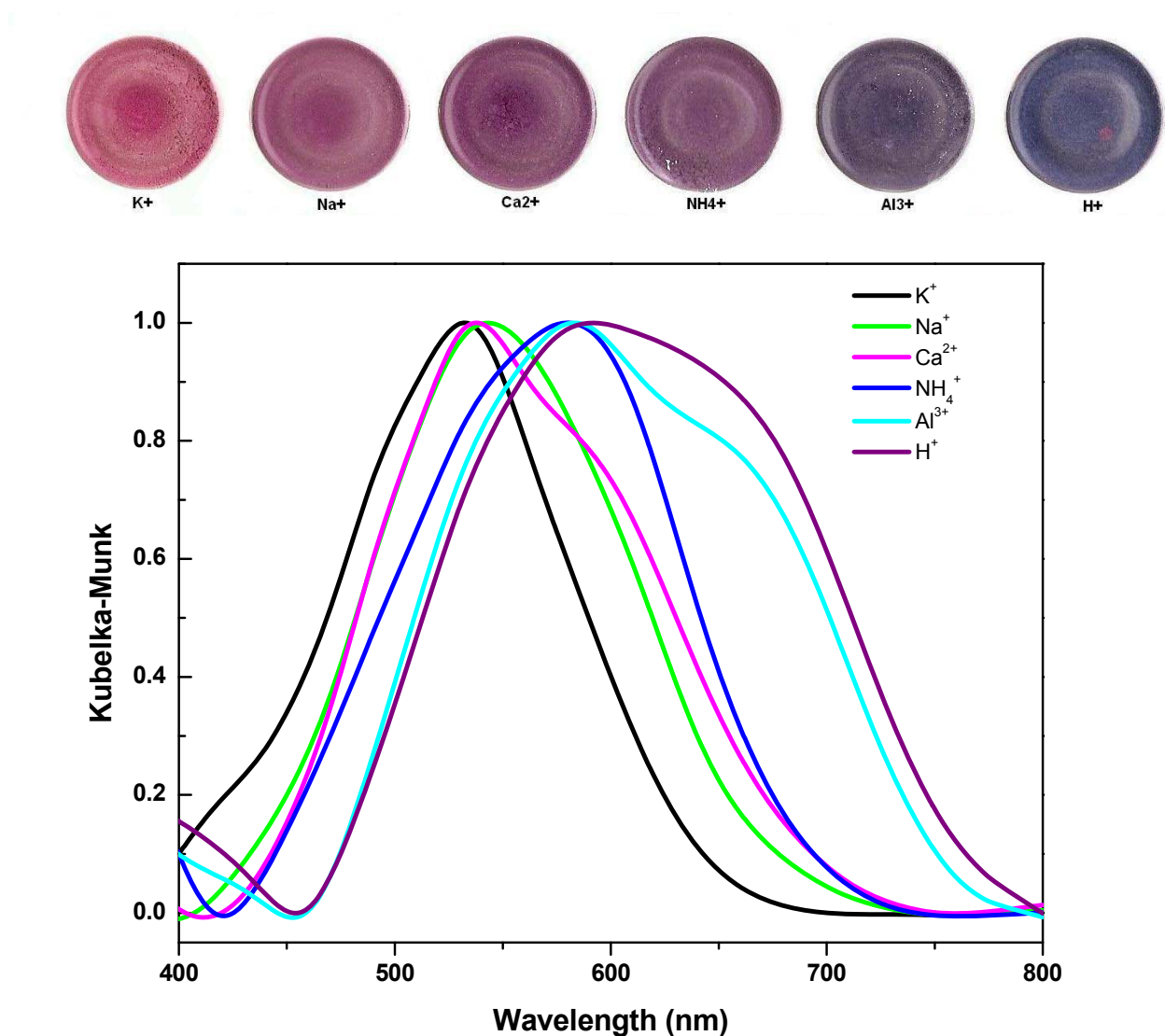


Figure 52 (Top) Color changes observed in heated samples of CBV21A (MOR) exchanged with different cations (K^+ , Na^+ , Ca^{2+} , NH_4^+ , Al^{3+} and H^+) and mixed with 0.5 mol% thioindigo. (Bottom) UV-Vis Spectra of the above mentioned samples.

Bathochromic shifts in the mixtures were observed after heat treatment at 413K for nine hours according to the cation. Exchanged cations with higher acidic strength such as aluminum and hydrogen ($\phi = 60.0 \text{ nm}^{-1}$ and $\phi > 60.0 \text{ nm}^{-1}$) were observed to present higher bathochromic shifts when compared to other cations with lower strength such as potassium ($\phi = 7.0 \text{ nm}^{-1}$).

Water Effect in Exchanged Mordenites (K^+ , Na^+ , Ca^{2+} , NH_4^+ , H^+ , Al^{3+} -MOR)

The absorption of water in most zeolites is one of the main applications among others.⁵¹ However, thioindigo color in this research has made the water absorption more visible than in raw zeolites. Thioindigo contact with the exchanged zeolites, such as faujasite and mordenite, displayed a variety of different color changes when heated. However, these colors were susceptible to hydration as shown in Figure 53.

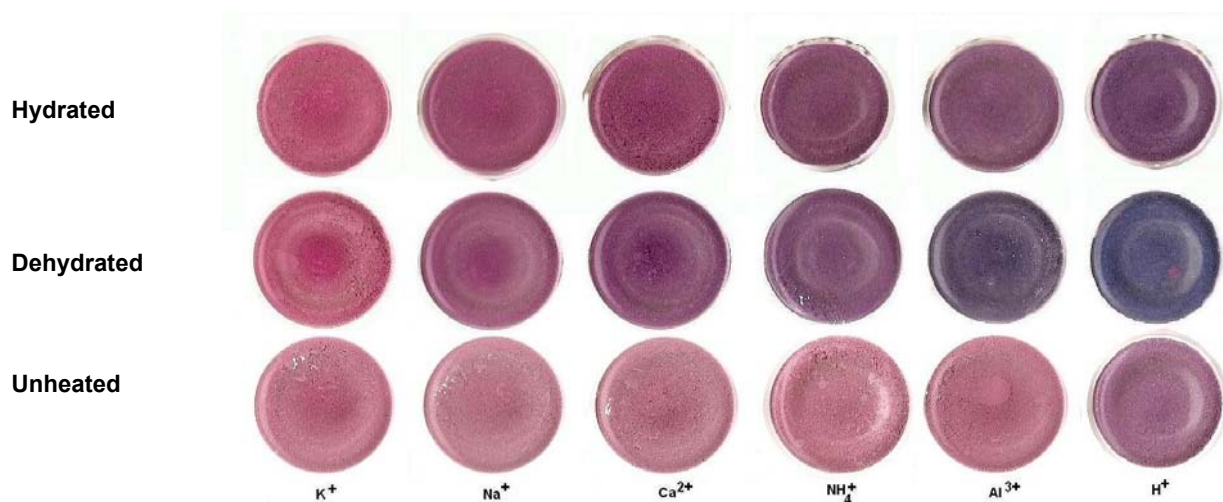


Figure 53 Color changes observed in 0.5 mol % thioindigo in exchanged zeolites unheated, dehydrated at 413K for nine hours and hydrated.

UV-Vis spectra of hydrated exchange mordenites (K^+ , Na^+ , Ca^{2+} , NH_4^+ , H^+ , Al^{3+} -MOR) exhibited a reduction in absorbance and hypsochromic shifts.

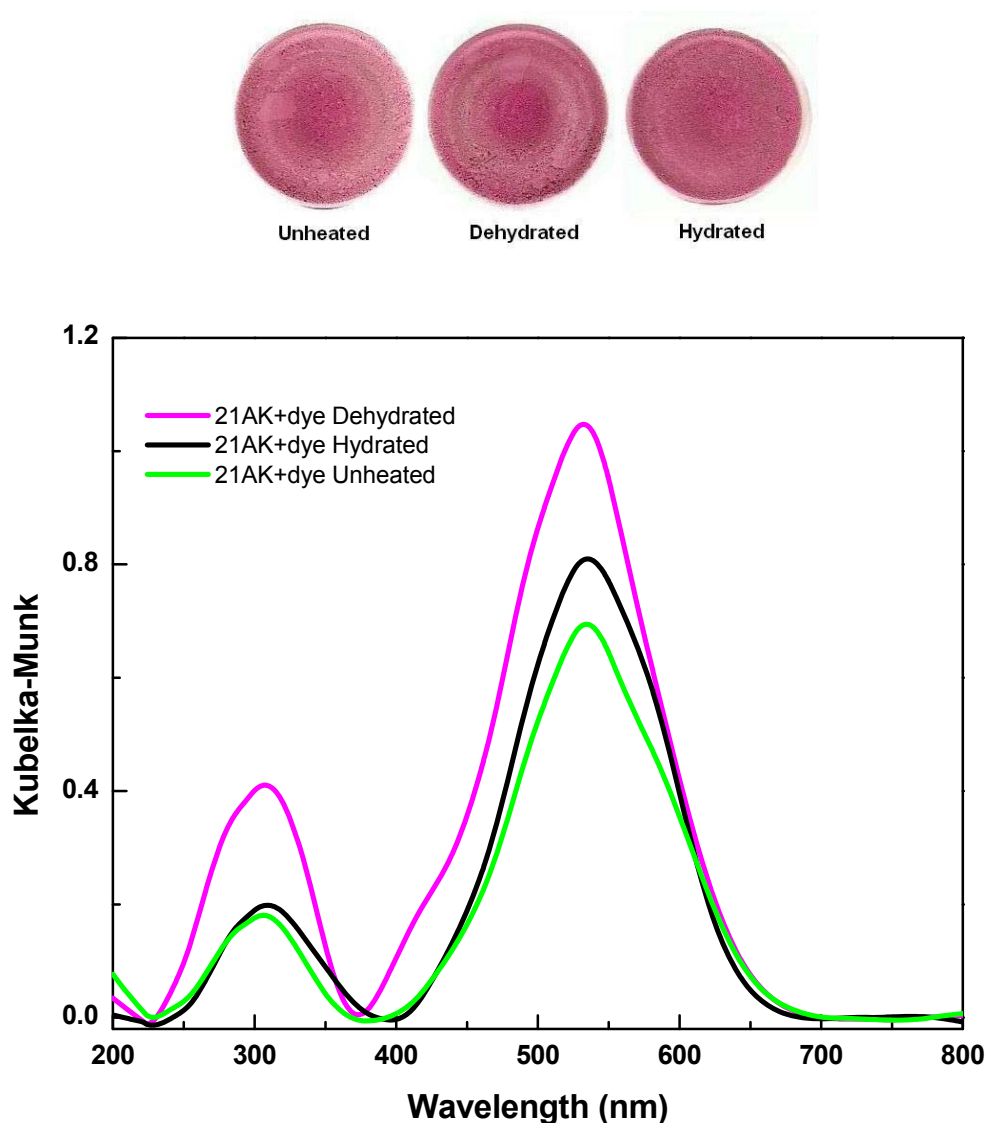


Figure 54 (Top) Color changes observed in 0.5 mol % thioindigo in K^+ -MOR unheated (21AK+dye Unheated), dehydrated at 413K for nine hours (21AK+dye Dehydrated) and hydrated (21AK+dye Hydrated). (Bottom) UV-Vis spectra of the above mentioned samples.

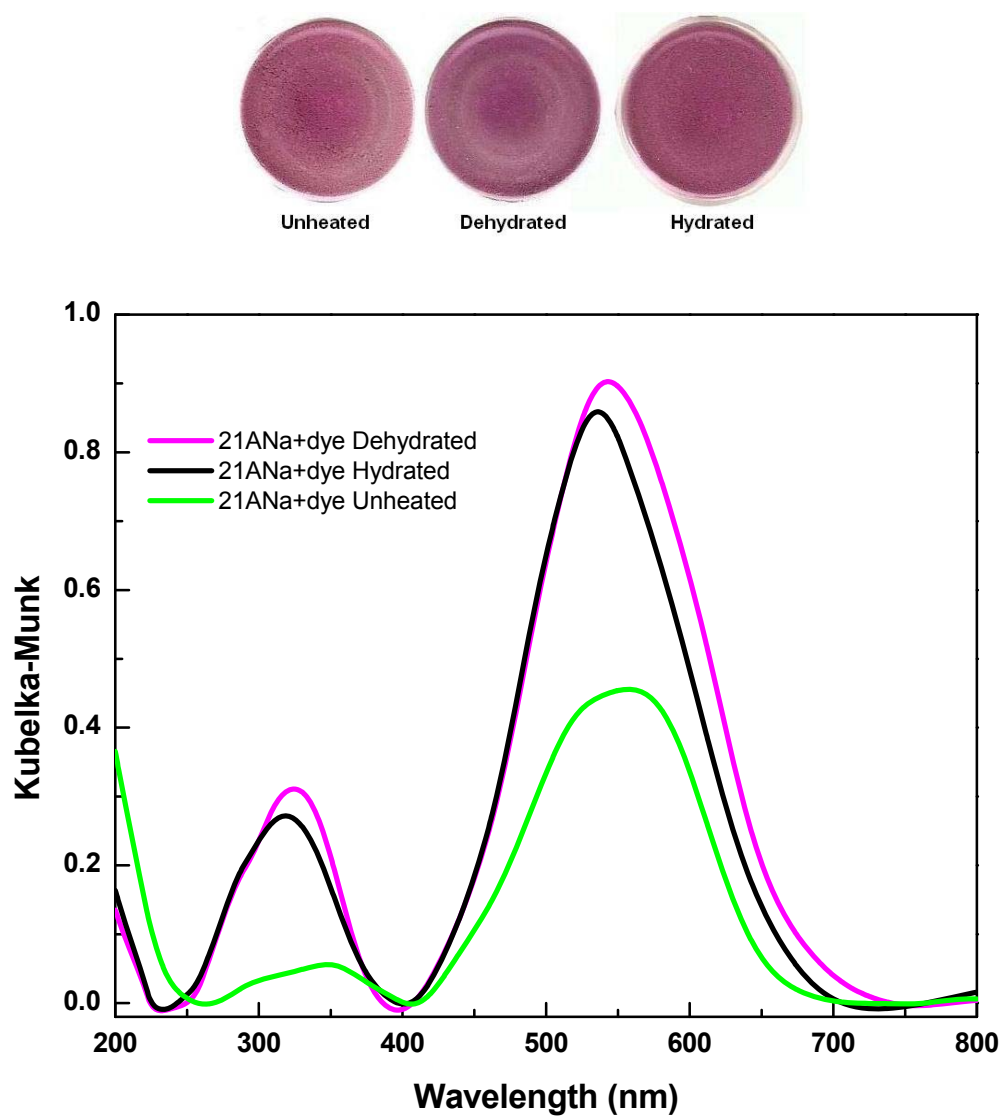


Figure 55 UV-Vis spectra of color change observed during hydration of 0.5 mol % thioindigo in Na⁺-MOR (21ANa+dye Hydrated). Hydrated sample was compared with heated mixture at 413K for nine hours (21ANa+dye Dehydrated) and unheated mixture (21ANa+dye Unheated).

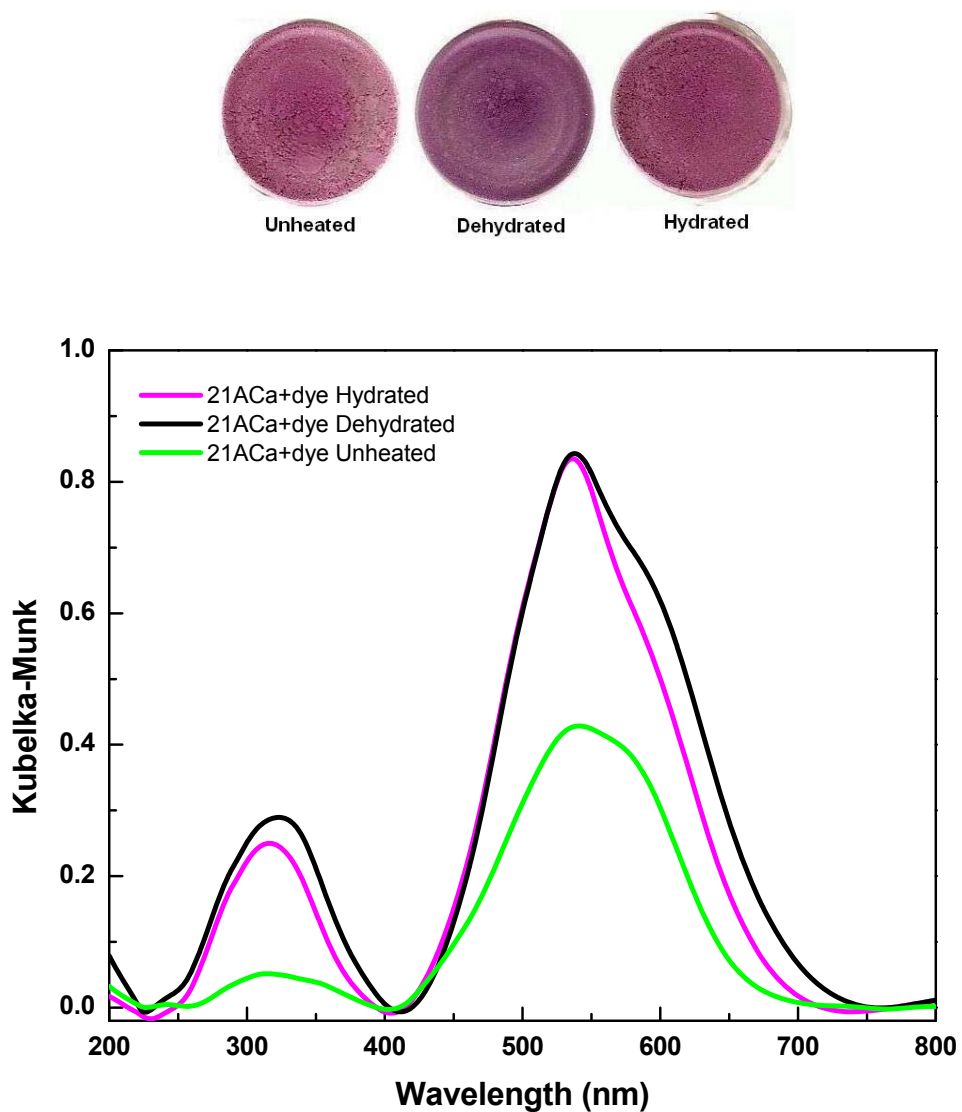


Figure 56 UV-Vis spectra of color change observed during hydration of 0.5 mol % thioindigo in Ca^{2+} MOR (21ACa^{2+} +dye Hydrated). Hydrated sample was compared with heated mixture at 413K for nine hours (21ACa^{2+} +dye Dehydrated) and unheated mixture (21ACa^{2+} +dye Unheated).

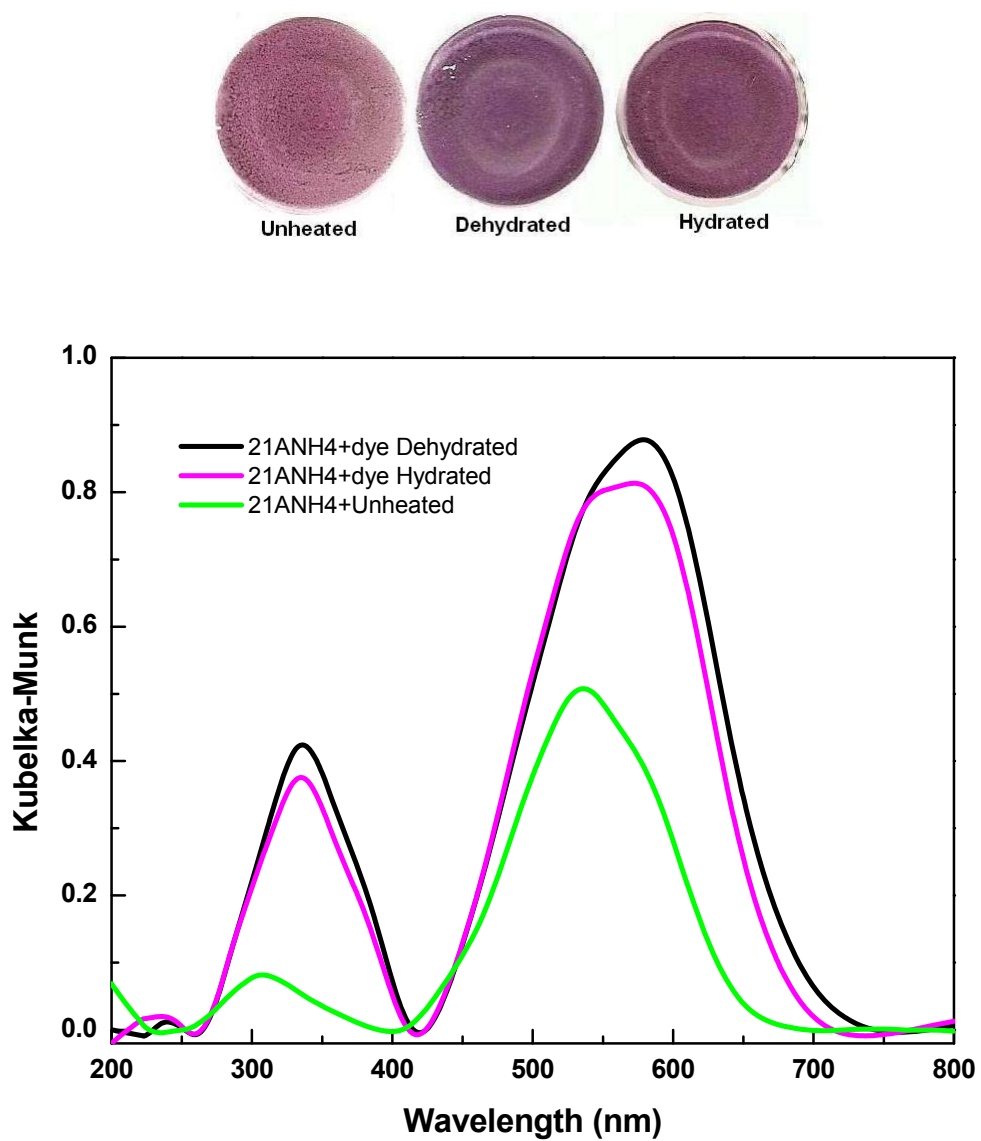


Figure 57 UV-Vis spectra of color change observed during hydration of 0.5 mol % thioindigo in NH_4^+MOR (21ANH_4^+ +dye Hydrated). Hydrated sample was compared with heated mixture at 413K for nine hours (21ANH_4^+ +dye Dehydrated) and unheated mixture (21ANH_4^+ +dye Unheated).

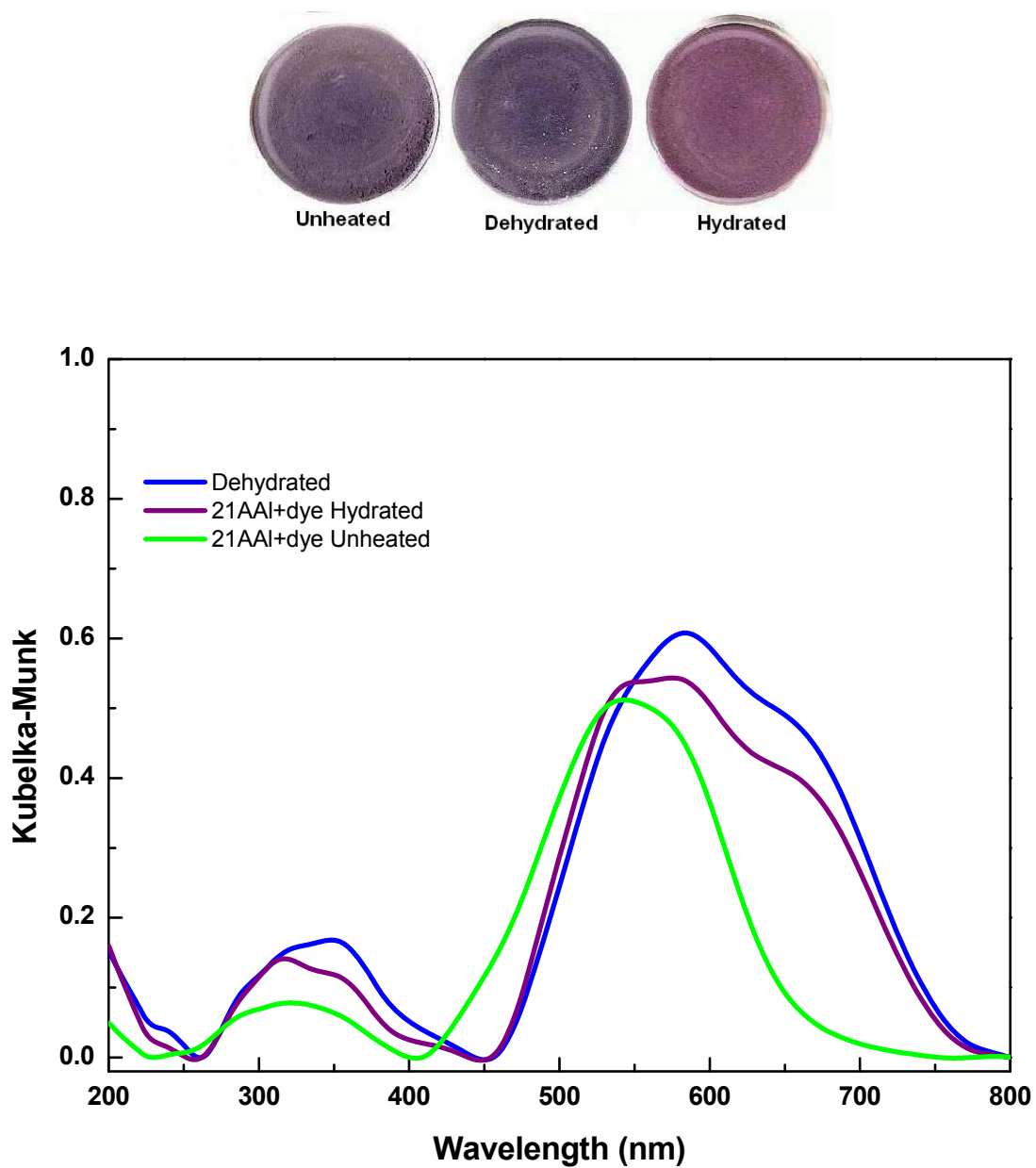


Figure 58 UV-Vis spectra of color change observed during hydration of 0.5 mol % thioindigo in Al^{3+} -MOR (21AAI+dye Hydrated). Hydrated sample was compared with heated mixture at 413K for nine hours (21AAI+dye Dehydrated) and unheated mixture (21AAI+dye Unheated).

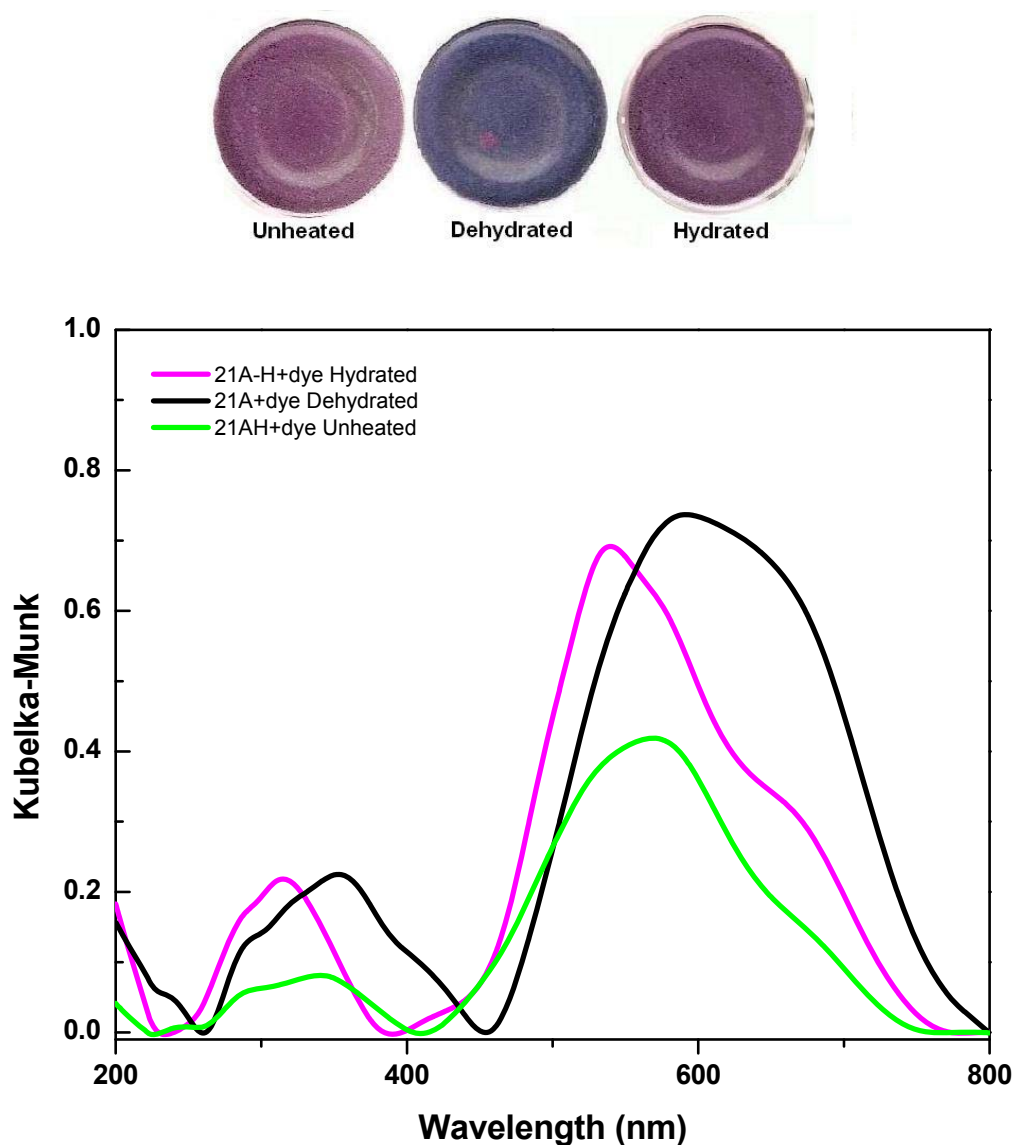


Figure 59 UV-Vis spectra of color change observed during hydration of 0.5 mol % thioindigo in H^+ -MOR (21AH+dye Hydrated). Hydrated sample was compared with heated mixture at 413K for nine hours (21AH+dye Dehydrated) and unheated mixture (21AH+dye Unheated).

4.4 Structural Analysis by Fourier-Transform Infrared Spectroscopy

4.4.1 Inorganic Host Materials

Palygorskite and Sepiolite

The position of the bands, identified in the FTIR spectra of the palygorskite sample, showed the existence of dioctahedral coordination, which was clearly noticed by the absence of the 3Mg-OH vibration (M3 and M1 positions) at 3680 cm^{-1} . Magnesium presence is found in the trioctahedral ends (M3 position) attached to coordinated water; however, M1 position is an empty occupancy. Stretching and bending vibrations of the Al-Al-OH vibration (M2 position) at 3620 and 913 cm^{-1} was detected, and that corresponding to Al-Fe³⁺-OH (M2 position) at 3589 and 863 cm^{-1} was identified as well. Data for the structural characterization of this clay was in accordance to the studies of M. Suarez *et al.*⁴⁴ for several palygorskite clays from different regions around the world. Structural arrangement is illustrated in Figure 9.

Sepiolite, on the other hand, revealed an intense peak in the 3Mg-OH (M3 and M1 positions) at 3680 cm^{-1} and (M1 position) Mg-OH bending mode in the 649 cm^{-1} region, thus trioctahedral coordination is believed to be present. In addition, another sharp vibration in the Fe-Al-Mg-OH was detected at 693 cm^{-1} .⁴⁴

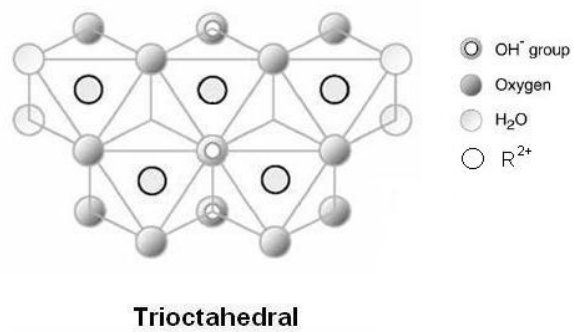


Figure 60 Trioctahedral arrangement for sepiolite clay [Image courtesy of Suarez *et al.*⁴⁴].

Impurities such as quartz and calcite were also visible in the spectrum correlating with the X-ray diffraction pattern (see Figure 98).

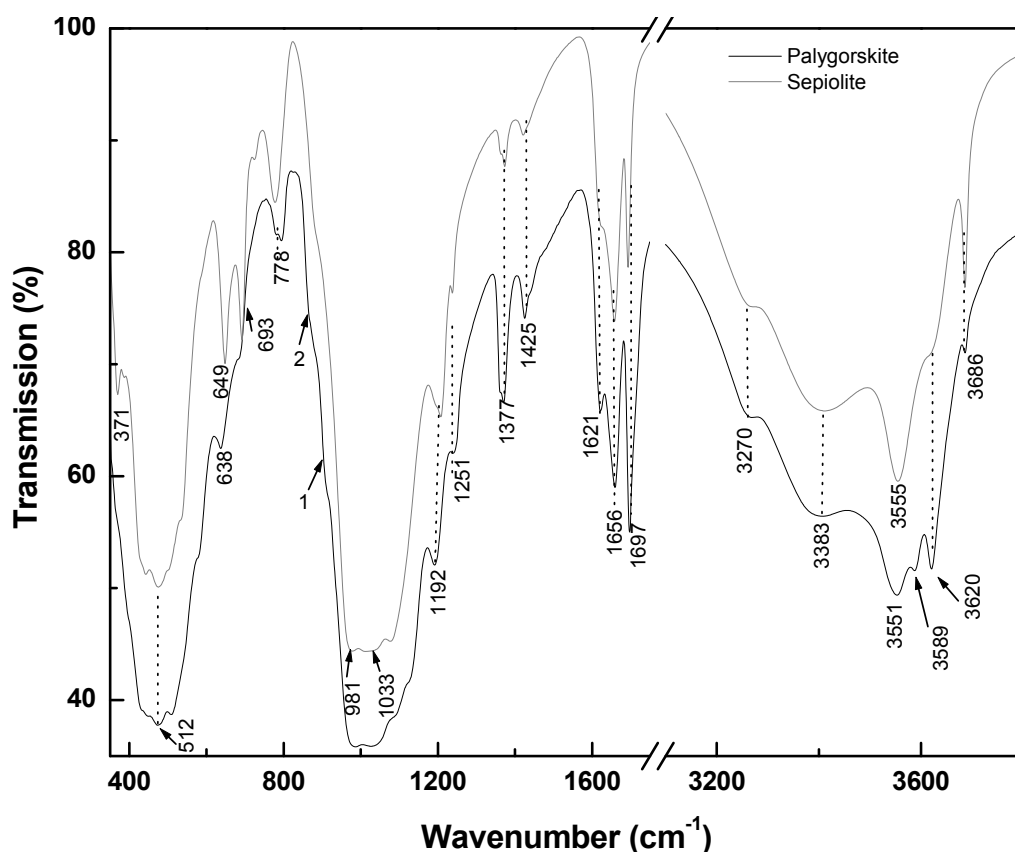


Figure 61 FTIR spectra for palygorskite and sepiolite clays with KBr support.

Table 2 Observed vibrational assignments for palygorskite and sepiolite clays.

Mode	Frequency (cm ⁻¹)		Ref.
	Palygorskite	Sepiolite	
Zeolitic Water	3270(sh), δ-3383(w), v-1621(w)	3240(sh), δ-3383(w), v-1619(sh), v-1621(w)	44,75,76
Mg-OH ₂	δ-3550(w), v-1656(s),	δ-3550(m), v-1656(s),	44,75,76, 48
Al-Fe ³⁺ -OH	δ-3589(m)	NA	44,75,76
Loosely bound H ₂ O	1697(w)	1697(w)	
Hydroxyl or hydrate water	1377(m)	1377(m)	77
Si-O-Si	v-1192(w), 500 region (vs)	v-1192(w), 500 region (vs)	44,75,76
2Al-OH	δ-3620(m), δ-913(sh)	δ-3620(sh)	44,75,76
3Mg-OH	δ-3686(s), 638(w)	δ-3686(s), 649(s)	44,75,76
Si-O quartz (impurity)	778(sh)	778(sh)	77
CaCO ₃ (impurity)	1425(m),	1425(m),	77
Si-O-Al	512(vs)	512(vs)	44
Si-O	v-1033(vs), 981(vs)	v-1033(vs), 981(vs)	44,75,76
Fe,Al,Mg-OH	693(m), δ-863(sh)	693(sh)	44,75,76

(vs):very strong, (s):strong, (m):medium, (w):weak, (sh):shoulder

(v)bending, (δ)stretching NA: Not Available

Low Charge Swelling Natural Occurring Clays (Smectite Group)

FTIR spectra of Na⁺-montmorillonite clays (Na⁺-MMT) [Kunipia and Wyoming deposits] and Ca²⁺-montmorillonite clays (Ca²⁺-MMT) [Bentolite L[®] and Texas deposit] revealed the absence of 3Mg-OH 3686 cm⁻¹ vibration mode indicative of no trioctahedral arrangement. Thus, these clays mostly have dioctahedral character due the presence of 2R³⁺-OH (R= Al³⁺ or Fe²⁺) at 3630 cm⁻¹ and the presence of Si-O-Fe²⁺ at 468 cm⁻¹.⁴⁴ The charge imbalance in these type of clays is mostly originated by divalent substitution in the octahedral sites as mentioned before in chapter 3, section 3.1.0. This occupancy was also confirmed by ²⁷Al-NMR. In addition, we may be tempted to assign vibrations similar to palygorskite and sepiolite; however, attention needs to be paid to changes in the water vibration, such as 1643 cm⁻¹ in Na⁺-MMT and 1638 cm⁻¹ in Ca²⁺-MMT. This vibration has been mentioned by H.W. van der Marel *et al.*⁷⁸ to be resistant up to 853K; therefore, it was assigned to hydroxyl groups instead of zeolitic water as in palygorskite and sepiolite.

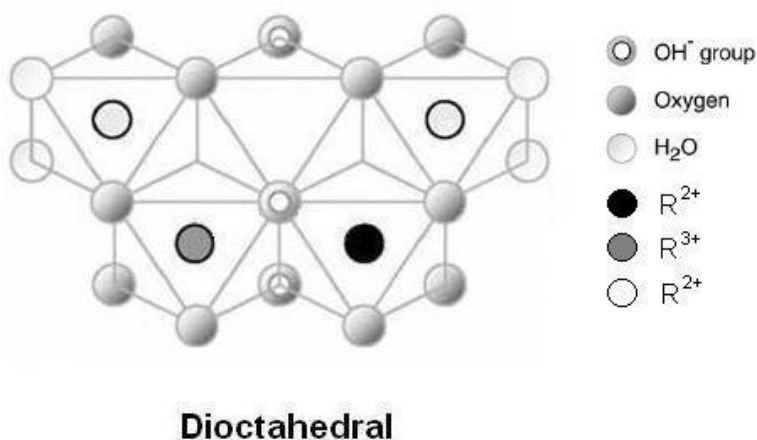


Figure 62 Dioctahedral arrangement in Na⁺ and Ca²⁺- Montmorillonite clays

The presence of quartz and calcite impurities in Na⁺-MMT clays and primarily quartz in Ca²⁺-MMT clays were also observed. These impurities were confirmed by X-ray diffraction. However, in some cases as in Kunipia deposit, the concentration of impurities in the sample probably was lower than 5% (xrd detection limit) since the characteristic peaks in the 2 theta (26 - 29 degrees) region were not detected (see Figure 99).

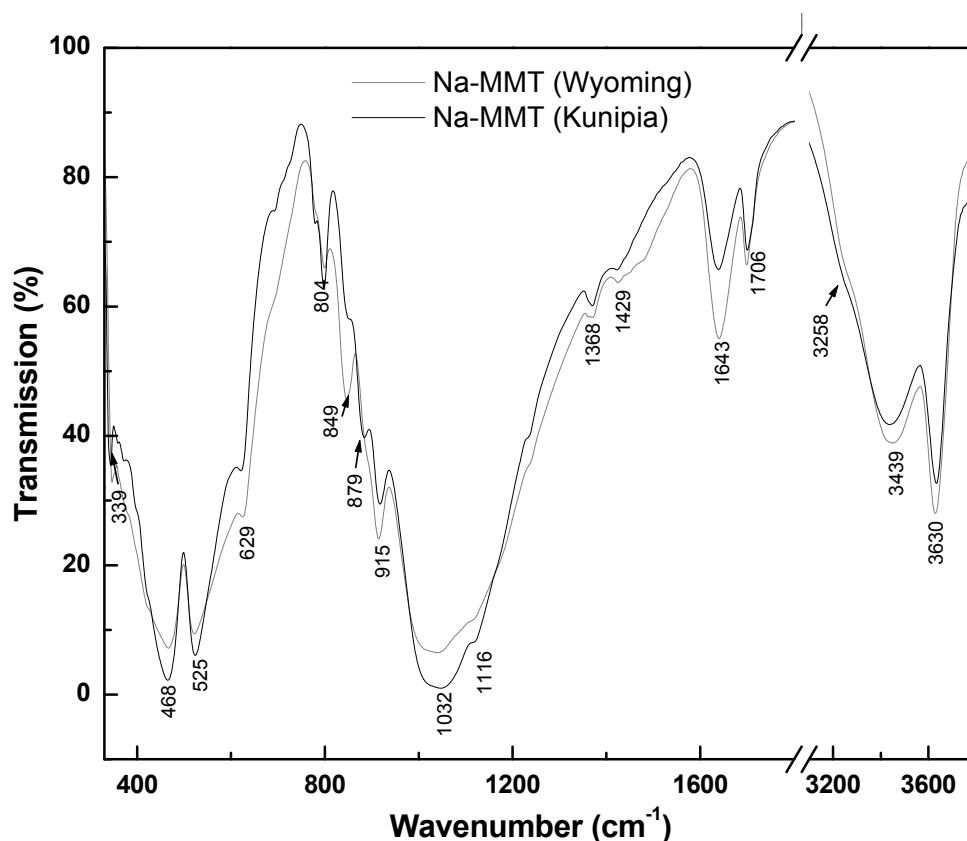


Figure 63 FTIR spectra for Na⁺-montmorillonite clays in KBr support.

Table 3 Observed vibrational assignments for Na⁺-montmorillonite clays.

Mode	Frequency (cm ⁻¹)		Ref.
	Na-MMT (Wyoming)	Na-MMT (Kunipia)	
Zeolitic H ₂ O	δ-3439(s), 3258(sh)	δ-3439(s), 3258(sh)	44,76
2Al-OH	δ-3630(m), δ-915(m)	δ-3630(m), δ-915(m)	44
Loosely Bound H ₂ O	1706(w)	1706(w)	
H-O-H deformation vibration	1643(m)	1643(m)	78
Hydrate H ₂ O	1368	1368	77
Si-O	1116(vs), v-1032(vs)	1116(vs), v-1032(vs)	75,77
CaCO ₃ (impurity)	1429(sh), δ-849(m), 879 (sh)	1429(sh), δ-849(sh), 879(w)	77
Si-O quartz (impurity)	804(m)	804(w)	77
Al-O	δ-629(w)	δ-629(w)	79
Si-O-Mg	δ-525(vs)	δ-525(vs)	79
Si-O-Fe	δ-468(vs)	δ-468(vs)	79

(vs):very strong, (s):strong, (m):medium, (w):weak, (sh):shoulder
(v)bending, (δ)stretching NA = Not available

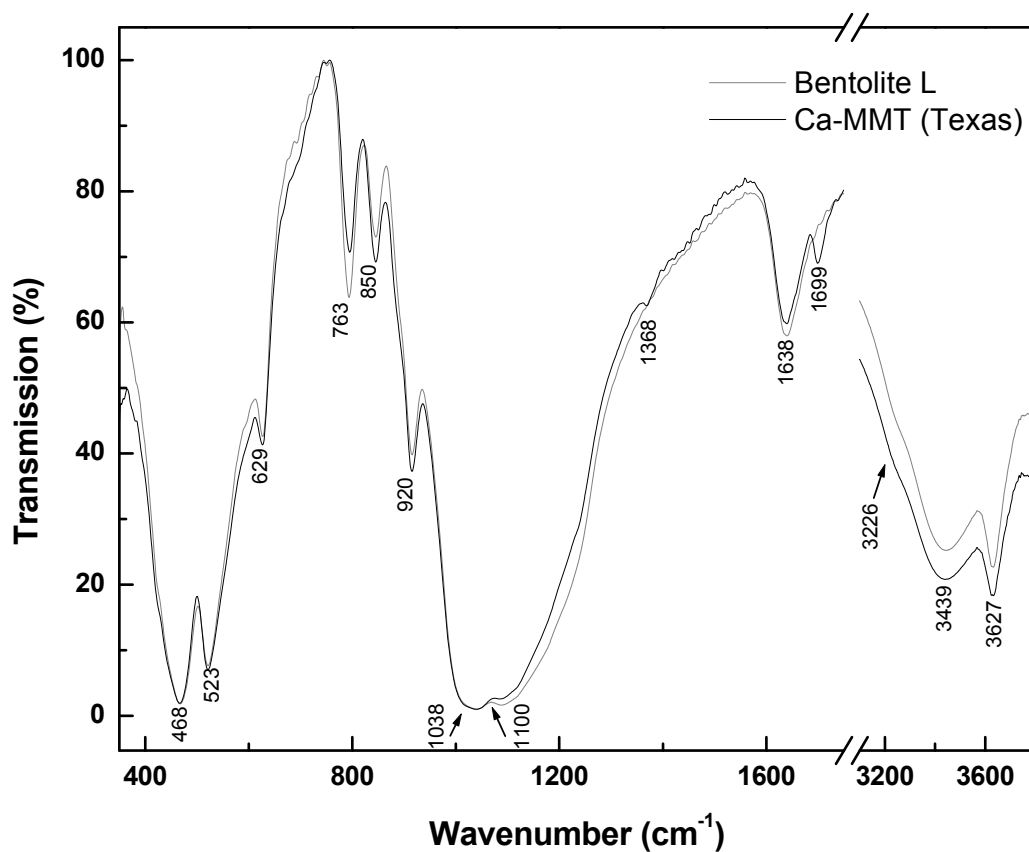


Figure 64 FTIR spectra for Ca²⁺-montmorillonite clays in KBr support.

Table 4 Observed vibrational assignments for Ca²⁺-montmorillonite clays.

Mode	Frequency (cm ⁻¹)		Ref.
	Ca-MMT (Texas)	Ca-MMT (Bentolite L [®])	
Zeolitic H ₂ O	δ-3439(m)	δ-3439(m)	76,79
2Al-OH	δ-3627(m), δ-920(m)	δ-3627(m), δ-920(m)	44
Loosely bound H ₂ O	1699(w)	NA	
H-O-H deformation vibration	1638(m)	1638(m)	78
Hydrate H ₂ O	1368(m)	1368(m)	75
Si-O	v-1038(vs), 1100(vs)	v-1038(vs), 1100(vs)	75
Mg-Al-Fe-OH	δ-850(m)	δ-850(m)	44
Si-O quartz (impurity)	763	763	77
Al-O	629(w)	629(w)	79
Si-O-Mg	v-523(vs)	v-523(vs)	79
Si-O-Fe	v-468(vs)	v-468(vs)	79

(vs):very strong, (s):strong, (m):medium, (w):weak, (sh):shoulder
(v)bending, (δ)stretching
NA = Not Available

Low Charge Synthetic Swelling Clays (Mica group)

FT-IR spectra of synthetic fluorinated Na⁺-micas (YN6, YN8 and sodium trisilicic [Na-Ts]) showed the absence of bridging acidic OH groups in the 3000 cm⁻¹ region, mostly due to the fluorine presence in the mineral formation. Therefore, most of the vibration modes present were in the low frequency region. FTIR measurements were in accordance with S. Sharma *et al.*²¹ in which hydrated mica displayed a strong water deformation at 1636 cm⁻¹ and symmetric water stretching at 3453 cm⁻¹. Si-O-Al deformation band was found near 624 cm⁻¹, Si-O-Al bending along with Mg-OH at 698 cm⁻¹, Si-O-Al in plane at 794 cm⁻¹, and a band due to Si-O at 1101, 996 and 895 cm⁻¹. These values are summarized in Table 5.

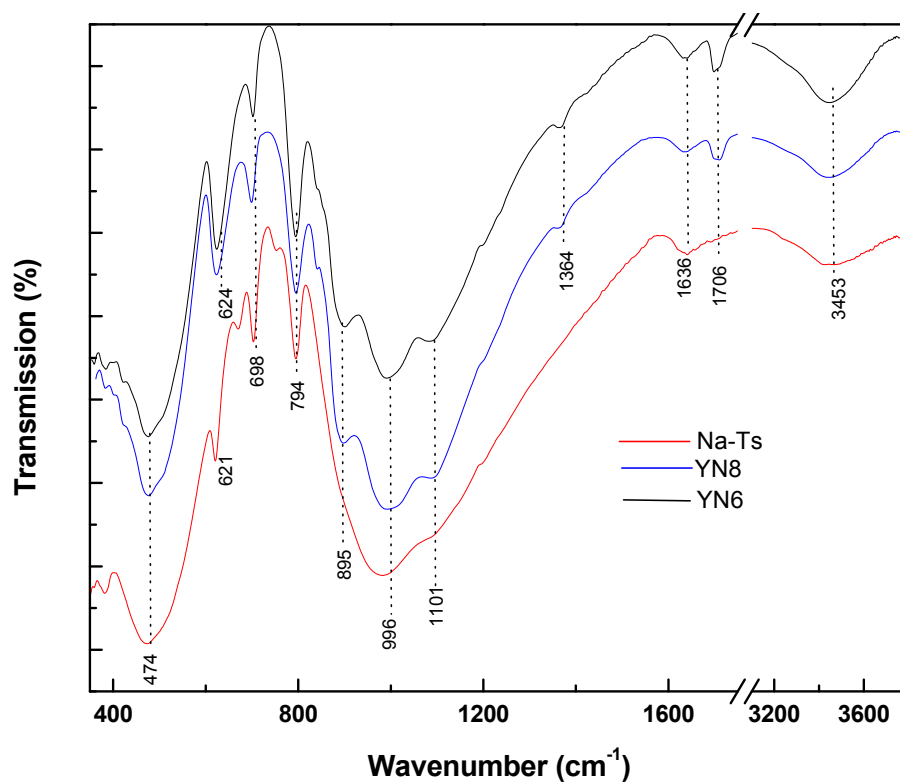


Figure 65 FTIR spectra for three low charge synthetic micas (YN6, YN8 and Na-Ts) in KBr support.

Table 5 Observed vibrational assignments for three low charge fluorinated micas.

Mode	Frequency (cm ⁻¹)			Ref.
	YN6	YN8	Na-Ts	
Zeolitic H ₂ O	δ-3453(w)	δ-3453(w)	δ-3453(w)	79
Loosely bound H ₂ O	1706(w)	1706(w)	NA	79
H-O-H	δ-1636(m)	δ-1636(m)	δ-1636(m)	79
Hydrated Water	1364(sh)	1364(sh)	NA	75
Si-O	v-1101(vs), 996(vs),895(vs)	v-1101(vs), 996(vs),895(vs)	v-1101(vs), 996(vs),895(vs)	75
Si-O-Al	v-794(m)	v-794(m)	v-794(m), δ-753(sh)	79
Mg-OH	698(w)	698(w)	698(m)	79
Si-O-Al	v- 624(m)	v- 624(m)	v-621(m)	44
Si-O	474(vs)	474(vs)	474(vs)	79

(vs):very strong, (s):strong, (m):medium, (w):weak, (sh):shoulder
(v)bending, (δ)stretching

NA: Not Available

Synthetic Zeolites (LTA, FAU, and MOR)

FTIR of synthetic zeolites revealed the presence of water by the $\delta(\text{OH})$ at 1635 cm^{-1} and a broad band around 3400 cm^{-1} . The absence of $\nu(\text{OH})$ in the ~ 3660 and $\sim 3550\text{ cm}^{-1}$ range indicates the deficiency of hydroxyl groups in the supercage and sodalite cages, confirming the pure cation. However, the large amount of zeolitic water generally covers these vibrations only visible when heated or under prolonged vacuum.⁸⁰

Different cations were present in the zeolites evaluated, therefore some differences in 3400 region and 1400 cm^{-1} were observed.

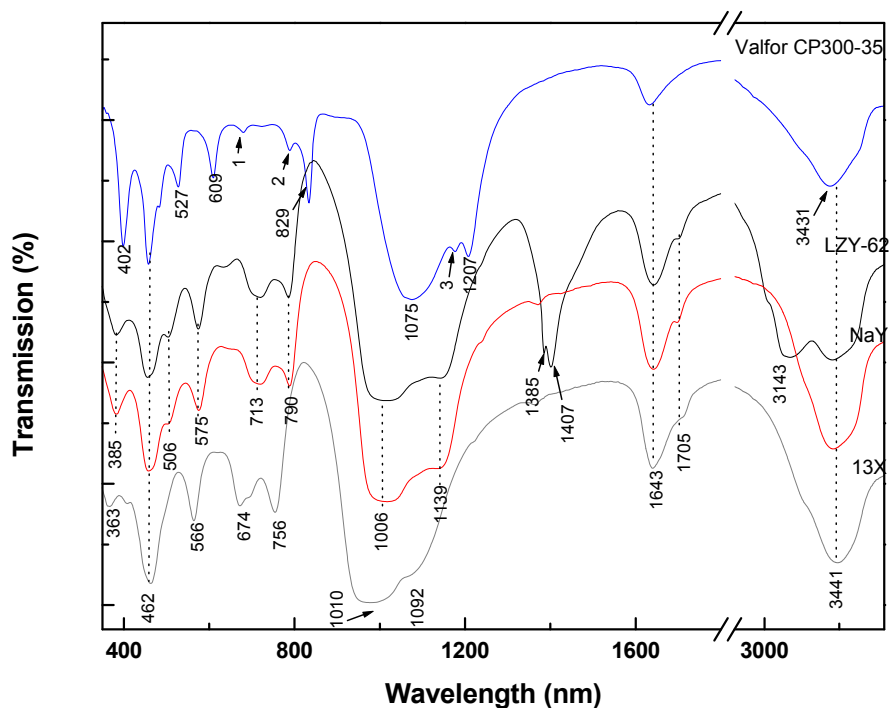


Figure 66 FTIR spectra of several faujasite sieves with different cations (KBr support): Valfor CP300-35 (H^+ -FAU), LZY-62 (NH_4^+ -FAU), NaY (Na^+ -FAU), 13X (Ca^{2+} , Na^+ -FAU).

Table 6 Observed vibrational assignments for several faujasite synthetic zeolites.

Mode	Frequency (cm^{-1})				Ref.
	NaY	Valfor CP300-35	LZY-62	13x	
Zeolitic H_2O	δ -3441(s)	δ -3431(s)	δ -3441(s)	δ -3441(s)	79,
NH_4^+	NA	NA	δ -3143(vs), v-1407(s)	NA	81,82
Loosely bound H_2O	1705(w)	NA	1705(sh)	NA	
H-O-H vibration	δ -1643(m)	δ -1643(m)	δ -1643(m)	δ -1643(m)	76,78
Hydrate H_2O	NA	NA	1385	NA	78
Asymmetrical stretch*	1139(vs), v- 1006(vs)	1207(m), 1180[3](sh), 1075(vs)	1139(vs), v-1006(vs)	1139(vs), 1092(vs), 1010(vs)	83
Symmetrical stretch**	v-790(w)	v-790(w), 829(m)	v-790(w)	NA	83
Symmetrical stretch*	713(w)	792[2](sh), 678[1](sh)	713(w)	674(w)	83
Double ring**	575(w)	609(w)	575(w)	566(w)	83
Tetrahedral cation -O bend*	506(sh), 462(m)	527(sh), 462(m)	506(sh), 462(m)	462(m)	83
Pore opening**	385(w)	402(m)	385(w)	363(w)	83

(vs):very strong, (s):strong, (m):medium, (w):weak, (sh):shoulder
(v)bending, (δ)stretching NA: Not Available

*Internal tetrahedral
** External linkages

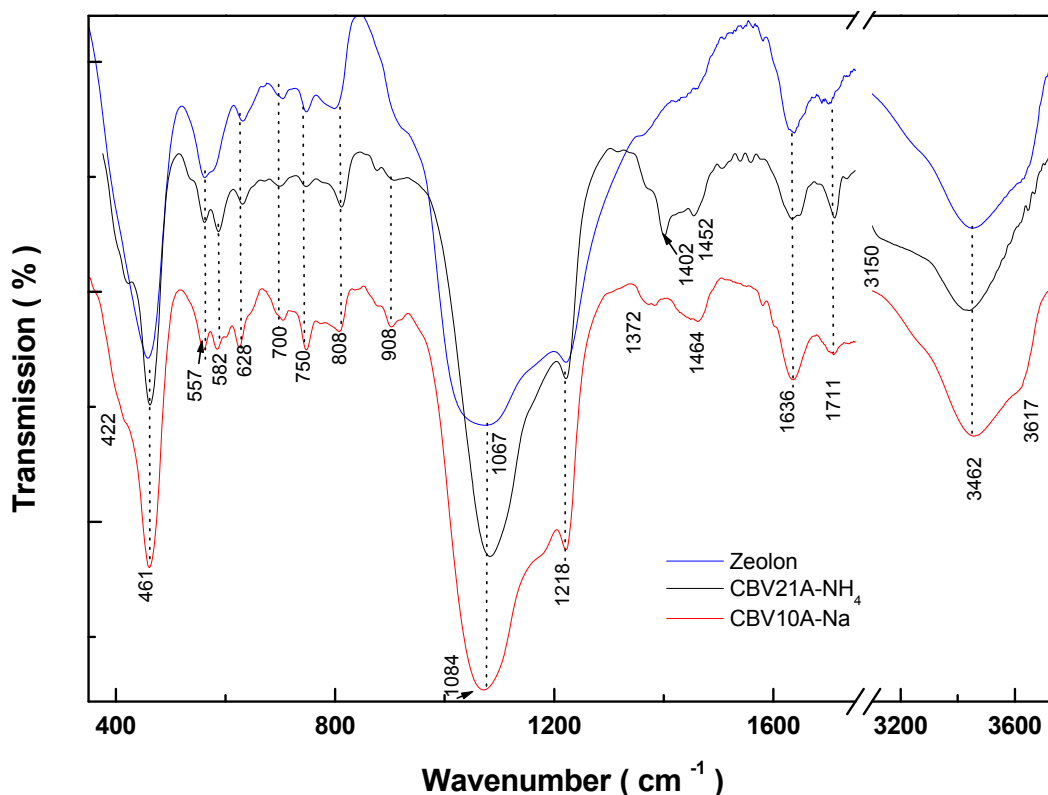


Figure 67 FTIR spectra of several mordenite synthetic zeolites with different cations (KBr support): Zeolon® (Na⁺-MOR), CBV21A (NH₄⁺-MOR), CBV10A (Na⁺-MOR).

Table 7 Observed vibrational assignments for mordenite synthetic zeolites.

Mode	Frequency (cm ⁻¹)			Ref.
	Zeolon®	CBV21A	CBV10A	
Supercages-OH	3617(sh)	NA	3617(sh)	83
Zeolitic H ₂ O	δ-3462(s)	δ-3462(s)	δ-3462(s)	,75
NH ₄ ⁺	NA	δ-3150(sh), 1452(w), v-1402(m)	NA	81,82
Loosely bound H ₂ O	1711(w)	1711(w)	1711(w)	
H-O-H vibration	1636(m)	1636(m)	1636(m)	79
	NA	NA	1464(m)	
hydrate H ₂ O	NA	1372(sh)	1372	78
Asymmetrical stretch*	1218(vs), v-1067(vs)	1218(vs), v-1084(vs)	1218(vs), v-1084(vs)	83
Symmetrical stretch**	908(w), 808(w), 750(m)	908(w), 808(w), 750(m)	908(w), 808(w), 750(m)	83
Double ring**	628(w), 582(w), 557(w)	628(w), 582(w), 557(w)	628(w), 582(w), 557(w)	83
Tetrahedral cation -O bend*	461(m),422(sh)	461(m),422(sh)	461(m),422(sh)	83
(vs):very strong, (s):strong, (m):medium, (w):weak, (sh):shoulder			*Internal tetrahedral	
(v)bending, (δ)stretching			**External linkages	
NA: Not Available				

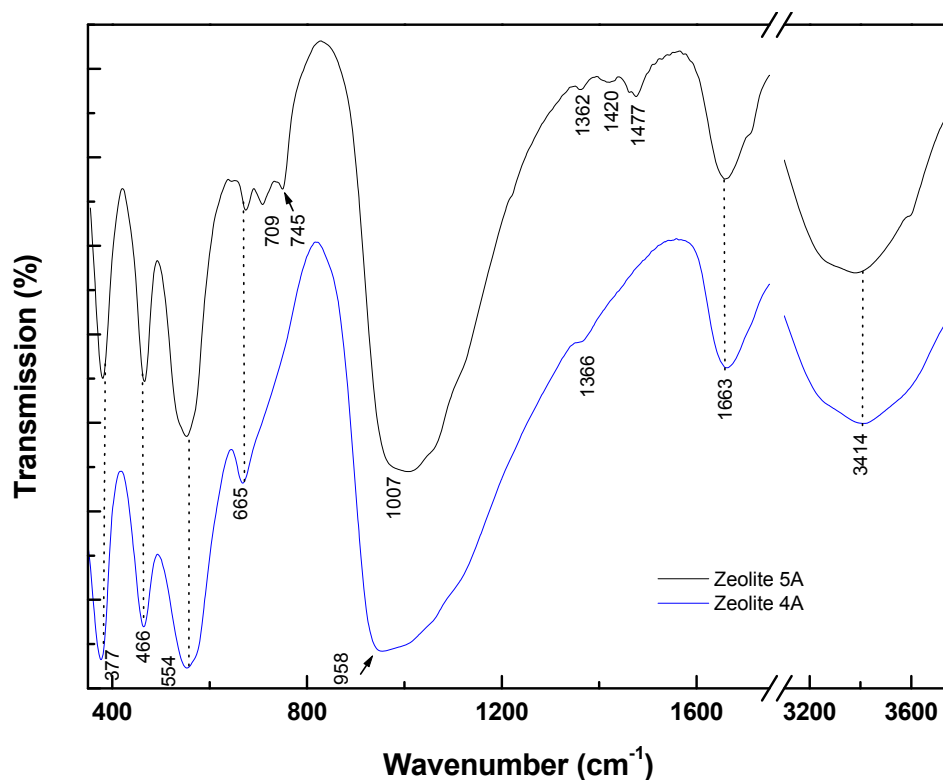


Figure 68 FTIR spectra of several LTA synthetic zeolites with different concentrations of sodium cation (KBr support): 4A (0.6 moles Na⁺-LTA), 5A (0.2moles Na⁺-LTA).

Table 8 Observed vibrational assignments for LTA synthetic zeolites.

Mode	Frequency (cm ⁻¹)		Ref.
	4A	5A	
Zeolitic H ₂ O	δ-3414(s)	δ-3414(s)	79,76
H-O-H deformation vibration	1633(m)	1633(m)	76
hydrate H ₂ O	1366(sh)	1477(w), 1420(sh), 1362(sh)	78
Asymmetrical stretch*	v-958(vs)	v-1007(vs)	83
Symmetrical stretch*	665(w), 554(vs)	745(w), 709(w), 665(w), 554(vs)	83
Tetrahedral cation -O bend*	466(m)	466(m)	83
Pore opening*	377(m)	377(m)	83
(vs):very strong, (s):strong, (m):medium, (w):weak, (sh):shoulder			*Internal tetrahedral
(v)bending, (δ)stretching NA= Not Available			** External linkages

4.4.2 Surface Acidity by Pyridine Adsorption

Pyridine (C_5H_5N) is a weak base used extensively in catalysis to evaluate the acidity of zeolites and clays⁸⁴. In this work the FTIR spectra of simulated pyridine was performed by Gaussian 3.0, and compared with reported data.^{85,86,87}

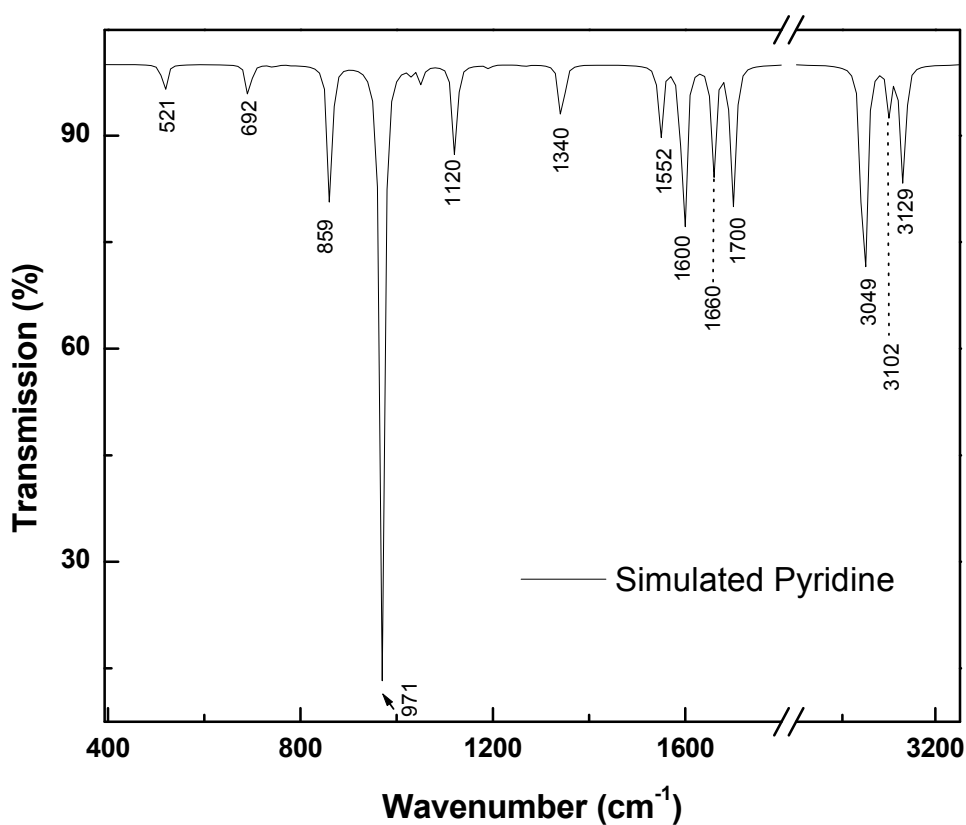


Figure 69 FTIR spectra of simulated pyridine by Gaussian 3.0.

Table 9 Fundamental frequencies (cm⁻¹) in pyridine.

Vibration No.	Symmetry	Form of Vibration	Frequency (cm ⁻¹)	Ref.
		v-C-H	3129(w)	87
14	B ₁	v-C-H	3102(m)	85
2,13	A ₁	v-C-H	3049(m)	86
		Overtones/combination	1700(m)	87
		Overtones/combination	1660(w)	87
8a	A ₁	C-C, CCH	1600(m)	86
19b	B ₁	C-C, CCH	1552(w)	86
14	B ₁	v-C-C	1340(w)	86
15	B ₁	CCH	1120(m)	85
1	A ₁	C-H	971(vs)	86
10b	B ₂	C-H	859(m)	86
11	B ₂	C-H	692(w)	85

(vs):very strong, (s):strong, (m):medium, (w):weak, (sh):shoulder

(v)bending, (δ)stretching

Palygorskite and Sepiolite

FTIR spectra of pyridine adsorption at 413K revealed the presence of pyridine – Lewis Acid sites⁸⁸ at 1447 cm^{-1} for palygorskite and 1445 cm^{-1} and 1596 cm^{-1} for sepiolite.

The origin of a Lewis acid in palygorskite ($\text{Si/Al} = 5.68$) could be primarily from extra-framework aluminum cations since the high concentration of potassium could not have any important effect due to its low acidity in comparison to aluminum.

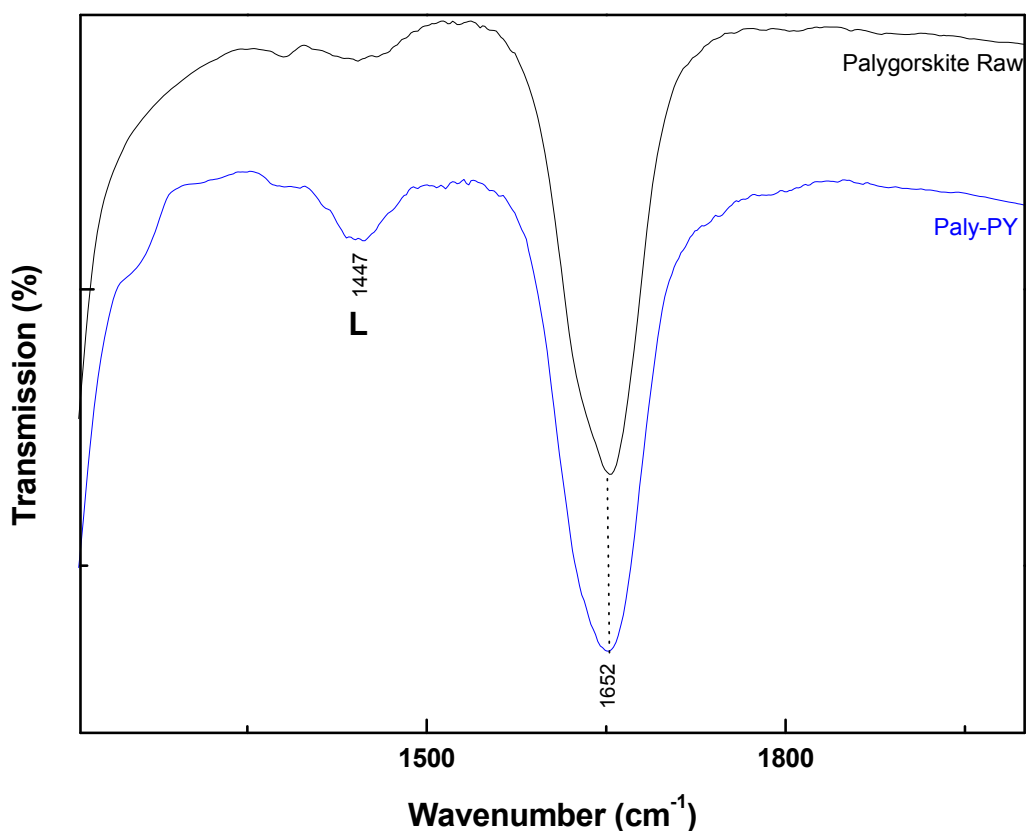


Figure 70 FTIR comparison of palygorskite raw material [Palygorskite Raw] and pyridine adsorption on palygorskite [Paly-PY] (KBR support).

In the case of sepiolite, two vibration modes of pyridinium-Lewis acids sites were detected by FTIR spectroscopy. Sepiolite (Si/Al = 15) contained a high concentration of Ca^{2+} to compensate the negative charge created by the aluminum substitution; therefore, the Lewis acid sites present in the FTIR spectra could be related to Ca^{2+} or Al^{3+} cations.

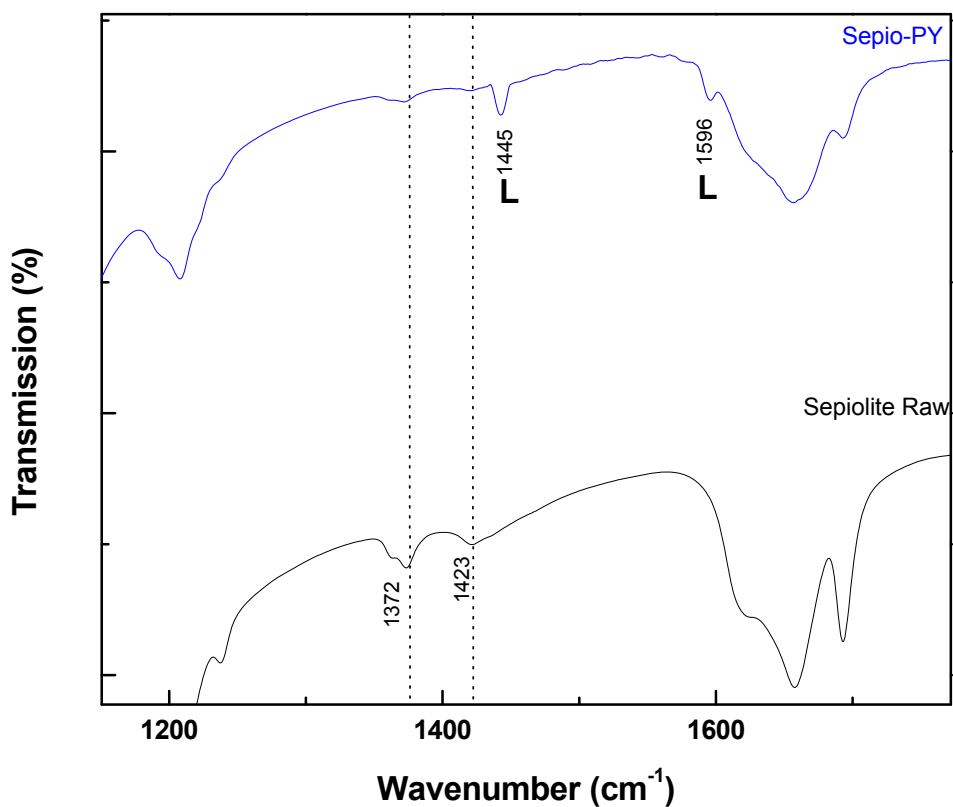


Figure 71 FTIR comparison of sepiolite raw material [Sepiolite Raw] and pyridine adsorption on sepiolite [Sepio-PY] (KBR support).

Montmorillonite Clays

Ca^{2+} -MMT

FTIR of pyridine adsorption of both Ca^{2+} -MMT clays (Bentolite L[®] Si/Al = 4.08 and Texas deposit Si/Al = 3.52) revealed the presence of Brønsted and Lewis acid sites. Brønsted acid sites were assigned to the protons from the framework and Lewis acid sites to the extra-framework aluminum.

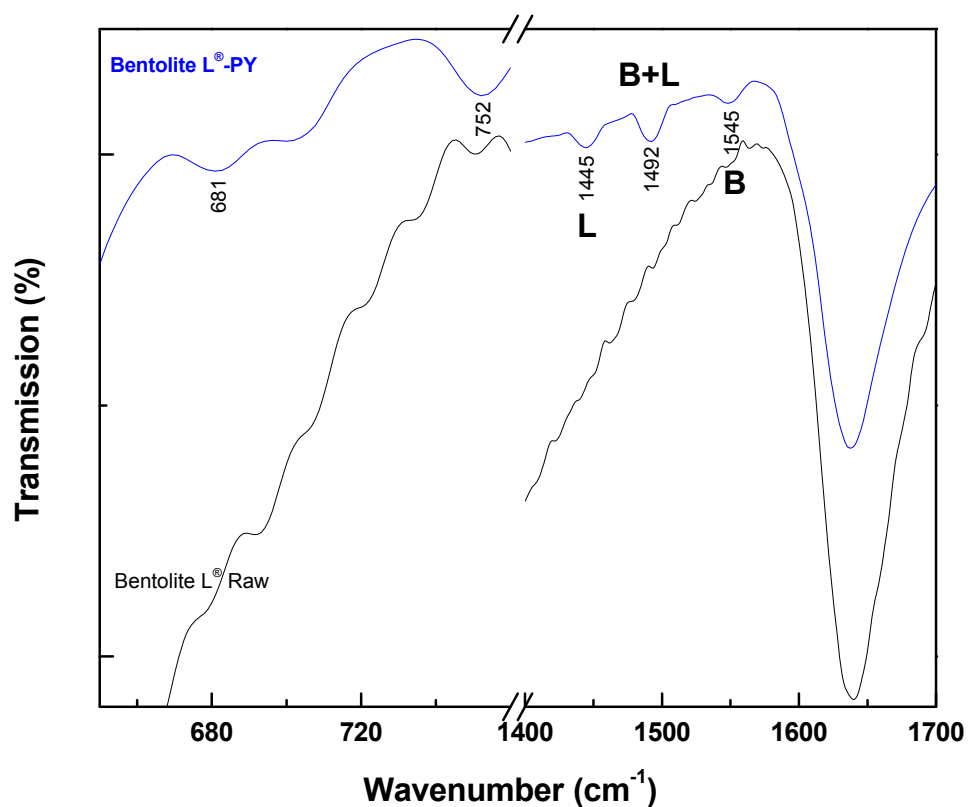


Figure 72 FTIR comparison of bentolite raw material [Bentolite L[®] Raw] and pyridine adsorption on bentolite [Bentolite L[®] -PY] (KBR support).

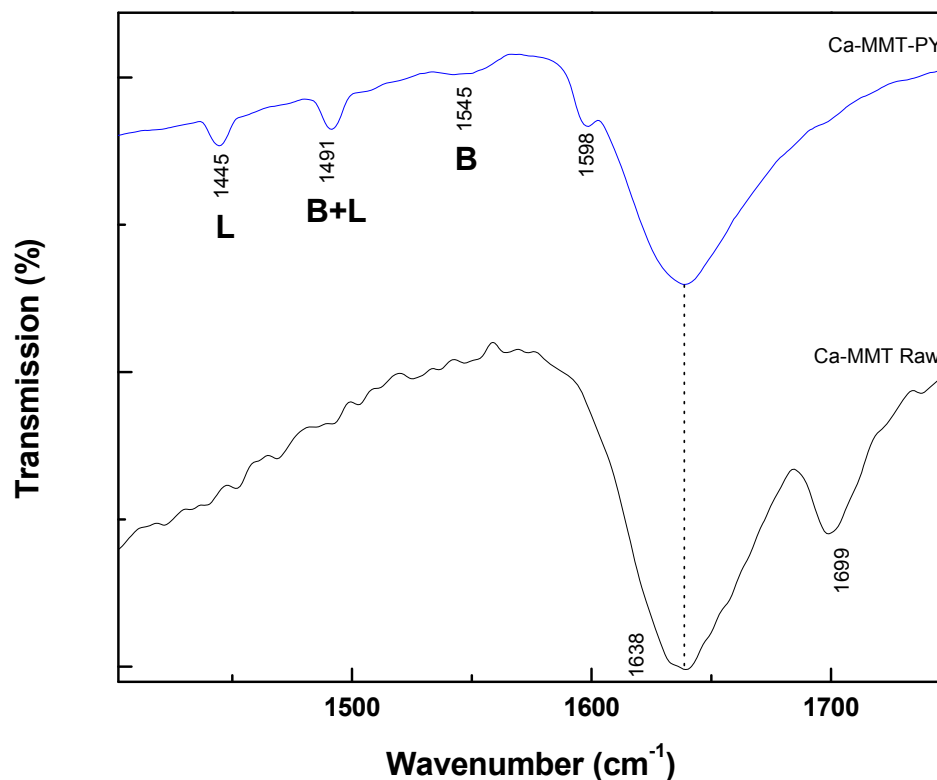


Figure 73 FTIR comparison of Ca^{2+} -MMT raw material [Ca-MMT Raw] and pyridine adsorption on Ca^{2+} -MMT [Ca-MMT -PY] (KBR support).

Na^{+} -MMT

FTIR of pyridine adsorption of both Na^{+} -MMT clays (Wyoming deposit, $\text{Si}/\text{Al} = 2.8$ and Kunipia deposit, $\text{Si}/\text{Al} = 2.4$) revealed a small amount of Lewis acid sites in Wyoming deposit and no Lewis acid sites in Kunipia deposit. This could be explained by the WD-XRF cation concentration in the samples. Na^{+} -MMT (Wyoming deposit) presented almost an equal amount of calcium when compared to sodium, which could be responsible for the small bands corresponding to the Lewis acid sites. On the other hand, a larger concentration of sodium was detected in Na^{+} -MMT (Kunipia deposit)

where no Lewis acids were observed. The color changes observed in both samples under UV-Vs spectroscopy agreed with the poor withdrawing effect of the cations present in both samples, as observed in cation exchanged modernites.

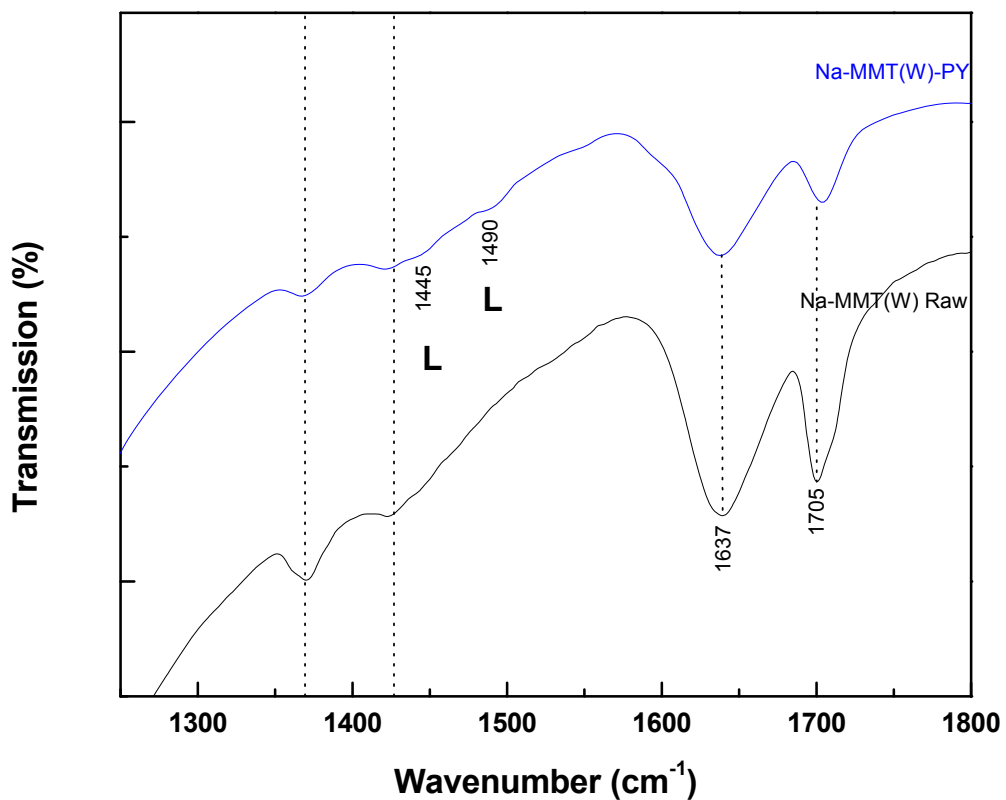


Figure 74 FTIR comparison of Na⁺-MMT (Wyoming deposit) raw material [Na-MMT(W) Raw] and pyridine adsorption [Na-MMT(W) -PY] (KBR support).

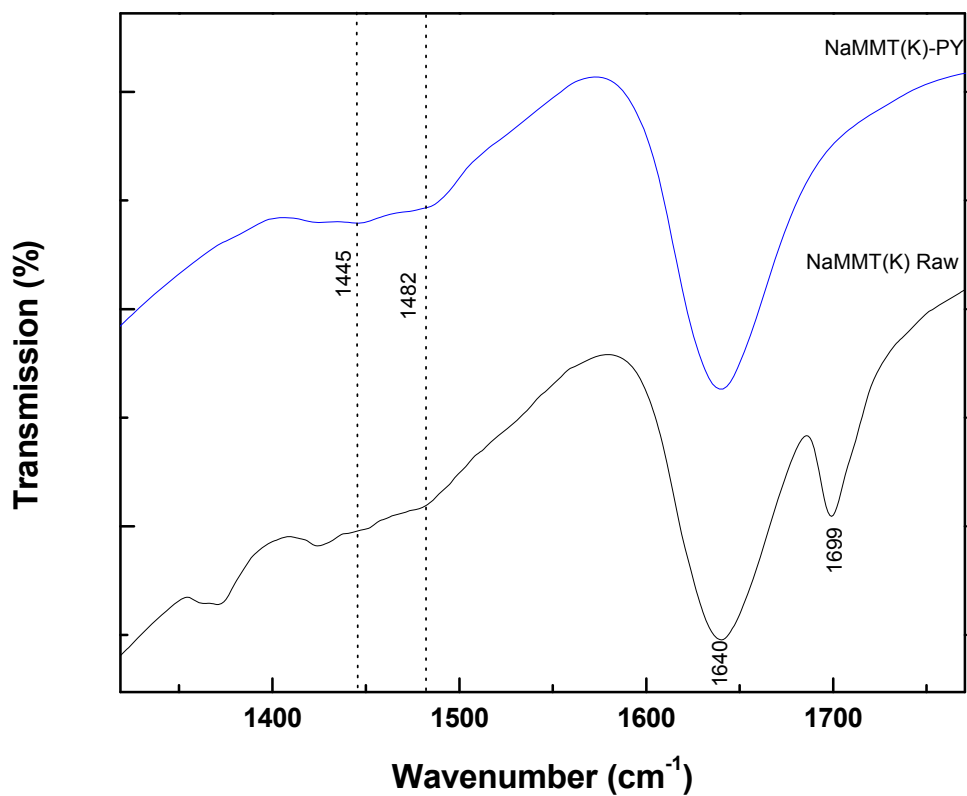


Figure 75 FTIR comparison of Na⁺-MMT (Kunipia deposit) raw material [Na-MMT(K) Raw] and pyridine adsorption [Na-MMT(K) -PY] (KBR support).

Synthetic zeolite, Faujasite (FAU)

FTIR pyridine adsorption spectra for Valfor CP300-35 (H^+ -MOR) displayed a large amount of Brønsted and Lewis acids, in accordance with the acidic characteristic of this zeolite.

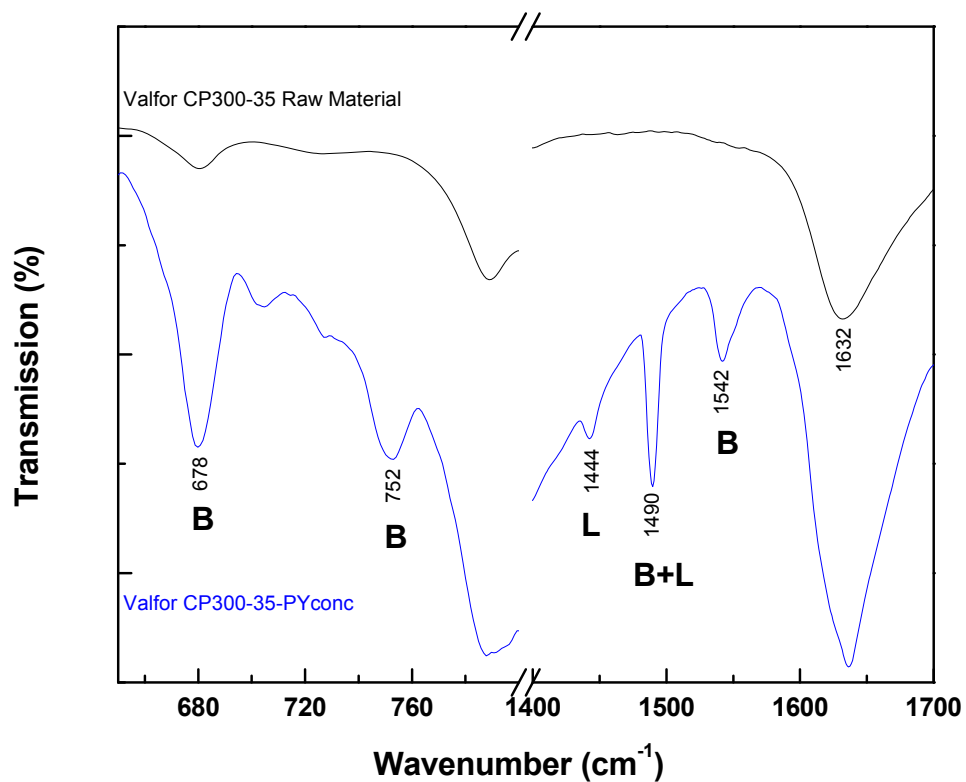
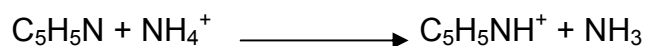


Figure 76 FTIR comparison of Valfor CP300-35 (H^+ -MOR) raw material [Valfor CP300-35Raw] and pyridine adsorption [Valfor CP300-35-PY] (KBR support).

Synthetic Zeolite, Mordenite (MOR)

Three mordenites were evaluated by this method: CBV21A (NH₄⁺ and Na⁺-MOR) and zeolon® (Na⁺-MOR).

FTIR spectra of CBV21A (NH₄⁺-MOR) Si/Al = 9.5 revealed the presence of Brønsted acids by the pyridinium vibration at 681, 755, 1490, and 1546 cm⁻¹ in accordance to Serratosa *et al.*⁸⁹ The presence of these vibrations could be explained by the acidic character of NH₄⁺ cation present in the zeolite, rather than OH vibrations present in the framework. The unshared pair of electrons of pyridine acted as Lewis base when in contact with the empty orbital of the acidic proton from NH₄⁺, thus producing pyridinium.



The effect of the acidic proton was an important factor in the color change observed in thioindigo; however, due to a poor electronegative neighboring atom such as nitrogen, this proton was not as acidic and therefore could not withdraw electrons as strongly as, for example, other protons attach to an oxygen atom.

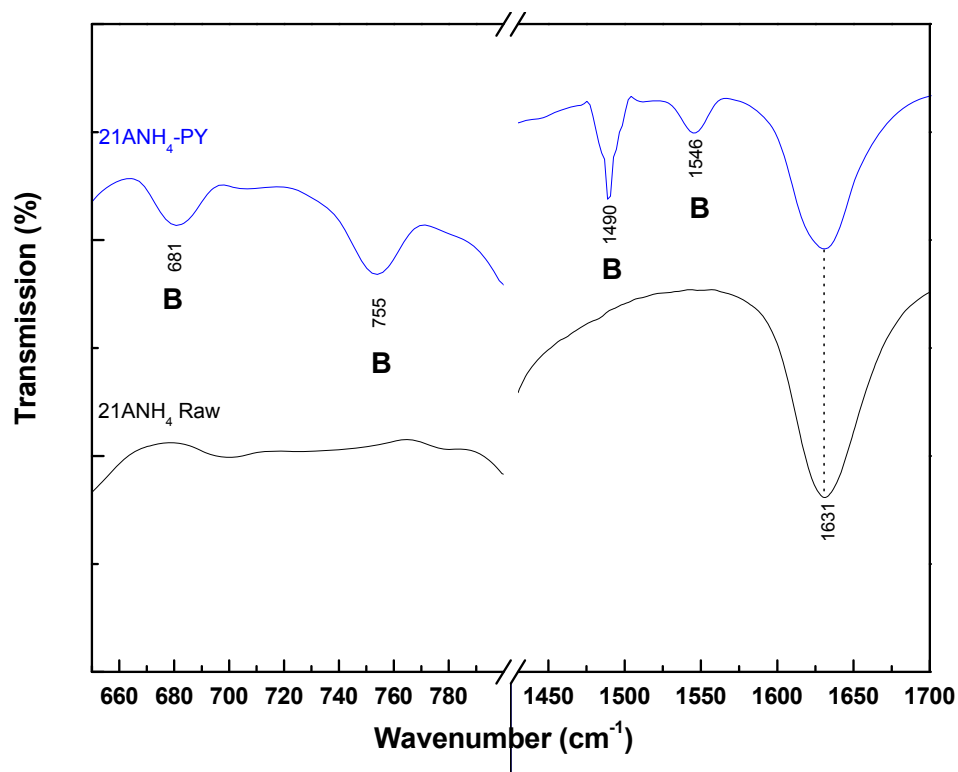


Figure 77 FTIR spectra of pyridine adsorption in CBV21A [NH_4^+ -MOR] (KBr support).

On the other hand, FTIR pyridine adsorption spectra of the Na^+ -MOR (cation exchanged form of CBV21A [NH_4^+ -MOR]) revealed the absence of almost all the Brønsted acids previously seen in the NH_4^+ -MOR. Thus, the previous hypothesis was confirmed in this experiment where the origin of the Brønsted acids in NH_4^+ -MOR was related primarily to the acidic proton of NH_4^+ rather than the framework. The Lewis acid present in the framework could be related to some residual extraframework aluminum; however, due to the low concentration of aluminum ($\text{Si}/\text{Al} = 9.5$) this may not be enough to display a drastic color change.

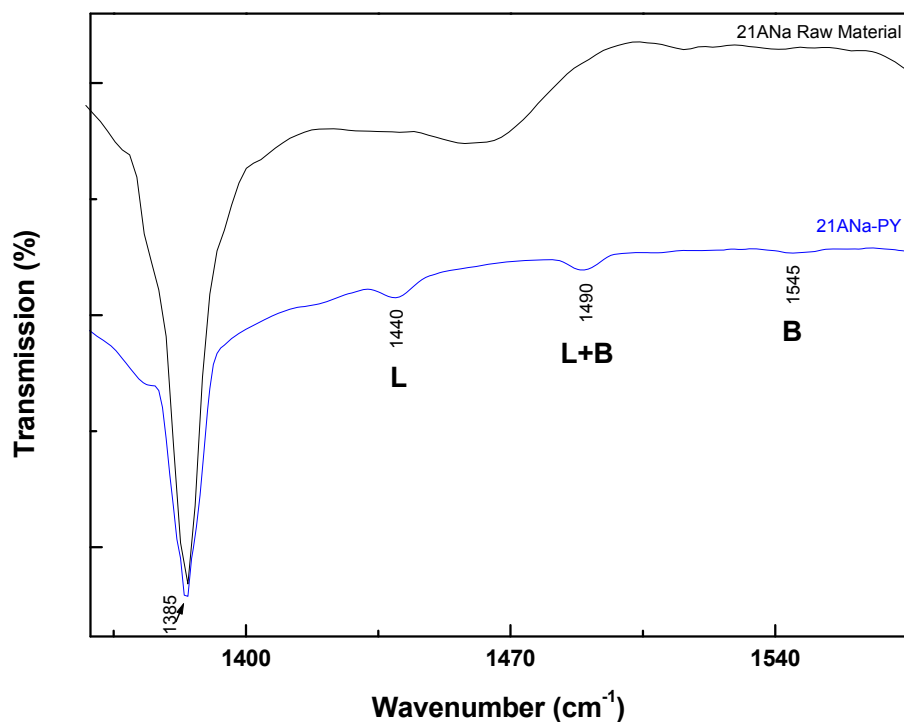


Figure 78 FTIR spectra of pyridine adsorption in CBV21A [Na⁺-MOR] (KBr support).

FTIR spectra of Zeolon[®] (Na⁺-MOR) with a Si/Al = 7.31 revealed a large concentration of Brønsted acids in the framework. The large aluminum substitution in the framework correlates with these findings, where sodium cations and Brønsted acids neutralized this imbalance charge; however, due to the large amount of sodium, color change is only purple instead of blue, which would be the case when a high concentration of protons were available.

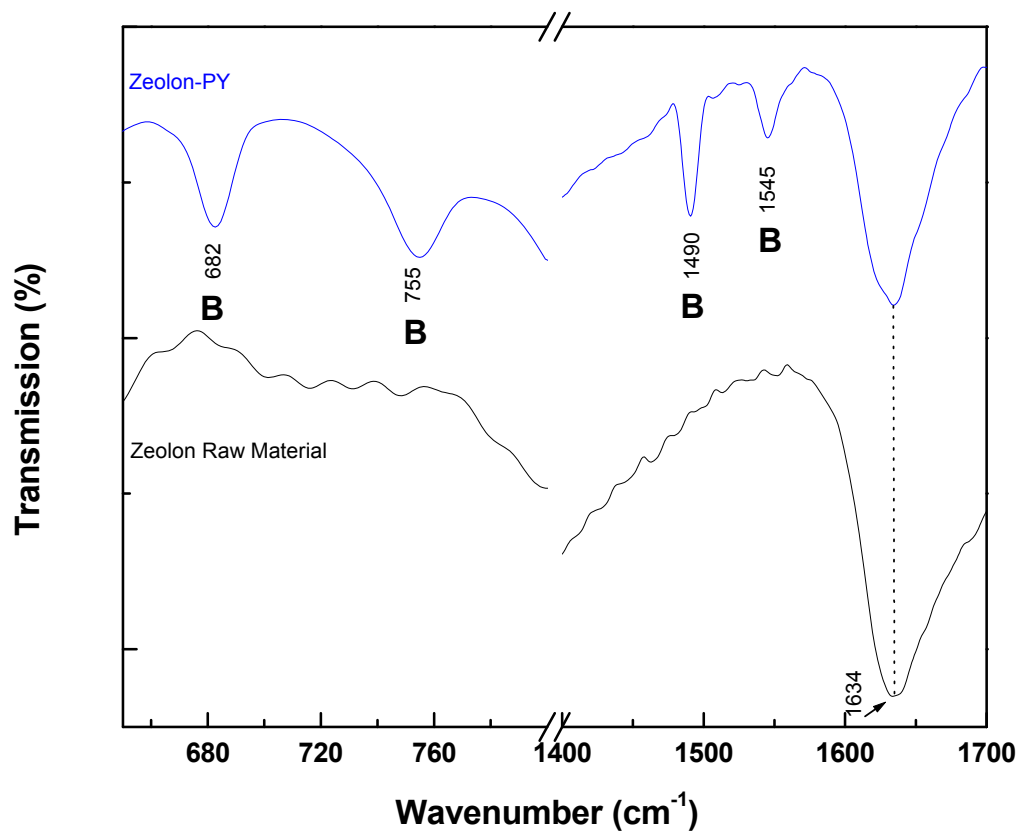


Figure 79 FTIR spectra of pyridine adsorption in Zeolon[®] (Na⁺-MOR) with KBr support.

4.4.3 Inorganic Host Materials Treated with Thioindigo

Palygorskite - Thioindigo Interaction

Palygorskite interaction with thioindigo unheated revealed the carbonyl vibration mode at 1655 cm^{-1} in agreement with thioindigo C=O vibration reported by Tatsch *et al.*⁹⁰ However, a downshift of this vibration mode to 1628 cm^{-1} was observed when the sample was heated at 413K for nine hours. This could be tentatively assigned to C=O stretching mode of thioindigo, with a possible downshifting from 1656 cm^{-1} , due to dye-clay interaction. This behavior has also been detected in indigo/palygorskite mixtures.⁹¹

The origin of the vibration mode at 1697 cm^{-1} in Figure 80 was not well understood, mostly because sometimes it would not disappear even under heating conditions. Therefore a change of support from KBr to mineral oil was pursued. FTIR spectra showed the absence of this vibration mode when the sample was immersed in mineral oil. Hence, this vibration mode could be related to the hygroscopic KBr support, nevertheless KBr water vibration mode was at 1638 cm^{-1} . The higher frequency of the water vibration could be correlated to the clay loosely bound water from the KBr support. The use of mineral oil avoided this misleading vibration mode, and also was able to capture the mixtures in their highest excitation state, as shown later in this section.

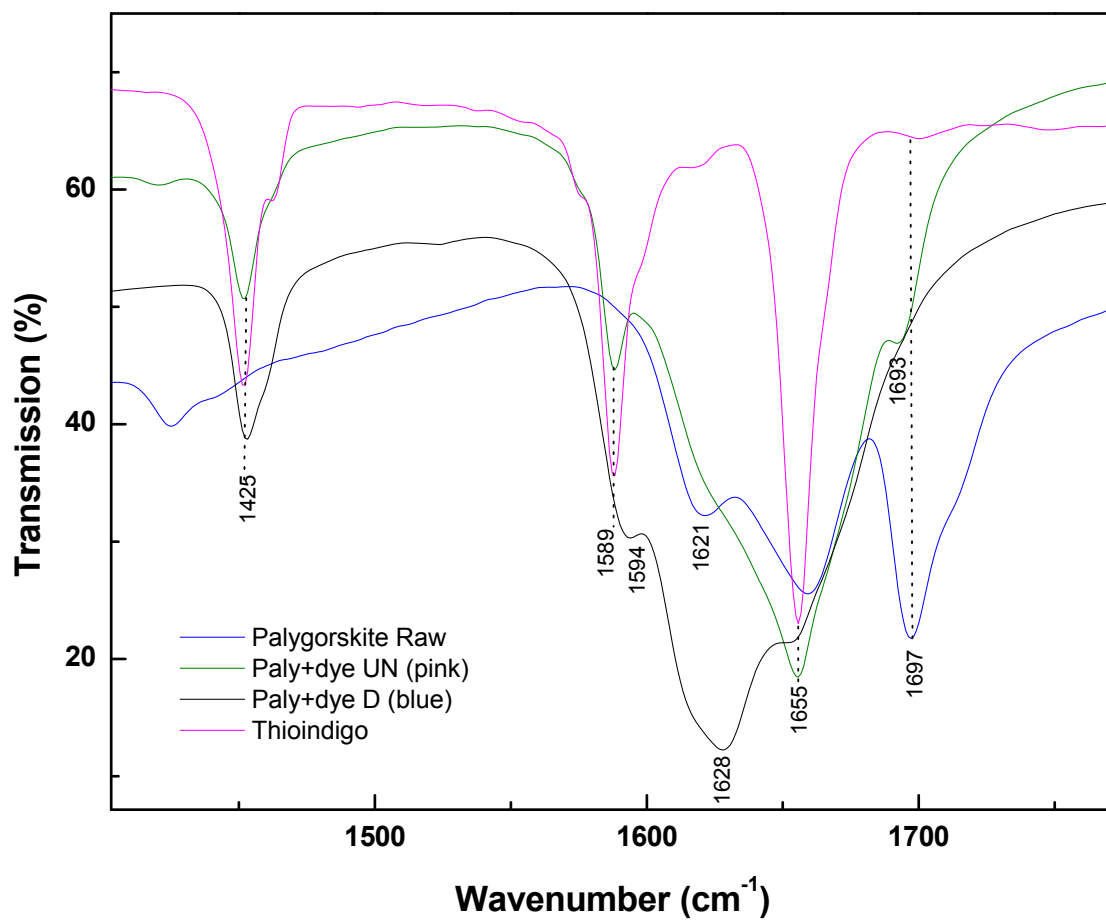


Figure 80 FTIR spectra of palygorskite raw material, thioindigo raw material, 0.5 mol % thioindigo/palygorskite mixture heated (paly+dye H), and unheated (paly+dye UN). All of the above mentioned samples mixed with KBr as support.

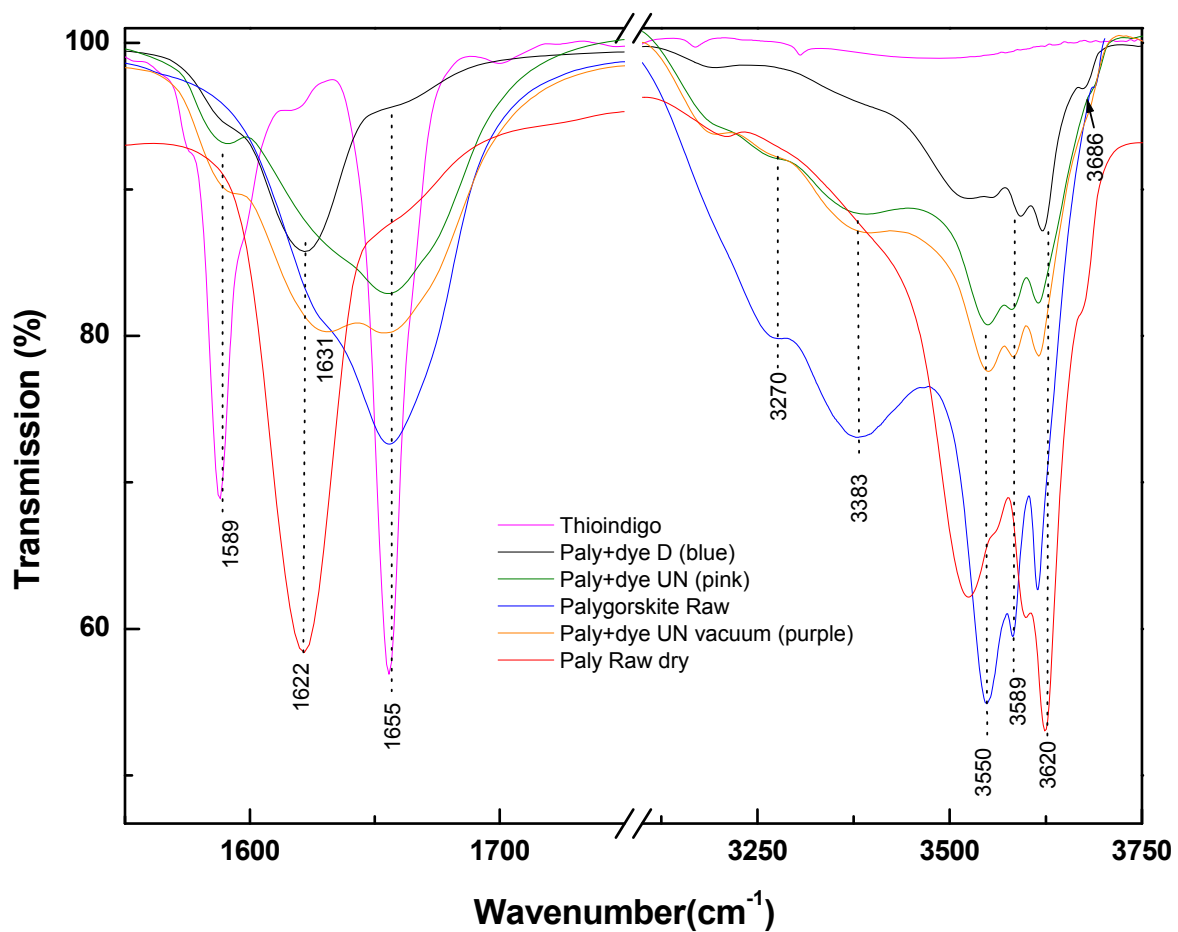


Figure 81 FTIR spectra of palygorskite raw material, thioindigo raw material, 0.5 mol % thioindigo/palygorskite mixture heated [paly+dye D (blue)], unheated [paly+dye UN (pink)] and vacuum [paly+dye UN vacuum (purple)]. Mineral oil as support.

Sepiolite - Thioindigo Interaction

In the case of sepiolite, 0.5 mol % thioindigo/sepiolite heated at 413K for nine hours displayed a magenta color at 1625 cm^{-1} vibration mode related to C=O-LAS, this peak was also assigned to the downshift of thioindigo free C=O at 1655 cm^{-1} . The disappearance of the 1655 , 3270 , and 3411 cm^{-1} water vibration modes of sepiolite related this interaction to the direct binding to LAS in the absence of water. Moreover, the downshift of the structural water (Mg-OH_2) from 3566 to 3543 cm^{-1} and hydroxyl groups (Mg-OH) from 3686 to 3677 cm^{-1} , could be an indicative of a less interaction of these sites with the zeolitic water. This displacement was also observed by E. Mendelovici⁹² where the 3590 cm^{-1} peak shifted to 3570 cm^{-1} on heating. Moreover, this hypothesis is confirmed in Figure 82, where the heated mixture was left to hydrate outside the desiccator (deep purple color), displaying the shift of 3000 cm^{-1} region peaks to their original positions, additionally the 1625 cm^{-1} vibration mode was shifted back slightly to higher frequencies at 1631 cm^{-1} . These changes could be related to the less interaction of thioindigo C=O with the active sites due to the hydration of the site C=O---H(OH)-LAS).

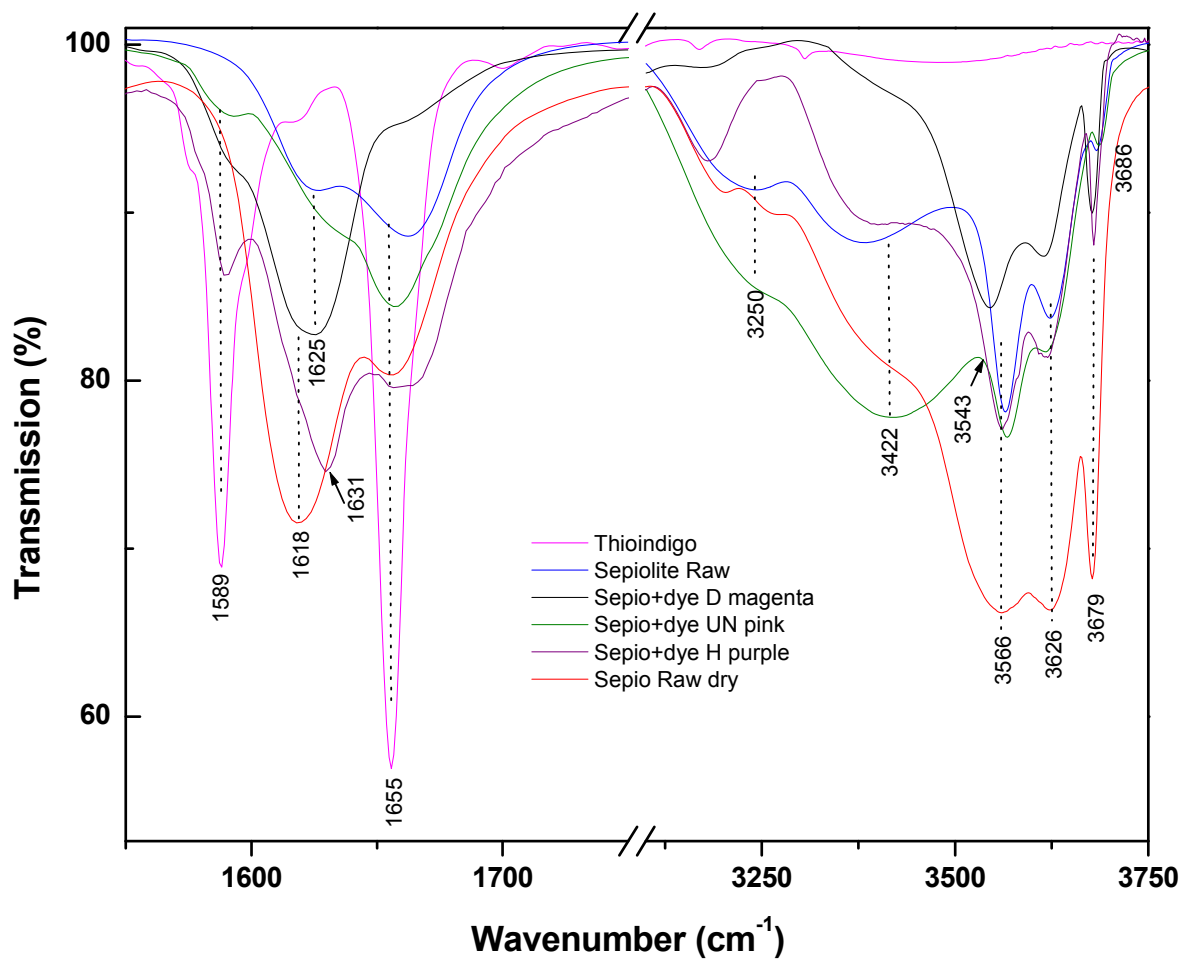


Figure 82 FTIR spectra of sepiolite raw material, thioindigo raw material, 0.5 mol % thioindigo/sepiolite mixture heated (sepio+dye D magenta) unheated (sepio+dye UN pink) and heated mixture hydrated (sepio+dye D purple). Mineral oil as support.

Ca²⁺-MMT – Thioindigo Interaction

The FT-IR spectra of Ca²⁺-MMT (Bentolite L[®] and Texas deposit) mixed with 0.5 mol % thioindigo and heated at 413K for nine hours shows no free C=O peak at 1655 cm⁻¹, and a C=O⁻LAS in 1632 cm⁻¹. This behavior is similar to palygorskite/thioindigo mixtures when heated or exposed to vacuum. Solids exposed to lower pressure exhibited water removal from the Lewis active sites (LAS), leaving direct interaction of the carbonyl group to the LAS. However, the blue color observed was not stable when exposed to moisture from the air (desiccator samples displayed no color change). Besides the open layer structure typical of montmorillonite clays, the susceptibility of Ca²⁺ cation to hydration due to its characteristic high hydration energy ($\Delta H_{\text{hyd}} = -1592$ KJ/mol) were two important factors in the instability of the color.

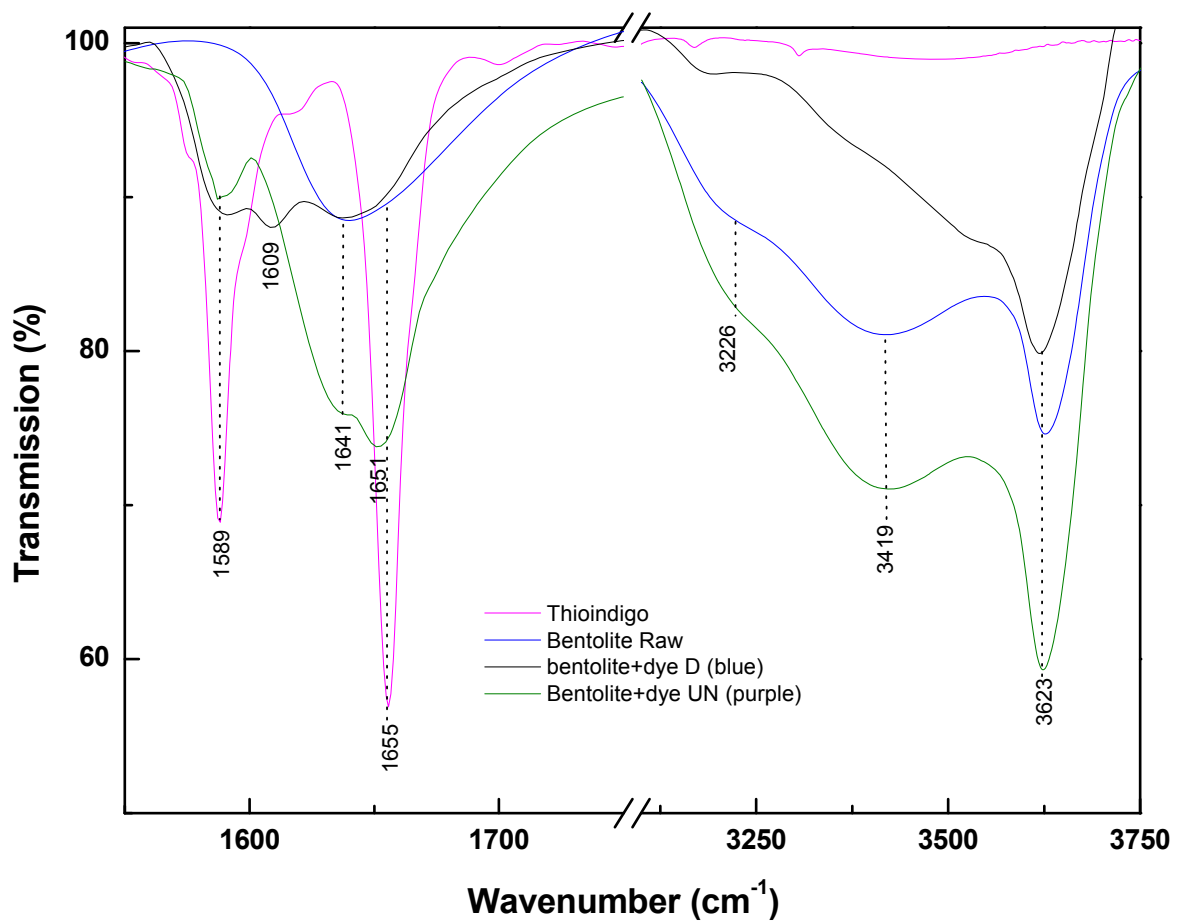


Figure 83 FTIR spectra of bentolite L[®] raw material, thioindigo raw material, 0.5 mol % thioindigo/bentolite L[®] mixture heated (bentolite L +dye D blue) and unheated (bentolite L+dye UN purple). Mineral oil as support.

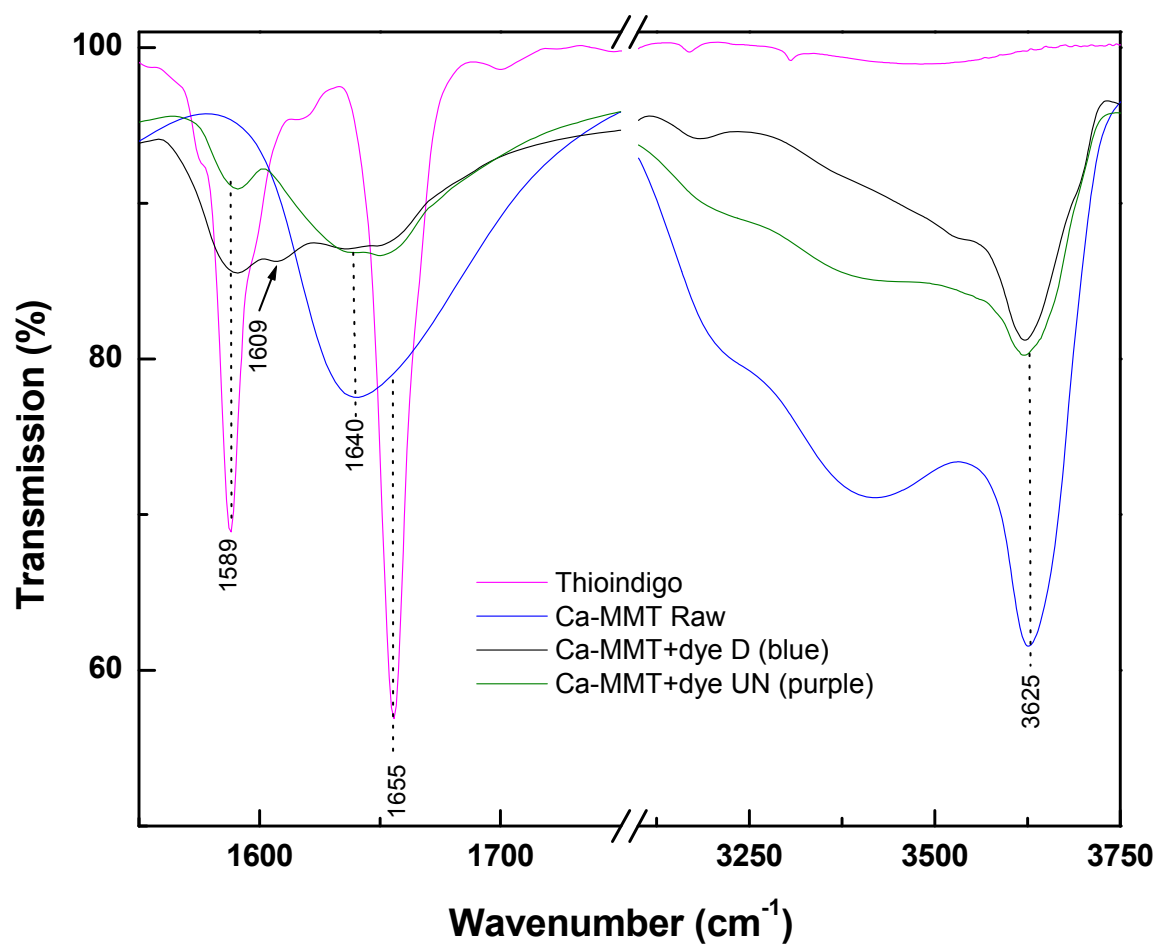


Figure 84 FTIR spectra of Ca-MMT (Texas deposit) raw material, thioindigo raw material, 0.5 mol % thioindigo/ Ca-MMT mixture heated (Ca-MMT +dye D blue) and unheated (Ca-MMT+dye UN purple). Mineral oil as support.

Na⁺-MMT- Thioindigo Interaction

For Na-MMT samples (Wyoming and Kunipia deposits), the FT-IR spectra shows a weak free C=O peak at 1655 cm⁻¹ and no water vibration at 1638 cm⁻¹.

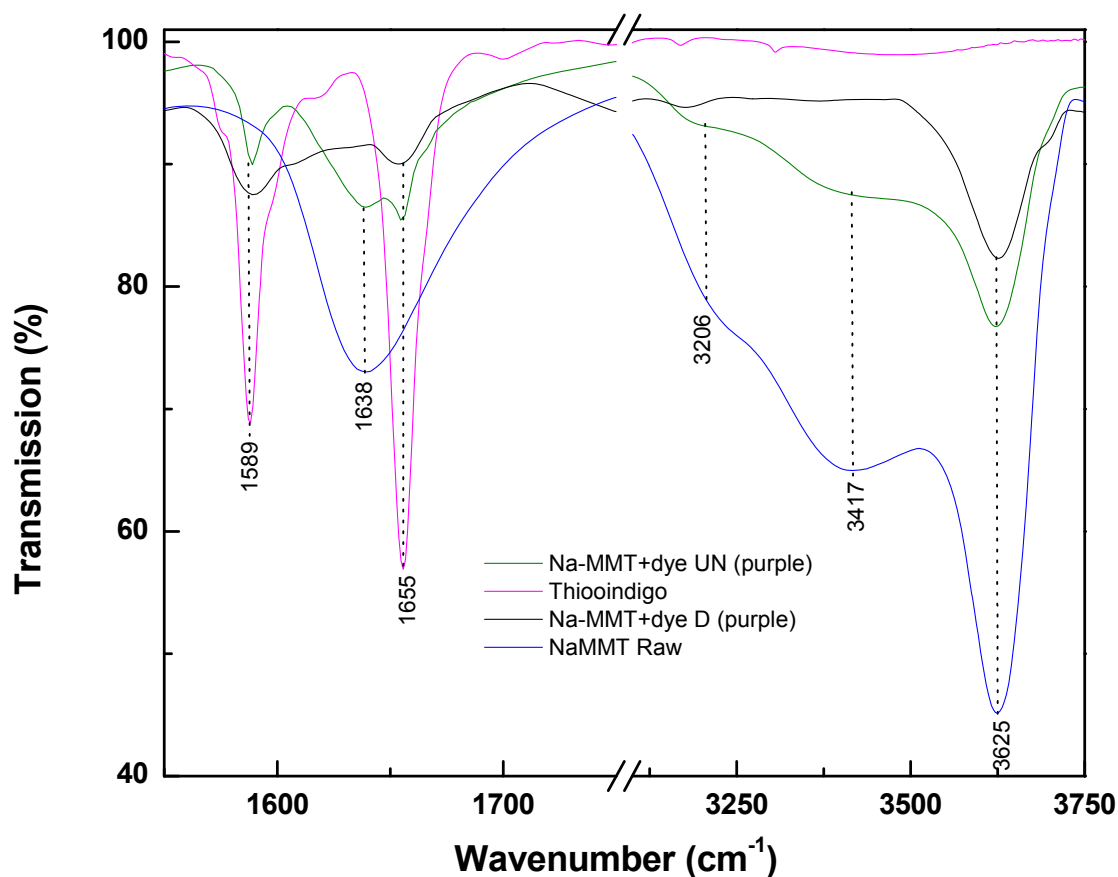


Figure 85 FTIR spectra of Na⁺-MMT (Wyoming deposit) raw material, thioindigo raw material, 0.5 mol % thioindigo/ Na⁺-MMT mixture heated (Na-MMT +dye D purple) and unheated (Na-MMT+dye UN purple). Mineral oil as support.

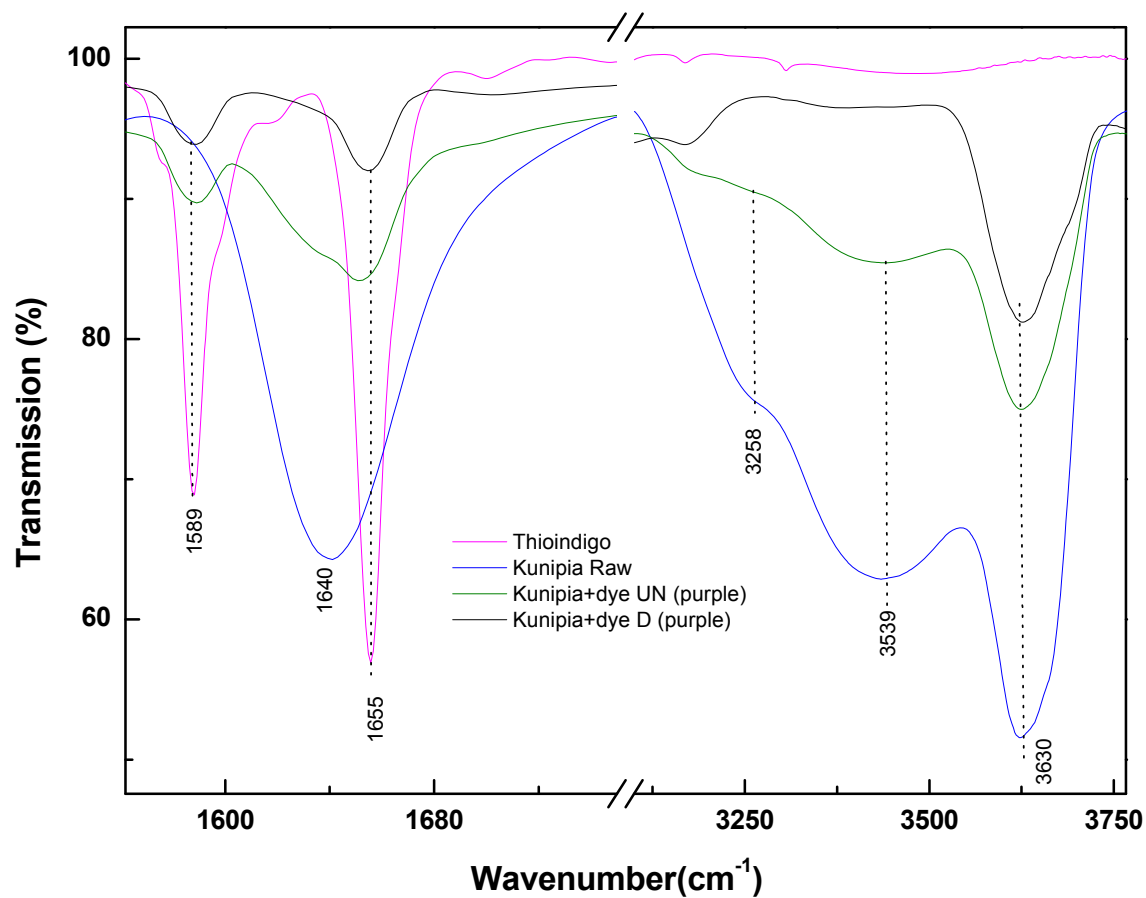


Figure 86 FTIR spectra of Na-MMT (Kunipia deposit) raw material, thioindigo raw material, 0.5 mol % thioindigo/ Na-MMT mixture heated (Na-MMT +dye D purple) and unheated (Na-MMT+dye UN purple). Mineral oil as support.

NaY(FAU) – Thioindigo Interaction

FTIR spectra of NaY (Si/Al = 2.5) revealed the displacement of C=O (1655 cm^{-1}) vibration mode to lower frequencies when 0.5 mol % thioindigo / zeolite unheated (NaY+dye UN pink) was exposed to thermal treatment at 413K for nine hours (NaY+dye D purple). Re-appearance of free C=O at 1655 cm^{-1} was detected when NaY+dye D purple was left to rehydrate (data not shown in Figure 87).

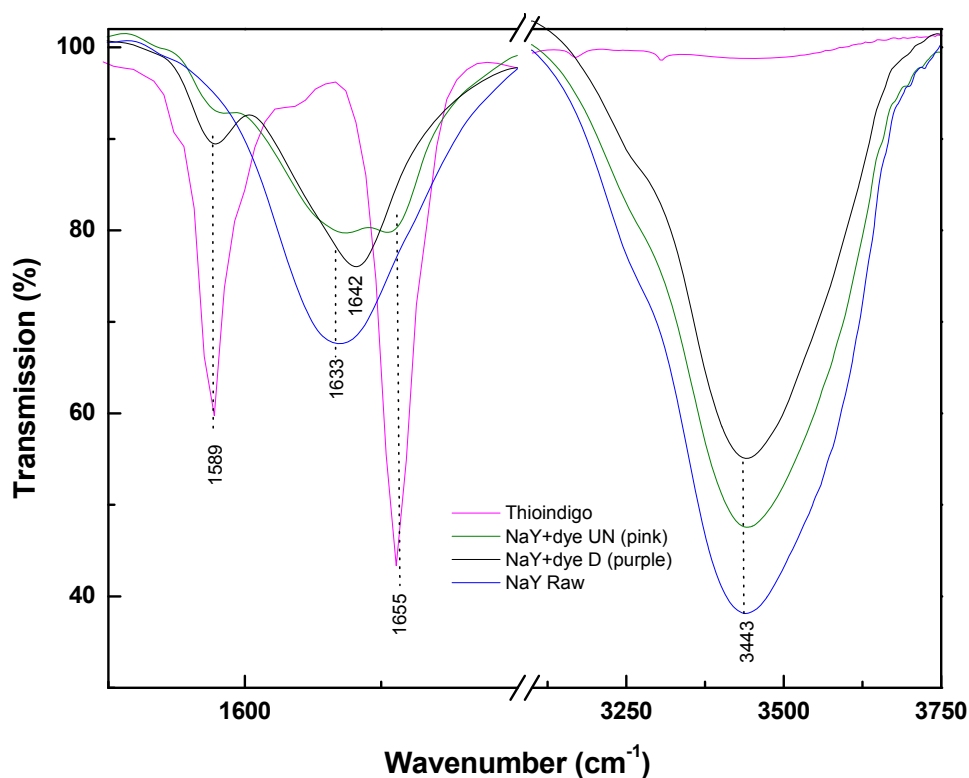


Figure 87 FTIR spectra of NaY raw material, thioindigo raw material, 0.5 mol % thioindigo/ NaY mixture heated (NaY +dye D purple) and unheated (NaY +dye UN red). Mineral oil as support.

As mentioned before, no Brønsted or Lewis acids were reported in zeolite NaY; therefore, color change from pink to purple of thioindigo-NaY mixture is considered to take place through sodium (a weak Lewis acid) interaction with carbonyl group ($\text{C}=\text{O} \cdots \text{Na}^+$). The high aluminum substitution ($\text{Si}/\text{Al} = 2.5$) indicated a large amount of sodium to compensate the negative charge in the framework; therefore, this zeolite had poor stability when exposed to moisture due to the high hydration energy of sodium ion ($\Delta H_{\text{hyd}} = -405 \text{ KJ/mol}$)⁶¹. A similar effect was noticed by Yoon *et al.*⁹³ with immobilized complexes inside NaY zeolite and moisture exposure.

Valfor CP300-35 (H^+ -FAU) - Thioindigo Interaction

Pyridine adsorption revealed a high concentration of Brønsted and small amount of Lewis acids in the zeolite (see Figure 76); moreover, the downshift of thioindigo $\text{C}=\text{O}$ to 1643 cm^{-1} could indicate a possible interaction ($\text{C}=\text{O} \cdots \text{H}^+$), mainly due to the strong acidity of hydrogen ion. High aluminum substitution ($\text{Si}/\text{Al} = 4.00$) indicated a large amount of protons to compensate the negative charge in the framework; therefore, this zeolite had poor stability when exposed to moisture due to the high hydration energy of hydrogen ion⁶¹. A similar effect was noticed by Yoon *et al.*⁹³ with immobilized complexes inside NaY zeolite and moisture exposure.

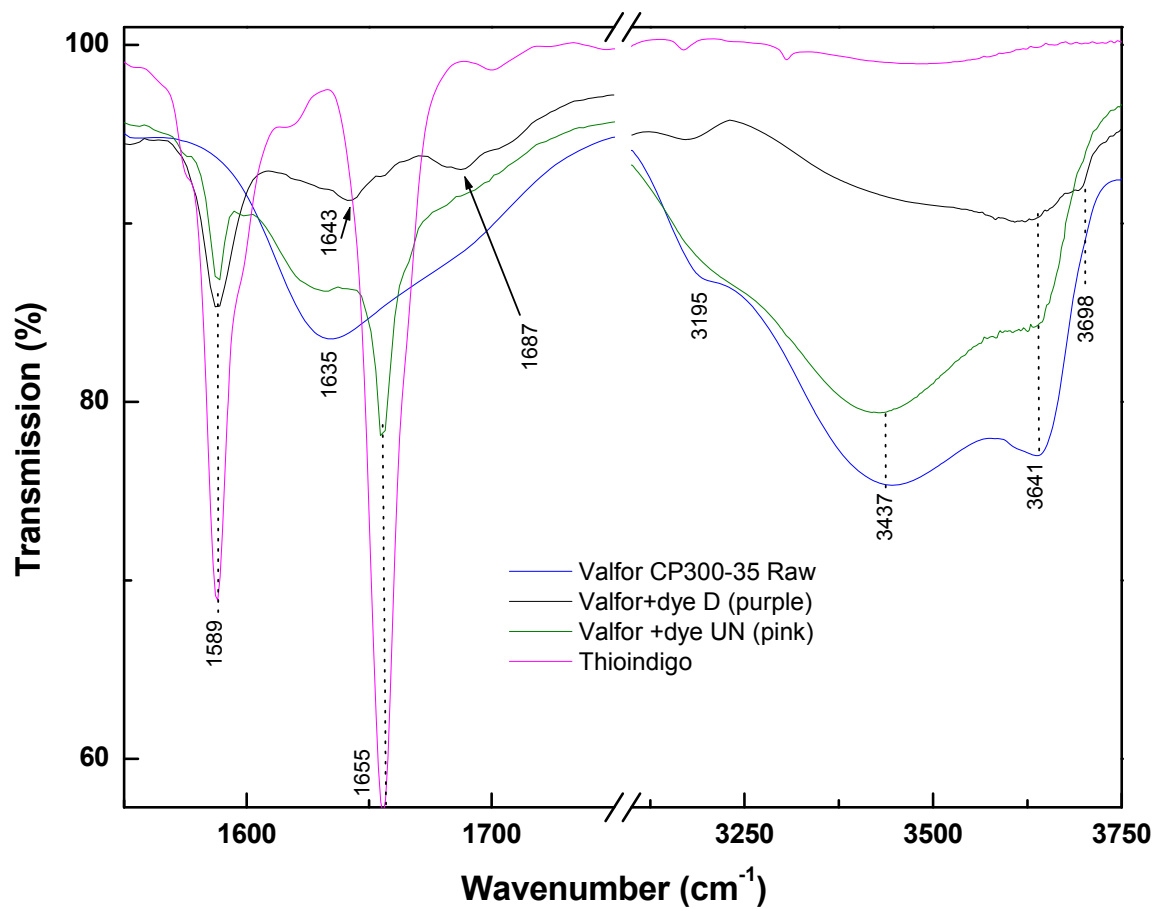


Figure 88 FTIR spectra of Valfor CP300-35 raw material, thioindigo raw material, 0.5 mol % thioindigo/Valfor mixture heated (Valfor +dye D purple), and hydrated (Valfor +dye UN pink). Mineral oil as support.

Na⁺ - MOR (Zeolon[®]) – Thioindigo Interaction

FTIR spectra of zeolon[®] revealed no disturbance in thioindigo C=O vibration mode at 1655 cm⁻¹. The band at 3631 cm⁻¹ corresponding to stretching OH mode showed a slight displacement to higher frequencies related to the removal of zeolitic water, since rehydration reversed this shift.

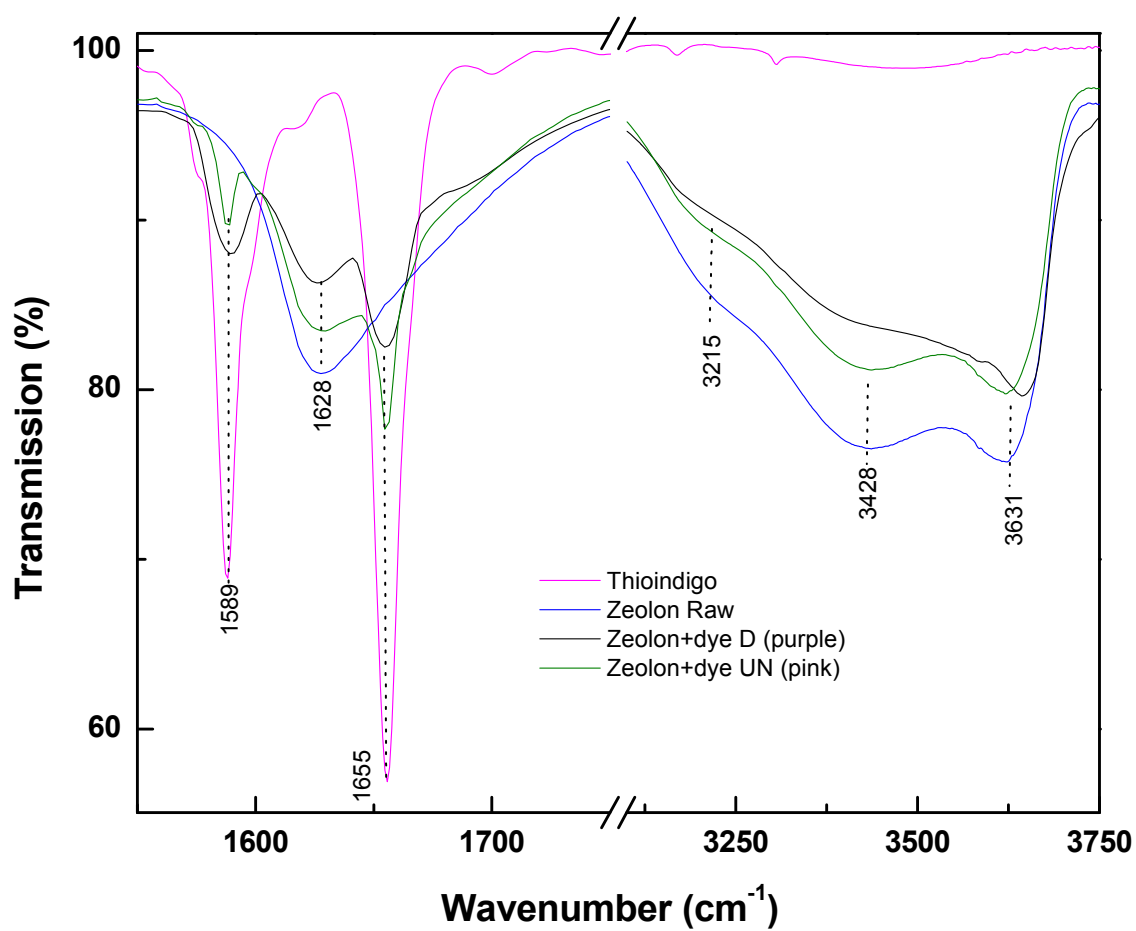


Figure 89 FTIR spectra of Zeolon[®] raw material, thioindigo raw material, 0.5 mol % thioindigo/Zeolon[®] mixture heated (Zeolon[®] +dye D purple), and hydrated (Zeolon[®] +dye UN pink). Mineral oil as support.

4.4.4 Cation Exchange Zeolite Treated with Thioindigo

FTIR spectra of exchanged mordenite (CBV21A) revealed a carbonyl shift to higher frequencies when heated. Water stretching vibration mode corresponding to zeolitic water, was observed to disappear after heat treatment. Moreover, a downshift of the bending water vibration mode at 1630 cm^{-1} was also observed. This behavior has been previously observed by Mendelovici *et al.*⁹²

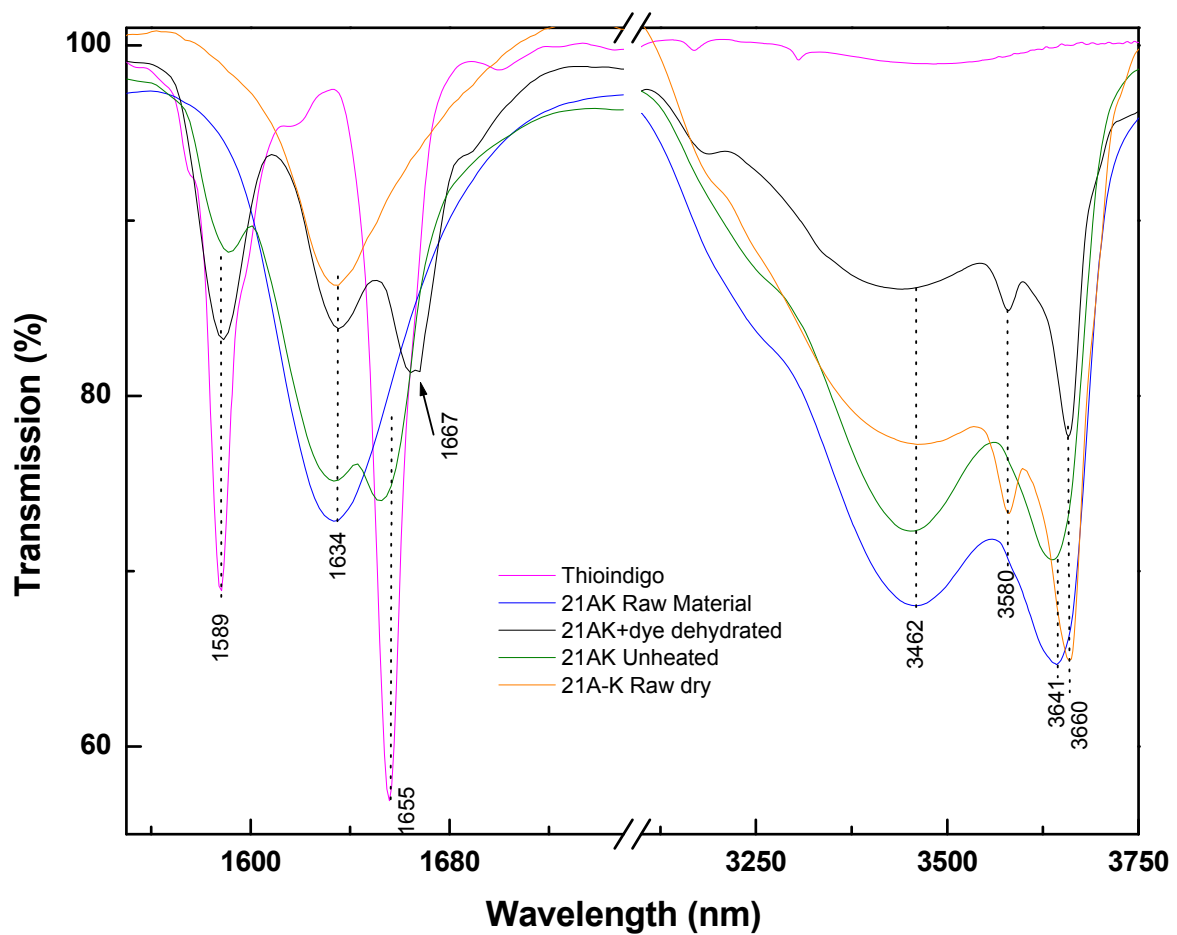


Figure 90 FTIR spectra of starting materials thioindigo and K^+ -MOR (21AK Raw) and 0.5 mol % thioindigo mixture with K^+ -MOR heated at 413K for nine hours (21AK+dye dehydrated) and unheated (21AK+dye Unheated) with Mineral Oil as support.

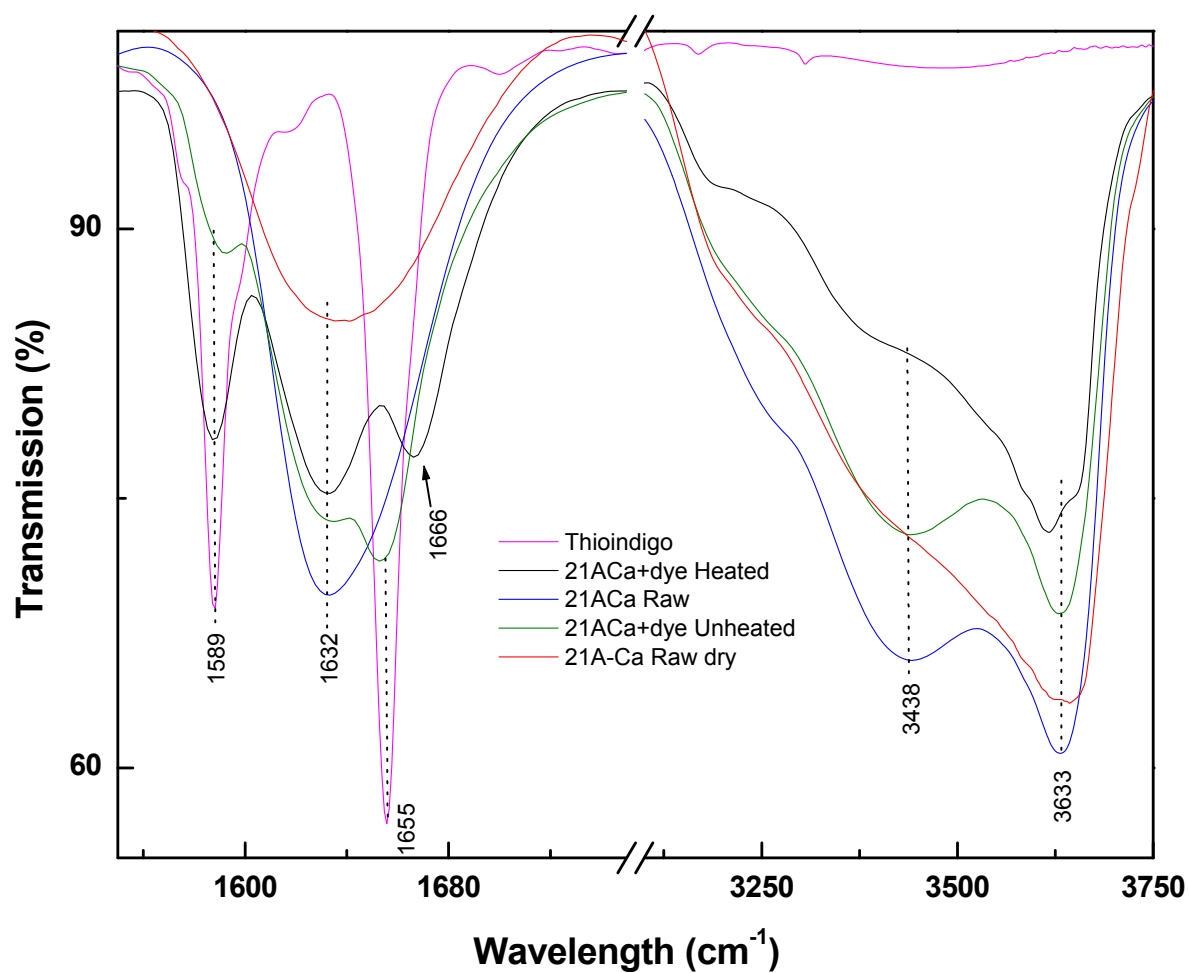


Figure 91 FTIR spectra of starting materials thioindigo and Ca²⁺-MOR (21ACa Raw) and 0.5 mol % thioindigo mixture with Ca²⁺-MOR heated at 413K for nine hours (21ACa+dye dehydrated) and unheated (21ACa+dye unheated) with Mineral Oil as support.

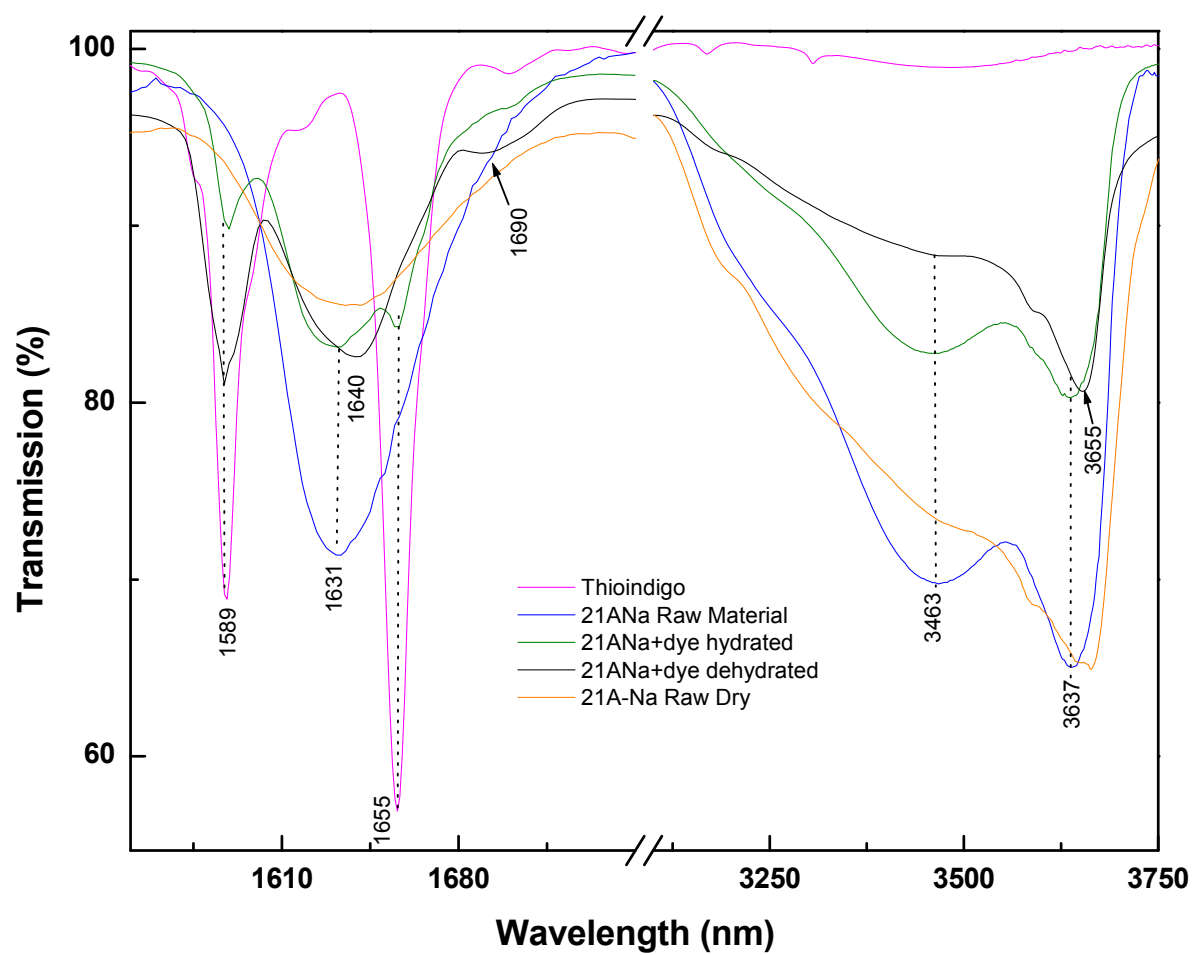


Figure 92 FTIR spectra of starting materials thioindigo and Na^+ -MOR (21ANa Raw) and 0.5 mol % thioindigo mixture with Na^{2+} -MOR heated at 413K for nine hours (21ANa+dye dehydrated) and unheated (21ANa+dye unheated) with Mineral Oil as support.

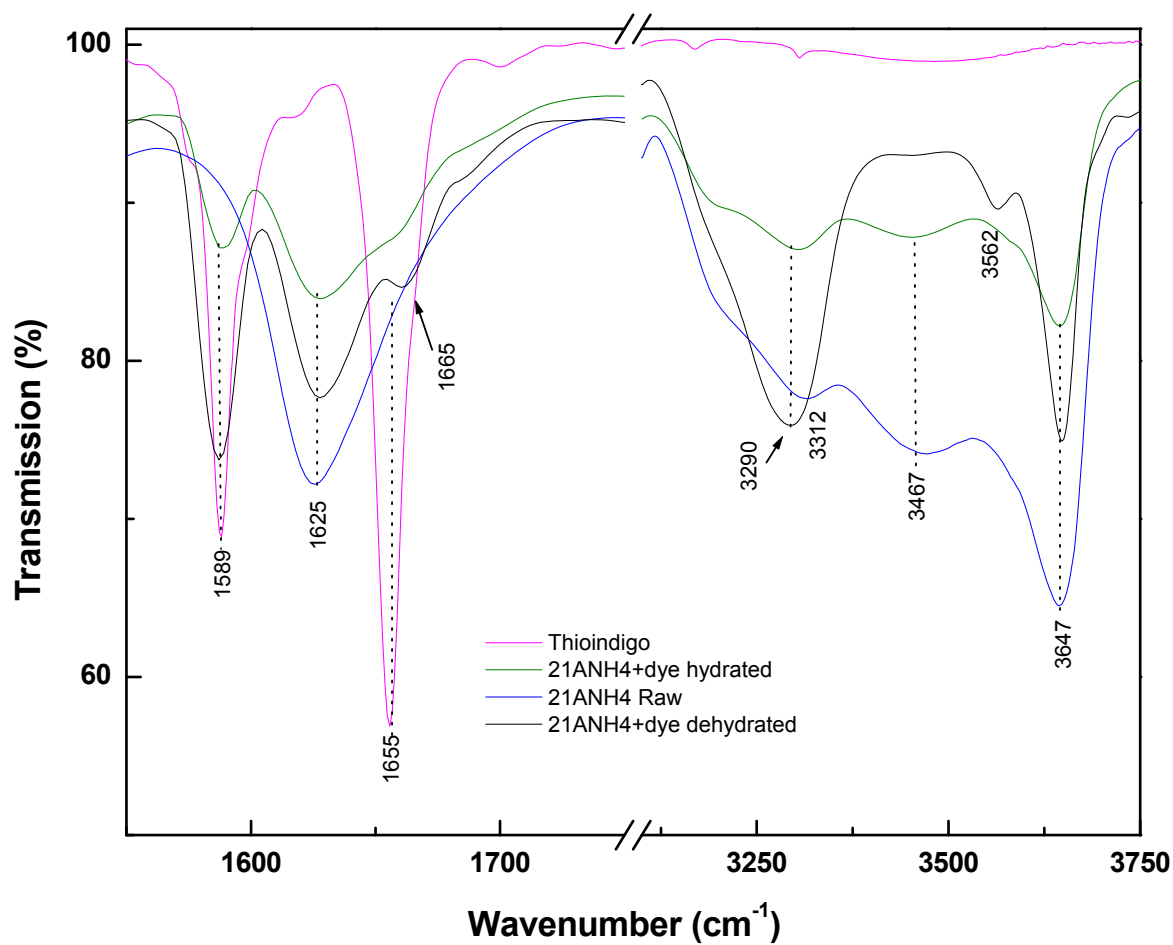


Figure 93 FTIR spectra of starting materials thioindigo and NH₄⁺-MOR (21ANH4 Raw) and 0.5 mol % thioindigo mixture with NH₄⁺-MOR heated at 413K for nine hours (21ANH4+dye dehydrated) and unheated (21ANH4+dye unheated) with Mineral Oil as support.

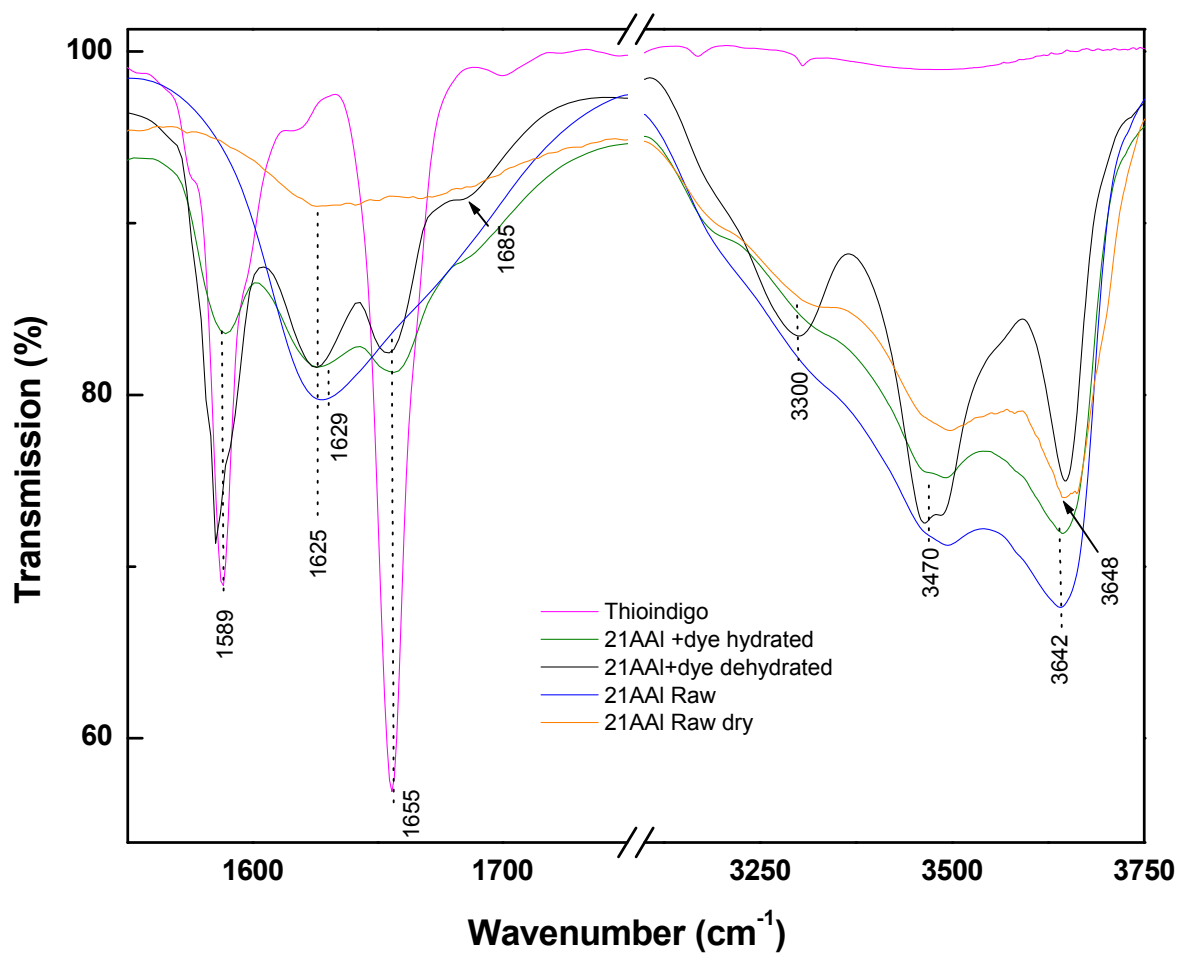


Figure 94 FTIR spectra of starting materials thioindigo and Al³⁺-MOR (21AAI Raw) and 0.5 mol % thioindigo mixture with Al³⁺-MOR heated at 413K for nine hours (21AAI+dye dehydrated) and unheated (21AAI+dye unheated) with Mineral Oil as support.

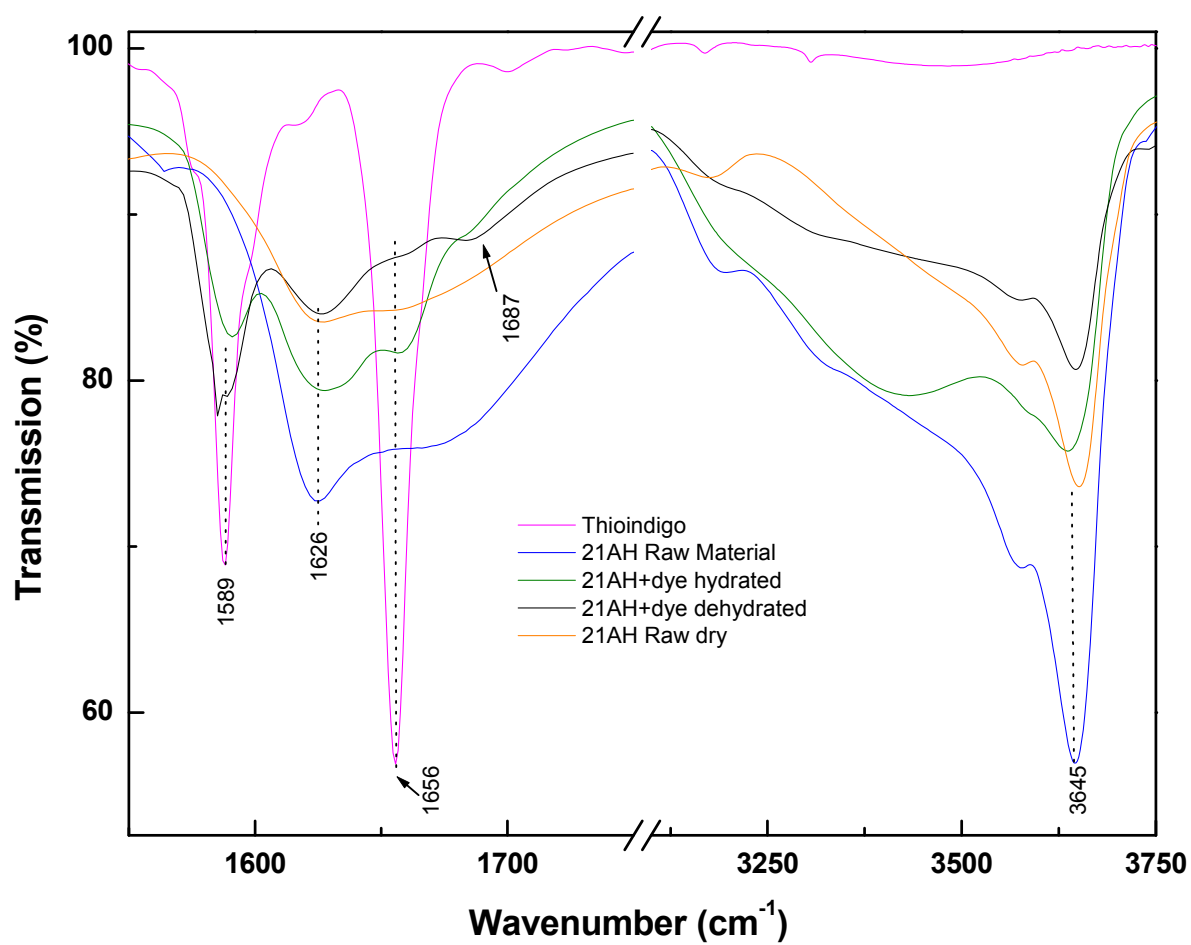


Figure 95 FTIR spectra of starting materials thioindigo and H⁺-MOR (21AH Raw) and 0.5 mol % thioindigo mixture with H⁺-MOR heated at 413K for nine hours (21AH+dye dehydrated) and unheated (21AH+dye unheated) with Mineral Oil as support.

4.5 Structural Analysis by X-ray Powder Diffraction

4.5.1 Thioindigo

X-ray powder diffraction of thioindigo was in agreement with the simulated triclinic unit cell, space group $P1$, investigated by H. von Eller⁹⁴ and built with Materials Studio v4.0 software. Thioindigo experimental reflections were slightly off the simulated structure. Lattice parameters adjustment should be performed in order to fit the simulated structure better to the experimental values.

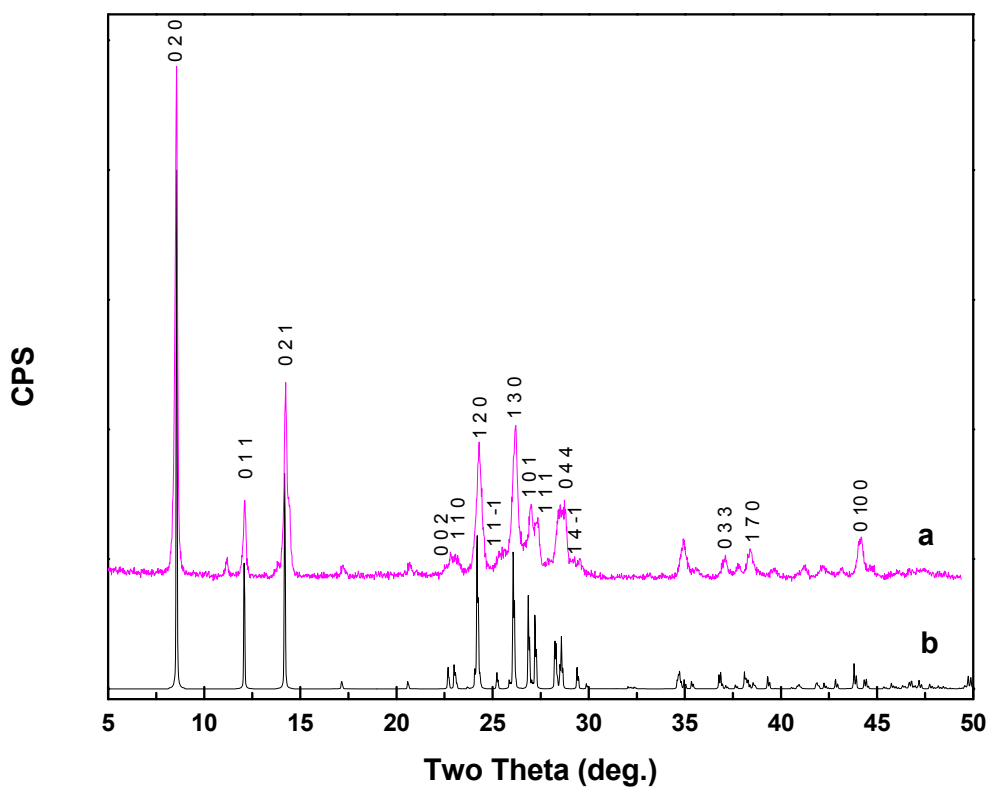


Figure 96 XRD pattern comparison of (a) thioindigo raw material, (b) thioindigo - triclinic simulated by Materials Studio v4.0 software.

4.5.2 Inorganic Host Materials

Palygorskite and Sepiolite

Palygorskite crystallizes in a mixture of two polymorphs (orthorhombic and monoclinic unit cell),³⁹ confirmed by the reflections of its diffraction pattern. Moreover, trigonal α -quartz was identified as an impurity. In the case of sepiolite, a monoclinic unit cell was identified. Impurities such as trigonal calcite and α -quartz were observed. These impurities were confirmed by FTIR. (see Figure 61).

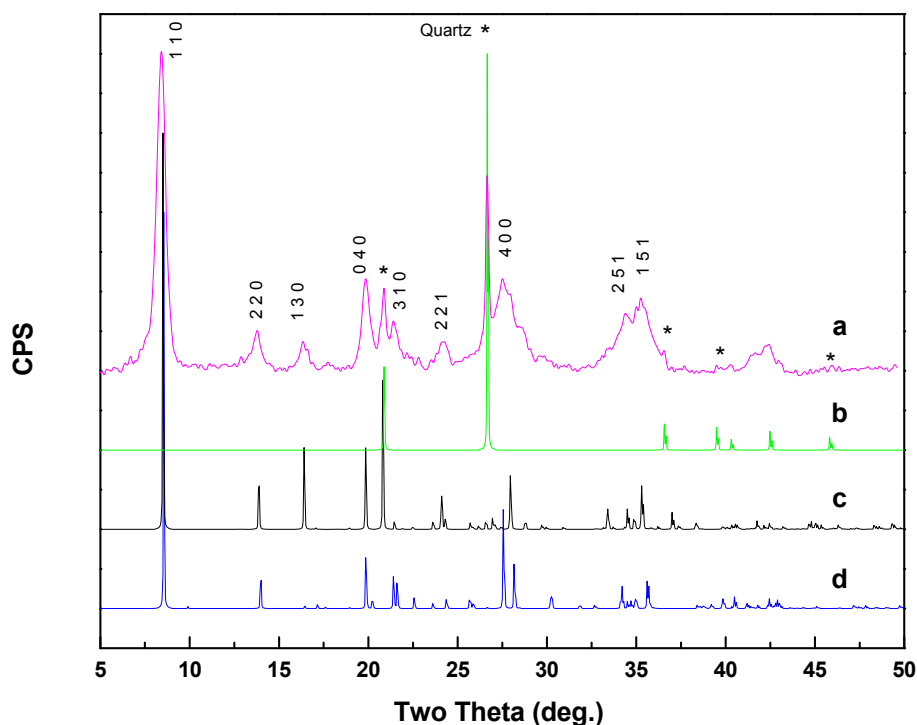


Figure 97 XRD pattern comparison of (a) palygorskite raw material, (b) palygorskite-orthorhombic (c) palygorskite -monoclinic and (d) α -quartz-trigonal. [Simulation of palygorskite and quartz unit cells by Cerius² accelrys software].

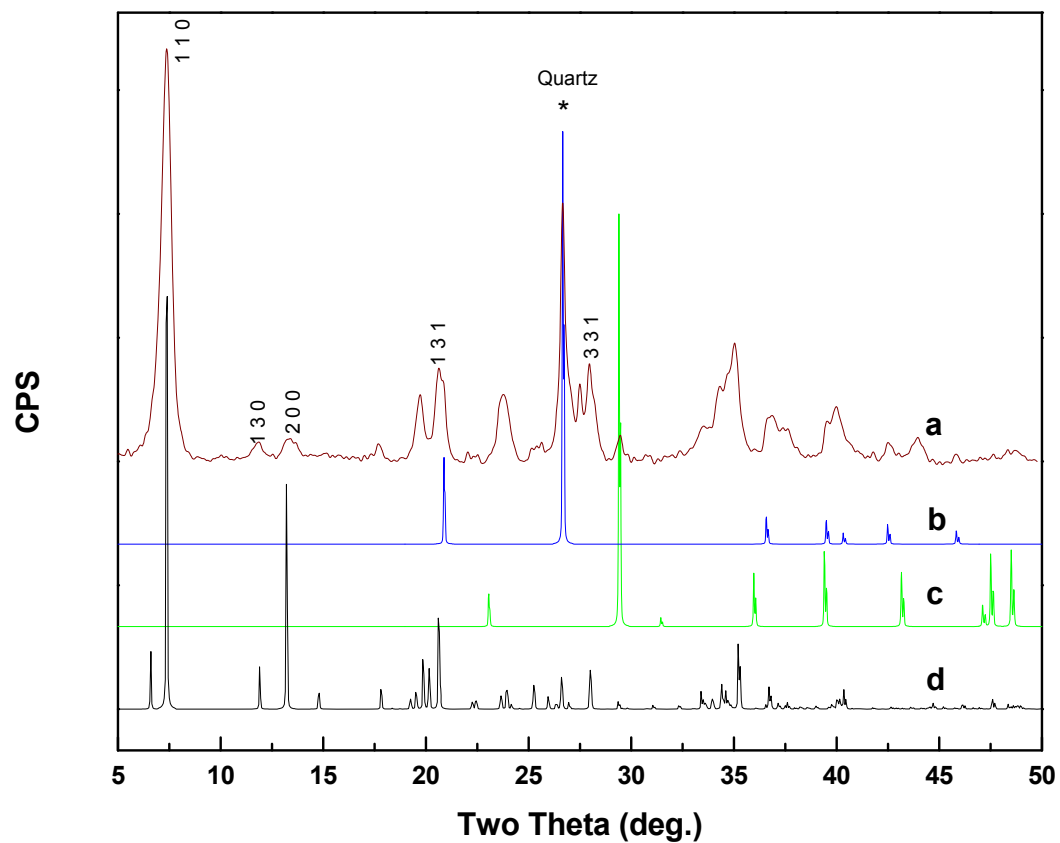


Figure 98 XRD pattern comparison of (a) sepiolite raw material, (b) α -quartz-trigonal, (c) calcite-trigonal, (d) sepiolite - monoclinic. [Simulation of sepiolite, quartz and calcite unit cells by Materials Studio v4.0 software].

Low Charge Swelling Natural Occurring Clays (Smectite Group)

Montmorillonite clays belong to the smectite group, which are characteristic of low framework charge and expandable or swelling layers.^{61,95} X-ray powder diffraction of these clays was of poor quality and reflections other than the basal were diffused. The basal reflection 001, corresponding to the most intense band, was identified in the four montmorillonite clays tested; however, d spacing values for this reflection was slightly higher for Ca-MMT than for Na-MMT. This behavior is probably in relation to the degree of hydration of the interlayer cations. Sodium with a $\Delta H_{\text{hyd}} = -405$ KJ / mol and a large ionic radius ($r = 0.1$ nm) generally requires one molecule of water to hydrate; calcium ($\Delta H_{\text{hyd}} = -1592$ KJ / mol), with a smaller ionic radius ($r = 0.05$ nm), requires two water molecules to hydrate.^{61,95} Consequently, Ca^{2+} -MMT would display larger d spacing values than Na^{+} -MMT. This behavior was observed in the samples tested as shown in Table 10. In the case of Wyoming deposit and based on the chemical analysis (appendix A) the larger d spacing value, when compared with Kunipia deposit, could be related to an equal amount of calcium in the interlayer. Therefore, Wyoming deposit could be considered a Na^{+} , Ca^{2+} -MMT clay.

Table 10 D spacing values for the studied montmorillonite clays.

SPECIMEN:	Ca^{2+} -MMT		$\text{Na}^{+}, \text{Ca}^{2+}$ -MMT	Na^{+} -MMT
	Bentolite L [®]	Texas deposit	Wyoming deposit	Kunipia deposit
Na moles*	-	-	1.18	0.105
Ca moles *	0.027	0.027	1.19	-
d spacing (Å)	13.3	13.6	11.1	10.4

*Values calculated from XRF measurements, appendix A.

Consistent with J. Thorez *et al.*⁹⁵, other reflections also observed in these montmorillonite clays were 8.5 Å (002), 5.7 Å (003), 4.2 Å (004), and 3.4 Å (005), as seen in Figure 99. However, some discrepancies were found for the 003 reflection which, in some references, has been reported to appear around 4.0 Å.²¹ Moreover, some impurities were identified in all samples such as α -quartz, calcite and mica⁹⁵. In the case of Kunipia deposit, no mica was identified; however, calcite and quartz were determined by FTIR, perhaps the levels were lower than 5% (XRD detection limit), and thus could not be detected by XRD.

The dioctahedral and trioctahedral character of montmorillonite clays is easily observed by the reflection 1.57 Å (060). Unfortunately, the experiments were only measured up to 50 degrees in the two theta scale; however, using FTIR, this characteristic could be confirmed.

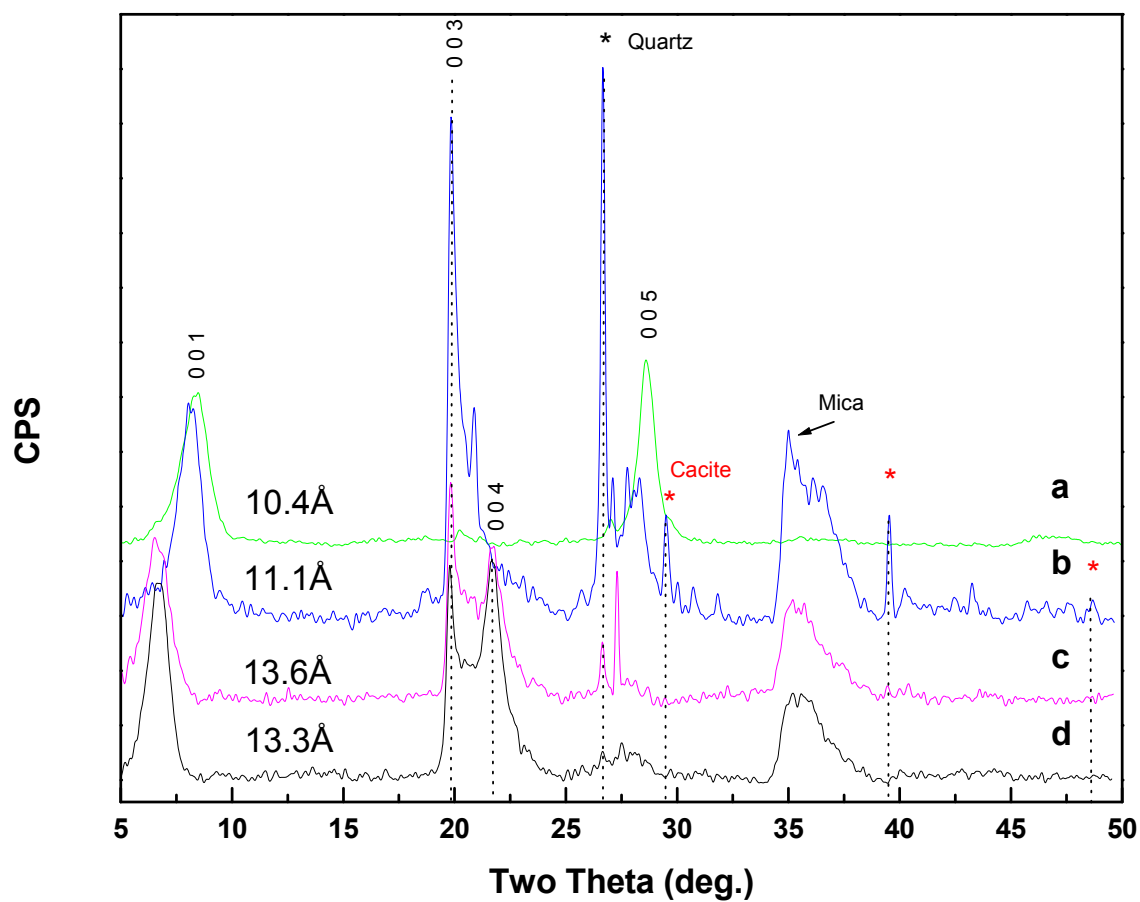


Figure 99 Powder X-ray diffraction pattern of (a) Na⁺-MMT (Kunipia deposit) raw material, (b) Na⁺-MMT (Wyoming deposit) raw material, (c) Ca²⁺-MMT (Texas deposit) raw material, and (d) Ca²⁺-MMT (bentolite L[®]).

Low Charge Synthetic Swelling Clays (Mica group)

X-ray powder diffraction for swelling Na⁺ micas (YN6, YN8 and Sodium Trisilic [Na-Ts]) displayed a strong symmetrical 001 reflection with d spacing values around 11 and 12.5 Å (as shown in Figure 100). These values were higher than the ones usually found in non-swelling natural micas (10 Å). The larger d-spacing was related to the introduction of a sodium cation instead of the potassium usually found in natural micas framework. Table 11 shows a comparison between concentration of ions and d-spacing of the Na⁺-Micas tested. D-spacing values are in agreement for YN6 and YN8, where at larger concentration of sodium, more displacement was observed. However, in the case of Na-Ts this effect was not observed.

A small 002 reflection was found in YN6 but not in YN8 and Na-Ts; this reflection is related to the dioctahedral character of the structure,⁹⁵ i.e. the substitution of trivalent atom in the octahedral sites. The absence of this reflection therefore is indicative of the trioctahedral character. This is also in agreement with the infrared spectrum of these samples (see Figure 65).

Table 11 d spacing values for the studied mica clays.

SPECIMEN:	Na ⁺ -Mica		
	YN6	NaTs	YN8
Na moles*	0.125	0.225	0.5
d spacing (Å)	12.3	11.6	12.5

* Values calculated from XRF measurements, appendix A.

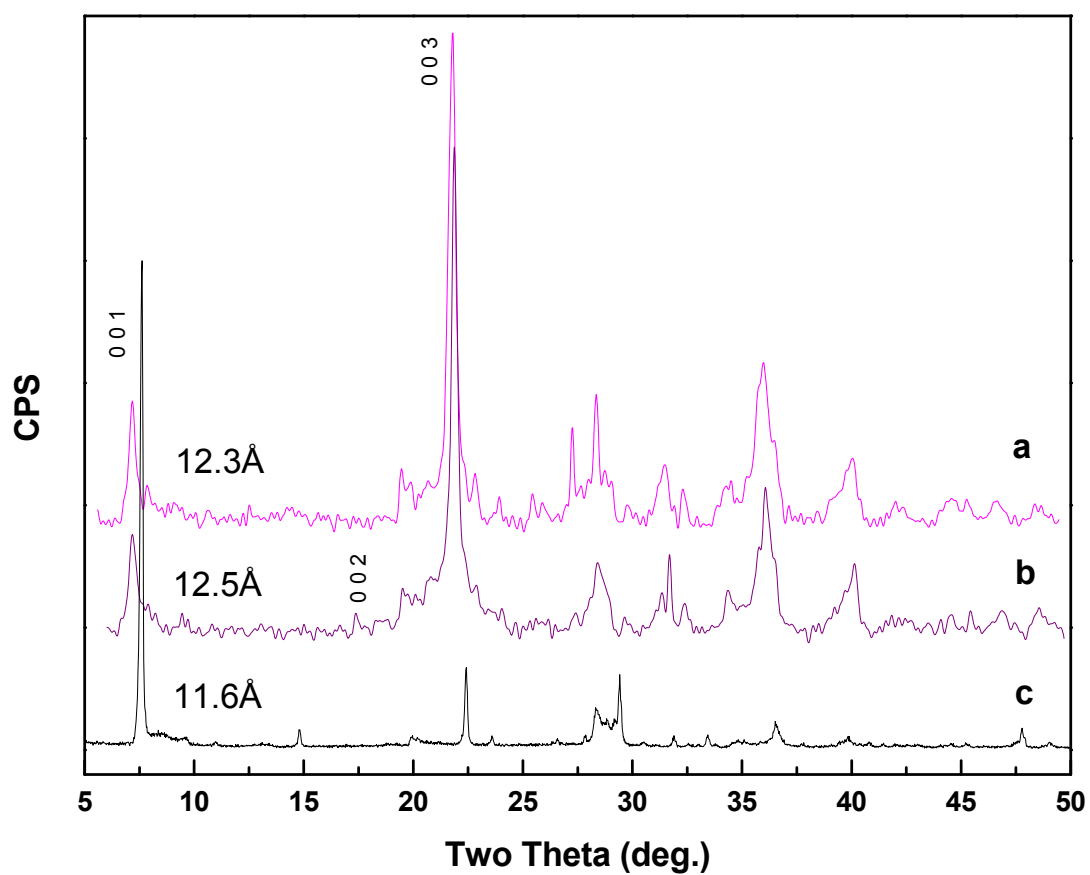


Figure 100 Powder X-ray diffraction pattern of (a) YN6 raw material, (b) YN8 raw material, and (c) Sodium Trisilic (Na-Ts) raw material.

Neutral Synthetic Talc

X-ray diffraction of Talc was identified by the index reflections reported by J. Thorez.⁹⁵ None of the crystallographic data available in the Inorganic Crystal Structure Database (ICSD) or Materials Studio v4.0 software gave a close match to these reflections.

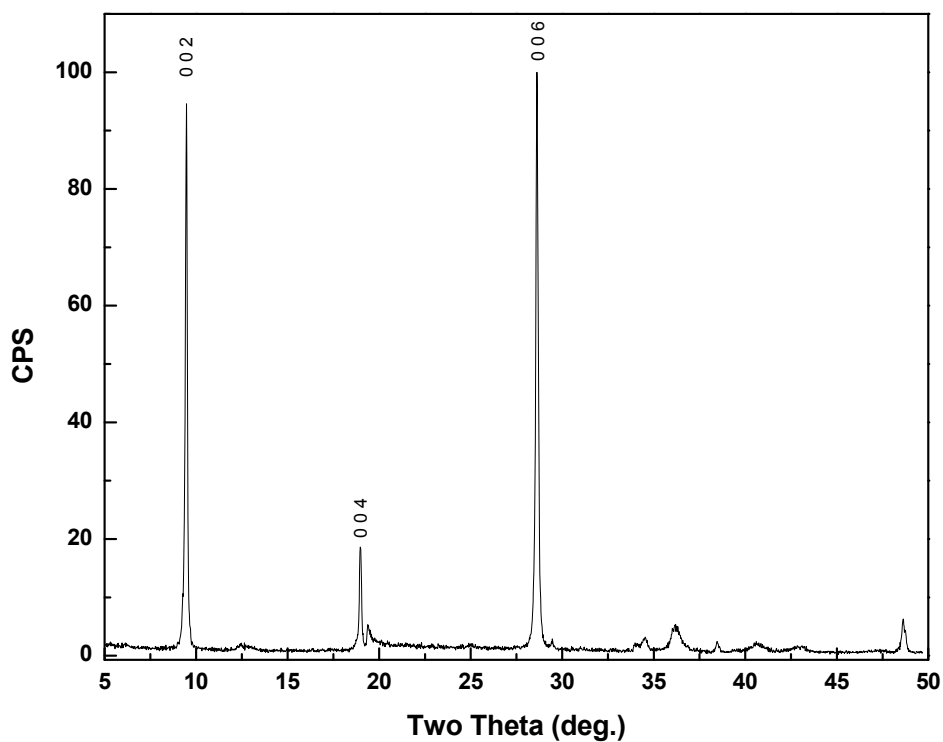


Figure 101 Powder X-ray diffraction pattern of Talc raw material.

Synthetic Zeolites (LTA, FAU and MOR)

Linde Type A (LTA)

X-ray powder diffraction of Linde Type A synthetic zeolites corresponded to a cubic unit cell and space group $F 4/m -3 2/c$. This crystal structure was in agreement with the LTA framework identified and available in Materials Studio v4.0 software.

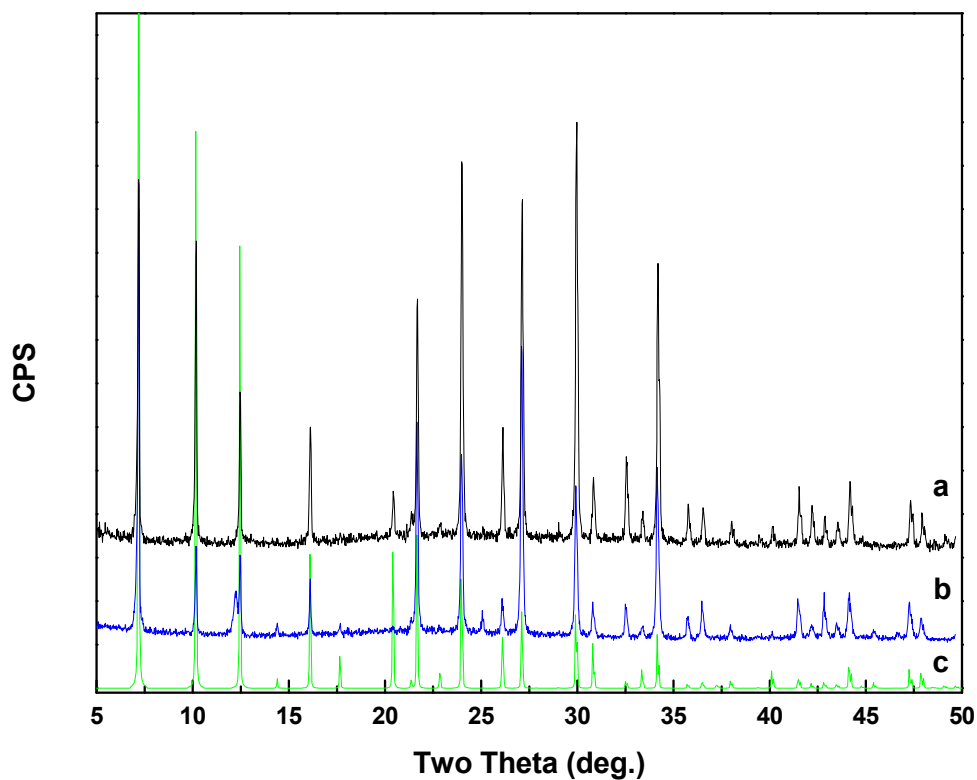


Figure 102 Powder X-ray diffraction pattern of (a) [Na⁺-LTA] 4A Raw material, (b) [Na⁺-LTA] 5A Raw material (c) LTA framework by Materials Studio v4.0 software.

Faujasite (FAU)

X-ray powder diffraction of faujasite synthetic zeolites corresponded to a cubic unit cell and space group $F2/D-3$. This crystal structure was in agreement with the faujasite framework measured and available in Materials Studio v4.0 software. Slight displacement of d-spacing values was observed for H^+ -FAU. This could be due to the proton present in the structure. The new cell parameters were not measured.

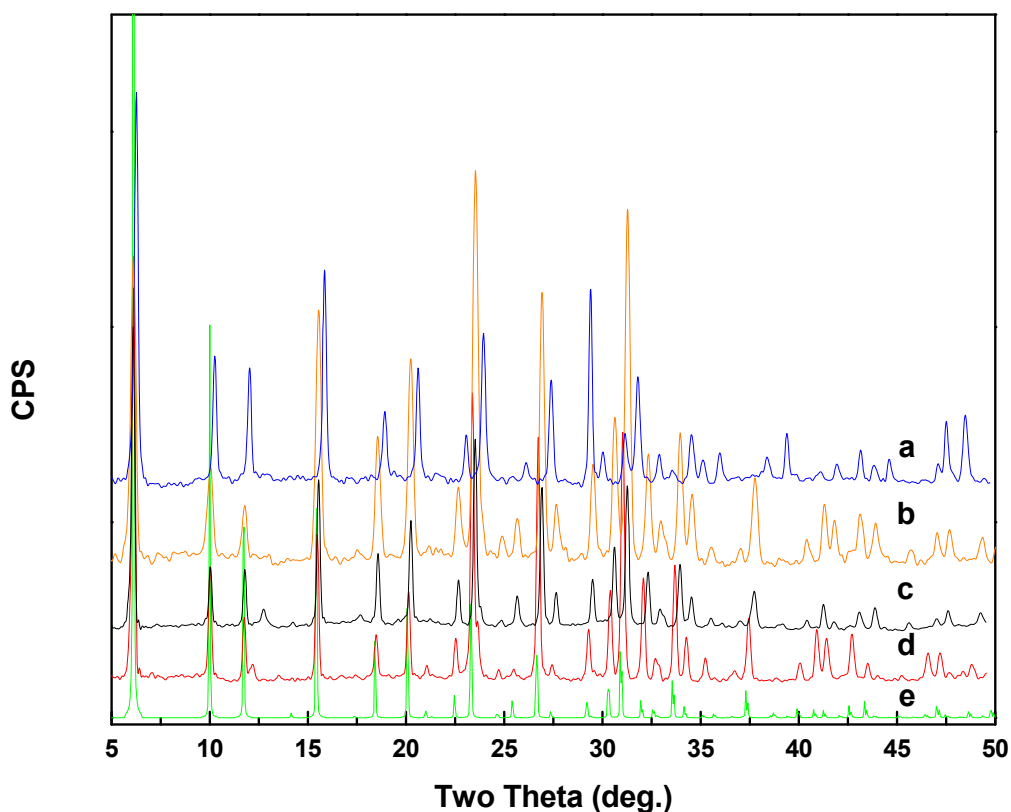


Figure 103 Powder X-ray diffraction pattern of (a) $[H^+]$ -FAU] Vallfor CP300-35[®] Raw material, (b) $[Na^+]$ -FAU] NaY Raw material (c) $[NH_4^+]$ -FAU] LZY-62 Raw material, (d) $[Na^+, Ca^{2+}]$ -FAU] 13X Raw material and (e) FAU framework by Materials Studio v4.0 software.

Mordenite (MOR)

X-ray powder diffraction of mordenite synthetic zeolites corresponded to an orthorhombic unit cell and space group $C 2/m 2/c 21/m$. This crystal structure was in agreement with the mordenite framework measured and available in Materials Studio v4.0 software.

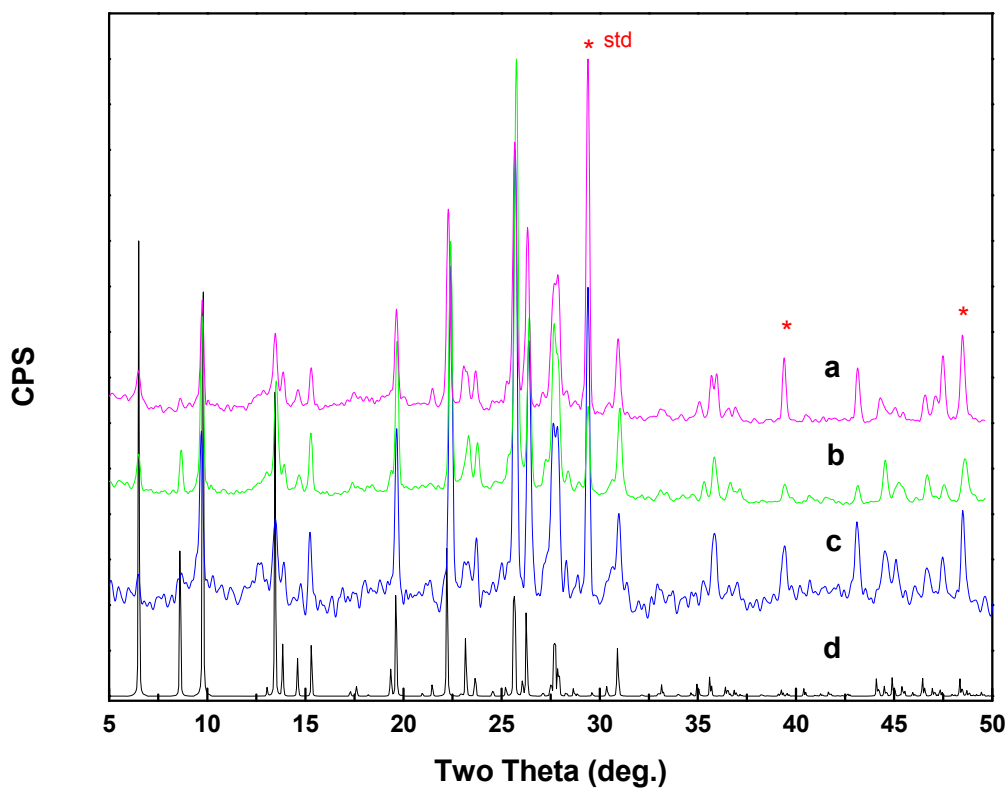


Figure 104 Powder X-ray diffraction pattern of (a) $[\text{Na}^+\text{-MOR}]$ CBV10A Raw material, (b) $[\text{NH}_4^+\text{-MOR}]$ CBV21A Raw material (c) $[\text{Na}^+\text{-MOR}]$ Zeolon[®] Raw material and (e) MOR framework by Materials Studio v4.0 software. (Calcite-standard).

Mesoporous Zeolites

X-ray powder diffraction of three mesoporous zeolites (MA-1, MAS-1 and MS-1) displayed broad and diffuse reflections indicative of a poorly crystalline structure, characteristic of sol-gel products before exposed to higher temperatures.

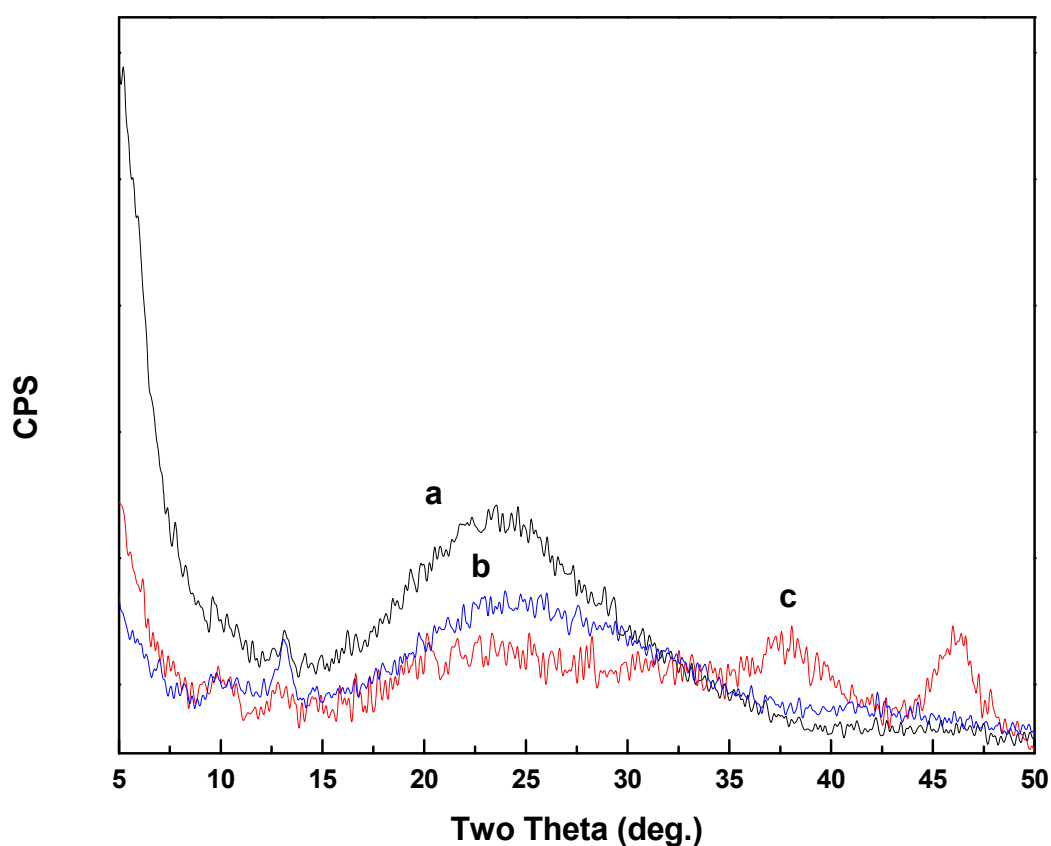


Figure 105 Powder X-ray diffraction pattern of (a) MS-1 Raw material, (b) MA-1 Raw material (c) MAS-1 Raw material.

4.5.3 Thermally Treated Inorganic Host Materials

CBV21A (NH₄⁺-MOR)

The procedure to prepare H⁺-MOR requested the calcination of NH₄⁺-MOR at 873K for three hours.⁹⁶ An X-ray diffraction pattern of the calcined sample was performed in order to corroborate no changes in the crystal structure. The X-ray powder diffraction of the H⁺-MOR displayed no major structural changes as shown in Figure 106.

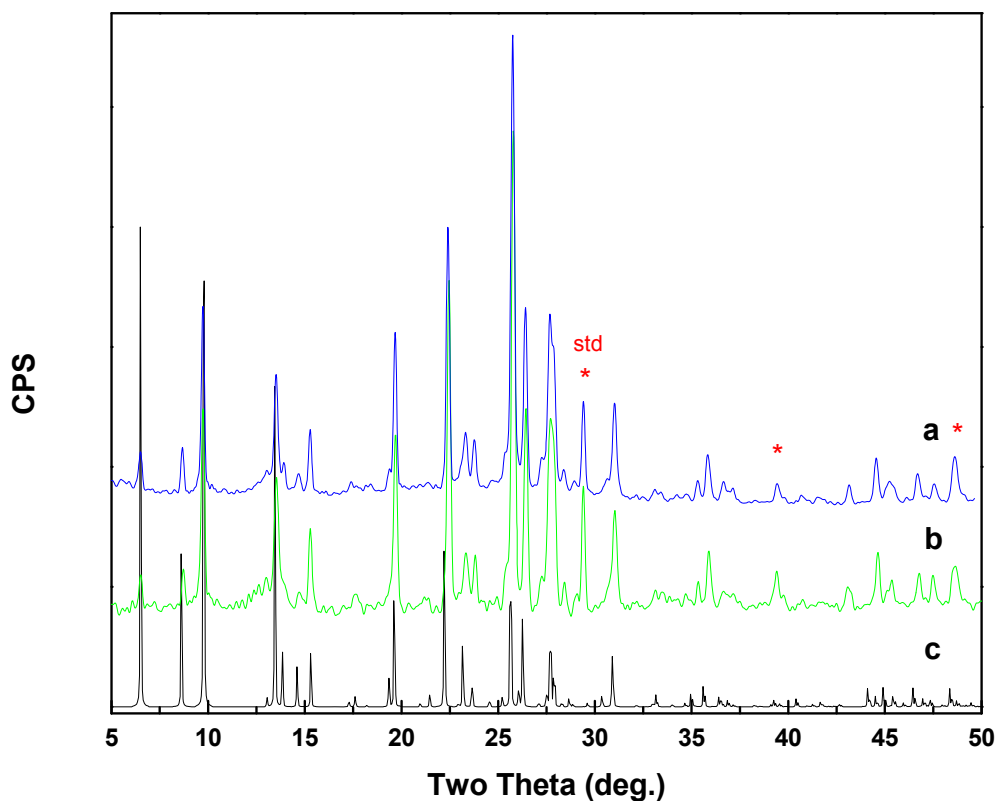


Figure 106 Powder X-ray diffraction pattern of (a) [NH₄⁺-MOR] CBV21A Raw material, (b) [H⁺-MOR] CBV21A (c) MOR framework by Materials Studio v4.0 software.

Zeolon® (Na⁺-MOR)

After thermal treatment at 1223K for sixteen hours zeolon® lost partially its crystal arrangement displayed by a broad diffuse peak. Only two reflection bands were resistant to this treatment.

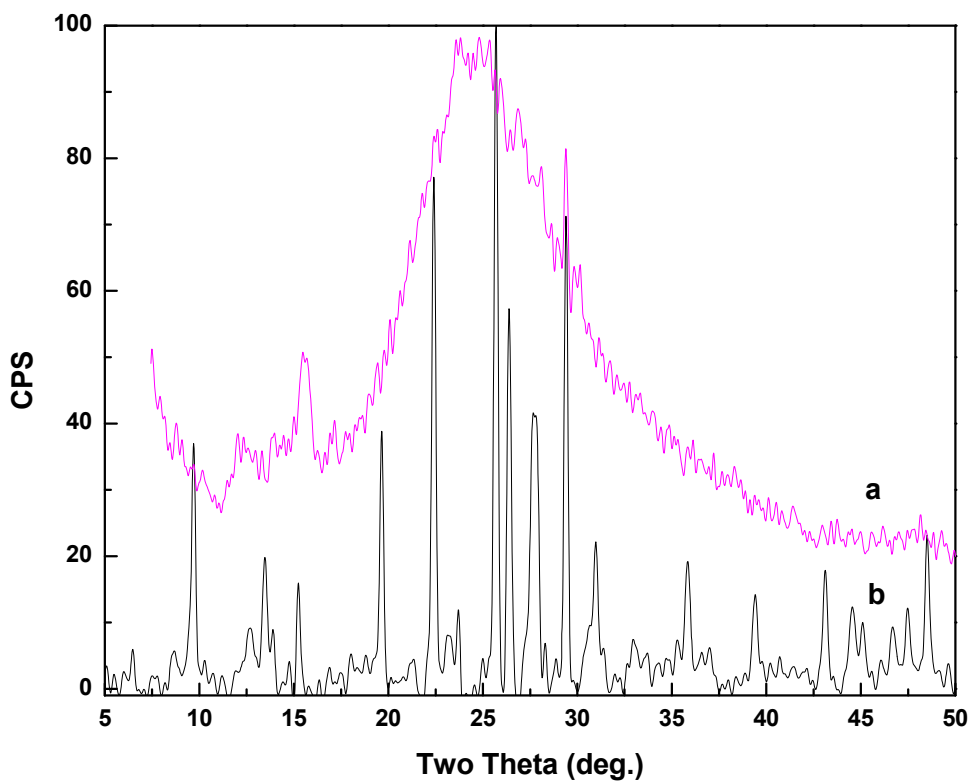


Figure 107 Powder X-ray diffraction pattern of (a) Zeolon® 1223K 16h, (b) Zeolon® Raw material.

Palygorskite

Disappearance of the 001 reflection corresponding to the pore channel of palygorskite structure was observed to disappear after thermal treatment at 833K for sixteen hours. This experiment was also performed with in-situ thermal X-ray powder diffraction by D. Williams,⁷⁴ where the reduction of the peak was monitored with time and temperature.

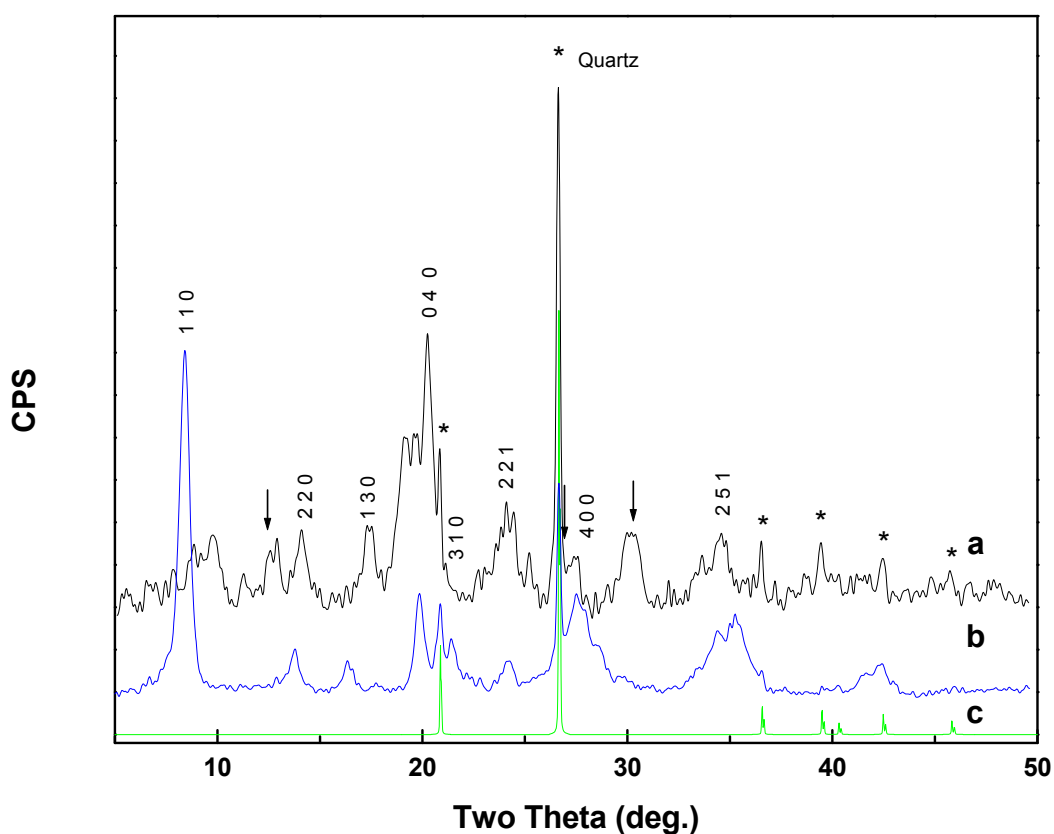


Figure 108 Powder X-ray diffraction pattern of (a) Palygorskite heated at 823K for sixteen hours. (b) Palygorskite raw material (c) trigonal α -Quartz simulated by Materials Studio v4.0. software.

4.5.4 Inorganic Host Materials Treated with Thioindigo

Palygorskite and Sepiolite

Mixtures of palygorskite and sepiolite with 0.5 mol % thioindigo displayed almost no thioindigo reflection bands in the unheated mixture and none in the heated sample or dehydrated at 413K for nine hours.

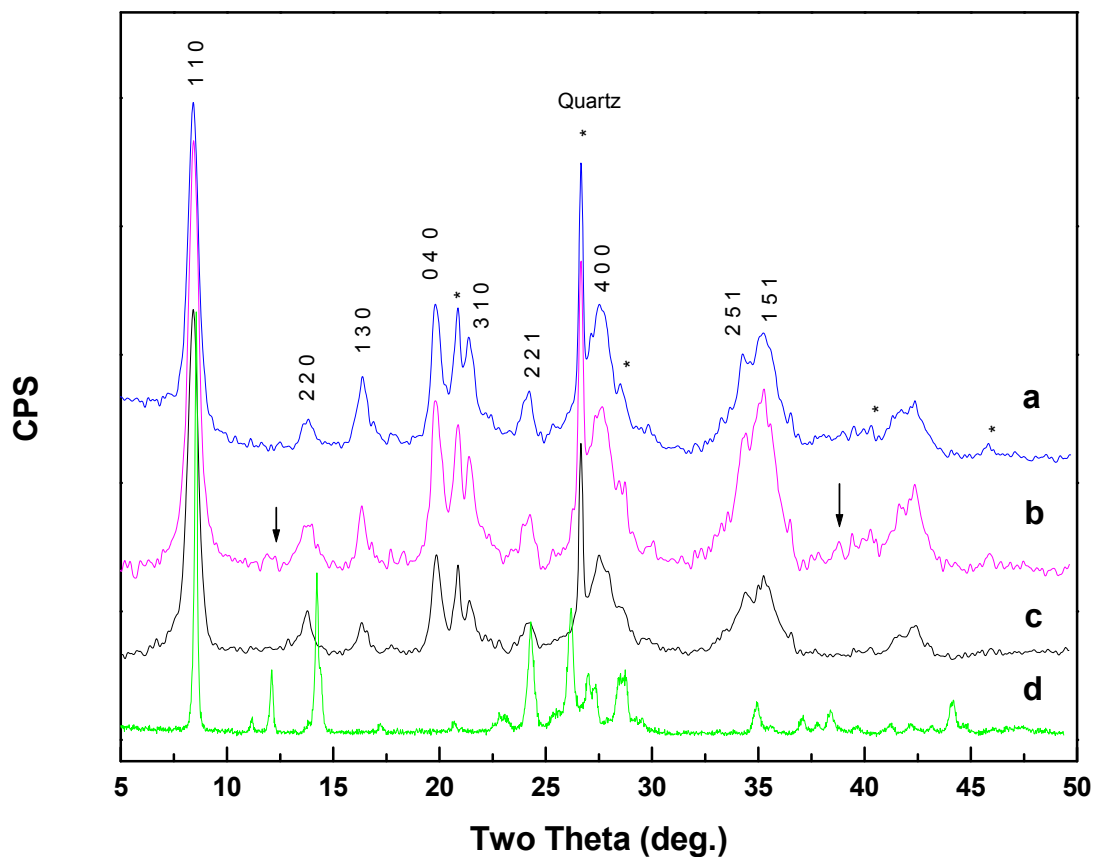


Figure 109 X-ray powder diffraction of (a) palygorskite +dye dehydrated [blue], (b) palygorskite +dye unheated [magenta], (c) palygorskite raw material and (d) thioindigo raw material.

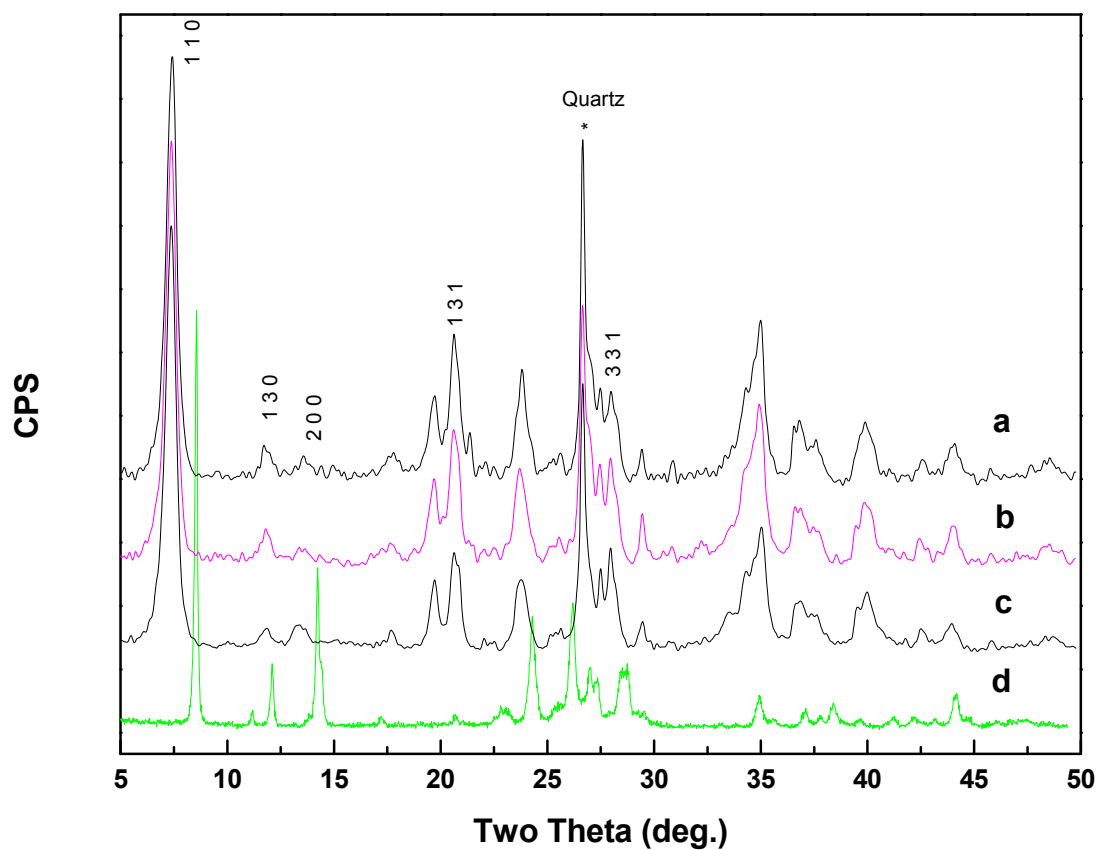


Figure 110 X-ray powder diffraction of (a) sepiolite +dye dehydrated [purple], (b) sepiolite +dye unheated [magenta], (c) sepiolite raw material and (d) thioindigo raw material.

Low Charge Swelling Natural Occurring Clays (Smectite Group)

As mentioned in chapter 4.1, mixtures with 0.5 % mol thioindigo presented color changes when exposed to different levels of humidity. This behavior was also confirmed by the displacement to higher d-spacing values in the hydrated samples, and to lower d spacing values for dehydrated samples. Moreover, purple samples indicative of a dehydrated state showed similar or less d-spacing values when compared to the raw material. The intercalation of thioindigo in the interlayer of the clays could be a feasible option based on the thioindigo molecules size (15.17 Å (length), 7.42 Å (width) and 3.4 Å (thickness)³² and the clay interlayer dimensions (10 Å when dehydrated⁶¹). The displacement of d spacing values and color changes in the layer materials could be an indication of a possible horizontal intercalation of the thioindigo molecules in the interlayer of the clays, therefore originating zero d-spacing changes when in contact with each other. This effect has also been observed for indigo carmine inserted in layer double hydroxides.⁹⁷

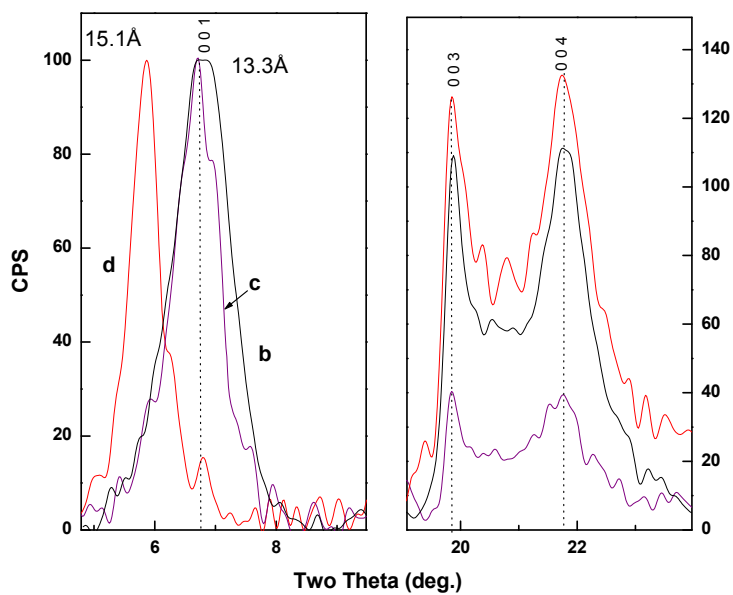
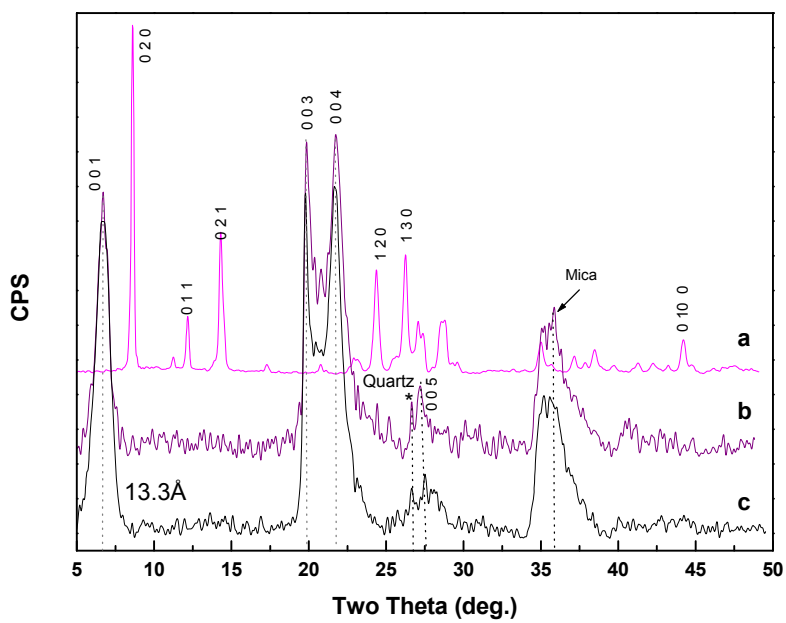


Figure 111 Powder X-ray diffraction pattern of (a) thioindigo, (b) bentolite L[®] +dye dehydrated [purple], (c) [Ca²⁺-MMT] bentolite L[®] raw material, and (d) bentolite L[®] +dye hydrated [red].

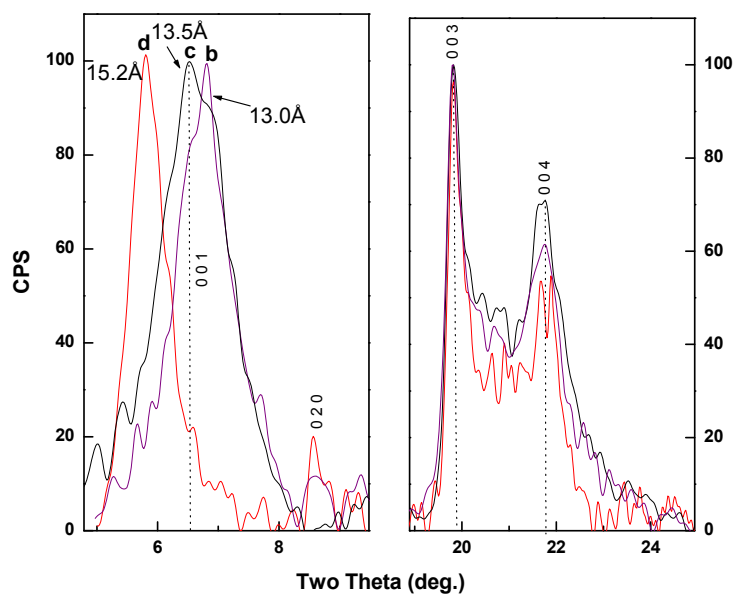
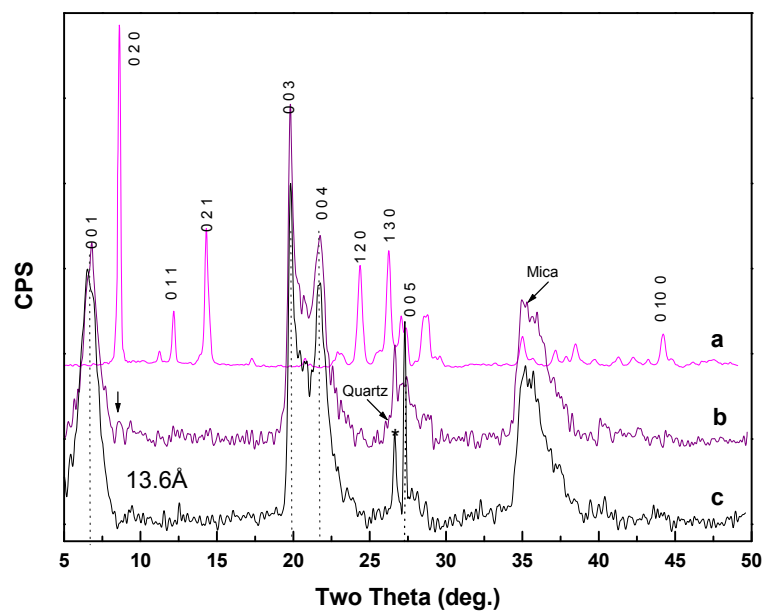


Figure 112 Powder X-ray diffraction pattern of (a) thioindigo, (b) Ca²⁺-MMT + dye dehydrated [purple], (c) Ca²⁺-MMT (Texas) raw material, and (d) Ca²⁺-MMT + dye hydrated [red].

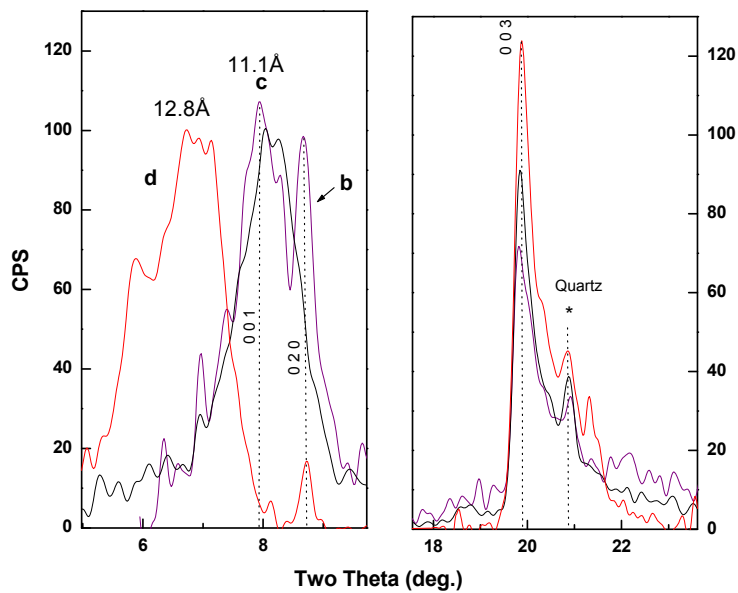
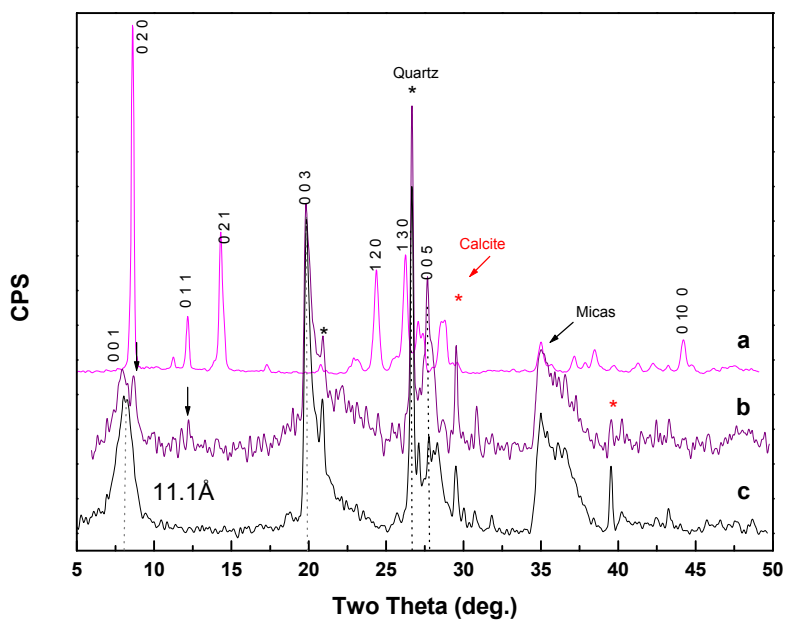


Figure 113 Powder X-ray diffraction pattern of (a) thioindigo, (b) Na⁺-MMT +dye dehydrated [purple], (c) Na⁺-MMT (Wyoming) raw material, and (d) Na⁺-MMT +dye hydrated [red].

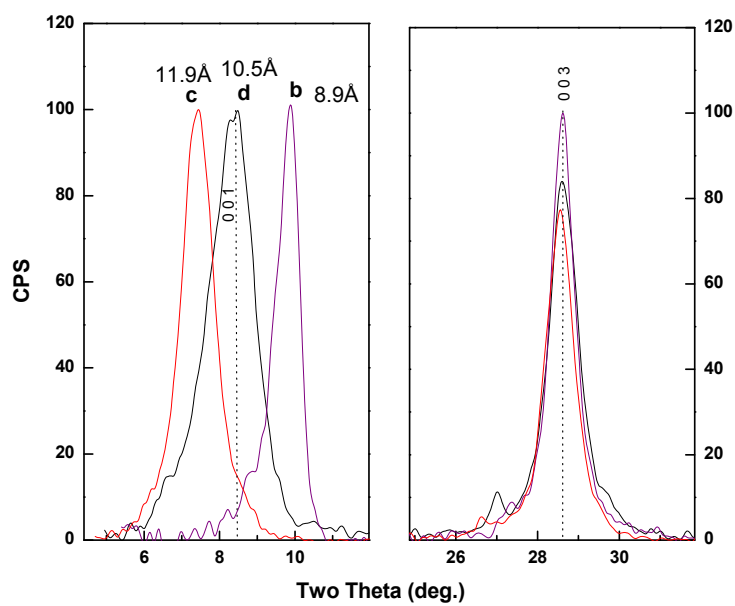
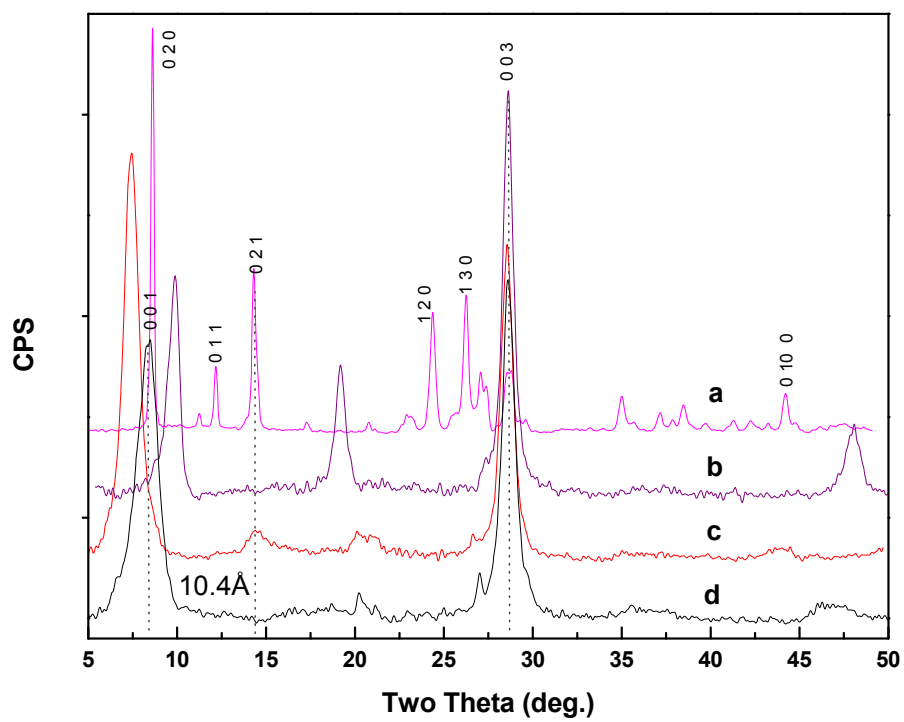


Figure 114 Powder X-ray diffraction pattern of (a) thioindigo, (b) Na⁺-MMT +dye dehydrated [purple], (c) Na⁺-MMT +dye hydrated [red],(d) Na⁺-MMT (Kunipia) raw material.

Low Charge Synthetic Swelling Clays (Mica group)-Thioindigo Interaction

X-ray powder diffraction of YN6 and YN8 displayed no change in the basal reflection (001) when thioindigo was incorporated in the mixture; moreover, thioindigo main reflections were still present after thermal treatment at 413K for nine hours. This could indicate a zero intercalation in the interlayer of the Na-Mica.

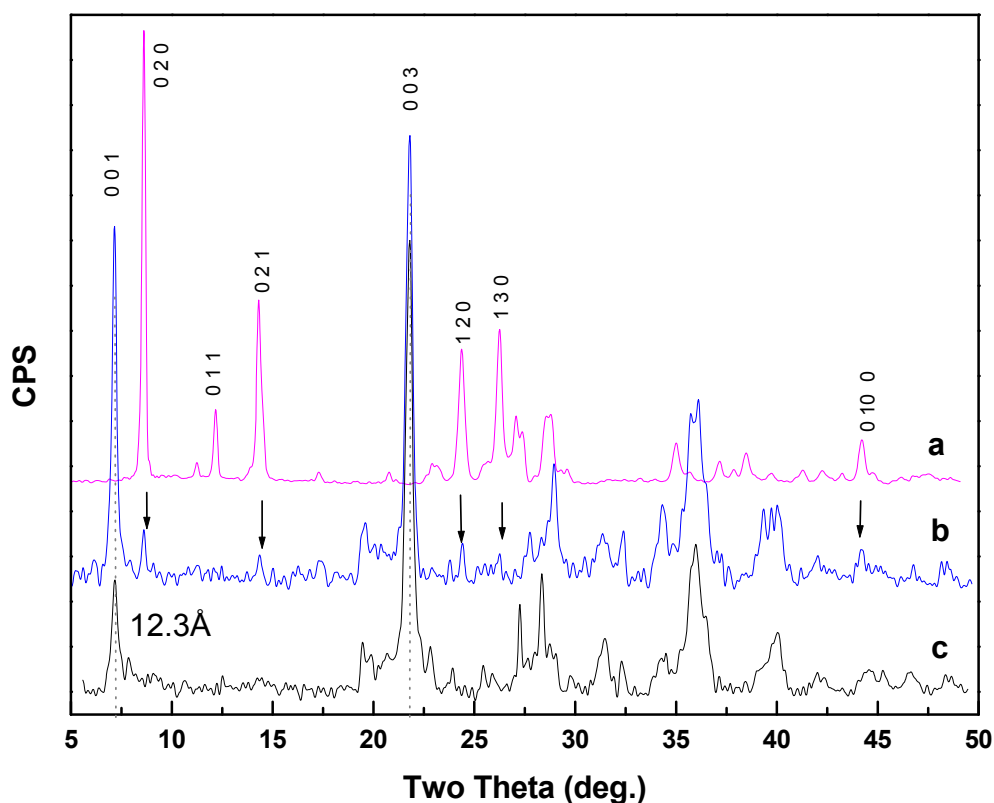


Figure 115 Powder X-ray diffraction pattern of (a) thioindigo, (b) YN8 +dye dehydrated [pink] and (c) [Na⁺-LTA] YN8 raw material.

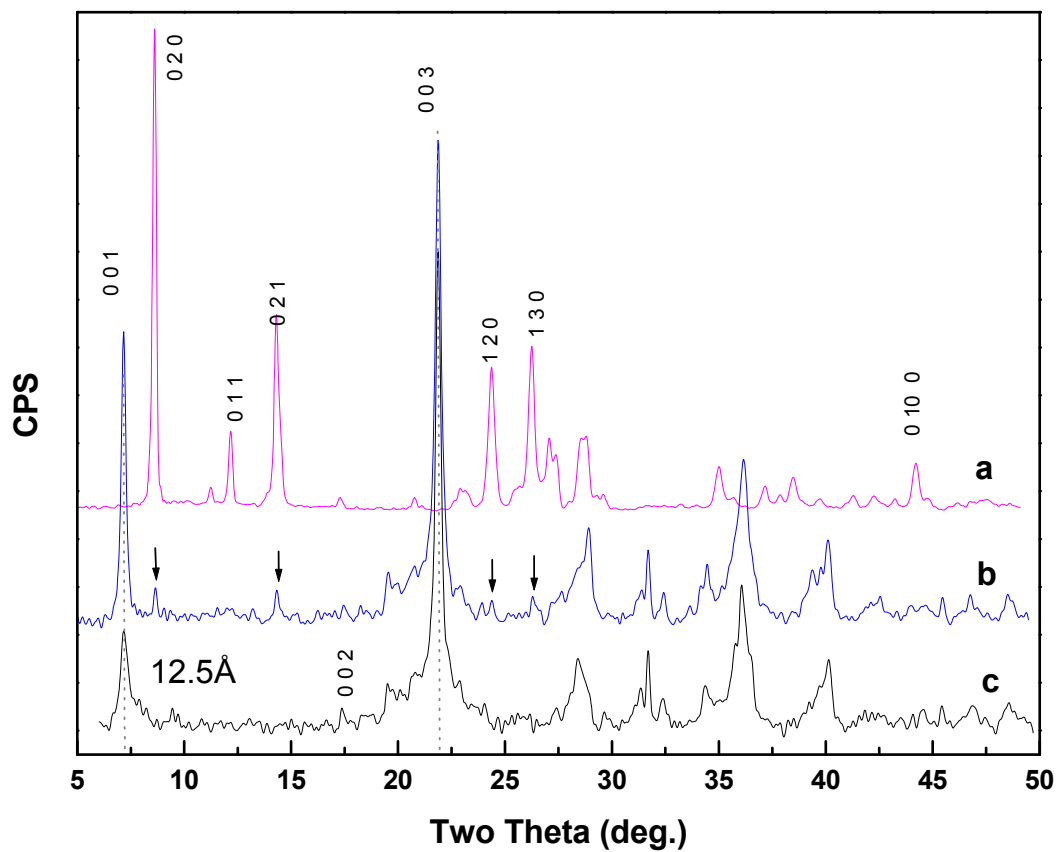


Figure 116 Powder X-ray diffraction pattern of (a) thioindigo, (b) YN6 +dye dehydrated [pink] and (c) [Na⁺-Mica] YN6 raw material.

4.6 Chemical Analysis by Energy Dispersive Analysis (EDAX)

Cation Exchange of Mordenite

The cation exchange in CBV21A-NH₄⁺ was carried out and confirmed by Energy Dispersive X-Ray Analysis.

Energy Dispersive X-Ray Analysis showed the presence of the cations exchange in the solution. In some cases, the temperature had an effect in the concentration of silicon of the zeolite, lowering the Si/Al ratio.

Table 12 Summary of Chemical Analysis for CBV21A exchanged with different cations by EDAX.

Specimen	wt. %						Si/Al EDAX	Si/Al XRF
CBV21A	O	Al	Si	Na	K	Ca		
K ⁺	40.05	5.11	47.3	-	7.54	-	9	9.48
Na ⁺	39.41	5.18	52.47	2.94	-	-	10	9.48
Ca ²⁺	42.62	4.78	47.43	-	2.3	2.88	10	9.48
*NH ₄ ⁺	40.59	5.21	54.2	-	-	-	10	9.48
Al ³⁺	40.23	7.36	52.41	-	-	-	7	9.48
H ⁺	44.16	5.33	50.51	-	-	-	9	9.48

* As received from Zeolyst International

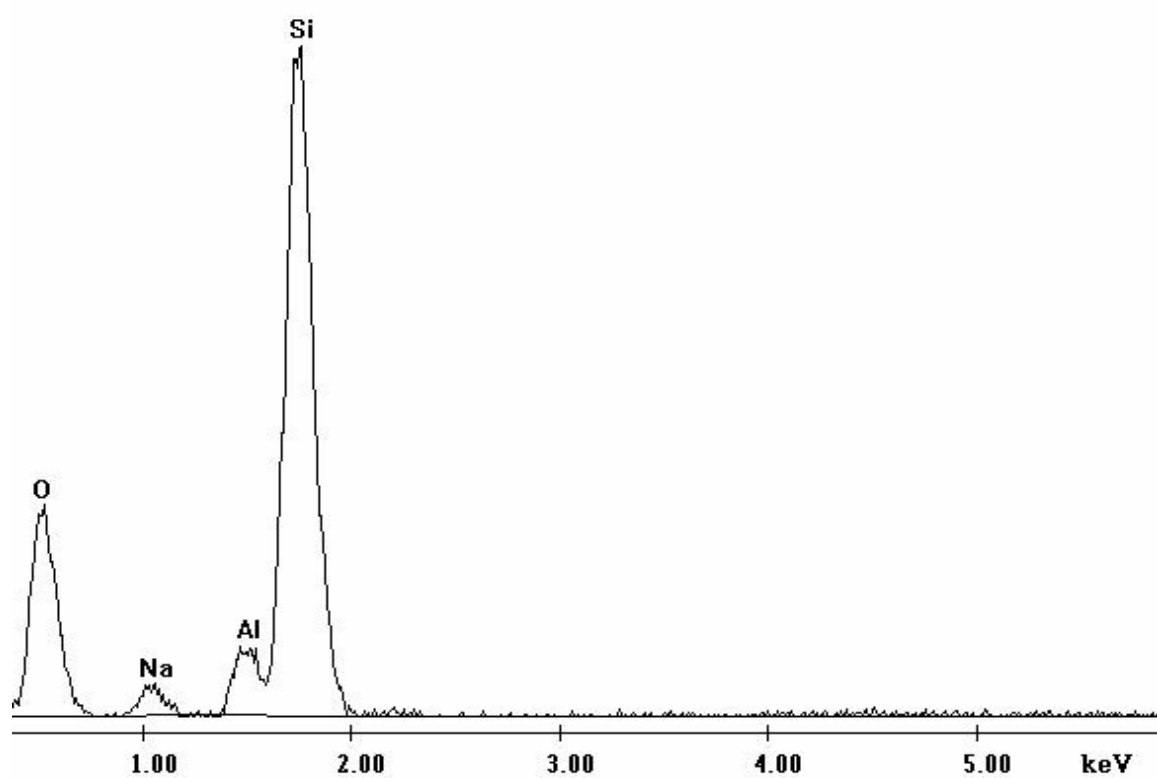


Figure 117 Sodium cation exchanged in Na⁺-MOR.

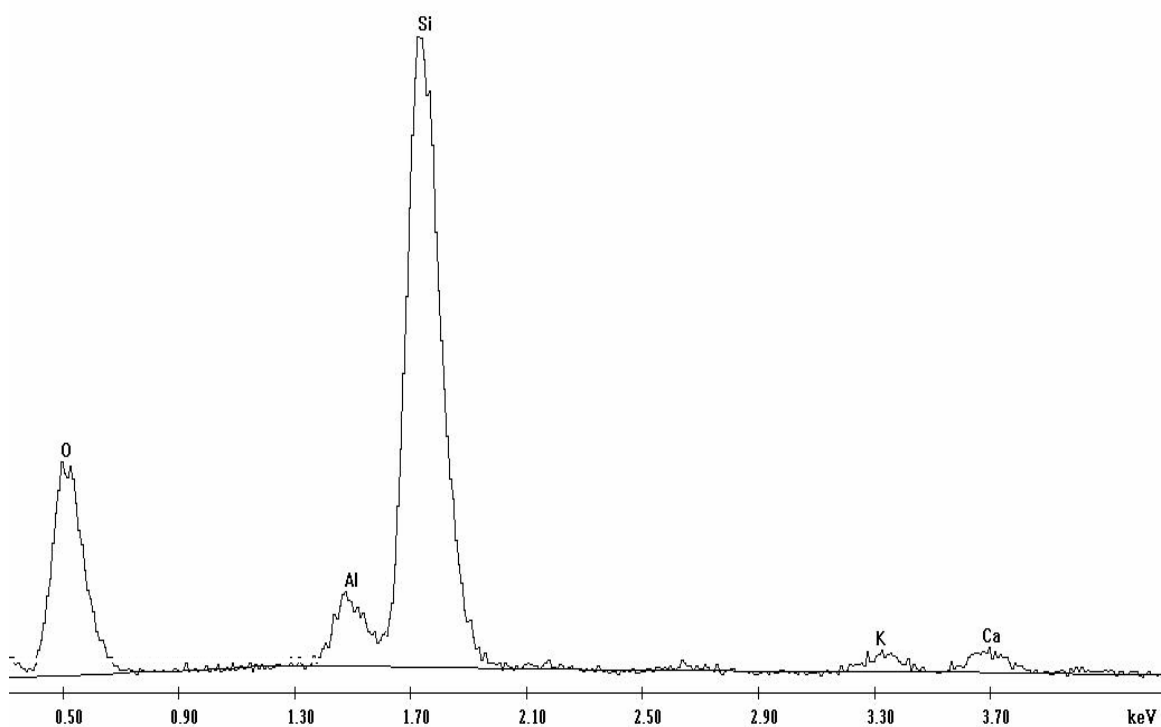


Figure 118 Calcium cation exchange for Ca^{2+} [MOR].

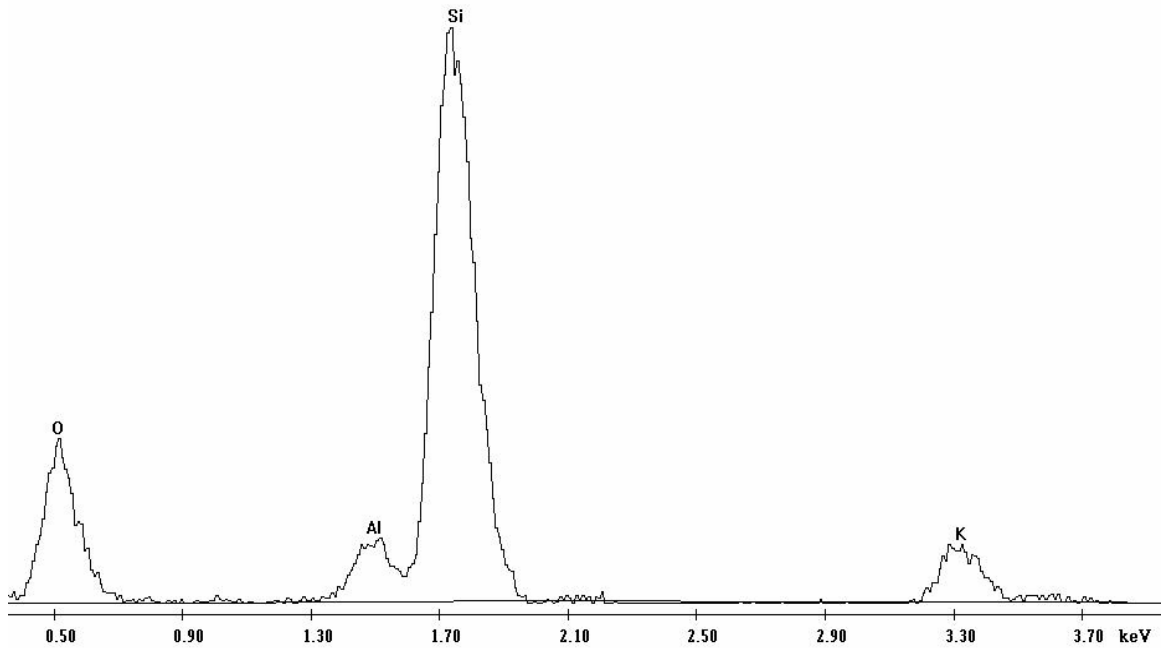


Figure 119 Potassium cation exchanged in K^+ -MOR.

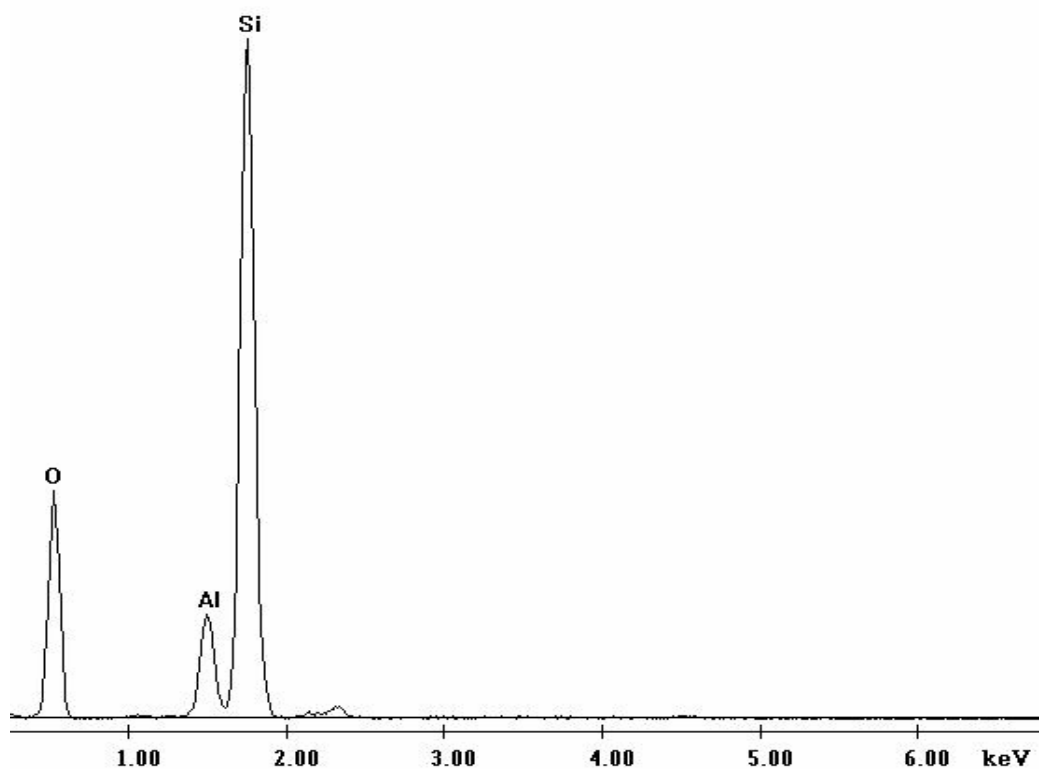


Figure 120 Aluminum cation exchanged in Al³⁺-MOR.

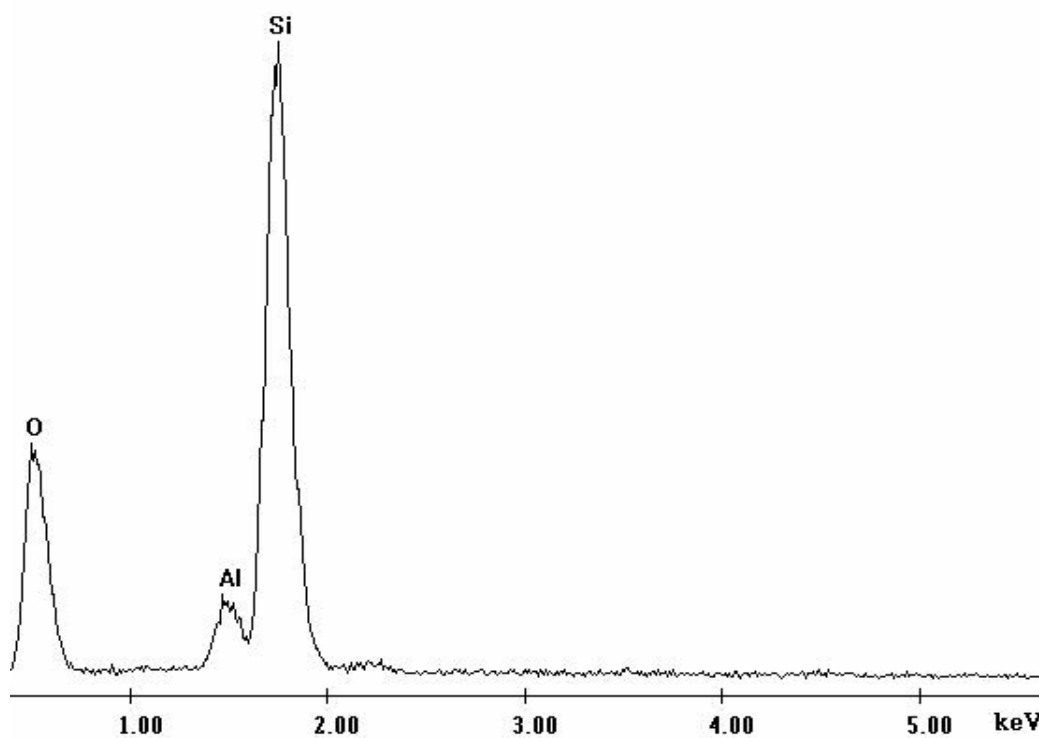


Figure 121 Hydrogen cation exchanged in H⁺-MOR.

4.7 Magic Angle Nuclear Magnetic Resonance

Palygorskite and sepiolite

^{27}Al NMR spectra for untreated palygorskite revealed two main resonances at 3.92 ppm (100% peak area) and 66.6 ppm (9.5 % peak area) representing octahedral and tetrahedral Al respectively. This is consistent with previous results of Al coordination in palygorskites.⁶⁷

On the other hand, untreated sepiolite showed two main resonances at 54.67 ppm (100% peak area) and 3.43 ppm (30.8% peak area) for tetrahedral and octahedral Al, respectively. This is in agreement with previous results of Al coordination in sepiolites.⁸⁷

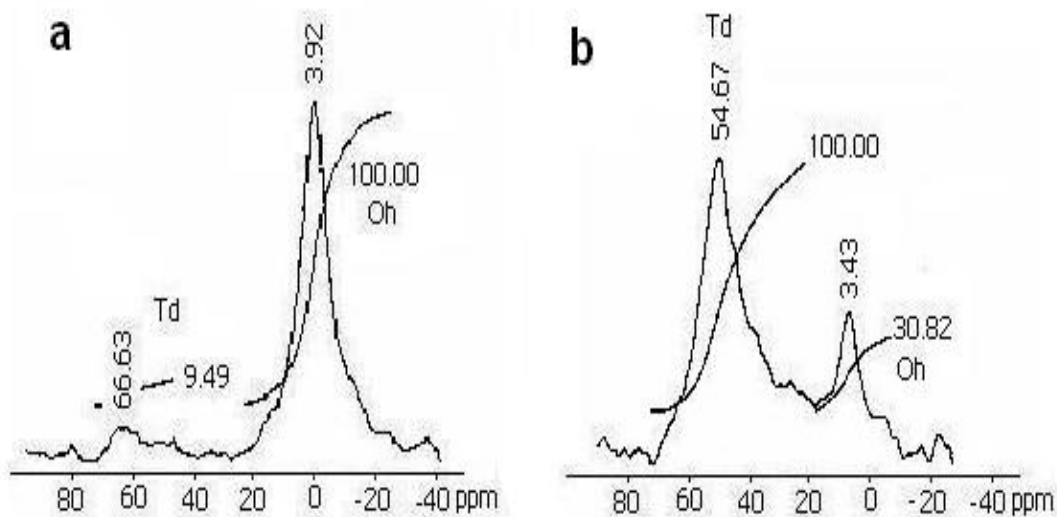


Figure 122 ^{27}Al magic angle spinning-nuclear magnetic resonance of (a) palygorskite and (b) sepiolite.

Montmorillonite Clays

Ca^{2+} -MMT (Bentolite L[®]) showed two main resonances at -0.63 ppm (100% peak area) and 52.2 ppm (9.75 % peak area) representing octahedral and tetrahedral Al, respectively (see Figure 123[a]). In the case of Ca^{2+} -MMT (Texas deposit) two main resonances at 0.90 ppm (100% peak area) and 53.1 ppm (9.56 % peak area) representing octahedral and tetrahedral Al were observed (see Figure 123[b]). This is in accordance with previous results of Al coordination in Ca^{2+} -MMT.⁹⁸

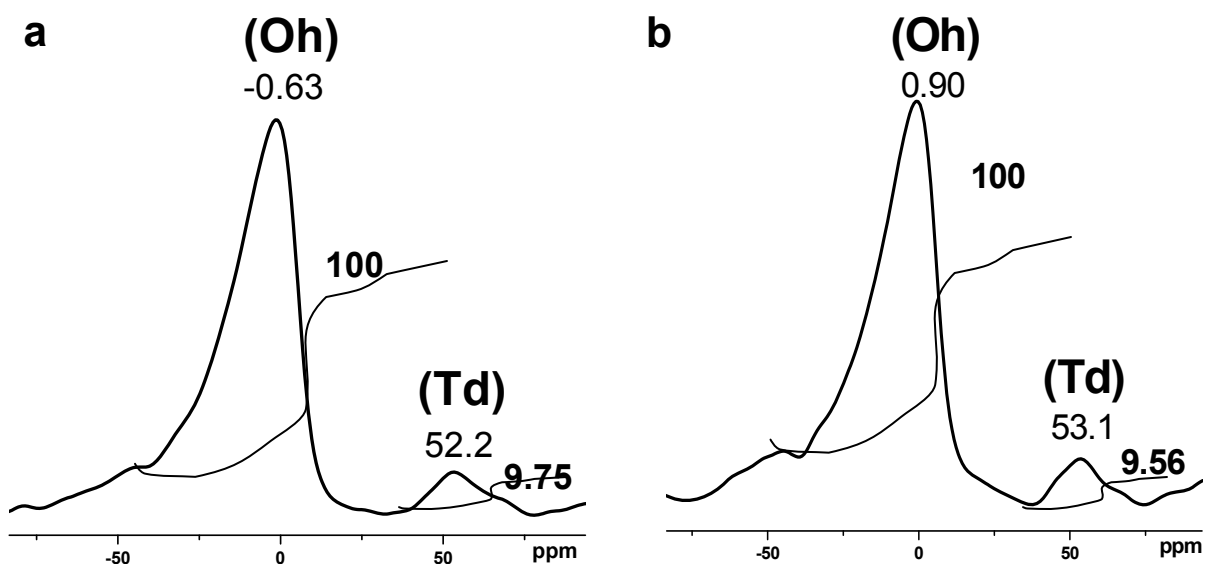


Figure 123 ^{27}Al magic angle spinning-nuclear magnetic resonance of (a) Ca^{2+} -MMT (Bentolite L[®]) and (b) Ca^{2+} -MMT (Texas deposit).

Na⁺-MMT (Kunipia deposit) showed two main resonances at 1.08 ppm (100% peak area) and 68.5 ppm (7.74% peak area) representing octahedral and tetrahedral Al, respectively (see Figure 124[a]). In the case of Na⁺-MMT (Wyoming deposit) two main resonances at -0.14 ppm (100% peak area) and 58.5 ppm (9.75% peak area) representing octahedral and tetrahedral Al were observed (see Figure 124[b]). This is consistent with previous results of Al coordination in Na⁺-MMT.⁹⁹

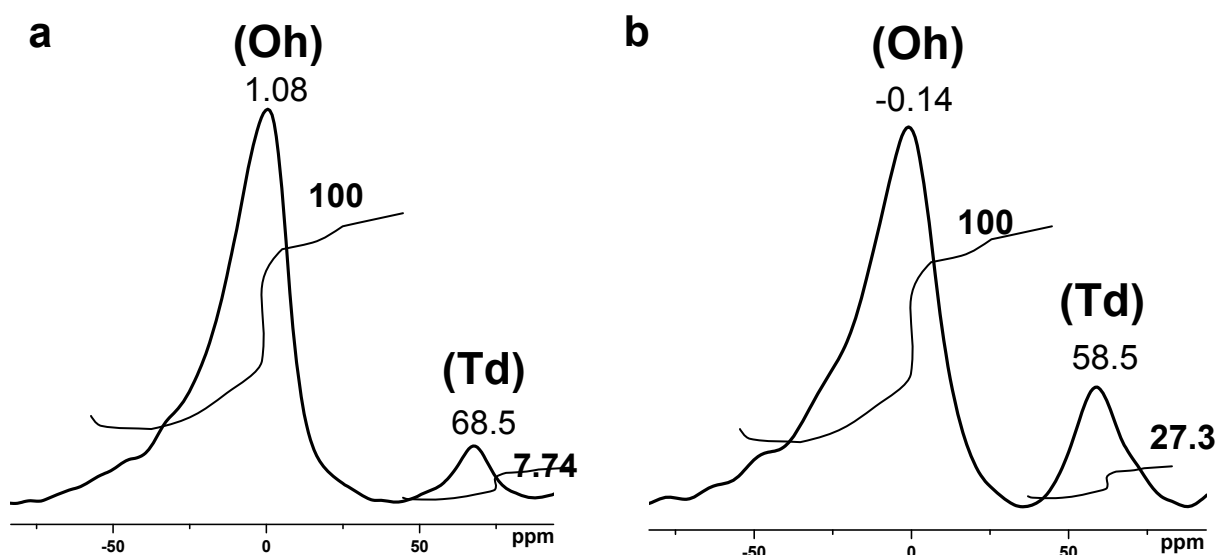


Figure 124 ²⁷Al magic angle spinning-nuclear magnetic resonance of (a) Na⁺-MMT (Kunipia deposit) and (b) Na⁺-MMT (Wyoming deposit).

Table 13 NMR resonances of several natural occurring clay minerals.

	Palygorskite	Sepiolite	CaMMT (Bentolite L [®])	CaMMT (Texas)	NaMMT (Wyoming)	NaMMT (Kunipia)
% Peak Area						
Octahedral	100	30.8	100	100	100	100
Tetrahedral	9.5	100	9.8	9.6	27.3	7.8

Palygorskite-Thioindigo Interaction

In this analysis two concentrations of thioindigo were studied: 0.5 mol % and 1 mol % thioindigo.

In the case of palygorskite / 1 mol % thioindigo after thermal treatment at 413K, slight changes in the peak areas of the tetrahedrally coordinated Al resonance were observed. However, more evident change with 0.5 mol % dye content was noted, as can be seen in Figure 125. Since the amount of tetrahedrally coordinated Al is very low in palygorskite, it is difficult to conclude any changes to the tetrahedral coordination of Al in the dye treated palygorskite samples. The accuracy of NMR measurements in the presence of metal atoms such as iron, is known to be reduced by its magnetic properties⁹⁹ and therefore a lack of resolution in the spectra was observed.

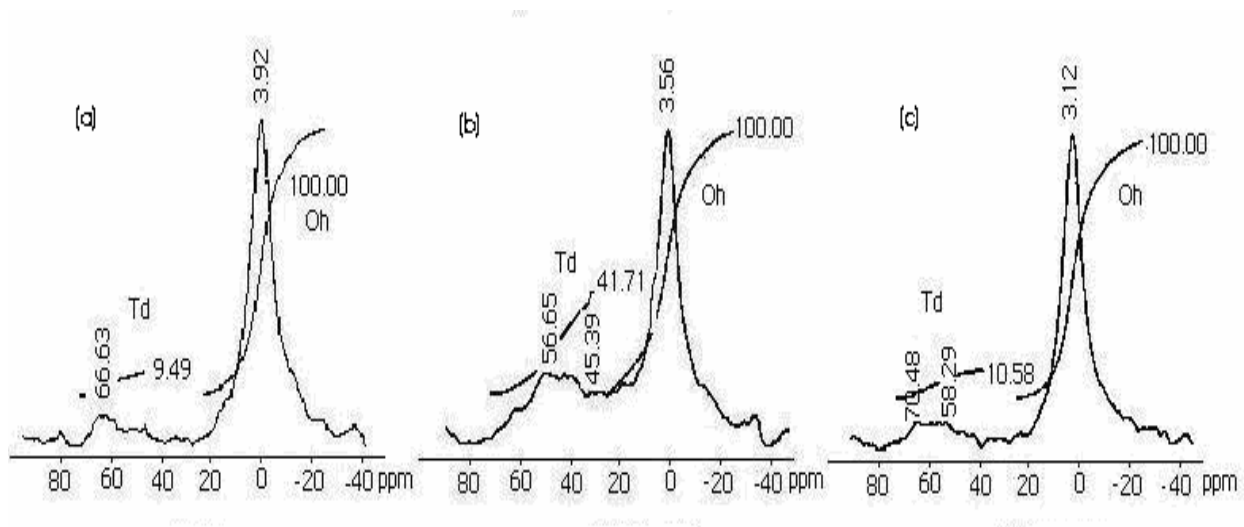


Figure 125 ^{27}Al magic angle spinning-nuclear magnetic resonance of (a) palygorskite from MinTech; (b) palygorskite / 0.5 mol % thioindigo heated at 413K for nine hours; (c) palygorskite/ 1 mol %thioindigo heated at 413K for nine hours.

Sepiolite-Thioindigo

After treatment with thioindigo dye at 413K, the peak areas of octahedrally coordinated Al resonance increased with an increase in dye content as can be seen in Figure 126. The peak areas of octahedrally coordinated Al are 30.8, 43.6 and 62.9 in untreated sepiolite, sepiolite treated with 0.5 mol % thioindigo and sepiolite treated with 1 mol % thioindigo, respectively. Thus it appears that the dye changes the coordination of some tetrahedral Al to octahedral Al.

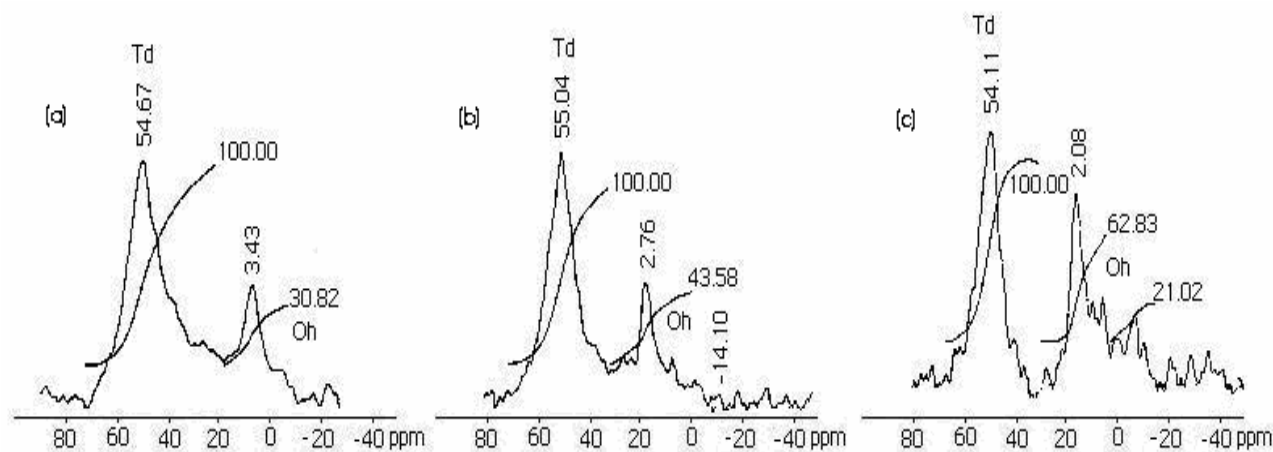


Figure 126 ^{27}Al magic angle spinning-nuclear magnetic resonance of (a) sepiolite (Pansil) from Tolsa; (b) Sepiolite / 0.5 mol % thioindigo heated at 413K for nine hours; (c) Sepiolite/ 1 mol % thioindigo heated at 413K for nine hours.

In order to prove these coordination changes were due to thioindigo addition, and no other factors, samples before heating were tested. A significant change was observed with and without heating as seen in Figure 127. This process is most likely to be unlinked to the organic additive.

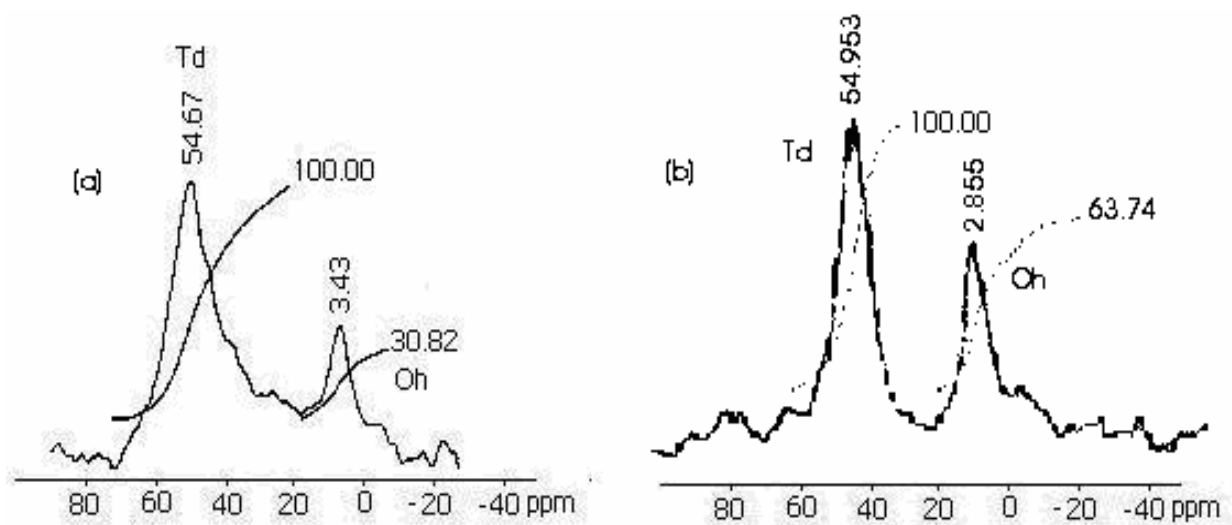


Figure 127 ^{27}Al magic angle spinning-nuclear magnetic resonance of (a) sepiolite (Pansil) from Tolsa; (b) Sepiolite dehydrated at 413K for nine hours

4.8 DFT Method for Calculation of Optical Spectra

The interaction of thioindigo with ammonium and hydrogen exchanged cations in an aluminum silicate framework was performed by MS (Materials Studio) modeling software. Two non-periodic superstructure fragments of an aluminum silicate tetrahedral framework with different cations substituted were modeled and optimized representing the active sites in the zeolite cavity. One thioindigo molecule was then located close to the two framework fragments, with two cations sites in the structure. The final interaction was again optimized and the optical spectra calculated with a semiempirical molecular orbital application called VAMP.¹⁰⁰ VAMP application was carried out with a Hamiltonian of neglect of diatomic differential overlap (NDDO) for best results.

NH_4^+ zeolite / thioindigo simulated interaction displayed a bathochromic shift under UV-Vis spectroscopy similar to the experimental values. Similar bathochromic shift was also observed with hydrogen cation. This simulation confirmed the effect of the cations in the electron withdrawing from thioindigo molecules when exposed to an acidic framework. However, the broadness of the peak was not as precise and more work in this area should be performed in order to acquire closer fittings to the experimental values and the rest of the cations tested in this research.

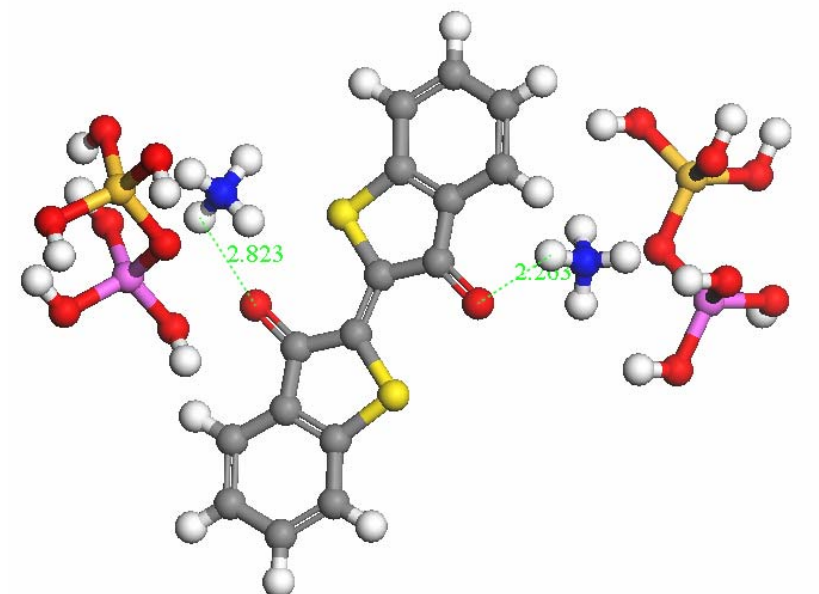


Figure 128 Ammonium cation interaction with one thioindigo molecule.

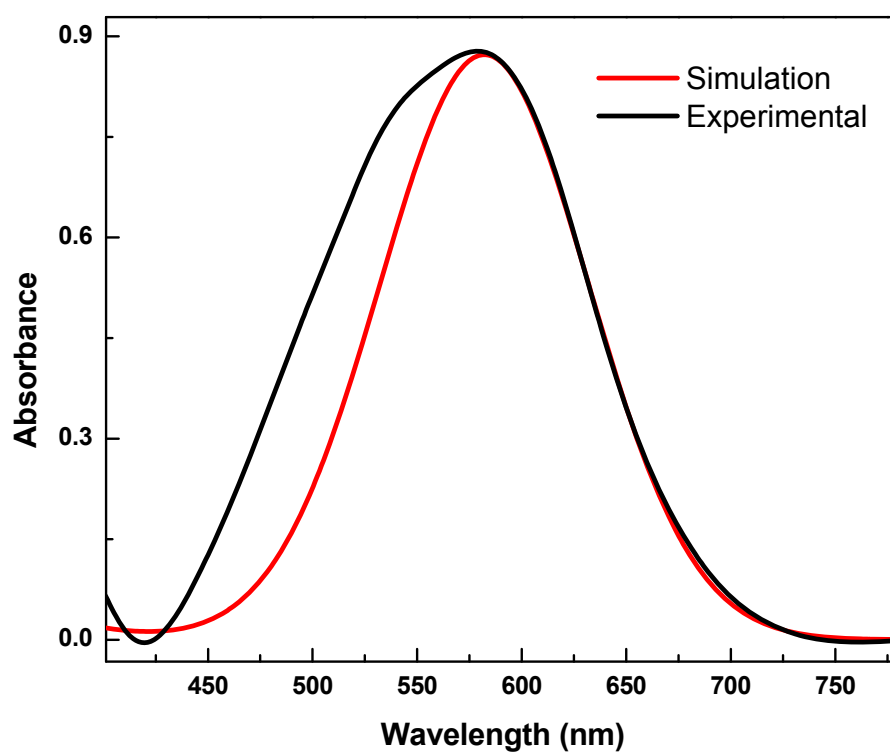


Figure 129 UV-Vis spectra simulated and experimental for 0.5 mol % thioindigo in NH_4^+ -MOR.

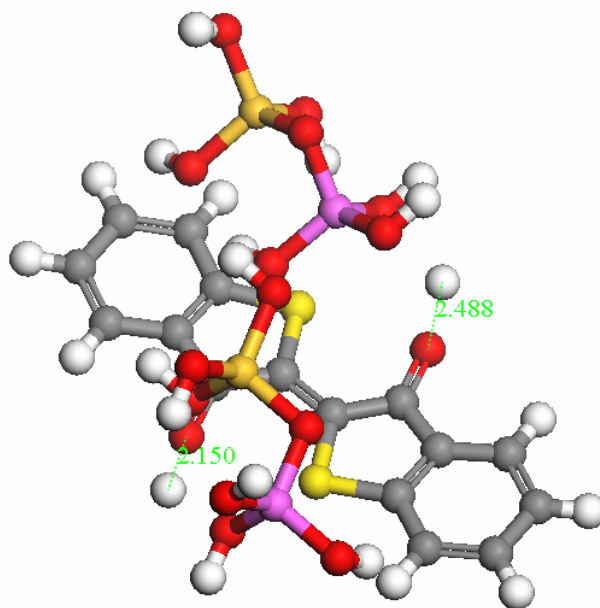


Figure 130 Hydrogen interaction with one thioindigo molecule.

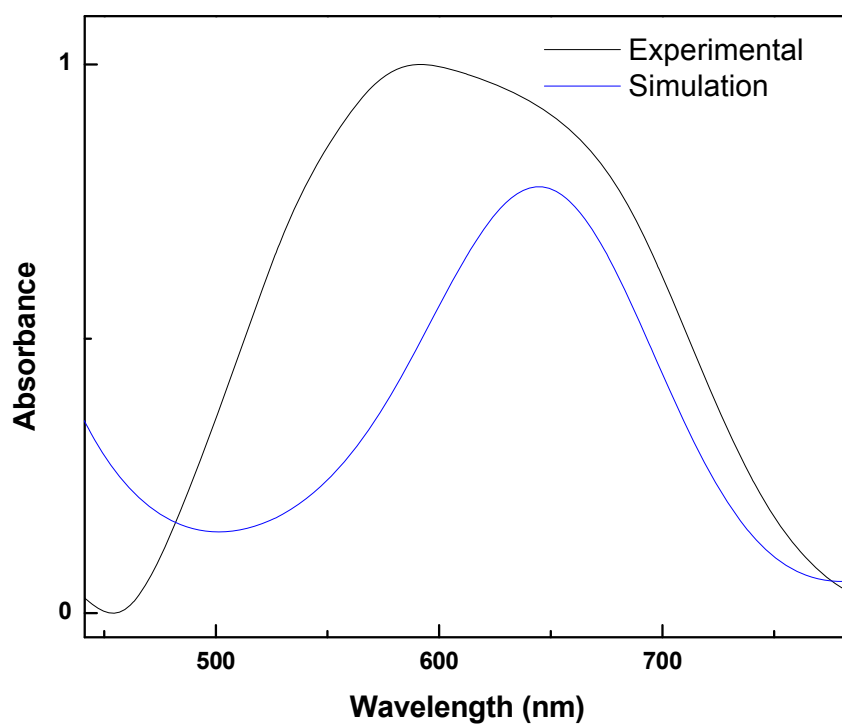


Figure 131 UV-Vis spectra simulated and experimental for 0.5 mol % thioindigo in H^+ -MOR.

CHAPTER 5

CONCLUSIONS

A reversible thioindigo excited state was obtained when immersed in some inorganic host materials after thermal treatment and upon moisture uptake. This excited state is related to a charge transfer of electron donor-acceptor complexes taking place with thioindigo C=O groups and Lewis acid sites (LAS). These acid sites were available in the materials tested. Charge transfer interactions (C=O---LAS) were confirmed by the increment in absorbance in most samples after thermal treatment or prolonged evacuation. Moreover, FTIR thioindigo C=O perturbation due to LAS polarizing effect was also observed. Similar complexes have been observed in dimmers of chlorophyll C=O group and magnesium metal.¹⁰¹

In general, there were three different LAS available depending on the nature of the inorganic host: (a) Proton acids, (b) Exchangeable cations^{40,102} and (c) Extra-framework aluminum originated by the disruption of the framework.^{103,104} In this work, different available LAS in the framework engendered color changes when in contact with thioindigo. The crystal structure of the inorganic host materials also played a significant role in the selectivity of the organic molecule; moreover, exchangeable cations were crucial for the moisture uptake in these materials.







LAS hydration was proved to reduce the absorbance of most samples; this effect could be explained as being mainly due to a highly polarized thin layer of water molecules absorbed around LAS. Blockage of the LAS could have interrupted direct interaction ($\text{C}=\text{O} \cdots [\text{LAS}]$) and only allowed hydrogen bonding interaction ($\text{C}=\text{O} \cdots \text{H}(\text{HO})[\text{LAS}]$) as revealed by FTIR (Chapter 4, section 4.3.3). Further hydration showed the presence of free thioindigo $\text{C}=\text{O}$ vibration mode perhaps due to the higher concentration of water molecules, thus it was less polarized due to larger distance from LAS.

Natural Occurring Clay Minerals

Palygorskite and Sepiolite

Palygorskite and sepiolite presented different color hues when in contact with thioindigo. This could be explained by the ratio of Al(VI) [aluminum occupancy in octahedral sites] and Al(IV) [aluminum occupancy in tetrahedral sites] available in both clays; however, 10% occupancy of Al(IV) seemed to be the ideal substitution for the blue color change to happen. The comparison with other clays, such as Ca^{2+} montmorillonites, confirmed this hypothesis. The iron concentration did not show any tendency in the samples evaluated.

Table 14 NMR spectra and color changes observed in several natural occurring clay minerals.

Specimen	Cation (moles)	Fe (moles)	Al(VI) (moles)	Al(IV) (moles)	Color
Palygorskite	K	0.067	0.15	0.015	
Sepiolite	Ca, Na	0.008	0.019	0.044	
CaMMT (Bentolite L [®])	Ca	0.011	0.24	0.026	
CaMMT (Texas)	Ca	0.024	0.27	0.029	
NaMMT (Wyoming)	Ca,Na	0.058	0.26	0.099	
NaMMT (Kunipia)	Na	0.029	0.37	0.031	

*Calculations based on WD-XRF chemical analysis (Table A.4)

Table 15 Cation content in natural occurring clay minerals.

Specimen	Na (moles)	Ca (moles)	K (moles)	TOTAL
Palygorskite	0.003	0.005	0.02	0.03
Sepiolite	0.02	0.02	0.02	0.05
Bentolite L [®]	0.007	0.03	0.002	0.04
CaMMT (Texas)	0.01	0.03	0.004	0.04
NaMMT (Wyoming)	0.05	0.03	0.012	0.09
NaMMT (Kunipia)	0.1	0.008	0.002	0.1

In the case of palygorskite and sepiolite, FTIR spectra of pyridine adsorbed in these clays revealed vibration modes at 1445 cm^{-1} and $1445, 1596\text{ cm}^{-1}$, respectively. These vibration modes were characteristic of LAS-pyridine interaction.¹⁰⁵ Nevertheless, this technique does not distinguish the cation responsible for this vibration; however the intensity of aluminum has been reported to be more intense than any other cation.⁵¹ In the case of palygorskite, the cation in higher concentration was potassium (0.02 moles K), which is known to be highly polarized by the framework⁶¹ and not very acidic ($\phi = 7\text{ nm}^{-1}$); thus this metal could not be responsible for this band. A more acidic metal also available in the surface of the framework is aluminum ($\phi = 60\text{ nm}^{-1}$) and could be accountable for the LAS-pyridine band in palygorskite, in agreement with the simulation previously done by L.A. Polette *et al.*¹¹ However, in the case of sepiolite, the LAS-pyridine could also be related to the calcium or sodium larger concentration and relatively strong ionic potential ($\phi_{\text{Ca}} = 20\text{ nm}^{-1}$ and $\phi_{\text{Na}} = 10.5\text{ nm}^{-1}$).

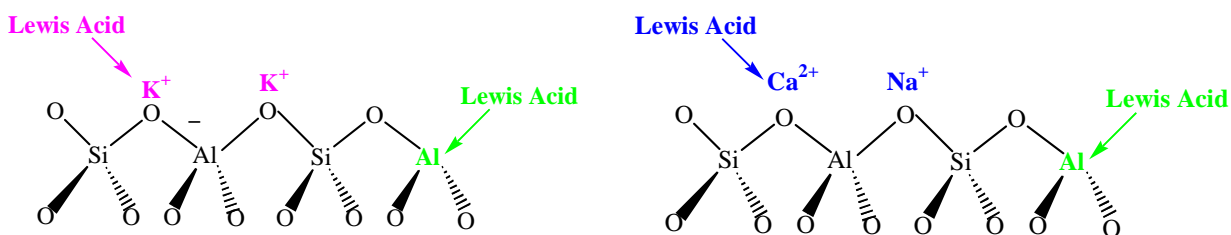


Figure 132 (Left) Lewis Acid Site (LAS) present in palygorskite. (Right) Lewis Acid Site (LAS) present in sepiolite.

The effect of temperature seemed to be a crucial factor for the stability of palygorskite – thioindigo interaction; the thermal energy given to the system at 413K appeared to be enough to drive thioindigo to further places in the structure where thioindigo bulky molecules could block the entrance of the channels for further hydration of the mixture. Besides temperature, moisture uptake due to a larger concentration of high energy hydration cations was another important factor in the stability of the mixture.

Sepiolite, with a larger channel size than palygorskite, managed to display bathochromic shifts only under slight hydration but not while heated. This behavior could be explained by the hydration of the LAS, where a thin layer of water surrounding the LAS, in a C=O---H(HO)LAS interaction with an acidic hydrogen; therefore a bathochromic shift was observed.

Furthermore, higher hydration loses strength by the distance of the water molecules from LAS, displayed as a hypsochromic shift to the original unheated sample and lower absorption.

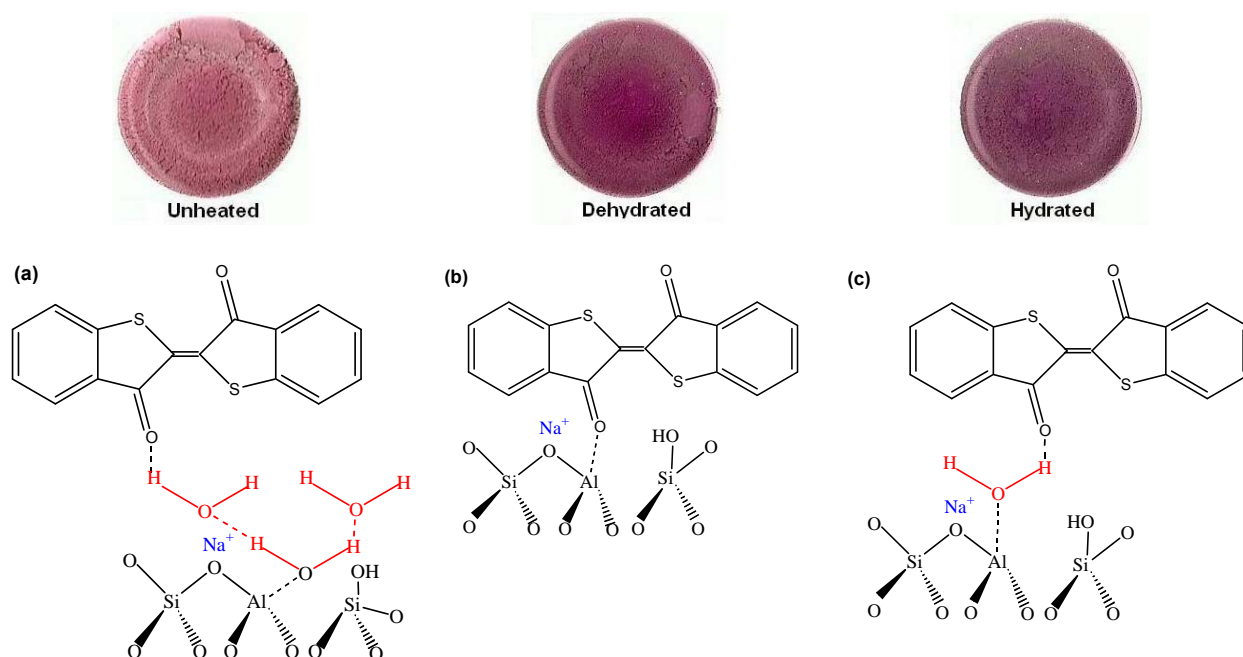


Figure 133 Schematic representation of possible explanation for color changes in sepiolite.

Montmorillonite Clays

Ca²⁺-MMT

Ca²⁺-montmorillonite clays (Bentolite L[®] and Texas deposit) behaved similarly to palygorskite when exposed to thioindigo; a bluer color was obtained under UV-Vis spectroscopy. This color could be explained by the presence of aluminum-LAS and Brønsted acids in these clays. Brønsted acid sites and Lewis acids were confirmed by FTIR pyridine adsorption.

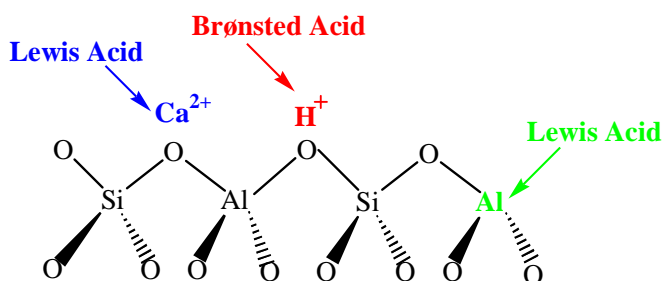
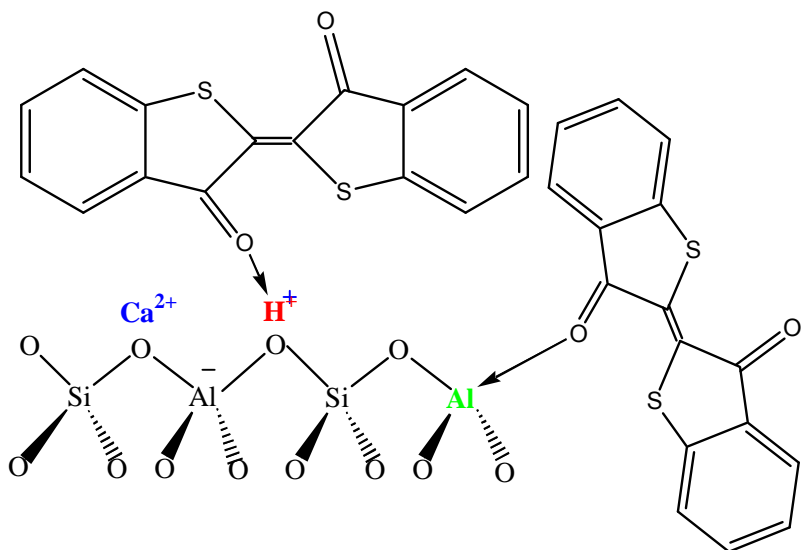


Figure 134 Acid Sites present in Ca^{2+} -Montmorillonite clays (Ca^{2+} -MMT).

The high concentration of calcium (1.1 wt.%) could have been overtaken by the acidic strength of aluminum ($\phi = 60.0 \text{ nm}^{-1}$) and hydrogen, therefore displaying a more intense blue ($\text{C}=\text{O} \cdots \text{Al}$ and $\text{C}=\text{O} \cdots \text{H}$). However, a FT-Raman analysis of these samples could help us draw more conclusions regarding the stress observed in the entire molecule. Color reversibility could be due to the high hydration energy of calcium ($\Delta H_{\text{hyd}} = -1,592 \text{ KJ} / \text{mol}^{-1}$)⁶¹ which was found in high concentration in these clays.



Heated



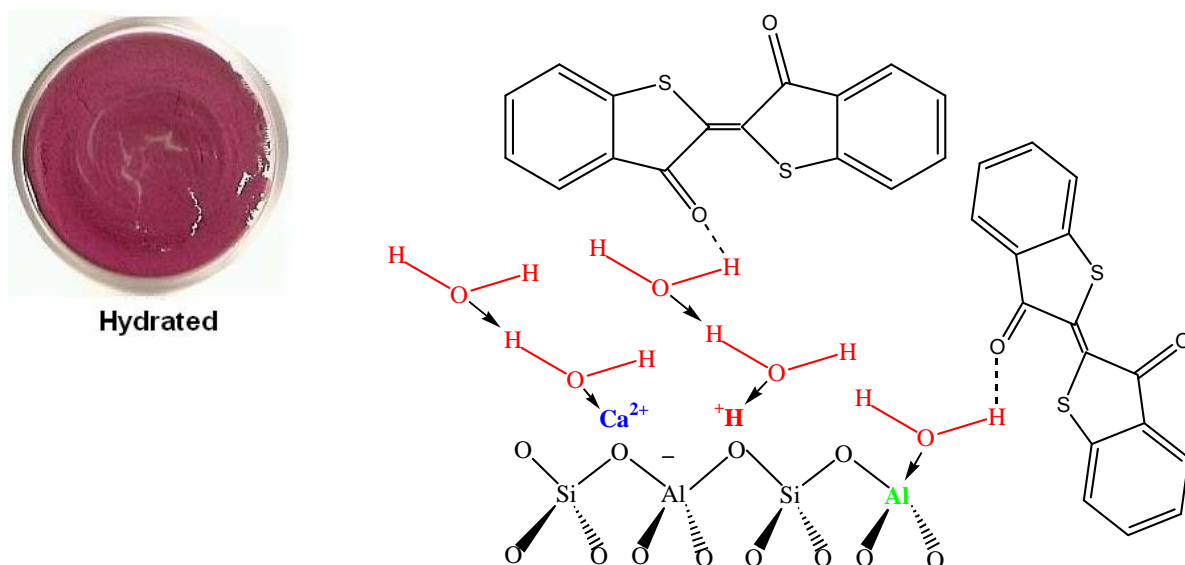


Figure 135 (Top) Schematic representation of tetrahedral sites in Ca^{2+} -MMT structure. Interaction with H and Al-LAS. (Bottom) Hydrated sites of $\text{C}=\text{O} \cdots \text{H}(\text{HO})\text{Al}$ -LAS interaction.

In addition, in these types of clays similar color changes were observed as in sepiolite, where after some time the unheated sample dehydrated due to the dry atmosphere in the region. Therefore, thioindigo molecules were drawn closer to the LAS, displaying a purple color and further dehydration displayed an intense blue. This behavior could be explained in a similar way as in sepiolite interaction shown in Figure 133.

Na⁺-MMT

On the other hand, Na⁺-montmorillonite clays (Wyoming and Kunipia deposits) exhibited only a slight bathochromic shift (purple color) when exposed to thermal treatment. FTIR of pyridine adsorption of these clays revealed no Brønsted acids and low aluminum-LAS (see Figure 74), thus the only available Lewis acids to withdraw thioindigo C=O electrons could be the large amount of sodium cations.

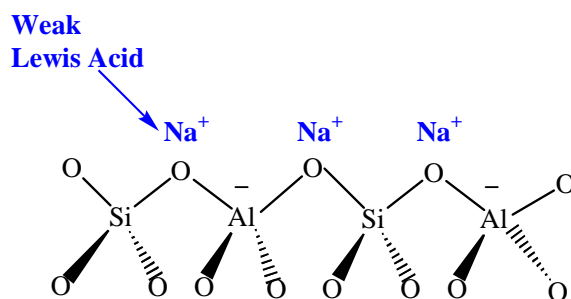
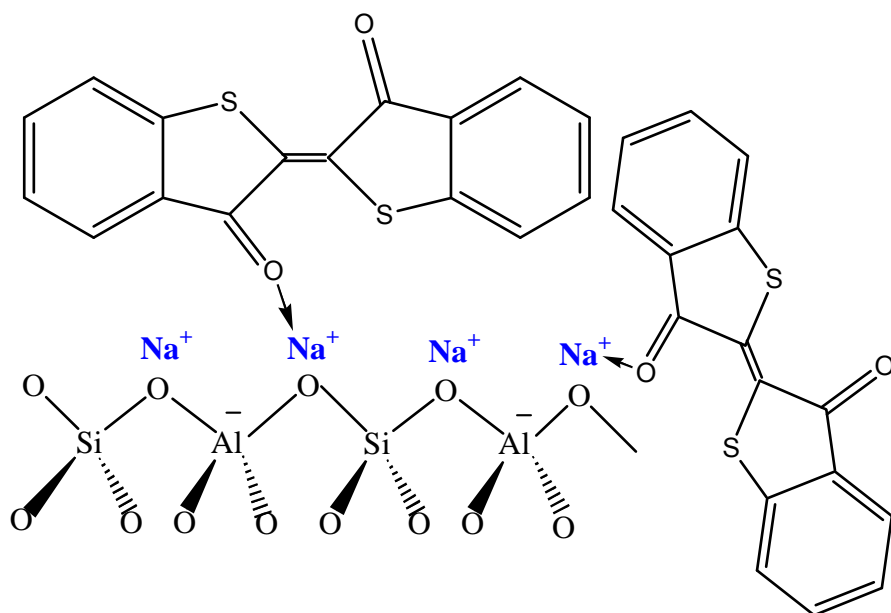


Figure 136 Acid Sites present in Na⁺-Montmorillonite clays (Na⁺-MMT).

Due to the weak Lewis acid character of sodium ($\phi = 10 \text{ nm}^{-1}$), color change (purple) was not as drastic as the purple-blue observed in aluminum ($\phi = 60 \text{ nm}^{-1}$). This effect was confirmed by the cation exchanged in mordenite (Na⁺-MOR) where sodium presented only a slight bathochromic shift. Other inorganic host materials with similar behavior were Zeolon[®] (Na⁺-MOR) and NaY (Na⁺-FAU). Color reversibility in these, Na⁺-MMT clays and zeolites, was obtained during hydration mostly due to the high hydration energy of sodium ($\Delta H_{\text{hyd}} = -405 \text{ KJ} / \text{mol}^{-1}$).⁶¹



Heated



Hydrated

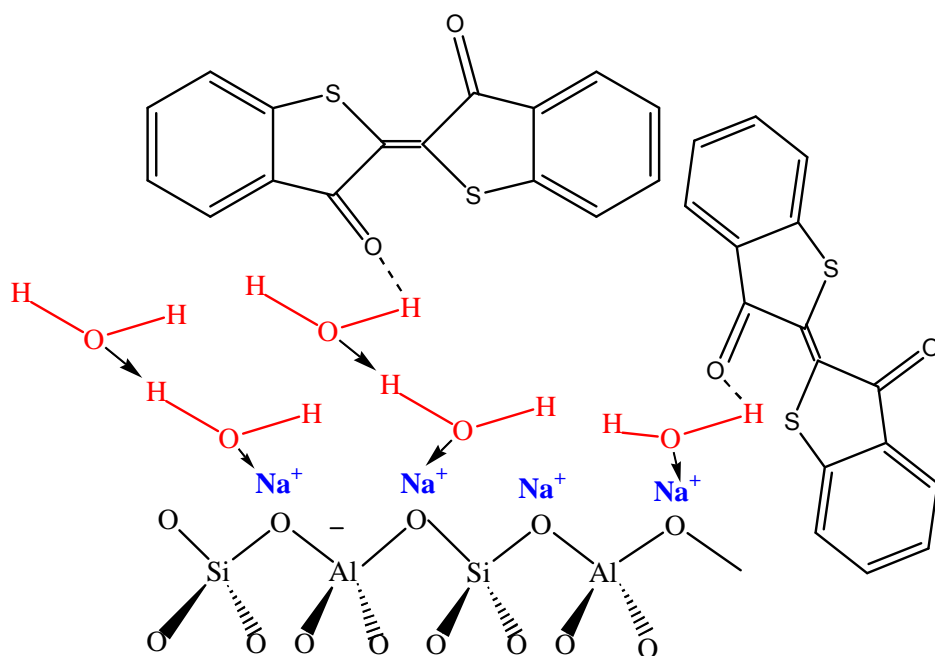


Figure 137 (Top) Schematic representations of tetrahedral sites in Na^+ -MMT structure. Interaction with Na^+ -LAS. (Bottom) Hydrated sites of $\text{C}=\text{O} \cdots \text{H}(\text{HO})\text{Na}^+$ -LAS interaction.

Synthetic Zeolites

Cation Exchange

As mentioned before, cations and protons acted as LAS in some of the inorganic host materials tested.

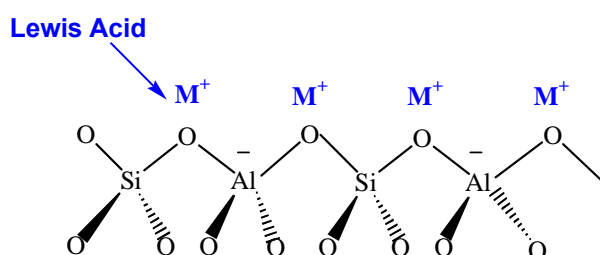








Figure 138 Acid Sites present in silicon-aluminum tetrahedral framework of synthetic zeolite.

Cation exchange H^+ , K^+ , Na^+ , NH_4^+ , Ca^{2+} , and Al^{3+} in mordenite synthetic zeolite (M^{n+} -MOR) demonstrated that a charge to radius ratio (ionic potential) of the cations increased the bathochromic shift of thioindigo when immersed in mordenite. In other words, HOMO-LUMO higher energy states were reached. Ionic potential is known to increase the strength of the electron shift when interacting with electron donor elements.⁶⁶ This was well demonstrated in this experiment where the cation strength was observed to decrease in order of exchange of ions $H^+ > Al^{3+} > Ca^{2+} > Na^+ > NH_4^+ > K^+$ -MOR (see Table 16).

Table 16 Color changes related to exchangeable cation.

Metal [M ⁿ⁺]	Charge [z ⁺]	Ionic Radius (nm) [r]	Ionic Potential (1/nm) ¹⁰⁶ [ϕ]	Color
K ⁺	1	0.142*	7.00	
NH ₄ ⁺	1	0.143**	6.99***	
Na ⁺	1	0.100*	10.0	
Ca ²⁺	2	0.100*	20.0	
Al ³⁺	3	0.050*	60.0	
H ⁺	1	-	-	

* Ionic radius calculated from ionic potential ** Value from ref.[107] *** Calculated from ref.[107]

Based on the ionic potential values, NH_4^+ displayed a larger bathochromic shift than expected. This could be explained by the proton acidity of the cation when attached to an electronegative neighboring atom. However, the shift was not as strong as the one observed in H^+ , since oxygen from the framework presented larger electronegativity as displayed in Figure 139.⁶⁶

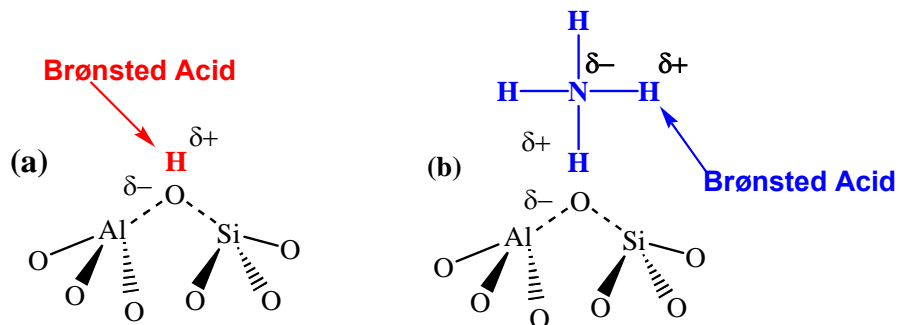
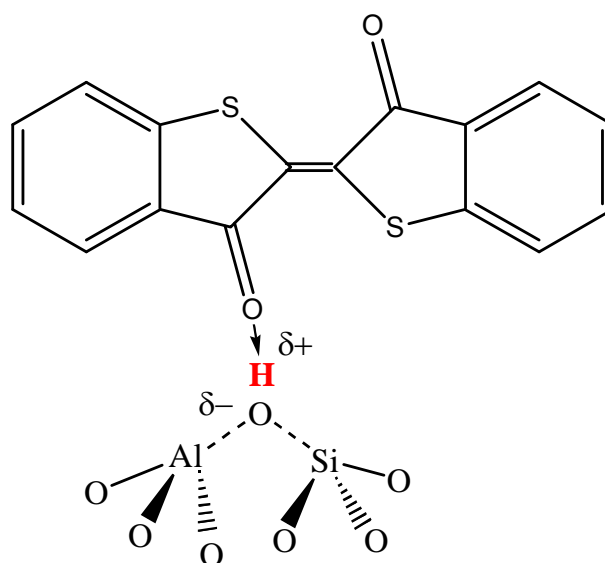


Figure 139 (a) Brønsted acid sites and (b) Ammonium exchange in silicon-aluminum tetrahedral framework.

This effect was also demonstrated by computer simulation (see Figure 129 and Figure 131) where structural models matched the experimental UV-Vis spectra. In addition, the acidic strength of the O-H bond was also tested in a solution where 100% sulfuric acid reacted with thioindigo to produce a bright blue-green color which was susceptible to humidity.



Heated



Unheated

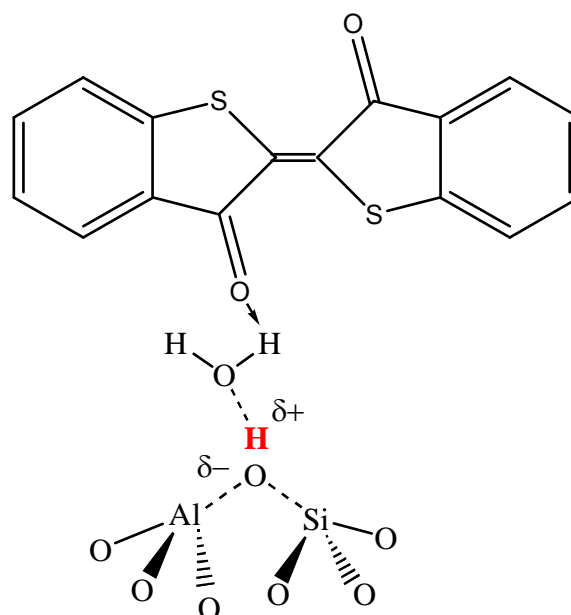
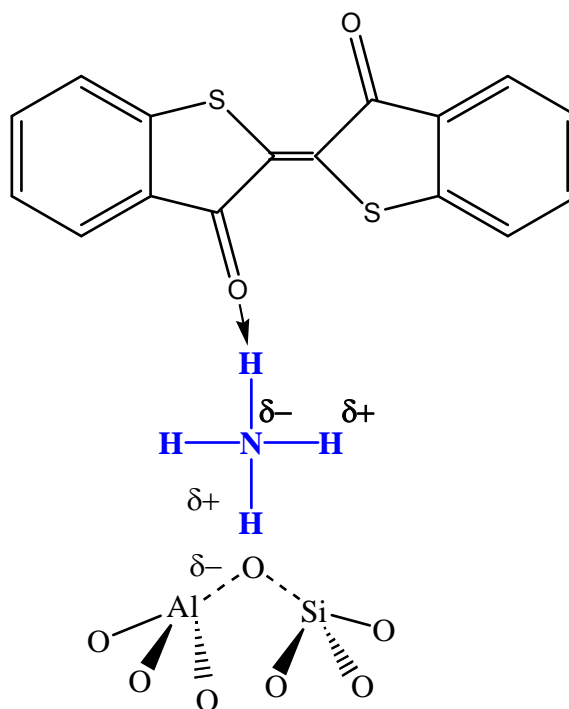


Figure 140 (Top) Schematic representation of tetrahedral sites in synthetic zeolites. Interaction with H^+ -LAS. (Bottom) Hydrated sites of $\text{C}=\text{O} \cdots \text{H}(\text{HO})\text{H}^+$ -LAS interaction.



Heated



Unheated

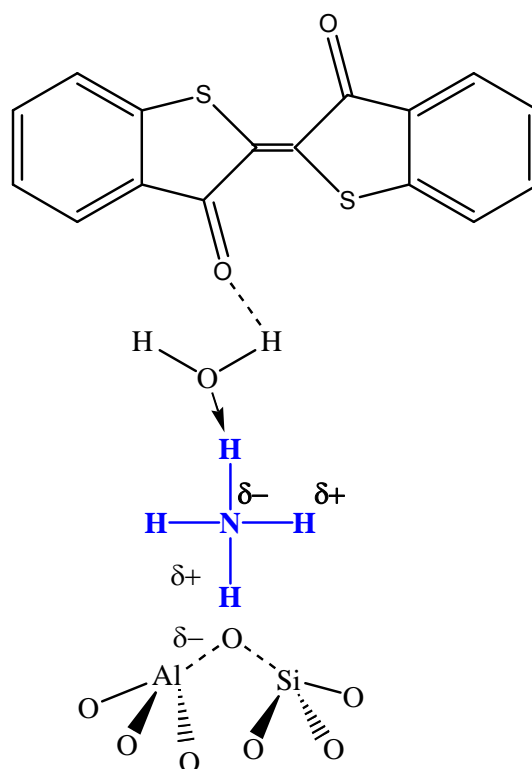


Figure 141 (Top) Schematic representation of tetrahedral sites in synthetic zeolites. Interaction with NH_4^+ -LAS. (Bottom) Hydrated sites of $\text{C}=\text{O} \cdots \text{H}(\text{HO}) \text{NH}_4^+$ -LAS interaction.

Influence of Channel Dimension in Zeolites

Surface interaction in zeolites appeared to be minimal; zeolites with channel size smaller than the size of thioindigo [15.17 Å (length), 7.42 Å (width) and 3.4 Å (thickness)³²] displayed no color changes. This effect was also confirmed by Monte Carlo sorption simulation¹⁰⁸ of the absorbed thioindigo molecules in three types of zeolites: faujasite (FAU) [11.7 molecules per unit cell], mordenite (MOR) [1 molecule per unit cell] and Linde type A (LTA) [0 molecules per unit cell], where FAU (channel size 7.4 Å⁵³) was able to accommodate more molecules than MOR (channel size 17.5 Å [length] x 6.5 Å [width]) and LTA (channel size 4.2 Å⁵³). Moreover, the destruction of the channel in Zeolon® (Na⁺-MOR) at 950°C did not display the characteristic purple obtained originally.

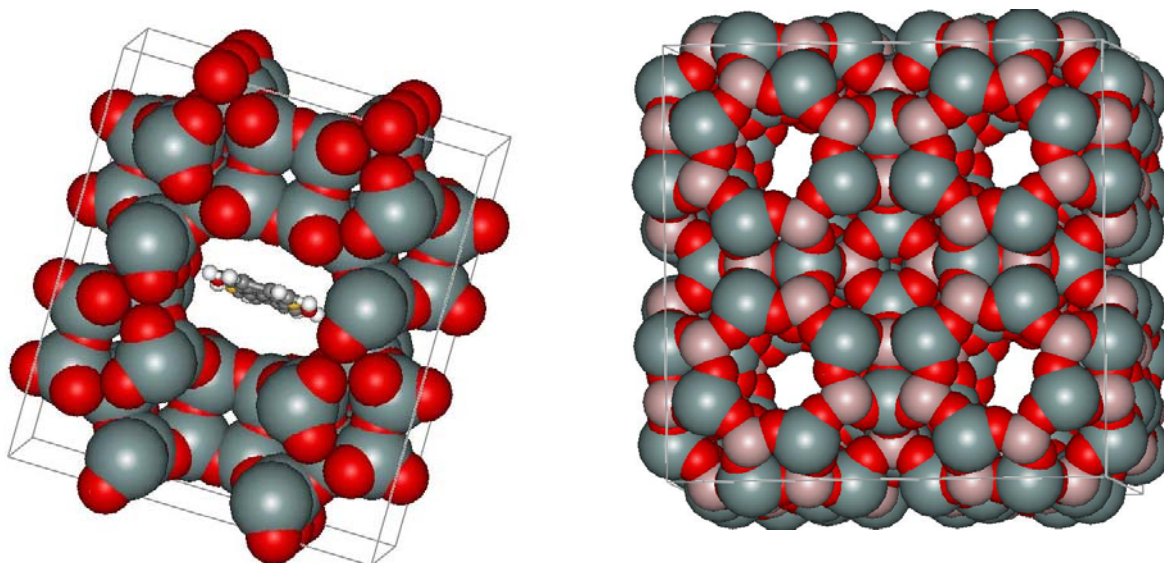


Figure 142 (Left) Mordenite (MOR) unit Cell with 1 molecule of thioindigo inserted in the channels. (Right) Linde Type A (LTA) unite cell with 0 molecules of thioindigo inserted in the channels by Monte Carlo Simulation [Cerius²-Software].

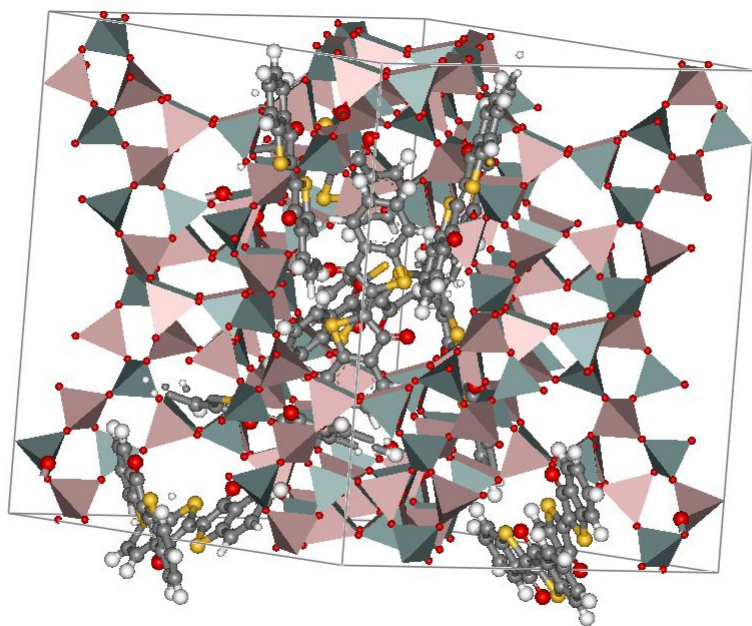


Figure 143 Faujasite (FAU) unit cell with 11.7 molecules of thioindigo inserted in the channels by Monte Carlo Simulation [Cerius² Software].

CHAPTER 6

INDUSTRIAL APPLICATION

6.1 Introduction

Hybrid materials color reversibility was observed to be water sensitive; therefore, a potential application could be their use as humidity sensors. A Water sensor, such as Co(II) chloride, is one of the main chemicals used in order to identify humidity in air tight compartments. The chemistry involved is the hydration of the salt to form $\text{Co}(\text{H}_2\text{O})_6^{2+}$. This salt is normally added to silica gel and used as indicator.¹⁰⁹ Nevertheless, hybrid materials chemistry is different since it is more related to the aluminum silicate framework acidity, thus withdrawing electrons from the organic molecule; however, the output is the same, i.e. color change when exposed to humidity. The use of clays is extensive and if this could have color changes depending on humidity, could be a beneficial point. A patent would be filed to limit the dissemination of this specific processing.

On the other hand, two materials with these reversible properties were tested in polyethylene resin in order to evaluate if the pigment would still go into reversible changes when immersed in a different matrix.

6.2 Experimental

Polyethylene resin RSN-001-01 was used as received. Reversible hybrid materials: Bentolite / 0.5 mol % thioindigo and Valfor CP300-35 / 0.5 % mol thioindigo heated at 413K for nine hours were used after thermal treatment.

40 g of polyethylene resin was treated with 0.4 g of reversible hybrid material and mixed inside a plastic container until a homogeneous cover on the polyethylene pellets was observed. These samples were then placed in a bench-top injection molding machine (Galmob, Inc, Model A-100) at 477K for 1 minute.

In order to obtain color changes previously observed in the hybrid material, the new composite was placed inside a furnace at 413K for 1 hour.

6.3 Results and Discussion

Chromatic samples were obtained after injection molding. However, no reversible color changes were observed (see Figure 144). Samples placed inside the furnace at 413K for 1 hour, displayed no color change. The absence of reversibility could be related to the matrix not allowing the free hydration and dehydration of the hybrid material, therefore no color change is observed.

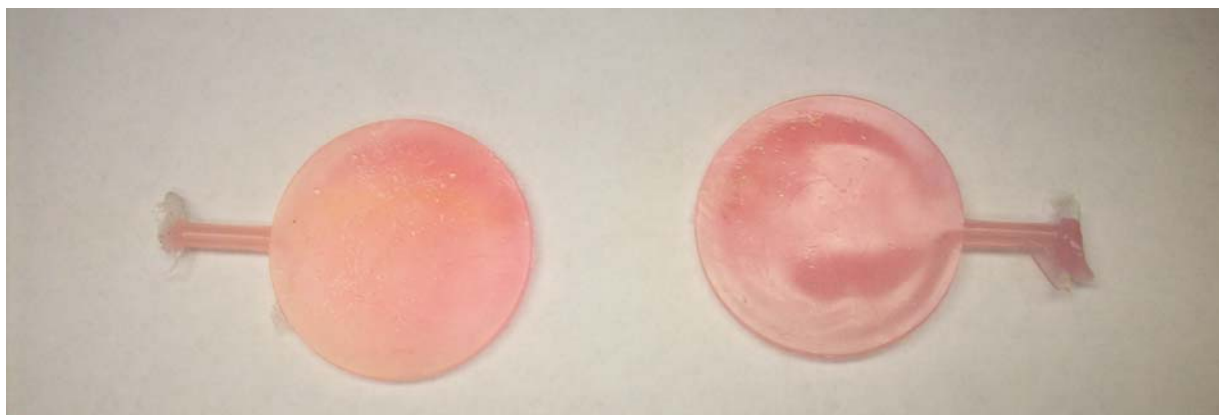


Figure 144 Injection molding samples (left) Valfor CP300-35 (H^+ -MMT) / 0.5 % thioindigo and (right). Bentolite L (Ca^{2+} -MMT) / 0.5 mol % thioindigo.

6.4 Conclusions

The use of this reversible hybrid material is exclusive to open systems, due to the major effect water molecules have on the color reversibility.

REFERENCES

-
- 1 R. J. Gettens, G.L. Stout (Eds.), *Paint Materials: A short Encyclopedia*. D. van Nostrand, New York, NY, 1946.
 - 2 L. A. Polette, Ph.D Thesis, University of Texas at El Paso, 2002.
 - 3 F. S. Manciu, L. Reza, L. A. Polette, B. Torres and R. R. Chianelli. *J.Raman Spectrosc.* 2007,38, 1193-1198.
 - 4 F. S. Manciu, A. Ramirez, W. Durrer, J. Govani and R. R. Chianelli, *J.Raman Spectrosc.* 2008, 39(9), 1257-1261.
 - 5 Silk, in *Student's Encyclopædia Britannica.*, 2007.
 - 6 Haymond Zwinger, in *Downcanyon*, The University of Arizona Press, 1995, pp. 69-70.
 - 7 A von Baeyer, *Berichte der Deutschen Chemischen Gesellschaft*, 1900, 33 (3), Supplement.
 - 8 M. Longhena, in *Grandes Civilizaciones del Pasado, Mexico Antiguo*, Folio, Barcelona, 1998, pp.31.
 - 9 D. E. Arnold, and B. F. Bohor, *American Antiquity*, 1977, 42(4), 575-82; D. E. Arnold, and B. F. Bohor, *Archeology*, 1975, 28, 23-9.
 - 10 R. Kebler, R. Masschelein-Kleiner, and J. Thissen. *Studies in Conservation*, 1967, 12(2), 41-56; H. van Olphen, *Science*, 1966, 154, 645-6.
 - 11 L. A. Polette-Niewold, F. S. Manciu; B. Torres; M. Jr. Alvarado; R. R. Chianelli, *Journal of Inorganic Biochemistry*, 2007,101 (11-12), 1958-73.

-
- 12 G. Chiari, R. Giustetto, J. Druzik, E. Doehnel and G. Ricchiardi, *Appl. Phys. A*, 2008, 90, 3-7.
- 13 B. Hubbard, W. Kuang, A. Moser, G. A. Facey and C. Detellier. *Clays and Clay Minerals*, 2003, 51(3), 318-326.
- 14 A. Domenech, M. T. Domenech-Carbo, and M. L.Vazquez de Agredos Pascual, *J. Phys. Chem. C*, 2007, 111, 4585-4595.
- 15 G. M. Schwab and E. Schneck, *Z. Phys. Chem. Neue Folge Bd*, 1958,18, 206.
- 16 H. D. Breuer and H. Jacob, *Chem. Phys. Letters*, 1980, 73(1), 172-174.
- 17 D. Reinen, P. Koehl and C. Mueller, *Z. Anorg. Allg. Chem.*, 2004, 630,97-103.
- 18 R. Hoppe, G. Schulz-Ekloff, D. Woehrle, C. Kirschhock and H. Fuess, *Langmuir*, 1994, 10, 1517-1523.
- 19 A. J. Gordon and R. A. Ford, in *The Chemist Companion, A Handbook of Practical Data, Technique and Reference*, Wiley Interscience, New York, 1972.
- 20 W. R. Brode and G. M. Wyman, *National Bureau of Standard*,1951,4267-4270.
- 21 S. Sharma, S. Komarneni, Synthesis and characterization of synthetic mica-bionanocomposites, *Applied Clay Science* ,2008, doi:10.1016/j.clay.2008.03.006.
- 22 S. Komarneni, R. Pidugu and V. C. Menon, *Journal of Porous Materials*, 1996, 3, 99-106.
- 23 M. A. Makarova,¹ A. E. Wilson, B. J. van Liemt, C. M. A. M. Mesters, A. W. deWinter, and C. Williams, *Journal of Catalysis*, 1997, 172, 170–177.
- 24 Xie Zaiku, Chen Qingling, Zhang Chengfang, Bao Jiaqing, and Cao Yuhua, *J. Phys. Chem. B* 2000, 104, 2853-2859.

-
- 25 C. Ravindra Reddy, Gopalpur Nagendrappa and B. S. Jai Prakash, *Catalysis Communications*, 2007, 8, 241–246.
- 26 K. F. J. Heinrich and D. E. Newbury in *ASM Handbook, Materials Characterization*, 1986, 10, p.516.
- 27 J. Ridley, M. C. Zerner, *Theor. Chem. Acta*, 1973, 32, 111; M. C. Zerner, K. B. Lipkowitz, D. B. Boyd (Eds.) in *Reviews of Computational Chemistry*, VCH New York 1991, 2 (8), pp. 313ff.
- 28 K. B. Stark, J. M. Gallas, G. W. Zajac, M. Eisner, T. J. Golab, *J. Phys.Chem. B* 107 (13) 2003 11558-11562.
- 29 J. A. Pople, D. P. Santry, *J. Chem. Phys.*, 1965, 43, p.129.
- 30 M. Sainsbury, in *Rodd's Chemistry of Carbon Compounds, Heterocyclic Compounds part B*, ed. S. Coffey, ch.14, 4, p.p.341-367.
- 31 M. Klessinger, *Tetrahedron*, 1966, 22, 3355-3365; D. Jaquemin, J. Preat, V. Wathelet, Michele Fontaine and E. A. Perpete, *J. Am. Chem. Soc.*, 2006, 128, 2072-2083.
- 32 MOPAC 2007, James .J. P. Stewart from *Stewart Computational Chemistry*, Version 8.032W. J. J. P. Stewart, *J. Mol. Mod.*, 2007, 13, 1173-1213. L. Pauling, in *The Nature of the Chemical Bond*, Cornell University Press, USA, 1945.
- 33 W. Haase-Wessel, M. Ohmasa and P. Suesse, *Naturwissenschaft*, 1977, 64, 435.
- 34 G. S. Egerton, *Nature*, 1959, 4658, 389-390.

-
- 35 . D. Jacquemin, J. Preat, V. Wathélet, M. Fontaine, and E. A. Perpete, *Journal of the American Chemical Society*, 2006, 128, 6, 2072-2083.
- 36 G. M. Wyman and W. R. Brode, *National Bureau of Standard*, 1951, 73, 1487-1493.
- 37 S. Y. Chai, R. Zhou, Z. W. An, A. Kimura, K. Fukuno and M. Matsumura, *Thin Solid Films*, 2005, 479, 282-287.
- 38 J. Fabian, L. A. Diaza, , G. Seifert and T. Niehaus, *Journal of Molecular Structure (Theochem)*, 2002, 594, 41–53
- 39 W. F. Bradley, *Am. Mineral.*, 1940, 25, 405-410; J. L. Ahlrichs, C. Serna and J. M. Serratosa, *Clays and Clay Minerals*, 1975, 23, 119-124.
- 40 B. Velde, in *Origin and Mineralogy of Clays*, Springer, New York, 1995, p.26, 31.
- 41 W. F. Bradley, *Am. Mineral.*, 1940, 25, 405-410. A. Pressinger, *Clays and Clay Minerals*, 1959, 61-67.
- 42 S. Caillère and S. Hénin, in G. Brown (Ed.), *The X-ray Identification and Crystal Structure of Clay Minerals*, Mineralogical Society, London, 1961 Chaps. VII and IX.
- 43 G. Chiari, R. Giustetto, J. Druzik, E. Doehnel and G. Ricchiardi, *Appl. Phys. A*, 2008, 90, 3-7.
- 44 M. Suarez,-Romero, M. Sanchez del Rio, P. Martinetto and E. Dooryhee, *Clay Minerals*, 2007, 42, 287-297.
- 45 Coastal and Marine Geology Program, Report number 01-041.

-
- 46 U. Shuali, M. Steinberg, S. Variv, M. Muller-Vonmoos, G. Kahr and A. Rub, Clay Minerals, 1990, 25, 107-119.
- 47 J. L. M. Vivaldi and P. F. Hach-Ali, in Differential Thermal Analysis, ed. R. C. Mackenzie, Academic Press, 1970, ch 20, pp.563-565.
- 48 C. Serna, G. E. VanScoyoc and J. L. Ahlrichs, American Mineralogist, 1977, 62, 784-792.
- 49 J. L. Ahlrichs, C. Serna and J. M. Serratos, Clays and Clay Minerals, 1975, 23, 119-124.
- 50 H. W. Van der Marel and H. Beutelspacher in Atlas of infrared Spectroscopy of Clay Minerals and their Admixtures, Elsevier, New York, 1976, p.118.
- 51 J. V. Smith, in Zeolite Chemistry and Catalysis, ed. J. A. Rabo, ACS Monographs 171, ch 1, 1976, pp.3-79.
- 52 W. M. Meier in Molecular Sieves, Society of the Chemical Industry, London, 1968, p.10.
- 53 L. Smart and E. Moore, in Solid State Chemistry, Chapman & Hall, London, ch. 5, pp.183-213.
- 54 G. Bergerhoff, G., W. H. Baur, and W. Nowacki, Über die Kristallstrukturen des Faujasits, 1958, 193-200.
- 55 T. B. Reed, and D. W. Breck, J. Am. Chem. Soc., 1956, 78, 5972-5977.
- 56 W. M. Meier, Z. Kristallogr., 1961, 115, 439-450.
- 57 T. C. Jorgensen and L. R. Wheelerley, Water Research, 2003, 37, 1723-1728.
- 58 James Girard in Principles of Environmental Chemistry, Jones & Bartlett Publishers, New York, 2004, pp. 570-571.

-
- 59 G. Wulfsberg in *Inorganic Chemistry*, University Science Books, New York, 2000, p.56-59.
- 60 M. W. Barsoum in *Fundamentals of Ceramics*, CRC Press, New York, 2003, p.92.
- 61 A. Meunier in *Clays*, Springer, Berlin, 2005, p.194.
- 62 G. Hill and J. Holman in *Chemistry in Context*, Nelson Thornes, New York, 2000, p.163.
- 63 J. Girard in *Principles of Environmental Chemistry*, Jones & Bartlett Publishers, New York, 2004, pp. 570-571.
- 64 E. Wiberg, N. Wiberg, A. F. Holleman in *Inorganic Chemistry*, Academic Press, 2001, p. XXXVI.
- 65 W. M. Latimer, K. S. Pitzer, C. M. Slansky, *J. Chem. Phys.* 1989, 7, 108. The original equation given by Latimer has been updated by Roger Todd to fit the more modern thermodynamic data and radii.
- 66 T. L. Brown, H. E. Lemay Jr, B. E. Bursten, J. R. Burdge, in *Chemistry the Central Science*, Prentice Hall, ed. 9th, ch.16, pp. 650-651.
- 67 W. Zhang, P. G. Smirniotis, M. Gangoda and R. N. Bose, *J. Phys. Chem. B*, 2000, 104, 4122-4129.
- 68 U. Shuali, L. Brain, M. Steinberg and S. Yariv. *Journal of Thermal Analysis*, 1991, 37, 1569-1578.
- 69 G. L. Woolery, G. H. Kuehl, H. C. Timken, A. W. Chester, and J. C. Vartuli, *Zeolites*, 1997, 19, 288-296.

-
- 70 F. Mauge, A. Sahibed-Dine, M. Gaillard and M. Ziolek, J. of Catalysis, 2002, 207, 353-360.
- 71 L. Pinard, P. Magnoux, P. Ayrault and M. Guisnet, J. of Catalysis, 2004, 221, 662-665.
- 72 M. Klessinger and W. Lüttke, Chem. Ber., 1966, 99, 2136-2145. W. Lüttke and M. Klessinger, Chem. Ber., 1964, 97, 2342-2357. G. S. Egerton, Nature, 1959, 389-390. R. Hoppe, G. Schulz-Ekloff, D. Wöhrle, Langmuir, 1994, 10, 1517-1523.
- 73 F. Abelès in Optical Properties of Solids, North Holland Publishing Company, London, 1972, p.184.
- 74 D. Williams, Masters Thesis, Durham University , 2008.
- 75 Hrachova, J. *et al.* Materials Letters, 2007, 61, 3361-3365.
- 76 U. Shuali, Thermochimica Acta, 1989, 148, 445-456.
- 77 P. G. Nahin, Calif. Dept. Nat. Resources, Div. Mines Bull., 1955, 169, 112-18.
- 78 H. W. Van der Marel and H. Beutelspacher in Atlas of infrared Spectroscopy of Clay Minerals and their Admixtures, Elsevier, New York, 1976, p.40, 118.
- 79 C. Yürüdü, S. Işçi, C. Ünlü, O. Atici, Ö. I. Ece and N. Güngör, Bull.Mater.Sci.,2005, 28,6,623-628.
- 80 F. Mauge, A. Sahibed-Dine, M. Gaillard and M. Ziolek, J. of Catalysis, 2002, 207, 353-360.
- 81 G. D. Chukin and P. Yu Serikov, Kinetics and Catalysis, 1999, 4, 567-574.
- 82 Shie-Ping Sheu, H. G. Karge and R. Schloegl, J. of Catalysis, 1997, 168, 278-291.

-
- 83 S. B. Weeds and J. B. Dixon, in *Minerals in Soil Enviroments*, Soil, Sci.Soc.Am., Madison, 1988, 13, p.p. 435-471.
- 84 J. A. Rabo, in *Zeolite Chemistry*, ACS Monographic 171, American Chemical Society, 1976, Washington D.C. 118-284.
- 85 I. S.; Perelygin, M. A. Klimchuk, *Zhurnal Prikladnoi Spektroskopii*, 1976, 24, 1, 65-68.
- 86 L. Bîrlădeanu in *Infrared Spectroscopy, Applications in Organic Chemistry*, Wiley Interscience, New York, 1966.
- 87 C. Yohannan Panicker, Hema Tresa Varghese, Daizy Philip, Helena I.S. Nogueira, *Spectrochimica Acta Part A*, 2006, 64, 744–747.
- 88 E. Jóna, M. Kubranová, A. Sirota and M. Kopcová, *Journal of Thermal Analysis and Calorimetry*, 2001, 63, 807-.813.
- 89 M. Serratos, J. M., *Clays and Clay Minererals*, 1966, 14, 385-389.
- 90 E. Tatsch and B. Schrader, *J. Raman Spectrosc.*, 1995, 26, 467-473.
- 91 F. S. Manciu, L. Reza, L. A. Polette, B. Torres and R. R. Chianelli, *J. Raman Spectrosc.* 2007; 38, 1193–1198.
- 92 E. Mendelovici, *Clays and Clay Minerals*, 1973, 21, 115-119.
- 93 K. B. Yoon and T. J. Huh, *Journal of Physical Chemistry*, 1995, 99, 7092-7053.
- 94 H. von Eller, *Bull. Soc. Chim. Fr.*, 1955, 1438-1449.
- 95 J. Thorez in *Practical Identification of Clay Minerals*, Editions G. Lelotte, Belgium, 1976, p. 16.

-
- 96 Xie Zaiku, Chen Qingling, Zhang Chengfang, Bao Jiaqing, and Cao Yuhua, J. Phys. Chem. B 2000, 104, 2853-2859.
- 97 Woo-Chan, Jung and Young-Duk Huh, Bull. Korean Chem. Soc. 1996, 17, 6, 547-550.
- 98 S. Komarneni, C. A. Fyfe, G. J. Kennedy and H. Strobl, J. Am. Ceram. Soc., 1986, 69, 3, C 45-47.
- 99 M. Matsumoto, M. Suzuki, H. Takahashi and Y. Saito, Bull. Chem. Soc. Jpn., 1986, 59, 303-304.
- 100 K. B. Stark, J. M. Gallas, G. W. Zajac, M. Eisner, T. J. Golab, J. Phys. Chem. B 107 (13) 2003 11558-11562.
- 101 E. Horn and G. Louis, in Inorganic Biochemistry, Elsevier Scientific, 1973, 1023-1066.
- 102 J. C. Davidtz, J. Catal., 1976, 43, 260-263.
- 103 B. C. Gates and H. Knözinger in Advances in Catalysis, Elsevier Academic Press, London, 2004, p. 260.
- 104 G. L. Woolery, G. H. Kuehl, H. C. Timken, A. W. Chester, and J. C. Vartuli, Zeolites, 1997, 19, 288-296.
- 105 E. Jóna, M. Kubranová, A. Sirota and M. Kopcová, Journal of Thermal Analysis and Calorimetry, 2001, 63, 807-813.
- 106 M. W. Barsoum in Fundamentals of Ceramics, CRC Press, 2003, p.92.
- 107 T. C. Jorgensen and L. R. Wheelerley, Water Research, 2003, 37, 1723-1728.

108 Metropolis, N.; Rosenbluth, A. W.; Rosenbluth, M. N.; Teller, A. H.; Teller, E.
J. Chem. Phys., 1953, 21, 1087.

109 The Merck Index, 7th edition, Merck & Co, Rahway, New Jersey, USA, 1960;
N. S. and F. B. Taylor, Inorg. Synth., 1967, 9: 136–142.

APPENDIX A

Table A. 1 WD-XRF chemical analysis clays and synthetic aluminosilicates used in this study.

Specimen :		Natural Occurring Clay Minerals				
	Sepiolite (Tolsa deposit)	Palygorskite (MinTech Inc.)	Bentolite L [®]	Na-MMT (Wyoming deposit)	Na-MMT (Kunipia deposit)	Ca-MMT (Texas deposit)
%SiO ₂	57.3	55.2	65.9	60.9	56.8	63.0
%Al ₂ O ₃	3.21	8.24	13.7	18.4	20.2	15.2
%Fe ₂ O ₃	0.5	4.27	0.68	3.72	1.86	1.53
%MgO	19.3	10.7	2.79	2.63	3.2	3.27
%CaO	0.83	0.29	1.49	1.66	0.46	1.53
%Na ₂ O	0.49	0.1	0.22	1.59	3.27	0.34
%K ₂ O	1.11	0.82	0.10	0.55	0.09	0.18
wt.% %TiO ₂	0.11	0.69	0.19	0.11	0.13	0.24
%P ₂ O ₅	0.05	0.07	0.03	0.06	0.02	0.04
%MnO	0.06	0.12	0.02	< 0.01	0.02	0.02
%Cr ₂ O ₃	0.01	0.01	< 0.01	0.05	< 0.01	0.01
%V ₂ O ₅	0.01	0.02	< 0.01	< 0.01	< 0.01	< 0.01
%LOI*	16.8	19	15.9	11.6	13.4	15.3
%Sum	99.8	99.5	101.0	101.2	99.4	100.7
Si / Al	15.1	5.68	4.08	2.80	2.39	3.52

*LOI = Loss of Ignition

*LOI = Loss of Ignition

Specimen : **Synthetic Zeolites**

	ZEOLON®	CBV10A	CBV21A	LZY-62	NaY	13X	4A	5A	VALFOR® CP300-35	MS-1	MAS-1	MA-1
%SiO ₂	75.0	65.7	78.3	51.2	49.0	39.5	33.5	36.3	73.8	100	50	0
%Al ₂ O ₃	8.73	13.9	7.01	17.4	16.8	26.5	28.7	31.2	15.7	0	50	100
%Fe ₂ O ₃	0.08	0.95	0.27	0.11	0.11	0.02	0.1	0.03	0.04	0	0	0
%MgO	0.02	0.26	0.09	< 0.01	0.03	< 0.01	< 0.01	< 0.01	0.06	0	0	0
%CaO	0.02	0.42	0.12	0.09	0.01	< 0.01	< 0.01	11.9	< 0.01	0	0	0
%Na ₂ O	0.63	5.00	0.19	2.05	10.4	15.7	17.3	5.7	0.08	0	0	0
%K ₂ O	0.02	0.12	0.04	< 0.01	0.03	0.02	0.01	0.21	< 0.01	0	0	0
%TiO ₂	0.32	0.35	0.41	0.06	0.04	< 0.01	0.02	< 0.01	0.03	0	0	0
%P ₂ O ₅	< 0.01	< 0.01	0.41	< 0.01	0.01	< 0.01	< 0.01	< 0.01	< 0.01	0	0	0
%MnO	< 0.01	< 0.01	< 0.01	< 0.01	< 0.01	< 0.01	< 0.01	0.01	< 0.01	0	0	0
%Cr ₂ O ₃	< 0.01	< 0.01	< 0.01	0.01	0.02	< 0.01	0.01	< 0.01	< 0.01	0	0	0
%V ₂ O ₅	< 0.00	< 0.01	< 0.01	0.01	0.02	< 0.00	0.00	< 0.01	< 0.01	0	0	0
%LOI*	16.1	12.2	5.77	29.7	24.3	18.4	20.8	14.5	9.96	0	0	0
%Sum	100.9	99.0	99.3	100.6	100.7	100.1	100.5	99.8	99.7	0	0	0
Si / Al	7.31	4.01	9.48	2.50	2.48	1.26	0.989	0.987	3.99	100%Si	1.00	100%Al

*LOI = Loss of Ignition

Table A. 2 WD-XRF Chemical analysis of synthetic zeolites used in this study.

Table A. 3 WD-XRF Chemical analysis of synthetic zeolites used in this study.

		Specimen:	Synthetic Swelling Micas		
		TALC	Na-Ts	YN6	YN8
	%SiO ₂	60.2	57.3		
	%Al ₂ O ₃	1.11	0.08		
	%Fe ₂ O ₃	1.57	0.05		
	%MgO	29.4	24.4		
	%CaO	0.72	0.11		
	%Na ₂ O	0.07	6.96		
	%K ₂ O	0.04	0.02		
	%TiO ₂	0.05	0.02		
	%P ₂ O ₅	0.02	0.01		
wt. %	%MnO	0.02	< 0.01		
	%Cr ₂ O ₃	<0.01	< 0.01		
	%V ₂ O ₅	<0.01	< 0.01		
	%LOI*	5.77	10.8		
	%Sum	98.9	99.8		
	Si / Al	46.0	71.6	63.0	15.0
	%Silicic Acid				
	%NaF				
	%MgCl ₂				
	%AlOOH				

*LOI= Loss on Ignition

Table A. 4 List of natural occurring clay minerals used in this research. Chemical formula derived from WD-XRF measurements, pore size and general structure based on literature.

Specimen	Chemical Formula							Cation	Si/Al	Pore Size (Å)	Structure	Ref.	Provider											
Natural Occurring Clay Minerals																								
Sepiolite	Si	0.953	Al	0.0629	Mg	0.479	Na	0.016	Ca	0.015	K	0.0236	H ₂ O	Ca,Na,K	15.1	10.7 x 3.7	channels	J.L.Ahrichs	Tolsa Inc.					
		0.933																						
Palygorskite	Si	0.918	Al	0.162	Fe	0.0669	Mg	0.266	K	0.017	O	2.48	H ₂ O	1.056	K	5.68	6.4 x 3.7	channels	W.F. Bradley	Mintech Inc.				
Smectites																								
Bentolite L [®]	Si	1.10	Al	0.269	Fe	0.011	Mg	0.0692	Ca	0.0266	O	2.72	H ₂ O	0.883	Ca	4.08	14.9 (l.s)	layer	G.Milton/ T.Kijima	Internationala				
Na-mont.	Si	1.01	Al	0.361	Fe	0.0583	Mg	0.0653	Ca	0.0296	Na	0.0513	K	0.012	Ca, Na, K	2.80	12.6 (l.s)	layer	G.Milton/ T.Kijima	Wyoming****				
Na-mont.	Si	0.945	Al	0.396	Fe	0.0292	Mg	0.0794	Na	0.105	O	2.67	H ₂ O	0.744	Na	2.39	12.6 (l.s)	layer	G.Milton/ T.Kijima	Kunipia, Japan				
Ca-mont.	Si	1.05	Al	0.298	Fe	0.0240	Mg	0.0811	Ca	0.0273	Na	0.011	O	2.70	Na, Ca	3.52	14.9 (l.s)	layer	G.Milton/ T.Kijima	Texas**				
(i.s.) interlayer spacing																								

**Clay Mineral Repository, University of Missouri, Columbia MO 65201, USA

Table A. 5 List of synthetic zeolites used in this research. Chemical formula derived from WD-XRF measurements, pore size and general structure based on literature.

Specimen	Chemical Formula	Cation	Si/Al	Pore Size (Å)	Structure	Ref.	Provider
<i>Synthetic Zeolites</i>							
ZEOLON®	Si _{1.25} Al _{0.171} Na _{0.020} O _{2.77} H ₂ O _{0.894}	Na	7.31	6.5 X 7.0	MOR	R.M.Barrer	Norton Co.
LZY-62	Si _{0.852} Al _{0.341} O _{2.26} H ₂ O _{1.65}	NH ₄	2.50	7.4	FAU	X.Qiao	Unknown
NaY	Si _{0.815} Al _{0.329} Na _{0.335} O _{2.30} H ₂ O _{1.35}	Na	2.48	7.4	FAU	L.Smart	Alfa Aesar
13X	Si _{0.657} Al _{0.520} Na _{0.506} O _{2.35} H ₂ O _{1.02}	Na	1.26	7.4	FAU	O.Cairon	Alfa Aesar
4A	Si _{0.557} Al _{0.563} Na _{0.558} O _{2.24} H ₂ O _{1.16}	Na	0.989	4.2	LTA	R.M.Barrer	Alfa Aesar
5A	Si _{0.604} Al _{0.612} Na _{0.212} O _{2.43} H ₂ O _{0.806}	Na	0.987	4.2	LTA	O.Cairon	Alfa Aesar
VALFOR® CP300-35	Si _{1.23} Al _{0.308} O _{2.92} H ₂ O _{0.553}	H+	3.99	7.4	FAU	US5320773	PQ corp.
MS-1		H	100% Si			S.Komarneni	PSU*
MAS-1		H	1			S.Komarneni	PSU*
MA-1		H	100% Al			S.Komarneni	PSU*
(i.s.) interlayer spacing							

*PSU: Synthesized by Penn State University

Table A. 6 List of synthetic swelling micas used in this research. Chemical formula derived from WD-XRF measurements, pore size and general structure based on literature.

Specimen	Chemical Formula	Cation Si/Al	Pore Size (Å)	Structure	Ref.	Provider
Talc		none	100	10 (i.s.)	layer	A. Maunier Alfa-aesar
Synthetic Swelling Micas						
YN6	$\text{Na}_{0.125} \text{Al}_{0.125} \text{Si}_{7.875} \text{Mg}_6 \text{O}_{20} \text{F}_4$	Na	63.0	10 (i.s.)	layer	A. Maunier PSU*
YN8	$\text{Na}_{0.5} \text{Al}_{0.5} \text{Si}_{7.5} \text{Mg}_6 \text{O}_{20} \text{F}_7$	Na	15	10 (i.s.)	layer	A. Maunier PSU*
Na-Ts (Sodium tetrasilicic Mica)	$\text{Na}_{0.225} \text{Si}_{0.953} \text{Mg}_{0.605} \text{O}_{2.63} \text{H}_2\text{O}_{0.600}$	Na	700	10 (i.s.)	layer	A. Maunier Topy Industries
(i.s.) interlayer spacing						

*PSU: Synthesized by Penn State University

APPENDIX B

STARTING MATERIALS AND SOLID SYNTHESIS

THIOINDIGO

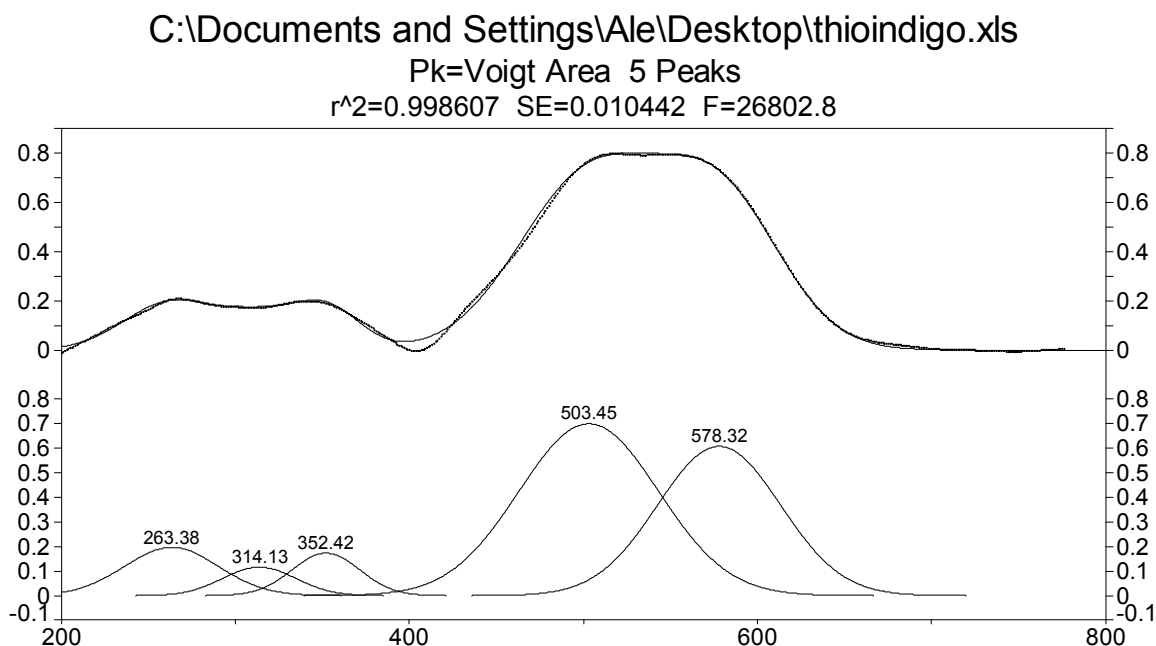


Figure B. 1 Peak fit of thioindigo.

Table B. 1 Peak fit statistics of thioindigo.

Description: C:\Documents and Settings\Ale\Desktop\thioindigo.xls

File Source: c:\documents and settings\ale\desktop\thesis final\peak fit\thioindigo\thioindigopeakfit.txt

Measured Values

Peak	Type	Amplitude	Center	FWHM	Asym50	FW Base	Asym10
1	Voigt Area	0.19673380	263.380218	64.1136498	0.99999996	128.497694	0.99999998
2	Voigt Area	0.11610336	314.127310	49.3864748	1.00000000	98.9812337	1.00000000
3	Voigt Area	0.17315124	352.421265	45.9126085	1.00000000	92.0188504	1.00000000
4	Voigt Area	0.69960119	503.452944	94.5548945	0.99999997	189.508568	0.99999998
5	Voigt Area	0.60778119	578.321831	83.2686853	1.00000003	166.888551	1.00000001
Peak	Type	Anlytc Area	% Area	Int Area	% Area	Centroid	Moment2
1	Voigt Area	13.4527459	8.81699403	13.3063493	8.73336015	264.222627	718.009543
2	Voigt Area	6.11553254	4.00814929	6.11293040	4.01210141	314.182129	458.961589
3	Voigt Area	8.47889082	5.55710561	8.47619913	5.56318628	352.457957	398.177587
4	Voigt Area	70.5530856	46.2408299	70.5168019	46.2823134	503.444666	1644.01767
5	Voigt Area	53.9772092	35.3769212	53.9500294	35.4090387	578.277981	1279.37320
	Total	152.577464	100.000000	152.362310	100.000000		

PALYGORSKITE

paly6%thioUnfresh - C:\COLOR\Data\ALE\pennstate\07.01.08UV\paly6%thioUn

Pk=Voigt Area 4 Peaks

$r^2=0.999125$ SE=0.00545353 F=55978.9

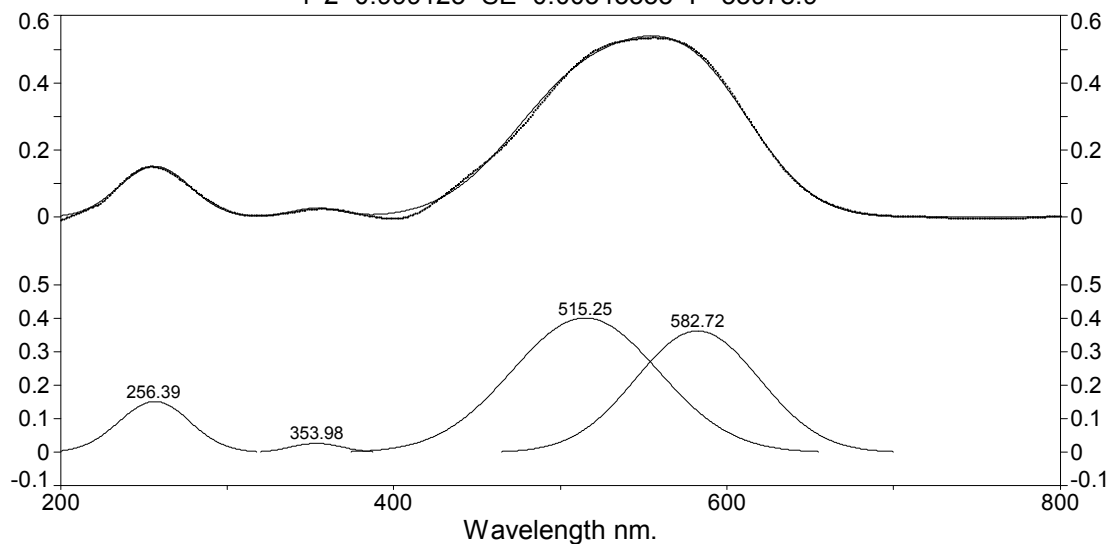


Figure B. 2 Peak fit of Palygorskite / 0.5 mol % thioindigo unheated.

Table B. 2 Peak fit statistics of Palygorskite / 0.5 mol % thioindigo unheated.

Description: paly6%thioUnfresh - smooth - C:\COLOR\Data\ALE\pennstate\07.01.08UV\paly6%thioUn

X Variable: Wavelength nm.

File Source: c:\documents and settings\ale\desktop\thesis final\peak fit\palygorskite\paly6%thioUnfreshpeakfit.txt

Measured Values

Peak	Type	Amplitude	Center	FWHM	Asym50	FW Base	Asym10
1	Voigt Area	0.15211084	256.371675	50.3723438	1.00000001	100.830735	1.00000001
2	Voigt Area	0.02685197	354.043975	35.5691791	0.99999998	71.1991184	0.99999999
3	Voigt Area	0.41331943	516.934846	104.545611	1.00000004	209.269810	1.00000002
4	Voigt Area	0.34897100	583.974142	85.8824648	1.00000002	171.911636	1.00000001

Peak	Type	Anlytc Area	% Area	Int Area	% Area	Centroid	Moment2
1	Voigt Area	8.15613714	9.36713861	8.12185351	9.33143881	256.637719	442.513822
2	Voigt Area	1.01667533	1.16762857	1.01667533	1.16808850	354.043975	228.156180
3	Voigt Area	45.9963994	52.8258220	45.9963994	52.8466299	516.934847	1971.04329
4	Voigt Area	31.9025981	36.6394108	31.9025981	36.6538428	583.974142	1330.12828
	Total	87.0718100	100.000000	87.0375263	100.000000		

Paly6%thio Dehydrated C:\COLOR\Data\ALE\pennstate\07.02.08U

Pk=Voigt Area 8 Peaks

$r^2=0.999702$ SE=0.00753644 F=80446.2

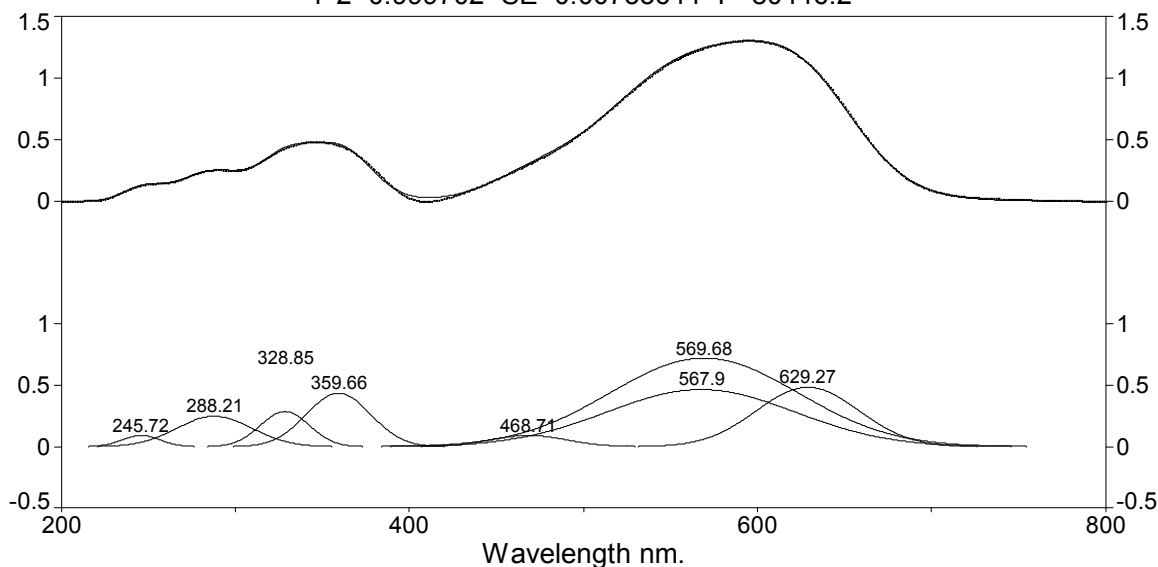


Figure B. 3 Peak fit of Palygorskite / 0.5 mol % thioindigo heated at 413K for nine hours.

Table B. 3 Peak fit statistics of Palygorskite / 0.5 mol % thioindigo heated at 413K for nine hours.

Description: Paly6%thio140C9hsuperfresh07.02 - smooth - C:\COLOR\Data\ALE\pennstate\07.02.08U

X Variable: Wavelength nm.

File Source: c:\documents and settings\ale\desktop\thesis final\peak

fit\palygorskite\paly6%thio140c9hsuperfresh07.02-peakfit.txt

Measured Values

Peak	Type	Amplitude	Center	FWHM	Asym50	FW Base	Asym10
1	Voigt Area	0.09222174	245.720727	25.7410876	1.00000000	51.5261469	1.00000000
2	Voigt Area	0.24860044	288.207231	51.4325904	1.00000007	102.953039	1.00000004
3	Voigt Area	0.28672104	328.850040	33.2172835	0.99999999	66.4913096	1.00000000
4	Voigt Area	0.43665143	359.660856	43.3850203	1.00000003	86.8441520	1.00000002
5	Voigt Area	0.09192203	468.707429	52.2915052	1.00000001	104.672336	1.00000000
6	Voigt Area	0.46547207	567.904808	127.518344	1.00000000	255.254519	1.00000000
7	Voigt Area	0.72166793	569.682576	127.635993	1.00000000	255.490016	1.00000000
8	Voigt Area	0.48409151	629.267832	69.3480978	1.00000000	138.814658	1.00000000

Peak	Type	Anlytc Area	% Area	Int Area	% Area	Centroid	Moment2
1	Voigt Area	2.52692545	1.01677249	2.52688903	1.01676614	245.721420	119.460173
2	Voigt Area	13.6104505	5.47650967	13.6100845	5.47640709	288.209736	476.826343
3	Voigt Area	10.1380841	4.07931506	10.1380841	4.07934836	328.850040	198.981535
4	Voigt Area	20.1654027	8.11406079	20.1654027	8.11412703	359.660856	339.440893
5	Voigt Area	5.11661787	2.05880086	5.11661787	2.05881767	468.707429	493.113438
6	Voigt Area	63.1827471	25.4231794	63.1821724	25.4231557	567.902592	2931.93069
7	Voigt Area	98.0489111	39.4524641	98.0478596	39.4523631	569.679981	2937.26084
8	Voigt Area	35.7350367	14.3788976	35.7350365	14.3790149	629.267832	867.268570
	Total	248.524176	100.000000	248.522147	100.000000		

Paly6%thio Hydrated- C:\COLOR\Data\ALE\pennstate\07.01.08\Paly

Pk=Voigt Area 8 Peaks

r²=0.999552 SE=0.00849342 F=53516.3

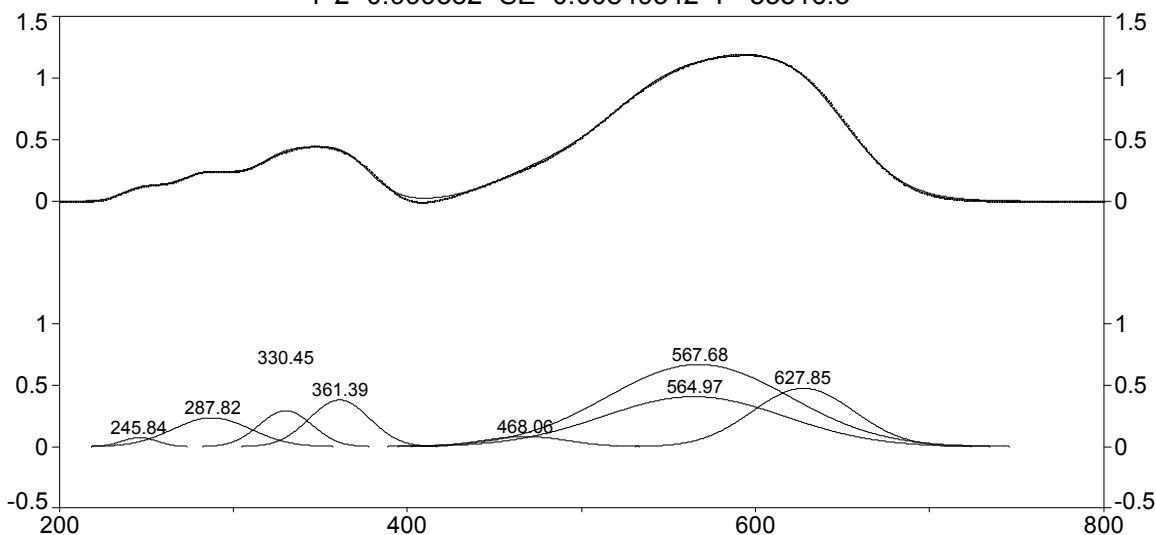


Figure B. 4 Peak fit of Palygorskite / 0.5 mol % thioindigo heated at 413K for nine hours / hydrated.

Table B. 4 Peak fit statistics of Palygorskite / 0.5 mol % thioindigo heated at 413K for nine hours / hydrated.

Description: Paly6%thio1409hnofreshswati - smooth - C:\COLOR\Data\ALE\pennstate\07.01.08\Paly

X Variable: Wavelength nm.

File Source: c:\documents and settings\ale\desktop\thesis final\peak

fit\palygorskite\paly6%thio1409hnofreshswatipeakfit.txt

Measured Values

Peak	Type	Amplitude	Center	FWHM	Asym50	FW Base	Asym10
1	Voigt Area	0.07407567	245.842960	24.0350994	1.00000007	48.1112562	1.00000004
2	Voigt Area	0.23627940	287.818471	53.1893558	1.00000000	106.469571	1.00000000
3	Voigt Area	0.29360231	330.451619	35.7085194	1.00000000	71.4780370	1.00000000
4	Voigt Area	0.38080033	361.391990	40.6664077	1.00000000	81.4022828	1.00000000
5	Voigt Area	0.08350229	468.055313	56.6016457	0.99999986	113.299980	0.99999992
6	Voigt Area	0.40730820	564.968252	123.166837	1.00000000	246.544071	1.00000000
7	Voigt Area	0.66934738	567.680252	123.769523	1.00000000	247.750472	1.00000000
8	Voigt Area	0.47495444	627.853606	69.0078352	1.00000006	138.133551	1.00000003

Peak	Type	Anlytc Area	% Area	Int Area	% Area	Centroid	Moment2
1	Voigt Area	1.89519416	0.84447359	1.89518746	0.84447552	245.843130	104.170319
2	Voigt Area	13.3777417	5.96094575	13.3770654	5.96067908	287.823174	509.779382
3	Voigt Area	11.1599826	4.97274148	11.1599826	4.97277040	330.451619	229.947259
4	Voigt Area	16.4841037	7.34509983	16.4841037	7.34514254	361.391990	298.233326
5	Voigt Area	5.03106193	2.24177503	5.03106193	2.24178807	468.055312	577.753612
6	Voigt Area	53.4009711	23.7947704	53.4007841	23.7948255	564.967391	2735.52079
7	Voigt Area	88.1855638	39.2943275	88.1851288	39.2943621	567.679053	2762.28292
8	Voigt Area	34.8885216	15.5458664	34.8885215	15.5459568	627.853606	858.778822
Total		224.423141	100.000000	224.421836	100.000000		

Paly+dyevacuum C:\COLOR\Data\ALE\pennstate\10.13.08UV\C6UNvacuum.spc

Pk=Voigt Area 8 Peaks

r^2=0.998613 SE=0.0128402 F=35285.6

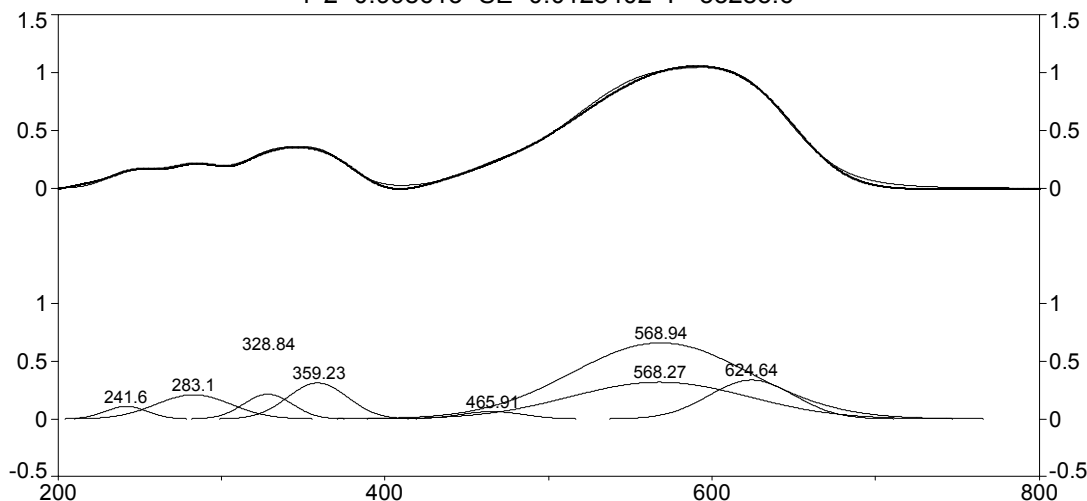


Figure B. 5 Peak fit of Palygorskite / 0.5 mol % thioindigo unheated / exposed to vacuum.

Table B. 5 Peak fit statistics of Palygorskite / 0.5 mol % thioindigo unheated / exposed to vacuum.

Description: C6UNvacuum - RawData - C:\COLOR\Data\ALE\pennstate\10.13.08UV\C6UNvacuum.spc

X Variable: Wavelength nm.

File Source: c:\documents and settings\ale\desktop\thesis final\peak fit\palygorskite\c6unvacuumpeakfit.txt

Measured Values

Peak	Type	Amplitude	Center	FWHM	Asym50	FW Base	Asym10
1	Voigt Area	0.10896347	241.604709	30.4981773	1.00000000	61.3535710	1.00000000
2	Voigt Area	0.21039471	283.103268	54.7522586	1.00000000	110.145815	1.00000000
3	Voigt Area	0.21502374	328.836305	34.8509705	0.99999984	70.1101404	0.99999991
4	Voigt Area	0.31297124	359.227903	43.0340822	0.99999995	86.5722102	0.99999997
5	Voigt Area	0.06495150	465.905076	45.3842063	1.00000000	91.2999848	1.00000000
6	Voigt Area	0.32019032	568.265244	127.802710	1.00000000	257.102337	1.00000000
7	Voigt Area	0.65969855	568.937324	128.346348	1.00000006	258.195979	1.00000003
8	Voigt Area	0.33733246	624.642553	61.4318733	1.00000000	123.583280	1.00000000

Peak	Type	Anlytc Area	% Area	Int Area	% Area	Centroid	Moment2
1	Voigt Area	3.56469889	1.79566889	3.55302308	1.79421980	241.888724	217.248901
2	Voigt Area	12.3567679	6.22455482	12.3238185	6.22333114	283.443220	624.243350
3	Voigt Area	8.03839459	4.04923263	8.02998295	4.05501289	328.974209	276.962410
4	Voigt Area	14.4472444	7.27760412	14.4311055	7.28747737	359.362000	404.025425
5	Voigt Area	3.16200062	1.59281507	3.15907503	1.59528234	465.936636	445.033324
6	Voigt Area	43.8951261	22.1115765	43.7703441	22.1033234	568.060807	3098.12789
7	Voigt Area	90.8232596	45.7509895	90.5633767	45.7330561	568.729306	3123.36623
8	Voigt Area	22.2290003	11.1975585	22.1953509	11.2082970	624.473675	775.413511
Total		198.516492	100.000000	198.026077	100.000000		

SEPIOLITE

sep6%thioUnfresh - smooth - C:\COLOR\Data\ALE\pennstate\07.01.08UV\sep6%thioUnfr

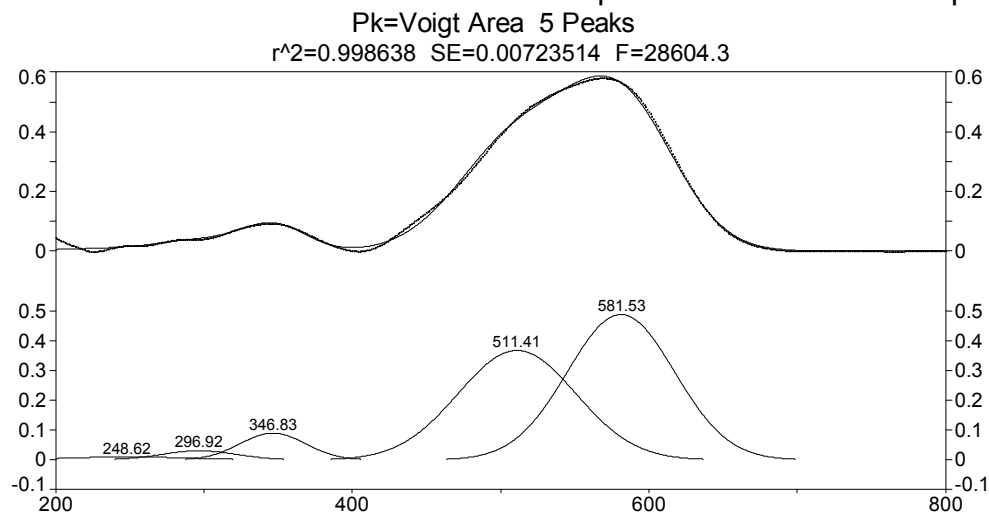


Figure B. 6 Peak fit of Sepiolite / 0.5 mol % thioindigo unheated.

Table B. 6 Peak fit statistics of Sepiolite / 0.5 mol % thioindigo unheated.

Description: sep6%thioUnfresh - smooth - C:\COLOR\Data\ALE\pennstate\07.01.08UV\sep6%thioUnfr

X Variable: Wavelength nm.

File Source: c:\documents and settings\ale\desktop\thesis final\peak fit\sepiolite\sep6%thioUnfreshpeakfit.txt

Measured Values

Peak	Type	Amplitude	Center	FWHM	Asym50	FW Base	Asym10
1	Voigt Area	0.01004950	248.624841	100.676707	1.00000000	201.525392	1.00000000
2	Voigt Area	0.03056664	296.915449	60.1097418	1.00000000	120.322165	1.00000000
3	Voigt Area	0.08995246	346.825970	51.7591453	1.00000000	103.606707	1.00000000
4	Voigt Area	0.36668014	511.414960	93.5073044	0.99999999	187.174341	1.00000000
5	Voigt Area	0.48736128	581.533473	85.0843139	1.00000001	170.313971	1.00000000
Peak	Type	Anlytc Area	% Area	Int Area	% Area	Centroid	Moment2
1	Voigt Area	1.07697503	1.21518398	0.93944537	1.06165423	258.865566	1225.03236
2	Voigt Area	1.95580171	2.20679110	1.95565831	2.21006243	296.922996	650.858325
3	Voigt Area	4.95601224	5.59202073	4.95601224	5.60072093	346.825970	483.124147
4	Voigt Area	36.4976695	41.1814407	36.4976695	41.2455118	511.414960	1576.79643
5	Voigt Area	44.1400413	49.8045635	44.1400413	49.8820506	581.533473	1305.52004
	Total	88.6264998	100.000000	88.4888267	100.000000		

Sepio+dye Dehydrated fiucha - C:\COLOR\Data\ALE\pennstate\10.27.08ir\A6fiucha.spc

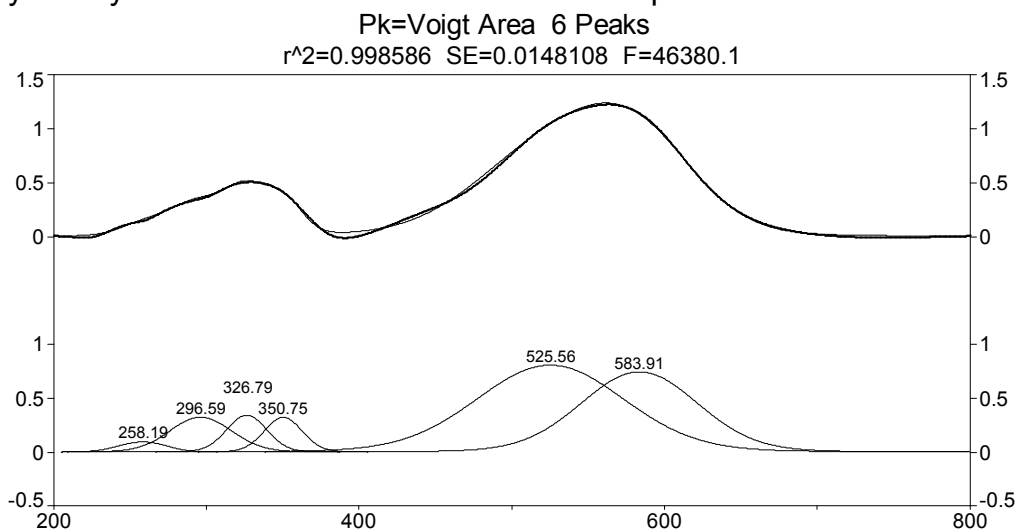


Figure B. 7 Peak fit of Sepiolite / 0.5 mol % thioindigo heated at 413K for nine hours.

Table B. 7 Peak fit statistics of Sepiolite / 0.5 mol % thioindigo heated at 413K for nine hours.

Description: A6Hfiucha - RawData - C:\COLOR\Data\ALE\pennstate\10.27.08ir\A6fiucha.spc

X Variable: Wavelength nm.

File Source: c:\documents and settings\ale\desktop\thesis final\peak fit\sepiolite\A6fiuchapeakfit.txt

Measured Values

Peak	Type	Amplitude	Center	FWHM	Asym50	FW Base	Asym10
1	Voigt Area	0.09648401	258.188754	37.3256552	1.00000000	77.0706300	1.00000000
2	Voigt Area	0.32452601	296.585843	48.5007027	1.00000003	100.145053	1.00000002
3	Voigt Area	0.34419506	326.787066	31.0969532	1.00000019	64.2095031	1.00000010
4	Voigt Area	0.32408086	350.749201	29.4074787	0.99999995	60.7210482	0.99999997
5	Voigt Area	0.80872230	525.564792	114.158381	1.00000000	235.716113	1.00000000
6	Voigt Area	0.74678747	583.909895	90.3659081	1.00000001	186.589021	1.00000000
Peak	Type	Anlytc Area	% Area	Int Area	% Area	Centroid	Moment2
1	Voigt Area	4.00553539	1.80625071	3.95258680	1.80355686	259.723013	599.817669
2	Voigt Area	17.5063396	7.89428509	17.3190492	7.90264494	298.033514	864.244410
3	Voigt Area	11.9047500	5.36831187	11.8405568	5.40282062	327.502807	472.128874
4	Voigt Area	10.6000761	4.77998396	10.5523388	4.81500954	351.308289	438.929375
5	Voigt Area	102.684531	46.3044238	101.295269	46.2208136	525.197534	3178.85306
6	Voigt Area	75.0584248	33.8467446	74.1952966	33.8551545	582.956513	2191.85885
Total		221.759657	100.000000	219.155097	100.000000		

Sepio-hydrated-purple C:\COLOR\Data\ALE\pennstate\10.27.08ir\A6Hpurple.spc

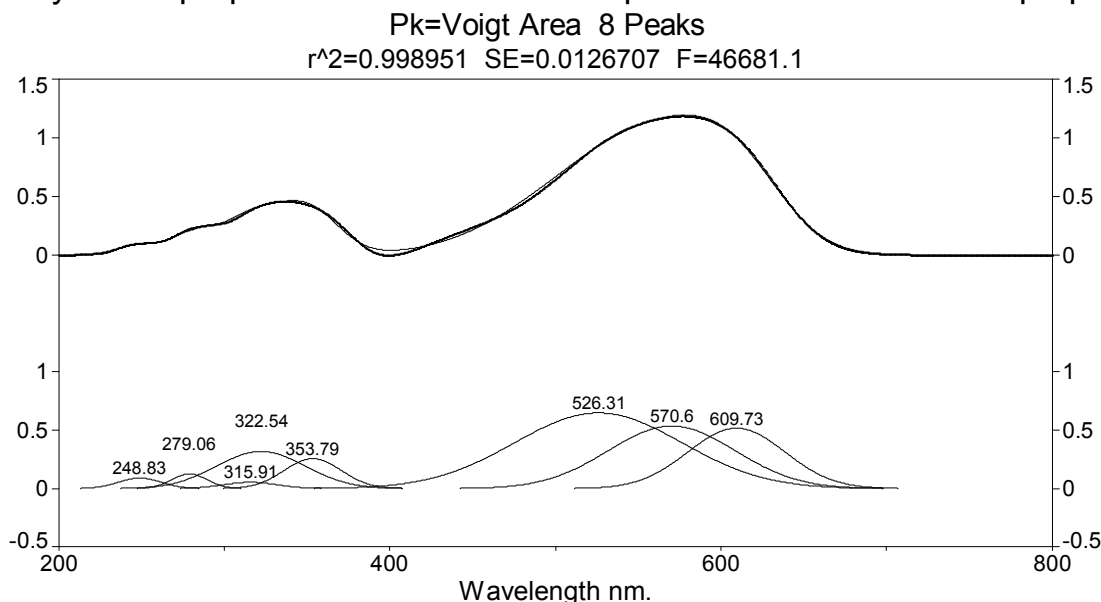


Figure B. 8 Peak fit of Sepiolite / 0.5 mol % thioindigo heated at 413K for nine hours / hydrated.

Table B. 8 Peak fit statistics of Sepiolite / 0.5 mol % thioindigo heated at 413K for nine hours / hydrated.

Description: A6Hpurple - RawData - C:\COLOR\Data\ALE\pennstate\10.27.08ir\A6Hpurple.spc

X Variable: Wavelength nm.

File Source: c:\documents and settings\ale\desktop\thesis final\peak fit\sepiolite\ale6hpurplepeakfit.txt

Measured Values

Peak	Type	Amplitude	Center	FWHM	Asym50	FW Base	Asym10
1	Voigt Area	0.08995595	248.831477	30.7527262	0.99999993	61.5579851	0.99999996
2	Voigt Area	0.12658618	279.064416	25.7220467	1.00000000	51.4880326	1.00000000
3	Voigt Area	0.05400393	315.909878	39.1762730	0.99999999	78.4194679	1.00000000
4	Voigt Area	0.31785701	322.540635	63.2571742	1.00000000	126.622406	1.00000000
5	Voigt Area	0.25706713	353.788305	40.6609498	1.00000000	81.3913577	1.00000000
6	Voigt Area	0.64803665	526.309761	118.959659	1.00000001	238.122529	1.00000000
7	Voigt Area	0.53547645	570.604429	90.3415813	0.99999998	180.837487	0.99999999
8	Voigt Area	0.51692074	609.729200	69.0441499	0.99999992	138.206243	0.99999995

Peak	Type	Anlytc Area	% Area	Int Area	% Area	Centroid	Moment2
1	Voigt Area	2.94473179	1.38420719	2.94445994	1.38408154	248.836272	170.315813
2	Voigt Area	3.46596379	1.62921866	3.46596379	1.62922118	279.064416	119.315152
3	Voigt Area	2.25206386	1.05861016	2.25206386	1.05861179	315.909878	276.777502
4	Voigt Area	21.4029579	10.0607221	21.4029036	10.0607121	322.540960	721.572850
5	Voigt Area	11.1264412	5.23011974	11.1264412	5.23012782	353.788305	298.153279
6	Voigt Area	82.0599959	38.5733046	82.0599934	38.5733630	526.309752	2552.01709
7	Voigt Area	51.4944325	24.2055877	51.4944324	24.2056251	570.604428	1471.83766
8	Voigt Area	37.9912038	17.8582299	37.9912038	17.8582575	609.729199	859.682973
Total		212.737791	100.000000	212.737462	100.000000		

MONTMORILLONITE CLAYS

BENTOLITE L[®]

bentolite-thio 6% UN - smooth - C:\COLOR\Data\ALE\pennstate\bentolite-thio 6% UN

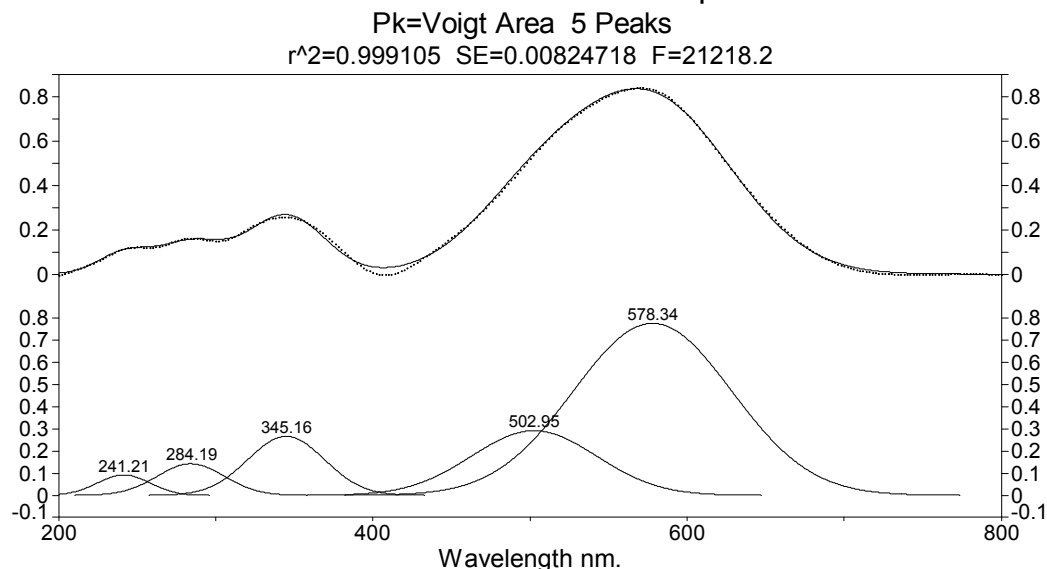


Figure B. 9 Peak fit of Bentolite L[®] / 0.5 mol % thioindigo unheated.

Table B. 9 Peak fit statistics of Bentolite L[®] / 0.5 mol % thioindigo unheated.

Description: bentolite-thio 6% UN - smooth - C:\COLOR\Data\ALE\pennstate\bentolite-thio 6% UN

X Variable: Wavelength nm.

File Source: c:\documents and settings\ale\desktop\thesis final\peak fit\bentolite\bentolite-thio 6% unpeakfit.txt

Measured Values

Peak	Type	Amplitude	Center	FWHM	Asym50	FW Base	Asym10
1	Voigt Area	0.09236533	241.214385	39.2082992	1.00000000	78.4835752	1.00000000
2	Voigt Area	0.14289789	284.192420	50.7218032	1.00000001	101.530251	1.00000000
3	Voigt Area	0.26635755	345.160308	57.5041864	0.99999994	115.106603	0.99999997
4	Voigt Area	0.29202568	502.952002	93.8000529	1.00000000	187.760338	1.00000000
5	Voigt Area	0.77729634	578.339184	118.690681	1.00000000	237.584113	1.00000000

Peak	Type	Anlytc Area	% Area	Int Area	% Area	Centroid	Moment2
1	Voigt Area	3.85495395	2.48325931	3.82929484	2.46715241	241.526807	264.256333
2	Voigt Area	7.71529830	4.96999097	7.71494038	4.97061066	284.196556	463.604718
3	Voigt Area	16.3040944	10.5026661	16.3040944	10.5044629	345.160308	596.325603
4	Voigt Area	29.1579064	18.7827516	29.1579064	18.7859651	502.952002	1586.68501
5	Voigt Area	98.2054193	63.2613320	98.2048822	63.2718089	578.337914	2540.21035
	Total	155.237672	100.000000	155.211118	100.000000		

bentolite - bentolite smooth - C:\COLOR\Data\ALE\pennstate\NEW RUNS WITH BaSo4\b

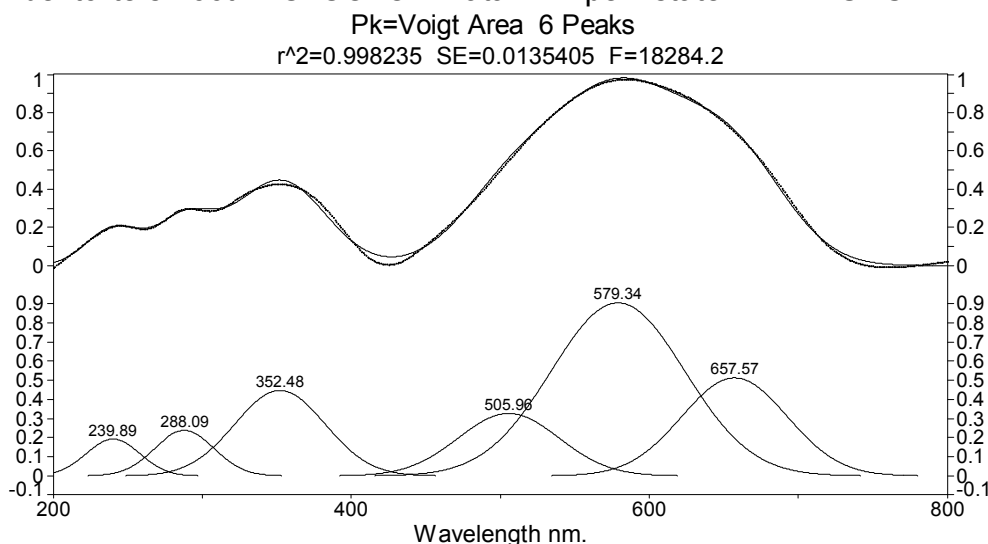


Figure B. 10 Peak fit of Bentolite L[®] / 0.5 mol % thioindigo heated at 413K for nine hours.

Table B. 10 Peak fit statistics of Bentolite L[®] / 0.5 mol % thioindigo heated at 413K for nine hours.

Description: bentolite - bentolite smooth - C:\COLOR\Data\ALE\pennstate\NEW RUNS WITH BaSo4\b

X Variable: Wavelength nm.

File Source: c:\documents and settings\ale\desktop\thesis final\peak fit\bentolite\bentolite-6%thio140c9h+10%humiditypeakfit.txt

Measured Values

Peak	Type	Amplitude	Center	FWHM	Asym50	FW Base	Asym10
1	Voigt Area	0.19229092	239.894377	42.2795971	1.00000000	84.6314175	1.00000000
2	Voigt Area	0.23763154	288.092514	47.2360070	1.00000001	94.5527038	1.00000001
3	Voigt Area	0.44635206	352.475518	71.3836836	1.00000000	142.889307	1.00000000
4	Voigt Area	0.32602170	505.955095	79.8620970	1.00000012	159.860617	1.00000006
5	Voigt Area	0.90464632	579.344614	105.562958	1.00000006	211.306242	1.00000004
6	Voigt Area	0.51243657	657.573544	83.3407902	1.00000000	166.823945	1.00000000

Peak	Type	Anlytc Area	% Area	Int Area	% Area	Centroid	Moment2
1	Voigt Area	8.65409854	3.77335291	8.54036117	3.72563187	240.509183	297.458476
2	Voigt Area	11.9483925	5.20972823	11.9483252	5.21231602	288.093033	402.329193
3	Voigt Area	33.9163191	14.7881655	33.9163108	14.7955907	352.475557	918.924153
4	Voigt Area	27.7152900	12.0843979	27.7152900	12.0904685	505.955097	1150.18042
5	Voigt Area	101.653558	44.3229005	101.653514	44.3451472	579.344517	2009.56927
6	Voigt Area	45.4600535	19.8214550	45.4587546	19.8308457	657.569248	1251.95162
	Total	229.347711	100.000000	229.232556	100.000000		

bentoliteL+dyered - RawData - C:\COLOR\Data\ALE\pennstate\11.25.08XRD\BentoliteL

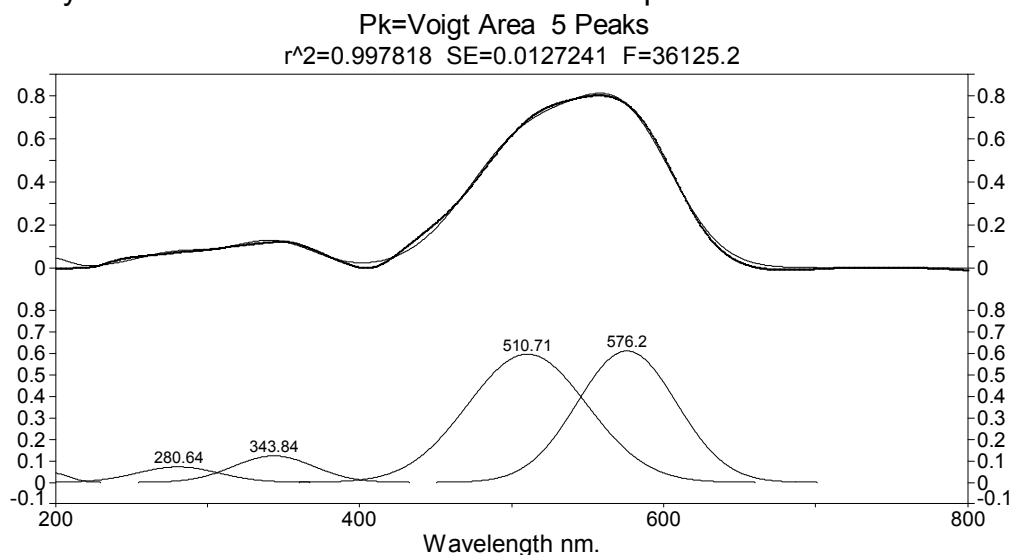


Figure B. 11 Peak fit of Bentolite L[®] / 0.5 mol % thioindigo heated at 413K for nine hours / hydrated.

Table B. 11 Peak fit statistics of Bentolite L[®] / 0.5 mol % thioindigo heated at 413K for nine hours / hydrated.

Description: bentoliteL+dyered - RawData - C:\COLOR\Data\ALE\pennstate\11.25.08XRD\BentoliteL

X Variable: Wavelength nm.

File Source: c:\documents and settings\ale\desktop\thesis final\peak fit\bentolite\bentolite+dyeredpeakfit.txt

Measured Values

Peak	Type	Amplitude	Center	FWHM	Asym50	FW Base	Asym10
1	Voigt Area	0.04280262	200.000004	23.8360525	0.81235910	47.4951537	0.89211319
2	Voigt Area	0.07242271	280.641665	63.7700239	1.00000006	127.648982	1.00000003
3	Voigt Area	0.12347202	343.839564	62.1875970	1.00000001	124.481425	1.00000000
4	Voigt Area	0.59729173	510.706198	92.4582930	1.00000000	185.074526	1.00000000
5	Voigt Area	0.61244506	576.199565	76.8793063	1.00000000	153.889940	1.00000000

Peak	Type	Anlytc Area	% Area	Int Area	% Area	Centroid	Moment2
1	Voigt Area	1.08832471	0.88422472	0.49108218	0.40095546	207.600724	34.2117528
2	Voigt Area	4.91613263	3.99418108	4.90899706	4.00806471	280.770090	722.988014
3	Voigt Area	8.17343362	6.64062106	8.17343341	6.67338962	343.839568	697.415767
4	Voigt Area	58.7847377	47.7604867	58.7847377	47.9961650	510.706198	1541.61630
5	Voigt Area	50.1197388	40.7204865	50.1197388	40.9214253	576.199565	1065.86810
Total		123.082367	100.000000	122.477989	100.000000		

Ca-MMT (Texas)

Ca-Mont. texas-thio 6% UN - smooth - C:\COLOR\Data\ALE\pennstate\Ca-Mont. texas-

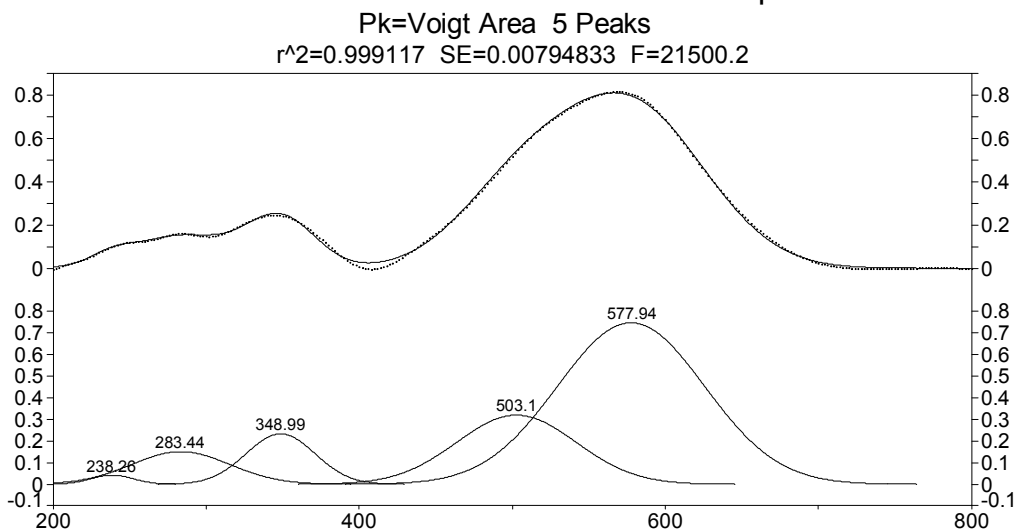


Figure B. 12 Peak fit of Ca-MMT (Texas) / 0.5 mol % thioindigo unheated.

Table B. 12 Peak fit statistics of Ca-MMT (Texas) / 0.5 mol % thioindigo unheated.

Description: Ca-Mont. texas-thio 6% UN - smooth - C:\COLOR\Data\ALE\pennstate\Ca-Mont. texas-

X Variable: Wavelength nm.

File Source: c:\documents and settings\ale\desktop\thesis final\peak fit\ca-mmt wyoming\ca-mont. texas-thio 6% unpeakfit.txt

Measured Values

Peak	Type	Amplitude	Center	FWHM	Asym50	FW Base	Asym10
1	Voigt Area	0.04213073	238.264111	32.4182642	1.00000009	64.8919061	1.00000005
2	Voigt Area	0.15099607	283.436149	76.1557838	1.00000002	152.441659	1.00000001
3	Voigt Area	0.23323649	348.987982	53.1184859	1.00000000	106.327710	1.00000000
4	Voigt Area	0.32006570	503.095821	91.9072486	1.00000000	183.971496	1.00000000
5	Voigt Area	0.74752837	577.943013	113.311406	0.99999993	226.816373	0.99999996

Peak	Type	Anlytc Area	% Area	Int Area	% Area	Centroid	Moment2
1	Voigt Area	1.45385458	0.97995662	1.44989644	0.97771450	238.379825	185.082876
2	Voigt Area	12.2405446	8.25062067	12.1800650	8.21343224	283.901155	1006.88591
3	Voigt Area	13.1878619	8.88915074	13.1878619	8.89302394	348.987982	508.833769
4	Voigt Area	31.3127428	21.1060514	31.3127428	21.1152478	503.095821	1523.29523
5	Voigt Area	90.1640719	60.7742206	90.1638945	60.8005816	577.942555	2315.32957
Total		148.359076	100.000000	148.294461	100.000000		

Ca-Mont.+dye dehydrated- C:\COLOR\Data\ALE\pennstate\NEW RUNS WITH B

Pk=Voigt Area 7 Peaks

$r^2=0.998665$ SE=0.0103645 F=20624.8

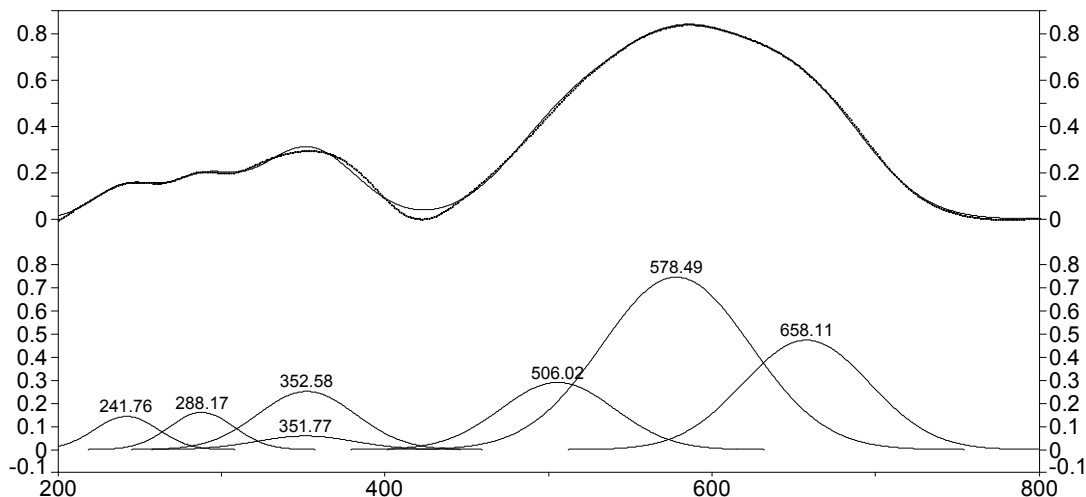


Figure B. 13 Peak fit of Ca-MMT (Texas) / 0.5 mol % thioindigo heated at 413K for nine hours.

Table B. 13 Peak fit statistics of Ca-MMT (Texas) / 0.5 mol % thioindigo heated at 413K for nine hours.

Description: Ca-Mont.+dye - Ca-Mont.+dye smooth - C:\COLOR\Data\ALE\pennstate\NEW RUNS WITH B

X Variable: Wavelength (nm)

Y Variable: Absorbance

File Source: c:\documents and settings\ale\desktop\thesis final\peak fit\ca-mmt wyoming\ca-mont.+dye\freshpeakfit.txt

Measured Values

Peak	Type	Amplitude	Center	FWHM	Asym50	FW Base	Asym10
1	Voigt Area	0.14413672	241.758353	45.7916067	1.00000000	91.6614359	1.00000000
2	Voigt Area	0.16164548	288.167857	47.3266688	1.00000001	94.7341823	1.00000001
3	Voigt Area	0.05941774	351.774673	70.6400996	1.00000000	141.400869	1.00000000
4	Voigt Area	0.25237078	352.575921	70.5461816	1.00000000	141.212872	1.00000000
5	Voigt Area	0.29145571	506.017412	82.0019298	1.00000003	164.143938	1.00000001
6	Voigt Area	0.74744248	578.490926	107.062215	1.00000000	214.307316	1.00000000
7	Voigt Area	0.47436286	658.108281	91.1952351	1.00000000	182.546252	1.00000000
Peak	Type	Anlytc Area	% Area	Int Area	% Area	Centroid	Moment2
1	Voigt Area	7.02575060	3.59816422	6.91417970	3.54315448	242.544209	344.709593
2	Voigt Area	8.14332386	4.17051760	8.14327705	4.17300241	288.168388	403.874186
3	Voigt Area	4.46786084	2.28816790	4.46785991	2.28954388	351.774706	899.880281
4	Voigt Area	18.9515522	9.70583797	18.9515488	9.71167485	352.575949	897.489795
5	Voigt Area	25.4406876	13.0291803	25.4406876	13.0370181	506.017413	1212.64226
6	Voigt Area	85.1816820	43.6249018	85.1816349	43.6511205	578.490799	2067.05048
7	Voigt Area	46.0484523	23.5832302	46.0427328	23.5944858	658.089490	1497.11768
Total		195.259309	100.000000	195.141921	100.000000		

CaMMT+dye HydratedRawData - C:\COLOR\Data\ALE\pennstate\11.25.08XRD\CaMMT+dyled.sp

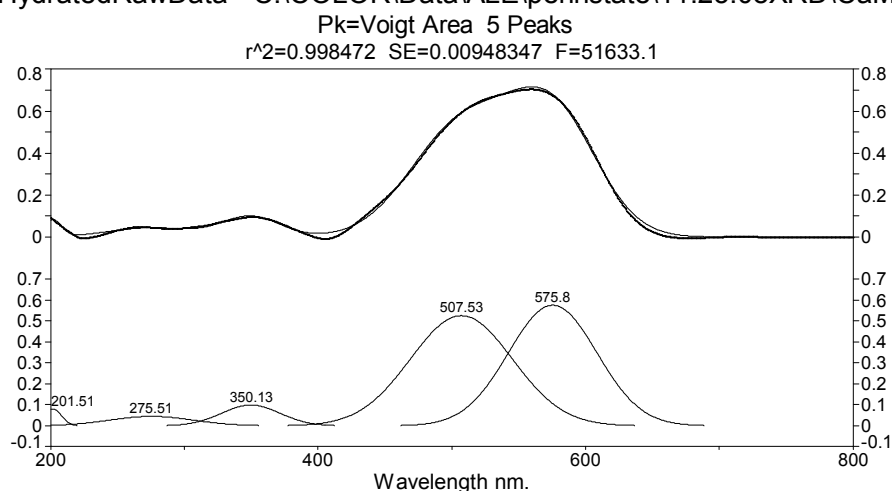


Figure B. 14 Peak fit of Ca-MMT (Texas) / 0.5 mol % thioindigo heated at 413K for nine hours / hydrated.

Table B. 14 Peak fit statistics of Ca-MMT (Texas) / 0.5 mol % thioindigo heated at 413K for nine hours / hydrated.

Description: NaMMT+dyled - RawData - C:\COLOR\Data\ALE\pennstate\11.25.08XRD\CaMMT+dyled.sp

X Variable: Wavelength nm.

File Source: c:\documents and settings\ale\desktop\thesis final\peak fit\ca-mmt wyoming\cammt+dyledpeakfit.txt

Measured Values

Peak	Type	Amplitude	Center	FWHM	Asym50	FW Base	Asym10
1	Voigt Area	0.07974030	201.513050	15.0943881	1.00000000	30.2145608	1.00000000
2	Voigt Area	0.04457826	275.511264	73.6761572	1.00000001	147.478170	1.00000001
3	Voigt Area	0.09854884	350.133126	51.4791990	1.00000009	103.046336	1.00000005
4	Voigt Area	0.52515087	507.534848	89.7758102	1.00000000	179.704978	1.00000000
5	Voigt Area	0.57450871	575.803493	77.8795744	0.99999995	155.892185	0.99999997
Peak	Type	Anlytc Area	% Area	Int Area	% Area	Centroid	Moment2
1	Voigt Area	1.28122553	1.18643321	0.76015277	0.70750720	205.704784	17.1751201
2	Voigt Area	3.49608737	3.23742702	3.46846603	3.22825197	276.194976	926.804917
3	Voigt Area	5.40027020	5.00072762	5.40027020	5.02626601	350.133127	477.912197
4	Voigt Area	50.1851967	46.4722116	50.1851967	46.7095421	507.534848	1453.46045
5	Voigt Area	47.6269091	44.1032006	47.6269091	44.3284327	575.803492	1093.78431
Total		107.989689	100.000000	107.440995	100.000000		

Na-MMT (Kunipia)

Na-Mont.Kunipia-thio 6% UN - smooth - C:\COLOR\Data\ALE\pennstate\Na-Mont.Kunipi

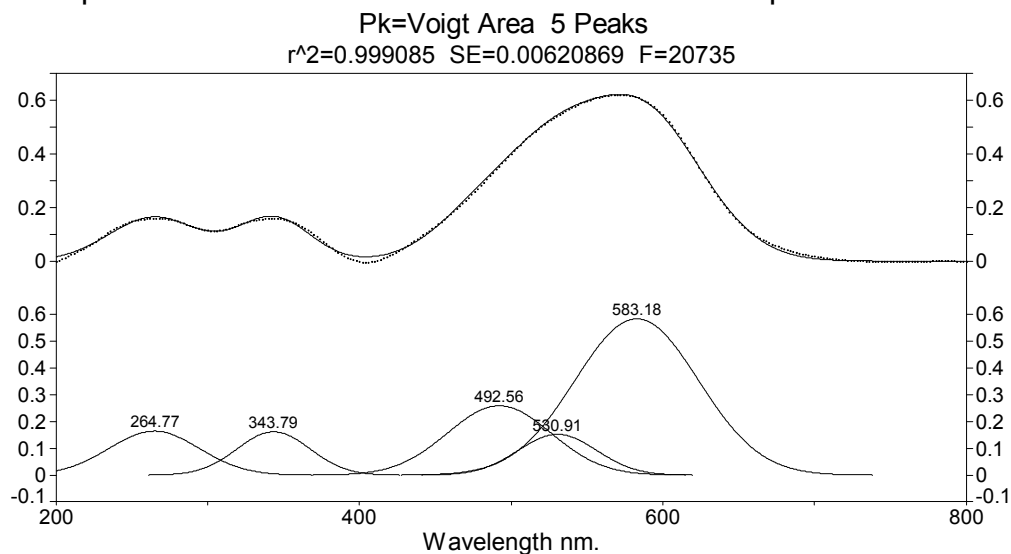


Figure B. 15 Peak fit of Na-MMT (Kunipia) / 0.5 mol % thioindigo unheated.

Table B. 15 Peak fit statistics of Na-MMT (Kunipia) / 0.5 mol % thioindigo unheated.

Description: Na-Mont.Kunipia-thio 6% UN - smooth - C:\COLOR\Data\ALE\pennstate\Na-Mont.Kunipi

X Variable: Wavelength nm.

File Source: c:\documents and settings\ale\desktop\thesis final\peak fit\kunipia\na-mont.kunipia-thio 6% unpeakfit.txt

Measured Values

Peak	Type	Amplitude	Center	FWHM	Asym50	FW Base	Asym10
1	Voigt Area	0.16449917	264.769767	70.9213803	0.99999994	141.963910	0.99999997
2	Voigt Area	0.16204670	343.790315	56.5349493	0.99999990	113.166473	0.99999994
3	Voigt Area	0.25910401	492.563884	80.4563644	1.00000001	161.050167	1.00000000
4	Voigt Area	0.15236692	530.906292	60.8947396	1.00000000	121.893501	1.00000000
5	Voigt Area	0.58412631	583.183374	95.8763968	0.99999998	191.916572	0.99999999
Peak	Type	Anlytc Area	% Area	Int Area	% Area	Centroid	Moment2
1	Voigt Area	12.4186135	10.9076984	12.2229556	10.7543272	265.978510	827.314932
2	Voigt Area	9.75190404	8.56543506	9.75190403	8.58018058	343.790313	576.392803
3	Voigt Area	22.1904829	19.4906697	22.1904829	19.5242232	492.563884	1167.36148
4	Voigt Area	9.87649132	8.67486438	9.87649132	8.68979830	530.906292	668.719684
5	Voigt Area	59.6143321	52.3613325	59.6143291	52.4514708	583.183362	1657.70527
	Total	113.851824	100.000000	113.656163	100.000000		

Kunipia Na-Mont dehydrated- C:\COLOR\Data\ALE\pennstate\NEW RUNS WITH Ba

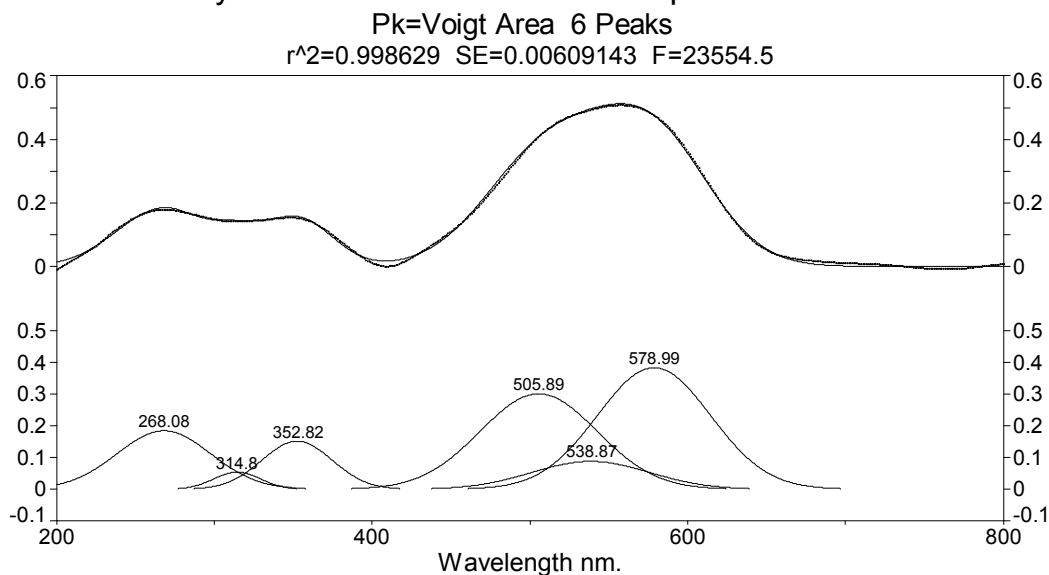


Figure B. 16 Peak fit of Na-MMT (Kunipia) / 0.5 mol % thioindigo heated at 413K for nine hours.

Table B. 16 Peak fit statistics of Na-MMT (Kunipia) / 0.5 mol % thioindigo heated at 413K for nine hours.

Description: Kunipia Na-Mont - Kunipia Na-Mont - C:\COLOR\Data\ALE\pennstate\NEW RUNS WITH Ba

X Variable: Wavelength nm.

File Source: c:\documents and settings\ale\desktop\thesis final\peak fit\kunipia\kunipia na-montpeakfit.txt

Measured Values

Peak	Type	Amplitude	Center	FWHM	Asym50	FW Base	Asym10
1	Voigt Area	0.18448811	268.078678	70.8419485	0.99999994	142.427942	0.99999997
2	Voigt Area	0.05457035	314.803469	34.9687589	1.00000002	70.3047909	1.00000001
3	Voigt Area	0.15173331	352.815365	52.4441734	1.00000000	105.439162	1.00000000
4	Voigt Area	0.30034899	505.888835	87.6737380	1.00000001	176.268304	1.00000000
5	Voigt Area	0.08815714	538.866860	87.6769274	1.00000000	176.274716	1.00000000
6	Voigt Area	0.38250043	578.993594	84.6888031	1.00000001	170.267083	1.00000001

Peak	Type	Anlytc Area	% Area	Int Area	% Area	Centroid	Moment2
1	Voigt Area	14.0065302	14.6206207	13.7954451	14.4513208	269.438097	933.081308
2	Voigt Area	2.04507219	2.13473460	2.04300334	2.14013368	314.939335	271.683827
3	Voigt Area	8.52805238	8.90194907	8.51747387	8.92241943	352.968766	569.200746
4	Voigt Area	28.2206737	29.4579569	28.1762809	29.5158635	505.879255	1496.27949
5	Voigt Area	8.28351134	8.64668658	8.27024375	8.66343527	538.803177	1496.29652
6	Voigt Area	34.7159937	36.2380522	34.6590357	36.3068274	578.866070	1400.50983
	Total	95.7998335	100.000000	95.4614826	100.000000		

kunipia-6%thio Hydrated- RawData - C:\COLOR\Data\ALE\pennstate\09.02.0

Pk=Voigt Area 4 Peaks

$r^2=0.998426$ SE=0.00914447 F=62786

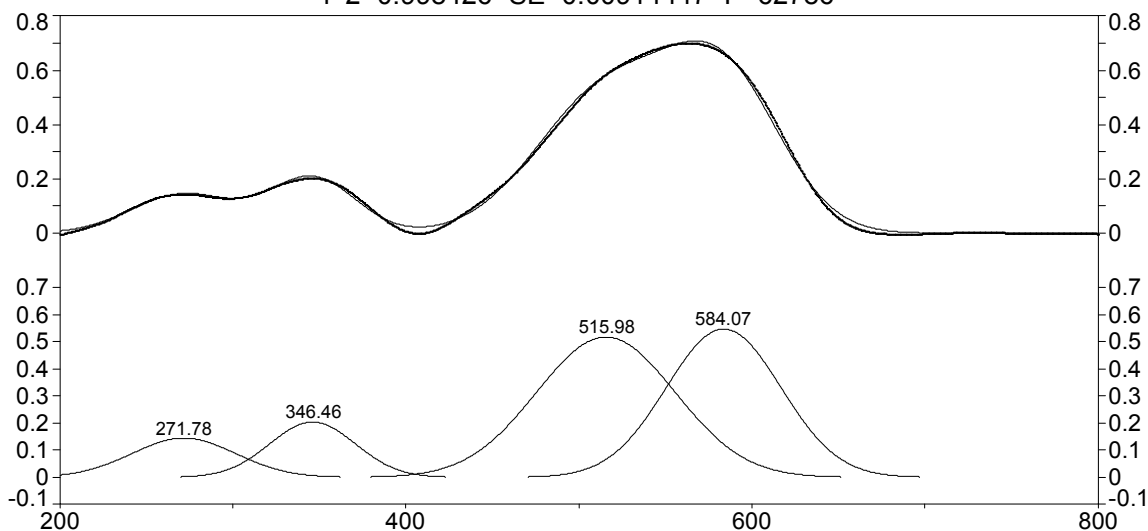


Figure B. 17 Peak fit of Na-MMT (Kunipia) / 0.5 mol % thioindigo heated at 413K for nine hours / hydrated.

Table B. 17 Peak fit statistics of Na-MMT (Kunipia) / 0.5 mol % thioindigo heated at 413K for nine hours / hydrated.

Description: kunipia-6%thio140C9h-90%humidity - RawData - C:\COLOR\Data\ALE\pennstate\09.02.0

Y Variable: Wavelength nm.

File Source: c:\documents and settings\ale\desktop\thesis final\peak fit\kunipia\kunipia-6%thio140c9h-90%humiditypeakfit.txt

Measured Values

Peak	Type	Amplitude	Center	FWHM	Asym50	FW Base	Asym10
1	Voigt Area	0.14474492	271.776518	71.1687987	1.00000005	142.459170	1.00000003
2	Voigt Area	0.20375652	346.464572	58.2614547	1.00000000	116.622433	1.00000000
3	Voigt Area	0.51672937	515.975302	94.4392698	1.00000000	189.039863	1.00000000
4	Voigt Area	0.54652207	584.073102	77.9489208	1.00000010	156.030996	1.00000005

Peak	Type	Anlytc Area	% Area	Int Area	% Area	Centroid	Moment2
1	Voigt Area	10.9654174	9.07023496	10.8691829	8.99779535	272.501452	860.847190
2	Voigt Area	12.6364489	10.4524576	12.6364489	10.4607846	346.464572	612.134949
3	Voigt Area	51.9455057	42.9676249	51.9455057	43.0018553	515.975302	1608.38418
4	Voigt Area	45.3471522	37.5096825	45.3471522	37.5395647	584.073104	1095.73306
Total		120.894524	100.000000	120.798290	100.000000		

Na-MMT (Wyoming)

Na-Mont. Wyoming-thio 6% -UN - C:\COLOR\Data\ALE\pennstate\Na-Mont. Wyoming

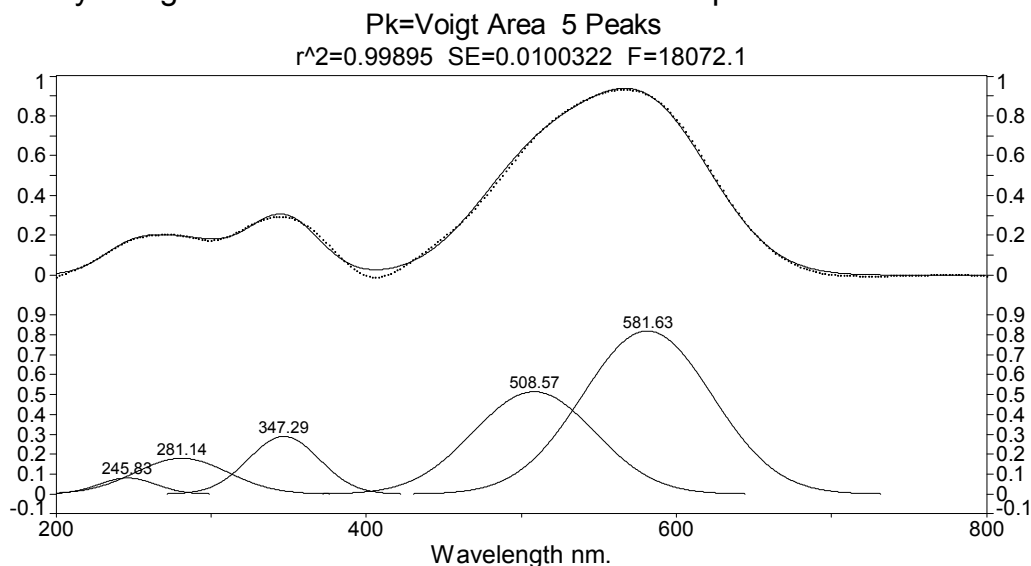


Figure B. 18 Peak fit of Na-MMT (Wyoming) / 0.5 mol % thioindigo unheated.

Table B. 18 Peak fit statistics of Na-MMT (Wyoming) / 0.5 mol % thioindigo unheated.

Description: Na-Mont. Wyoming-thio 6% - smooth - C:\COLOR\Data\ALE\pennstate\Na-Mont. Wyoming

X Variable: Wavelength nm.

File Source: c:\documents and settings\ale\Desktop\thesis final\peak fit\n-mmt wyoming\Na-Mont. Wyoming-thio 6% unpeakfit.txt

Measured Values

Peak	Type	Amplitude	Center	FWHM	Asym50	FW Base	Asym10
1	Voigt Area	0.08044765	245.829591	43.2204546	1.00000009	86.5147396	1.00000005
2	Voigt Area	0.17955382	281.138142	70.9462051	1.00000000	142.013602	1.00000000
3	Voigt Area	0.28960003	347.294894	53.7344343	1.00000000	107.560659	1.00000000
4	Voigt Area	0.51389546	508.570419	92.1079194	1.00000000	184.373180	1.00000000
5	Voigt Area	0.81925658	581.630271	98.2915981	1.00000000	196.751101	1.00000000

Peak	Type	Anlytc Area	% Area	Int Area	% Area	Centroid	Moment2
1	Voigt Area	3.70113497	2.17805629	3.67795524	2.16532245	246.155790	321.814762
2	Voigt Area	13.5598856	7.97976684	13.5118907	7.95485488	281.459131	881.553663
3	Voigt Area	16.5646971	9.74804838	16.5646971	9.75213348	347.294894	520.702800
4	Voigt Area	50.3853136	29.6509179	50.3853136	29.6633437	508.570419	1529.95443
5	Voigt Area	85.7173121	50.4432106	85.7173049	50.4643455	581.630252	1742.27342
Total		169.928343	100.000000	169.857162	100.000000		

Na-Mont+dye Dehydrated- C:\COLOR\Data\ALE\pennstate\NEW RUNS WITH Ba

Pk=Gauss Amp 5 Peaks

r²=0.999078 SE=0.007295 F=45369.7

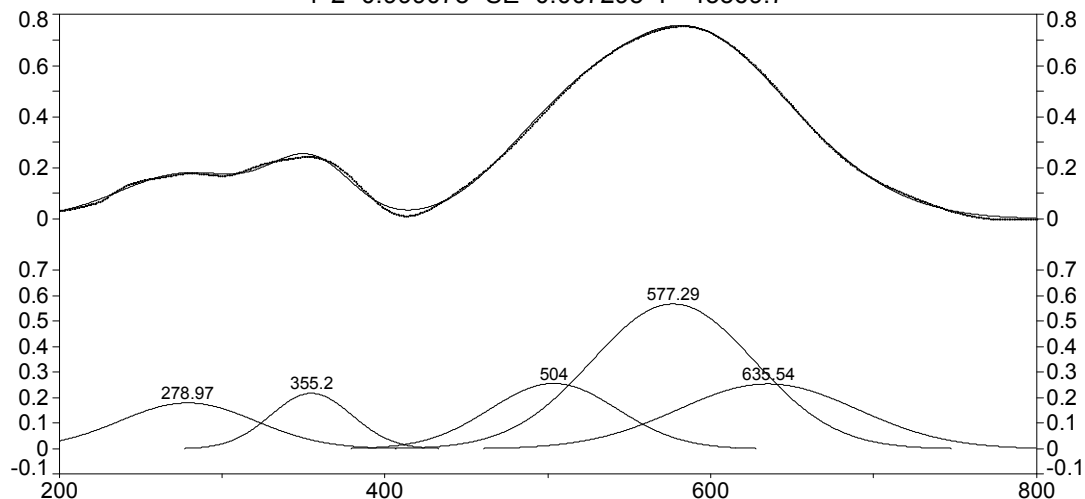


Figure B. 19 Peak fit of Na-MMT (Wyoming) / 0.5 mol % thioindigo heated at 413K for nine hours.

Table B. 19 Peak fit statistics of Na-MMT (Wyoming) / 0.5 mol % thioindigo heated at 413K for nine hours.

Description: Na-Mont.+dye - Na-Mont+dye smooth - C:\COLOR\Data\ALE\pennstate\NEW RUNS WITH Ba

X Variable: Wavelength (nm)

Y Variable: Absorbance

File Source: c:\documents and settings\ale\desktop\thesis final\peak fit\n-mmt wyoming\na-mont.+dyebaselinepeakfit.txt

Measured Values

Peak	Type	Amplitude	Center	FWHM	Asym50	FW Base	Asym10
1	Gauss Amp	0.17969161	278.965068	98.7336066	1.00000002	197.635873	1.00000001
2	Gauss Amp	0.21723063	355.196551	58.6329794	1.00000000	117.366117	1.00000000
3	Gauss Amp	0.25586799	504.004105	92.1185353	1.00000000	184.394430	1.00000000
4	Gauss Amp	0.56689634	577.286146	117.636246	1.00000000	235.473442	1.00000000
5	Gauss Amp	0.25414571	635.535406	129.605113	1.00000000	259.431620	1.00000000
Peak	Type	Anlytc Area	% Area	Int Area	% Area	Centroid	Moment2
1	Gauss Amp	18.8853493	11.5448990	18.3220476	11.2426603	281.891628	1518.32189
2	Gauss Amp	13.5579878	8.28820254	13.5579878	8.31936771	355.196551	619.966860
3	Gauss Amp	25.0896839	15.3377024	25.0896839	15.3953750	504.004105	1530.30712
4	Gauss Amp	70.9867060	43.3952446	70.9864127	43.5582387	577.285183	2495.33899
5	Gauss Amp	35.0620357	21.4339515	35.0128373	21.4843583	635.282349	2987.52318
Total		163.581763	100.000000	162.968969	100.000000		

NaMMT+dyered hydrated- C:\COLOR\Data\ALE\pennstate\11.25.08XRD\NaMMT+dyered.sp

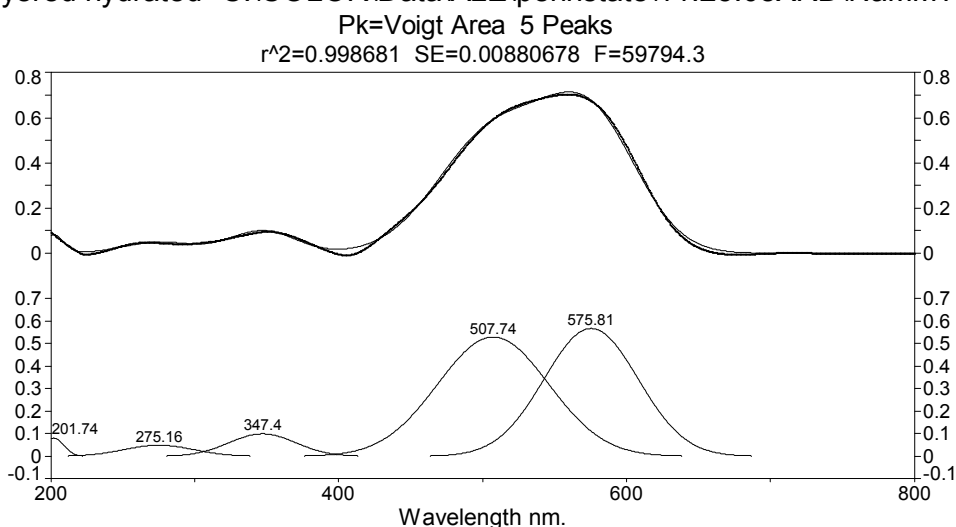


Figure B. 20 Peak fit of Na-MMT (Wyoming) / 0.5 mol % thioindigo heated at 413K for nine hours / hydrated.

Table B. 20 Peak fit statistics of Na-MMT (Wyoming) / 0.5 mol % thioindigo heated at 413K for nine hours / hydrated.

Description: NaMMT+dyered - RawData - C:\COLOR\Data\ALE\pennstate\11.25.08XRD\NaMMT+dyered.sp

X Variable: Wavelength nm.

File Source: c:\documents and settings\ale\desktop\thesis final\peak fit\n-mmt wyoming\nammt+dyeredpeakfit.txt

Measured Values

Peak	Type	Amplitude	Center	FWHM	Asym50	FW Base	Asym10
1	Voigt Area	0.08090252	201.744863	16.6199852	0.99999998	33.2683612	0.99999999
2	Voigt Area	0.04954067	275.155165	57.1283075	1.00000006	114.354203	1.00000004
3	Voigt Area	0.09977380	347.397778	54.4512565	1.00000001	108.995528	1.00000000
4	Voigt Area	0.52854074	507.738953	90.7627116	1.00000000	181.680467	1.00000000
5	Voigt Area	0.56663627	575.807841	76.8061283	1.00000002	153.743459	1.00000001
Peak	Type	Anlytc Area	% Area	Int Area	% Area	Centroid	Moment2
1	Voigt Area	1.43128093	1.32996229	0.85537938	0.79912630	206.314453	20.9588963
2	Voigt Area	3.01262761	2.79936735	3.00969169	2.81176267	275.235019	582.547573
3	Voigt Area	5.78304554	5.37367074	5.78304554	5.40272998	347.397778	534.687907
4	Voigt Area	51.0643894	47.4496031	51.0643894	47.7061967	507.738953	1485.59174
5	Voigt Area	46.3268158	43.0473965	46.3268158	43.2801843	575.807842	1063.83996
	Total	107.618159	100.000000	107.039322	100.000000		

YN6

YN6-6%THIOUN - YN6-6%THIOUNsmooth - C:\COLOR\Data\ALE\pennstate\YN6-6%THIOUN.spc

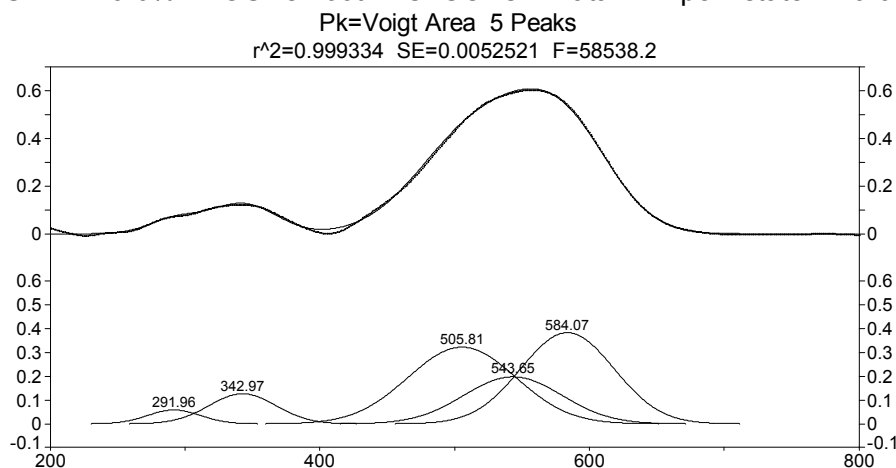


Figure B. 21 Peak fit of YN6 / 0.5 mol % thioindigo unheated.

Table B. 21 Peak fit statistics of YN6 / 0.5 mol % thioindigo unheated.

Description: YN6-6%THIOUN - YN6-6%THIOUNsmooth - C:\COLOR\Data\ALE\pennstate\YN6-6%THIOUN.spc

X Variable: Wavelength nm.

File Source: c:\documents and settings\ale\desktop\thesis final\peak fit\yn6\yn6-6%thiounpeakfit.txt

Measured Values

Peak	Type	Amplitude	Center	FWHM	Asym50	FW Base	Asym10
1	Voigt Area	0.05875281	291.963910	46.2618648	1.00000007	92.6027555	1.00000004
2	Voigt Area	0.12648480	342.973091	58.6222113	0.99999989	117.344563	0.99999994
3	Voigt Area	0.32283747	505.812173	94.0066268	1.00000000	188.173838	1.00000000
4	Voigt Area	0.19813877	543.645919	85.6485299	1.00000000	171.443367	1.00000000
5	Voigt Area	0.38358293	584.068314	81.3688737	1.00000005	162.876744	1.00000003

Peak	Type	Anlytc Area	% Area	Int Area	% Area	Centroid	Moment2
1	Voigt Area	2.89323700	3.06553267	2.89323287	3.06552843	291.964047	385.937230
2	Voigt Area	7.89283014	8.36285747	7.89283010	8.36285780	342.973090	619.739071
3	Voigt Area	32.3053620	34.2291844	32.3053620	34.2291859	505.812173	1593.68135
4	Voigt Area	18.0643184	19.1400699	18.0643184	19.1400707	543.645919	1322.89196
5	Voigt Area	33.2238370	35.2023556	33.2238370	35.2023572	584.068315	1193.99129
Total		94.3795846	100.000000	94.3795804	100.000000		

YN6 DEHYDRATED C:\COLOR\Data\ALE\pennstate\NEW RUNS WITH BaSo4\YN6.spc

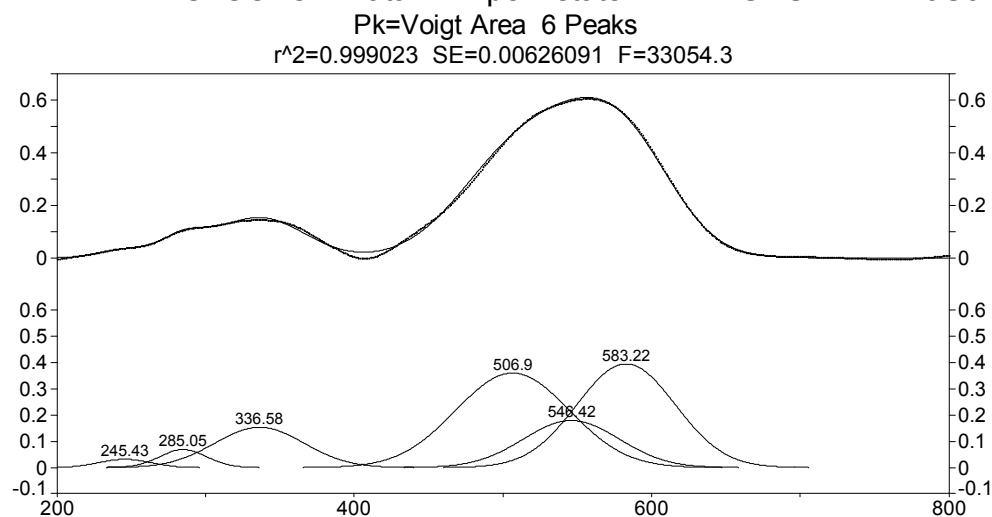


Figure B. 22 Peak fit of YN6 / 0.5 mol % thioindigo heated at 413K for nine hours.

Table B. 22 Peak fit statistics of YN6 / 0.5 mol % thioindigo heated at 413K for nine hours.

Description: YN6 - YN6 SMOOTH - C:\COLOR\Data\ALE\pennstate\NEW RUNS WITH BaSo4\YN6.spc

X Variable: Wavelength (nm)

Y Variable: Absorbance

File Source: c:\documents and settings\ale\desktop\thesis final\peak fit\yn6\yn6peakfit.txt

Measured Values

Peak	Type	Amplitude	Center	FWHM	Asym50	FW Base	Asym10
1	Voigt Area	0.03163075	245.431472	40.3318865	0.99999999	80.7326691	0.99999999
2	Voigt Area	0.06859617	285.045525	37.6910386	1.00000002	75.4464621	1.00000001
3	Voigt Area	0.15340126	336.584138	70.7283863	1.00000000	141.577593	1.00000000
4	Voigt Area	0.36034535	506.901166	89.9124235	1.00000000	179.978438	1.00000000
5	Voigt Area	0.17922412	546.416967	75.9969647	1.00000000	152.123750	1.00000000
6	Voigt Area	0.39530716	583.222629	78.0463545	0.99999993	156.226030	0.99999996
Peak	Type	Anlytc Area	% Area	Int Area	% Area	Centroid	Moment2
1	Voigt Area	1.35797018	1.39296979	1.35254626	1.38748371	245.634927	284.062307
2	Voigt Area	2.75213776	2.82306990	2.75213761	2.82322774	285.045530	256.188765
3	Voigt Area	11.5492793	11.8469444	11.5492480	11.8475752	336.584525	902.083164
4	Voigt Area	34.4882244	35.3771057	34.4882244	35.3790855	506.901166	1457.88732
5	Voigt Area	14.4985616	14.8722398	14.4985616	14.8730722	546.416967	1041.54262
6	Voigt Area	32.8412377	33.6876704	32.8412377	33.6895557	583.222628	1098.47404
	Total	97.4874110	100.000000	97.4819556	100.000000		

YN-8

YN8-6%thioUN - YN8-6%THIOUN - C:\COLOR\Data\ALE\pennstate\YN8-6%THIOUN.spc

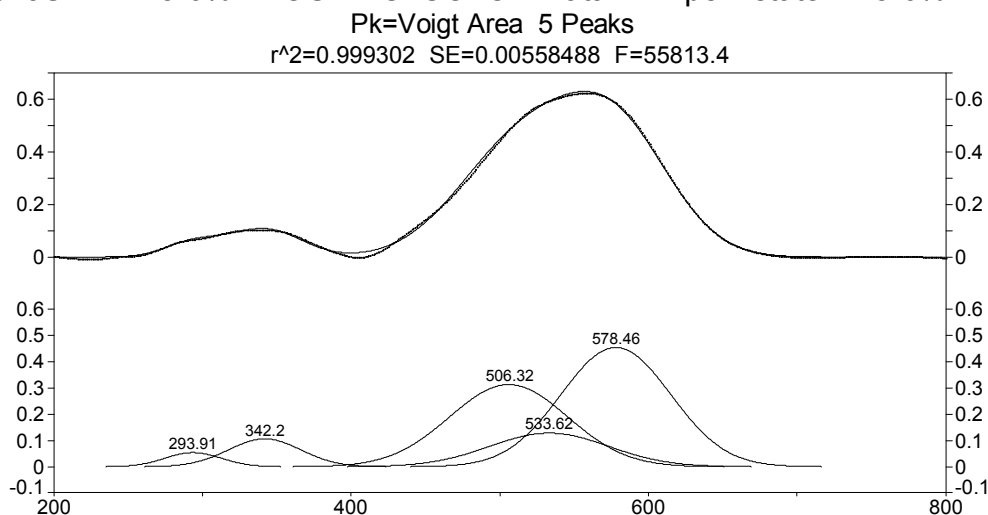


Figure B. 23 Peak fit of YN8 / 0.5 mol % thioindigo unheated.

Table B. 23 Peak fit statistics of YN8 / 0.5 mol % thioindigo unheated.

Description: YN8-6%thioUN - YN8-6%THIOUN - C:\COLOR\Data\ALE\pennstate\YN8-6%THIOUN.spc

X Variable: Wavelength nm.

File Source: c:\documents and settings\ale\desktop\thesis final\peak fit\yn8\yn8-6%thiounpeakfit.txt

Measured Values

Peak	Type	Amplitude	Center	FWHM	Asym50	FW Base	Asym10
1	Voigt Area	0.05419404	293.909236	44.5658217	1.00000003	89.2077720	1.00000001
2	Voigt Area	0.10631909	342.202173	57.3706954	0.99999992	114.839393	0.99999995
3	Voigt Area	0.31331584	506.323407	93.6432717	1.00000000	187.446507	1.00000000
4	Voigt Area	0.12819316	533.616882	94.4301140	1.00000000	189.021536	1.00000000
5	Voigt Area	0.45486948	578.456891	86.9094928	1.00000001	173.967447	1.00000001
Peak	Type	Anlytc Area	% Area	Int Area	% Area	Centroid	Moment2
1	Voigt Area	2.57090294	2.69877615	2.57090204	2.69877524	293.909270	358.166134
2	Voigt Area	6.49282314	6.81576734	6.49282313	6.81576739	342.202173	593.560155
3	Voigt Area	31.2313771	32.7847833	31.2313771	32.7847836	506.323407	1581.38534
4	Voigt Area	12.8856871	13.5266036	12.8856871	13.5266038	533.616882	1608.07233
5	Voigt Area	42.0810170	44.1740696	42.0810169	44.1740700	578.456891	1362.13128
Total		95.2618072	100.000000	95.2618063	100.000000		

YN8 DEHYDRATED C:\COLOR\Data\ALE\pennstate\NEW RUNS WITH BaSo4\YN8.spc

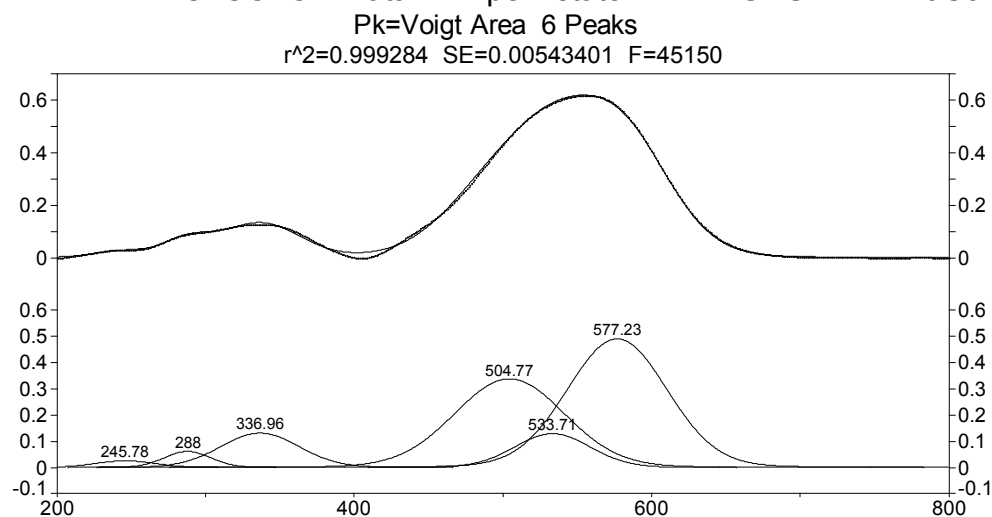


Figure B. 24 Peak fit of YN8 / 0.5 mol % thioindigo heated at 413K for nine hours.

Table B. 24 Peak fit statistics of YN8 / 0.5 mol % thioindigo heated at 413K for nine hours.

Description: YN8 - YN8 SMOOTH - C:\COLOR\Data\ALE\pennstate\NEW RUNS WITH BaSo4\YN8.spc

X Variable: Wavelength nm.

File Source: c:\documents and settings\ale\desktop\thesis final\peak fit\yn8\yn8peakfit.txt

Measured Values

Peak	Type	Amplitude	Center	FWHM	Asym50	FW Base	Asym10
1	Voigt Area	0.02580232	245.780970	47.4240686	1.00000000	96.7419607	1.00000000
2	Voigt Area	0.06173674	288.004394	37.3783023	0.99999995	76.2492624	0.99999997
3	Voigt Area	0.13144556	336.957307	62.4028923	1.00000000	127.297770	1.00000000
4	Voigt Area	0.33844428	504.773396	87.2624821	1.00000000	178.009687	1.00000000
5	Voigt Area	0.12921681	533.712227	60.1423129	1.00000000	122.686337	1.00000000
6	Voigt Area	0.49052991	577.225489	79.1394783	1.00000000	161.439297	1.00000000

Peak	Type	Anlytc Area	% Area	Int Area	% Area	Centroid	Moment2
1	Voigt Area	1.33926401	1.39274373	1.30686334	1.36783387	247.787501	652.310662
2	Voigt Area	2.52564294	2.62649734	2.51156264	2.62873733	288.744722	474.360130
3	Voigt Area	8.97758026	9.33607450	8.91808073	9.33414573	337.826756	1047.39915
4	Voigt Area	32.3238732	33.6146355	32.1160281	33.6143724	504.741568	1821.69482
5	Voigt Area	8.50565538	8.84530465	8.46776977	8.86282592	533.560590	989.928673
6	Voigt Area	42.4881022	44.1847442	42.2222441	44.1920848	576.749488	1546.79368
	Total	96.1601180	100.000000	95.5425487	100.000000		

Na-Ts

Na-Ts6%THIOUN - Na-Ts6%THIOUNsmooth - C:\COLOR\Data\ALE\pennstate\Na-Ts6%THIOUN.

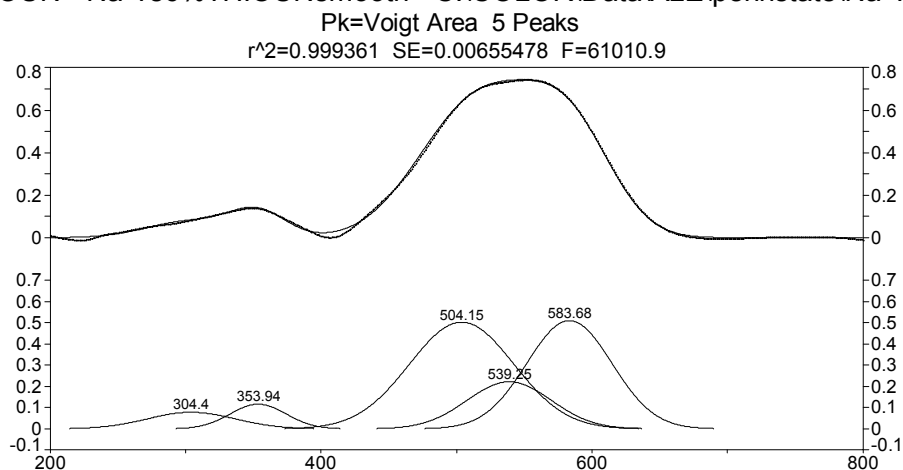


Figure B. 25 Peak fit of Na-Ts / 0.5 mol % thioindigo unheated.

Table B. 25 Peak fit statistics of Na-Ts / 0.5 mol % thioindigo unheated.

Description: Na-Ts6%THIOUN - Na-Ts6%THIOUNsmooth - C:\COLOR\Data\ALE\pennstate\Na-Ts6%THIOUN.

X Variable: Wavelength nm.

File Source: c:\documents and settings\ale\desktop\thesis final\peak fit\na-ts\na-ts6%thiounpeakfit.txt

Measured Values

Peak	Type	Amplitude	Center	FWHM	Asym50	FW Base	Asym10
1	Voigt Area	0.07825086	304.396268	76.5964786	1.00000004	153.323801	1.00000002
2	Voigt Area	0.11632009	353.938850	48.6000332	0.99999995	97.2830863	0.99999997
3	Voigt Area	0.50247306	504.145096	90.7487751	1.00000000	181.652570	1.00000000
4	Voigt Area	0.22189072	539.253320	73.2039603	1.00000013	146.532970	1.00000007
5	Voigt Area	0.50966221	583.682038	73.9918277	1.00000000	148.110050	1.00000000

Peak	Type	Anlytc Area	% Area	Int Area	% Area	Centroid	Moment2
1	Voigt Area	6.38013854	5.39006204	6.37589645	5.38667130	304.471548	1050.17563
2	Voigt Area	6.01760263	5.08378483	6.01760263	5.08396703	353.938850	425.949079
3	Voigt Area	48.5384345	41.0061900	48.5384345	41.0076597	504.145096	1485.13555
4	Voigt Area	17.2904353	14.6072877	17.2904353	14.6078112	539.253323	966.392845
5	Voigt Area	40.1419438	33.9126754	40.1419438	33.9138908	583.682038	987.306649
Total		118.368555	100.000000	118.364313	100.000000		

Na-TS+dye - Na-TS+dye dehydrated C:\COLOR\Data\ALE\pennstate\NEW RUNS WITH BaSo4\N

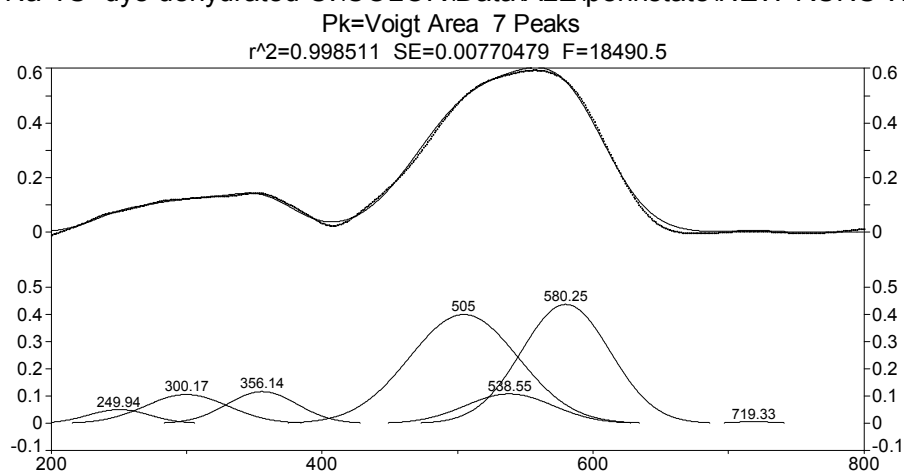


Figure B. 26 Peak fit of Na-Ts / 0.5 mol % thioindigo heated at 413K for nine hours.

Table B. 26 Peak fit statistics of Na-Ts / 0.5 mol % thioindigo heated at 413K for nine hours.

Description: Na-TS+dye - Na-TS+dye smooth - C:\COLOR\Data\ALE\pennstate\NEW RUNS WITH BaSo4\N

X Variable: Wavelength (nm)

Y Variable: Absorbance

File Source: c:\documents and settings\ale\desktop\thesis final\peak fit\na-ts\na-ts+dyebaselinepeakfit.txt

Measured Values

Peak	Type	Amplitude	Center	FWHM	Asym50	FW Base	Asym10
1	Voigt Area	0.05090272	249.940556	53.5012786	1.00000000	107.243599	1.00000000
2	Voigt Area	0.10588818	300.166661	72.3517594	1.00000000	145.029488	1.00000000
3	Voigt Area	0.11680777	356.137279	60.8739931	1.00000000	122.022245	1.00000000
4	Voigt Area	0.39895227	505.004554	94.5432151	1.00000000	189.512380	1.00000000
5	Voigt Area	0.10830546	538.553633	76.1485823	1.00000002	152.640240	1.00000001
6	Voigt Area	0.43604781	580.247660	77.1043451	0.99999988	154.556072	0.99999993
7	Voigt Area	0.00678781	719.328792	36.5895642	1.00000000	73.3439771	1.00000000

Peak	Type	Anlytc Area	% Area	Int Area	% Area	Centroid	Moment2
1	Voigt Area	2.90524979	2.79806328	2.86166725	2.75878638	250.879290	498.420903
2	Voigt Area	8.17287653	7.87134579	8.16170836	7.86828372	300.336381	967.986554
3	Voigt Area	7.58545951	7.30560098	7.58197426	7.30939186	356.193530	694.939580
4	Voigt Area	40.2373771	38.7528562	40.2153494	38.7695522	505.001705	1649.25151
5	Voigt Area	8.79813349	8.47353448	8.79421256	8.47804852	538.536215	1077.71378
6	Voigt Area	35.8666921	34.5434236	35.8494679	34.5606302	580.210039	1104.36199
7	Voigt Area	0.26495076	0.25517565	0.26482809	0.25530716	719.268808	258.530719
	Total	103.830739	100.000000	103.729208	100.000000		

Talc

TALC-6%THIOUN - RawData - C:\COLOR\Data\ALE\pennstate\09.02.08\TALC-6%THIOUN.spc

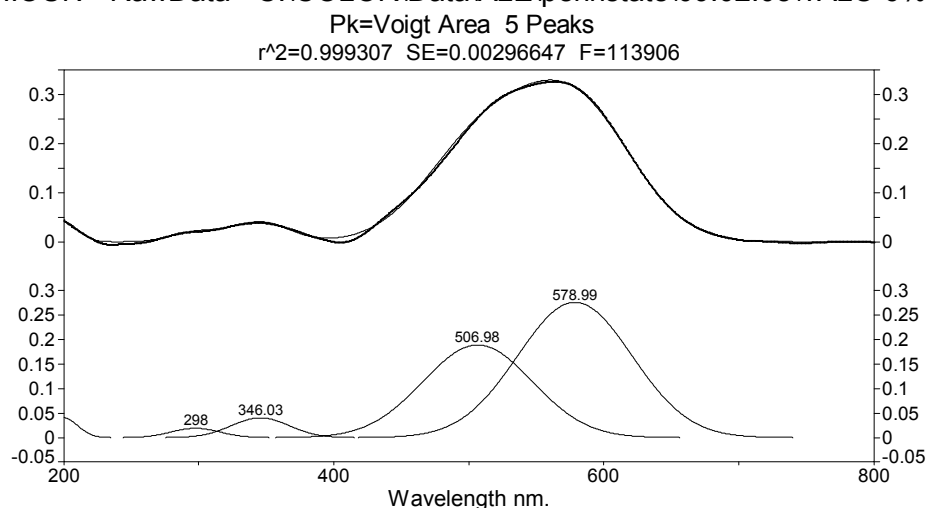


Figure B. 27 Peak fit of Talc / 0.5 mol % thioindigo unheated.

Table B. 27 Peak fit statistics of Talc / 0.5 mol % thioindigo unheated.

Description: TALC-6%THIOUN - RawData - C:\COLOR\Data\ALE\pennstate\09.02.08\TALC-6%THIOUN.spc

X Variable: Wavelength nm.

File Source: c:\documents and settings\ale\desktop\thesis final\peak fit\talc\talc-6%thiounpeakfit.txt

Measured Values

Peak	Type	Amplitude	Center	FWHM	Asym50	FW Base	Asym10
1	Voigt Area	0.04087402	200.000004	25.4591700	0.87944053	50.8725459	0.93190900
2	Voigt Area	0.01911446	298.004128	42.3097131	0.99999989	84.6917008	0.99999994
3	Voigt Area	0.04033893	346.026243	50.4602154	1.00000011	101.006628	1.00000006
4	Voigt Area	0.18909019	506.980350	95.4186363	1.00000000	191.000269	1.00000000
5	Voigt Area	0.27617880	578.990908	99.5826791	1.00000000	199.335468	1.00000000
Peak	Type	Anlytc Area	% Area	Int Area	% Area	Centroid	Moment2
1	Voigt Area	1.10859324	2.10688203	0.52085698	1.00107090	208.318502	40.4178917
2	Voigt Area	0.86086362	1.63607176	0.86086360	1.65455305	298.004129	322.822938
3	Voigt Area	2.16673450	4.11788007	2.16673450	4.16439629	346.026245	459.179775
4	Voigt Area	19.2058890	36.5008022	19.2058890	36.9131210	506.980350	1641.91611
5	Voigt Area	29.2756371	55.6383639	29.2756346	56.2668587	578.990888	1788.34417
Total		52.6177175	100.000000	52.0299786	100.000000		

Talc-6%thio Dehydrated- C:\COLOR\Data\ALE\pennstate\09.03.08UV\Talc-6%th

Pk=Voigt Area 4 Peaks

$r^2=0.996904$ SE=0.00734519 F=31874.5

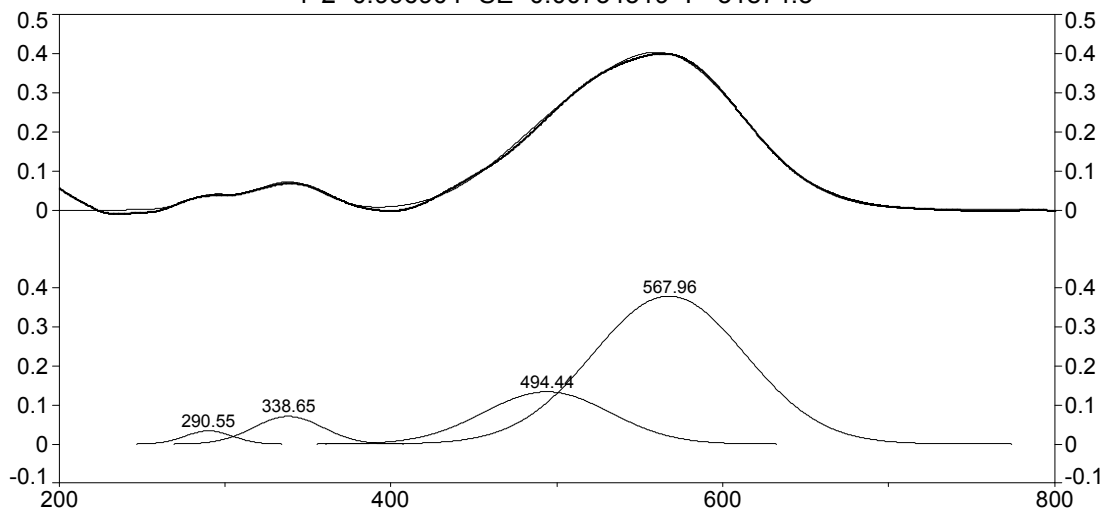


Figure B. 28 Peak fit of Talc / 0.5 mol % thioindigo heated at 413K for nine hours.

Table B. 28 Peak fit statistics of Talc / 0.5 mol % thioindigo heated at 413K for nine hours.

Description: Talc-6%thio140C9hrs - RawData - C:\COLOR\Data\ALE\pennstate\09.03.08UV\Talc-6%th

X Variable: Wavelength nm.

File Source: c:\documents and settings\ale\desktop\thesis final\peak fit\talc\talc-6%thio140c9hrspeakfit.txt

Measured Values

Peak	Type	Amplitude	Center	FWHM	Asym50	FW Base	Asym10
1	Voigt Area	0.03399256	290.550898	34.0144312	1.00000000	68.4241441	1.00000000
2	Voigt Area	0.07114341	338.647885	48.8722995	1.00000000	98.3125440	1.00000000
3	Voigt Area	0.13433262	494.440527	89.5392830	1.00000001	180.119102	1.00000001
4	Voigt Area	0.37941865	567.964105	108.554478	1.00000000	218.370469	1.00000000
Peak	Type	Anlytc Area	% Area	Int Area	% Area	Centroid	Moment2
1	Voigt Area	1.24018121	1.99872286	1.23850932	2.00034597	290.730078	264.659025
2	Voigt Area	3.72937046	6.01039427	3.72418385	6.01501826	338.827784	508.174768
3	Voigt Area	12.9012907	20.7922072	12.8779656	20.7995097	494.450940	1571.39746
4	Voigt Area	44.1778403	71.1986756	44.0740967	71.1851260	567.801328	2265.99502
	Total	62.0486826	100.000000	61.9147555	100.000000		

Zeolite 4A

4A-6%THIOUN - 4A-6%THIOUNsmooth - C:\COLOR\Data\ALE\pennstate\4A-6%THIOUN.spc

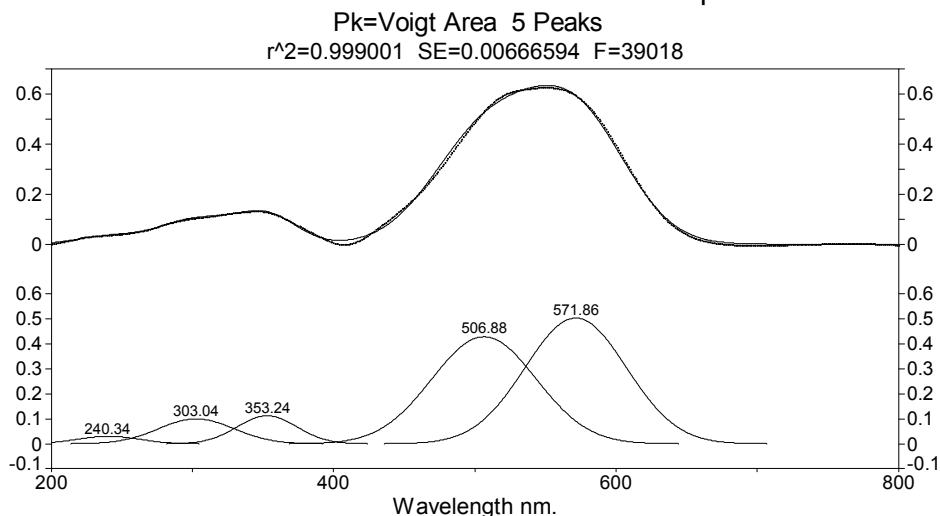


Figure B. 29 Peak fit of 4A / 0.5 mol % thioindigo unheated.

Table B. 29 Peak fit statistics of 4A / 0.5 mol % thioindigo unheated.

Description: 4A-6%THIOUN - 4A-6%THIOUNsmooth - C:\COLOR\Data\ALE\pennstate\4A-6%THIOUN.spc

X Variable: Wavelength nm.

File Source: c:\documents and settings\ale\desktop\thesis final\peak fit\4a\4a-6%thiounpeakfit.txt

Measured Values

Peak	Type	Amplitude	Center	FWHM	Asym50	FW Base	Asym10
1	Voigt Area	0.03015407	240.341628	52.0066540	1.00000000	104.102147	1.00000000
2	Voigt Area	0.09980015	303.040763	63.5203609	1.00000000	127.149229	1.00000000
3	Voigt Area	0.11225608	353.241510	49.9384384	0.99999999	99.9621830	0.99999999
4	Voigt Area	0.42899294	506.882325	86.9976226	1.00000000	174.143857	1.00000000
5	Voigt Area	0.50395405	571.864376	84.5320826	1.00000002	169.208565	1.00000001
Peak	Type	Anlytc Area	% Area	Int Area	% Area	Centroid	Moment2
1	Voigt Area	1.66931014	1.67839730	1.61275860	1.62246780	242.061298	415.424214
2	Voigt Area	6.74802002	6.78475398	6.74756960	6.78819158	303.048064	726.877511
3	Voigt Area	5.96728846	5.99977238	5.96728846	6.00321296	353.241510	449.732701
4	Voigt Area	39.7273630	39.9436255	39.7273630	39.9665312	506.882325	1364.89525
5	Voigt Area	45.3465991	45.5934508	45.3465991	45.6195964	571.864377	1288.62837
	Total	99.4585807	100.000000	99.4015788	100.000000		

4A6%THIO140C9hfreshpink - 4A6%THIO140C9hfreshpink - C:\COLOR\Data\ALE\pennstate\
Pk=Voigt Area 4 Peaks
 $r^2=0.999237$ SE=0.00603397 F=64196.4

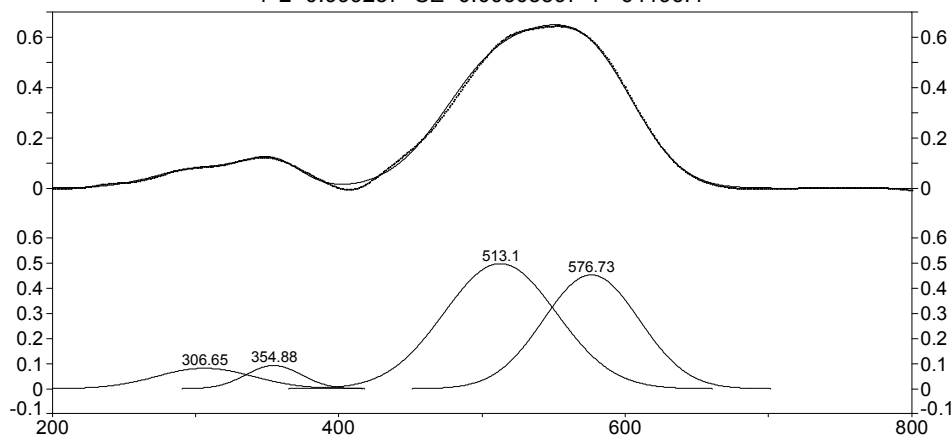


Figure B. 30 Peak fit of 4A / 0.5 mol % thioindigo heated at 413K for nine hours.

Table B. 30 Peak fit statistics of 4A / 0.5 mol % thioindigo heated at 413K for nine hours.

Description: 4A6%THIO140C9hfreshpink - 4A6%THIO140C9hfreshpink - C:\COLOR\Data\ALE\pennstate\
Y Variable: Wavelength nm.
File Source: c:\documents and settings\ale\desktop\thesis final\peak fit\4a\4a6%thio140c9hfreshpinkdeconvolution.txt

Measured Values

Peak	Type	Amplitude	Center	FWHM	Asym50	FW Base	Asym10
1	Voigt Area	0.08167473	306.651422	79.4195010	1.00000000	158.974668	1.00000000
2	Voigt Area	0.09268293	354.878642	45.4027989	0.99999990	90.8831561	0.99999995
3	Voigt Area	0.49887500	513.099060	92.4021257	1.00000005	184.962095	1.00000003
4	Voigt Area	0.45398560	576.727392	78.8236887	1.00000008	157.782026	1.00000004

Peak	Type	Anlytc Area	% Area	Int Area	% Area	Centroid	Moment2
1	Voigt Area	6.90473560	7.00670446	6.89933088	7.00160393	306.742157	1127.78189
2	Voigt Area	4.47934556	4.54549636	4.47934556	4.54574567	354.878641	371.748996
3	Voigt Area	49.0688542	49.7935010	49.0688542	49.7962321	513.099061	1539.74384
4	Voigt Area	38.0917605	38.6542981	38.0917605	38.6564183	576.727394	1120.46440
	Total	98.5446959	100.000000	98.5392911	100.000000		

Zeolite 5A

5A-6%THIOUN - 5A-6%THIOUNsmooth - C:\COLOR\Data\ALE\pennstate\5A-6%THIOUN.spc

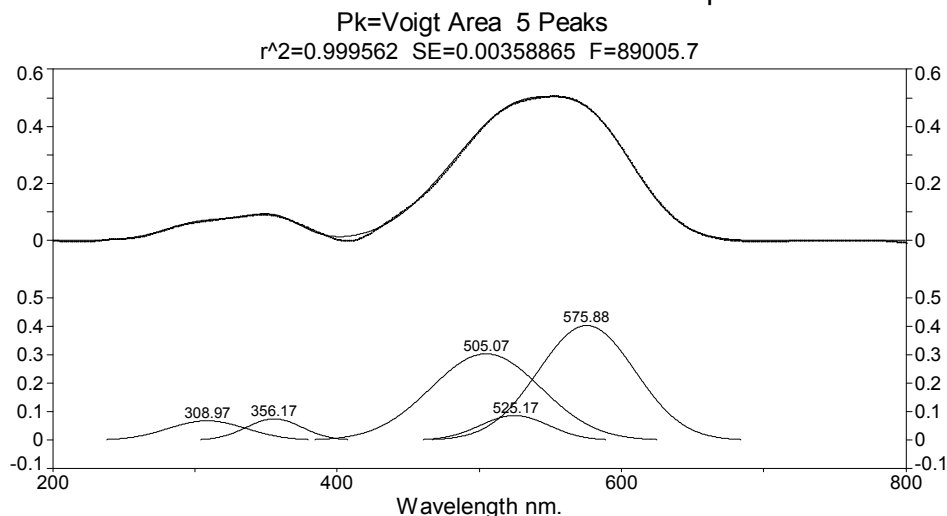


Figure B. 31 Peak fit of 5A / 0.5 mol % thioindigo unheated.

Table B. 31 Peak fit statistics of 5A / 0.5 mol % thioindigo unheated.

Description: 5A-6%THIOUN - 5A-6%THIOUNsmooth - C:\COLOR\Data\ALE\pennstate\5A-6%THIOUN.spc

X Variable: Wavelength nm.

File Source: c:\documents and settings\ale\desktop\thesis final\peak fit\5a\5a-6%thiounpeakfit.txt

Measured Values

Peak	Type	Amplitude	Center	FWHM	Asym50	FW Base	Asym10
1	Voigt Area	0.06807938	308.970255	64.9160157	1.00000001	129.942923	1.00000001
2	Voigt Area	0.07496297	356.166582	46.1963474	1.00000001	92.4716087	1.00000001
3	Voigt Area	0.30290185	505.071673	91.1103447	1.00000000	182.376327	1.00000000
4	Voigt Area	0.08666541	525.167026	56.5397645	0.99999999	113.176112	1.00000000
5	Voigt Area	0.40214821	575.883305	79.9097400	0.99999986	159.955984	0.99999992

Peak	Type	Anlytc Area	% Area	Int Area	% Area	Centroid	Moment2
1	Voigt Area	4.70435032	6.09447499	4.70416869	6.09425403	308.974705	759.470769
2	Voigt Area	3.68626583	4.77554888	3.68626583	4.77556011	356.166582	384.857389
3	Voigt Area	29.3766200	38.0573434	29.3766200	38.0574330	505.071673	1496.99356
4	Voigt Area	5.21593289	6.75722903	5.21593289	6.75724493	525.167026	576.491015
5	Voigt Area	34.2072424	44.3154037	34.2072424	44.3155079	575.883302	1151.55315
Total		77.1904114	100.000000	77.1902298	100.000000		

Molecularsieve5A+thio - molecularsieve5A+thio smooth - C:\COLOR\Data\ALE\pennsta

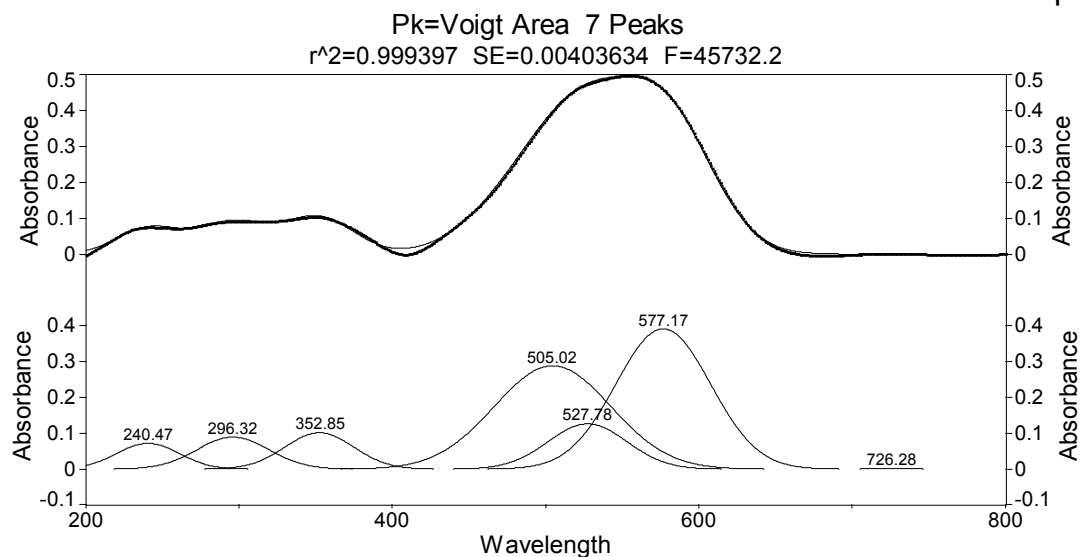


Figure B. 32 Peak fit of 5A / 0.5 mol % thioindigo heated at 413K for nine hours.

Table B. 32 Peak fit statistics of 5A / 0.5 mol % thioindigo heated at 413K for nine hours.

Description: Molecularsieve5A+thio - molecularsieve5A+thio smooth - C:\COLOR\Data\ALE\pennsta

X Variable: Wavelength

Y Variable: Absorbance

File Source: c:\documents and settings\ale\desktop\thesis final\peak fit\5a\molecularsieve5a+thiobaselinepeakfit.txt

Measured Values

Peak	Type	Amplitude	Center	FWHM	Asym50	FW Base	Asym10
1	Voigt Area	0.07194437	240.470831	48.1075355	0.99999999	96.2972496	1.00000000
2	Voigt Area	0.08919315	296.315487	55.9199689	1.00000000	111.935462	1.00000000
3	Voigt Area	0.10159687	352.852295	52.8998459	0.99999991	105.890057	0.99999995
4	Voigt Area	0.28840081	505.015964	89.5449349	1.00000000	179.242833	1.00000000
5	Voigt Area	0.12643811	527.781147	60.6730158	1.00000000	121.449675	1.00000000
6	Voigt Area	0.39141917	577.172750	72.7847143	0.99999986	145.693762	0.99999992
7	Voigt Area	0.00254620	726.284479	25.4526549	1.00000000	50.9487887	1.00000000

Peak	Type	Anlytc Area	% Area	Int Area	% Area	Centroid	Moment2
1	Voigt Area	3.68419072	4.56162370	3.59652519	4.45792573	241.644245	368.493991
2	Voigt Area	5.30921863	6.57367095	5.30908605	6.58066052	296.318025	563.676766
3	Voigt Area	5.72093406	7.08344121	5.72093406	7.09114987	352.852294	504.653588
4	Voigt Area	27.4896818	34.0366700	27.4896818	34.0737109	505.015964	1445.99437
5	Voigt Area	8.16593246	10.1107445	8.16593246	10.1217477	527.781147	663.858800
6	Voigt Area	30.3259546	37.5484343	30.3259546	37.5892970	577.172747	955.355297
7	Voigt Area	0.06898562	0.08541536	0.06898562	0.08550831	726.284479	116.829019
	Total	80.7648979	100.000000	80.6770997	100.000000		

Zeolite NaY

NaY-6%THIOUN - NaY-6%THIOUNsmooth - C:\COLOR\Data\ALE\pennstate\NaY-6%THIOUN.spc

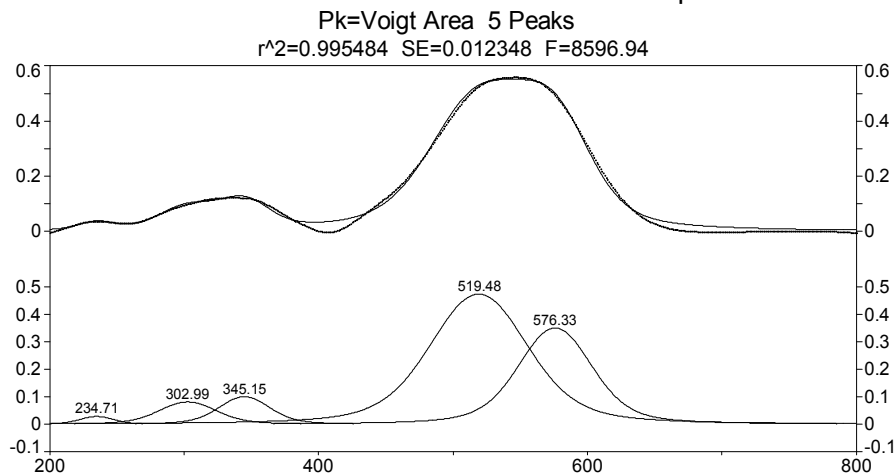


Figure B. 33 Peak fit of NaY / 0.5 mol % thioindigo unheated.

Table B. 33 Peak fit statistics of NaY / 0.5 mol % thioindigo unheated.

Description: NaY-6%THIOUN - NaY-6%THIOUNsmooth - C:\COLOR\Data\ALE\pennstate\NaY-6%THIOUN.spc

X Variable: Wavelength nm.

File Source: c:\documents and settings\ale\desktop\thesis final\peak fit\nay\nay+6%thiounpeakfit.txt

Measured Values

Peak	Type	Amplitude	Center	FWHM	Asym50	FW Base	Asym10
1	Voigt Area	0.02913582	234.712165	30.6867389	1.00000001	70.3963860	1.00000001
2	Voigt Area	0.08170583	302.989118	51.4798202	1.00000001	118.096397	1.00000000
3	Voigt Area	0.10096789	345.147303	45.0686376	1.00000000	103.388933	1.00000000
4	Voigt Area	0.47282556	519.479229	86.1429326	1.00000010	197.614714	1.00000005
5	Voigt Area	0.35007399	576.327046	65.0052662	1.00000000	149.124214	1.00000000
Peak	Type	Anlytc Area	% Area	Int Area	% Area	Centroid	Moment2
1	Voigt Area	1.10358256	1.22246044	1.03699914	1.18627100	240.320316	1169.88676
2	Voigt Area	5.19178849	5.75104780	5.00489308	5.72532735	308.012344	2027.48055
3	Voigt Area	5.61674389	6.22177938	5.48150668	6.27054756	348.260203	1753.38492
4	Voigt Area	50.2744714	55.6900360	48.5685658	55.5598159	518.785202	3639.24221
5	Voigt Area	28.0889368	31.1146763	27.3247501	31.2580382	574.266137	2636.82850
Total		90.2755232	100.000000	87.4167148	100.000000		

NaY6%thio140C9hfresh - smooth - C:\COLOR\Data\ALE\pennstate\07.01.08\NaY6%thio14
Pk=Voigt Area 6 Peaks

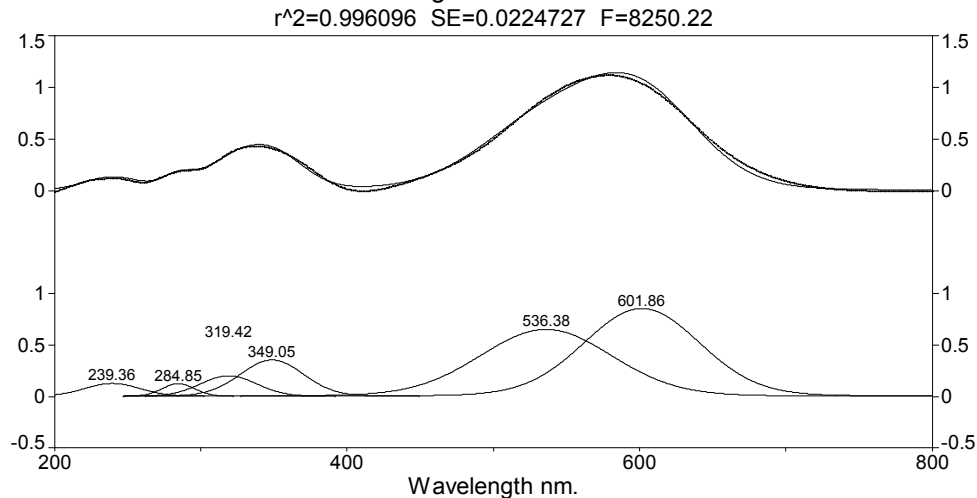


Figure B. 34 Peak fit of NaY / 0.5 mol % thioindigo heated at 413K for nine hours.

Table B. 34 Peak fit statistics of NaY / 0.5 mol % thioindigo heated at 413K for nine hours.

Description: NaY6%thio140C9hfresh - smooth - C:\COLOR\Data\ALE\pennstate\07.01.08\NaY6%thio14

X Variable: Wavelength nm.

File Source: c:\documents and settings\ale\desktop\thesis final\peak fit\nay\nay+6%thio1409hfreshpeakfit.txt

Measured Values

Peak	Type	Amplitude	Center	FWHM	Asym50	FW Base	Asym10
1	Voigt Area	0.12782082	239.363117	44.9908091	1.00000000	92.9788848	1.00000000
2	Voigt Area	0.12514881	284.849369	27.0629220	1.00000000	55.9287631	1.00000000
3	Voigt Area	0.20193828	319.417070	45.5290115	1.00000000	94.0911445	1.00000000
4	Voigt Area	0.35563090	349.048884	51.1584737	1.00000000	105.725101	1.00000000
5	Voigt Area	0.65177800	536.379094	106.499784	1.00000000	220.094534	1.00000000
6	Voigt Area	0.85450070	601.858015	93.8952690	1.00000000	194.045797	1.00000000
Peak	Type	Anlytc Area	% Area	Int Area	% Area	Centroid	Moment2
1	Voigt Area	6.40333704	3.08893406	6.14281625	3.00225514	242.550765	758.233731
2	Voigt Area	3.77122428	1.81921755	3.74615023	1.83090269	285.727942	400.329807
3	Voigt Area	10.2373569	4.93844383	10.1496655	4.96057253	320.573021	802.477801
4	Voigt Area	20.2580681	9.77237903	20.0923615	9.81999023	350.080146	946.444639
5	Voigt Area	77.2910821	37.2847868	76.2859103	37.2841636	535.883227	2863.65685
6	Voigt Area	89.3381782	43.0962387	88.1898322	43.1021158	600.594628	2343.66764
	Total	207.299247	100.000000	204.606736	100.000000		

NaY140C9houtsidedessicator - smooth - C:\COLOR\Data\ALE\pennstate\07.01.08UV\NaY

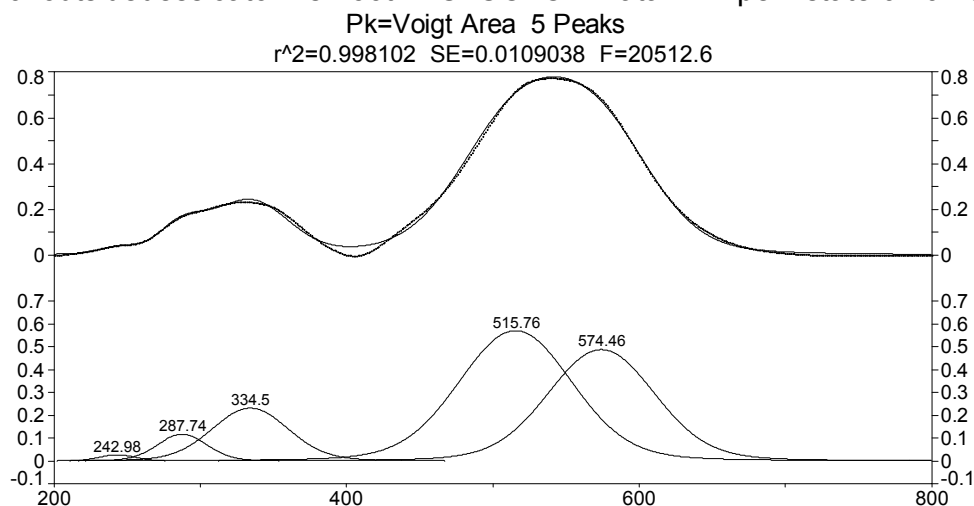


Figure B. 35 Peak fit of NaY / 0.5 mol % thioindigo heated at 413K for nine hours / hydrated.

Table B. 35 Peak fit statistics of NaY / 0.5 mol % thioindigo heated at 413K for nine hours / hydrated.

Description: NaY140C9houtsidedessicator - smooth - C:\COLOR\Data\ALE\pennstate\07.01.08UV\NaY

X Variable: Wavelength nm.

File Source: c:\documents and settings\ale\desktop\thesis final\peak fit\nay\nay140c9houtsidedessicatorpeakfit.txt

Measured Values

Peak	Type	Amplitude	Center	FWHM	Asym50	FW Base	Asym10
1	Voigt Area	0.02790974	242.980751	29.5973980	1.00000011	62.3175753	1.00000006
2	Voigt Area	0.11764641	287.744893	40.4489794	1.00000000	85.1656730	1.00000000
3	Voigt Area	0.23196982	334.497367	61.4861740	1.00000000	129.459667	1.00000000
4	Voigt Area	0.57016775	515.761700	91.2754291	1.00000001	192.181199	1.00000001
5	Voigt Area	0.48764704	574.461556	86.0335479	0.99999998	181.144373	0.99999999

Peak	Type	Anlytc Area	% Area	Int Area	% Area	Centroid	Moment2
1	Voigt Area	0.94067534	0.72560326	0.92053863	0.72185747	245.140826	593.362639
2	Voigt Area	5.41896961	4.17999902	5.33923584	4.18686095	289.715746	872.465176
3	Voigt Area	16.2419965	12.5284942	15.9818938	12.5324988	336.626970	1504.86565
4	Voigt Area	59.2634586	45.7137089	58.2926949	45.7112994	515.492059	2612.74347
5	Voigt Area	47.7753514	36.8521946	46.9892376	36.8474834	573.236871	2399.40741
	Total	129.640451	100.000000	127.523601	100.000000		

Zeolite 13X

13x6%THIOUN - 13x6%THIOUNsmooth - C:\COLOR\Data\ALE\pennstate\13x6%THIOUN.spc

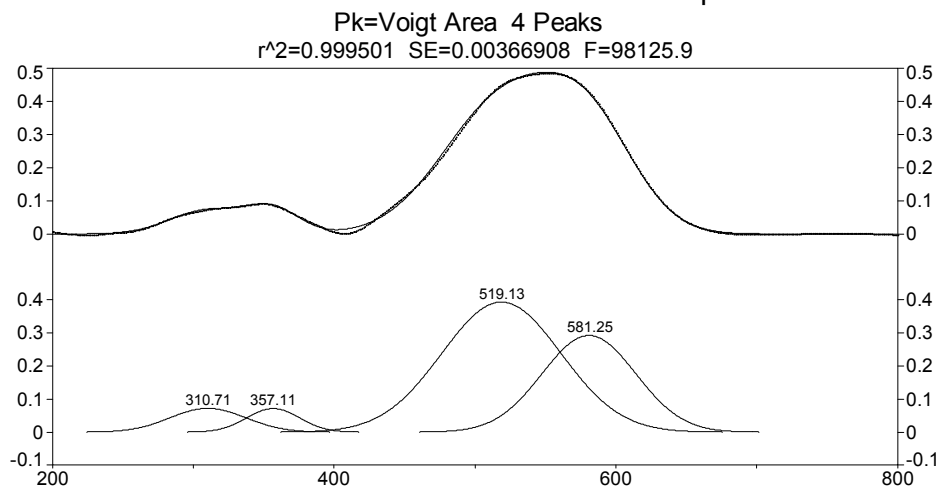


Figure B. 36 Peak fit of 13X / 0.5 mol % thioindigo unheated.

Table B. 36 Peak fit statistics of 13X / 0.5 mol % thioindigo unheated.

Description: 13x6%THIOUN - 13x6%THIOUNsmooth - C:\COLOR\Data\ALE\pennstate\13x6%THIOUN.spc

X Variable: Wavelength nm.

File Source: c:\documents and settings\ale\desktop\thesis final\peak fit\13x\13x6%thiounpeakfit.txt

Measured Values

Peak	Type	Amplitude	Center	FWHM	Asym50	FW Base	Asym10
1	Voigt Area	0.07199158	310.707324	63.3951795	1.00000000	126.898652	1.00000000
2	Voigt Area	0.07149622	357.107111	44.2948220	1.00000000	88.6653096	1.00000000
3	Voigt Area	0.39365779	519.129554	99.5756009	1.00000002	199.321300	1.00000001
4	Voigt Area	0.29255734	581.254332	78.2158429	1.00000012	156.565296	1.00000007

Peak	Type	Anlytc Area	% Area	Int Area	% Area	Centroid	Moment2
1	Voigt Area	4.85814149	6.53742723	4.85804631	6.53730751	310.709610	724.511674
2	Voigt Area	3.37107360	4.53633316	3.37107360	4.53633897	357.107111	353.826595
3	Voigt Area	41.7257350	56.1488290	41.7257350	56.1489009	519.129555	1788.09432
4	Voigt Area	24.3577929	32.7774106	24.3577929	32.7774526	581.254334	1103.25019
	Total	74.3127430	100.000000	74.3126478	100.000000		

13x6%thio1409hfresh - 13x6%thio1409hfreshsmooth - C:\COLOR\Data\ALE\pennstate\05

Pk=Voigt Area 6 Peaks

r²=0.999116 SE=0.00857157 F=36552.3

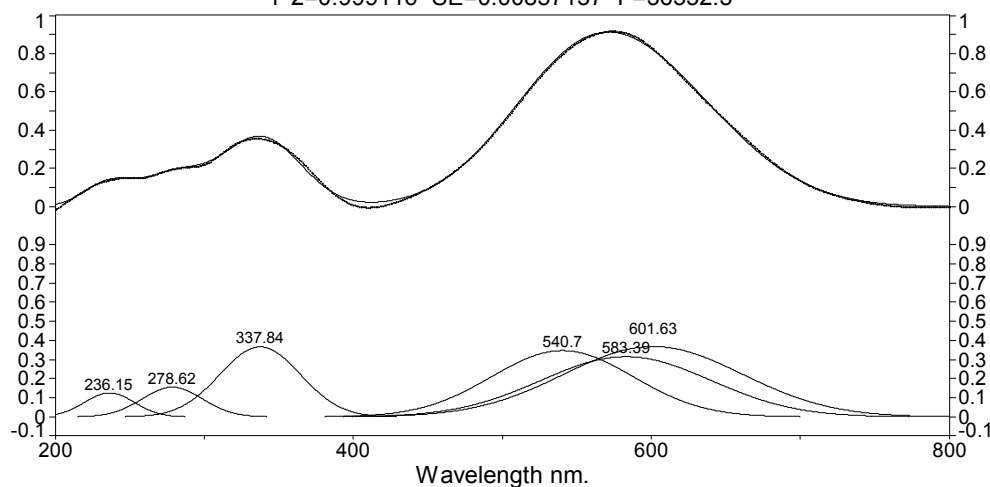


Figure B. 37 Peak fit of 13X / 0.5 mol % thioindigo heated at 413K for nine hours.

Table B. 37 Peak fit statistics of 13X / 0.5 mol % thioindigo heated at 413K for nine hours.

Description: 13x6%thio1409hfresh - 13x6%thio1409hfreshsmooth - C:\COLOR\Data\ALE\pennstate\05

X Variable: Wavelength nm.

File Source: c:\documents and settings\ale\desktop\thesis final\peak fit\13x\13x6%thiohfreshpeakfit.txt

Measured Values

Peak	Type	Amplitude	Center	FWHM	Asym50	FW Base	Asym10
1	Voigt Area	0.12540388	236.149146	39.3521147	0.99999994	78.7714518	0.99999997
2	Voigt Area	0.15568243	278.616450	48.1220652	1.00000000	96.3263338	1.00000000
3	Voigt Area	0.36621949	337.838045	63.5455646	1.00000000	127.199680	1.00000000
4	Voigt Area	0.34664791	540.700794	111.882261	1.00000000	223.955642	1.00000000
5	Voigt Area	0.31467172	583.386385	134.329743	1.00000004	268.888951	1.00000002
6	Voigt Area	0.36785691	601.633174	141.043321	0.99999997	282.327577	0.99999998
Peak	Type	Anlytc Area	% Area	Int Area	% Area	Centroid	Moment2
1	Voigt Area	5.25304673	2.92637417	5.17286095	2.88346389	236.801549	255.258212
2	Voigt Area	7.97473159	4.44257395	7.97425489	4.44502110	278.621434	417.220222
3	Voigt Area	24.7718768	13.7999496	24.7718727	13.8083744	337.838069	728.204111
4	Voigt Area	41.2840246	22.9985586	41.2840236	23.0126022	540.700787	2257.39052
5	Voigt Area	44.9947774	25.0657497	44.9914861	25.0792215	583.369557	3250.43953
6	Voigt Area	55.2285512	30.7667939	55.2029605	30.7713169	601.533926	3567.78369
	Total	179.507008	100.000000	179.397459	100.000000		

zeolite13x - zeolite13x - C:\COLOR\Data\ALE\pennstate\NEW RUNS WITH BaSo4\zeolit

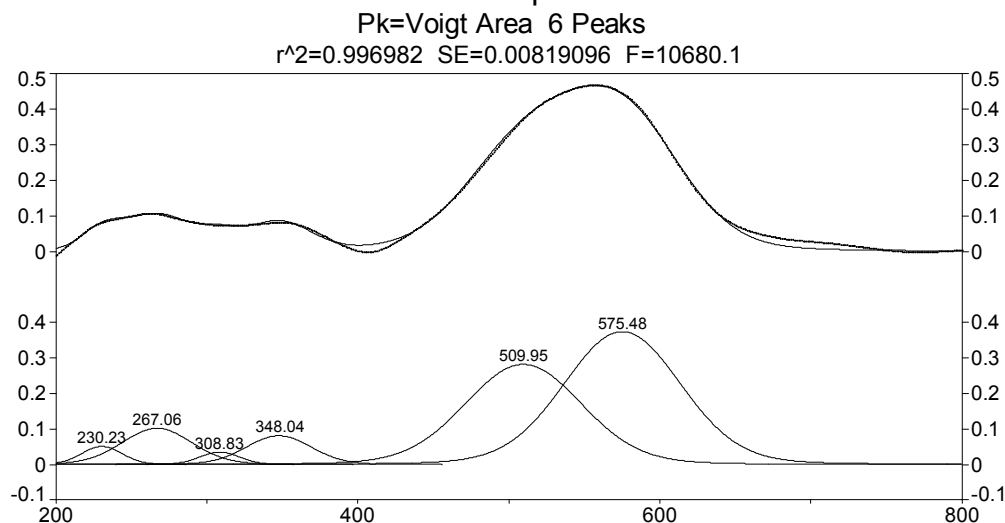


Figure B. 38 Peak fit of 13X / 0.5 mol % thioindigo heated at 413K for nine hours / hydrated.

Table B. 38 Peak fit statistics of 13X / 0.5 mol % thioindigo heated at 413K for nine hours / hydrated.

Description: zeolite13x - zeolite13x - C:\COLOR\Data\ALE\pennstate\NEW RUNS WITH BaSo4\zeolit

X Variable: Wavelength (nm)

Y Variable: Absorbance

File Source: c:\documents and settings\ale\desktop\thesis final\peak fit\13x\zeolite13xnofreshpeakfit.txt

Measured Values

Peak	Type	Amplitude	Center	FWHM	Asym50	FW Base	Asym10
1	Voigt Area	0.05126669	230.233174	31.5573743	0.99999985	65.3177655	0.99999992
2	Voigt Area	0.10232289	267.061497	55.2722908	1.00000000	114.403134	1.00000000
3	Voigt Area	0.03523924	308.825383	31.2207187	1.00000000	64.6209524	1.00000000
4	Voigt Area	0.08126491	348.037213	50.8400586	1.00000000	105.229256	1.00000000
5	Voigt Area	0.28216332	509.953540	90.8984254	1.00000000	188.142460	1.00000000
6	Voigt Area	0.37425867	575.484927	91.2212790	1.00000000	188.810706	1.00000000

Peak	Type	Anlytc Area	% Area	Int Area	% Area	Centroid	Moment2
1	Voigt Area	1.80494827	2.23787335	1.74576601	2.19239344	232.492073	492.374217
2	Voigt Area	6.30970281	7.82311385	6.17910288	7.75993150	269.536428	1062.74072
3	Voigt Area	1.22743387	1.52183949	1.21942788	1.53139979	309.708187	495.242808
4	Voigt Area	4.60932919	5.71489784	4.57005582	5.73923446	349.115415	958.419957
5	Voigt Area	28.6144606	35.4777696	28.2900810	35.5276640	509.835936	2264.94891
6	Voigt Area	38.0887461	47.2245058	37.6238836	47.2493768	574.563892	2274.90632
	Total	80.6546208	100.000000	79.6283172	100.000000		

Zeolites LZY62

LZY-62-6%THIOUN - LZY-62-6%THIOUNsmooth - C:\COLOR\Data\ALE\pennstate\LZY-62-6%T

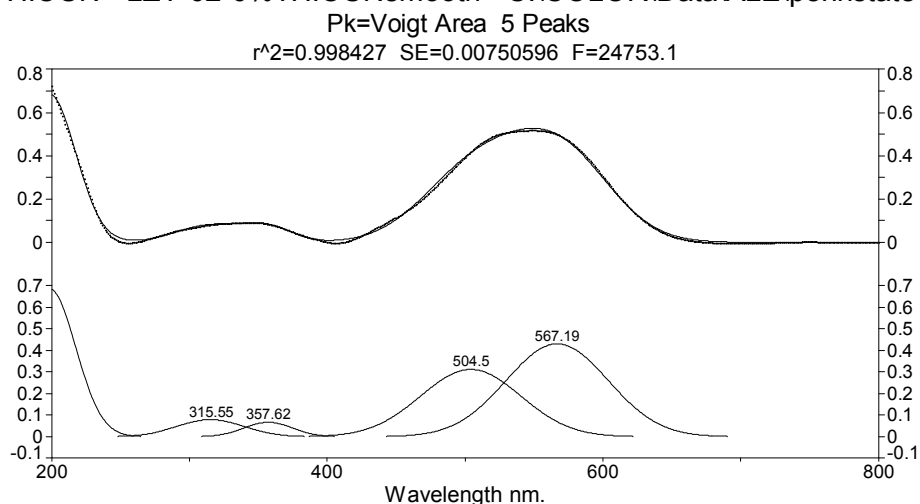


Figure B. 39 Peak fit of LZY62 / 0.5 mol % thioindigo unheated.

Table B. 39 Peak fit statistics of LZY62 / 0.5 mol % thioindigo unheated.

Description: LZY-62-6%THIOUN - LZY-62-6%THIOUNsmooth - C:\COLOR\Data\ALE\pennstate\LZY-62-6%T

X Variable: Wavelength nm.

File Source: c:\documents and settings\ale\desktop\thesis final\peak fit\lzy-62\lzy-62-6%thiounpeakfit.txt

Measured Values

Peak	Type	Amplitude	Center	FWHM	Asym50	FW Base	Asym10
1	Voigt Area	0.68191935	200.000003	44.8591391	0.85560129	89.5634166	0.91793853
2	Voigt Area	0.07942000	315.551167	57.2471737	1.00000000	114.592139	1.00000000
3	Voigt Area	0.06715937	357.615739	41.4249757	1.00000000	82.9207146	1.00000000
4	Voigt Area	0.31160323	504.503716	85.3790327	1.00000000	170.903912	1.00000000
5	Voigt Area	0.42976426	567.187251	87.2260048	1.00000000	174.601011	1.00000000

Peak	Type	Anlytc Area	% Area	Int Area	% Area	Centroid	Moment2
1	Voigt Area	32.6010228	30.0124819	15.1069222	16.5771904	214.536501	124.019857
2	Voigt Area	4.83967430	4.45540124	4.83966946	5.31068611	315.551288	590.993116
3	Voigt Area	2.96142726	2.72628814	2.96142726	3.24964561	357.615739	309.463245
4	Voigt Area	28.3194873	26.0709029	28.3194873	31.0756569	504.503716	1314.57998
5	Voigt Area	39.9032697	36.7349259	39.9032697	43.7868210	567.187251	1372.07076
	Total	108.624881	100.000000	91.1307758	100.000000		

LZY-62-6%THIO1409hfresh - LZY-62-6%THIO1409hfreshsmooth - C:\COLOR\Data\ALE\penn

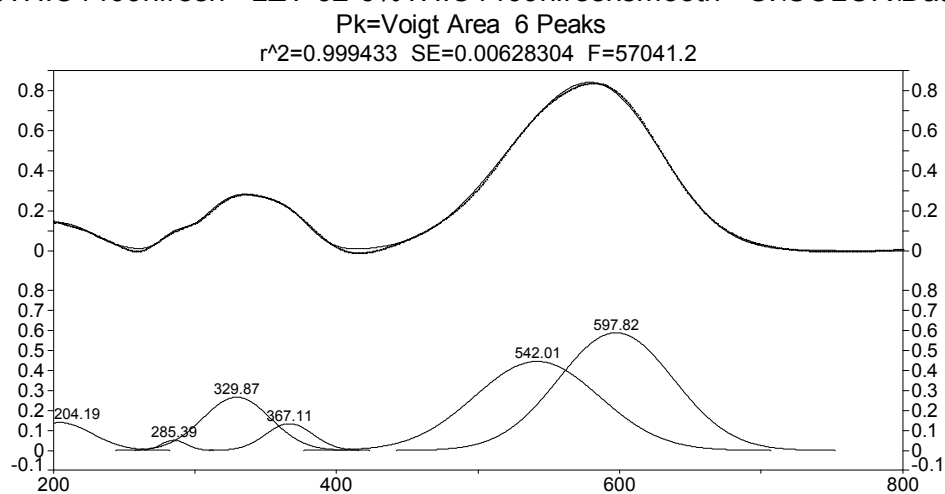


Figure B. 40 Peak fit of LZY62 / 0.5 mol % thioindigo heated at 413K for nine hours.

Table B. 40 Peak fit statistics of LZY62 / 0.5 mol % thioindigo heated at 413K for nine hours.

Description: LZY-62-6%THIO1409hfresh - LZY-62-6%THIO1409hfreshsmooth - C:\COLOR\Data\ALE\penn

X Variable: .spc

Y Variable: Wavelength nm.

File Source: c:\documents and settings\ale\desktop\thesis final\peak fit\lzy-62\lzy-62-6%thio1409hfreshpeakfit.txt

Measured Values

Peak	Type	Amplitude	Center	FWHM	Asym50	FW Base	Asym10
1	Voigt Area	0.13960887	204.187351	53.9235657	1.00000000	107.939245	1.00000000
2	Voigt Area	0.05087037	285.386031	21.2401603	0.99999979	42.5166037	0.99999989
3	Voigt Area	0.26676912	329.869377	56.2290889	1.00000007	112.554230	1.00000004
4	Voigt Area	0.13426558	367.113376	38.9663769	1.00000000	77.9993173	1.00000000
5	Voigt Area	0.44552208	542.005651	103.957805	1.00000000	208.093193	1.00000000
6	Voigt Area	0.58919967	597.821192	95.7835890	1.00000000	191.730798	1.00000000

Peak	Type	Anlytc Area	% Area	Int Area	% Area	Centroid	Moment2
1	Voigt Area	8.01352904	5.72087540	4.58811423	3.35757141	219.878676	212.451959
2	Voigt Area	1.15015100	0.82109524	1.15015100	0.84167785	285.386030	81.3579755
3	Voigt Area	15.9672020	11.3990194	15.9672016	11.6847613	329.869382	570.172529
4	Voigt Area	5.56912468	3.97580994	5.56912468	4.07547259	367.113376	273.819647
5	Voigt Area	49.3013193	35.1963166	49.3013192	36.0785916	542.005651	1948.94109
6	Voigt Area	60.0738981	42.8868834	60.0738780	43.9619253	597.821122	1654.48581
	Total	140.075224	100.000000	136.649789	100.000000		

ZeoliteLZY-62 - ZeoliteLZY-62 - C:\COLOR\Data\ALE\pennstate\NEW RUNS WITH BaSo4\

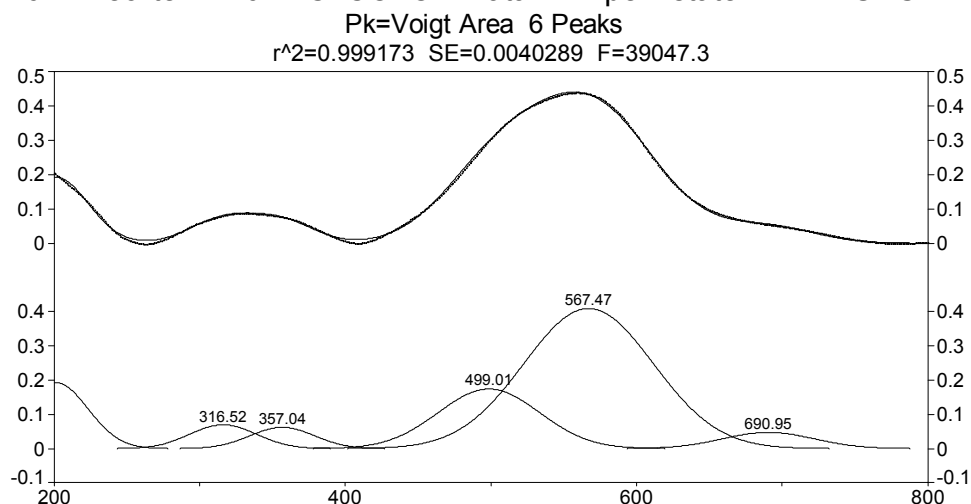


Figure B. 41 Peak fit of LZY62 / 0.5 mol % thioindigo heated at 413K for nine hours / hydrated.

Table B. 41 Peak fit statistics of LZY62 / 0.5 mol % thioindigo heated at 413K for nine hours / hydrated.

Description: ZeoliteLZY-62 - ZeoliteLZY-62 - C:\COLOR\Data\ALE\pennstate\NEW RUNS WITH BaSo4\

X Variable: Wavelength (nm)

Y Variable: Absorbance

File Source: c:\documents and settings\ale\desktop\thesis final\peak fit\lzy-62\zeolitelzy-62nofreshpeakfit.txt

Measured Values

Peak	Type	Amplitude	Center	FWHM	Asym50	FW Base	Asym10
1	Voigt Area	0.19291279	201.000665	51.8461176	1.00000000	103.780800	1.00000000
2	Voigt Area	0.06969555	316.515449	53.8996005	1.00000000	107.891274	1.00000000
3	Voigt Area	0.06222878	357.042902	52.1694486	1.00000000	104.428014	1.00000000
4	Voigt Area	0.17429479	499.013157	81.7135798	1.00000006	163.566745	1.00000003
5	Voigt Area	0.40925127	567.470327	104.815190	1.00000000	209.809428	1.00000000
6	Voigt Area	0.04749470	690.946525	74.0684609	1.00000000	148.263448	1.00000000
Peak	Type	Anlytc Area	% Area	Int Area	% Area	Centroid	Moment2
1	Voigt Area	10.6465639	12.8788258	5.51625666	7.11445525	217.935659	181.008866
2	Voigt Area	3.99873684	4.83715084	3.99873613	5.15727077	316.515470	523.906228
3	Voigt Area	3.45572974	4.18029159	3.45572974	4.45694175	357.042902	490.814116
4	Voigt Area	15.1604063	18.3390843	15.1604063	19.5527582	499.013158	1204.12903
5	Voigt Area	45.6611113	55.2348632	45.6611073	58.8902810	567.470306	1981.21648
6	Voigt Area	3.74464544	4.52978417	3.74366033	4.82829309	690.915732	985.993798
Total		82.6671935	100.000000	77.5358965	100.000000		

Zeolites Zeolon®

Zeolon-thio 6% UN - smooth - C:\COLOR\Data\ALE\pennstate\Zeolon-thio 6% UN.spc

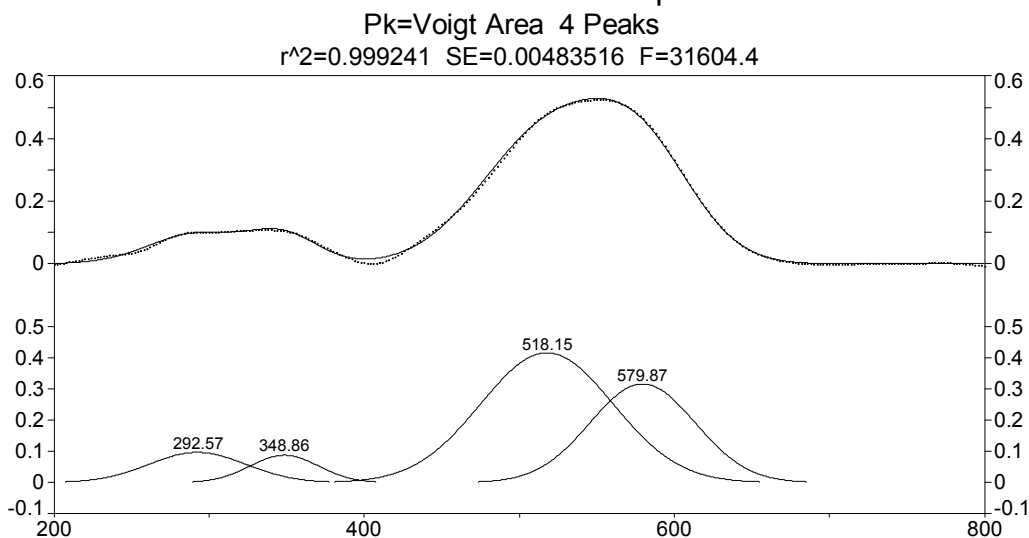


Figure B. 42 Peak fit of Zeolon® / 0.5 mol % thioindigo unheated.

Table B. 42 Peak fit statistics of Zeolon® / 0.5 mol % thioindigo unheated.

Description: Zeolon-thio 6% UN - smooth - C:\COLOR\Data\ALE\pennstate\Zeolon-thio 6% UN.spc

X Variable: Wavelength nm.

File Source: c:\documents and settings\ale\desktop\thesis final\peak fit\zeolon\ zeolon-thio 6% unpeakfit.txt

Measured Values

Peak	Type	Amplitude	Center	FWHM	Asym50	FW Base	Asym10
1	Voigt Area	0.09672127	292.568863	74.1929854	0.99999994	148.512709	0.99999997
2	Voigt Area	0.08757476	348.861874	52.0912432	1.00000002	104.271470	1.00000001
3	Voigt Area	0.41511489	518.153477	100.632037	1.00000005	201.435976	1.00000003
4	Voigt Area	0.31565849	579.866555	79.9032076	1.00000007	159.942908	1.00000004
Peak	Type	Anlytc Area	% Area	Int Area	% Area	Centroid	Moment2
1	Voigt Area	7.63865749	9.11429457	7.62604304	9.10061302	292.736968	977.092601
2	Voigt Area	4.85596882	5.79404565	4.85596882	5.79491786	348.861874	489.343694
3	Voigt Area	44.4668924	53.0570139	44.4668924	53.0650009	518.153478	1826.23674
4	Voigt Area	26.8481215	32.0346459	26.8481215	32.0394683	579.866557	1151.36488
	Total	83.8096402	100.000000	83.7970258	100.000000		

Storage 045540 PM - zeolon smooth - C:\COLOR\Data\ALE\pennstate\NEW RUNS WITH Ba
Pk=Voigt Area 6 Peaks

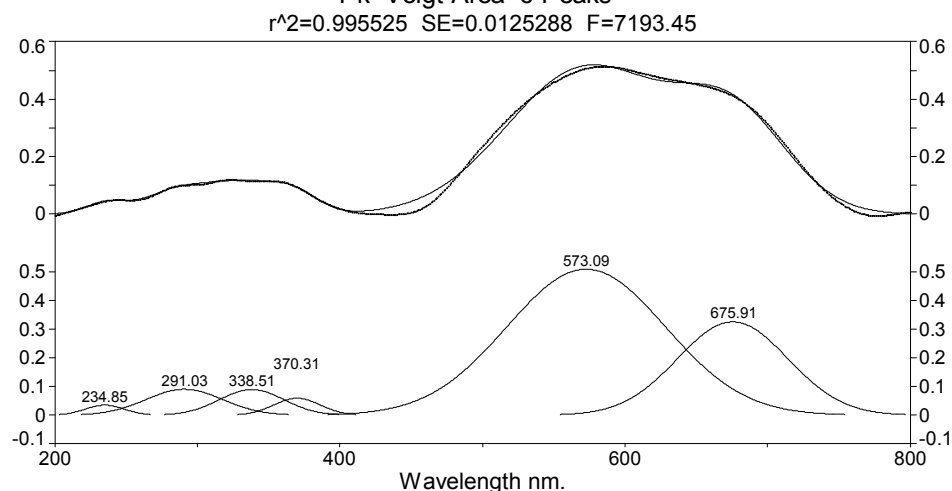


Figure B. 43 Peak fit of Zeolon® / 0.5 mol % thioindigo heated at 413K for nine hours.

Table B. 43 Peak fit statistics of Zeolon® / 0.5 mol % thioindigo heated at 413K for nine hours.

Description: Storage 045540 PM - zeolon smooth - C:\COLOR\Data\ALE\pennstate\NEW RUNS WITH Ba

X Variable: Wavelength nm.

File Source: c:\documents and settings\ale\Desktop\thesis final\peak fit\zeolon\zeolonpeakfit.txt

Measured Values

Peak	Type	Amplitude	Center	FWHM	Asym50	FW Base	Asym10
1	Voigt Area	0.03536145	234.854111	32.3386923	1.00000006	64.7326264	1.00000003
2	Voigt Area	0.09054805	291.034251	63.8521616	1.00000008	127.813397	1.00000004
3	Voigt Area	0.08946758	338.510603	53.4401565	1.00000000	106.971601	1.00000000
4	Voigt Area	0.05905424	370.312004	38.4519276	1.00000000	76.9695398	1.00000000
5	Voigt Area	0.50819670	573.085689	130.826340	1.00000000	261.876161	1.00000000
6	Voigt Area	0.32516975	675.907497	91.0842968	1.00000000	182.324186	1.00000000

Peak	Type	Anlytc Area	% Area	Int Area	% Area	Centroid	Moment2
1	Voigt Area	1.21726389	1.03882424	1.21047811	1.03331387	235.074088	180.879223
2	Voigt Area	6.15441700	5.25223628	6.15199478	5.25159560	291.072869	731.734357
3	Voigt Area	5.08938885	4.34333142	5.08938884	4.34451149	338.510603	515.015127
4	Voigt Area	2.41713767	2.06280760	2.41713767	2.06336806	370.312004	266.637227
5	Voigt Area	70.7716372	60.3971685	70.7700732	60.4122432	573.080402	3085.36181
6	Voigt Area	31.5272334	26.9056320	31.5061772	26.8949678	675.817608	1484.97513
	Total	117.177078	100.000000	117.145250	100.000000		

zeolonH-6%thio 140C 9hrs - RawData - C:\COLOR\Data\ALE\pennstate\09.11.08UV\zeol

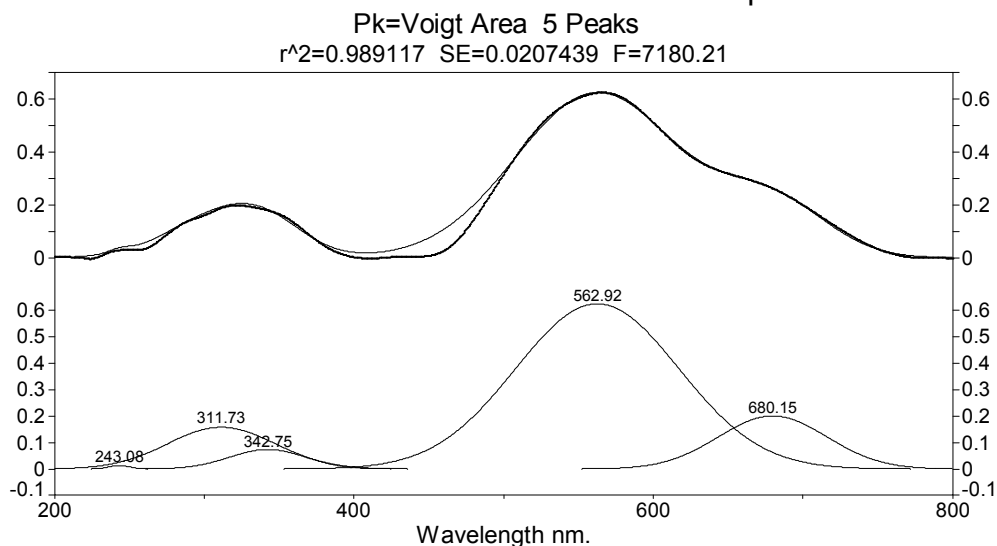


Figure B. 44 Peak fit of Zeolon® / 0.5 mol % thioindigo heated at 413K for nine hours / hydrated.

Table B. 44 Peak fit statistics of Zeolon® / 0.5 mol % thioindigo heated at 413K for nine hours / hydrated.

Description: zeolonH-6%thio 140C 9hrs - RawData - C:\COLOR\Data\ALE\pennstate\09.11.08UV\zeol

X Variable: Wavelength nm.

File Source: c:\documents and settings\ale\desktop\thesis final\peak fit\zeolon\zeolonh-6%thio 140c 9hrsnofreshpeakfit.txt

Measured Values

Peak	Type	Amplitude	Center	FWHM	Asym50	FW Base	Asym10
1	Voigt Area	0.01312961	243.083781	16.5890890	1.00000000	33.2065160	1.00000000
2	Voigt Area	0.15831218	311.730603	84.7422190	1.00000001	169.629197	1.00000000
3	Voigt Area	0.07392560	342.754550	59.7795515	1.00000001	119.661220	1.00000000
4	Voigt Area	0.62545880	562.922013	128.766787	0.99999998	257.753537	0.99999999
5	Voigt Area	0.20078092	680.149856	85.2844537	1.00000000	170.714593	1.00000000

Peak	Type	Anlytc Area	% Area	Int Area	% Area	Centroid	Moment2
1	Voigt Area	0.23184968	0.18822885	0.23184968	0.18826362	243.083781	49.6283253
2	Voigt Area	14.2805973	11.5938069	14.2670005	11.5849076	311.846547	1282.07515
3	Voigt Area	4.70413451	3.81908585	4.70413447	3.81979121	342.754552	644.450737
4	Voigt Area	85.7303857	69.6008378	85.7297625	69.6131871	562.920205	2989.71668
5	Voigt Area	18.2273917	14.7980406	18.2188654	14.7938505	680.089315	1304.40958
Total		123.174359	100.000000	123.151613	100.000000		

Zeolite CBV21A

CBV21A - CBV21 SMOOTH - C:\COLOR\Data\ALE\pennstate\06.04.08\CBV21A6%THIOUN.spc

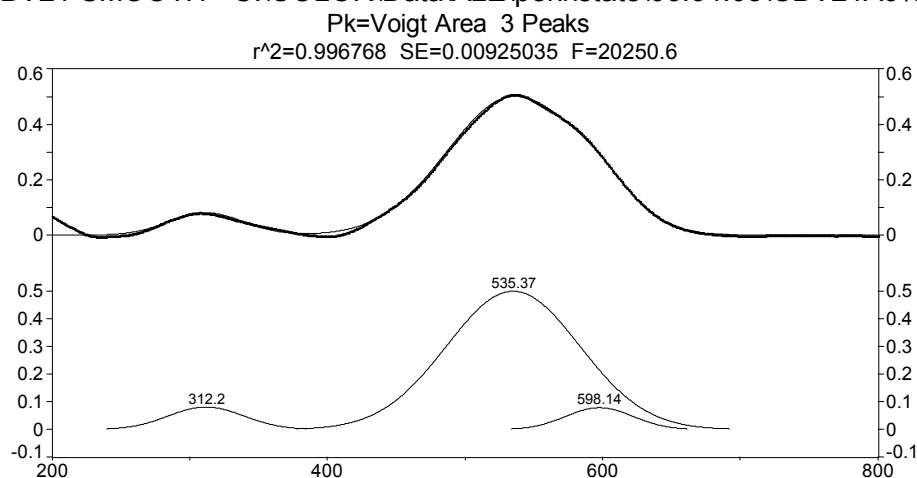


Figure B. 45 Peak fit of CBV21A / NH₄ / 0.5 mol % thioindigo unheated.

Table B. 45 Peak fit statistics of CBV21A / NH₄ / 0.5 mol % thioindigo unheated.

Description: CBV21A - CBV21 SMOOTH - C:\COLOR\Data\ALE\pennstate\06.04.08\CBV21A6%THIOUN.spc

X Variable: Wavelength nm.

File Source: c:\documents and settings\ale\desktop\thesis final\peak fit\21anh4\cbv21a6%thiounpeakfit.txt

Measured Values

Peak	Type	Amplitude	Center	FWHM	Asym50	FW Base	Asym10
1	Voigt Area	0.08097301	312.198664	64.8553589	1.00000000	129.821506	1.00000000
2	Voigt Area	0.49868760	535.374931	113.574930	1.00000001	227.343872	1.00000001
3	Voigt Area	0.07881087	598.136264	57.0986827	1.00000000	114.294903	1.00000000

Peak	Type	Anlytc Area	% Area	Int Area	% Area	Centroid	Moment2
1	Voigt Area	5.59008461	7.91013495	5.58995533	7.90996662	312.201400	758.229136
2	Voigt Area	60.2897188	85.3117341	60.2897176	85.3118899	535.374926	2326.21168
3	Voigt Area	4.79009852	6.77813099	4.79009852	6.77814351	598.136264	587.945038
Total		70.6699020	100.000000	70.6697715	100.000000		

CBV21A6%thioH1409h - smooth - C:\COLOR\Data\ALE\pennstate\06.05.08\CBV21A6%thioH

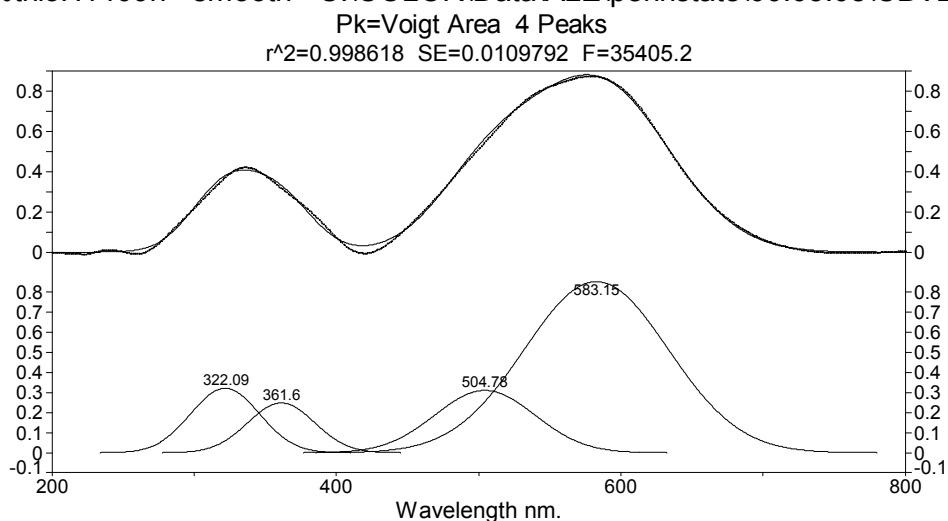


Figure B. 46 Peak fit of CBV21A / NH₄ / 0.5 mol % thioindigo heated at 413K for nine hours.

Table B. 46 Peak fit statistics of CBV21A / NH₄ / 0.5 mol % thioindigo heated at 413K for nine hours.

Description: CBV21A6%thioH1409h - smooth - C:\COLOR\Data\ALE\pennstate\06.05.08\CBV21A6%thioH

X Variable: Wavelength nm.

File Source: c:\documents and settings\ale\Desktop\thesis final\peak fit\21anh4\cbv21a6%thioh1409hpeakfit.txt

Measured Values

Peak	Type	Amplitude	Center	FWHM	Asym50	FW Base	Asym10
1	Voigt Area	0.32143501	322.090411	56.8371236	1.00000000	113.771338	1.00000000
2	Voigt Area	0.24867313	361.597560	55.0801947	1.00000000	110.254479	1.00000000
3	Voigt Area	0.31106716	504.781640	82.5756274	1.00000000	165.292313	1.00000000
4	Voigt Area	0.85269416	583.147826	118.832051	1.00000000	237.867094	1.00000000
Peak	Type	Anlytc Area	% Area	Int Area	% Area	Centroid	Moment2
1	Voigt Area	19.4472176	11.4916335	19.4472135	11.4916947	322.090438	582.567562
2	Voigt Area	14.5799669	8.61550686	14.5799669	8.61555456	361.597560	547.111049
3	Voigt Area	27.3425020	16.1570677	27.3425020	16.1571572	504.781640	1229.66926
4	Voigt Area	107.859671	63.7357919	107.858739	63.7355936	583.145858	2546.12049
	Total	169.229358	100.000000	169.228421	100.000000		

CBV21ANH4-6%thio1409hno-fresh - smooth - C:\COLOR\Data\ALE\pennstate\06.21.08UV\

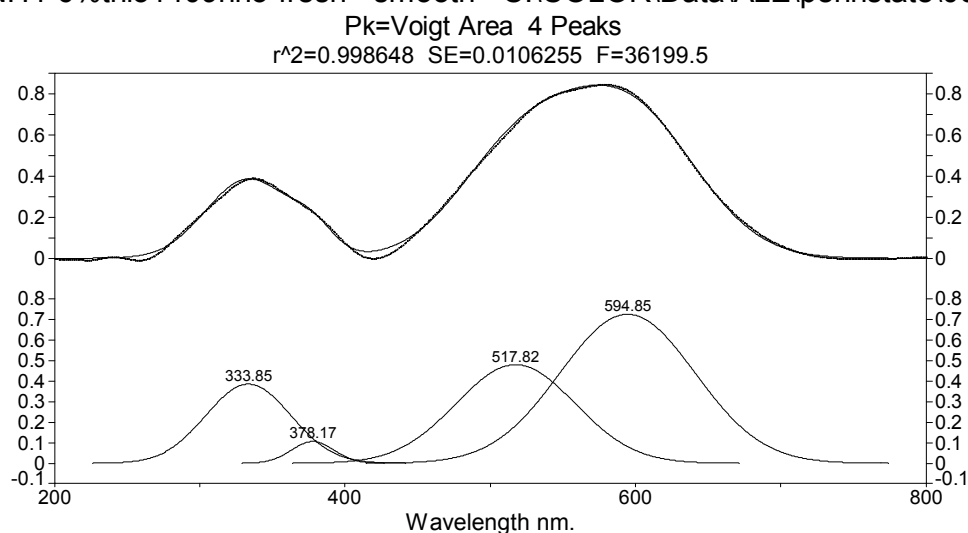


Figure B. 47 Peak fit of CBV21A / NH₄ / 0.5 mol % thioindigo heated at 413K for nine hours / hydrated.

Table B. 47 Peak fit statistics of CBV21A / NH₄ / 0.5 mol % thioindigo heated at 413K for nine hours / hydrated.

Description: CBV21ANH4-6%thio1409hno-fresh - smooth - C:\COLOR\Data\ALE\pennstate\06.21.08UV\

X Variable: Wavelength nm.

File Source: c:\documents and settings\ale\desktop\thesis final\peak fit\21anh4\cbv21anh4-6%thio1409hno-freshpeakfit.txt

Measured Values

Peak	Type	Amplitude	Center	FWHM	Asym50	FW Base	Asym10
1	Voigt Area	0.38613846	333.851645	68.6654942	1.00000001	137.448285	1.00000000
2	Voigt Area	0.10598914	378.172386	34.4157413	0.99999999	68.8902724	0.99999999
3	Voigt Area	0.48073856	517.819016	96.3441754	0.99999995	192.852928	0.99999997
4	Voigt Area	0.72642478	594.854486	109.515800	1.00000000	219.218677	1.00000000

Peak	Type	Anlytc Area	% Area	Int Area	% Area	Centroid	Moment2
1	Voigt Area	28.2236919	16.9927609	28.2236294	16.9927743	333.851955	850.238009
2	Voigt Area	3.88285097	2.33776497	3.88285097	2.33777198	378.172386	213.598800
3	Voigt Area	49.3022376	29.6836126	49.3022376	29.6837016	517.819015	1673.92301
4	Voigt Area	84.6836633	50.9858615	84.6832278	50.9857521	594.853381	2162.68165
	Total	166.092444	100.000000	166.091946	100.000000		

21A-Al6%thio UN - RawData - C:\COLOR\Data\ALE\pennstate\10.20.08UV\21A-Al6%thio

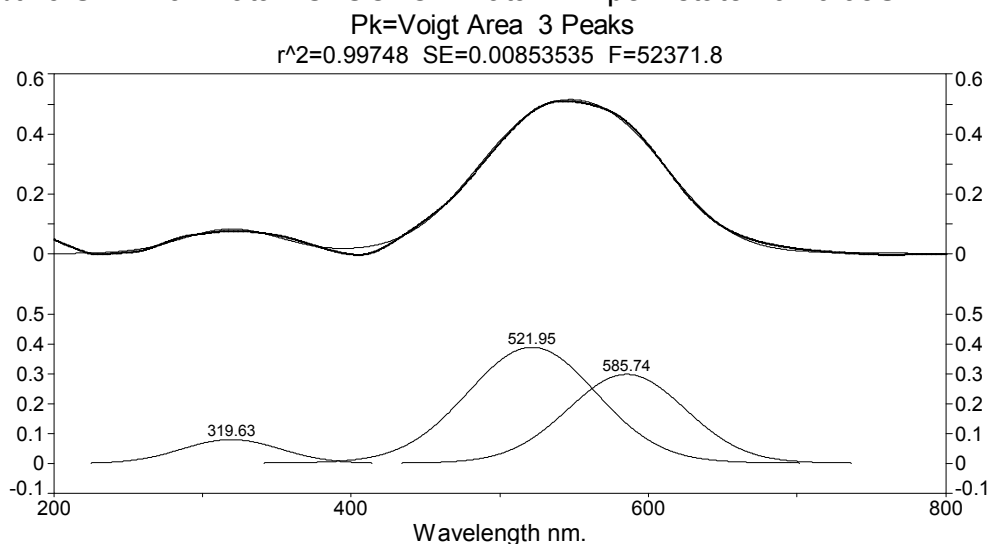


Figure B. 48 Peak fit of CBV21A / Al / 0.5 mol % thioindigo unheated.

Table B. 48 Peak fit statistics of CBV21A / Al / 0.5 mol % thioindigo unheated.

Description: 21A-Al6%thio UN - RawData - C:\COLOR\Data\ALE\pennstate\10.20.08UV\21A-Al6%thio

X Variable: Wavelength nm.

File Source: c:\documents and settings\ale\desktop\thesis final\peak fit\21a-al\21a-al6%thio unpeakfit.txt

Measured Values

Peak	Type	Amplitude	Center	FWHM	Asym50	FW Base	Asym10
1	Voigt Area	0.08085046	319.633786	79.1929063	1.00000002	162.633116	1.00000001
2	Voigt Area	0.38911112	521.952278	102.487627	1.00000000	210.471908	1.00000000
3	Voigt Area	0.29858905	585.741327	93.8635136	1.00000000	192.761150	1.00000000
Peak	Type	Anlytc Area	% Area	Int Area	% Area	Centroid	Moment2
1	Voigt Area	7.07133239	8.61649121	6.97968522	8.59379009	321.407045	1670.34921
2	Voigt Area	44.0430642	53.6669265	43.5973421	53.6795563	521.719222	2551.32572
3	Voigt Area	30.9530276	37.7165823	30.6407491	37.7266536	584.887006	2208.31347
	Total	82.0674241	100.000000	81.2177764	100.000000		

21A-AI6%thio H - RawData - C:\COLOR\Data\ALE\pennstate\10.20.08UV\21A-AI6%thio H

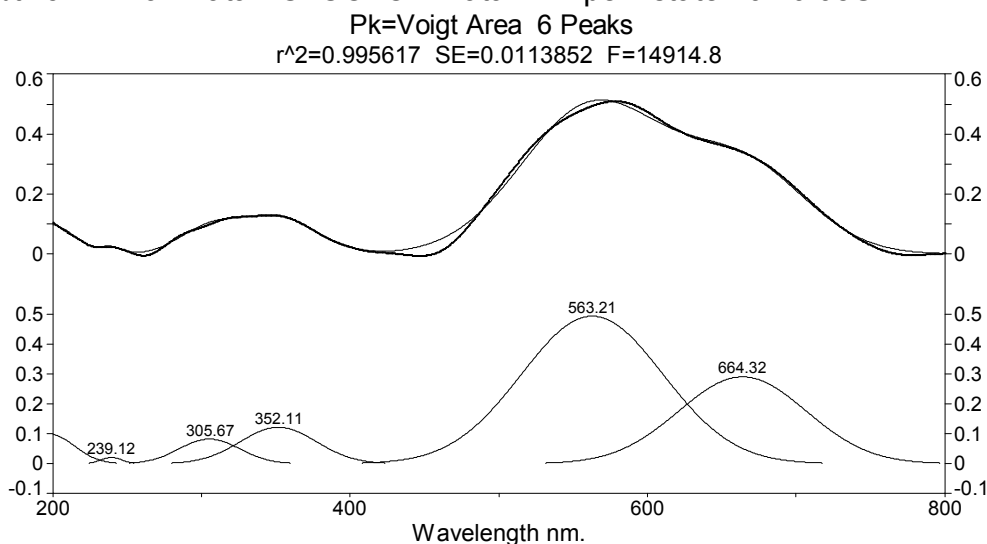


Figure B. 49 Peak fit of CBV21A / AI / 0.5 mol % thioindigo heated at 413K for nine hours.

Table B. 49 Peak fit statistics of CBV21A / AI / 0.5 mol % thioindigo heated at 413K for nine hours.

Description: 21A-AI6%thio H - RawData - C:\COLOR\Data\ALE\pennstate\10.20.08UV\21A-AI6%thio H

X Variable: Wavelength nm.

File Source: c:\documents and settings\ale\desktop\thesis final\peak fit\21a-ai\21a-ai6%thio hpeakfit.txt

Measured Values

Peak	Type	Amplitude	Center	FWHM	Asym50	FW Base	Asym10
1	Voigt Area	0.09731791	200.000004	38.8344076	0.81735952	77.4010035	0.89513293
2	Voigt Area	0.02133084	239.121603	16.9067855	0.99999993	33.8424517	0.99999996
3	Voigt Area	0.08268036	305.674984	48.0893456	1.00000007	96.2608388	1.00000004
4	Voigt Area	0.12187120	352.109497	60.3242489	1.00000000	120.751545	1.00000000
5	Voigt Area	0.49291851	563.214041	112.096412	1.00000000	224.384309	1.00000000
6	Voigt Area	0.29029392	664.320691	100.974371	1.00000000	202.121228	1.00000000

Peak	Type	Anlytc Area	% Area	Int Area	% Area	Centroid	Moment2
1	Voigt Area	4.03096250	3.78524860	1.82467903	1.75011054	212.407337	91.0678016
2	Voigt Area	0.38388500	0.36048466	0.38388499	0.36819690	239.121604	51.5473449
3	Voigt Area	4.23236833	3.97437741	4.23236784	4.05940520	305.674997	417.043074
4	Voigt Area	7.82573665	7.34870610	7.82573664	7.50592510	352.109497	656.248579
5	Voigt Area	58.8164828	55.2312281	58.8164636	56.4128325	563.213961	2266.02303
6	Voigt Area	31.2019191	29.2999552	31.1776558	29.9035298	664.206028	1823.11238
	Total	106.491354	100.000000	104.260788	100.000000		

21A-A1weekoutsidedesiccator - RawData - C:\COLOR\Data\ALE\pennstate\10.30.08UV\

Pk=Voigt Area 7 Peaks

$r^2=0.998668$ SE=0.00754647 F=42083.6

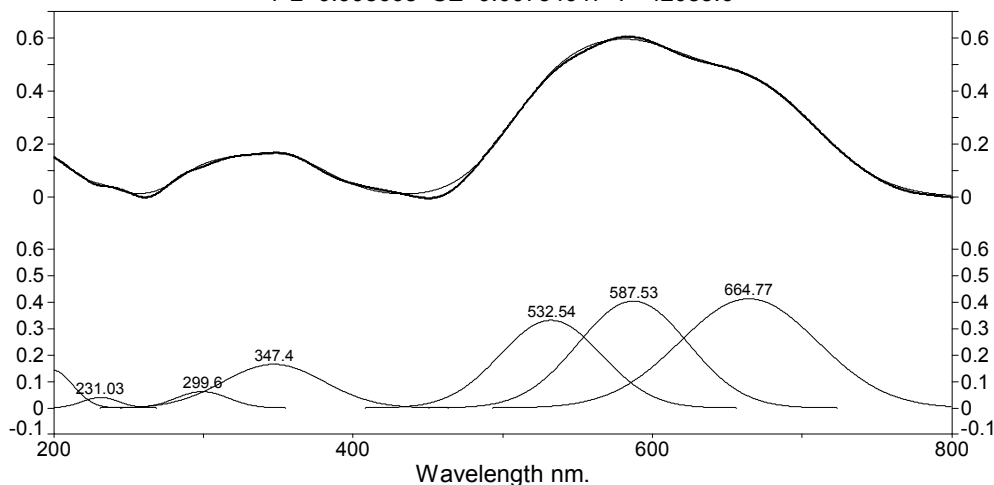


Figure B. 50 Peak fit of CBV21A / Al / 0.5 mol % thioindigo heated at 413K for nine hours / hydrated.

Table B. 50 Peak fit statistics of CBV21A / Al / 0.5 mol % thioindigo heated at 413K for nine hours / hydrated.

Description: 21A-A1weekoutsidedesiccator - RawData - C:\COLOR\Data\ALE\pennstate\10.30.08UV\

X Variable: Wavelength nm.

File Source: c:\documents and settings\ale\desktop\thesis final\peak fit\21a-al\21a-al1weekoutsidedesiccator-bluepeakfit.txt

Measured Values

Peak	Type	Amplitude	Center	FWHM	Asym50	FW Base	Asym10
1	Voigt Area	0.14359680	200.000004	31.9483185	0.87823182	63.8367665	0.93120501
2	Voigt Area	0.03971647	231.030888	29.0240155	1.00000003	58.0976107	1.00000002
3	Voigt Area	0.06200886	299.603389	41.1310576	1.00000003	82.3323763	1.00000001
4	Voigt Area	0.16542419	347.397959	79.0786536	1.00000000	158.292391	1.00000000
5	Voigt Area	0.33216095	532.540761	79.8633059	1.00000000	159.863037	1.00000000
6	Voigt Area	0.40478568	587.534074	86.3442716	1.00000002	172.836039	1.00000001
7	Voigt Area	0.41353506	664.769783	108.509550	1.00000000	217.204459	1.00000000

Peak	Type	Anlytc Area	% Area	Int Area	% Area	Centroid	Moment2
1	Voigt Area	4.88743464	3.59472576	2.29471500	1.72170581	210.434482	63.6107042
2	Voigt Area	1.22704458	0.90249570	1.21979627	0.91520312	231.238804	145.419569
3	Voigt Area	2.71491236	1.99682781	2.71491235	2.03697643	299.603390	305.087363
4	Voigt Area	13.9248491	10.2417766	13.9247699	10.4476404	347.398838	1127.59524
5	Voigt Area	28.2376189	20.7688703	28.2376189	21.1864535	532.540761	1150.21525
6	Voigt Area	37.2041062	27.3637540	37.2041061	27.9139351	587.534073	1344.47138
7	Voigt Area	47.7652998	35.1315498	47.6855624	35.7780856	664.521484	2089.70541
Total		135.961266	100.000000	133.281481	100.000000		

21A-Al1weekoutsidedesiccator-purplechange - RawData - C:\COLOR\Data\ALE\pennstat

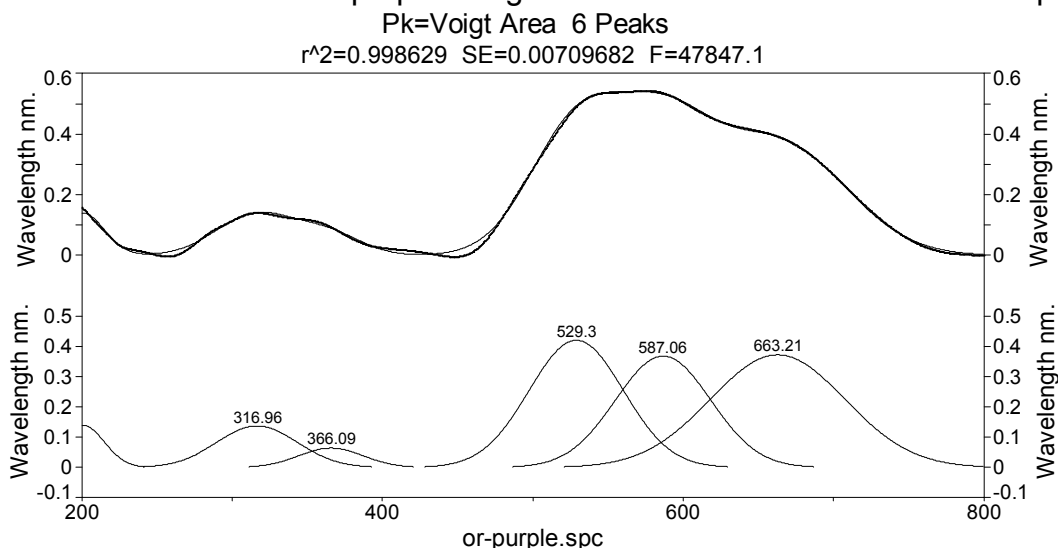


Figure B. 51 Peak fit of CBV21A / Al / 0.5 mol % thioindigo heated at 413K for nine hours / hydrated for 1 week.

Table B. 51 Peak fit statistics of CBV21A / Al / 0.5 mol % thioindigo heated at 413K for nine hours / hydrated for 1 week.

Description: 21A-Al1weekoutsidedesiccator-purplechange - RawData - C:\COLOR\Data\ALE\pennstat

X Variable: or-purple.spc

Y Variable: Wavelength nm.

File Source: c:\documents and settings\ale\desktop\thesis final\peak fit\21a-al\21a-al1weekoutsidedesiccator-purplepeakfit.txt

Measured Values

Peak	Type	Amplitude	Center	FWHM	Asym50	FW Base	Asym10
1	Voigt Area	0.13995387	200.297018	34.0115595	0.99999998	68.0812184	0.99999999
2	Voigt Area	0.13712459	316.962245	63.1975969	1.00000000	126.503150	1.00000000
3	Voigt Area	0.06411486	366.088254	50.3290456	1.00000000	100.744065	1.00000000
4	Voigt Area	0.41966824	529.298291	73.8103646	1.00000000	147.746814	1.00000000
5	Voigt Area	0.36750829	587.055673	74.5450284	1.00000001	149.217397	1.00000000
6	Voigt Area	0.37165222	663.206847	105.308236	1.00000000	210.796362	1.00000000

Peak	Type	Anlytc Area	% Area	Int Area	% Area	Centroid	Moment2
1	Voigt Area	5.06691573	4.16953296	2.57502369	2.16417376	211.632748	76.7455147
2	Voigt Area	9.22461222	7.59087515	9.22455172	7.75275695	316.963049	720.159964
3	Voigt Area	3.43486446	2.82652827	3.43486446	2.88682530	366.088254	456.795632
4	Voigt Area	32.9727872	27.1330984	32.9727872	27.7119163	529.298291	982.469899
5	Voigt Area	29.1620491	23.9972661	29.1620491	24.5091887	587.055673	1002.12506
6	Voigt Area	41.6611522	34.2826991	41.6148708	34.9751390	663.040839	1977.16794
	Total	121.522381	100.000000	118.984147	100.000000		

21ACa-6%thioUNpink(outside desiccator) - RawData - C:\COLOR\Data\ALE\pennstate\1

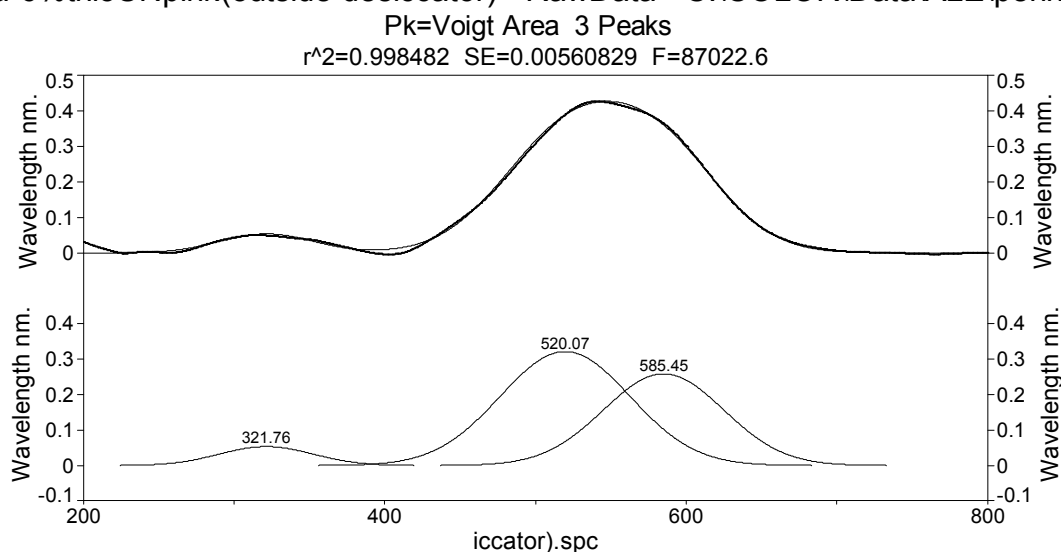


Figure B. 52 Peak fit of CBV21A / Ca / 0.5 mol % thioindigo unheated.

Table B. 52 Peak fit statistics of CBV21A / Ca / 0.5 mol % thioindigo unheated.

Description: 21ACa-6%thioUNpink(outside desiccator) - RawData - C:\COLOR\Data\ALE\pennstate\1

X Variable: iccatort).spc

Y Variable: Wavelength nm.

File Source: c:\documents and settings\ale\desktop\thesis final\peak fit\21aca\21aca-6%thiounpink(outside desiccator)peakfit.txt

Measured Values

Peak	Type	Amplitude	Center	FWHM	Asym50	FW Base	Asym10
1	Voigt Area	0.05360005	321.757198	72.9526656	1.00000000	146.260487	1.00000000
2	Voigt Area	0.32175512	520.065472	101.558278	0.99999999	203.610972	1.00000000
3	Voigt Area	0.25881710	585.449635	93.9526666	1.00000001	188.362724	1.00000000
Peak	Type	Anlytc Area	% Area	Int Area	% Area	Centroid	Moment2
1	Voigt Area	4.17259958	6.42040677	4.16920716	6.41955590	321.866564	993.442089
2	Voigt Area	34.8691330	53.6533673	34.8458031	53.6539856	520.051460	1904.07599
3	Voigt Area	25.9479126	39.9262260	25.9304038	39.9264585	585.392969	1633.59037
	Total	64.9896452	100.000000	64.9454140	100.000000		

21A-Ca H fresh - RawData - C:\COLOR\Data\ALE\pennstate\10.20.08UV\21A-Ca H fresh

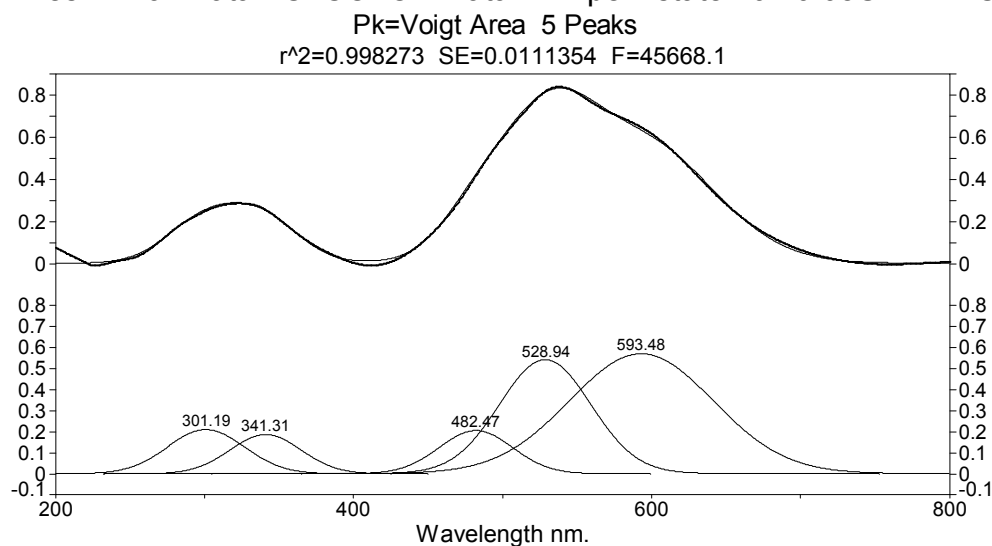


Figure B. 53 Peak fit of CBV21A / Ca / 0.5 mol % thioindigo heated at 413K for nine hours.

Table B. 53 Peak fit statistics of CBV21A / Ca / 0.5 mol % thioindigo heated at 413K for nine hours.

Description: 21A-Ca H fresh - RawData - C:\COLOR\Data\ALE\pennstate\10.20.08UV\21A-Ca H fresh

X Variable: Wavelength nm.

File Source: c:\documents and settings\ale\desktop\thesis final\peak fit\21aca\21a-ca h freshpeakfit.txt

Measured Values

Peak	Type	Amplitude	Center	FWHM	Asym50	FW Base	Asym10
1	Voigt Area	0.21077794	301.186267	61.4687607	1.00000000	124.378727	1.00000000
2	Voigt Area	0.18736514	341.306179	56.4199354	1.00000000	114.162701	1.00000000
3	Voigt Area	0.20624323	482.474604	58.3261411	1.00000000	118.019806	1.00000000
4	Voigt Area	0.54330286	528.944931	72.5787837	1.00000000	146.859260	1.00000000
5	Voigt Area	0.57138126	593.477038	114.193993	1.00000000	231.065396	1.00000000
Peak	Type	Anlytc Area	% Area	Int Area	% Area	Centroid	Moment2
1	Voigt Area	14.0183260	9.23880885	13.9478339	9.23345096	301.865076	879.491403
2	Voigt Area	11.4376792	7.53802783	11.3986356	7.54588448	341.746463	761.117631
3	Voigt Area	13.0154589	8.57786704	12.9828156	8.59460990	482.519162	806.995725
4	Voigt Area	42.6646533	28.1182344	42.5301532	28.1549156	528.852023	1180.42977
5	Voigt Area	70.5969279	46.5270619	70.1982097	46.4711391	592.950577	2658.48145
Total		151.733045	100.000000	151.057648	100.000000		

21A-Ca1weekoutsidedesiccator - RawData - C:\COLOR\Data\ALE\pennstate\10.30.08UV\

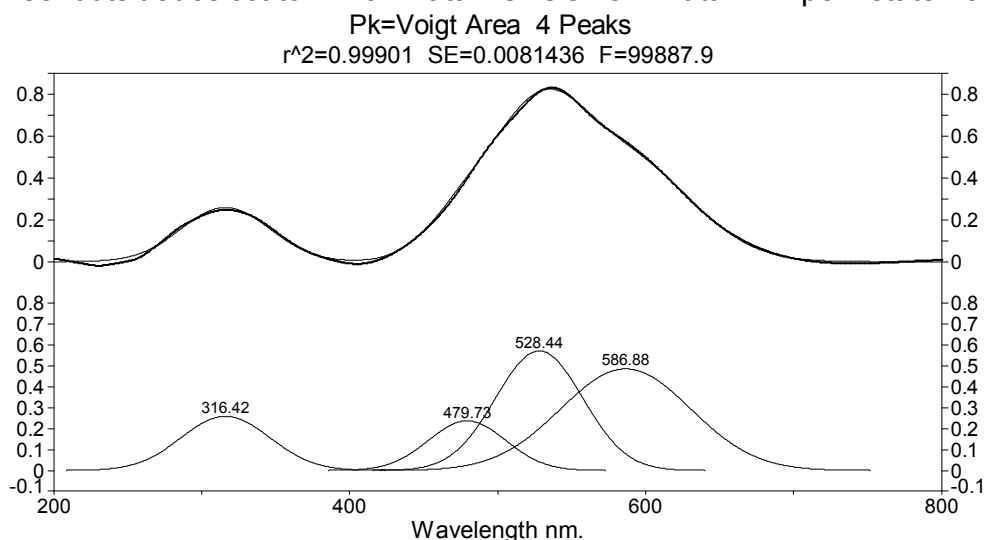


Figure B. 54 Peak fit of CBV21A / Ca / 0.5 mol % thioindigo heated at 413K for nine hours / hydrated.

Table B. 54 Peak fit statistics of CBV21A / Ca / 0.5 mol % thioindigo heated at 413K for nine hours / hydrated.

Description: 21A-Ca1weekoutsidedesiccator - RawData - C:\COLOR\Data\ALE\pennstate\10.30.08UV\

X Variable: Wavelength nm.

File Source: c:\documents and settings\ale\desktop\thesis final\peak fit\21aca\21a-ca1weekoutsidedesiccatorpeakfit.txt

Measured Values

Peak	Type	Amplitude	Center	FWHM	Asym50	FW Base	Asym10
1	Voigt Area	0.25933297	316.416057	70.6514272	1.00000000	141.423543	1.00000000
2	Voigt Area	0.23742477	479.729827	61.5739445	0.99999999	123.253071	0.99999999
3	Voigt Area	0.57243254	528.437667	69.3306287	1.00000000	138.779690	1.00000000
4	Voigt Area	0.48671625	586.880374	103.408641	1.00000001	206.993927	1.00000001

Peak	Type	Anlytc Area	% Area	Int Area	% Area	Centroid	Moment2
1	Voigt Area	19.5034250	14.9010768	19.5024070	14.9004186	316.422496	899.424309
2	Voigt Area	15.5616347	11.8894560	15.5616347	11.8895514	479.729827	683.720347
3	Voigt Area	42.2456173	32.2766482	42.2456173	32.2769073	528.437667	866.831789
4	Voigt Area	53.5753340	40.9328190	53.5753014	40.9331227	586.880240	1928.37615
Total		130.886011	100.000000	130.884960	100.000000		

21AKCI-6%thioUN - RawData - C:\COLOR\Data\ALE\pennstate\10.09.08\21AKCI-6%thioUN

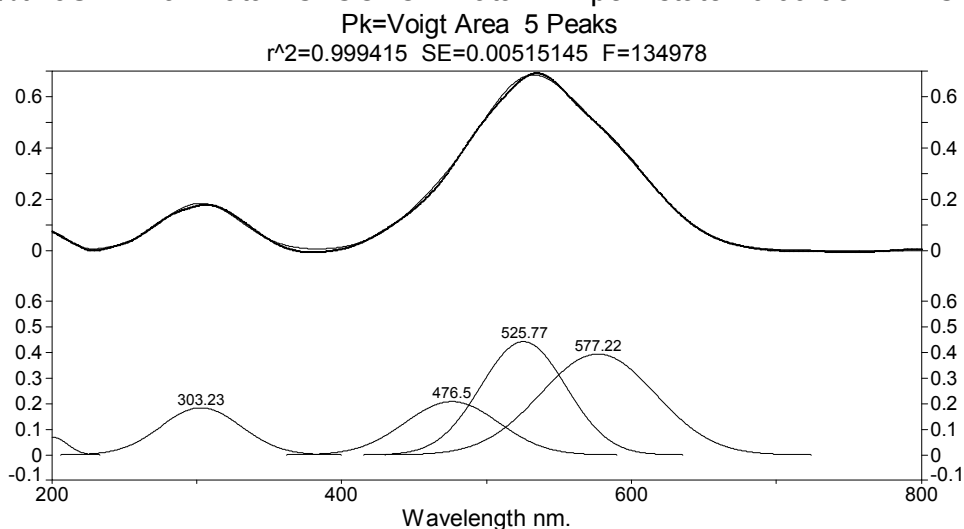


Figure B. 55 Peak fit of CBV21A / K / 0.5 mol % thioindigo unheated.

Table B. 55 Peak fit statistics of CBV21A / K / 0.5 mol % thioindigo unheated.

Description: 21AKCI-6%thioUN - RawData - C:\COLOR\Data\ALE\pennstate\10.09.08\21AKCI-6%thioUN

X Variable: Wavelength nm.

File Source: c:\documents and settings\ale\desktop\thesis final\peak fit\21ak\21akci-6%thiounpink(outside desiccator)peakfit.txt

Measured Values

Peak	Type	Amplitude	Center	FWHM	Asym50	FW Base	Asym10
1	Voigt Area	0.06893987	200.549250	23.6554272	0.99999998	47.3512632	0.99999999
2	Voigt Area	0.18445491	303.226670	65.2895443	1.00000000	130.690618	1.00000000
3	Voigt Area	0.20854540	476.500770	75.9224951	0.99999999	151.974683	1.00000000
4	Voigt Area	0.44293195	525.774743	69.1872323	1.00000000	138.492652	1.00000000
5	Voigt Area	0.39459887	577.218032	93.2923942	1.00000000	186.744153	1.00000000

Peak	Type	Anlytc Area	% Area	Int Area	% Area	Centroid	Moment2
1	Voigt Area	1.73593508	1.68183963	0.90581388	0.88471293	208.218069	37.8898917
2	Voigt Area	12.8193519	12.4198735	12.8180906	12.5194929	303.237481	767.610421
3	Voigt Area	16.8540123	16.3288053	16.8540123	16.4613978	476.500770	1039.50240
4	Voigt Area	32.6208430	31.6043079	32.6208430	31.8609399	525.774743	863.249763
5	Voigt Area	39.1863024	37.9651736	39.1863021	38.2734565	577.218030	1569.55629
Total		103.216445	100.000000	102.385062	100.000000		

21A-K H fresh - RawData - C:\COLOR\Data\ALE\pennstate\10.20.08UV\21A-K H fresh.s

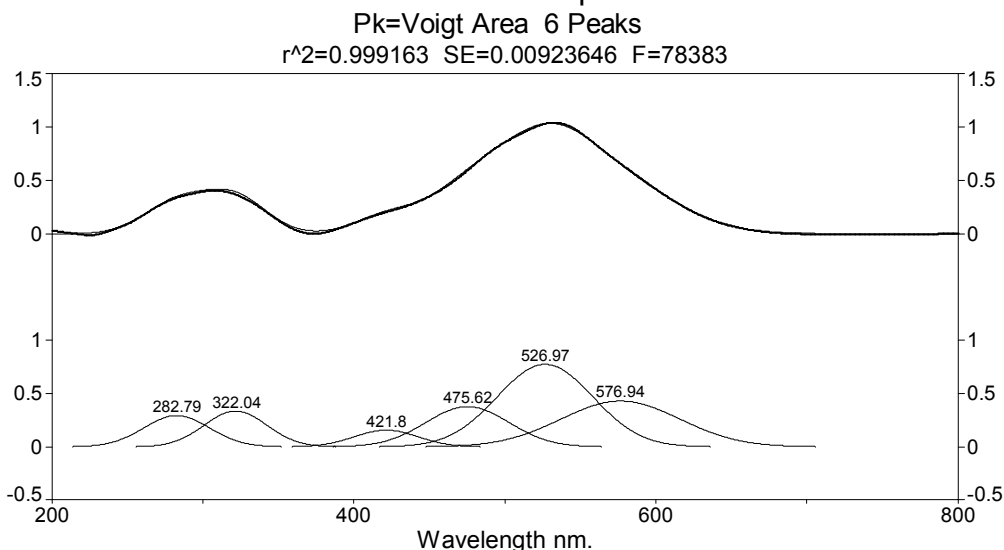


Figure B. 56 Peak fit of CBV21A / K / 0.5 mol % thioindigo heated at 413K for nine hours.

Table B. 56 Peak fit statistics of CBV21A / K / 0.5 mol % thioindigo heated at 413K for nine hours.

Description: 21A-K H fresh - RawData - C:\COLOR\Data\ALE\pennstate\10.20.08UV\21A-K H fresh.s

X Variable: Wavelength nm.

File Source: c:\documents and settings\ale\desktop\thesis final\peak fit\21ak\21a-k h freshpeakfit.txt

Measured Values

Peak	Type	Amplitude	Center	FWHM	Asym50	FW Base	Asym10
1	Voigt Area	0.29449484	282.787838	51.6434355	1.00000000	103.375090	1.00000000
2	Voigt Area	0.33555884	322.039125	48.8134251	1.00000000	97.7102345	1.00000000
3	Voigt Area	0.15682380	421.804506	49.5553323	0.99999996	99.1953163	0.99999998
4	Voigt Area	0.37744642	475.618825	64.7935500	1.00000000	129.697782	1.00000000
5	Voigt Area	0.77397219	526.965187	74.6831973	1.00000001	149.493970	1.00000000
6	Voigt Area	0.42979010	576.938187	92.8204835	1.00000001	185.799526	1.00000000

Peak	Type	Anlytc Area	% Area	Int Area	% Area	Centroid	Moment2
1	Voigt Area	16.1891864	9.41646224	16.1878909	9.41577966	282.794879	480.383518
2	Voigt Area	17.4357317	10.1415170	17.4357317	10.1415934	322.039125	429.697755
3	Voigt Area	8.27245800	4.81168641	8.27245800	4.81172268	421.804506	442.858859
4	Voigt Area	26.0327052	15.1419583	26.0327052	15.1420724	475.618825	757.091033
5	Voigt Area	61.5290867	35.7884767	61.5290867	35.7887464	526.965188	1005.84337
6	Voigt Area	42.4651283	24.6998994	42.4651279	24.7000854	576.938186	1553.71764
Total		171.924296	100.000000	171.923000	100.000000		

21AK-6%thioHbrightpink(outside desiccator) - RawData - C:\COLOR\Data\ALE\pennsta

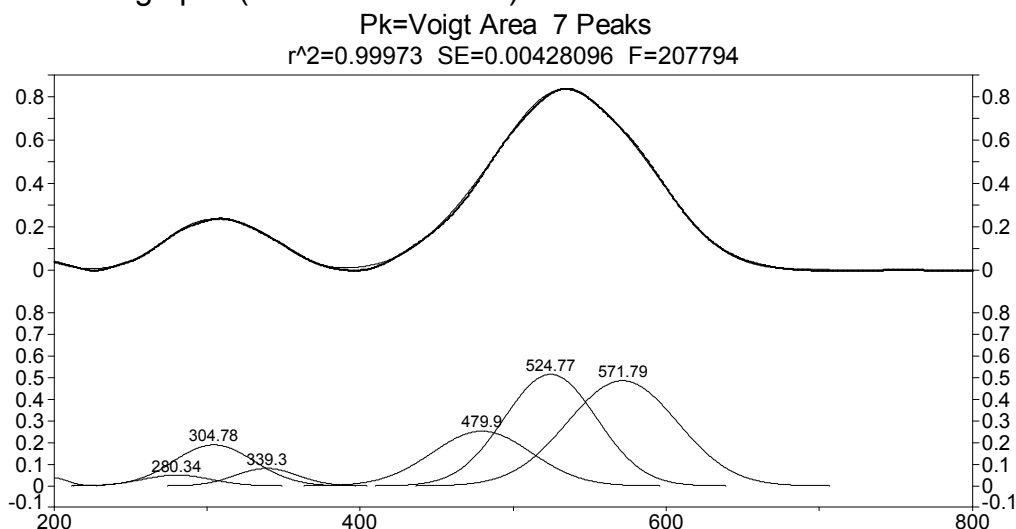


Figure B. 57 Peak fit of CBV21A / K / 0.5 mol % thioindigo heated at 413K for nine hours / hydrated.

Table B. 57 Peak fit statistics of CBV21A / K / 0.5 mol % thioindigo heated at 413K for nine hours / hydrated.

Description: 21AK-6%thioHbrightpink(outside desiccator) - RawData - C:\COLOR\Data\ALE\pennsta

X Variable: side desiccator).spc

Y Variable: Wavelength nm.

File Source: c:\documents and settings\ale\desktop\thesis final\peak fit\21ak\21ak-6%thiohbrightpink(outside desiccator)peakfit.txt

Measured Values

Peak	Type	Amplitude	Center	FWHM	Asym50	FW Base	Asym10
1	Voigt Area	0.03686810	200.000003	22.3066382	0.87732623	44.5702034	0.93067728
2	Voigt Area	0.05007527	280.337641	52.4347510	1.00000010	104.959073	1.00000005
3	Voigt Area	0.18956165	304.778922	61.9196710	1.00000001	123.945115	1.00000001
4	Voigt Area	0.08088137	339.296497	47.4469331	0.99999990	94.9749164	0.99999995
5	Voigt Area	0.25306379	479.904894	76.4708753	1.00000000	153.072380	1.00000000
6	Voigt Area	0.51624698	524.770112	71.1904121	1.00000001	142.502434	1.00000000
7	Voigt Area	0.48667727	571.790594	84.5498051	1.00000004	169.244041	1.00000002

Peak	Type	Anlytc Area	% Area	Int Area	% Area	Centroid	Moment2
1	Voigt Area	0.87615056	0.70787325	0.41115213	0.33343944	207.283220	30.9965893
2	Voigt Area	2.79495413	2.25814302	2.79452279	2.26632447	280.350886	494.754648
3	Voigt Area	12.4942828	10.0945762	12.4938608	10.1323713	304.782662	691.027964
4	Voigt Area	4.08496995	3.30039276	4.08496995	3.31286165	339.296496	405.976452
5	Voigt Area	20.5995763	16.6431316	20.5995763	16.7060094	479.904894	1054.57306
6	Voigt Area	39.1211163	31.6073436	39.1211163	31.7267562	524.770112	913.960793
7	Voigt Area	43.8011870	35.3885395	43.8011870	35.5222375	571.790594	1289.16876
	Total	123.772237	100.000000	123.306385	100.000000		

21ANa-6%thioUN - RawData - C:\COLOR\Data\ALE\pennstate\09.11.08UV\21ANa-6%thioUN

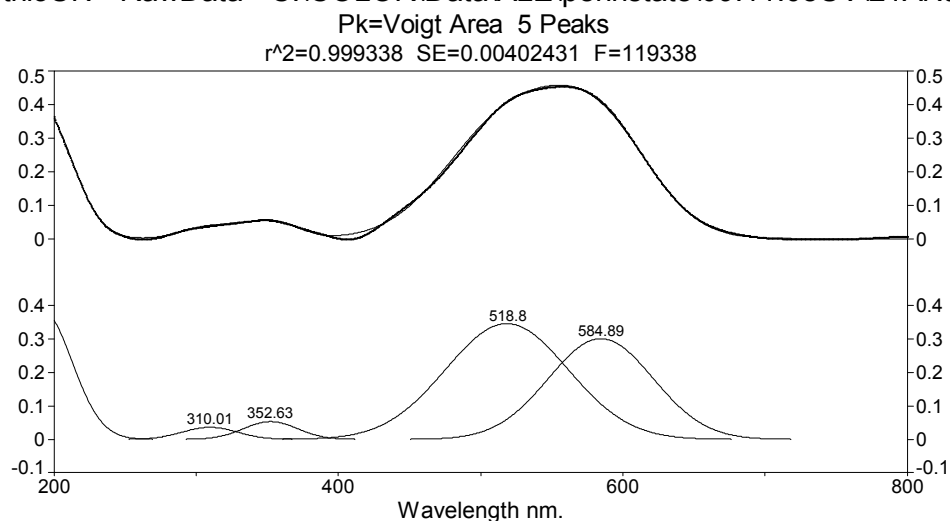


Figure B. 58 Peak fit of CBV21A / Na / 0.5 mol % thioindigo unheated.

Table B. 58 Peak fit statistics of CBV21A / Na / 0.5 mol % thioindigo unheated.

Description: 21ANa-6%thioUN - RawData - C:\COLOR\Data\ALE\pennstate\09.11.08UV\21ANa-6%thioUN

X Variable: Wavelength nm.

File Source: c:\documents and settings\ale\desktop\thesis final\peak fit\21ana\21ana-6%thiounpeakfit.txt

Measured Values

Peak	Type	Amplitude	Center	FWHM	Asym50	FW Base	Asym10
1	Voigt Area	0.37570620	196.360485	50.1341332	0.67486625	98.7464254	0.80515157
2	Voigt Area	0.03626078	310.009682	45.2342598	1.00000002	90.5457901	1.00000001
3	Voigt Area	0.05325863	352.634467	44.5695102	1.00000000	89.2151552	1.00000000
4	Voigt Area	0.34601111	518.796347	101.226627	1.00000000	202.626171	1.00000000
5	Voigt Area	0.30109807	584.888456	86.6732951	1.00000002	173.494648	1.00000001
Peak	Type	Anlytc Area	% Area	Int Area	% Area	Centroid	Moment2
1	Voigt Area	20.2097638	22.5692505	9.57651061	12.1356350	209.535214	139.598227
2	Voigt Area	1.74597006	1.94981178	1.74597005	2.21254442	310.009683	368.994127
3	Voigt Area	2.52673731	2.82173349	2.52673731	3.20195559	352.634467	358.228615
4	Voigt Area	37.2835295	41.6363756	37.2835295	47.2467816	518.796347	1847.88134
5	Voigt Area	27.7795685	31.0228287	27.7795684	35.2030835	584.888455	1354.73743
Total		89.5455692	100.000000	78.9123160	100.000000		

21A-Na H fresh - RawData - C:\COLOR\Data\ALE\pennstate\10.20.08UV\File 081020 03

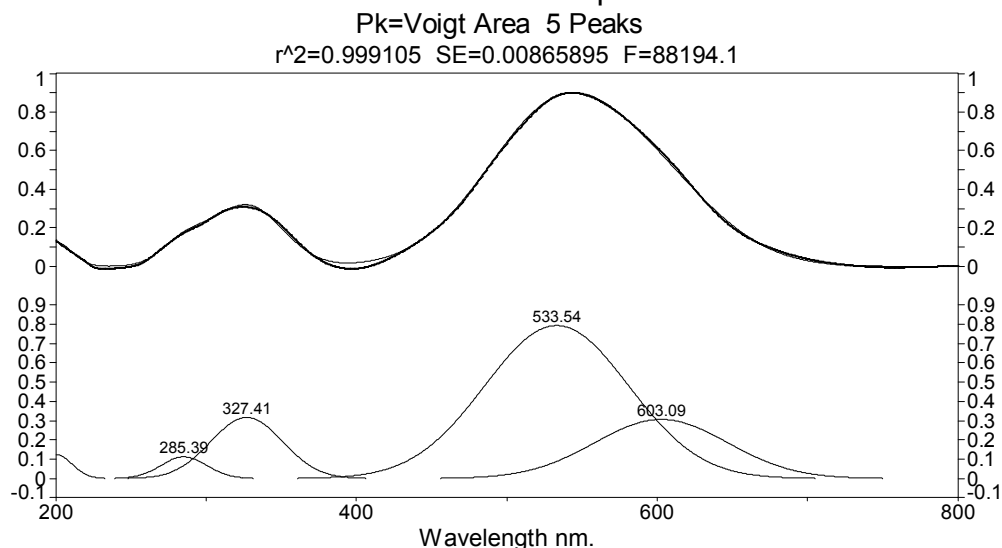


Figure B. 59 Peak fit of CBV21A / Na / 0.5 mol % thioindigo heated at 413K for nine hours.

Table B. 59 Peak fit statistics of CBV21A / Na / 0.5 mol % thioindigo heated at 413K for nine hours.

Description: 21A-Na H fresh - RawData - C:\COLOR\Data\ALE\pennstate\10.20.08UV\File 081020 03

X Variable: Wavelength nm.

File Source: c:\documents and settings\ale\desktop\thesis final\peak fit\21ana\21a-na h freshpeakfit.txt

Measured Values

Peak	Type	Amplitude	Center	FWHM	Asym50	FW Base	Asym10
1	Voigt Area	0.12446024	200.000000	24.9656100	0.99699645	49.9738188	0.99835095
2	Voigt Area	0.11249870	285.391888	36.3138196	1.00000000	72.6896716	1.00000000
3	Voigt Area	0.31681132	327.411854	56.1285683	1.00000000	112.353017	1.00000000
4	Voigt Area	0.79328775	533.542249	112.751127	1.00000000	225.694858	1.00000000
5	Voigt Area	0.30621764	603.092505	104.209853	1.00000000	208.597720	1.00000000

Peak	Type	Anlytc Area	% Area	Int Area	% Area	Centroid	Moment2
1	Voigt Area	3.30754092	2.12344362	1.65143377	1.07161633	208.452279	40.8007156
2	Voigt Area	4.34862202	2.79181842	4.34862196	2.82182331	285.391889	237.808956
3	Voigt Area	18.9285290	12.1521290	18.9285281	12.2827329	327.411860	568.135469
4	Voigt Area	95.2102811	61.1250679	95.2102799	61.7820058	533.542246	2292.58872
5	Voigt Area	33.9680950	21.8075411	33.9679488	22.0418217	603.091619	1958.22863
	Total	155.763068	100.000000	154.106813	100.000000		

21A-Na1weekoutsidedessicant - RawData - C:\COLOR\Data\ALE\pennstate\10.30.08UV\2

Pk=Voigt Area 5 Peaks

$r^2=0.999336$ SE=0.00687897 F=118982

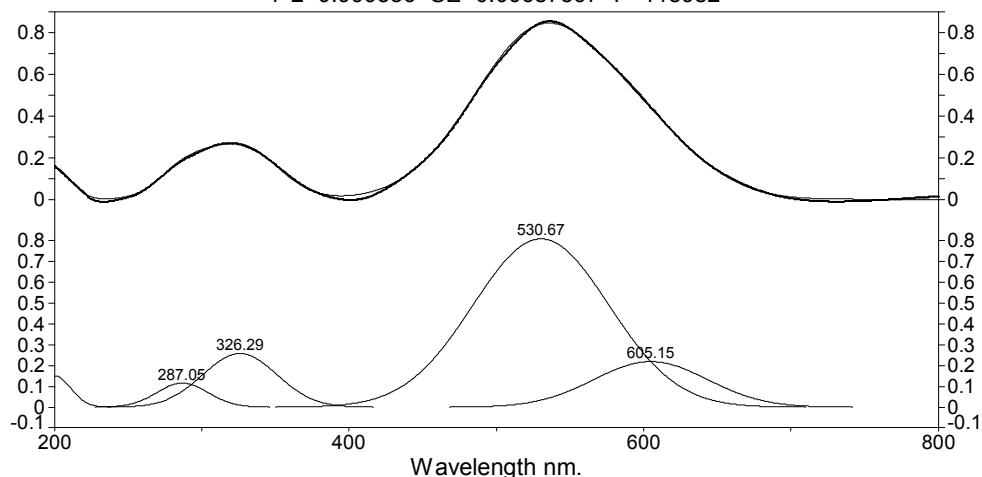


Figure B. 60 Peak fit of CBV21A / Na / 0.5 mol % thioindigo heated at 413K for nine hours / hydrated.

Table B. 60 Peak fit statistics of CBV21A / Na / 0.5 mol % thioindigo heated at 413K for nine hours / hydrated.

Description: 21A-Na1weekoutsidedessicant - RawData - C:\COLOR\Data\ALE\pennstate\10.30.08UV\2

X Variable: Wavelength nm.

File Source: c:\documents and settings\ale\desktop\thesis final\peak fit\21ana\21a-na1weekoutsidedesiccatorpeakfit.txt

Measured Values

Peak	Type	Amplitude	Center	FWHM	Asym50	FW Base	Asym10
1	Voigt Area	0.15081575	200.000000	25.7532751	0.98650090	51.5495288	0.99257081
2	Voigt Area	0.11566597	287.046074	41.4729465	1.00000006	83.0167382	1.00000003
3	Voigt Area	0.25764032	326.294974	59.2534817	1.00000000	118.608182	1.00000000
4	Voigt Area	0.80928867	530.671114	108.664062	1.00000000	217.513747	1.00000000
5	Voigt Area	0.21909306	605.154643	90.8032406	1.00000001	181.761594	1.00000000

Peak	Type	Anlytc Area	% Area	Int Area	% Area	Centroid	Moment2
1	Voigt Area	4.13442611	2.94731571	2.05401608	1.48629292	208.694070	43.2519143
2	Voigt Area	5.10625724	3.64010670	5.10625527	3.69490342	287.046109	310.177354
3	Voigt Area	16.2502452	11.5843412	16.2502410	11.7587288	326.295008	633.154001
4	Voigt Area	93.6098617	66.7318289	93.6098615	67.7364095	530.671114	2129.39574
5	Voigt Area	21.1768902	15.0964075	21.1768856	15.3236654	605.154599	1486.91022
Total		140.277680	100.000000	138.197259	100.000000		

CBV21AH6%THIOUN - SMOOTH - C:\COLOR\Data\ALE\pennstate\06.12.08IR\CBV21AH6%THIOU

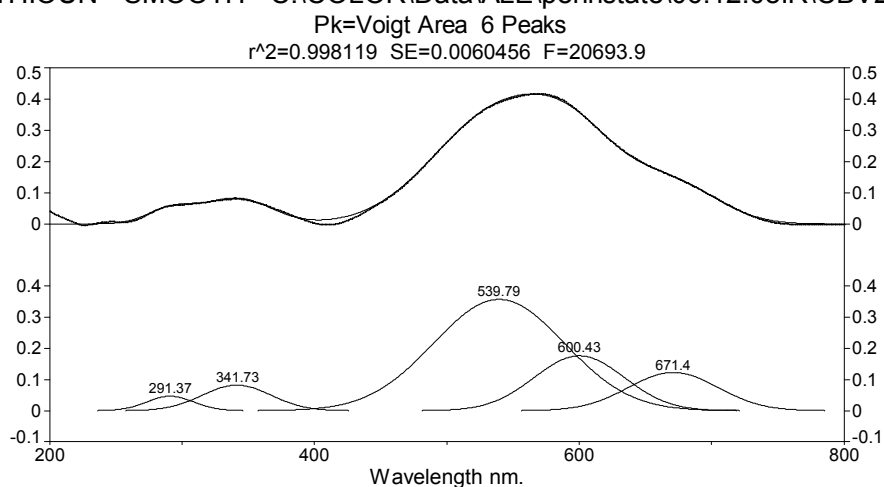


Figure B. 61 Peak fit of CBV21A / H / 0.5 mol % thioindigo unheated.

Table B. 61 Peak fit statistics of CBV21A / H / 0.5 mol % thioindigo unheated.

Description: CBV21AH6%THIOUN - SMOOTH - C:\COLOR\Data\ALE\pennstate\06.12.08IR\CBV21AH6%THIOU

X Variable: Wavelength nm.

File Source: c:\documents and settings\ale\desktop\thesis final\peak fit\21ah\cbv21ah6%thiounpeakfit.txt

Measured Values

Peak	Type	Amplitude	Center	FWHM	Asym50	FW Base	Asym10
1	Voigt Area	0.04650847	291.365992	42.2272624	1.00000007	84.5266586	1.00000004
2	Voigt Area	0.08221155	341.728068	61.0612349	1.00000002	122.226776	1.00000001
3	Voigt Area	0.35733486	539.793899	116.425950	1.00000000	233.050782	1.00000000
4	Voigt Area	0.17627318	600.425692	80.0729431	1.00000002	160.282669	1.00000001
5	Voigt Area	0.12288866	671.398165	79.8106656	0.99999999	159.757666	0.99999999

Peak	Type	Anlytc Area	% Area	Int Area	% Area	Centroid	Moment2
1	Voigt Area	2.09053394	2.74484541	2.09053358	2.78394045	291.366009	321.564702
2	Voigt Area	5.34355907	7.01602747	5.34355895	7.11595836	341.728072	672.380965
3	Voigt Area	44.2850755	58.1457605	44.2850723	58.9739411	539.793880	2444.46178
4	Voigt Area	15.0246455	19.7271751	15.0246454	20.0081542	600.425692	1156.26160
5	Voigt Area	10.4401071	13.7077325	10.4393346	13.9019464	671.388057	1147.39946
Total		76.1621743	100.000000	75.0926113	100.000000		

21A- H fresh - RawData - C:\COLOR\Data\ALE\pennstate\10.20.08UV\21A- H fresh.spc

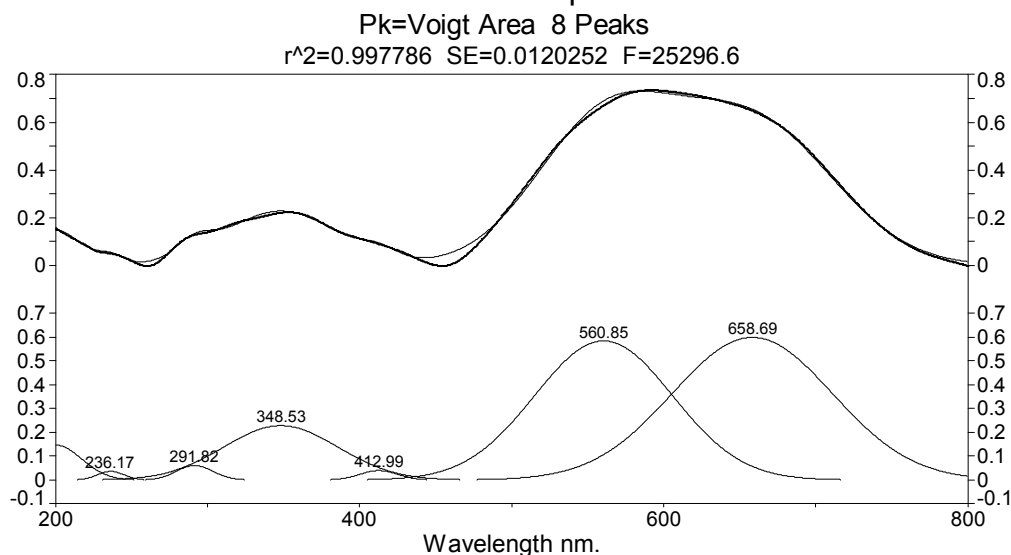


Figure B. 62 Peak fit of CBV21A / H / 0.5 mol % thioindigo heated at 413K for nine hours.

Table B. 62 Peak fit statistics of CBV21A / H / 0.5 mol % thioindigo heated at 413K for nine hours.

Description: 21A- H fresh - RawData - C:\COLOR\Data\ALE\pennstate\10.20.08UV\21A- H fresh.spc

X Variable: Wavelength nm.

File Source: c:\documents and settings\ale\desktop\thesis final\peak fit\21ah\21a- h freshpeakfit.txt

Measured Values

Peak	Type	Amplitude	Center	FWHM	Asym50	FW Base	Asym10
1	Voigt Area	0.14739319	200.000004	40.3945562	0.96605477	80.8478497	0.98122983
2	Voigt Area	0.03643336	236.173896	20.4968095	1.00000000	41.0286321	1.00000000
3	Voigt Area	0.06081708	291.824148	28.4608680	1.00000000	56.9703536	1.00000000
4	Voigt Area	0.22807007	348.530861	88.3297976	1.00000000	176.810483	1.00000000
5	Voigt Area	0.03968472	412.985862	29.2071134	1.00000000	58.4641193	1.00000000
6	Voigt Area	0.58351902	560.850874	106.901532	1.00000000	213.985676	1.00000000
7	Voigt Area	0.59808398	658.692539	124.091080	1.00000000	248.394135	1.00000000
Peak	Type	Anlytc Area	% Area	Int Area	% Area	Centroid	Moment2
1	Voigt Area	6.33807673	5.63258541	3.11763299	2.90975833	213.558916	105.599192
2	Voigt Area	0.79490958	0.70642819	0.79489670	0.74189531	236.174513	75.7406724
3	Voigt Area	1.84249338	1.63740545	1.84249338	1.71964131	291.824148	146.076661
4	Voigt Area	21.4440962	19.0571539	21.4432917	20.0135157	348.536753	1406.14071
5	Voigt Area	1.23379825	1.09646417	1.23379825	1.15153219	412.985862	153.837363
6	Voigt Area	66.4004707	59.0094343	66.4004661	61.9730769	560.850857	2060.87453
7	Voigt Area	79.0014279	70.2077790	78.7119394	73.4636572	658.113283	2694.74604
Total		112.525177	100.000000	107.144053	100.000000		

C:\Documents and Settings\Ale\Desktop\Peak Fit\CBV21AH+6%thioHnofresh.xls

Pk=Voigt Area 9 Peaks

$r^2=0.999087$ SE=0.00664156 F=23098.7

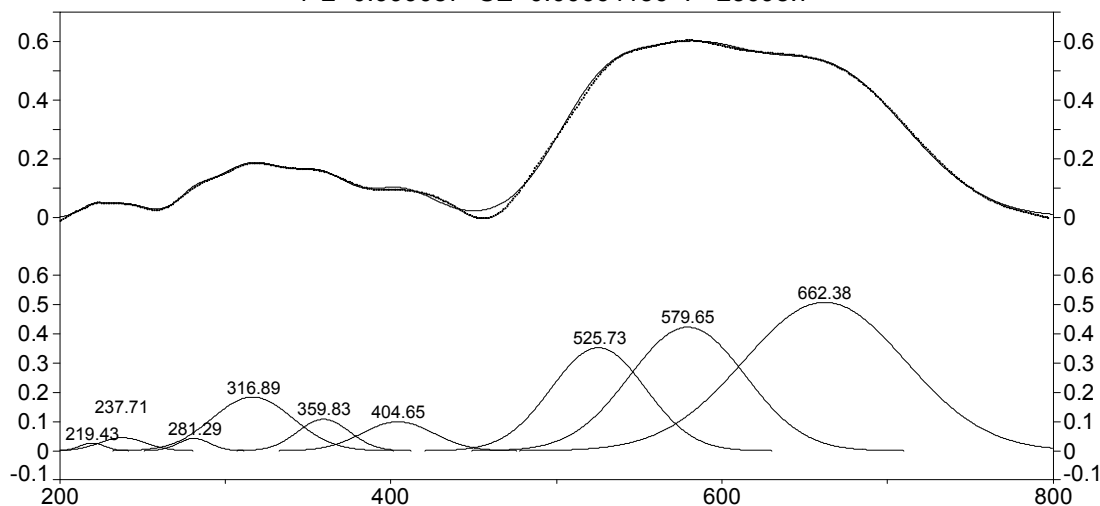


Figure B. 63 Peak fit of CBV21A / H / 0.5 mol % thioindigo heated at 413K for nine hours / hydrated.

Table B. 63 Peak fit statistics of CBV21A / H / 0.5 mol % thioindigo heated at 413K for nine hours / hydrated.

Description: C:\Documents and Settings\Ale\Desktop\Peak Fit\CBV21AH+6%thioHnofresh.xls

File Source: c:\documents and settings\ale\desktop\thesis final\peak fit\21ah\cbv21ah6%thioh-nofreshpeakfit.txt

Measured Values

Peak	Type	Amplitude	Center	FWHM	Asym50	FW Base	Asym10
1	Voigt Area	0.02696635	219.434092	17.4677450	0.99999978	34.9653288	0.99999988
2	Voigt Area	0.04489275	237.705729	32.9425847	1.00000006	65.9414429	1.00000003
3	Voigt Area	0.04231074	281.290837	23.3957882	1.00000003	46.8315416	1.00000001
4	Voigt Area	0.18433985	316.885256	57.2061960	1.00000000	114.510113	1.00000000
5	Voigt Area	0.10819985	359.827017	36.9565229	0.99999986	73.9761760	0.99999992
6	Voigt Area	0.09951622	404.648007	50.9325004	1.00000000	101.952005	1.00000000
7	Voigt Area	0.35301709	525.729582	67.0861416	0.99999989	134.286881	0.99999994
8	Voigt Area	0.42308691	579.653779	82.4352516	0.99999999	165.011321	1.00000000
9	Voigt Area	0.50871233	662.378963	114.828978	1.00000003	229.854110	1.00000002

Peak	Type	Anlytc Area	% Area	Int Area	% Area	Centroid	Moment2
1	Voigt Area	0.50140793	0.33759807	0.49920286	0.33653729	219.530170	53.1483292
2	Voigt Area	1.57422240	1.05992431	1.56868705	1.05752937	237.853893	190.095529
3	Voigt Area	1.05370856	0.70946222	1.05370856	0.71035695	281.290837	98.7097183
4	Voigt Area	11.2252109	7.55793715	11.2252025	7.56746308	316.885347	590.150604
5	Voigt Area	4.25647396	2.86588492	4.25647396	2.86949920	359.827015	246.301331
6	Voigt Area	5.39536783	3.63270244	5.39536783	3.63728377	404.648007	467.815435
7	Voigt Area	25.2092979	16.9734263	25.2092979	16.9948321	525.729580	811.615216
8	Voigt Area	37.1257098	24.9967492	37.1257098	25.0282735	579.653779	1225.49201
9	Voigt Area	62.1807526	41.8663154	62.0014305	41.7982247	661.947168	2319.55168
Total		148.522152	100.000000	148.335081	100.000000		

21AHCl0.2M100Ctwice+6%thioUN - RawData - C:\COLOR\Data\ALE\pennstate\10.10.08UV\

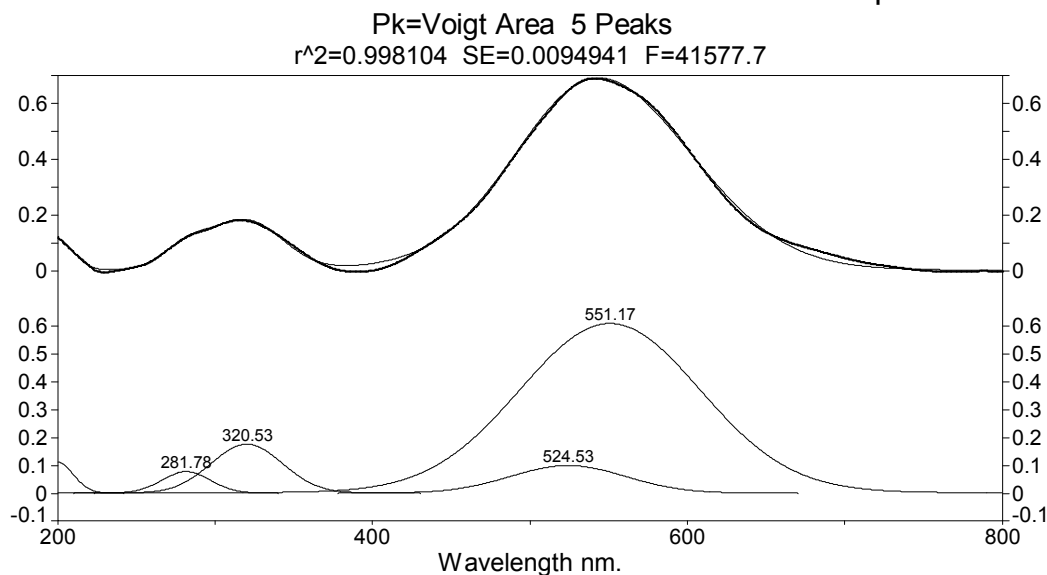


Figure B. 64 Peak fit of CBV21A / H(HCL) / 0.5 mol % thioindigo unheated.

Table B. 64 Peak fit statistics of CBV21A / H(HCL) / 0.5 mol % thioindigo unheated.

Description: 21AHCl0.2M100Ctwice+6%thioUN - RawData - C:\COLOR\Data\ALE\pennstate\10.10.08UV\

X Variable: Wavelength nm.

File Source: c:\documents and settings\ale\desktop\thesis final\peak

fit\21ahcl\21ahcl0.2m100ctwice+6%thiounpeakfit.txt

Measured Values

Peak	Type	Amplitude	Center	FWHM	Asym50	FW Base	Asym10
1	Voigt Area	0.11322369	200.000003	24.3642130	0.89209724	49.3678584	0.94002487
2	Voigt Area	0.07818056	281.784994	36.9299357	1.00000000	74.9320389	1.00000000
3	Voigt Area	0.17661597	320.528634	53.6691810	1.00000000	108.896511	1.00000000
4	Voigt Area	0.09987272	524.531101	86.8435442	1.00000003	176.208372	1.00000001
5	Voigt Area	0.61032639	551.174155	135.678648	0.99999999	275.296384	1.00000000
Peak	Type	Anlytc Area	% Area	Int Area	% Area	Centroid	Moment2
1	Voigt Area	2.99849744	2.58923528	1.41950597	1.25149422	209.261723	252.101016
2	Voigt Area	3.13631728	2.70824422	3.12285164	2.75323309	282.345447	406.395659
3	Voigt Area	10.2966890	8.89130337	10.2497180	9.03656848	321.142439	741.983674
4	Voigt Area	9.42165213	8.13569949	9.37736389	8.26746560	524.412195	1686.67540
5	Voigt Area	89.9531389	77.6755176	89.2554520	78.6912386	550.746033	3731.57363
	Total	115.806295	100.000000	113.424891	100.000000		

21AHCl0.2M100Ctwice+6%thioHblue - RawData - C:\COLOR\Data\ALE\pennstate\10.10.08

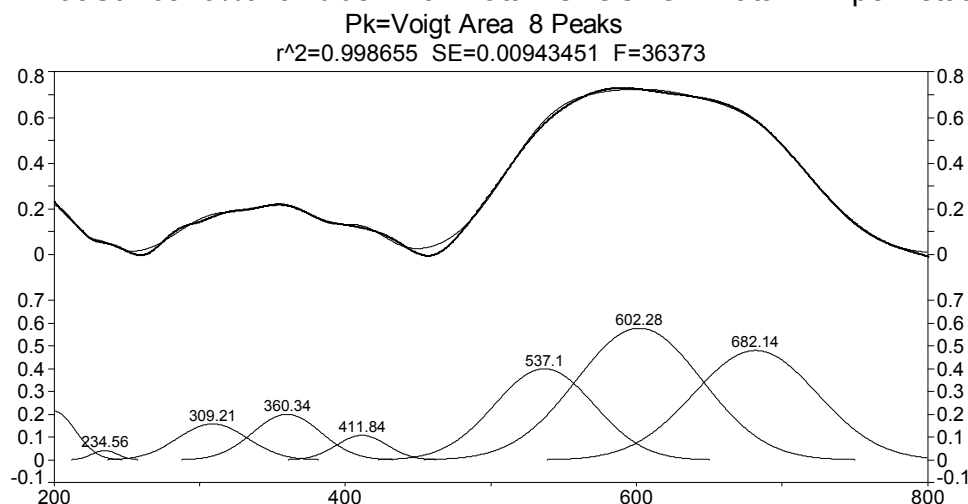


Figure B. 65 Peak fit of CBV21A / H(HCL) / 0.5 mol % thioindigo heated at 413K for nine hours.

Table B. 65 Peak fit statistics of CBV21A / H(HCL) / 0.5 mol % thioindigo heated at 413K for nine hours.

Description: 21AHCl0.2M100Ctwice+6%thioHblue - RawData - C:\COLOR\Data\ALE\pennstate\10.10.08

Y Variable: Wavelength nm.

File Source: c:\documents and settings\ale\desktop\thesis final\peak

fit\21ahcl\21ahcl0.2m100ctwice+6%thiohbluepeakfit.txt

Measured Values

Peak	Type	Amplitude	Center	FWHM	Asym50	FW Base	Asym10
1	Voigt Area	0.21417300	200.000004	34.7192416	0.96717640	69.4895509	0.98185480
2	Voigt Area	0.04168303	234.559233	21.0399830	1.00000000	42.1159071	1.00000000
3	Voigt Area	0.15822601	309.210601	56.4165880	1.00000000	112.929548	1.00000000
4	Voigt Area	0.20060651	360.341526	54.7349227	1.00000008	109.563345	1.00000005
5	Voigt Area	0.10842235	411.836443	40.8089137	1.00000000	81.6875383	1.00000000
6	Voigt Area	0.39981627	537.096246	80.6352876	1.00000000	161.408319	1.00000000
7	Voigt Area	0.57781538	602.279294	101.727614	1.00000000	203.629001	1.00000000
8	Voigt Area	0.48014119	682.140983	99.9316298	1.00000001	200.033965	1.00000000
Peak	Type	Anlytc Area	% Area	Int Area	% Area	Centroid	Moment2
1	Voigt Area	7.91572186	4.33238469	3.89581719	2.18191476	211.657660	78.0444828
2	Voigt Area	0.93354844	0.51094405	0.93349720	0.52282005	234.561244	79.7621985
3	Voigt Area	9.50204127	5.20059937	9.50201679	5.32175655	309.210895	573.949789
4	Voigt Area	11.6880416	6.39702773	11.6880416	6.54607470	360.341527	540.273380
5	Voigt Area	4.70983915	2.57776048	4.70983915	2.63782078	411.836443	300.327168
6	Voigt Area	34.3176712	18.7825388	34.3176712	19.2201609	537.096246	1172.55934
7	Voigt Area	62.5691373	34.2449592	62.5689897	35.0427639	602.278807	1866.12123
8	Voigt Area	51.0745024	27.9537856	50.9345118	28.5266884	681.782107	1758.47807
	Total	182.710503	100.000000	178.550385	100.000000		

21AHCl0.2M100Ctwice+6%thiopurple - RawData - C:\COLOR\Data\ALE\pennstate\10.10.0

Pk=Voigt Area 9 Peaks

$r^2=0.995939$ SE=0.0120557 F=10654.8

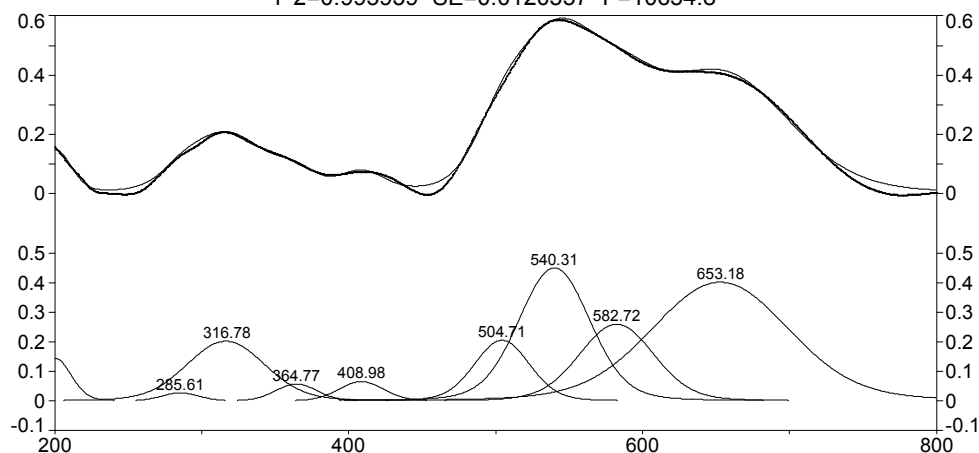


Figure B. 66 Peak fit of CBV21A / H(HCL) / 0.5 mol % thioindigo heated at 413K for nine hours / hydrated.

Table B. 66 Peak fit statistics of CBV21A / H(HCL) / 0.5 mol % thioindigo heated at 413K for nine hours / hydrated.

Description: 21AHCl0.2M100Ctwice+6%thiopurple - RawData - C:\COLOR\Data\ALE\pennstate\10.10.0

X Variable: pc

Y Variable: Wavelength nm.

File Source: c:\documents and settings\ale\Desktop\thesis final\peak

fit\21ahcl\21ahcl0.2m100ctwice+6%thiopurplepeakfit.txt

Measured Values

Peak	Type	Amplitude	Center	FWHM	Asym50	FW Base	Asym10
1	Voigt Area	0.14439283	200.102362	25.7976374	1.00000001	54.4894222	1.00000000
2	Voigt Area	0.02775760	285.606515	31.0842423	0.99999989	65.6557178	0.99999994
3	Voigt Area	0.20228112	316.779231	63.0384850	1.00000000	133.149039	1.00000000
4	Voigt Area	0.05784998	364.773810	33.4372546	0.99999983	70.6257188	0.99999991
5	Voigt Area	0.06592012	408.975428	36.1191335	1.00000001	76.2903472	1.00000000
6	Voigt Area	0.20541716	504.706250	44.3457086	1.00000011	93.6664082	1.00000006
7	Voigt Area	0.44971783	540.314828	57.2167376	0.99999998	120.852422	0.99999999
8	Voigt Area	0.25961703	582.719726	60.0065208	1.00000000	126.744965	1.00000000
9	Voigt Area	0.40152056	653.183393	109.824461	1.00000001	231.969746	1.00000001

Peak	Type	Anlytc Area	% Area	Int Area	% Area	Centroid	Moment2
1	Voigt Area	4.25708618	3.20647798	2.13821862	1.66833269	213.119891	781.078187
2	Voigt Area	0.98607313	0.74271970	0.97422816	0.76013588	287.204908	654.792163
3	Voigt Area	14.5729677	10.9764985	14.2897760	11.1495149	319.446285	1597.67598
4	Voigt Area	2.21065350	1.66508534	2.19333415	1.71133626	365.693595	716.015762
5	Voigt Area	2.72108541	2.04954753	2.70090267	2.10736366	409.615744	787.132323
6	Voigt Area	10.4105864	7.84135317	10.3244965	8.05562856	504.666763	1017.08623
7	Voigt Area	29.4069565	22.1496006	29.0866559	22.6946947	539.871509	1412.85395
8	Voigt Area	17.8040376	13.4101712	17.5873164	13.7224017	581.741403	1503.65711
9	Voigt Area	50.3957307	37.9585459	48.8700733	38.1305916	649.118732	3431.77772
Total		132.765177	100.000000	128.165002	100.000000		

Zeolite CBV10A

CBV10AH6%THIOUN - SMOOTH - C:\COLOR\Data\ALE\pennstate\06.13.08\CBV10AH6%THIOUN.

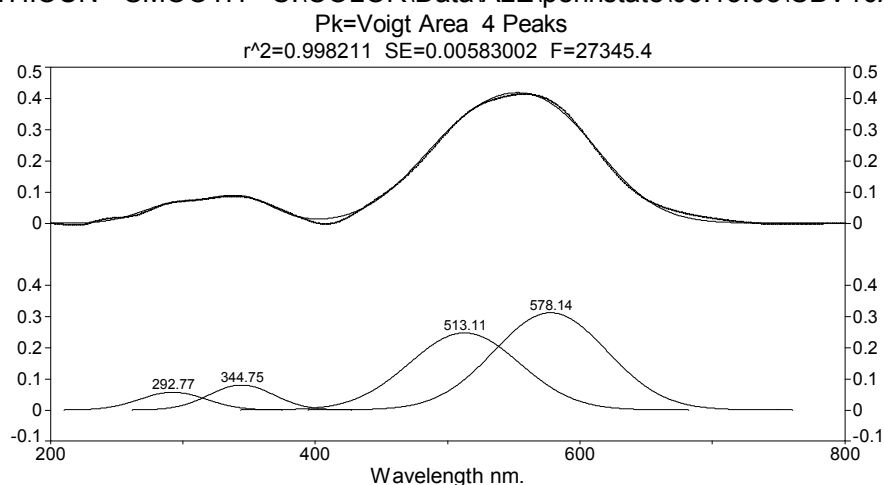


Figure B. 67 Peak fit of CBV10A / H / 0.5 mol % thioindigo unheated.

Table B. 67 Peak fit statistics of CBV10A / H / 0.5 mol % thioindigo unheated.

Description: CBV10AH6%THIOUN - SMOOTH - C:\COLOR\Data\ALE\pennstate\06.13.08\CBV10AH6%THIOUN.

X Variable: Wavelength nm.

File Source: c:\documents and settings\ale\desktop\thesis final\peak fit\10ah\cbv10ah6%thiounpeakfit.txt

Measured Values

Peak	Type	Amplitude	Center	FWHM	Asym50	FW Base	Asym10
1	Voigt Area	0.05745569	292.768517	59.8061075	1.00000000	120.334500	1.00000000
2	Voigt Area	0.08074007	344.745805	57.6446878	1.00000012	115.985557	1.00000007
3	Voigt Area	0.24793317	513.110902	98.2547767	1.00000000	197.696188	1.00000000
4	Voigt Area	0.31263031	578.135375	100.573815	1.00000000	202.362272	1.00000000
Peak	Type	Anlytc Area	% Area	Int Area	% Area	Centroid	Moment2
1	Voigt Area	3.68693636	5.37801545	3.67701643	5.37535517	293.122936	738.470711
2	Voigt Area	4.99384989	7.28436817	4.98549521	7.28819355	344.959148	692.229441
3	Voigt Area	26.1381812	38.1269240	26.0837002	38.1312282	513.082401	1880.43046
4	Voigt Area	33.7367366	49.2106924	33.6588761	49.2052231	577.955143	1964.88309
	Total	68.5557041	100.000000	68.4050880	100.000000		

CBV10AH-6%THIOH140C9H - SMOOTH - C:\COLOR\Data\ALE\pennstate\06.14.08\CBV10AH-6%

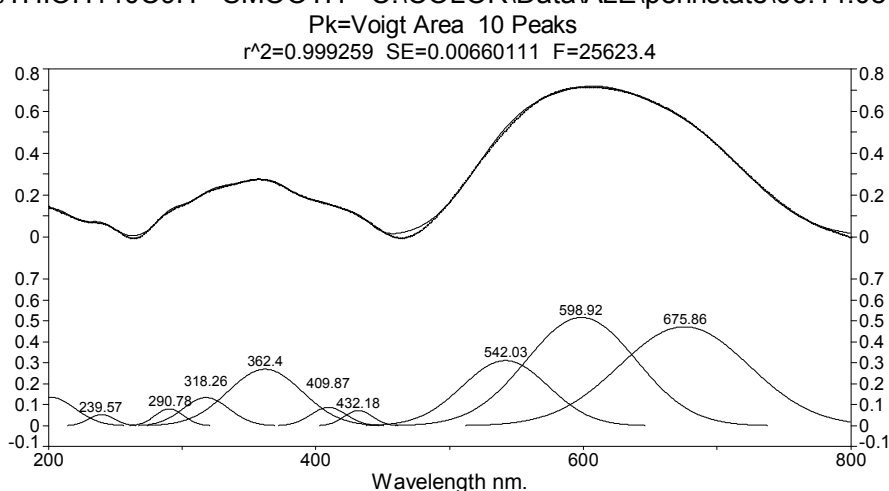


Figure B. 68 Peak fit of CBV10A / H / 0.5 mol % thioindigo heated at 413K for nine hours.

Table B. 68 Peak fit statistics of CBV10A / H / 0.5 mol % thioindigo heated at 413K for nine hours.

Description: CBV10AH-6%THIOH140C9H - SMOOTH - C:\COLOR\Data\ALE\pennstate\06.14.08\CBV10AH-6%

X Variable: Wavelength nm.

File Source: c:\documents and settings\ale\desktop\thesis final\peak fit\10ah\cbv10ah-6%thioh140c9hpeakfit.txt

Measured Values

Peak	Type	Amplitude	Center	FWHM	Asym50	FW Base	Asym10
1	Voigt Area	0.13629738	201.378725	43.1951568	1.00000001	86.4641008	1.00000000
2	Voigt Area	0.05376669	239.569823	22.3943701	1.00000001	44.8269949	1.00000000
3	Voigt Area	0.08052480	290.778214	25.1964074	1.00000000	50.4358559	1.00000000
4	Voigt Area	0.13448427	318.256474	40.3994473	1.00000001	80.8679061	1.00000000
5	Voigt Area	0.26931254	362.399624	65.3550794	1.00000000	130.821800	1.00000000
6	Voigt Area	0.08775509	409.867023	31.1008719	1.00000000	62.2548712	1.00000000
7	Voigt Area	0.07268991	432.175269	24.7974138	1.00000000	49.6371873	1.00000000
8	Voigt Area	0.31089662	542.025947	75.7614977	1.00000000	151.652413	1.00000000
9	Voigt Area	0.51596387	598.916355	96.6995566	1.00000006	193.564298	1.00000003
10	Voigt Area	0.47225107	675.860050	114.332975	0.99999997	228.861257	0.99999998

Peak	Type	Anlytc Area	% Area	Int Area	% Area	Centroid	Moment2
1	Voigt Area	6.26692911	3.58708020	3.32120441	1.93702523	215.148278	127.891436
2	Voigt Area	1.28169408	0.73361919	1.28167377	0.74751027	239.570483	90.4142296
3	Voigt Area	2.15973513	1.23619447	2.15973513	1.25962179	290.778214	114.488481
4	Voigt Area	5.78334550	3.31028543	5.78334550	3.37301917	318.256474	294.330589
5	Voigt Area	18.7356224	10.7239414	18.7356224	10.9271724	362.399625	770.270398
6	Voigt Area	2.90520700	1.66288948	2.90520700	1.69440316	409.867023	174.433414
7	Voigt Area	1.91872495	1.09824448	1.91872495	1.11905748	432.175269	110.891264
8	Voigt Area	25.0724496	14.3510300	25.0724496	14.6229986	542.025947	1035.09844
9	Voigt Area	53.1099613	30.3992095	53.1099355	30.9752946	598.916254	1686.27440
10	Voigt Area	57.4746942	32.8975059	57.1711183	33.3438973	675.118950	2264.81970
	Total	174.708363	100.000000	171.459017	100.000000		

CBV10AH-6%THIOH140C9H - SMOOTH - C:\COLOR\Data\ALE\pennstate\06.19.08XRD\CBV10AH

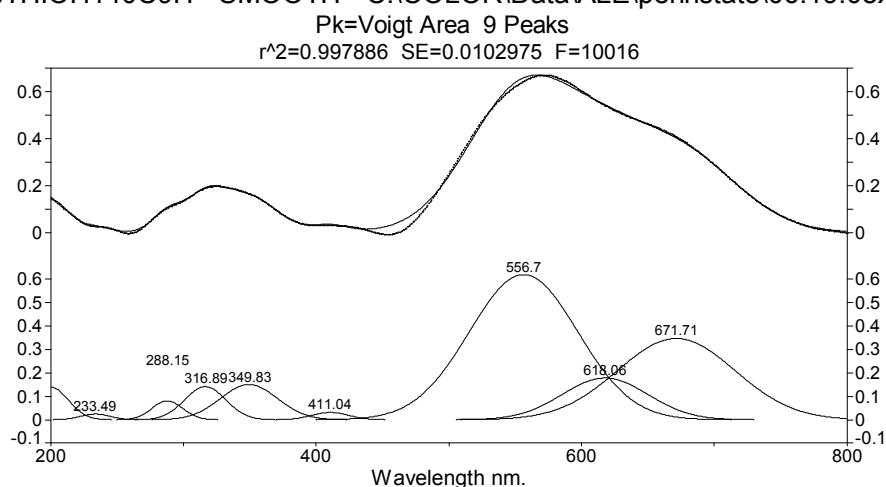


Figure B. 69 Peak fit of CBV10A / H / 0.5 mol % thioindigo heated at 413K for nine hours / hydrated.

Table B. 69 Peak fit statistics of CBV10A / H / 0.5 mol % thioindigo heated at 413K for nine hours / hydrated.

Description: CBV10AH-6%THIOH140C9H - SMOOTH - C:\COLOR\Data\ALE\pennstate\06.19.08XRD\CBV10AH

X Variable: Wavelength nm.

File Source: c:\documents and settings\ale\desktop\thesis final\peak fit\10ah\cbv10ah-6%thioh140c9hno-freshpeakfit.txt

Measured Values

Peak	Type	Amplitude	Center	FWHM	Asym50	FW Base	Asym10
1	Voigt Area	0.13906688	200.000004	31.1278980	0.99404522	62.3087329	0.99672843
2	Voigt Area	0.02408952	233.489058	26.0797896	1.00000000	52.2041295	1.00000000
3	Voigt Area	0.08021758	288.148712	27.5665660	0.99999982	55.1802219	0.99999990
4	Voigt Area	0.14142168	316.887990	36.2824892	0.99999999	72.6269571	1.00000000
5	Voigt Area	0.15030289	349.830312	50.3738779	0.99999989	100.833806	0.99999994
6	Voigt Area	0.03097258	411.037614	32.5493408	1.00000025	65.1542832	1.00000013
7	Voigt Area	0.61957708	556.697159	96.2488066	0.99999992	192.662028	0.99999996
8	Voigt Area	0.17820140	618.056597	75.8757099	1.00000004	151.881033	1.00000002
9	Voigt Area	0.34682234	671.709450	104.093191	1.00000000	208.364197	1.00000000

Peak	Type	Anlytc Area	% Area	Int Area	% Area	Centroid	Moment2
1	Voigt Area	4.60793638	3.32642805	2.29750506	1.68757254	210.530160	63.3614873
2	Voigt Area	0.66875093	0.48276531	0.66791632	0.49060055	233.534800	121.123178
3	Voigt Area	2.35388072	1.69924543	2.35388072	1.72898181	288.148711	137.040801
4	Voigt Area	5.46191922	3.94291062	5.46191922	4.01191059	316.887990	237.398899
5	Voigt Area	8.05944098	5.81803834	8.05944098	5.91985259	349.830311	457.609805
6	Voigt Area	1.07312851	0.77468187	1.07312851	0.78823861	411.037616	191.059636
7	Voigt Area	63.4779520	45.8241657	63.4779519	46.6260773	556.697157	1670.61062
8	Voigt Area	14.3928264	10.3900526	14.3928263	10.5718759	618.056596	1038.22138
9	Voigt Area	38.4292227	27.7417120	38.3580267	28.1748901	671.447526	1920.34977
	Total	138.525058	100.000000	136.142596	100.000000		

10AHCl0.2M100Ctwice+6%thioUN - RawData - C:\COLOR\Data\ALE\pennstate\10.10.08UV\

Pk=Voigt Area 5 Peaks

r^2=0.998123 SE=0.00785796 F=42019.9

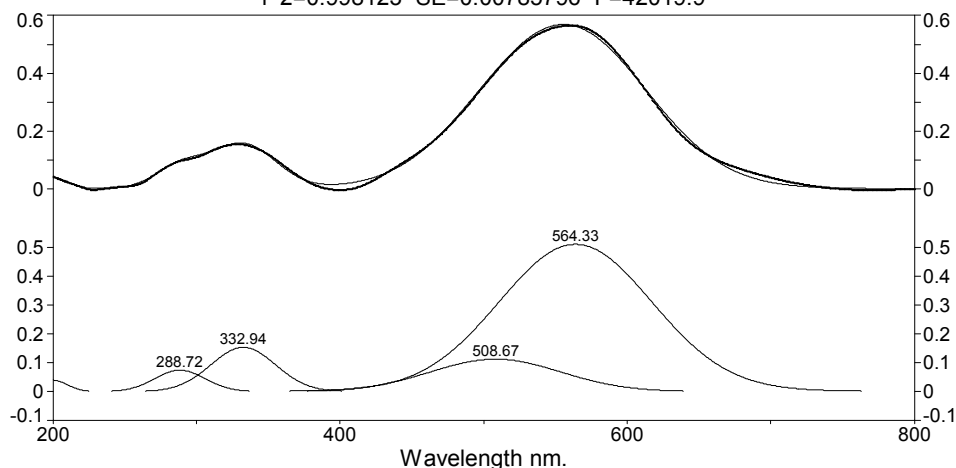


Figure B. 70 Peak fit of CBV10A / H(HCl) / 0.5 mol % thioindigo unheated.

Table B. 70 Peak fit statistics of CBV10A / H(HCl) / 0.5 mol % thioindigo unheated.

Description: 10AHCl0.2M100Ctwice+6%thioUN - RawData - C:\COLOR\Data\ALE\pennstate\10.10.08UV\

X Variable: Wavelength nm.

File Source: c:\documents and settings\ale\desktop\thesis final\peak
fit\10ahcl\10ahcl0.2m100ctwice+6%thiounpeakfit.txt

Measured Values

Peak	Type	Amplitude	Center	FWHM	Asym50	FW Base	Asym10
1	Voigt Area	0.04058650	200.000002	25.0915367	0.86682262	50.7259465	0.92538429
2	Voigt Area	0.07465696	288.717926	41.9510025	0.99999992	84.9925250	0.99999996
3	Voigt Area	0.15341291	332.936623	53.2109214	1.00000000	107.805065	1.00000000
4	Voigt Area	0.11262566	508.672799	107.359554	1.00000000	217.509928	1.00000000
5	Voigt Area	0.50944801	564.330073	126.080980	1.00000000	255.439445	1.00000000
Peak	Type	Anlytc Area	% Area	Int Area	% Area	Centroid	Moment2
1	Voigt Area	1.10495488	1.15005173	0.51573918	0.54334584	209.332910	238.830822
2	Voigt Area	3.39485573	3.53341096	3.38097736	3.56195538	289.260470	477.998056
3	Voigt Area	8.84853497	9.20967281	8.81545959	9.28733631	333.428705	708.516372
4	Voigt Area	13.1065003	13.6414197	13.0382666	13.7361831	508.625177	2412.77999
5	Voigt Area	69.6238657	72.4654448	69.1686955	72.8711794	563.888504	3225.33265
Total		96.0787116	100.000000	94.9191383	100.000000		

10AHCl0.2M100Ctwice+6%thioH - RawData - C:\COLOR\Data\ALE\pennstate\10.10.08UV\1

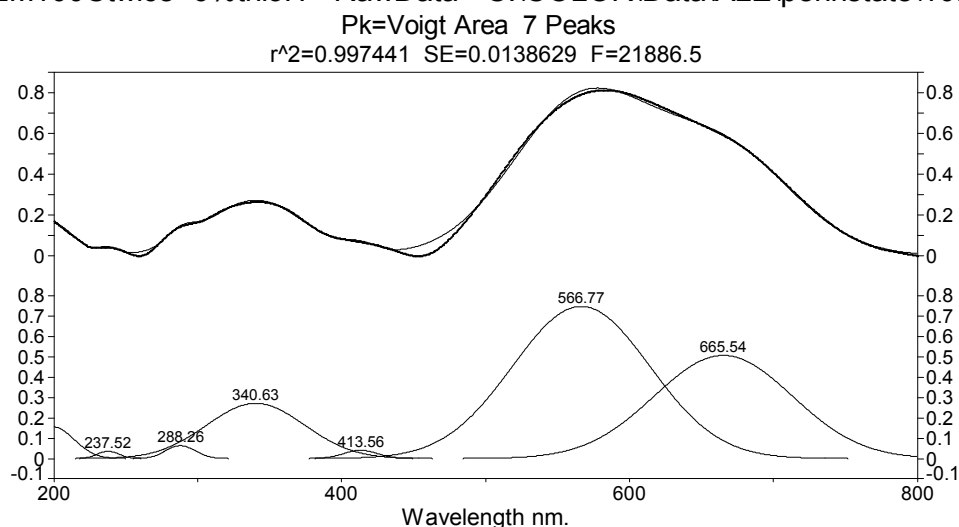


Figure B. 71 Peak fit of CBV10A / H(HCl) / 0.5 mol % thioindigo heated at 413K for nine hours.

Table B. 71 Peak fit statistics of CBV10A / H(HCl) / 0.5 mol % thioindigo heated at 413K for nine hours.

Description: 10AHCl0.2M100Ctwice+6%thioH - RawData - C:\COLOR\Data\ALE\pennstate\10.10.08UV\1

X Variable: Wavelength nm.

File Source: c:\documents and settings\ale\desktop\thesis final\peak

fit\10ahcl\10ahcl0.2m100ctwice+6%thiohbluepeakfit.txt

Measured Values

Peak	Type	Amplitude	Center	FWHM	Asym50	FW Base	Asym10
1	Voigt Area	0.15643136	200.000003	34.3883022	0.90607039	68.7641648	0.94730477
2	Voigt Area	0.03598569	237.519641	17.7303210	1.00000010	35.4909295	1.00000006
3	Voigt Area	0.06345876	288.256388	24.3995397	1.00000000	48.8407593	1.00000000
4	Voigt Area	0.27180383	340.630555	80.1491834	1.00000000	160.435280	1.00000000
5	Voigt Area	0.04037809	413.560931	27.8137630	1.00000027	55.6750383	1.00000015
6	Voigt Area	0.74915668	566.773394	112.459496	0.99999998	225.111098	0.99999999
7	Voigt Area	0.50801589	665.536766	112.919587	1.00000000	226.032066	1.00000000
Peak	Type	Anlytc Area	% Area	Int Area	% Area	Centroid	Moment2
1	Voigt Area	5.72890470	3.12738418	2.73175716	1.51736029	211.335060	74.6525555
2	Voigt Area	0.67917023	0.37075608	0.67917002	0.37724642	237.519653	56.6910171
3	Voigt Area	1.64818297	0.89973592	1.64818297	0.91548672	288.256388	107.361314
4	Voigt Area	23.1892599	12.6589162	23.1888425	12.8802916	340.633220	1158.08970
5	Voigt Area	1.19546734	0.65260043	1.19546734	0.66402486	413.560933	139.509587
6	Voigt Area	89.6811148	48.9565309	89.6810681	49.8135389	566.773267	2280.71600
7	Voigt Area	61.0630914	33.3340763	60.9090330	33.8320512	665.160577	2248.72027
Total		183.185191	100.000000	180.033521	100.000000		

10AHCl0.2M100Ctwice+6%thiopurple - RawData - C:\COLOR\Data\ALE\pennstate\10.10.0
Pk=Voigt Area 7 Peaks

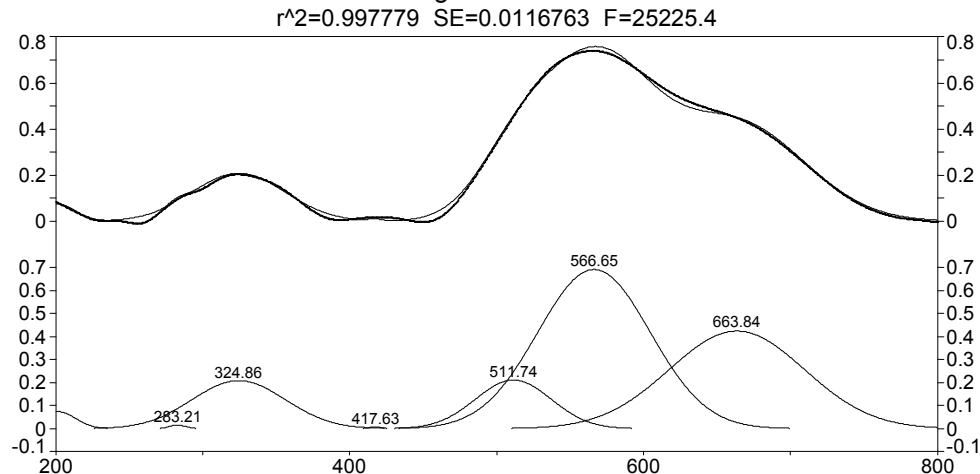


Figure B. 72 Peak fit of CBV10A / H(HCl) / 0.5 mol % thioindigo heated at 413K for nine hours / hydrated.

Table B. 72 Peak fit statistics of CBV10A / H(HCl) / 0.5 mol % thioindigo heated at 413K for nine hours / hydrated.

Description: 10AHCl0.2M100Ctwice+6%thiopurple - RawData - C:\COLOR\Data\ALE\pennstate\10.10.0
X Variable: pc
Y Variable: Wavelength nm.
File Source: c:\documents and settings\ale\desktop\thesis final\peak
fit\10ahcl\10ahcl0.2m100ctwice+6%thiopurplepeakfit.txt

Measured Values

Peak	Type	Amplitude	Center	FWHM	Asym50	FW Base	Asym10
1	Voigt Area	0.07468376	201.075699	28.4661408	0.99999999	56.9809081	0.99999999
2	Voigt Area	0.01560014	283.214902	13.7486515	0.99999963	27.5207889	0.99999980
3	Voigt Area	0.20865128	324.857960	74.6042807	1.00000000	149.336002	1.00000000
4	Voigt Area	0.00785083	417.629850	10.0401161	0.99999961	20.0973831	0.99999978
5	Voigt Area	0.21127480	511.736328	60.7520779	1.00000003	121.607934	1.00000002
6	Voigt Area	0.69095317	566.653780	90.0895346	0.99999999	180.332963	0.99999999
7	Voigt Area	0.42377874	663.839929	108.370725	0.99999989	216.926573	0.99999994

Peak	Type	Anlytc Area	% Area	Int Area	% Area	Centroid	Moment2
1	Voigt Area	2.26301251	1.52953482	1.21173761	0.82528352	210.046678	56.0022555
2	Voigt Area	0.22830785	0.15430971	0.22830785	0.15549464	283.214901	34.0882543
3	Voigt Area	16.5697904	11.1992626	16.5691183	11.2848030	324.863319	1003.04967
4	Voigt Area	0.08390474	0.05670990	0.08390474	0.05714537	417.629849	18.1786666
5	Voigt Area	13.6628419	9.23450146	13.6628419	9.30541237	511.736329	665.590057
6	Voigt Area	66.2605701	44.7844847	66.2605700	45.1283807	566.653779	1463.63649
7	Voigt Area	48.8858709	33.0411968	48.8103480	33.2434805	663.608880	2086.40244
Total		147.954298	100.000000	146.826828	100.000000		

CBV10ANH46%THIOUN - SMOOTH - C:\COLOR\Data\ALE\pennstate\06.12.08IR\CBV10ANH46%T

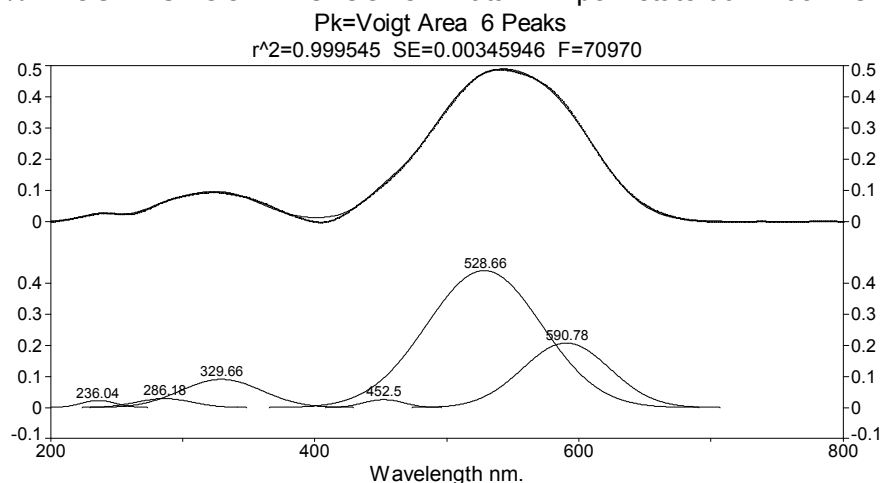


Figure B. 73 Peak fit of CBV10A / NH₄ / 0.5 mol % thioindigo unheated.

Table B. 73 Peak fit statistics of CBV10A / NH₄ / 0.5 mol % thioindigo unheated.

Description: CBV10ANH46%THIOUN - SMOOTH - C:\COLOR\Data\ALE\pennstate\06.12.08IR\CBV10ANH46%T

X Variable: Wavelength nm.

File Source: c:\documents and settings\ale\desktop\thesis final\peak fit\10anh4\cbv10anh46%thiounpeakfit.txt

Measured Values

Peak	Type	Amplitude	Center	FWHM	Asym50	FW Base	Asym10
1	Voigt Area	0.02299728	236.040381	30.8737921	0.99999985	61.8003236	0.99999992
2	Voigt Area	0.02923699	286.181002	50.4642904	1.00000000	101.014785	1.00000000
3	Voigt Area	0.09119571	329.660293	71.7386503	1.00000000	143.599846	1.00000000
4	Voigt Area	0.02589628	452.497785	35.7252691	0.99999997	71.5115651	0.99999998
5	Voigt Area	0.44101712	528.662987	102.369098	1.00000000	204.913066	1.00000000
6	Voigt Area	0.20820253	590.778046	77.6263833	1.00000015	155.385370	1.00000008
Peak	Type	Anlytc Area	% Area	Int Area	% Area	Centroid	Moment2
1	Voigt Area	0.75578581	1.00056307	0.75352610	0.99760290	236.160328	167.558128
2	Voigt Area	1.57054004	2.07919274	1.57049463	2.07919806	286.183633	459.027157
3	Voigt Area	6.96401687	9.21946141	6.96394444	9.21965572	329.661709	927.908171
4	Voigt Area	0.98479322	1.30373939	0.98479322	1.30378043	452.497784	230.163032
5	Voigt Area	48.0569870	63.6212613	48.0569870	63.6232639	528.662987	1889.82810
6	Voigt Area	17.2039259	22.7757821	17.2039258	22.7764990	590.778049	1086.68395
	Total	75.5360488	100.000000	75.5336712	100.000000		

CBV10ANH4-6%THIOH - SMOOTH - C:\COLOR\Data\ALE\pennstate\06.13.08\CBV10ANH4-6%TH

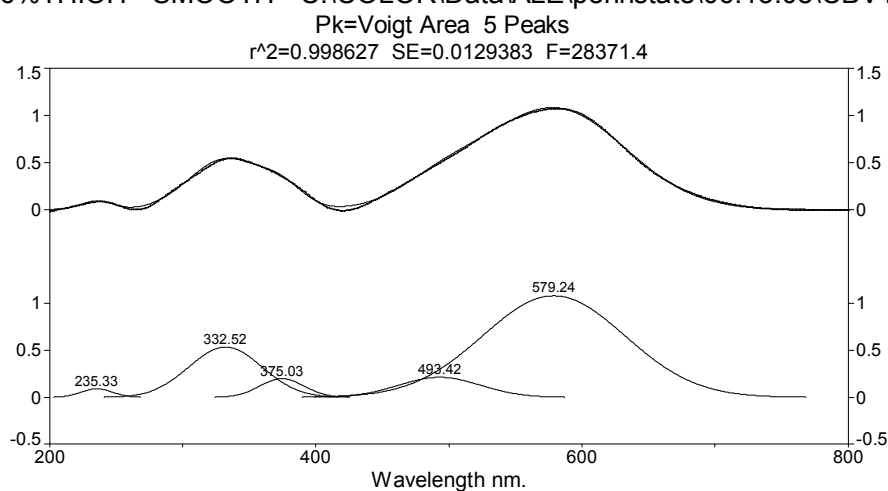


Figure B. 74 Peak fit of CBV10A / NH₄ / 0.5 mol % thioindigo heated at 413K for nine hours.

Table B. 74 Peak fit statistics of CBV10A / NH₄ / 0.5 mol % thioindigo heated at 413K for nine hours.

Description: CBV10ANH4-6%THIOH - SMOOTH - C:\COLOR\Data\ALE\pennstate\06.13.08\CBV10ANH4-6%TH

X Variable: Wavelength nm.

File Source: c:\documents and settings\ale\desktop\thesis final\peak fit\10anh4\cbv10anh4-6%thiohpeakfit.txt

Measured Values

Peak	Type	Amplitude	Center	FWHM	Asym50	FW Base	Asym10
1	Voigt Area	0.09100772	235.325279	27.6701780	1.00000000	55.3876229	1.00000000
2	Voigt Area	0.53591889	332.517521	64.6092581	1.00000007	129.328884	1.00000004
3	Voigt Area	0.19847583	375.034693	39.1818078	1.00000000	78.4305471	1.00000000
4	Voigt Area	0.21289969	493.424488	72.5248630	1.00000000	145.173615	1.00000000
5	Voigt Area	1.08186473	579.242342	125.880117	1.00000000	251.975265	1.00000000
Peak	Type	Anlytc Area	% Area	Int Area	% Area	Centroid	Moment2
1	Voigt Area	2.68054057	1.28122703	2.67699618	1.27957084	235.376448	136.262732
2	Voigt Area	36.8575131	17.6169099	36.8574879	17.6174202	332.517616	752.777907
3	Voigt Area	8.27797874	3.95665344	8.27797874	3.95677075	375.034693	276.855714
4	Voigt Area	16.4359251	7.85593462	16.4359251	7.85616753	493.424488	948.545976
5	Voigt Area	144.964717	69.2892750	144.962084	69.2900707	579.238119	2856.65051
	Total	209.216674	100.000000	209.210471	100.000000		

C:\Documents and Settings\Ale\Desktop\Peak Fit\10ANH4\Outside Desiccator.xls

Pk=Voigt Area 6 Peaks

$r^2=0.999229$ SE=0.00841246 F=41891.4

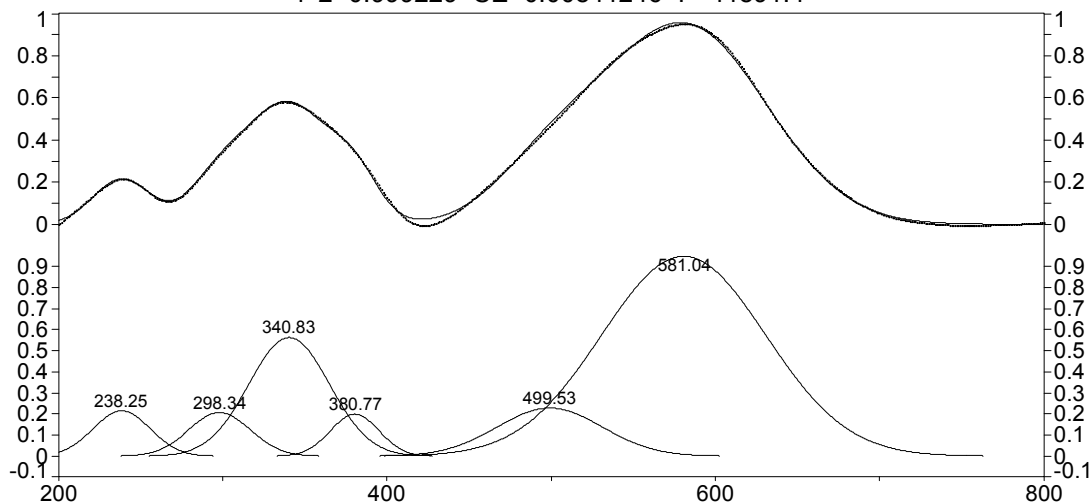


Figure B. 75 Peak fit of CBV10A / NH₄ / 0.5 mol % thioindigo heated at 413K for nine hours / hydrated.

Table B. 75 Peak fit statistics of CBV10A / NH₄ / 0.5 mol % thioindigo heated at 413K for nine hours / hydrated.

Description: C:\Documents and Settings\Ale\Desktop\Peak Fit\10ANH4\Outside Desiccator.xls

File Source: c:\documents and settings\ale\desktop\thesis final\peak fit\10anh4\cbv10anh4-6%thiohnofreshpeakfit.txt

Measured Values

Peak	Type	Amplitude	Center	FWHM	Asym50	FW Base	Asym10
1	Voigt Area	0.21487981	238.249311	40.8856362	0.99999999	81.8411143	0.99999999
2	Voigt Area	0.20648325	298.341244	44.3750137	1.00000000	88.8258300	1.00000000
3	Voigt Area	0.56282709	340.833366	57.8612164	0.99999988	115.821273	0.99999993
4	Voigt Area	0.19919798	380.771657	34.7941932	1.00000016	69.6478229	1.00000009
5	Voigt Area	0.22822256	499.533754	75.2583637	1.00000001	150.645286	1.00000000
6	Voigt Area	0.94792693	581.043492	117.643316	1.00000000	235.487594	1.00000000

Peak	Type	Anlytc Area	% Area	Int Area	% Area	Centroid	Moment2
1	Voigt Area	9.35187264	4.71988627	9.22283480	4.65781071	238.869773	277.340260
2	Voigt Area	9.75338903	4.92253143	9.75338815	4.92575622	298.341253	355.107994
3	Voigt Area	34.6652843	17.4955547	34.6652841	17.5070177	340.833365	603.753412
4	Voigt Area	7.37774964	3.72354721	7.37774964	3.72598687	380.771658	218.322298
5	Voigt Area	18.2829199	9.22738214	18.2829199	9.23342791	499.533754	1021.39586
6	Voigt Area	118.706454	59.9110983	118.705758	59.9500006	581.042148	2495.55908
Total		198.137669	100.000000	198.007935	100.000000		

CBV10ANa-6%thio UN - smooth - C:\COLOR\Data\ALE\pennstate\06.21.08UV\CBV10ANa-6%

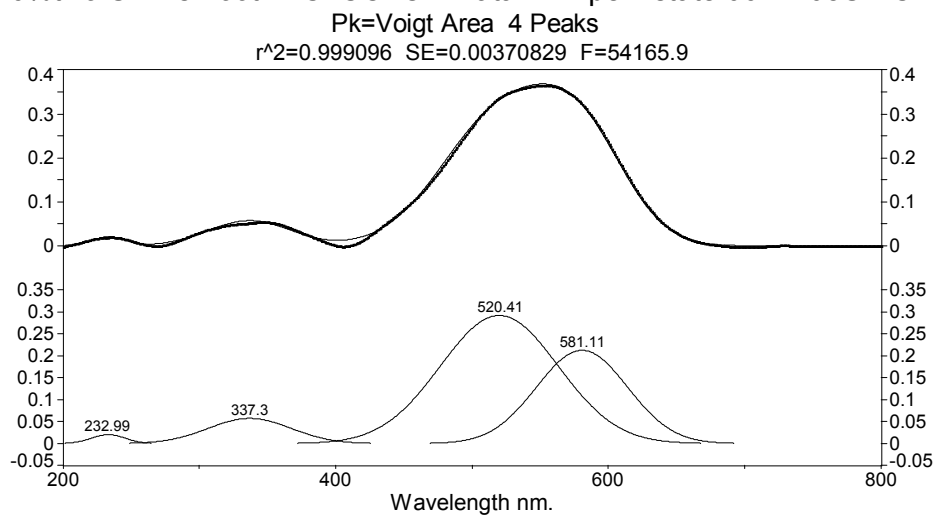


Figure B. 76 Peak fit of CBV10A / Na / 0.5 mol % thioindigo unheated.

Table B. 76 Peak fit statistics of CBV10A / Na / 0.5 mol % thioindigo unheated.

Description: CBV10ANa-6%thio UN - smooth - C:\COLOR\Data\ALE\pennstate\06.21.08UV\CBV10ANa-6%

X Variable: Wavelength nm.

File Source: c:\documents and settings\ale\desktop\thesis final\peak fit\10ana\cbv10ana-6%thiounfreshpeakfit.txt

Measured Values

Peak	Type	Amplitude	Center	FWHM	Asym50	FW Base	Asym10
1	Voigt Area	0.02044872	232.985673	29.4177280	1.00000006	58.8857082	1.00000003
2	Voigt Area	0.05745185	337.302830	71.4972478	1.00000005	143.116629	1.00000003
3	Voigt Area	0.29156584	520.413033	101.720733	1.00000000	203.615228	1.00000000
4	Voigt Area	0.21235926	581.109662	78.5453847	1.00000010	157.224943	1.00000006

Peak	Type	Anlytc Area	% Area	Int Area	% Area	Centroid	Moment2
1	Voigt Area	0.64033524	1.17842546	0.63768419	1.17360421	233.138939	150.984955
2	Voigt Area	4.37245740	8.04674608	4.37244402	8.04711604	337.303270	921.795954
3	Voigt Area	31.5702729	58.0995873	31.5702729	58.1024363	520.413033	1865.96507
4	Voigt Area	17.7551396	32.6752412	17.7551396	32.6768435	581.109664	1112.56628
Total			54.3382052	100.000000	54.3355407	100.000000	

CBV10A6%thioH1409h - smooth - C:\COLOR\Data\ALE\pennstate\06.05.08\CBV10A6%thioH
Pk=Voigt Area 4 Peaks

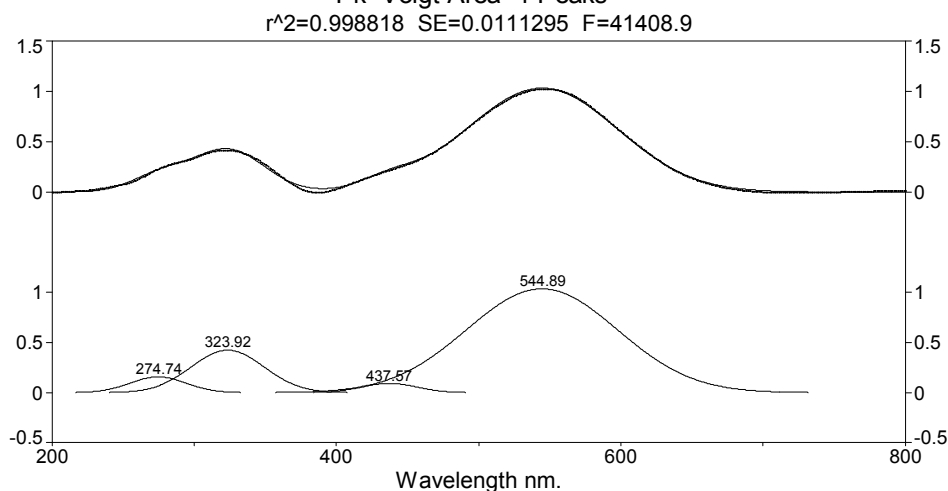


Figure B. 77 Peak fit of CBV10A / Na / 0.5 mol % thioindigo heated at 413K for nine hours.

Table B. 77 Peak fit statistics of CBV10A / Na / 0.5 mol % thioindigo heated at 413K for nine hours.

Description: CBV10A6%thioH1409h - smooth - C:\COLOR\Data\ALE\pennstate\06.05.08\CBV10A6%thioH

X Variable: Wavelength nm.

File Source: c:\documents and settings\ale\desktop\thesis final\peak fit\10ana\cbv10a6%thioh1409hpeakfit.txt

Measured Values

Peak	Type	Amplitude	Center	FWHM	Asym50	FW Base	Asym10
1	Voigt Area	0.15865833	274.737848	46.5100785	1.00000000	93.0996068	1.00000000
2	Voigt Area	0.42356029	323.916235	60.2884866	1.00000000	120.679960	1.00000000
3	Voigt Area	0.09251262	437.565764	45.5732162	1.00000000	91.2242818	1.00000000
4	Voigt Area	1.03495952	544.893313	124.954009	1.00000000	250.121469	1.00000000

Peak	Type	Anlytc Area	% Area	Int Area	% Area	Centroid	Moment2
1	Voigt Area	7.85492731	4.43319806	7.85432120	4.43287421	274.743975	389.644482
2	Voigt Area	27.1820266	15.3411104	27.1820089	15.3411636	323.916319	655.460390
3	Voigt Area	4.48789666	2.53289864	4.48789666	2.53290906	437.565764	374.544918
4	Voigt Area	137.659368	77.6927929	137.659262	77.6930531	544.893110	2815.63898
Total			177.184218	100.000000	177.183489	100.000000	

CBV10ANa-6%thio1409hnofresh - smooth - C:\COLOR\Data\ALE\pennstate\06.21.08UV\CB

Pk=Voigt Area 4 Peaks

$r^2=0.999215$ SE=0.00908397 F=62406.8

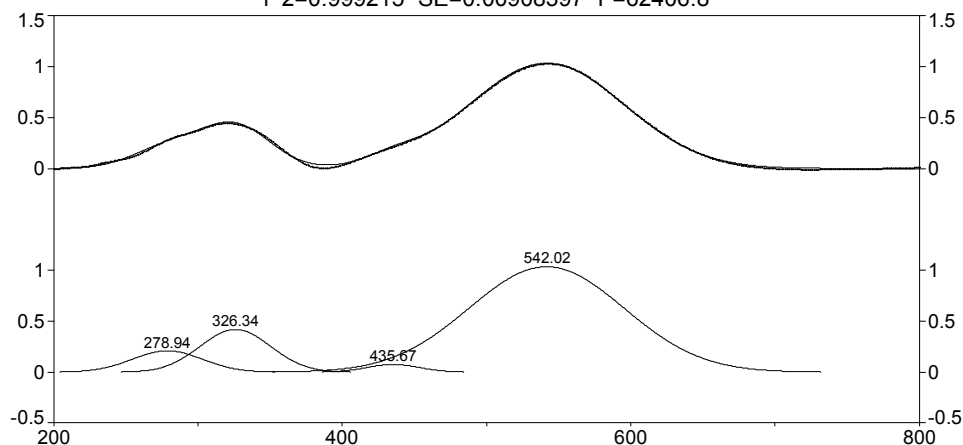


Figure B. 78 Peak fit of CBV10A / Na / 0.5 mol % thioindigo heated at 413K for nine hours / hydrated.

Table B. 78 Peak fit statistics of CBV10A / Na / 0.5 mol % thioindigo heated at 413K for nine hours / hydrated.

Description: CBV10ANa-6%thio1409hnofresh - smooth - C:\COLOR\Data\ALE\pennstate\06.21.08UV\CB

X Variable: Wavelength nm.

File Source: c:\documents and settings\ale\desktop\thesis final\peak fit\10ana\cbv10ana-6%thio1409hnofreshpeakfit.txt

Measured Values

Peak	Type	Amplitude	Center	FWHM	Asym50	FW Base	Asym10
1	Voigt Area	0.21053311	278.937689	57.5957381	1.00000000	115.289863	1.00000000
2	Voigt Area	0.41920372	326.337957	57.3980562	1.00000000	114.894161	1.00000000
3	Voigt Area	0.07512069	435.672367	42.8948158	1.00000004	85.8629056	1.00000002
4	Voigt Area	1.03528511	542.017553	126.720903	0.99999999	253.658275	1.00000000
Peak	Type	Anlytc Area	% Area	Int Area	% Area	Centroid	Moment2
1	Voigt Area	12.9075247	7.10766653	12.8994624	7.10354689	278.991120	594.005361
2	Voigt Area	25.6126503	14.1038798	25.6126475	14.1045135	326.337971	594.124697
3	Voigt Area	3.43001934	1.88877683	3.43001934	1.88886191	435.672367	331.813587
4	Voigt Area	139.649838	76.8996769	139.649724	76.9030777	542.017333	2895.82680
	Total	181.600033	100.000000	181.591853	100.000000		

MESOPOROUS ZEOLITES

MA-1

MA1-6%thioUN - MA1-6%thioUNsmooth - C:\COLOR\Data\ALE\pennstate\MA1-6%thioUN.spc

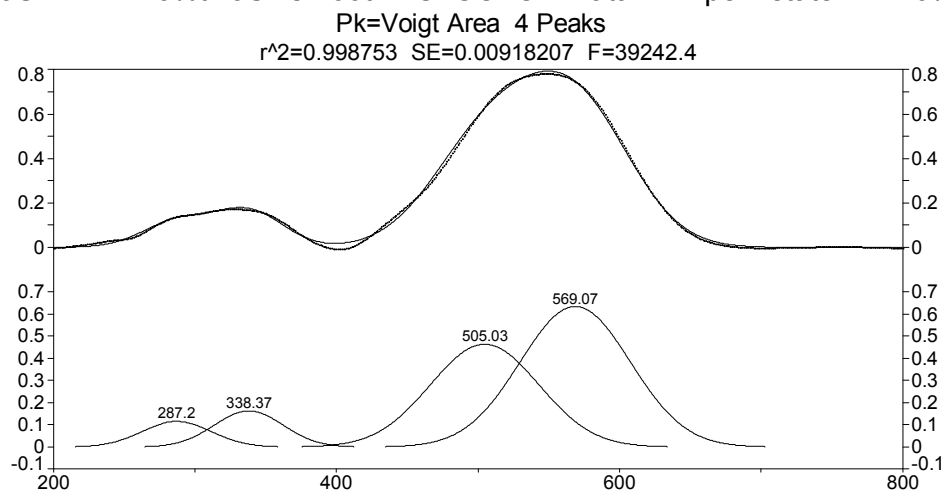


Figure B. 79 Peak fit of MA-1 / 0.5 mol % thioindigo unheated.

Table B. 79 Peak fit statistics of MA-1 / 0.5 mol % thioindigo unheated.

Description: MA1-6%thioUN - MA1-6%thioUNsmooth - C:\COLOR\Data\ALE\pennstate\MA1-6%thioUN.spc

X Variable: Wavelength nm.

File Source: c:\documents and settings\ale\desktop\thesis final\peak fit\ma-1\ma1-6%thiounpeakfit.txt

Measured Values

Peak	Type	Amplitude	Center	FWHM	Asym50	FW Base	Asym10
1	Voigt Area	0.11538273	287.199858	57.8681172	1.00000000	115.835086	1.00000000
2	Voigt Area	0.16273627	338.368079	57.3317832	1.00000004	114.761502	1.00000002
3	Voigt Area	0.46292969	505.025612	90.2647015	1.00000000	180.683596	1.00000000
4	Voigt Area	0.63331406	569.065792	91.5558992	1.00000000	183.268197	1.00000000

Peak	Type	Anlytc Area	% Area	Int Area	% Area	Centroid	Moment2
1	Voigt Area	7.10742663	5.76711574	7.10604935	5.76606263	287.217943	602.320178
2	Voigt Area	9.93143540	8.05857596	9.93143533	8.05866598	338.368081	592.755179
3	Voigt Area	44.4800426	36.0920438	44.4800426	36.0924472	505.025612	1469.33374
4	Voigt Area	61.7216710	50.0822645	61.7216709	50.0828241	569.065792	1511.67070
	Total	123.240576	100.000000	123.239198	100.000000		

MA-1+dye - MA-1+dye sDEHYDRATED\COLOR\Data\ALE\pennstate\NEW RUNS WITH BaSo4\MA-

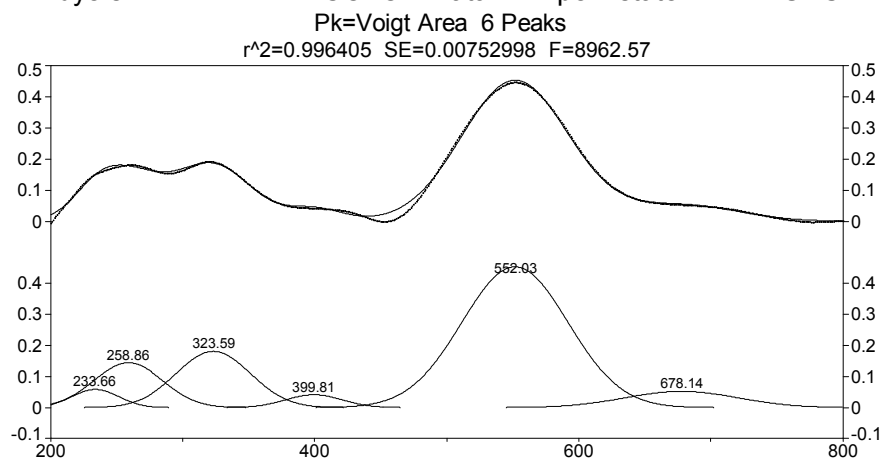


Figure B. 80 Peak fit of MA-1 / 0.5 mol % thioindigo heated at 413K for nine hours.

Table B. 80 Peak fit statistics of MA-1 / 0.5 mol % thioindigo heated at 413K for nine hours.

Description: MA-1+dye - MA-1+dye smooth - C:\COLOR\Data\ALE\pennstate\NEW RUNS WITH BaSo4\MA-

X Variable: Wavelength (nm)

Y Variable: Absorbance

File Source: c:\documents and settings\ale\desktop\thesis final\peak fit\ma-1\ma-1+dyepeakfit.txt

Measured Values

Peak	Type	Amplitude	Center	FWHM	Asym50	FW Base	Asym10
1	Voigt Area	0.05859871	233.658051	41.8237904	1.00000000	83.7190253	1.00000000
2	Voigt Area	0.14472730	258.857592	61.3329927	1.00000000	122.770756	1.00000000
3	Voigt Area	0.18121306	323.592046	66.3159265	1.00000000	132.745136	1.00000000
4	Voigt Area	0.04136652	399.808427	50.6535923	0.99999999	101.393713	1.00000000
5	Voigt Area	0.45328860	552.030482	94.6017951	1.00000000	189.365192	1.00000000
6	Voigt Area	0.05235762	678.138419	100.460604	1.00000000	201.092818	1.00000000
Peak	Type	Anlytc Area	% Area	Int Area	% Area	Centroid	Moment2
1	Voigt Area	2.60881707	3.33074001	2.53305146	3.24230538	234.869607	273.204087
2	Voigt Area	9.44880347	12.0635165	9.33619762	11.9503311	259.675997	629.540574
3	Voigt Area	12.7920323	16.3318978	12.7919594	16.3737055	323.592785	792.994655
4	Voigt Area	2.23044476	2.84766291	2.23044476	2.85496885	399.808427	462.705918
5	Voigt Area	45.6463845	58.2778460	45.6463845	58.4273633	552.030482	1613.92482
6	Voigt Area	5.59896684	7.14833673	5.58697417	7.15132585	677.849955	1784.78400
	Total	78.3254490	100.000000	78.1250119	100.000000		

MS-1

MS1-6%thio UnheatedC:\COLOR\Data\ALE\pennstate\MS1-6%THIOUN.spc

Pk=Voigt Area 5 Peaks

$r^2=0.999246$ SE=0.00638544 F=51664.8

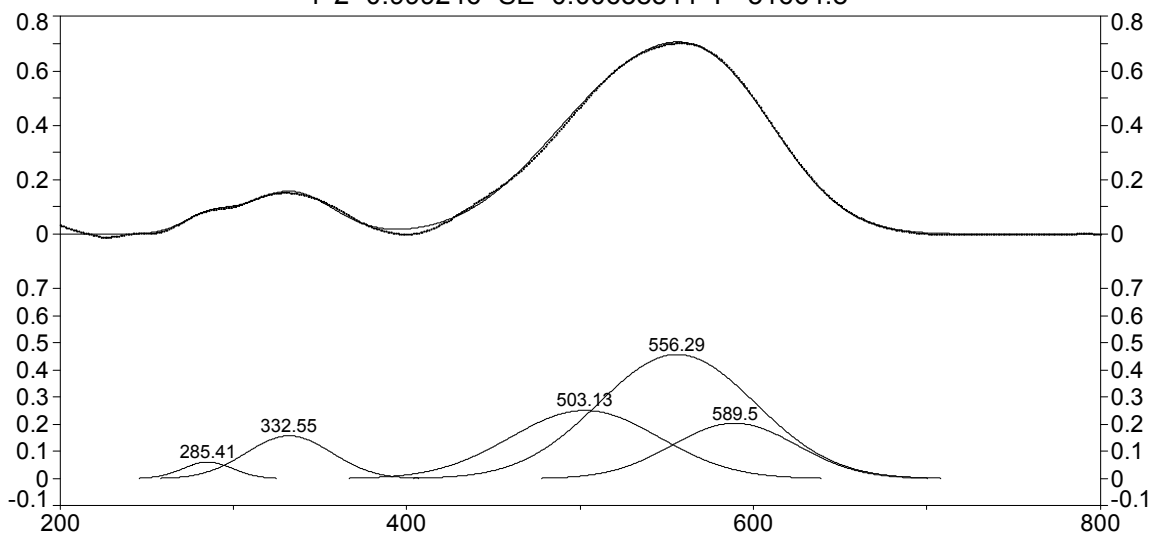


Figure B. 81 Peak fit of MS-1 / 0.5 mol % thiondigo unheated.

Table B. 81 Peak fit statistics of MS-1 / 0.5 mol % thioindigo unheated.

Description: MS1-6%THIOUN - MS1-6%THIOUNsmooth - C:\COLOR\Data\ALE\pennstate\MS1-6%THIOUN.spc

X Variable: Wavelength nm.

File Source: c:\documents and settings\ale\desktop\thesis final\peak fit\ms-1\ms1-6%thiounpeakfit.txt

Measured Values

Peak	Type	Amplitude	Center	FWHM	Asym50	FW Base	Asym10
1	Voigt Area	0.06106366	285.412905	34.6497638	1.00000000	69.3587172	1.00000000
2	Voigt Area	0.15752210	332.553285	57.9530635	1.00000000	116.005124	1.00000000
3	Voigt Area	0.25117404	503.127687	101.048754	1.00000000	202.270122	1.00000000
4	Voigt Area	0.45696470	556.286414	106.730400	1.00000000	213.643119	1.00000000
5	Voigt Area	0.20411405	589.498280	84.4481129	0.99999998	169.040482	0.99999999
Peak	Type	Anlytc Area	% Area	Int Area	% Area	Centroid	Moment2
1	Voigt Area	2.25224345	2.06152792	2.25224344	2.06152795	285.412905	216.513539
2	Voigt Area	9.71740050	8.89455021	9.71740015	8.89455008	332.553290	605.671140
3	Voigt Area	27.0170501	24.7292996	27.0170501	24.7293001	503.127687	1841.39296
4	Voigt Area	51.9162125	47.5200501	51.9162105	47.5200493	556.286405	2054.28328
5	Voigt Area	18.3482673	16.7945722	18.3482672	16.7945725	589.498279	1286.06943
Total		109.251174	100.000000	109.251171	100.000000		

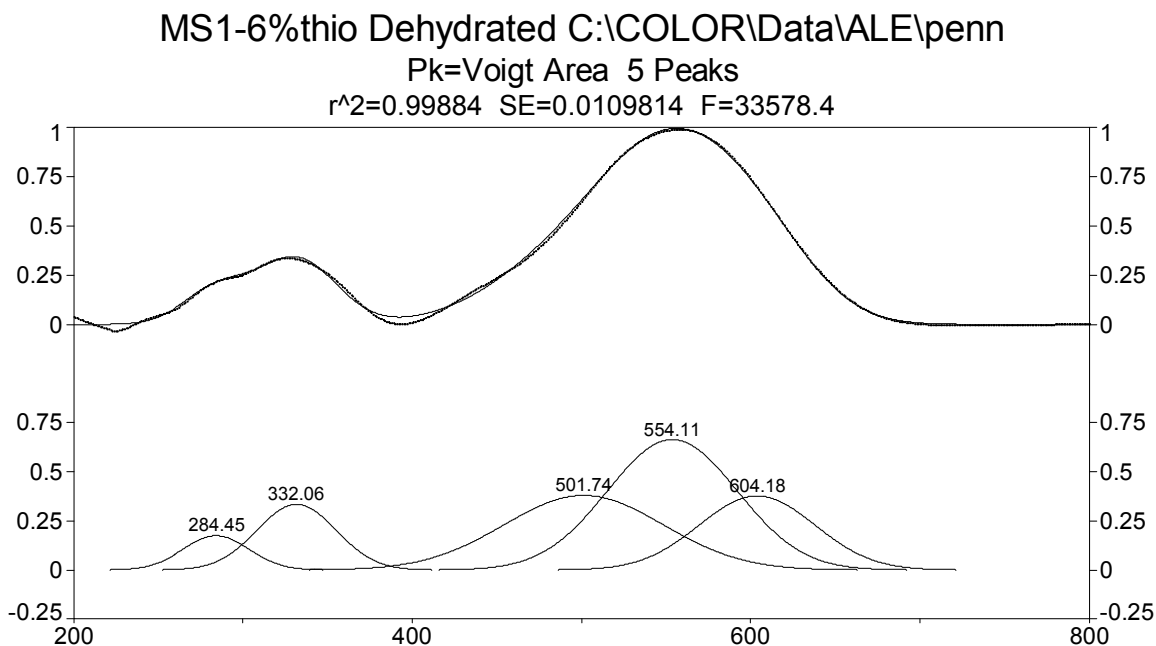


Figure B. 82 Peak fit of MS-1 / 0.5 mol % thioindigo heated at 413K for nine hours.

Table B. 82 Peak fit statistics of MS-1 / 0.5 mol % thioindigo heated at 413K for nine hours.

Description: MS1-6%thio1409hfreshfiucha - MS1-6%thio1409hfreshfiucha - C:\COLOR\Data\ALE\penn

X Variable: iucha.spc

Y Variable: Wavelength nm.

File Source: c:\documents and settings\ale\desktop\thesis final\peak fit\ms-1\ms1-6%thio1409hfreshfiuchapeakfit.txt

Measured Values

Peak	Type	Amplitude	Center	FWHM	Asym50	FW Base	Asym10
1	Voigt Area	0.17479236	284.453668	46.0739641	1.00000006	92.2266330	1.00000003
2	Voigt Area	0.33465543	332.055144	55.0316302	1.00000000	110.157267	1.00000000
3	Voigt Area	0.37963722	501.738239	110.819975	1.00000000	221.829256	1.00000000
4	Voigt Area	0.66392372	554.105659	90.3508753	1.00000000	180.856090	1.00000000
5	Voigt Area	0.37762657	604.180213	80.4584938	1.00000007	161.054429	1.00000004

Peak	Type	Anlytc Area	% Area	Int Area	% Area	Centroid	Moment2
1	Voigt Area	8.57255409	5.06786152	8.57248611	5.06782338	284.454371	382.761627
2	Voigt Area	19.6038996	11.5892939	19.6038995	11.5892984	332.055145	546.146550
3	Voigt Area	44.7836044	26.4748525	44.7836044	26.4748632	501.738239	2214.72927
4	Voigt Area	63.8532141	37.7482887	63.8532141	37.7483039	554.105659	1472.14056
5	Voigt Area	32.3419831	19.1197034	32.3419830	19.1197110	604.180213	1167.42308
	Total	169.155255	100.000000	169.155187	100.000000		

MAS-1

MAS1-6%THIOUN - C:\COLOR\Data\ALE\pennstate\MAS1-6%THIOUN.

Pk=Voigt Area 5 Peaks

$r^2=0.999457$ SE=0.00633179 F=71738

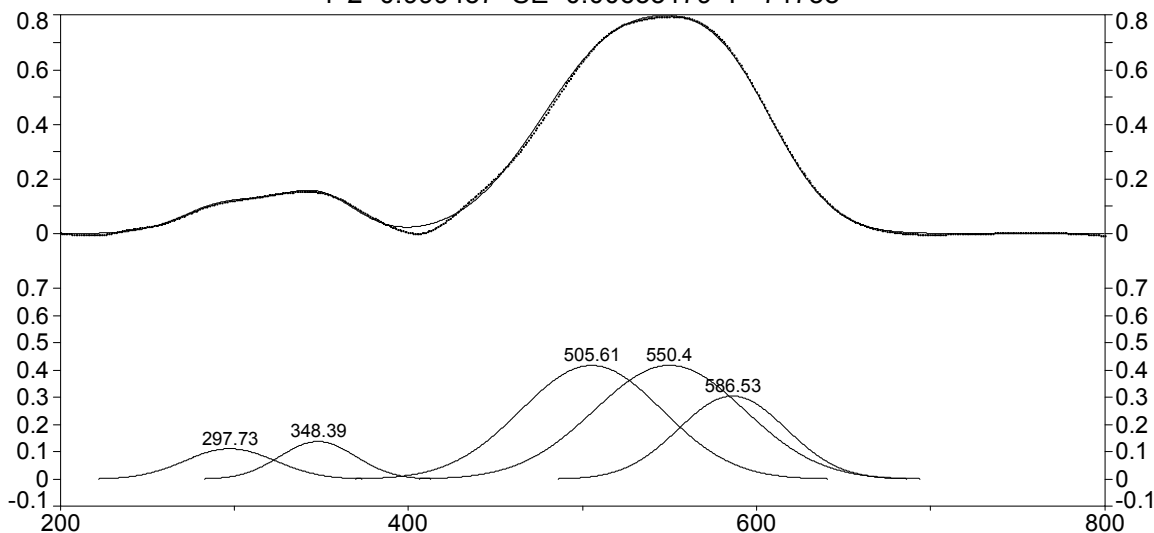


Figure B. 83 Peak fit of MAS-1 / 0.5 mol % thioindigo unheated.

Table B. 83 Peak fit statistics of MAS-1 / 0.5 mol % thioindigo unheated.

Description: MAS1-6%THIOUN - MAS1-6%THIOUNsmooth - C:\COLOR\Data\ALE\pennstate\MAS1-6%THIOUN.

X Variable: Wavelength nm.

File Source: c:\documents and settings\ale\desktop\thesis final\peak fit\mas-1\mas1-6%thiounpeakfit.txt

Measured Values

Peak	Type	Amplitude	Center	FWHM	Asym50	FW Base	Asym10
1	Voigt Area	0.11184971	297.728681	61.5406050	1.00000001	123.186335	1.00000001
2	Voigt Area	0.13854345	348.394056	51.2640817	0.99999998	102.615734	0.99999999
3	Voigt Area	0.41704501	505.610895	95.8400705	1.00000000	191.843858	1.00000000
4	Voigt Area	0.41761055	550.403542	101.734739	1.00000000	203.643264	1.00000000
5	Voigt Area	0.30507173	586.531369	72.7111663	1.00000015	145.546540	1.00000008
Peak	Type	Anlytc Area	% Area	Int Area	% Area	Centroid	Moment2
1	Voigt Area	7.32704488	5.80267572	7.32636948	5.80217188	297.738265	682.043441
2	Voigt Area	7.56016713	5.98729761	7.56016713	5.98732964	348.394056	473.926416
3	Voigt Area	42.5463454	33.6947091	42.5463454	33.6948894	505.610895	1656.45179
4	Voigt Area	45.2244133	35.8156132	45.2244132	35.8158047	550.403541	1866.47873
5	Voigt Area	23.6121369	18.6997044	23.6121369	18.6998044	586.531372	953.425524
Total		126.270108	100.000000	126.269432	100.000000		

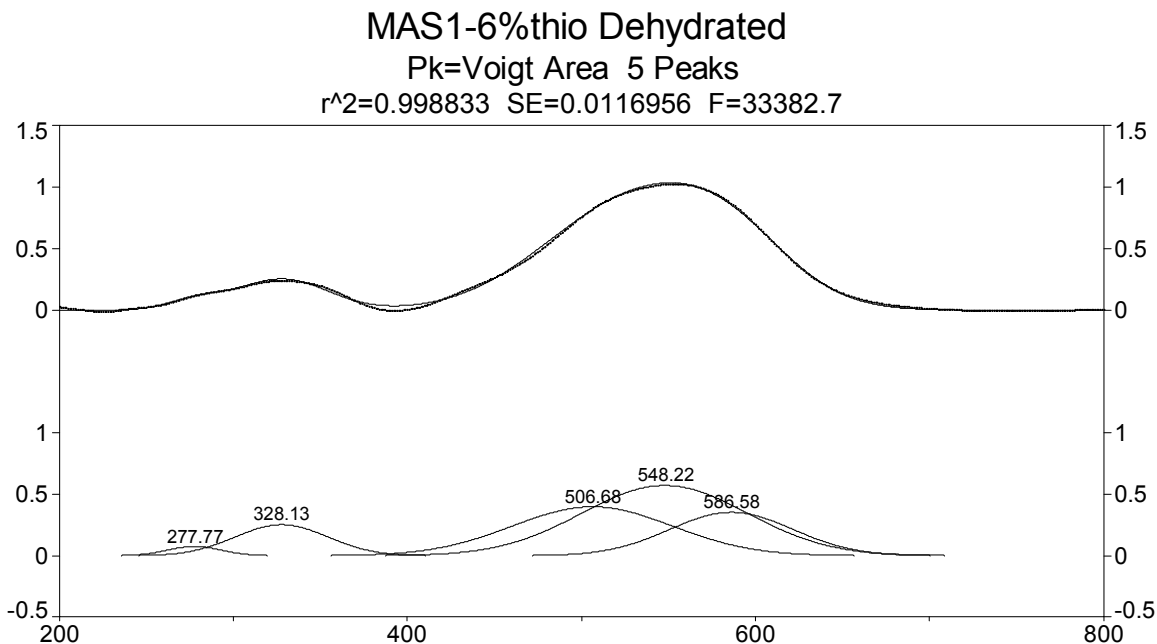


Figure B. 84 Peak fit of MAS-1 / 0.5 mol % thioindigo heated at 413K for nine hours.

Table B. 84 Peak fit statistics of MAS-1 / 0.5 mol % thioindigo heated at 413K for nine hours.

Description: MAS1-6%thio1409hfreshredlila - MAS1-6%thio1409hfreshredlila - C:\COLOR\Data\ALE\
X Variable: reshredlila.spc
Y Variable: Wavelength nm.
File Source: c:\documents and settings\ale\desktop\thesis final\peak fit\mas-1\mas1-6%thio1409hfreshredlilapeakfit.txt

Measured Values

Peak	Type	Amplitude	Center	FWHM	Asym50	FW Base	Asym10
1	Voigt Area	0.07598992	277.766286	36.8912774	1.00000001	73.8976677	1.00000001
2	Voigt Area	0.25345125	328.126416	62.4865637	1.00000000	125.168106	1.00000000
3	Voigt Area	0.39848643	506.679177	108.490330	1.00000000	217.319185	1.00000000
4	Voigt Area	0.57234484	548.221928	111.868494	0.99999992	224.086054	0.99999996
5	Voigt Area	0.35387989	586.575529	83.4757654	0.99999996	167.212003	0.99999998

Peak	Type	Anlytc Area	% Area	Int Area	% Area	Centroid	Moment2
1	Voigt Area	2.98738294	1.80349928	2.98665077	1.80362205	277.797700	254.144705
2	Voigt Area	16.8768846	10.1886667	16.8721773	10.1890155	328.163502	717.855964
3	Voigt Area	46.0697398	27.8125517	46.0549908	27.8123568	506.676923	2143.14331
4	Voigt Area	68.2302179	41.1909524	68.2069665	41.1898136	548.204817	2277.67521
5	Voigt Area	31.4794754	19.0043299	31.4710454	19.0051920	586.552987	1273.90950
	Total	165.643701	100.000000	165.591831	100.000000		

PRETREATED PALYGORSKITE AT 833K

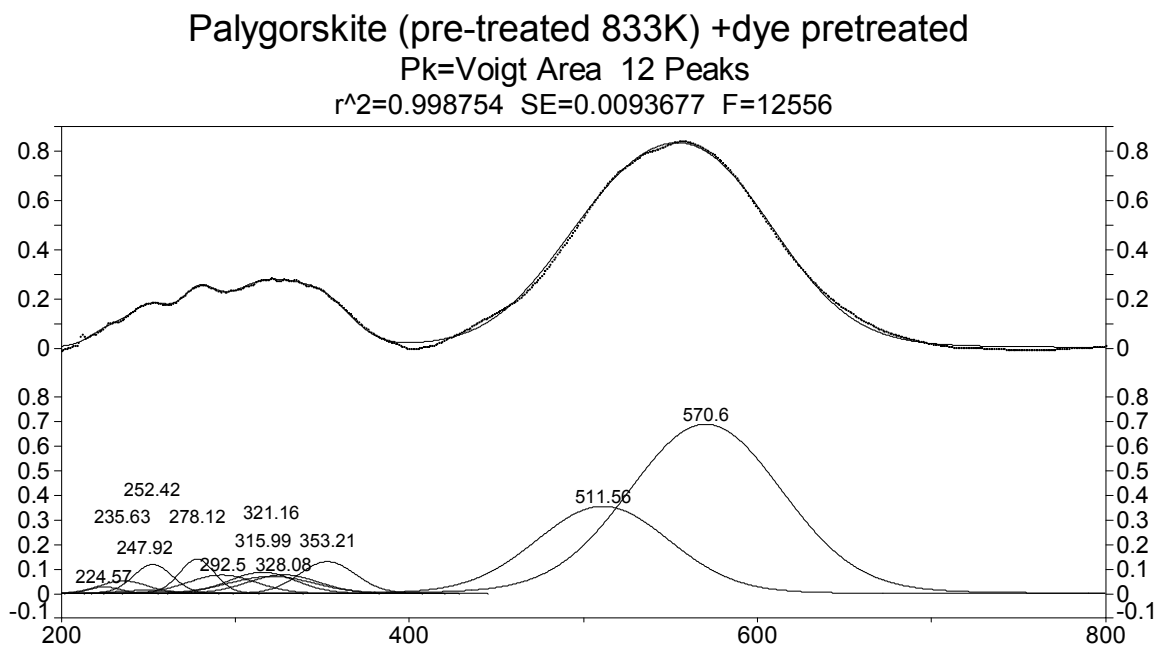


Figure B. 85 Peak fit of pretreated palygorskite / 0.5 mol % thioindigo heated at 413K for nine hours.

Table B. 85 Peak fit statistics of pretreated palygorskite / 0.5 mol % thioindigo heated at 413K for nine hours.

Description: C:\Documents and Settings\Ale\Desktop\THESIS FINAL\Peak Fit\Palygorskite\paly550
File Source: c:\documents and settings\ale\desktop\thesis final\peak fit\palygorskite\paly550peakfit.txt

Measured Values

Peak	Type	Amplitude	Center	FWHM	Asym50	FW Base	Asym10
1	Voigt Area	0.02796468	224.566092	21.8819129	0.99999999	45.0159073	1.00000000
2	Voigt Area	0.05221477	235.625667	33.2529526	0.99999998	68.4086367	0.99999999
3	Voigt Area	0.01381041	247.918473	42.1271122	0.99999999	86.6647346	0.99999999
4	Voigt Area	0.11888305	252.415306	26.4567489	1.00000006	54.4273510	1.00000003
5	Voigt Area	0.14191873	278.124760	24.2795354	0.99999997	49.9483440	0.99999998
6	Voigt Area	0.07592791	292.500867	47.2987291	1.00000000	97.3038880	1.00000000
7	Voigt Area	0.08759440	315.988559	45.3345484	1.00000000	93.2631364	1.00000000
8	Voigt Area	0.07070699	321.155008	58.0251136	1.00000000	119.370420	1.00000000
9	Voigt Area	0.07714054	328.081668	48.2958939	1.00000000	99.3552754	1.00000000
10	Voigt Area	0.13087373	353.211911	38.1967600	1.00000014	78.5791358	1.00000007
11	Voigt Area	0.35604904	511.561580	90.6235250	1.00000007	186.432521	1.00000004
12	Voigt Area	0.69021650	570.598014	103.766006	0.99999993	213.469494	0.99999996

Peak	Type	Anlytc Area	% Area	Int Area	% Area	Centroid	Moment2
1	Voigt Area	0.67736693	0.45734650	0.66409888	0.45311979	225.814830	275.340171
2	Voigt Area	1.92199555	1.29769834	1.87938515	1.28231897	237.384033	473.117038
3	Voigt Area	0.64401666	0.43482897	0.63138577	0.43079938	249.835703	657.276920
4	Voigt Area	3.48165077	2.35075072	3.45083822	2.35453351	253.403947	354.190044

5	Voigt Area	3.81424761	2.57531439	3.79305269	2.58802908	278.844633	317.105678
6	Voigt Area	3.97538955	2.68411466	3.93699702	2.68624340	293.798579	787.367086
7	Voigt Area	4.39576436	2.96794450	4.36239467	2.97649550	317.015410	742.031547
8	Voigt Area	4.54158145	3.06639769	4.49836559	3.06926950	322.441815	1063.81162
9	Voigt Area	4.12402855	2.78447315	4.09311318	2.79276266	329.080120	813.138425
10	Voigt Area	5.53360054	3.73619192	5.50496647	3.75608104	353.850037	583.217586
11	Voigt Area	35.7173766	24.1157584	35.3808640	24.1406361	511.448227	2126.74968
12	Voigt Area	79.2810192	53.5291807	78.3659786	53.4697111	569.769966	2641.72044
	Total	148.108038	100.000000	146.561440	100.000000		

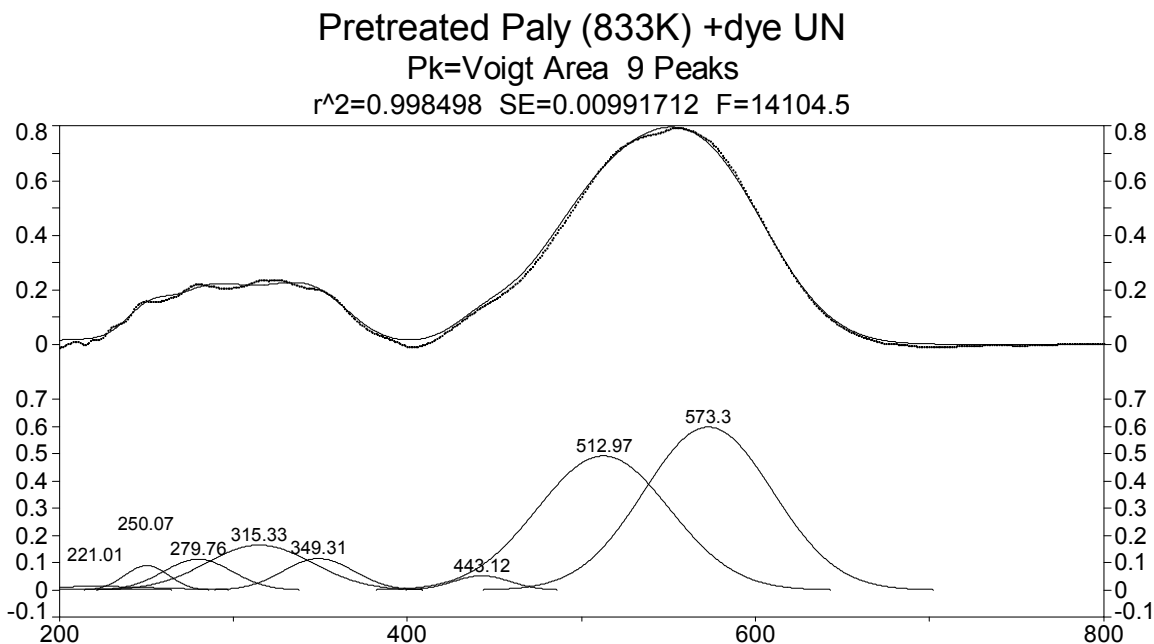


Figure B. 86 Peak fit of pretreated palygorskite / 0.5 mol % thioindigo unheated.

Table B. 86 Peak fit statistics of pretreated palygorskite / 0.5 mol % thioindigo unheated.

Description: C:\Documents and Settings\Ale\Desktop\THESIS FINAL\Peak Fit\Palygorskite\paly550
File Source: c:\documents and settings\ale\desktop\thesis final\peak fit\palygorskite\paly550unpeakfit.txt

Measured Values

Peak	Type	Amplitude	Center	FWHM	Asym50	FW Base	Asym10
1	Voigt Area	0.00421682	200.000002	118.896279	0.86319909	237.784260	0.92251289
2	Voigt Area	0.01378179	221.014380	87.3231936	1.00000000	175.041730	1.00000000
3	Voigt Area	0.09021031	250.065440	29.5459850	1.00000003	59.2257348	1.00000002
4	Voigt Area	0.11409861	279.761138	46.8187798	0.99999995	93.8495244	0.99999997
5	Voigt Area	0.16537339	315.328002	71.8436709	1.00000000	144.012603	1.00000000
6	Voigt Area	0.11594099	349.314457	47.7072464	0.99999996	95.6304799	0.99999998
7	Voigt Area	0.05294747	443.118744	38.4339460	1.00000000	77.0418957	1.00000000
8	Voigt Area	0.49180364	512.971592	89.5236520	1.00000000	179.452609	1.00000000
9	Voigt Area	0.59766536	573.299414	87.1395297	1.00000002	174.673570	1.00000001

Peak	Type	Anlytc Area	% Area	Int Area	% Area	Centroid	Moment2
1	Voigt Area	0.53542170	0.40065376	0.24916808	0.18747036	238.977593	958.920037

2	Voigt Area	1.28387016	0.96071452	0.91659349	0.68963130	238.859127	741.412621
3	Voigt Area	2.84341613	2.12771606	2.84163680	2.13800525	250.130898	171.461005
4	Voigt Area	5.69883635	4.26441473	5.69512791	4.28492952	279.843553	416.421273
5	Voigt Area	12.6747645	9.48447177	12.6647699	9.52878450	315.433802	959.951430
6	Voigt Area	5.90074845	4.41550469	5.89856014	4.43798890	349.360797	432.352946
7	Voigt Area	2.17093056	1.62449800	2.17043323	1.63300167	443.131539	284.535360
8	Voigt Area	46.9694295	35.1470221	46.9448981	35.3206430	512.964586	1481.57418
9	Voigt Area	55.5595928	41.5750043	55.5294678	41.7795455	573.259988	1404.84507
	Total	133.637010	100.000000	132.910656	100.000000		

LIQUID INTERACTION

THIOINDIGO- 98.7% SULFURIC ACID

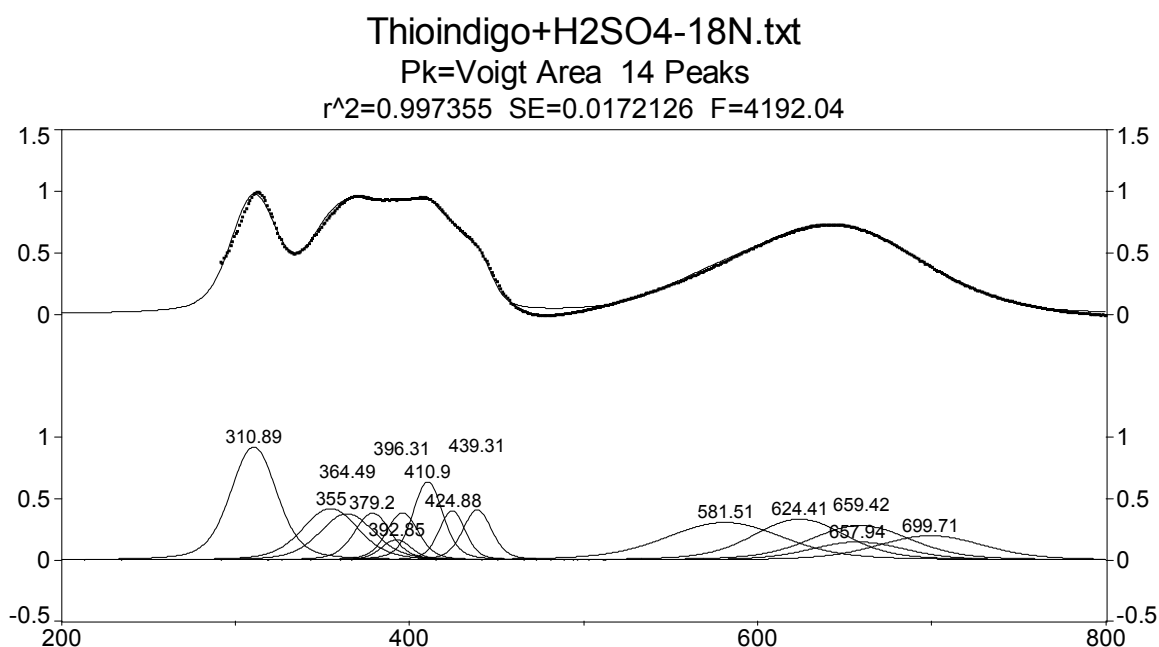


Figure B. 87 Peak fit of thioindigo in concentrated sulfuric acid.

Table B. 87 Peak fit statistics of thioindigo in concentrated sulfuric acid.

Description: C:\Documents and Settings\Ale\Desktop\09.12.08UV Varian\thioH2SO4-18N.txt

File Source: c:\documents and settings\ale\Desktop\thesis final\peak fit\thioindigo-h2so4\thioh2so4- 0.18npeakfit.txt

Measured Values

Peak	Type	Amplitude	Center	FWHM	Asym50	FW Base	Asym10
1	Voigt Area	0.92152715	310.886514	31.2097055	0.99999988	70.7812818	0.99999994
2	Voigt Area	0.42015120	354.999262	38.1839338	0.99999998	86.5983108	0.99999999
3	Voigt Area	0.37837549	364.490791	36.9370536	0.99999999	83.7704797	0.99999999
4	Voigt Area	0.38292399	379.196930	24.4244088	0.99999998	55.3927356	0.99999999

5	Voigt Area	0.16594762	392.845588	20.6519931	0.99999999	46.8371785	1.00000000
6	Voigt Area	0.38480328	396.308345	21.5768105	1.00000036	48.9345953	1.00000017
7	Voigt Area	0.63756998	410.902415	20.2545776	1.00000000	45.9358696	1.00000000
8	Voigt Area	0.40227895	424.875322	17.6312882	0.99999990	39.9864452	0.99999995
9	Voigt Area	0.40972434	439.310716	19.6380285	1.00000000	44.5375825	1.00000000
10	Voigt Area	0.30656651	581.509713	79.8528931	1.00000000	181.100399	1.00000000
11	Voigt Area	0.33401586	624.414815	62.8718495	1.00000000	142.588660	1.00000000
12	Voigt Area	0.14834300	657.942105	64.2307943	1.00000001	145.670646	1.00000000
13	Voigt Area	0.28117085	659.419022	68.2133731	1.00000000	154.702837	1.00000000
14	Voigt Area	0.19879272	699.713794	72.4355066	1.00000000	164.278321	1.00000000
Peak	Type	Anlytc Area	% Area	Int Area	% Area	Centroid	Moment2
1	Voigt Area	35.1737379	14.6362234	30.6789051	13.3574789	318.420127	988.526027
2	Voigt Area	19.6203610	8.16427268	18.8601049	8.21161815	359.346748	1197.63606
3	Voigt Area	17.0925147	7.11240486	16.5294335	7.19685265	368.295403	1154.59228
4	Voigt Area	11.4381911	4.75957150	11.2271624	4.88826395	381.339437	736.416934
5	Voigt Area	4.19134803	1.74407128	4.13302836	1.79950487	394.439716	615.422089
6	Voigt Area	10.1542237	4.22529691	10.0102322	4.35841715	397.924177	644.813916
7	Voigt Area	15.7932594	6.57176877	15.6019398	6.79302543	412.226823	602.786309
8	Voigt Area	8.67425259	3.60946281	8.58936450	3.73977673	425.880868	520.383431
9	Voigt Area	9.84034590	4.09468852	9.73965527	4.24060897	440.277437	583.316517
10	Voigt Area	29.9389166	12.4579501	28.8781449	12.5734348	580.176101	2795.77747
11	Voigt Area	25.6828986	10.6869689	24.9071111	10.8444617	622.087250	2109.85111
12	Voigt Area	11.6528204	4.84888139	11.2461194	4.89651775	654.381472	2159.08373
13	Voigt Area	23.4563556	9.76047704	22.5787825	9.83071628	655.552207	2314.60662
14	Voigt Area	17.6105408	7.32796184	16.6958797	7.26932270	693.450931	2467.72730
	Total	240.319767	100.000000	229.675864	100.000000		

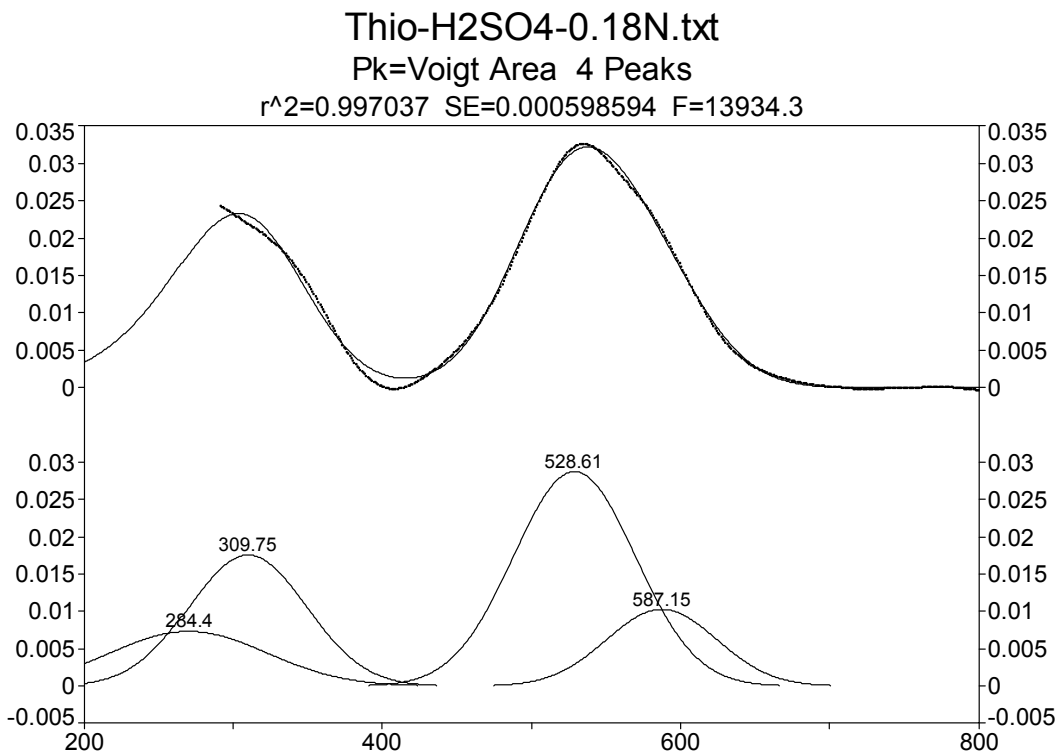


Figure B. 88 Peak fit of thioindigo interaction with concentrated sulfuric acid, after water addition.

Table B. 88 Peak fit statistics of thioindigo interaction with concentrated sulfuric acid, after water addition.

Description: C:\Documents and Settings\Ale\Desktop\09.12.08UV Varian\ThioH2SO4-0.18N.txt

File Source: c:\documents and settings\ale\desktop\thesis final\peak fit\thioindigo-h2so4\thioh2so4- 0.18npeakfit.txt

Measured Values

Peak	Type	Amplitude	Center	FWHM	Asym50	FW Base	Asym10
1	Voigt Area	0.00705337	284.395604	126.262696	0.63233168	247.292670	0.77646319
2	Voigt Area	0.01754570	309.752700	92.3603611	1.00000001	184.878495	1.00000001
3	Voigt Area	0.02873348	528.609858	96.0735959	1.00000001	192.311307	1.00000000
4	Voigt Area	0.01029158	587.152487	86.8591891	1.00000000	173.866753	1.00000000

Peak	Type	Anlytc Area	% Area	Int Area	% Area	Centroid	Moment2
1	Voigt Area	0.95848765	14.5810321	0.42250994	7.69456810	317.647279	-11768.285
2	Voigt Area	1.72499750	26.2415942	1.17846683	21.4617278	330.197755	738.184261
3	Voigt Area	2.93849201	44.7019283	2.93849200	53.5145441	528.609859	1664.53373
4	Voigt Area	0.95154689	14.4754455	0.95154689	17.3291600	587.152486	1360.55478
	Total	6.57352405	100.000000	5.49101566	100.000000		

CURRICULUM VITAE

Alejandra Ramirez earned her Bachelor of Science degree in Chemistry from the Universidad Autonoma de Nuevo Leon in 1995. She received her Master of Science degree in Materials Science and Engineering in 2000 from the University Autonoma de Nuevo Leon. In 2008 she will graduate from the PhD of Materials Science and Engineering program at the University of Texas at El Paso (UTEP). Alejandra Ramirez was the recipient of a study abroad scholarship from the UTEP International Office to perform research in Berlin, Germany at the Hahn- Meitner Institute. While pursuing her degree, she worked as a research associate and teaching assistant for the department of Materials Science and Engineering. In addition, as part of her academic training, she had the opportunity to teach Chemistry at El Paso Community College. Alejandra Ramirez has presented her research at international conferences and workshops such as the 2008 Pan American Advanced Studies Institute. Her dissertation entitled, "A Study of the Interaction of Thioindigo Dye, with Several Inorganic Host Materials", was supervised by Dr. Russell Chianelli and Dr. Pannell. After graduation, she will pursue her academic career with a postdoctoral position overseas at the Helmholtz-Zentrum Berlin für Materialien und Energie in Germany.

This dissertation was typed by Alejandra Ramirez